PETROCHEMICAL AND Sr ISOTOPIC STUDIES OF LAVAS AND XENOLITHS FROM TONGARIRO VOLCANIC CENTRE - IMPLICATIONS FOR CRUSTAL CONTAMINATION OF CALC-ALKALINE MAGMAS.

by

IAN J. GRAHAM

A thesis submitted for the degree of Doctor of Philosophy,

Research School of Earth Sciences,

Victoria University of Wellington.

March, 1985.

FRONTISPIECE: BEI photograph of TYPE IX xenolith (hydrothermal nodule) from Whakapapa Formation flow, Ruapehu. Minerals are natroalunite (blades), quartz (rounded aggregates) and rutile (white patches on quartz, LHS). Natroalunite is zoned with K-rich cores (lighter) and Na-rich rims (darker) Scale bar = .1mm; field of view = 1.9mm.

****

ABSTRACT

****

Petrogenesis of Tongariro Volcanic Centre lavas, particularly those from Mount Ruapehu and nearby vents, is investigated through a detailed petrochemical and Sr isotope study. The importance and nature of crustal contamination as a process is assessed from metasedimentary xenoliths and their relationship to local sedimentary basement lithologies. These results are tested by least squares modelling of processes such as crystal fractionation, crystal accumulation, combined assimilation and fractional crystallisation (AFC) and magma mixing.

Sedimentary basement lithologies near the TVC provide a guide to the composition of potential crustal contaminants and a genetic link to some xenoliths. The rocks are of three main types (i) Torlesse terrane greywackes and argillites, (ii) Waipapa terrane greywackes and (iii) Late Tertiary marine sandstones, siltstones and conglomerates.

Torlesse terrane flysch sediments, which form the Kaimanawa ranges on the eastern margin, have dominantly granitic bulk compositions and comprise a chemical continuum between Si-, Na-, Sr-rich greywackes and Al-, Fe- and K-rich argillites. A Rb-Sr whole-rock isochron age for the latter of 141 (3) Ma is interpreted as the time of low-grade metamorphism; similar rocks from Otaki Forks, north of Wellington yield an age of 182 (13) Ma which is some 40 Ma younger than the depositional age as inferred from fossil evidence. These data suggest that metamorphism and uplift of Torlesse terrane sequences are local events unrelated to major phases of the Rangitata Orogeny.

Waipapa terrane greywackes occur to the NW and west of the TVC. These have intermediate calc-alkaline chemistries and low Sr isotopic ratios (.70500 to .70850) which give a whole-rock isochron age of 205 (17) Ma. By comparison with a similar rock suite from Coffs Harbour Block, northern

N.S.W., Austalia, this age is interpreted to be the timing of low-grade (prehnite-pumpellyite facies) metamorphism.

Late Tertiary marine sediments form a thin veneer over older basement on the margins of TVC. These rocks are chemically similar to Torlesse terrane metasediments and have Sr isotopic compositions ranging between .707 and .710.

Xenoliths of metasedimentary, igneous and metaigneous origin occur in most TVC lavas and are abundant in some. They are classified according to petrography and presumed origin, and are of six main types: (1) Upper crustal xenoliths (TYPE UCX) include porcellanite, metagreywacke and calcsilicate and can be related to known sedimentary basement on the basis of mineralogy, bulk-rock chemistry and Sr isotopic composition (2) Vitrified xenoliths (TYPE VX) occur only in Ngauruhoe 1954 and Pukeonake lavas and are of two chemically distinct types. Of these, TYPE VXa xenoliths are chemically similar to Torlesse terrane metasediments and usually contain more than 50% glass, representing advanced partial melting. Retention of their original bulk-rock chemistry implies derivation from shallow depths and rapid transport to the surface. TYPE VXb xenoliths are less vitrified and are chemically different from any known basement lithology (3) Quartz-rich xenoliths (TYPE QX) are conspicuous and abundant in most lavas and are mainly quartzo-feldspathic gneisses (TYPE QXa) or quartzites (TYPE QXb). The latter probably represent TYPE QXa xenoliths modified by extraction of partial granitic melt and subsequent recrystallisation. Both are interpreted to be restite assemblages derived initially from greywacke-gneiss (probably from the Torlesse terrane). Several rare TYPE QX xenoliths (TYPES QXc to QXf) with unusual mineral assemblages and obscure origins also occur (4) Quartz-poor xenoliths (TYPE QPX) have biotite-, spinel-rich or feldspar-rich assemblages and are interpreted to be restites after partial melting of the feldspathic and micaceous layers of greywacke-gneiss (5) Igneous xenoliths (TYPE IX), include variably altered blocks of surface volcanics, a natroalunite-bearing nodule and a variety of cognate cumulate nodules and show little evidence of pyrometamorphism or of an extended history (6) Meta-igneous xenoliths (TYPE MIX) have broadly calc-alkaline chemistries but are texturally, mineralogically and isotopically different from host lavas. Some (TYPE MIXa) are coarse-grained with high Cr and Ni contents and may be basic cumulates. Others (TYPES MIXb and MIXc) are finer-grained and are chemically similar to low-K orogenic andesites. All may have originated from the base of the continental crust and represent the original oceanic crust on which the Torlesse terrane was deposited.

Cation exchange equilibria pertaining to certain key assemblages indicates that equilibration of most xenoliths occurred at temperatures of 800 °C to 1000 °C (reliable pressure estimates are unattainable). The occurrence of granitic partial melt in some xenoliths and the dominance of quartz-rich and quartz-poor xenolith types indicate that crustal contamination (by assimilation of partial melt) is a widespread phenomenum.

Ruapehu lavas and those of nearby vents are dominantly calc-alkaline, medium-K andesites. They are porphyritic with phenocrysts of plagioclase, augite, olivine (mainly in basalts and basic andesites), orthopyroxene (mainly in acid andesites and dacites) and titanomagnetite (or chromian spinel in basic lavas). Hydrous minerals are rare. The lavas can be catagorised into six petrographically and chemically distinct groups: TYPE 1 are plagioclase-pyroxene-rich and are the dominant type, being represented by all Ruapehu Group Formations, Red Crater basalt and Ngauruhoe 1954 andesite. Compositions range from basalt to dacite and show decreasing Fe, Mg, Ca, Cr, Ni, constant Ti, Al, Na, Sr, increasing LILE and increasing $^{87}Sr/^{86}Sr$ with increasing silica. TYPE 2 are characterised by high modal plagioclase and TYPES 3 & 4 by high mafic mineral contents, but each is otherwise similar to TYPE 1. TYPE 5 lavas are olivine andesites from Pukekaikiore, Ohakune and Hauhungatahi. They characteristically contain no plagioclase phenocrysts and have high Mg, Ca and Sr contents and low $^{87}Sr/^{86}Sr$ ratios. TYPE 6 lavas show disequilibrium features (such as strongly reversed-zoned phenocrysts) which are normally considered evidence for magma mixing. All have high Cr and Ni contents, and low $^{87}Sr/^{86}Sr$ ratios.

Potential parental magmas for TVC lavas include high-alumina basalts restricted to the extensional zone of rhyolitic volcanism in Taupo Volcanic Zone, low-alumina basalts occurring at the southern end of the extensional zone and directly associated with andesites and one example of magnesian quartz tholeiite (Waimarino basalt). The latter, from east of Lake Taupo, has primary chemical characteristics but is highly porphyritic and contains quartzose xenoliths. Compositional data indicate that neither low-alumina nor high-alumina basalt can be generated directly from tholeiite by any reasonable process and therefore each represents a distinct magma type.

Petrochemical and isotopic data of TVC lavas and xenoliths provide an excellent framework for petrogenetic modelling. Least squares analysis shows that evolved TYPE 1 lavas can be generated from low-alumina basalt (e.g. Ruapehu basalt) or from less-evolved TYPE 1 lavas by AFM, involving POAM fractionation plus assimilation of granitic partial melt of greywacke-gneiss. Additional selective contamination may be required to explain the high Sr isotopic ratios of some lavas (e.g. Ngauruhoe 1954). TYPE 2 lavas can be generated from TYPE 1 either by POAM fractionation (where plagioclase removal is suppressed) or, better, by plagioclase addition. TYPE 3 can be generated from TYPE 1 by olivine + clinopyroxene addition. However, their higher LILE and lower $^{87}Sr/^{86}Sr$ ratios may rather suggest an alternative genesis from an unknown parent. TYPE 5 lavas can be generated from a Waimarino basalt-type parent by POAM fractionation without addition of a crustal contaminant. The somewhat higher $^{87}Sr/^{86}Sr$ ratio of Waimarino basalt indicates that although tholeiitic basalt has occurred in small amounts throughout the history of the TVC, its isotopic composition (and

LILE content) has varied with time. TYPE 4 are chemically and isotopically intermediate to TYPES 3 and 5 and, although internally consistent, these lavas cannot be easily generated from any known basalt type (Red Crater basalt gives the best-fit model). For TYPE 6 lavas, the high Cr and Ni contents and low $^{87}Sr/^{86}Sr$ imply that a Waimarino basalt-type parent must be one endmember; best-fit models are achieved when Mangawhero Formation dacite is the other.

Each petrogenetic model is consistent with petrographic, chemical and Sr isotopic constraints. They show that it is feasible to generate most Ruapehu lavas from low-alumina basalt by processes of crystal fractionation with or without crustal assimilation. However, some spatially and volumetrically restricted lava types are better derived from a more tholeiitic parent by crystal fractionation or hybridisation with dacite.

CONTENTS

LIST OF TABLES ("F" denotes facing page)

LIST OF FIGURES ("F" denotes facing page)

LIST OF PLATES

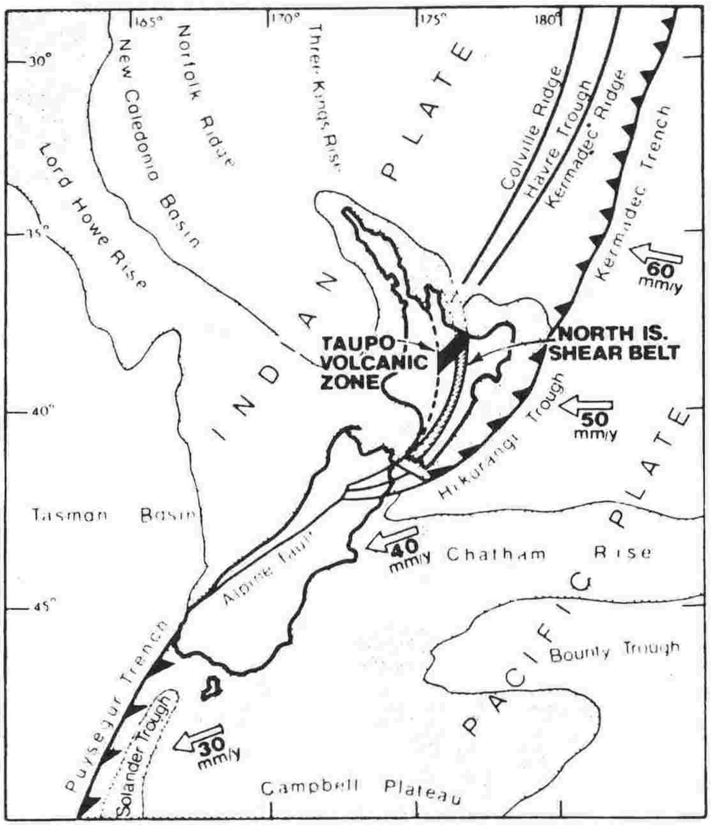

Fig.1.1: Major components of the Pacific-Indian plate boundary in the New Zealand region. Stipple represents continental crust. Arrows show motion of the Pacific plate relative to the Indian plate (after Cole, 1984).

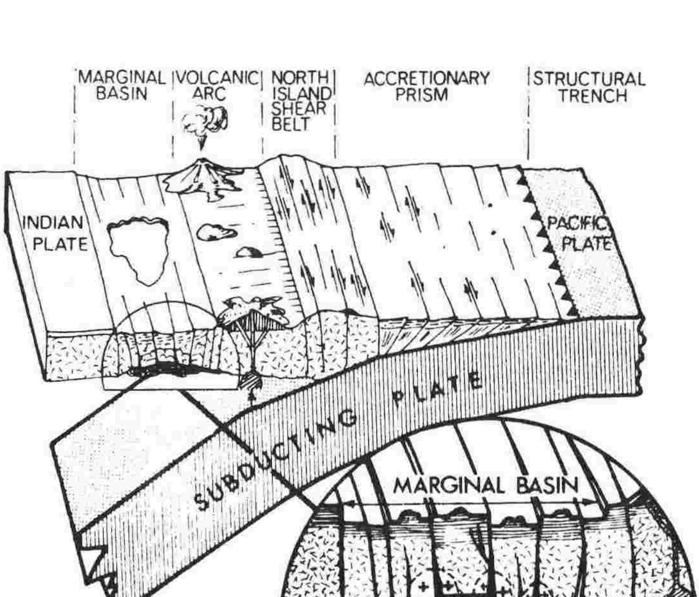

Fig.1.2: Diagrammatic model of the major structural elements of the Taupo-Hikurangi oblique-subduction margin (used by permission Dr.J.W.Cole, 1985).

****

CHAPTER 1: INTRODUCTION

****

1.1 TECTONIC SETTING OF TAUPO VOLCANIC ZONE

The Taupo Volcanic Zone (TVZ), a volcanic arc and marginal basin of the Taupo-Hikurangi subduction system (Cole and Lewis, 1981; Cole, 1984), is a southward extension of the Tonga-Kermadec arc into the continental crustal environment of North Island, New Zealand, representing oblique subduction of the Pacific plate beneath the Indian plate (Fig.1.1). The Hikurangi trough to the east is a structural trench marking the plate boundary and is a topographic expression of the west-dipping seismic zone (Fig.1.2). West of this is a 150km-wide accretionary prism characterised by imbricate thrust faults in Upper Cretaceous to Quaternary turbidites. The accretionary prism is bounded by a frontal ridge of Upper Paleozoic to Mesozoic greywacke, which forms the main axial ranges of the North Island. The North Island Shear Belt, a zone of dextral transcurrent faults, cuts obliquely across the frontal ridge. Thus, oblique convergence is manifested by compressional features to the east and dextral strike-slip features to the west (Cole and Lewis, 1981).

The TVZ (Fig.1.3) extends approximately 300km NNE across the centre of the North Island from Ohakune to White Island. It is up to 40km wide in the central part but narrows northwards and southwards. The zone is essentially a graben structure filled with 2-4km of predominantly rhyolitic pyroclastic debris; in the centre of it is the Taupo Fault Belt (Grindley, 1960), a series of linear faults many of which have been active within the past 10,000 years (Nairn, 1971). Surrounding the zone are plateaux formed of flat-lying sheets of ignimbrite covering a total area of approximately 20,000km^2. This volcano-tectonic depression (Taupo-Rotorua depression;

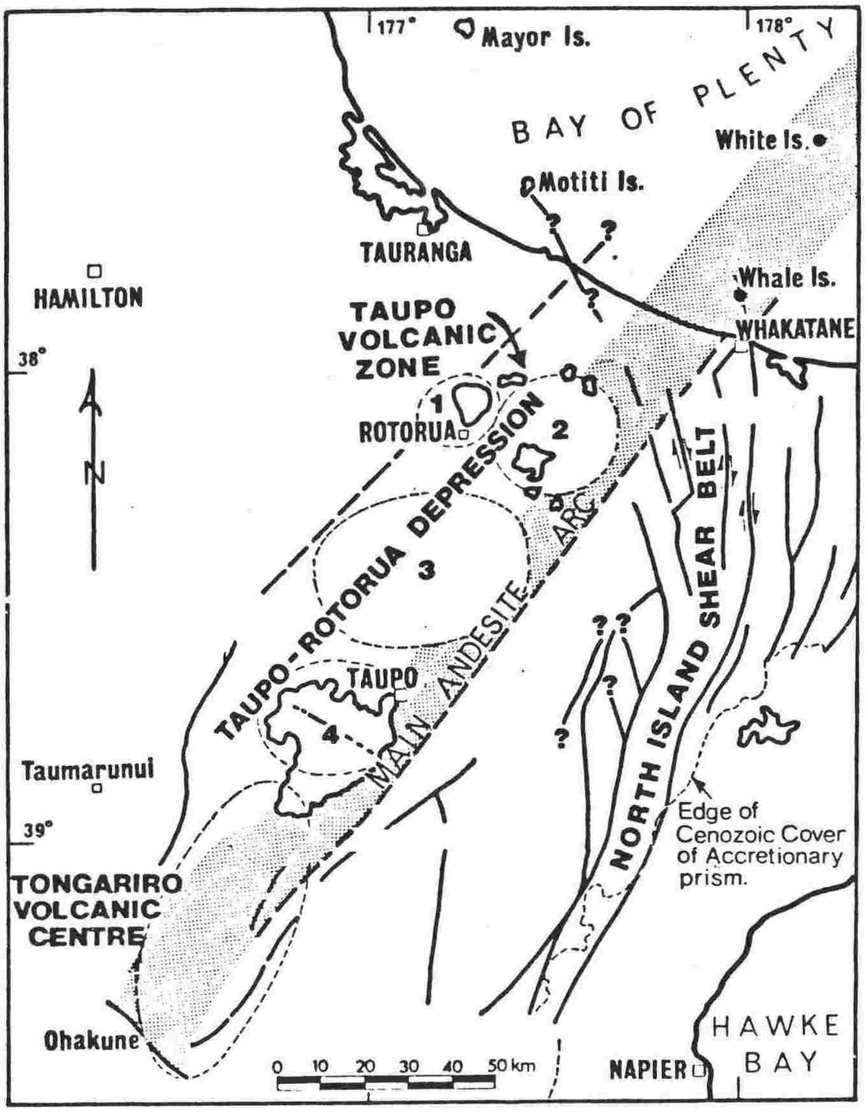

Fig.1.3: Volcanic centres within Taupo Volcanic Zone : 1 = Rotorua, 2 = Okataina, 3 = Maroa, 4 = Taupo. Shaded area is main andesite arc (used by permission, Dr.J.W.Cole, 1985).

Grindley, 1960) is interpreted as an ensialic marginal basin (Cole and Lewis, 1981), and comprises four volcanic centres: Rotorua, Okataina, Maroa and Taupo (Fig.1.3). The fifth centre, Tongariro, is part of a young (<250ka) andesite-dacite volcanic arc extending along the eastern side of the zone and has no associated rhyolitic volcanism (Cole and Lewis, 1981; Cole, 1984). Tongariro Volcanic Centre (TVC) lavas are calc-alkaline but differ chemically from those of Tonga, in particular by having higher alkali element and light REE contents and higher Sr isotopic ratios (Cole, 1981); this suggests some crustal contamination (Ewart and Stipp, 1968, Cole, 1982).

1.2 THESIS ORGANISATION

This thesis uses petrographic and chemical evidence, particularly Sr isotope data, to provide information on petrogenetic models for TVC lavas. This involves a close examination of three integral components, namely parental magmas, crustal contaminants and contaminated magma. Organisation of the study is as follows:

Chapter 2 gives details of the analytical methods employed, and, in particular, stresses the importance of precision and accuracy required for chemical or isotopic data used in petrogenetic modelling. Much time was spent during the early part of this study in developing Sr isotopic analysis techniques at the Institute of Nuclear Sciences. Hence the main features of that system and the experimental methods employed are discussed in full.

Chapter 3 describes chemical and Sr isotopic compositions of the dominant sedimentary basement lithologies. Of particular interest are Torlesse terrane greywackes which occur to the east of the TVC, since these are considered to be the most likely source of crustal contaminants.

Chapter 4 contains a compilation of published and unpublished data on lavas of Ruapehu and nearby vents. W.R.Hackett provided much of this material including detailed stratigraphic and petrographic data, but this study extends beyond his work by using bulk-rock chemistry and Sr isotope systematics to more closely define lava types. Part 2 of the chapter reviews and discusses all basaltic lavas reported from the TVZ, in the hope of identifying suitable parental magma compositions from which to model andesites and dacites of the TVC.

Crustal xenoliths, which provide important information concerning the nature of contaminants and the assimilation process, are described in Chapter 5. Such detailed studies are rarely attempted but, as shown here, provide much data which can be used either in support of, or to argue against, many of the simplistic models for andesite petrogenesis that have been presented in the literature.

Chapter 6 discusses possible petrogenetic models for TVC lavas and the relative importance to them of crystal fractionation, assimilation and fractional crystallisation, selective contamination and magma mixing.

The final chapter summarises and discusses the findings of Chapters 3 to 6 and makes suggestions for further study in certain areas.

1.4 ACKNOWLEDGEMENTS

I wish to acknowledge and to thank the many people from INS, Victoria University and elsewhere who have provided technical information and/or helpful critisism during the course of this work. In particular, each of my supervisors, Dr.J.W.Cole, Dr.J.A.Gamble (Victoria University) and Dr.C.J.D.Adams (INS) contributed greatly and gave unstintingly of time and energy. I thank all INS staff, particularly Dr.B.J.O'Brien (Director) who allowed full use of facilities during my time of research, Dr.J.R.Hulston who was supervisor (by proxy) for a time and who was always available to assist when things went wrong, P.F.Whitla who contributed to an amiable working relationship in the Rb-Sr lab. and R.Ditchburn who shared his technical expertise on matters relating to chemical preparation. All academic and technical staff at Victoria University offered cooperation and helpful discussion during my four years as Junior Lecturer, particularly Dr.R.J.Korsch who found time to pursue joint research (Coffs Harbour Block Rb-Sr geochronology), Dr.R.H.Grapes who combined in the study of xenoliths, J.Carter who created many fine thin-sections, K.Palmer whose expertise in XRF and microprobe analysis was of great assistence, E.Hardy and P.A.Hoverd who drew up the more complicated figures and C.Wallace who willingly undertook a number of gruelling tasks relating to data presentation. I acknowledge also the helpful discussions and suggestions made by visiting geologists Prof.A.R.Duncan (Cape Town); Dr.M.T.McCulloch (ANU), Dr.M.A.Menzies (Open University) and Dr.P.Koons (Otago). Finally, a special mention for my wife Lesley who eased domestic responsibilities when that was most needed, and my parents for their emotional and financial support.

****

CHAPTER 2: ANALYTICAL METHODS

****

2.1 SAMPLE SELECTION & PREPARATION

Basement sediment and metasediment samples (Chapter 3) were selected from drill-core and tunnel cuttings procured through geological investigations relating to the Tongariro Power Project. Only material with minimum exterior weathering and post-depositional veining or sulphide mineralisation was analysed. Lava samples (Chapter 4) from Ruapehu, Ohakune, Hauhungatahi, Pukeonake and Waimarino were collected and prepared for analysis by W.R.Hackett; those from Ngauruhoe 1954 flows were collected by Prof.R.H.Clark and those from other localities by Dr.J.W.Cole. Xenoliths (Chapter 5) from Ruapehu, Ohakune and Pukeonake lavas were recovered by W.R.Hackett and the author and those from Ngauruhoe 1954 lava by Dr.A.Steiner (N.Z.G.S.) and Prof.R.H.Clark. Some of the smaller examples showed minor exterior alteration, while others contained traces of host lava extruded along fractures. All were carefully cleaned prior to analysis by removing external rinds and by hand-picking.

Rock crushing for both geochemical and isotopic analysis was carried out using a tungsten carbide 'Tema' swing mill; 200-500g of clean chips were ground for 60-90s and between crushings, the barrel washed in warm water and dried with acetone.

Table 2.1: Instrument settings for Siemens SRS-1 XRF spectrometer. (a) Major elements (b) Trace elements

Element	Crystal	Coll	Aperture	Time(s)	Cps	LLD %	Bgd %
Fe	LiF200	0.4	small	20	1100	.008	.20
Mn	LiF200	0.15	large	40	220	.022	.43
Ti	LiF200	0.15	large	20	6300	.002	.07
Ca	PET	0.15	small	20	2600	.004	.08
K	PET	0.4	small	20	3700	.002	.02
P	PET	0.4	large	40	200	.010	.08
Si	PET	0.4	small	100	150	.020	.34
Al	PET	0.4	small	100	140	.013	.13
Mg	TAP	0.4	large	100	40	.031	.46
Na	TAP	0.4	large	200	15	.068	1.62

NOTES: Coll = fine (0.15mm) or coarse (0.40mm) primary collimator. Aperture = aperture over x-ray tube window. Cps = count rate (counts/second per percent element in sample). LLD = Lower Level of Detection; Bgd = apparent background (%) obtained from a disc of SPEX SiO_2 (SPEX $CaCO_3$ for Si).

Element	Line	Tube	kV/mA	Crystal	Detector	Path	Count Times (s) PEAK	BACKGD
Ga	Kα	Mo	55/44	LiF200	S	a	40	20x2
Pb	Lα	Mo	55/44	LiF220	S	a	40	40x2
Rb	Kα	Mo	55/44	LiF220	S	a	40	40x2
Sr	Kα	Mo	55/44	LiF220	S	a	40	20x2
Th	Lα	Mo	55/44	LiF220	S	a	200	100x2
U	Lα	Mo	55/44	LiF220	S	a	200	100x2
Y	Kα	Mo	55/44	LiF220	S	a	40	20x2
Cu	Kα	Au	55/44	LiF200	S	a	100	40x2
Nb	Kα	Au	55/44	LiF220	S	a	100	40x2
Ni	Kα	Au	55/44	LiF200	S	a	100	40x2
Zn	Kα	Au	55/44	LiF200	S	a	40	40
Zr	Kα	Au	55/44	LiF220	S	a	40	40,20
Ba	Lα	Au	50/48	LiF200	F	v	200	100
Ce	Lα	Au	50/48	LiF220	F	v	200	100,200
Cr	Kα	Au	50/48	LiF220	F	v	100	100
La	Kα	Au	50/48	LiF220	F	v	200	200
Mn	Kα	Au	50/48	LiF220	F	v	10	100
Sc	Kα	Au	50/48	LiF200	F	v	100	100
Ti	Kα	Au	50/48	LiF220	F	v	10	100
V	Kα	Au	50/48	LiF220	F	v	100	100,200

NOTES: S = scintillation, F = flow counter; v = vaccuum, a = air.

2.2 X-RAY FLUORESCENCE SPECTROMETRY

2.2.1 Operating Conditions:

Bulk-rock chemical compositions of crushed rock samples were determined by X-ray spectrometry (XRF), using the methods of Norrish and Hutton (1969) and Norrish and Chappell (1977). Analyses were carried out on an automated Siemens SRS-1 X-ray spectrometer at the Analytical Facility, Victoria University of Wellington. This instrument has a ten position sample changer and on-line data reduction allowing analysis in duplicate. For major elements, lithium borate glass discs were made up with ammonium nitrate to enable sodium to be analysed simultaneously; for trace elements, 4cm diameter, boric-acid backed, pressed powder pellets with 3.5g powder were used. Instrumental settings are given in Table 2.1a (major elements) and Table 2.1b (trace elements).

Backgrounds under peaks were calculated by linear extrapolation from one or more measured background positions. Non-linear backgrounds (caused by instrument-induced interferences e.g. Cu in Au tube) were determined using "Spectrosil" ultrapure silica glass. All analyses were corrected for mass absorption at an appropriate wavelength, using the power curve relationship between mass absorption and the scattered anode radiation (Compton peak). Corrections for the absorption edge effects of Fe, Mn, Cr and Ti were used in the mass absorption computations. All spectral interferences including Ti kα on Ba, V kβ on Cr, Ti kβ on V, Rb kβ on Y and Sr kβ on Zr were corrected iteratively after calculation of peak minus background count rates.

Table 2.2: XRF major element compositions of some standard rocks, compared to published values.

		SiO_2	TiO_2	Al_2O_3	Fe_2O_3T	MnO	MgO	CaO	Na_2O	K_2O	P_2O_5
AGV-1	VUW	59.65	1.05	17.19	6.89	0.12	1.50	4.97	4.17	2.95	0.50
	p	.36	.01	.08	.08	.01	.06	.02	.16	.02	.01
	REF1	59.61	1.06	17.19	6.78	0.10	1.52	4.94	4.32	2.92	0.50
BCR-1	VUW	54.69	2.25	13.67	13.37	0.18	3.46	7.03	3.30	1.73	0.38
	p	.37	.01	.08	.12	.01	.08	.02	.15	.02	.01
	REF1	54.53	2.26	13.72	13.41	0.18	3.48	6.97	3.30	1.70	0.36
STM-1	VUW	59.38	0.12	18.44	5.26	0.22	0.13	1.14	8.98	4.26	0.16
	p	.37	.01	.09	.06	.01	.01	.02	.17	.02	.01
	REF2	59.66	0.13	18.44	5.20	0.22	0.10	1.09	8.95	4.29	0.16
BE-N	VUW	38.17	2.66	10.07	12.78	0.20	13.25	13.99	3.26	1.40	1.07
	p	.39	.01	.07	.11	.01	.11	.03	.15	.01	.01
	REF3	38.39	2.62	10.12	12.90	0.20	13.22	13.94	3.20	1.40	1.06
AN-G	VUW	46.51	0.21	30.33	3.34	0.04	1.84	15.96	1.68	0.15	0.01
	p	.39	.01	.11	.05	.01	.08	.03	.13	.01	.01
	REF3	46.35	0.22	29.83	3.36	0.04	1.80	15.92	1.63	0.13	0.01
NIM-G	VUW	76.18	0.09	12.14	2.01	0.01	0.06	0.78	3.29	5.02	0.01
	p	.36	.01	.08	.04	.01	.01	.01	.15	.02	.01
	REF1	75.70	0.09	12.08	2.02	0.02	0.06	0.78	3.36	4.99	0.01
NIM-L	VUW	52.13	0.48	13.51	9.90	0.77	0.27	3.14	8.66	5.39	0.07
	p	.38	.01	.08	.10	.01	.01	.02	.17	.02	.01
	REF1	52.40	0.48	13.64	9.96	0.77	0.28	3.22	8.37	5.51	0.06
NIM-S	VUW	63.76	0.03	17.29	1.44	0.02	0.48	0.68	0.39	15.28	0.11
	p	.36	.01	.08	.03	.01	.01	.01	.01	.02	.01
	REF1	63.63	0.04	17.34	1.40	0.01	0.46	0.68	0.43	15.35	0.12

NOTES: VUW = Victoria University Analytical Facility (compiled 1984). precision (p) is for the 95% confidence interval. REF1 = Abbey (1980); REF2 = Abbey (1982); REF3 = Govindaraju (1980)

Table 2.3: XRF trace element compositions of some standard rocks, compared to published values.

		Ga	Pb	Rb	Sr	Th	U	Y
AGV-1	TS	20 (3)	38 (2)	69 (1)	664 (4)	7 (2)	2 (1)	21 (1)
(86)	ROSER	20 (2)	36 (2)	68 (4)	645 (6)	-	-	21 (2)
	REF1	21	36	67	662	7	2	21
BCR-1	TS	22 (2)	15 (2)	48 (1)	326 (2)	7 (1)	2 (1)	38 (1)
(23)	ROSER	22 (2)	15 (2)	48 (4)	332 (4)	-	-	-
	REF1	22	14	47	330	6	2	39
BHVO-1	TS	21 (3)	3 (2)	9 (1)	390 (3)	3 (2)	1 (1)	28 (2)
(8)	KENN1	21 (3)	4 (3)	9 (2)	407 (2)	2 (2)	ND	29 (1)
	REF2	22 (12)	4 (4)	10 (4)	378*	1 (1)	.4 (.1)	28 (4)
MAG-1	TS	21 (3)	22 (1)	150 (1)	133 (2)	11 (2)	2 (1)	29 (2)
(5)	KENN1	21 (2)	24 (4)	149 (2)	134 (3)	11 (2)	2 (1)	29 (1)
	REF2	21 (1)	25 (8)	152 (6)	144*	13 (1)	3 (.1)	?
QLO-1	TS	17 (2)	28 (6)	73 (1)	328 (2)	6 (2)	2 (1)	25 (1)
(5)	KENN1	18 (1)	28 (7)	72 (3)	328 (5)	5 (1)	2 (2)	26 (2)
	REF2	18 (2)	21 (2)	77 (18)	329*	5 (2)	2 (.1)	28
RGM-1	TS	16 (1)	24 (2)	151 (2)	100 (1)	15 (2)	5 (1)	25 (1)
(11)	KENN1	16 (3)	25 (2)	151 (2)	99 (1)	16 (1)	7 (1)	25 (2)
	REF2	14 (4)	22 (2)	156 (8)	107*	16 (4)	6 (.1)	27
SCO-1	TS	15 (3)	32 (3)	109 (1)	156 (3)	10 (2)	3 (1)	25 (1)
(5)	KENN1	15 (2)	31 (2)	109 (6)	157 (1)	10 (1)	3 (1)	24 (3)
	REF2	12 (4)	29 (4)	118 (9)	170*	10 (1)	3 (.2)	26
SDC-1	TS	21 (2)	26 (3)	124 (1)	175 (1)	13 (2)	3 (1)	40 (1)
(9)	KENN1	21 (1)	25 (3)	124 (3)	174 (1)	13 (1)	4 (2)	41 (2)
	REF2	25 (10)	24	128 (14)	186*	12 (1)	3 (.2)	?
STM-1	TS	35 (4)	18 (2)	115 (1)	685 (3)	31 (1)	8 (1)	47 (2)
(5)	KENN1	34 (2)	19 (2)	115 (6)	678 (8)	35 (1)	10 (2)	50 (2)
	REF2	37 (2)	17 (2)	120 (12)	716*	33 (10)	9 (.1)	53
BE-N	TS	15 (3)	5 (2)	49 (2)	1380 (6)	13 (2)	3 (2)	32 (2)
(12)	KENN2	-	5 (3)	49 (3)	1337 (16)	12 (2)	ND	30 (1)
	REF3	17	4	47	1370	11	2	30
AN-G	TS	19 (2)	2 (1)	1 (1)	76 (1)	1 (2)	1 (3)	8 (1)
(5)	KENN2	-	6 (3)	3 (1)	76 (3)	1 (1)	1 (2)	10 (1)
	REF3	18	2	1	76	-	-	8

NOTE: * XRF data only included in mean.

Table 2.3 cont:

		Cu	Nb	Ni	Zn	Zr
AGV-1	TS	57 (2)	13 (2)	18 (3)	87 (2)	227 (5)
(34)	ROSER	53 (2)	14 (2)	20 (4)	87 (2)	231 (2)
	REF1	60 (12)	15 (6)	17 (8)	88 (4)	225 (36)
BCR-1	TS	19 (2)	11 (2)	16 (4)	127 (2)	187 (4)
(51)	ROSER	-	13 (2)	-	127 (2)	191 (4)
	REF1	19 (8)	14 (6)	13 (8)	129 (2)	191 (5)
BHVO-1	TS	135 (4)	17 (3)	127 (4)	108 (3)	176 (5)
(10)	KENN1	128 (2)	18 (1)	116 (3)	99 (2)	175 (1)
	REF2	137 (12)	19 (4)	117 (36)	102 (14)	180 (60)
MAG-1	TS	27 (2)	15 (1)	45 (3)	131 (3)	121 (6)
(6)	KENN1	33 (2)	14 (1)	51 (2)	134 (1)	124 (1)
	REF2	30 (6)	10 (3)	54 (16)	126 (36)	130 (20)
QLO-1	TS	27 (1)	9 (2)	6 (4)	62 (2)	180 (4)
(8)	KENN1	35 (3)	9 (1)	10 (1)	59 (1)	185 (2)
	REF2	29 (6)	11 (4)	2 (2)	61 (8)	190 (40)
RGM-1	TS	10 (1)	8 (2)	4 (2)	34 (1)	208 (2)
(10	KENN1	14 (1)	8 (2)	7 (1)	31 (1)	221 (3)
	REF2	11 (1)	9 (4)	-	32 (14)	210 (20)
SCO-1	TS	25 (2)	10 (2)	28 (2)	104 (2)	155 (5)
(5)	KENN1	31 (2)	10 (1)	25 (2)	99 (2)	166 (3)
	REF2	30 (4)	9 (2)	28 (4)	106 (18)	160 (48)
SDC-1	TS	26 (2)	17 (2)	32 (1)	105 (1)	276 (4)
(8)	KENN1	33 (2)	17 (2)	34 (3)	102 (2)	288 (0)
	REF2	30 (4)	18 (6)	41 (20)	102 (16)	270 (60)
STM-1	TS	3 (2)	247 (2)	5 (1)	240 (5)	1226 (18)
(5)	KENN1	12 (2)	262 (3)	5 (2)	232 (2	1267 (16)
	REF2	4 (4)	270 (40)	2 (1)	230 (60)	1260 (160)
BE-N	TS	73 (3)	109 (3)	280 (3)	122 (2)	272 (8)
(5)	KENN2	81 (4)	109 (2)	261 (8)	117 (3)	241 (5)
	REF3	72	100	267	120	265

Table 2.3 cont:

		Ba	Ce	Cr	La	Sc	V
AGV-1	TS	1201 (6)	70 (5)	14 (3)	36 (4)	14 (2)	125 (4)
(5)	ROSER	1258 (14)	-	8 (4)	-	-	124 (4)
	REF1	1221 (32)	66 (12)	12 (6)	38 (6)	12 (2)	123 (24)
BCR-1	TS	731 (10)	55 (3)	15 (5)	26 (7)	32 (2)	419 (4)
(3)	ROSER	776 (28)	-	7 (4)	-	-	410 (6)
	REF1	678 (32)	54 (2)	16 (8)	25 (.2)	33 (3)	404 (80)
BHVO-1	TS	142 (5)	41 (3)	307 (3)	20 (7)	35 (4)	340 (6)
(5)	KENN1	150 (10)	-	310 (2)	-	-	323 (6)
	REF2	142 (36)	41 (8)	300 (60)	17 (2)	30 (4)	314 (24)
MAG-1	TS	462 (6)	69 (2)	106 (2)	39 (6)	16 (1)	144 (3)
(5)	KENN1	472 (8)	-	117 (1)	-	-	151 (4)
	REF2	490 (70)	94 (14)	105 (26)	46 (4)	17 (4)	142 (6)
SCo-1	TS	531 (24)	47 (2)	76 (5)	27 (5)	11 (2)	140 (9)
(5)	KENN1	551 (16)	-	86 (3)	-	-	145 (4)
	REF2	580 (100)	62 (12)	67 (10)	35 (10)	11 (2)	122 (32)
SDC-1	TS	665 (12)	80 (4)	63 (1)	39 (4)	13 (3)	101 (1)
(3)	KENN1	621 (18)	-	75 (1)	-	-	97 (3)
	REF2	620 (120)	104 (12)	69 (14)	-	17 (4)	110 (60)
BE-N	TS	1061 (24)	145 (5)	372 (7)	82 (4)	27 (3)	258 (6)
(5)	KENN2	1031 (31)	-	415 (7)	-	-	239 (8)
	REF3	1025	152	360	82	22	235

NOTES: Number of repeat analyses used for the compilation is given in brackets below each standard rock name. Other bracketted numbers give the analytical precision, expressed as two standard deviations. All concentrations in ppm. TS = this study; ROSER = Roser (1983); REF1 = Gladney et al. (1983); KENN1 = Kennedy et al (1981); REF2 = Gladney and Goode (1981); KENN2 = Kennedy et al (1980); REF3 = Govindaraju (1980); REF4 = Abbey (1980).

Table 2.4: Comparison of trace element analyses 1973-1984.

	COLE (1973)				:	COLE (1978)			
	No.	MEAN	VAR%	RATIO	:	No.	MEAN	VAR%	RATIO
Ba	-	-	-	-		50	319	5.2	1.053
Cr	5	72	23.2	1.152		48	121	10.1	.959
Cu	5	41	16.7	1.016		43	51	6.7	1.015
Ga	5	19	4.2	1.189		50	18	7.2	1.012
Ni	5	38	4.7	1.077		19	40	9.6	1.000
Pb	-	-	-	-		29	10	17.3	1.672
Rb	5	9	6.8	.807		35	58	4.7	1.535
Sr	5	353	1.8	1.046		48	298	5.3	1.554
V	5	268	4.9	1.191		50	180	2.4	1.183
Zr	5	98	7.8	.854		46	114	2.2	1.000

	HACKETT (1980)			
	No.	MEAN	VAR%	RATIO
Ba	96	328	2.8	.994
Cr	93	152	4.9	.967
Cu	78	60	8.2	.889
Ga	64	18	6.7	1.026
Ni	68	71	6.1	1.032
Pb	153	9	27.2	.846
Rb	138	50	3.7	.959
Sr	153	281	1.7	1.006
V	96	197	2.6	1.008
Y	152	21	4.4	.968
Zn	82	80	2.1	1.020
Zr	81	105	5.2	1.009

NOTES: No.= number of samples; MEAN = average elemental concentration (ppm); VAR% = percentage difference between new analysis and corrected old analysis after calibration adjustment (estimated from RATIO). RATIO = ratio of new analysis / old analysis.

2.2.2 Precision and Accuracy:

Analytical precision was determined from the results of repeated analysis of a wide range of international rock standards, including those provided by the U.S.G.S. (AGV-1, BCR-1; BHVO-1, MAG-1, QLO-1, RGM-1, SCo-1, SDC-1, STM-1), Association Nationale de la Recherche Technique, Paris / Centre de Recherches Petrographiques et Geochemiques (BE-N, AN-G) and the South African National Institute of Metallurgy (NIM-G, NIM-L, NIM-S). Precision is given (for the 95% confidence interval) from five or more repeat analyses (Tables 2.2 & 2.3).

All analyses were calibrated against standard rocks, one of which was included in each run block (consisting of Spectrosil, one rock standard and seven unknowns). A compilation of standard rock data generated between 1982 and 1984 (TS) (Tables 2.2 and 2.3) include recent compilations made by Kennedy et al. (1980), Kennedy et al. (1981) and Roser (1983) and "best" published values from Abbey (1980), Govindaraju (1980) and Gladney and Goode (1983). These data give a measure of both the internal consistency of the methods used (i.e. precision) and also the accuracy (as may be assessed from comparisons with "best" published values). On both counts, the results are considered acceptable.

Re-analysis of lava samples previously analysed for J.W.Cole and W.R.Hackett was carried out to assess the quality of this data. As shown in Table 2.4, most of the data compare well and only one serious analytical discrepancy has occurred since 1973, involving Rb-Sr-Pb-Y. This resulted from a calibration error (Dr.J.W.Cole, pers. comm., 1985) and highlights the need for careful monitoring of data generated by the XRF method <<note that this error occurred during a previous tenure (K.Palmer, Tech. Officer, Analytical Facility, Victoria University, pers.comm., 1985)>>.

Table 2.5: Electron microprobe analyses of two mineral standards.

	PX-1 (21)			OR-1 (18)		
	MEAN	p	REF.	MEAN	p	REF.
SiO_2	53.98	1.22	53.94	64.63	.55	64.39
TiO_2	.23	.06	.26	nd	-	nd
Al_2O_3	.61	.10	.66	18.53	.05	18.58
Cr_2O_3	.23	.08	.21	nd	-	nd
FeO	2.90	.53	2.93	nd	-	nd
MnO	.08	.09	.07	nd	-	nd
MgO	16.80	.37	16.93	nd	-	nd
CaO	24.70	.55	24.55	nd	-	nd
BaO	nd	-	nd	.91	.38	.82
Na_2O	.22	.06	.24	1.05	.11	1.14
K_2O	nd	-	nd	14.90	.62	14.92
Total	99.75		99.79	100.02		99.85

NOTES: Analysis by K.Palmer (1983). Number of repeated analyses is given in brackets after the mineral name. Precision (p) is given as one standard deviation. REF = Goldich et al. (1967). n.d. = not detected.

2.3 ELECTRON PROBE MICROANALYSIS (EPMA)

All mineral analyses were made using the Jeol 733 Superprobe of the Analytical Facility, Victoria University of Wellington. Polished mounts were first carbon-coated, then analysed with an accelerating potential of 25kV and specimen current of 1.2 x 10^{-8} amps; for glasses, the current was lowered to 0.8 x 10^{-8} amps and beam diameter increased from 3 to 10 microns to reduce Na-loss.

The instrument was initially calibrated against pure oxide and/or mineral standards. Analyses are corrected empirically using the method of Bence and Albee (1968), with alpha correction factors after Kushiro and Nakamura (1970). Additional corrections are made for dead-time, background and probe current drift. In the analysis of unknowns, three 10s counts were made on peaks, and single 10s counts on each of two background positions. For glasses, count time was reduced to a single 10s count and two 5s counts on background.

Analytical precision and accuracy was estimated from replicate analyses of mineral standards including Amelia albite, OR-1 (orthoclase) PX-1 (pyroxene), Kakanui augite and Engels hornblende. Statistical parameters for two of these are given in Table 2.5 (compiled by K.Palmer, 1983). For unknowns, only those analyses with oxide totals in the range 98.5% to 100.5% were accepted (see Appendix 3), unless the amount of any non-analysed component (i.e. trace elements, volatiles) could not be accurately assessed. For a mineral of known stochiometry, agreement with the accepted cation total was used to test accuracy.

2.4 Rb-Sr ISOTOPIC ANALYSIS

The rubidium or strontium isotopic composition of a rock or mineral is usually determined by solid-source mass spectrometry. For this, a sample is first dissolved in strong acids, then the desired element is separated by cation exchange chromatography. For precise determination of Rb or Sr concentrations, the isotope dilution method is used in which a known amount of tracer or "spike" (artificially enriched isotopic standard) is added prior to analysis (Faure, 1977).

The following account of analytical procedures in Rb-Sr analysis refers to methods currently employed at the Institute of Nuclear Sciences (INS), Lower Hutt, New Zealand (Graham, 1983a, 1983b).

2.4.1 Sample Preparation:

Rock dissolution - Approximately 50mg of finely-ground sample is dissolved in 8ml HF (40%) + 2ml HNO_3 (69%) + 1ml $HClO_4$ (70%) (the addition of perchloric acid oxidises and decomposes any carbonaceous material present). After gentle heating for 2-3hr, 10ml H_3BO_3 (saturated) is added to ensure complete dissolution of insoluble BF_6 complexes. Finally, 10ml de-ionised water is added to prevent excess boric acid crystallising during cooling of the solution. For the isotope dilution procedure only, sample and spike weights are accurately measured prior to dissolution.

Solutions of the isotopic standards NBS987 ($SrCO_3$) and NBS984 (RbCl) are made up gravimetrically in weak acid (0.1M HCl) and are used to calibrate the spike solutions, NBS988 (^{84}Sr -enriched) and ORNL 190101 (^{87}Rb -enriched).

Cation Exchange Chromatography: Cation exchange resins used for the separation of Rb and Sr have open, permeable molecular structures, low solubility in both water and organic solvents and contain counter ions that exchange reversibly. The ionic selectivity of resins for one ion over another is determined by the degree of cross-linking of the polymer chains

Table 2.6: Distribution coefficients of selected cations in HCl solutions of differing molarity.

Ion	0.1M	0.2M	0.5M	1.0M	2.0M	3.0M
Sr^{2+}	4700	1070	217	60.2	17.8	10.0
Al^{3+}	8200	1900	318	60.8	12.5	4.7
Ca^{2+}	3200	790	151	42.3	12.2	7.3
Rb^{+}	120	72	33	15.4	8.1	?
K^{+}	108	64	29	13.9	7.4	?
Mg^{2+}	1720	530	88	21.0	6.2	3.5
Fe^{3+}	9000	3400	225	35.5	5.2	3.6
Fe^{2+}	1820	370	66	19.8	4.1	2.7
Na^{+}	52	28	12	5.6	3.6	?

NOTES: $k = [R^+ \text{(resin)}]/[R^+ \text{(solution)}]$ for any cation R^+.

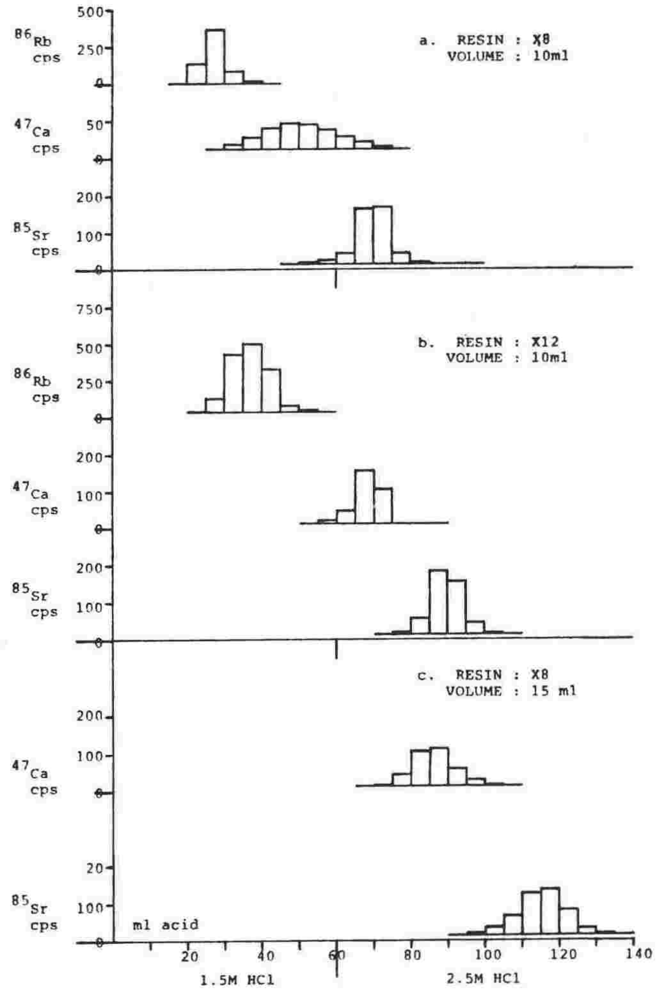

Fig.2.1: Calibration of cation exchange columns using 100mg of a typical rock sample (Mangawhero Formation basic andesite 14822). Note: acid strength changes at 60ml.

and by the pH of the eluent. In general, selectivity increases with increasing valency, ionic radius and concentration of the exchanging ion.

Columns used for Rb-Sr separation at INS are made of FEP tubing (500mm long and 11mm internal diameter) filled to 100mm with DOWEX 50W-X8, 200-400 mesh, hydrogen-form sulphonic acid styrene resin. The base of each column is filter-plugged with sufficient Teflon "wool" to minimise resin loss while allowing for a flow-rate of about .75ml per minute. Ultimate flow control is by means of a Teflon stopcock at the lower end of the column.

When a rock solution is eluted through a resin column, cations are progressively removed and replaced by hydrogen ions until the proportion of original cations in the eluent becomes indetectible. Cations with different affinities for the resin become, in this way, distributed along the column (normally in the uppermost 10%) and may then be selectively removed by eluting acid (2.0M HCl) through the column. The more loosely-held cations are exchanged first and each can be collected in turn as the eluent emerges from the base of the column. Calculated distribution coefficients with HCl at differing pH are given in Table 2.6 for the main cationic species found in a typical rock. As shown, using 2.0M HCl as eluent, Sr will be selectively absorbed only slightly more than Al or Ca (making these difficult to separate) but much more than Rb.

In order to achieve optimum separation of Sr from other cations in solution, the ionic exchange method was tried in several different ways with varying success. Initially, flame photometry was used to monitor the experiments, but this required samples to be "doped" with additional amounts of Rb and Sr to obtain suitable flame intensity. In later trials, appropriate radioactive tracers with very short half-lives (^{86}Rb T=18.6d, ^{47}Ca T=7.5d, ^{85}Sr T=65d) allowed better, quantitative analysis. Results can be summarised as follows:

i. Varying acid strength - as seen in Table 2.6, separation of Rb and Sr may be improved by lowering the pH of the HCl eluent, though this has little effect on the separation of Sr and Ca. Several schemes using different acid strengths were tried and one of the best possibilities is illustrated in Fig.2.1a. Although the results of changing the acid strength part-way through were satisfactory, this procedure was later abandoned and a double pass through the column tried instead. The latter is simpler and has a lower margin of error in guaging the cut-off point for Sr collection.

ii. Changing resin type - resins with higher degrees of cross-linking such as DOWEX X12 (12% cross-linking compared to 8% for DOWEX X8), effectively accentuate small differences in distribution coefficients and so improve separation (Fig.2.1b). However, flowrates through such resins are slow and, since cations are more strongly-held, more eluent is required, further increasing the effective run-time.

iii. Increasing the size of the resin bed - separation of Rb and Sr is also improved by using a larger resin bed (Fig.2.1c), but again the flow-rate is lowered and the run-time increased.

For the procedure finally adopted, samples are loaded as weak acid solutions and are twice passed through a 10ml column of DOWEX X8 resin using 2.0M HCl as eluent. During the first pass, 50ml HCl is eluted then 20ml is collected, evaporated to dryness and the precipitate taken up in de-ionised water. For the second pass, 55ml HCl is eluted, then 15ml is collected. This yields a concentrated, contaminant-free Sr solution which is evaporated to dryness for later mass spectrometric analysis.

For Rb separation, dissolution procedures and cation exchange set-up are similar to those described above. The elution procedure is different, requiring five identical passes of 20 ml 2.0M HCl and collection of the final 10ml. This sample, when evaporated to dryness, is highly enriched in KCl and NaCl but, nevertheless, contains sufficient Rb for subsequent isotopic analysis.

Filament preparation: For mass spectrometric analysis, purified Rb and Sr samples are evapourated on to a metal filament placed in the source of the

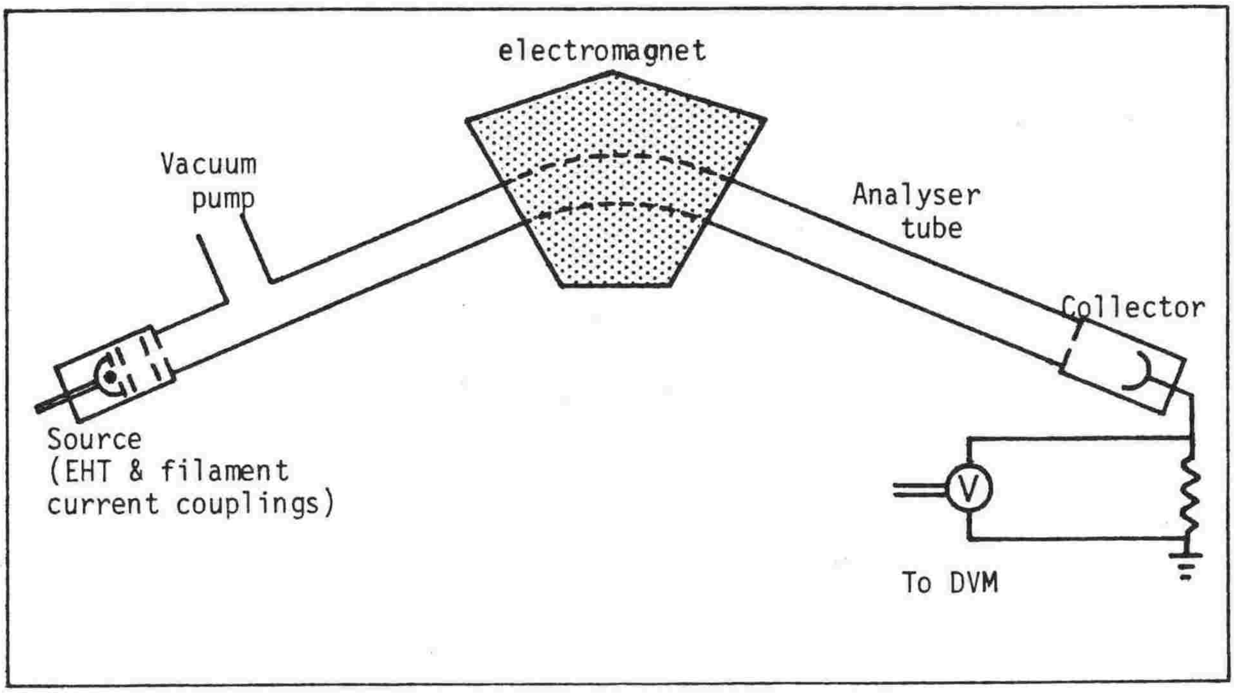

Fig.2.2: Schematic diagram of a 60° sector mass spectrometer. EHT is accelerating voltage; DVM is digital voltmeter.

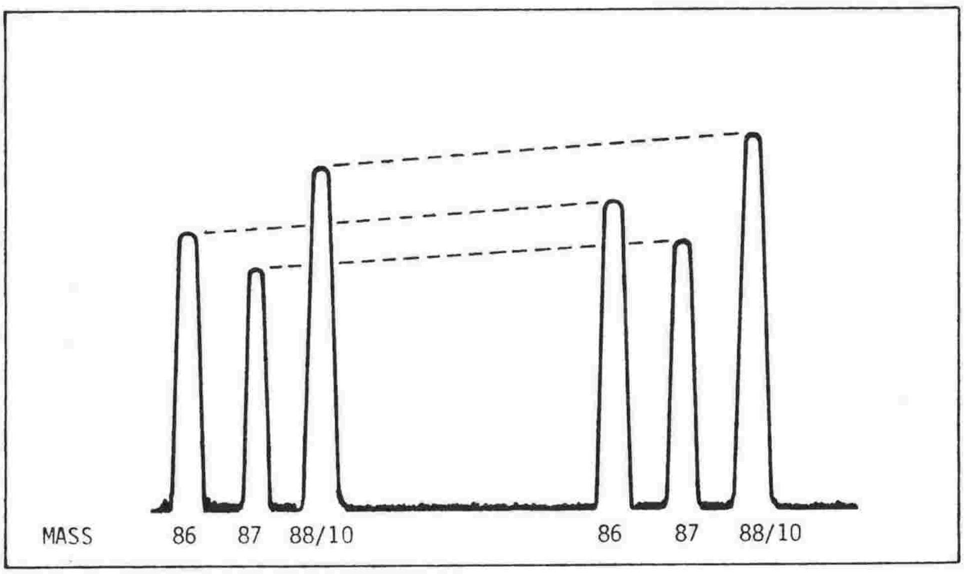

Fig.2.3: Mass spectrum of Sr obtained on a 60° sector, 15.24cm radius Nier-type mass spectrometer (note that the height of the ^{88}Sr peak is one-tenth true height). Lines demonstrate interpolation of successive peaks which is necessay to compensate for temporal changes in intensity.

mass spectrometer. Triple filament beads, constructed of Kodial with Nilo K pins (Cathodeon, Cambridge) are used as single filaments. Beads are normally re-cycled up to five times, unless they have been used for Rb analysis. Prior to re-use, the beads are rinsed several times in hot de-ionised water and dried at 105 °C for 6 hr. Tantalum ribbon (.77mm wide, .03mm thick, high purity) is then spot-welded to the pins ensuring the filament surface is flat and parallel to the base of the bead. Filaments are routinely outgassed in vaccuo before sample loading. This removes water and absorbed gases from the filament and bead surfaces and is achieved by passing 4amp through the Ta ribbon for 15-20min in a vaccuum of less than 10^{-3} torr.

Rb and Sr samples are loaded onto outgassed filaments using micro-pipettes made from pyrex tubing of 3-4mm internal diameter, 5-6mm external diameter. These are first cleaned in nitric acid, then in de-ionised water. After evaporating one drop (about .1ml) of .1M H_3PO_4 from the centre of the filament to etch the surface, the sample is dissolved in a tiny drop (about .001ml) of de-ionised water and so transferred to the centre of the cold filament. This is then heated to a dull red colour by passing 3amp through it for 10-15s. Only if the sample is concentrated in the central part of the filament will a strong, stable Rb or Sr ion beam be obtained.

2.4.2 Mass Spectrometry:

The solid-source mass spectrometer at INS is a Micromass 30B (30cm radius) made by Vaccuum Generators (UK) Ltd. Such an instrument is designed to separate charged Rb or Sr atoms on the basis of their slightly differing masses which is done by varying the motions of charged particles in a magnetic field. The essential parts of a Nier-type mass spectrometer similar to MM30B are shown in Fig.2.2. For isotopic analysis, six samples loaded onto filament beads are placed in a barrel which is secured in the source, then both source and analyser are evacuated to pressures less than 10^{-7} Torr by triode ion pumps and titanium sublimation pumps. All samples are then de-gassed by briefly pre-heating the filaments with a low current. For each analysis, the filament current is increased slowly to about 2.5amp so that Sr is volatilised from the filament and partly ionised at temperatures close to 1400 °C. Ions in the source barrel are extracted through the source slit (.2mm) by an adjustable voltage (EHT) of about 8.3 kV and are collimated into a tight, rectangular beam by various focus plates (D-focus, D-bias, Z-focus, Z-bias). The magnetic field strength (typically 2.6 kGauss) is set by the Field Memory Unit (FMU) so that ions of a particular mass (e.g. 86, 87, 88) pass directly through the analyser, to the collector slit (.6mm). The ion beam then enters a Faraday collector cup and the small current generated there is amplified to give the ion beam current (IBC). This is interrogated by the system microcomputer (INS-developed units called "HAL" with 16k total capacity) and is displayed on a digital voltmeter (DVM). A typical scan of the ion beam intensity of several Sr isotopes obtained by continually increasing the magnetic field strength is shown on a chart recording (Fig.2.3).

Details of the semi-automation of MM30B using HAL-system micro-computers is contained in Plummer (1980). The computer links two units, namely the DANA 5900 Multimeter (DVM) and the Field Memory Unit (FMU). All logic, control, data acquisition and data processing is under machine code or BASIC language control. Description of the BASIC programs which handle data acquisition and analysis is given in Appendix 4.2 and only those important features which pertain to the methods employed are now discussed.

For Sr isotopic composition analysis (Sr IA), six mass positions are measured in each scan in the following sequence: 84.5 - 85 - 86 - 87 - 88 - 84 (channels 1 to 6). At each mass position, the ion beam DANA signal (IBC) is read rapidly 27 times and the average value is stored in an array. At the completion of the second (and all subsequent) scans, successive IBC averages are interpolated between scans to a common time plane, arbitrarily chosen as channel 6. This is done to compensate for long-term drift in the

Table 2.7: Variables used in Sr ID recalculations.

VARIABLE	RATIO	LOCALITY	VALUE INS	VALUE NBS	SOURCE
A4	84/86	tracer	1779	1698	calibration
A7	87/86	tracer	0.119	0.166	calibration
A8	88/86	tracer	0.948	0.655	calibration
B4	84/86	common	0.0568		handbook
B7	87/86	unspiked sample	calculated		MM 30B
B8	88/86	common	8.375		handbook
C4	84/86	spiked sample	measured		MM 30B
C7	87/86	spiked sample	measured		MM 30B
C8	88/86	spiked sample	measured		MM 30B

NOTES: A4, A7, A8 are Sr isotopic ratios for NBS 988 standard as derived from calibration runs (INS values are used); values for B4 and B8 are from the Handbook of Chemistry and Physics, 55th Ed. (1974-1975), other ratios are measured during an ID analysis or are calculated from it (B7).

$$D1 = \frac{1}{2} \begin{vmatrix} (B4 - 3C4) & (B8 + C8) \\ (B4 - A4) & (B8 - A8) \end{vmatrix}$$

$$D2 = \begin{vmatrix} -C4 & C8 \\ (B4 - C4) & (B8 - C8) \end{vmatrix}$$

$$D3 = \begin{vmatrix} C4 & C8 \\ (C4 - A4) & (C8 - A8) \end{vmatrix}$$

Fig.2.4: Determinants used in Sr ID solution of Russell (1977) - see Table 2.7 and text for values of constants.

ion beam intensity (Fig.2.3). The presence of contaminating Rb isotopes in the Sr beam is monitored at channel 2 (mass 85). Because ^{85}Sr is radioactive with a half-life of only a few months, the mass 85 signal must be entirely attributable to ^{85}Rb which can thus be used to calculate the amount (if any) that ^{87}Rb is contributing to the total mass 87 signal. Rb correction is made after background (taken as the interpolated IBC mean of channel 1) has been subtracted from the interpolated IBC means of each of the other channels, and requires that the value for channel 4 (mass 87) be reduced by .3857 of the value for channel 2 (mass 85). The corrected values for channels 3, 4 and 5 form the ratios 86/88 ($^{86}Sr/^{88}Sr$) and 87/86 ($^{87}Sr/^{86}Sr$) which are then used to calculate 87/86N ($^{87}Sr/^{86}Sr$ normalised): 87/86N = ((86/88+.1194)/.2388)*87/86. Normalisation of the measured $^{87}Sr/^{86}Sr$ ratio against the internationally accepted $^{86}Sr/^{88}Sr$ ratio of .1194 is necessary to compensate for mass fractionation within the source which is caused by the tendency for isotopes of lower mass to volatilise to a greater extent during an analysis than those of higher mass. Since neither ^{86}Sr nor ^{88}Sr are radiogenic nor the products of radioactive decay of another isotope, their ratio is assumed to be constant in time and space and can thus be used to correct instrument-induced fractionation in any other Sr isotopic ratio. For the measured $^{87}Sr/^{86}Sr$ ratio, this will correspond to half the fractionation experienced by $^{88}Sr/^{86}Sr$ since the latter pair of isotopes has twice the atomic mass difference as the former.

For Sr isotope dilution analysis (Sr ID), the same sequence of masses are measued as for Sr IA. The ratios 84/86 ($^{84}Sr/^{86}Sr$), 87/86m ($^{87}Sr/^{86}Sr$ of the unspiked sample) and Sr(sample)/Sr(spike) are calculated after the method of Russell (1977), whose equations find a specific geometric solution in closed form using a ^{86}Sr-enriched spike (the method applies equally well to the ^{84}Sr-enriched spike composition used at INS). Matrix determinants and variables used in the solution are given in Fig.2.4 and

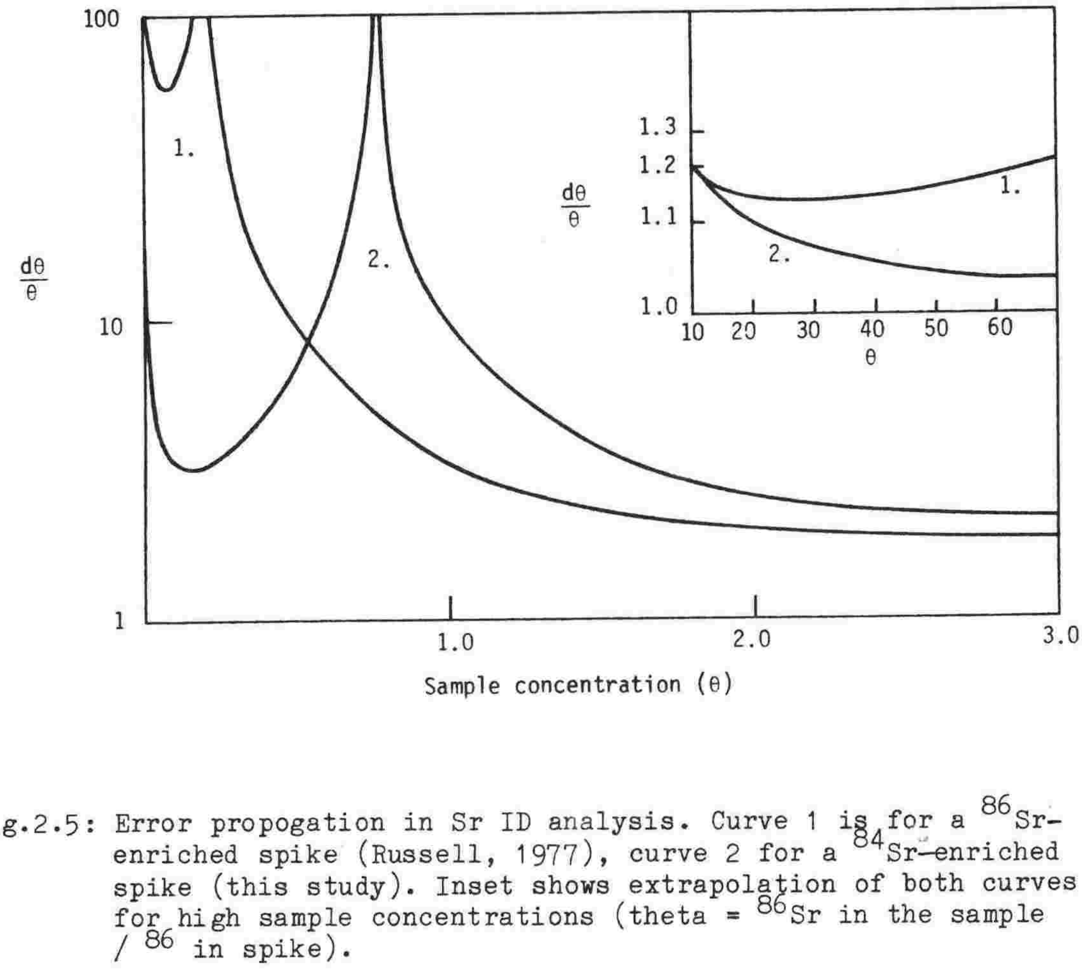

Fig.2.5: Error propogation in Sr ID analysis. Curve 1 is for a ^{86}Sr-enriched spike (Russell, 1977), curve 2 for a ^{84}Sr-enriched spike (this study). Inset shows extrapolation of both curves for high sample concentrations (theta = ^{86}Sr in the sample / ^{86} in spike).

Table 2.7 respectively. From these, the following ratios are defined:

87/86m = (D1/D2)*C7-(D2/D3)*A7;

Sr(sample)/Sr(spike) = (D3*(1+B4+B7+B8))/(D2*(1+A4+A7+A8)).

The ratio 87/86m provides an good estimate of the $^{87}Sr/^{86}Sr$ ratio of the sample and compares favourably with repeat unspiked (Sr IA) analyses (see Table 2.9). E1 is used to calculate the Sr concentration of the sample:

Sr(ppm)=(E1*A1*W1)/W2 where W1 = spike weight; W2 = sample weight

A1 = Sr concentration of the spike (NBS 988)

Russell also pointed out that significant error magnification can occur if ^{86}Sr (sample) / ^{86}Sr (spike) falls below 1.0 (Fig.2.5). However, for samples with Sr concentrations greater than 1ppm, these errors are negligible providing that suitable proportions of spike to sample are used (e.g. 1g spike solution @ 2ppm + .05g sample).

For Rb isotope dilution analysis (Rb ID), only two isotopes need be measured, namely ^{85}Rb and ^{87}Rb and these enable the ratios 85/87 ($^{85}Rb/^{87}Rb$) and Rb(sample)/Rb(spike) to be calculated. The 85/87 ratio gives an indication of the extent of instrument-induced mass fractionation during an analysis (which cannot be corrected for since Rb has only one stable isotope). Thus it is important that Rb analyses be undertaken in a way which minimises variation in the 85/87 ratio; this is best achieved by maintaining low beam intensity and by reducing the number of total scans (across the sequence 84.5 - 85 87 - 84). The ratio Rb(sample)/Rb(spike) (K6) is used to calculate the Rb concentration in the sample:

Rb(ppm)=(K6*A1*W1)/W2 where W1 = spike weight; W2 = sample weight

A1 = Rb concentration of the spike (ORNL 190101)

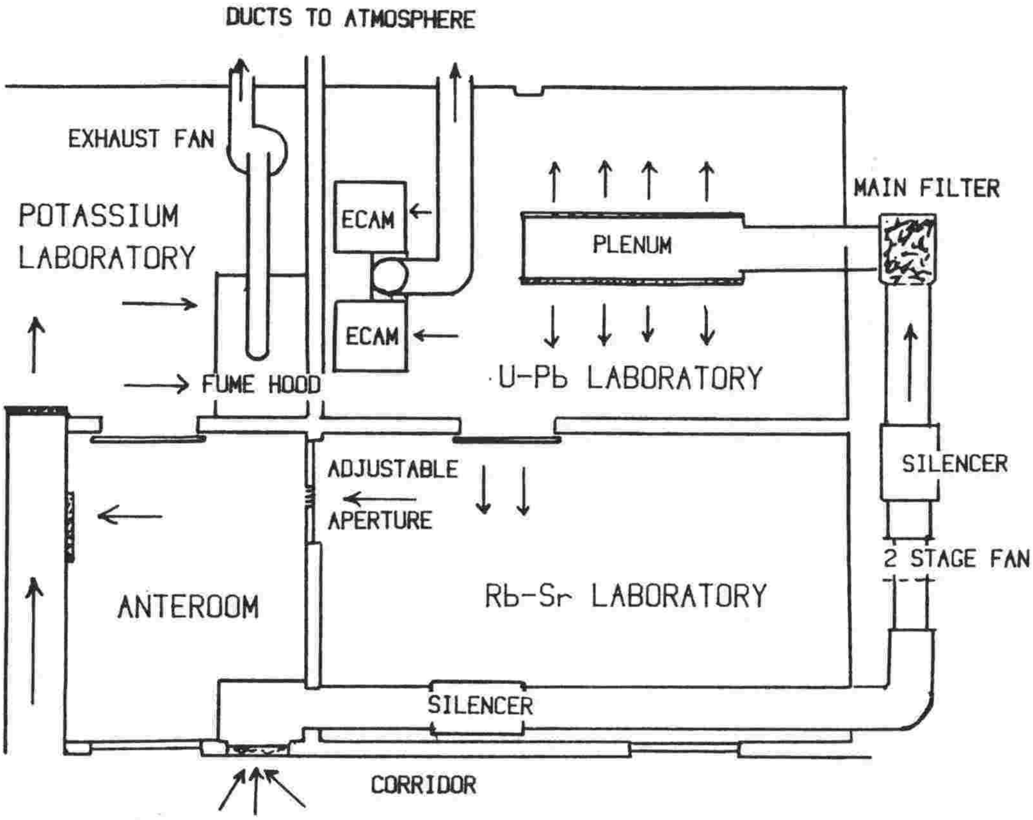

Fig.2.6: Layout of Clean Laboratories at INS, including details of the ventilation system - air movement is shown by arrows (used by permission W.H.Heald, 1977).

2.4.3 Data treatment:

At the completion of a scan, a running mean and standard deviation for each of ratio is calculated. Occasionally during an analysis on MM30B (and indeed on most mass spectrometers), spurious data is generated as the result of a re-focus operation, a computer crash, an EHT surge or a mains power fluctuation causing a current surge in either the source filament or in another part of the electronics. Since data so generated are not part of a normal Gaussian distribution, it would be illogical to include them in the mean and error calculations. Therefore these are removed automatically in the Grand Mean procedure (c.f.Appendix 4.2), by means of the following cycle:

1. the mean, standard deviation and skewness of the distribution is calculated,
2. all data outside 2.5 standard deviations of the mean are excluded from the distribution,
3. a new mean, standard deviation and skewness is calculated.

The final mean and error is given when the skewness is minimised, so achieving a distribution from the raw data which more closely corresponds to normality. An option is also available in the program to edit spurious data before the Grand Mean cycle begins and to calculate Grand Means of successive blocks of ten ratios in order to assess any drift in the normalised data during the period of the analysis.

It is clear from discussions with geochronologists from other laboratories that data "treatment" is an integral part of most established systems. For example, at the "Lunatic Asylum" (C.I.T) (Papanastassiou and Wasserburg, 1969, 1973), data is grouped in sets of ten and the mean and standard deviation are calculated. All blocks for which the standard deviation is greater than .05% of the mean are then rejected outright. This seems unreasonably subjective, excluding large quantities of data which, but for a few outliers, might be considered acceptable. The procedure

Table 2.8: Comparison of standard rock isotopic data.

	Rb			Sr			$^{87}Sr/^{86}Sr$	$^{87}Sr/^{86}Sr$
method	XRF	XRF	ID	XRF	XRF	ID	IA	IA
origin	P&O	VIC	INS	P&O	VIC	INS	P&O	INS
G2	169	-	169.9	476	-	476.4	.70974	.70980
AGV-1	67	69	66.8	662	664	658.1	.70395	.70405
BCR-1	47	48	47.4	332	330	331.7	.70497	.70502

NOTES: International rock standards from U.S. Geol. Surv.
XRF = by X-ray fluorescence spectrometry; ID = by isotope dilution analysis; IA = by isotopic composition analysis.
P & O = Pankhurst and O`Nions (1973); VIC = Victoria University Analytical Facility; INS = Institute of Nuclear Sciences.
Trace element contents in ppm. Isotopic analyses from INS are normalised to NBS987=.71025; those from P & O to .71039.

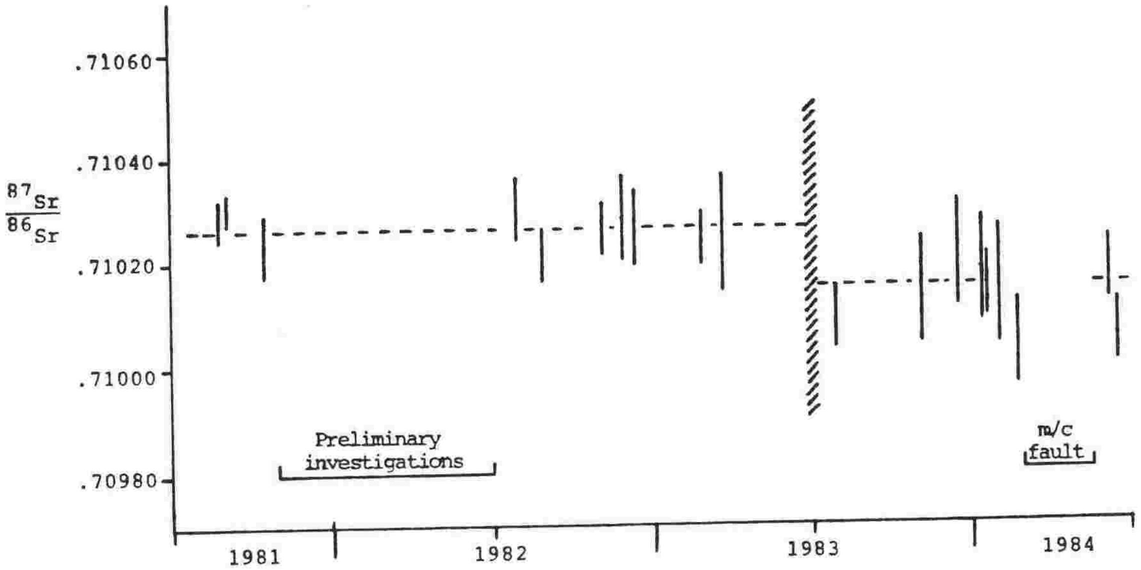

Fig.2.7: Variation in $^{87}Sr/^{86}Sr$ ratio of NBS987 from July 1981 to June 1984. Analytical breaks resulted from (i) developmental work (preliminary investigations) and (ii) machine down-time.

adopted here is novel, but the application of skewness measurements at least brings an element of objectivity into a difficult area of data treatment.

2.4.4 Data Control:

During chemical preparation, external contamination (blank) of a sample must be kept to a minimum especially if the sample has a low Sr content (less than 10ppm). Blank is derived from dust particles in the atmosphere, from impurities in the chemicals used for dissolution and cation exchange chromatography and from handling (Stille, 1981). To maintain low blank levels, a clean laboratory system operates at INS, reducing particulate contamination (i.e. atmospheric blank) (F.g.2.6). In addition to this, all water is distilled and only acids of analytical grade are used. Despite these precautions, total blank measures 10-12ng for Sr, somewhat high by international standards. However, for samples with Sr contents greater than 50ppm, a blank of 10ng will contribute a change in the $^{87}Sr/^{86}Sr$ ratio of only .00002 to .00005 (for most rock compositions considered here), well within average precision. Steps are presently being taken to further reduce blank levels in the INS laboratory by imposing stricter clean-room regulations and by re-distilling acid solutions.

Sample contamination can often be difficult to detect since it is not possible to analyse a known standard concurrently with an unknown sample. Systematic (long-term) blank problems can be detected by regular standard analysis, whereas duplicate analysis of unknowns provides best control over random contamination. Although time-consuming in a semi-automated system, this procedure was often applied here (c.f. Table 4.4) with excellent results.

Long term drift in normalised isotopic ratios is regularly monitored using the internationally accepted standard, NBS987 (National Bureau of Standards $SrCO_3$). Usually one analysis is made each week. All $^{87}Sr/^{86}Sr$ ratios are calibrated against a value for NBS987 of .71025. Although this

$$t = \frac{1}{\lambda} \ln \left[\frac{\frac{^{87}Sr}{^{86}Sr} - \frac{^{87}Sr}{^{86}Sr}_o}{\frac{^{87}Rb}{^{86}Sr}} + 1 \right] \qquad \text{(i)}$$

Where t = time elapsed
λ = decay constant of ^{87}Rb

$$\frac{^{87}Sr}{^{86}Sr}_o = \text{initial isotopic ratio}$$

$$\frac{^{87}Rb}{^{86}Sr} = \frac{Rb}{Sr} \times \frac{Ab\ ^{87}Rb \times WSr}{Ab\ ^{86}Sr \times WRb} \qquad \text{(ii)}$$

where Ab = isotopic abundances
W = atomic weight

Fig.2.8: Equations for radioactive decay in the Rb-Sr system.

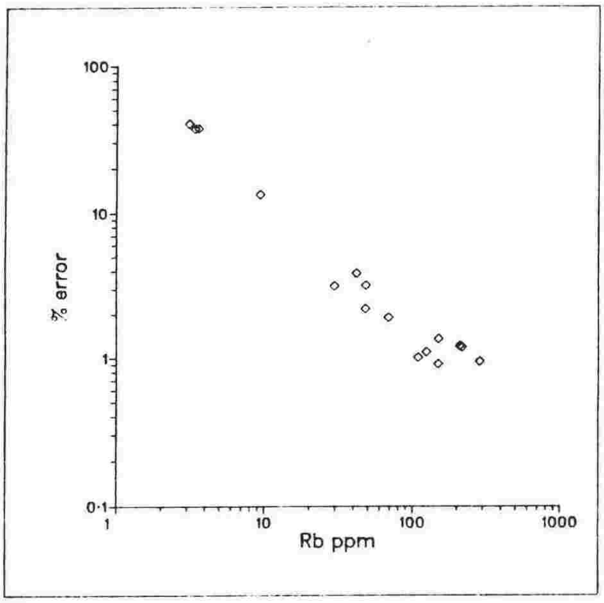

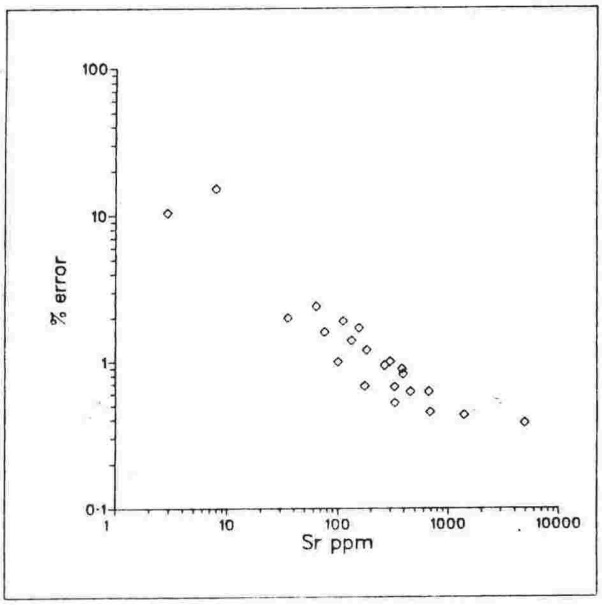

Fig.2.9: % error (precision) vs.concentration for XRF analysis of Rb (a) and Sr (b). Errors are for the 95% confidence interval; concentrations are the means of at least 5 repeat analyses.

is about .00010 greater than that quoted by most laboratories, it corresponds to the average value at INS from 1981 to mid-1983 (Fig.2.7). After that, the value has fluctuated about a lower mean of .71015 (15) (the reason for the drop in the ratio is unclear). A more serious drop (to .70920), which occurred in mid-1983, was eventually traced to an electronic fault in the collector amplifier. An external check of the accuracy of Rb-Sr isotopic analyses at INS is made using International Rock Standards. Table 2.8 gives the results for three U.S.G.S. old-series standards (G2, AGV-1, BCR-1) and these data indicate good agreement with the Rb-Sr laboratory at Oxford (Pankhurst and O'Nions, 1973). Isotope dilution analyses also agree well with XRF determinations made at Victoria University Analytical Facility (Table 2.9) for a range of xenolith, sediment and lava samples.

2.4.5 Geochronology:

The Rb-Sr radioactive decay scheme (Fig.2.8) involves the breakdown of ^{87}Rb to ^{87}Sr with the emission of a beta particle. The decay constant used here is that recommended by Steiger and Jäger (1977), 1.42×10^{-11} a^{-1}, and is equivalent to a half-life for ^{87}Rb of 4.88×10^{4} Ma. Equation (i), which is only valid when decay has taken place in a closed system, may be solved for "t" if the concentrations of Rb and Sr and the $^{87}Sr/^{86}Sr$ are known. If all the components of a system have the same initial $^{87}Sr/^{86}Sr$ ratio (i.e. the same ratio when equilibration took place) then after time t, each should plot on a straight line on an isochron diagram, in coordinates of $^{87}Rb/^{86}Sr$ (x) and $^{87}Sr/^{86}Sr$ (y). The line has a slope $e^{\lambda t}-1$ and y-intercept equal to the initial $^{87}Sr/^{86}Sr$ value. Calculation of these variables requires a least squares cubic regression analysis similar to that proposed by McIntyre et al. (1966) and York (1966, 1967, 1969). For this study, a computer program after York (1969) was developed jointly by R.M.Renner (Statistics and Operations Research, Victoria University of Wellington) and the author (Appendix 4.3).

Least squares cubic regression analysis of Rb-Sr data has been the subject of intensive discussion in recent years and from this several important points have emerged:

i) Error Assignment to x and y variables: Brooks et al. (1972) pointed out that "....a basic assumption in any application of least squares analysis is that all errors (i.e. both experimental and geological) affecting the fit of the regression line are normally distributed". This they demonstrated for a large number of replicate analyses. For Rb/Sr isochrons where the Sr isotopic ratios and concentration are measured together (Sr ID), error correlation is possible especially if $^{87}Sr/^{86}Sr >$ 1.0 (Butler, 1982). However, such correlations can be avoided if Rb/Sr is measured by XRF analysis (as is done here). Errors in Rb and Sr content can be assessed either from replicate analyses (at least five) or from the average analytical error derived from replicate analyses of a range of suitable standard rocks. Since the first option is impractical at INS (which is without an on-site XRF spectrometer), the second option is adopted. Some Rb and Sr standard data generated by XRF at Victoria University Analytical Facility (Table 2.3) is plotted on Fig.2.9 in coordinates of elemental concentration (ppm) and % error (95% confidence interval). For the purposes of isochron calculation, the error in X is taken to be the combined % error in Rb and Sr for the 68% confidence interval. The conversion of Rb/Sr to $^{87}Rb/^{86}Sr$ uses the $^{87}Sr/^{86}Sr$ ratio which has an associated error, but this error is negligible compared to those associated with the Rb and Sr concentrations and can be ignored. Further refinement of these error estimates will occur as more standard rock data becomes available.

For isotope dilution analysis of Rb or Sr, error calculations are much more complex. For example, there are fixed errors in estimating the spike concentration (six replicate analyses gave a value for the current spike solution of 2.141 ppm Sr (s.d.=.00184) and in measuring sample and spike

Table 2.9: Comparison between XRF and isotope dilution analyses of Rb and Sr in selected rocks.

	XRF1	XRF2	ID	p%	$^{87}Sr/^{86}Sr$ (ID)	$^{87}Sr/^{86}Sr$ (IA)
Strontium						
17835	527	526	525.6	.50	.70546 (11)	.70545 (13)
17836	442	444	443.6	.38	.70534 (11)	.70531 (13)
17837	210	211	212.6	.34	.70826 (9)	.70836 (13)
17838	569	563	569.4	.41	.70489 (8)	.70478 (8)
17839	419	419	417.7	.38	.70507 (10	.70502 (5)
G2	-	-	476.4	.35	.70979 (7)	.70979 (4)
Rubidium						
17836	70	69	69.4	2.19		
17837	106	108	112.4	2.18		
17839	47	47	47.3	2.96		
17840	51	50	51.0	2.44		

NOTES: XRF1, XRF2 are repeat analyses (of the same pellet), ID = isotope dilution analysis; IA = isotopic composition analysis. p% = precision (68% confidence interval). precision of Sr isotopic analyses (given in brackets) corresponds to two standard errors of the mean. Samples are Waipapa terrane greywackes (Appendix 2.1).

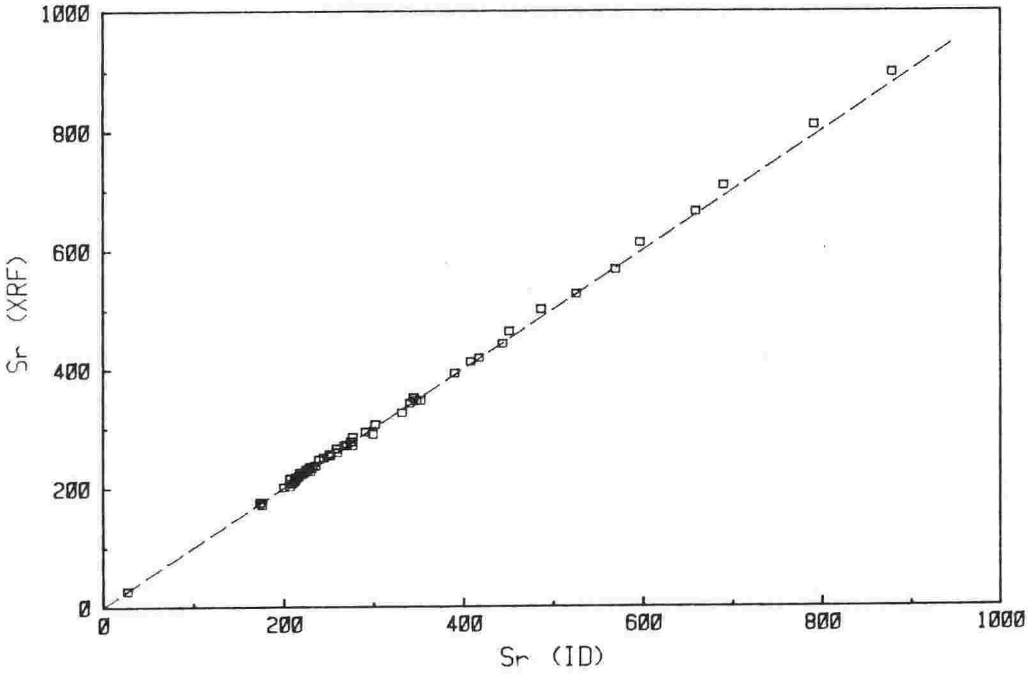

Fig.2.10: Comparison between XRF and isotope dilution analyses of Sr in selected rocks. Reference line is 1:1.

weights (precision > .00005). The other variable in the equation (c.f. section 2.4.2), E1 = Sr (Rb) in sample / Sr (Rb) in spike, is derived from mass spectrometric analysis and represents a normal Gaussian distribution with an associated error expressed as the standard deviation. Because individual errors involved in isotope dilution analysis are complicated to calculate it may be better to assess them in a way similar to that adopted for XRF analysis (i.e. from replicate analyses of standard rock samples). Clearly this will not be possible until much more standard data becomes available.

Comparison between XRF and isotope dilution methods of analysis of Rb and Sr (Table 2.8 and 2.9) indicates no clear bias for the few data so far compiled (Fig.2.10). Some minor disagreements are probably the result of sample inhomogeneity (which greatly affects isotope dilution analysis because of the small sample weights used).

The error in a strontium isotopic ratio is given in two ways: in compilations, it is normally the standard error of the mean (for the 95% confidence interval); for regression analysis, the standard deviation (68% confidence interval) is used since weights are assigned as the inverse of the variance (see Appendix 4.3). When a sample is analysed in duplicate, the mean and standard deviation of the combined analyses may be used since both distributions are considered to be independent estimates of the population (provided that blank and instrumental drift are fully taken into account):

Mc = SUM(Mi*(ni-1)) / SUM(ni-1) where Mc = combined mean
Mi = individual mean
ni = number of ratios measured
i = sample number

Vc = SUM(Vi*(ni-1)) / SUM(ni-1) where Vc = combined variance
Vi = individual variance

ii) Goodness of fit: The scatter of data points about an isochron must be contained within the limits of the assigned experimental errors alone (Brooks et al., 1972). For the regression treatment used here, RMSWD (Root Mean Square of the Weighted Deviations - formerly MSWD after McIntyre et al., 1966) is calculated as an index of fit. If the value exceeds that calculated from the errors assigned to both x and y variables then the excess scatter about an isochron must be due to geological error and the isochron is invalid and is termed an errorchron. Brooks et al. (1972) point out, however, that although under ideal conditions the RMSWD must be 1 or less, the relatively few data points used in most isochrons and the minimal replication of individual analyses implies that the cut-off value for RMSWD between isochron and errorchron will, in most cases, be considerably greater than unity.

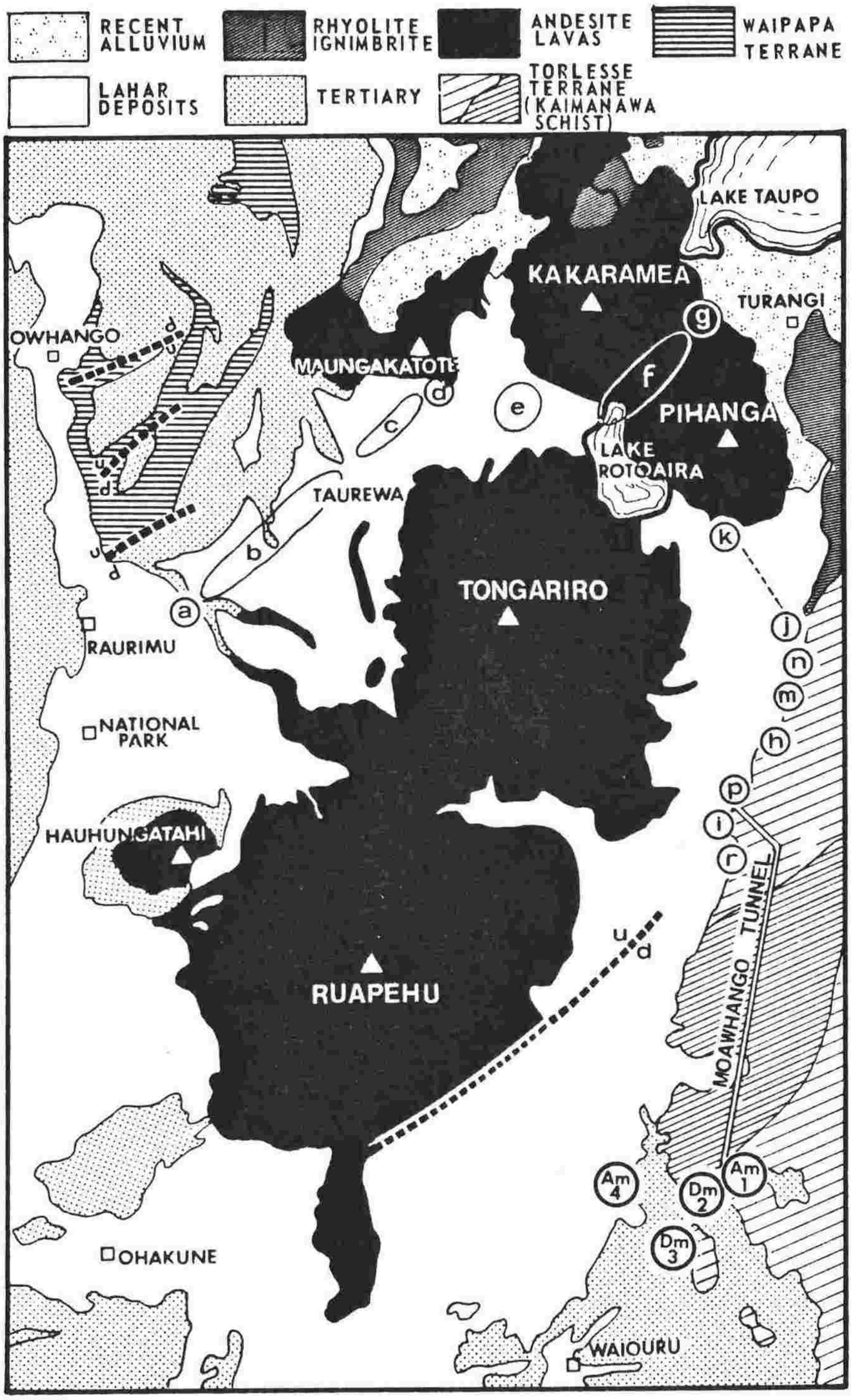

Fig.3.1: Geologic map of Tongariro Volcanic Centre showing distribution of sedimentary basement and recent volcanics. Borehole localities (c.f. Table 3.1) are lettered.

****

CHAPTER 3: PETROGRAPHY, GEOCHEMISTRY AND Rb-Sr GEOCHRONOLOGY OF EXPOSED SEDIMENTARY BASEMENT LITHOLOGIES

****

PART 1 describes the petrographic, chemical and isotopic characteristics of sedimentary basement in the vicinity of Tongariro Volcanic Centre. Lithologies include greywacke and argillite of the Torlesse terrane (i.e. "Rangipo Torlesse suite"), greywacke of the Waipapa terrane ("Rangipo Waipapa suite") and Late Tertiary fossiliferous siltstone, sandstone and conglomerate ("Rangipo Tertiary suite"). These provide a framework to discuss the origin of metasedimentary crustal xenoliths (Chapter 5) and hence to better understand contamination processes involved in petrogenesis of TVC lavas (Chapter 4 & 6).

Part 2 is a Rb-Sr whole-rock geochronological study of volcanogenic greywacke and argillite from the Coffs Harbour Block, northern N.S.W., Australia. This was undertaken to compare with a similar study of Waipapa terrane rocks (section 3.3) and to further examine the Rb-Sr systematics of coarse-grained rocks in relation to their fine-grained counterparts.

Table 3.1: Tongariro Power Development cores.

BORE	ELEVATION (m)	VOLCANICS min.	VOLCANICS max.	TERTIARY min.	TERTIARY max.	GREYWACKE min.	GREYWACKE max.
a	700	0	3	0	97	-	-
b	(750)	0	152	110	175	46	137
c	(700)	0	116	61	76	-	-
d	600	0	73	15	76	-	-
e	600	0	61	-	-	-	-
f	(800)	0	318	-	-	-	-
g	500	0	137	-	-	-	-
k	650	0	46	-	-	-	-
j	625	0	85	-	-	-	-
n	800	0	122	-	-	91	107
m	800	0	73	-	-	73	88
h	850	0	31	-	-	15	41
p	850	0	72	-	-	72	76
i	900	0	77	-	-	77	102
r	850	0	30	-	-	0	305
DM-2	800	-	-	0	30	-	-
DM-3	900	0	5	0	24	0	63
AM-1	900	0	34	-	-	0	19
AM-4	900	0	56	49	116	-	-

NOTES: Borehole locations are plotted on Fig.3.1.
Elevation = height above sea-level (averages in brackets).
Min. and max. = depth ranges from ground surface.

PART 1: SEDIMENTARY BASEMENT OF TONGARIRO VOLCANIC CENTRE

3.1 INTRODUCTION

The oldest rocks in the TVC are unfossiliferous greywackes and argillites forming the Kaimanawa Mountains to the east and the hills to the NW (Fig.3.1). Gregg (1960) considered all of these to belong to the Alpine Facies (Wellman, 1952). Eastern lithologies are quartzo-feldspathic with a chlorite-rich matrix and reach subschist rank (Chlorite 2 subzone) at the axis of a gently plunging anticline (i.e. "Kaimanawa schist"). Those to the NW are of lower metamorphic grade and dominated by breccias of angular lithic fragments in a sandy matrix. Evidence from this study indicates that the latter belong to the Shelf Facies (Wellman, 1952), and the boundary between the two facies (referred to here as Waipapa and Torlesse terranes of the Torlesse Supergroup; Suggate, 1978) must lie somewhere beneath the main line of volcanic vents. Late Tertiary marine sediments occur extensively on the the NW and south margins, forming a thin wedge between Mesozoic greywacke basement and Recent volcanic cover.

Outcrop geology of the TVC and the location of drill-cores (see Chapter 2.1) are given in Fig.3.1. Brief core-logs (Table 3.1) indicate a very uneven topography above the Mesozoic basement, resulting in variable thickness of both Tertiary sediments and volcanics. Mesozoic basement is reached in boreholes "b" (Waipapa) and "n" (Torlesse) but not in any in between (to maximum drilled depth of 350m). Therefore, major depression of the basement, probably caused by faulting, may occur beneath the TVC. This might result from, or be the cause of, the sudden change from Waipapa to Torlesse terrane lithologies?

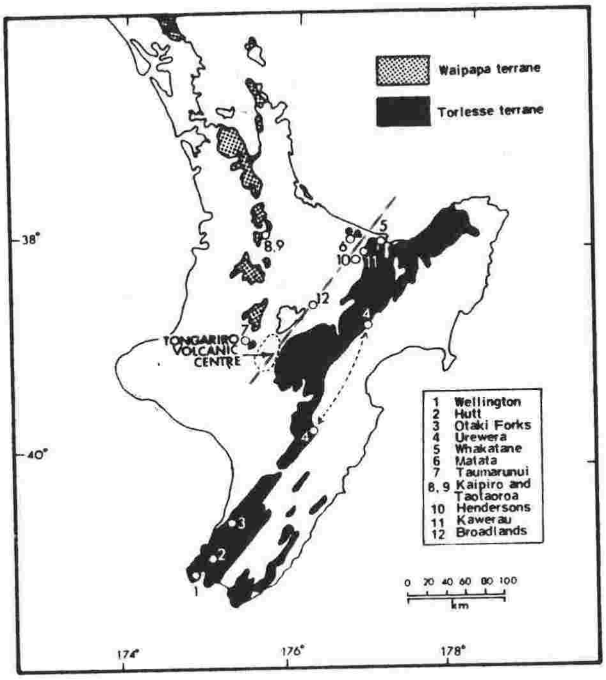

Fig.3.2:
Distribution of Torlesse and Waipapa terranes in the North Island (Suggate 1978). Referenced localities are plotted and assumed Waipapa-Torlesse boundary shown.

Fig.3.3:
Distribution of Torlesse terrane near Tongariro Volcanic Centre. Fossil localities are shown.

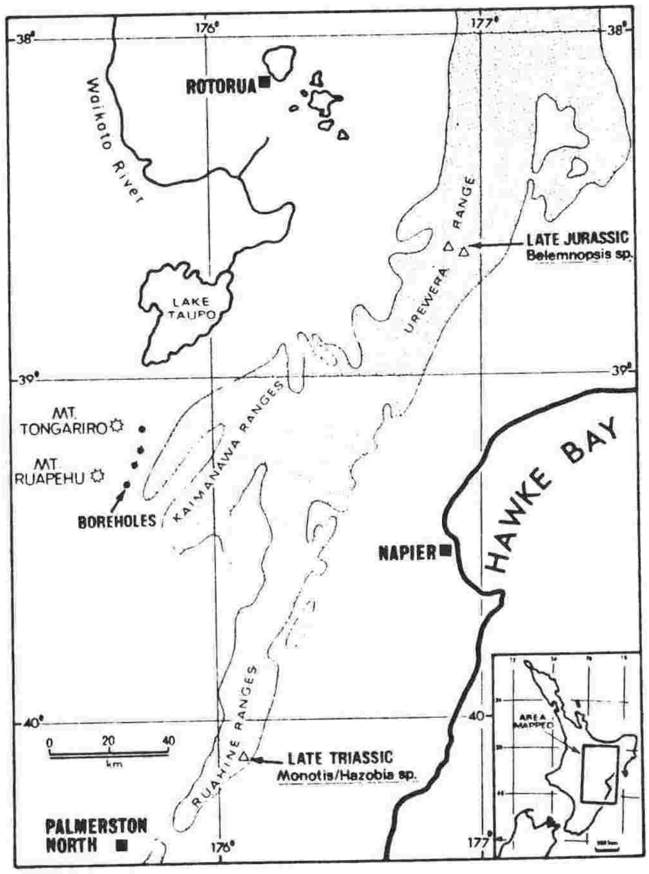

3.2 TORLESSE TERRANE (RANGIPO TORLESSE SUITE)

3.2.1 Introduction:

Torlesse terrane rocks of the North Island make up much of the exposed Mesozoic basement central to and east of the main ranges (Fig.3.2). The terrane consists mainly of interbedded quartzo-feldspathic greywacke and argillite (flysch) sequences with minor amounts of chert, conglomerate, limestone and basic volcanics. The rocks are intensely deformed, sometimes forming zones of melange (Sporli, 1978).

Speden (1976) listed the sparse fossil fauna of these rocks. He noted that (with few exceptions), although the faunal zones become younger to the east, within each zone, the dominant younging direction is to the west. This is in agreement with an accretionary prism model corresponding to a west-dipping subduction zone (Taupo-Hikurangi system - c.f. Chapter 1.1) and provenance from the south or east (Korsch and Wellman, in press). The closest known fossil localities to the TVC, which might give an indication of the age of the rocks in that area (Fig.3.3), are: Ruatahuna, Urewera range (Belemnopsis sp., Late Jurassic; Stevens, 1963) and Oroua, Ruahine range (Monotis and Halobia sp., Late Triassic; Grant-Taylor and Waterhouse, 1963). However, these localities are somewhat distant from the TVC and therefore offer a poor indication of the depositional age there.

3.2.2 Petrography:

The Rangipo Torlesse suite ranges from well-indurated and foliated quartzo-feldspathic greywackes (defined as coarse-medium sand grade rocks with a dominance of poorly-sorted angular detritus) to micaceous argillites (defined as fine sand to silt grade rocks in which original clay matrix has been reconstituted to sericite + chlorite). Some rocks of intermediate grainsize are hand-specimen-scale melanges (tectonic mixes) of greywacke and argillite Brief petrographic descriptions of all thirty samples examined are given in Appendix 2.1.

Table 3.2: Modal analyses of the coarse-detrital and matrix components of Rangipo Torlesse suite metasediments.

	COARSE-DETRITAL	MATRIX
Quartz	33	28
K-Feldspar	5	-
Plagioclase	45	10
Rock Fragments	12	0
Detrital Accessories	5	12
White Mica	0	15
Chlorite	0	33
Metamorphic Accessories	0	2
TOTAL	100	100

NOTES: Matrix feldspar is given as plagioclase. Rock fragments include metamorphics and plutonics (8%), acid volcanics (2%) and basic volcanics (2%). Detrital accessories include hornblende, pyroxene, zircon, sphene, apatite, Fe-Ti oxides and mica. Metamorphic accessories include calcite, prehnite and epidote.

Microscopic examination shows that the coarse detrital fraction consists of quartz, feldspar and lithic fragments, whereas the finer matrix (i.e. material less than .02mm) consists mainly of muscovite, chlorite and minor heavy minerals. Approximate modal compositions of these two fractions are given in Table 3.2 and the data agree well with Reed (1957), McKean (1976) and Rowe (1980) for Torlesse terrane rocks near Wellington and Reid (1982) and Roser (1983) for other North Island occurrences.

Plagioclase (An_0 to An_{10}) occurs as subangular, variably-altered grains up to 1mm across. Alteration varies from partial sericitisation, through replacement by prehnite and/or calcite to total recrystallisation of fresh albite. Alkali feldspar is ubiquitous but minor, making up about 10% of total feldspar content. Quartz, which comprises 20% to 30% of the coarse fraction, is usually strained and pitted about grain margins. This indicates pressure solution during metamorphism and might explain the widespread occurrence of quartz-rich veins. Minor detrital components (i.e. detrital accessories in Table 3.2) are pyroxene, hornblende, mica, zircon, sphene, apatite, monazite, magnetite and ilmenite. Lithics are important components of the detrital mode and include clasts of igneous metamorphic and sedimentary origin. Some are very altered and blend into the matrix making identification difficult. Many others are internally recrystallised, or at their borders.

Chlorite and 2M muscovite (McKean, 1976) are the main secondary minerals. Prehnite occurs as tabular crystals in the matrix, as replacement fillings in quartz and plagioclase and, with quartz and calcite, as vein fillings. Calcite and epidote are minor components which occur in veins and in the matrix of many samples. Pumpellyite is rarely observed in greywackes, but is a more important constituent of the matrix (Rowe, 1980; McKean, 1976). The occurrence of calcite replacing prehnite, embayed quartz and partially altered plagioclase suggests that metamorphic equilibrium may be localised to the more porous regions of rocks, to domains much smaller

Table 3.3: Calculated end-member chemistry of Rangipo Torlesse suite metasediments and chemistry of metabasite sample 17822.

	ARGILLITE	p	GREYWACKE	p	PCC	REF	17822
major elements (weight %)							
SiO_2	55.00	.38	75.00	.36	-.981	.73	46.99
TiO_2	.94	.01	.30	.01	+.996	3.11	3.20
Al_2O_3	21.02	.09	12.26	.07	+.962	1.71	14.57
Fe_2O_3	7.06	.07	2.53	.04	+.894	2.79	14.64
MnO	.10	.02	.04	.02	+.445	2.50	.51
MgO	2.29	.07	.77	.06	+.903	2.97	3.10
CaO	1.33	.02	1.33	.02	-	1.00	6.48
Na_2O	1.60	.13	3.92	.15	-.630	.41	1.73
K_2O	5.67	.02	1.79	.01	+.848	3.17	2.27
P_2O_5	.19	.02	.08	.02	+.522	2.38	1.59
LOI	4.54	.05	1.70	.05	+.927	2.67	4.67
Total	99.74	-	99.72	-	-	-	99.75
trace elements (ppm)							
Rb	247	3	69	2	+.849	3.59	88
Sr	156	4	256	4	-.431	.61	301
Ba	991	16	468	12	+.517	2.12	709
Pb	25	2	25	2	-	1.00	12
V	162	3	26	2	+.980	6.17	140
Cr	68	2	16	2	+.985	4.38	18
Ni	26	3	7	3	+.631	3.69	28
Nb	16	2	6	2	+.929	2.88	68
Zn	123	2	55	2	+.636	2.23	200
Ga	28	2	12	2	+.948	2.35	28
Sc	18	2	4	2	+.918	4.63	24
La	32	3	17	3	+.523	1.93	54
Ce	75	3	36	3	+.623	2.09	117
Y	35	2	18	2	+.686	1.95	75
Th	23	2	10	2	+.878	2.34	6
Zr	182	4	182	4	-	1.00	455

NOTES: End-member compositions for argillite and greywacke were calculated by least squares regression analysis of 30 samples (Appendix 2.1), using Ti as the dependent variable (Ti=5791ppm for argillite and 1517ppm for greywacke).
All Pearson Correlation Coefficients (PCC) listed are significant within the 95 confidence interval - where PCC was not significant (Ca, Pb, Zr), average concentrations were assigned to each end-member composition.
Analytical precision (p) for the 95% confidence interval were estimated from replicate analyses of International rock standards.
Relative enrichment factors (REF) are given as concentration in argillite / concentration in greywacke.
LOI is loss on ignition at 1000 °C.

than that of a typical thin-section (Zen and Thompson, 1974). It is thus probable that a mobile fluid phase was an important agent during alteration.

3.2.3 Bulk-rock chemistry:

End-member chemical compositions of Rangipo Torlesse suite metasediments (Table 3.3) were calculated by least squares linear regression of each element for all thirty samples. For this, titanium was chosen as the dependent variable because it is considered to be a relatively immobile element during weathering processes (Correns, 1978) and can be analysed with high precision (i.e. less than 5% error). The statistical method simplifies data presentation and is considered appropriate since the sample suite represents a petrographic and chemical continuum between greywacke and argillite. The well-defined chemical trends exhibited by the rocks (Fig.3.4) allow relative enrichment factors (REF) to be calculated where, for any element, REF = the concentration in the argillitic end-member / concentration in the greywacke end-member. These data give a good estimate of the partitioning of elements into each of the end-member compositions (Table 3.3).

Comparison of Tables 3.2 and 3.3 shows that chemical trends are closely linked to changes in modal composition. Greywackes with high high proportions of quartz and albitic plagioclase, are rich in SiO_2 and Na_2O whereas argillites, dominated by a micaceous matrix, are rich in Al_2O_3, MgO and K_2O . Efficient mixing of detritus followed by hydraulic sorting in turbidity currents, best explains these trends (Roser, 1983). Detrital modes and bulk-chemistry of Torlesse terrane sediments suggest derivation from a dominantly granitic source region, but lithic clasts also indicate a minor basic and acid volcanic input (Table 3.2).

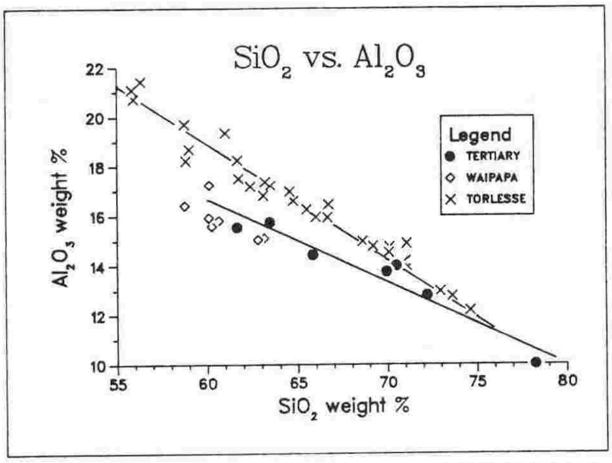

SiO2 vs. Al2O3
Al2O3 weight %
SiO2 weight %
Legend
TERTIARY
WAIPAPA
TORLESSE

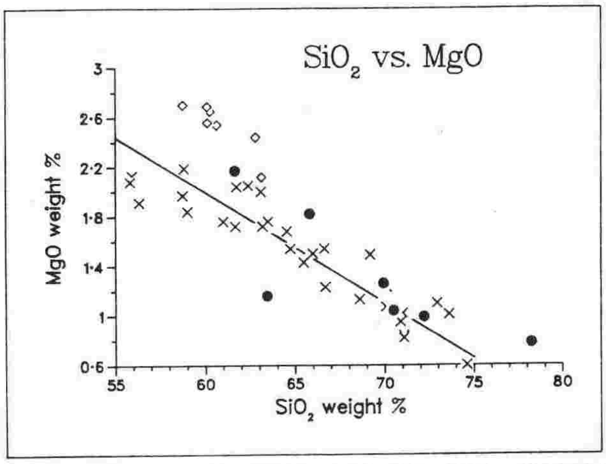

SiO2 vs. MgO
MgO weight %
SiO2 weight %

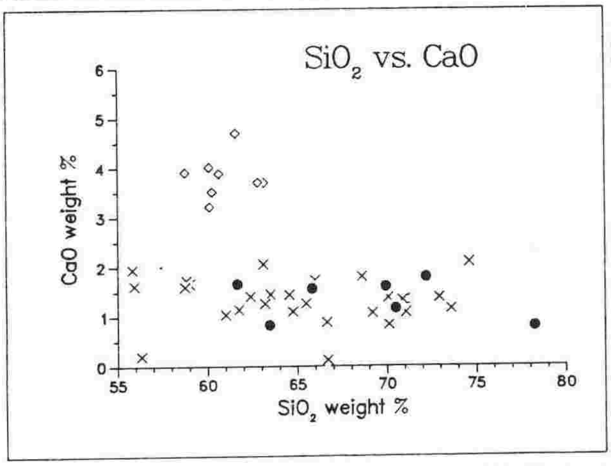

SiO2 vs. CaO
CaO weight %
SiO2 weight %

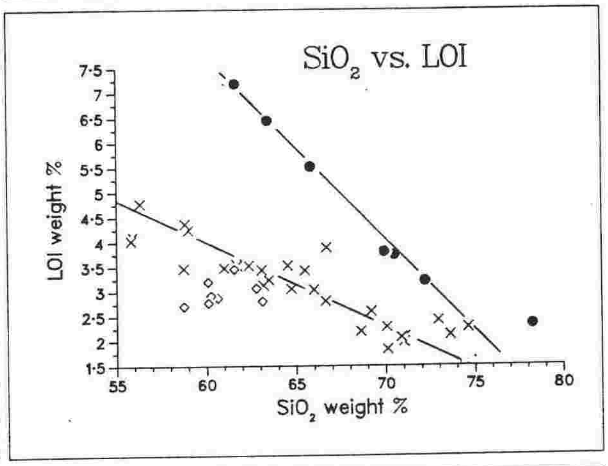

SiO2 vs. LOI
LOI weight %
SiO2 weight %

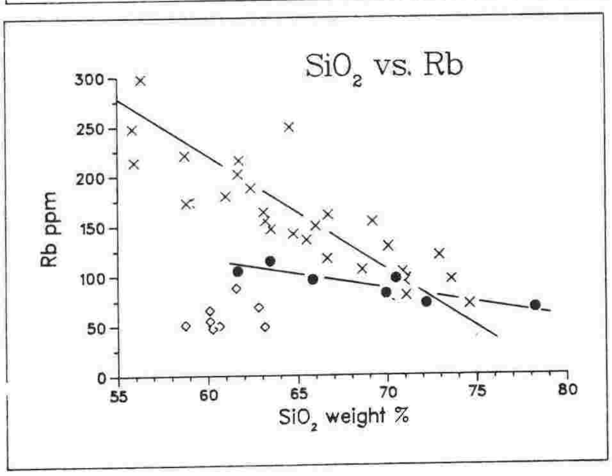

SiO2 vs. Rb
Rb ppm
SiO2 weight %

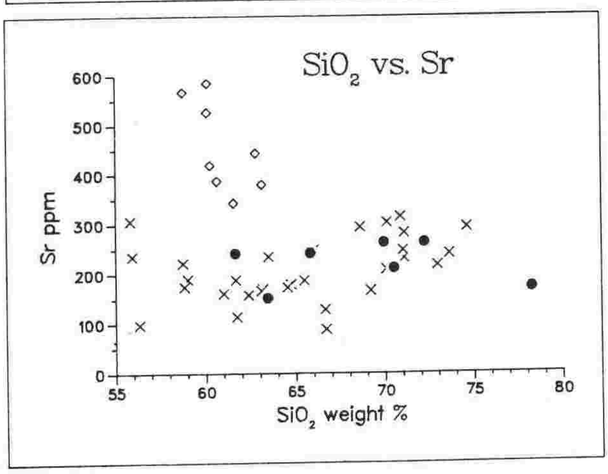

SiO2 vs. Sr
Sr ppm
SiO2 weight %

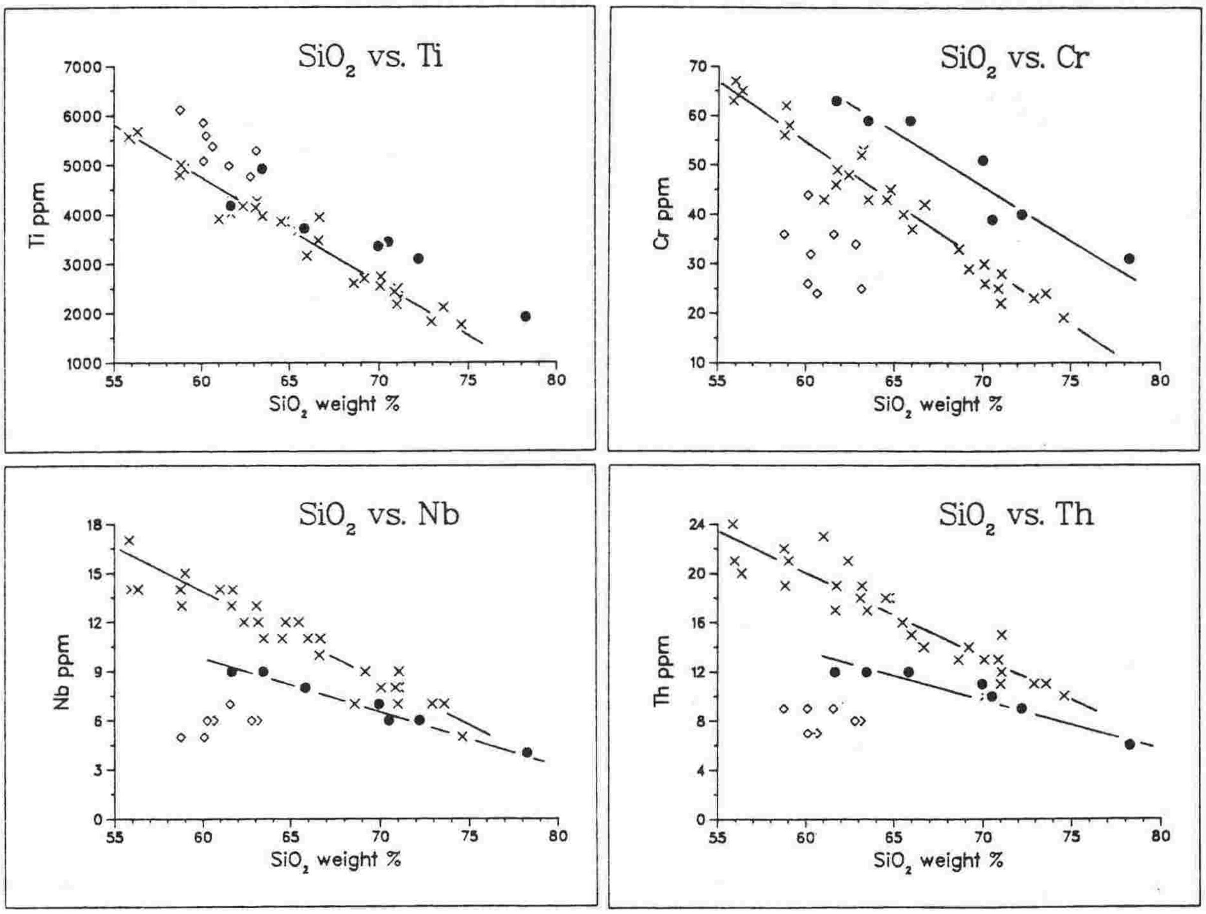

Fig.3.4: Harker variation diagrams of Rangipo suite sediments showing Torlesse suite chemical trends, field of Waipapa suite and Tertiary suite chemical trends. All trend lines are calculated by least squares regression analysis.

Table 3.4: Rb-Sr whole-rock isotopic data of Rangipo Torlesse suite lithologies.

VUW	Rb	Sr	1/Sr	$^{87}Rb/^{86}Sr$ (p)	$^{87}Sr/^{86}Sr$ (p)
Argillite					
17504	249	173	.0058	4.166 (0.9)	.71525 (.072)
17505	216	114	.0088	5.495 (1.1)	.71773 (.069)
17515	298	98	.0102	8.812 (1.0)	.72455 (.080)
17820	221	223	.0045	2.878 (0.9)	.71265 (.112)
17823	164	166	.0060	2.858 (1.2)	.71258 (.094)
17831	161	88	.0114	5.317 (1.5)	.71743 (.099)
Intermediates & Greywackes					
17501	248	307	.0033	2.345 (0.7)	.71231 (.040)
17502	120	217	.0046	1.601 (1.1)	.71074 (.100)
17503	214	236	.0042	2.619 (0.9)	.71282 (.077)
17506	188	158	.0063	3.456 (1.1)	.71415 (.074)
17507	173	175	.0057	2.858 (1.1)	.71325 (.083)
17508	179	161	.0062	3.224 (1.1)	.71423 (.064)
17509	145	235	.0043	1.810 (1.1)	.71095 (.051)
17510	154	166	.0060	2.693 (1.2)	.71246 (.094)
17511	136	187	.0053	2.099 (1.2)	.71152 (.083)
17512	96	239	.0042	1.157 (1.2)	.70962 (.084)
17513	116	128	.0078	2.640 (1.3)	.71350 (.062)
17514	142	179	.0056	2.290 (1.2)	.71220 (.045)
17516	150	248	.0040	1.747 (1.1)	.71100 (.079)
17517	80	281	.0036	.826 (1.4)	.70924 (.070)
17518	174	190	.0053	2.649 (1.0)	.71289 (.074)
17519	154	170	.0059	2.623 (1.3)	.71287 (.036)
17824	97	231	.0043	1.212 (1.2)	.70921 (.053)
17825	106	294	.0034	1.041 (1.1)	.70930 (.050)
17826	94	247	.0041	1.099 (1.0)	.70922 (.064)
17827	201	188	.0053	3.101 (1.2)	.71334 (.046)
17828	129	209	.0048	1.784 (1.2)	.71058 (.060)
17829	104	314	.0032	.962 (1.5)	.70908 (.072)
17830	71	293	.0034	.697 (1.1)	.70867 (.067)
17832	79	303	.0033	.755 (1.3)	.70820 (.069)
Metabasite					
17822	88	301	.0033	.843 (1.2)	.70880 (.069)

NOTES: Errors (p) are given for the 68% confidence interval and are expressed as percentages. Samples listed as argillites are plotted on Fig.3.6.

Because of uncertainty about the precise nature of the source, the effects of weathering, diagenesis and metamorphism on different minerals, it is not possible to trace reliably the chemical history of these rocks. However, some observations become important in discussions of Rb-Sr isotope geochronology (section 3.2.4).

The matrix is partly derived directly from the source region and partly by subsequent decomposition of detritus in-situ (Rowe, 1980). It is dominated by chlorite and M2 muscovite resulting from low-grade metamorphic reconstitution of clays such as illite and smectite. Since Ti is contained mainly in detrital Fe-Ti oxides which are also concentrated (with other heavy minerals) in the matrix (Roser, 1983), there are strong positive correlations between Ti and MgO, Ti and Fe_2O_3, Ti and K_2O and Ti and volatile content (LOI) (Table 3.3 and Fig.3.4). Similar trends occur for the relatively immobile elements Cr, Ni, Nb and V, all of which are contained in both heavy minerals and the micaceous component of the matrix and which, as a consequence, have the highest REFs. The rare earth elements La and Ce, together with Y, Th and Zr are probably contained in detrital minerals such as apatite, monazite and zircon, none of which are well partitioned by the hydraulic sorting processes (Roser, 1983). These elements thus show poor correlations with Ti (Zr is uncorrelated), and have relatively low REFs. Al_2O_3 shows a strong positive correlation with Ti as it is controlled mainly by the micaceous component of the matrix. However, it also occurs in feldspars concentrated in the coarse fraction and thus has only a moderate REF compared to most other elements. The partitioning of felsic detrital minerals into greywacke endmembers of the suite is well illustrated by the negative correlations between Ti and SiO_2, Ti and Na_2O and Ti and Sr.

Correlations between Ti and mobile elements such as Ba, K, Rb, Na and Sr are poor compared to others. This may be due to factors such as source heterogeneity, but more probably results from interaction of hydrothermal

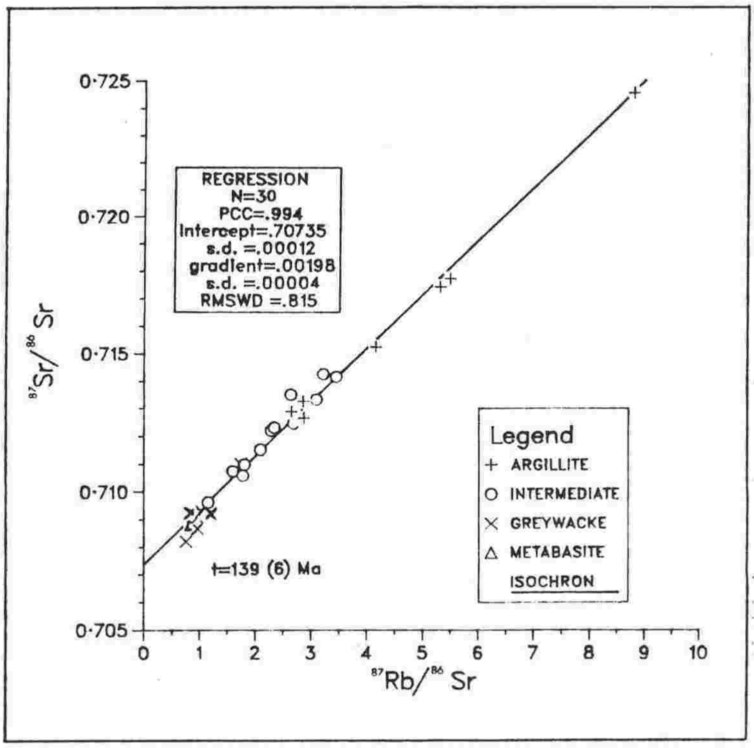

Fig.3.5: Rb-Sr whole-rock isochron plot of Rangipo Torlesse suite metasediments. REGRESSION = statistical data for the isochron: N = number of samples; PCC = Pearson correlation coefficient; s.d. = standard deviation; RMSWD = root mean square of weighted deviations. Error on age is for the 95% confidence interval.

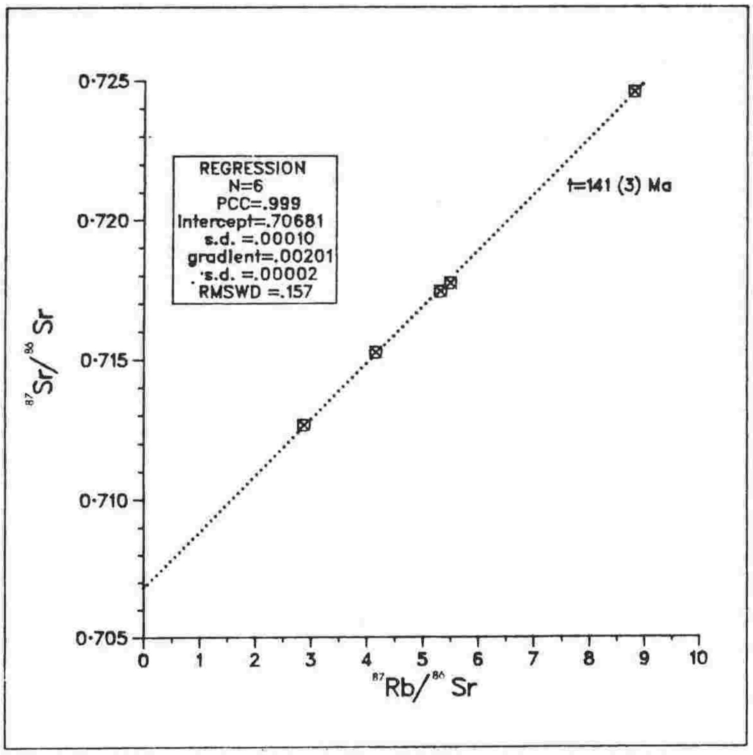

Fig.3.6: Rb-Sr whole-rock isochron plot of Rangipo Torlesse suite argillites (see Table 3.4). One point is obscured.

fluids with the sedimentary pile during diagenesis and metamorphism. The lack of significant correlation between Ti and CaO mainly reflects similar concentrations of the latter in both the matrix and the coarse component of the rocks, although widespread occurrence of calcite and prehnite in veins and in the groundmass of many samples indicates that this element has also been mobile during metamorphism.

To summarise, erosion of a dominantly granitic source region produced detritus made up mainly of quartz, feldspar, mixed-layer clays and lithics. During sedimentation, the felsic-detrital and the clay-rich / heavy mineral fractions were hydraulically separated to produce Ti-, Al-, Fe-, Mg- and K-rich argillites, and Si- and Na-rich greywackes. Subsequent diagenetic and low-grade metamorphic alteration of the rocks has not altered the chemical trends except for the most mobile elements. Na and Sr are those most-affected by interaction with pore-fluids, though Ca, Ba, and Rb concentrations may also have been slightly modified.

3.2.4 Rb-Sr geochronology:

Rb-Sr whole-rock dating of metasedimentary rocks is now commonplace (e.g. Moorbath, 1969; Gebauer and Grünenfelder, 1974 & 1976; Chaudhuri, 1976; Criscione et al., 1978; Priem et. al., 1978; Clauer and Kröner, 1979; Clauer, 1982) and is used to determine either (1) the time of compaction and diagenesis of sediments or (2) the time of subsequent metamorphism. The technique is here applied to the Rangipo Torlesse suite to test the use of coarse-grained greywacke samples in Rb-Sr geochronology and also to provide a data base for crustal contamination models and to compare with metasedimentary xenoliths.

Strontium isotopic data for all samples examined (Table 3.4) are plotted on an isochron diagram in Fig.3.5. This reveals what appears to be an acceptable whole-rock isochron (RMSWD=.815), giving an age of 139 (6) Ma and intercept of .70735 (24) (errors in brackets are for the 95% confidence interval). A corresponding plot of six argillites, being those with the

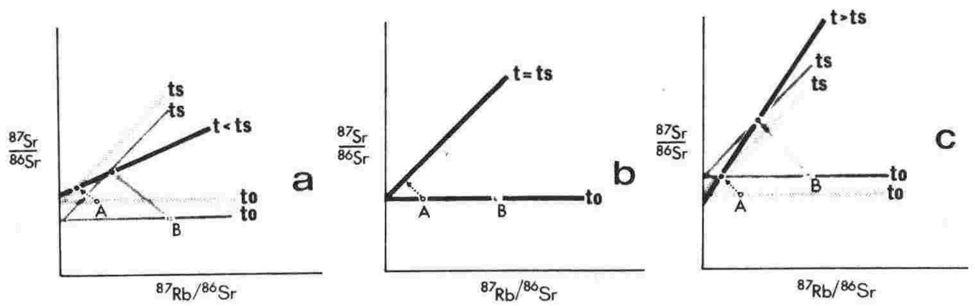

Fig.3.7: Theoretical pseudo-isochrons generated by mixing two components with (a) low Rb/Sr and high $^{87}Sr/^{86}Sr$ (A) & high Rb/Sr and low $^{87}Sr/^{86}Sr$ (B) respectively, giving a lower age than expected; (b) different Rb/Sr but the same $^{87}Sr/^{86}Sr$ giving the time of mixing and (c) low Rb/Sr and high $^{87}Sr/^{86}Sr$ (A) and high Rb/Sr and high $^{87}Sr/^{86}Sr$ (B) respectively, giving a higher age than expected.
to = initial age; t = isochron age; ts = evolved age.

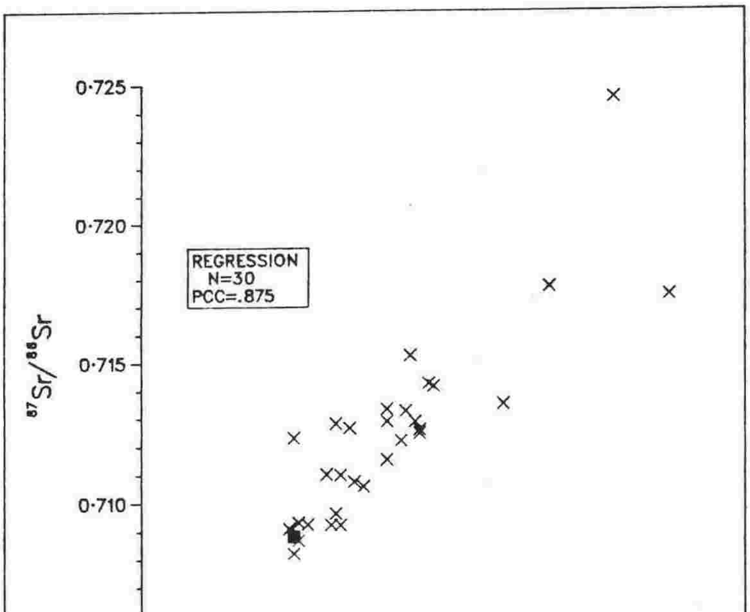

Fig.3.8: $^{87}Sr/^{86}Sr$ vs. 1/Sr plot of Rangipo Torlesse suite lithologies. Metabasite 17822 is filled square.

smallest average grainsize and highest matrix content, yield an isochron (RMSWD=.157) giving an age of 141 (3) Ma and intercept of .70681 (29) (Fig.3.6). Comparison of these two isochrons suggests that the greywacke samples plot on a line which is slightly curved and steeper than that of the argillite samples. However, these differences are small and there is clear overlap between the calculated ages.

The lines shown as "isochrons" in Fig.3.5 and Fig.3.6 could be produced by several geological processes such as (i) mixing of a binary source, (ii) unmixing of detritus from a homogeneous source or (iii) metamorphic re-equilibration. Each is discussed and evaluated below.

(i) Mixing of a binary source: Mixing of a coarse-grained, quartzo-feldspathic component (low Rb/Sr) with a finer-grained, micaceous component (high Rb/Sr) could produce the mineralogical and chemical trends described previously. However, the isotopic correlation produced has no geological meaning and is a pseudo-isochron. Such arrays which result from mixing of isotopically different components can yield "ages" that are either younger or older than the actual source age (Fig.3.7a, Fig.3.7c) - only if both components had the same initial $^{87}Sr/^{86}Sr$ ratio would the age refer to the time of mixing (Fig.3.7b). For the data presented here, binary mixing is improbable for the following reasons:

1. The wide variety of lithic fragments in the mode (Table 3.2) makes a simple mixing hypothesis unlikely (see also Roser, 1983; MacKinnon, (1983).

2. The mineralogical and chemical trends described above are better related to hydraulic sorting of detritus in turbidity currents than to mixing of petrographically and chemically distinct endmembers.

3. Faure (1977) showed that mixing of two components having differing $^{87}Sr/^{86}Sr$ ratios and Sr contents follow a hyperbolic relationship. The mixing equation is derived from plots of $^{87}Sr/^{86}Sr$ vs. 1/Sr. For the Rangipo Torlesse suite (Fig.3.8), there is a broad relationship between the two parameters but the correlation (PCC=.875) is poorer than that between

$^{87}Sr/^{86}Sr$ and Rb/Sr (PCC=.994), and is considered to be merely a consequence of the petrological and chemical trends resulting from the hydraulic sorting process.

4. A metabasite sample (17822) plots close to the isochron in Fig.3.5. Such rocks are accidental inclusions of oceanic crust in the predominantly sedimentary sequence and hence have no genetic or temporal relationship to them (Roser, 1983). Given such an origin, it is unlikely that 17822 would have an initial Sr isotopic ratio as high as the metasedimentary members of the Rangipo Torlesse suite and its present $^{87}Sr/^{86}Sr$ ratio requires an alternative explanation.

5. K-Ar whole-rock ages for nine argillite samples from the Rangipo area are similar to the Rb-Sr ages discussed here. The ages (B.Hegan (NZGS) and C.J.D.Adams (INS) pers. comm., 1984) range from 132.6 (1) to 146.6 (1) Ma, with a mean of 138.4 (4) Ma (analytical methods employed for K-Ar dating at INS are described in Adams (1975) and recalculations use the decay constants recommended by Steiger and Jäger (1977)). Age agreement between these two independent techniques strongly suggests that mixing is not the best explanation for the Rb-Sr isochron. Erosion and alteration of source detritus would have a severe effect on K-Ar systematics since the most important K-bearing phases are clays resulting from feldspar breakdown. These are susceptable to recrystallisation and consequent Ar loss during diagenesis and anchimetamorphism. Although Rb and radiogenic Sr occur in similar lattice sites to K and Ar, displacement of them does not imply immediate loss from the system and consequent isotopic resetting.

ii. Un-mixing of detritus from a homogeneous source: The strong chemical trends exhibited by the Rangipo Torlesse suite are interpreted to be the result of hydraulic sorting of detritus in turbidity currents. This process produces a spectrum from clay-rich argillites (with high Rb/Sr and high $^{87}Sr/^{86}Sr$) to quartzo-feldspathic greywackes (with low Rb/Sr and low $^{87}Sr/^{86}Sr$) - a result similar to that produced by mixing detritus from a binary source. If post-depositional re-equilibration of Sr isotopes did not occur in the system, the resultant whole-rock isochron should represent the average age of the source terrane (see Fig.3.7b). However, a source-age interpretation has similar difficulties to a binary mixing interpretation:

1. The source terrane was not entirely homogeneous.
2. There is a poor correlation between $^{87}Sr/^{86}Sr$ and 1/Sr.
3. Metabasite sample 17822, which is unrelated to the sedimentary source, plots close to the isochron.
4. It is highly unlikely that K-Ar ages of various minerals in the source would be maintained during erosion, transport, deposition and metamorphism of the rocks, even if the Rb-Sr isotopic system were, at the same time, preserved.

A further point is that the Torlesse terrane spans the period Permian - Lower Cretaceous (Speden, 1976) and during this time, bulk-rock composition of sediments remained remarkably constant (Reid, 1982; Roser, 1983). The age of the source terrane must therefore be Permian or older, conflicting with the younger 141 Ma (Late Jurassic) age.

iii. Metamorphic re-equilibration: Moorbath (1969) obtained a 761 Ma whole-rock isochron for Torridonian sediments from NW Scotland which he interpreted as the time of diagenesis, closely following deposition and compaction. However, Dasch (1969) studied Sr isotopes in deep-sea sediment profiles and showed that, although alumino-silicate detritus increase their Rb/Sr ratios as a result of Rb fixation, there was little evidence for significant equilibration of Sr isotopes even after prolonged contact with sea water and interstitial brines. In a study of Miocene shales off the coast of Louisiana, Perry and Turekian (1974) showed that diagenetic changes involved the breakdown of detrital feldspars and micas and the formation of illite-rich clays. These processes release Sr which then partially equilibrates with interstitial fluids and with Sr adsorbed on the clays. They noted a trend towards Sr homogenisation, but even those samples from depths greater than 5km were not completely equilibrated. Chaudhuri (1976) also found incomplete homogenisation of Sr isotopes in Lower Permian shales of the Havensville Formation (Kansas and northern Oklahoma) and concluded that the ages obtained were between the age of the source terrane and the time of sedimentation and/or diagenesis. On the other hand, Priem et al. (1978) showed that complete equilibration of Sr isotopes is possible in water-laid pyroclastics during re-ordering and albitisation of feldspars.

The above studies suggest that it is unlikely that the Rangipo Torlesse suite, with its high proportion of coarse-grained lithologies, could be completely equilibrated for Sr isotopes during diagenesis unless partial or complete albitisation of plagioclase occurred during this early stage of burial. However, other studies suggest that equilibration is much more likely to happen during anchimetamorphism (deep burial). Gebauer and Grünenfelder (1974) discussed the Rb-Sr ages of Paleozoic sediments from Montagne Noire and showed that data from least deformed rocks yielded poor Rb-Sr whole rock isochrons. This they related to incomplete equilibration of Sr in detrital micas. However, the more schistose, folded parts of the sequence yielded isochron ages corresponding to the known age of folding and anchimetamorphism. Minerals separated from psammites between equilibrated pelitic layers showed that, while detrital micas were only partly isotopically equilibrated, albites were completely equilibrated. Such evidence suggests that at least partial equilibration of Rangipo Torlesse suite greywacke could have occurred during deep burial. All the rocks are highly deformed and the detrital component is dominated by albitised plagioclase. The size of any equilibrated domain is difficult to assess but drill-core logs indicate that the full range of sediment lithology (and therefore bulk-rock chemistry) is repeated over distances of only a few hundred metres. Thus it is only necessary to equilibrate relatively small volumes to reset effectively the whole-rock isotopic

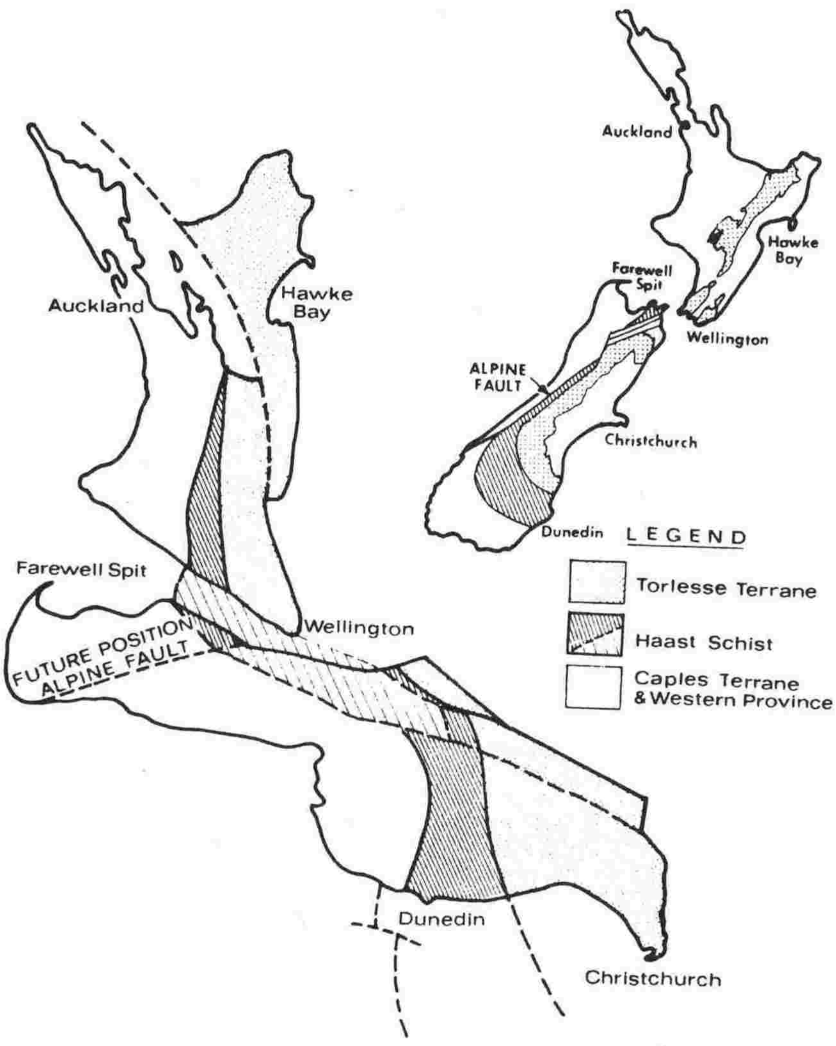

Fig.3.9: Plate tectonic reconstruction of New Zealand in the Mesozoic (after Korsch and Wellman, in press), showing continuation of Haast schist through central North Island.

system over a much larger region (Roddick and Compston, 1977). Rare lithologies such as metabasite would have only a minor effect on the isotopic composition of each domain and would be equilibrated to its mean value.

It is difficult to distinguish isotopic equilibration during burial metamorphism from that during a subsequent tectonic event. Textural evidence for more than one event is absent in the Rangipo area, but the rocks are clearly more foliated than those from other regions and there is structural evidence for polyphase deformation elsewhere within the Torlesse terrane (Sporli, 1978). MacKinnon (1983) correlated the Kaimanawa schist belt (Fig.3.1) with the more highly metamorphosed Haast Schist terrane of the South Island, a link which is supported by plate tectonic reconstruction of New Zealand in the Mesozoic (Fig.3.9) (Korsch and Wellman, in press). Rb-Sr geochronological data for Haast Schist is limited (Aronson, 1965) to a mineral isochron age of 119 (13) Ma from near Cromwell, Otago. This falls within the error limits for the age of the Rangipo Torlesse suite but is not conclusive support for a correlation between the two terranes. However, recent K-Ar ages (Sheppard et al., 1975; Adams, 1980) indicate that the main metamorphism of the Haast Schist terrane occurred at 190-200 Ma. There were later tectonic events (Rangitata II, Bradshaw et al., 1980) at about 120-140 Ma, which affected the western part of the Torlesse accretionary prism in Late Jurassic times. Subsequent movement along the Alpine Fault has separated the Haast Schist terrane from its equivalents in Marlborough and the central North island.

In summary, the 141 Ma Rb-Sr whole rock age of Torlesse terrane sediments in the vicinity of the TVC probably dates the timing of low-grade metamorphism and uplift of the sequence. During diagenesis, strontium isotopes were equilibrated with pore fluids as a result of alteration of feldspar and re-crystallisation of clays in the matrix. This process continued during anchimetamorphism and ended at about 140 Ma as a result of

Table 3.5: Bulk-rock chemistry of Torlesse terrane metasediments from various North Island localities.

LOC	Wellington	Hutt	Otaki	Ureweras	Whakatane	Matata
SAMPLES	4	3	4	6	3	5
major elements (weight%)						
SiO_2	59.3	69.1	59.2	71.0	65.8	72.7
TiO_2	.8	.5	.9	.5	.6	.5
Al_2O_3	18.0	14.5	19.5	14.4	16.0	13.4
Fe_2O_3	6.8	3.7	7.0	3.2	5.0	3.1
MnO	.1	.1	.1	.0	.1	.1
MgO	2.6	1.4	2.0	.9	1.5	1.1
CaO	1.6	1.3	.5	1.5	.8	1.1
Na_2O	1.9	4.0	1.5	3.9	3.3	3.2
K_2O	4.4	2.6	3.6	2.5	3.3	2.6
P_2O_5	.2	.1	.1	.1	.1	.1
LOI	4.1	2.5	5.5	1.7	3.3	1.9
Total	99.8	99.8	99.9	99.8	99.8	99.8
trace elements (ppm)						
Ba	552	585	610	659	760	680
Rb	224	93	180	88	99	84
Sr	218	284	97	276	345	232
V	126	81	179	63	86	57
Cr	70	54	86	41	48	41

NOTES: Samples = number of individual analyses used for each mean.
Sources: Wellington (Horokiwi Quarry), Hutt (Rimutaka Road) - Roser (1983); Ureweras, Whakatane, Matata - Reid (1983); Otaki Forks - McKean (1976).

critical reduction in porosity and/or uplift. In a rapidly accreting continental margin, like that in New Zealand during the Mesozoic, these processes might operate over a short time span, uplift post-dating sedimentation by only a few million years (Korsch and Wellman, in press). Isotopic equilibration was not completely effective for greywackes or intermediate lithologies although deviation of data points from the isochron is small. Interpretation that the 140 Ma age represents uplift directly related to the Rangitata II orogeny is equivocal. Given the accretionary prism model for the Torlesse terrane as a whole, it is possible that individual crustal blocks were metamorphosed and uplifted in separate events. The Rb-Sr whole-rock ages derived from each block might therefore relate only to a local event.

3.2.5 Regional Variations:

Torlesse terrane sediments of the North Island are chemically similar regionally (Table 3.5 and Fig.3.10) but show significant differences in their Sr isotopic compositions (Table 3.6). These reflect either different metamorphic ages, isotopically different sources, variable degrees of post-depositional alteration or equilibration in domains of differing size. Rb-Sr whole-rock isotopic data for selected samples are plotted on an isochron diagram (Fig.3.11) which shows data from some areas (e.g. Ureweras) falling close to the Rangipo isochron, suggesting similar metamorphic and/or tectonic histories. However, samples from geothermal regions (e.g. Broadlands) are markedly displaced from the isochron, probably as a result of hydrothermal alteration and consequent disturbance of the whole-rock Sr isotopic systems. These data indicate that application of Rb-Sr geochronology to Torlesse rocks may be impossible in areas where geothermal activity is, or has been present.

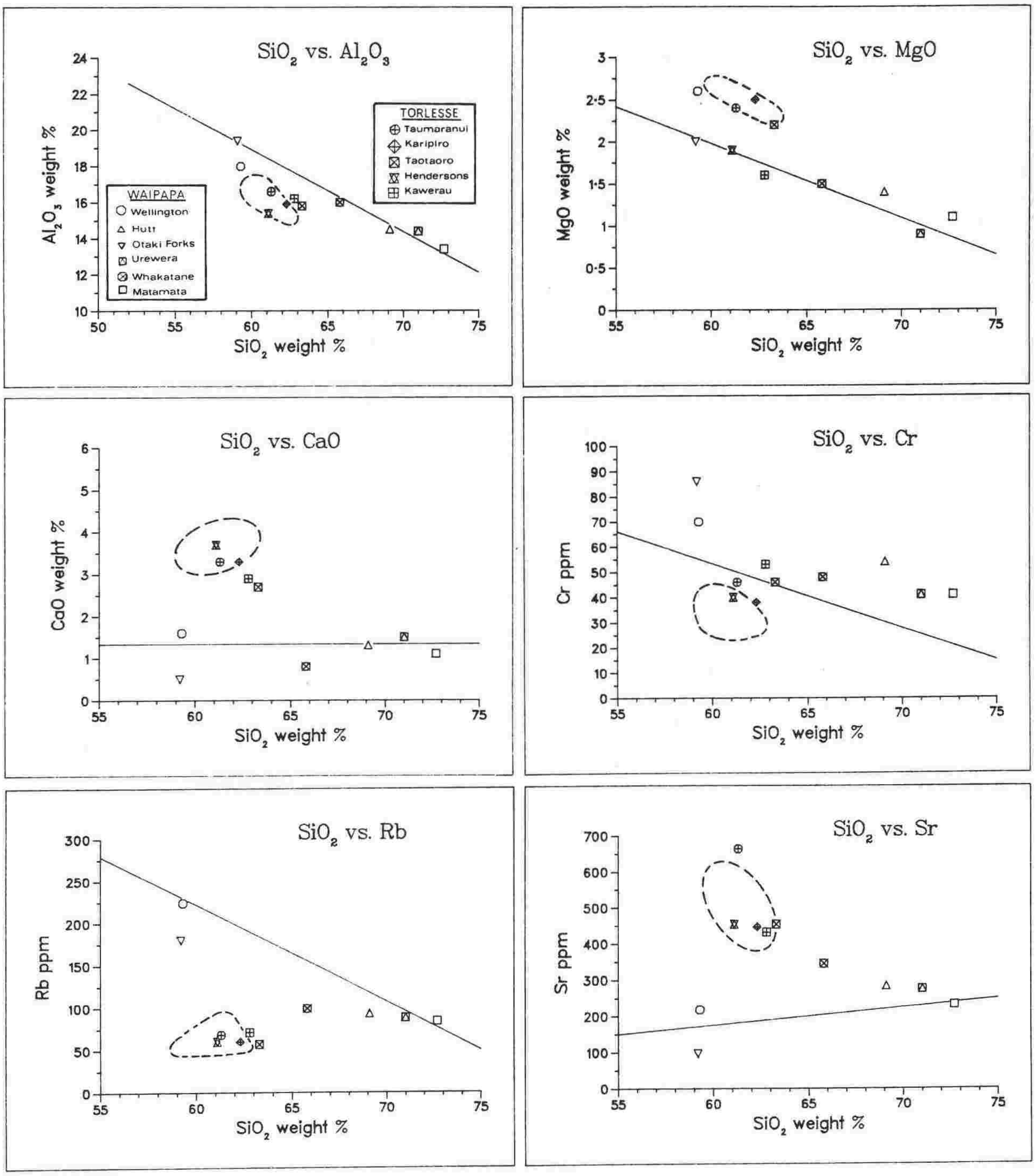

Fig.3.10: Harker variation diagrams of Torlesse and Waipapa terrane metasediments from various North Island localities. Regression lines are of Rangipo Torlesse suite (Table 3.3); fields are of Rangipo Waipapa suite (Fig.3.4).

Table 3.6: Rb-Sr whole-rock isotopic data of Torlesse terrane metasediments from various North Island localities.

VUW	Rb	Sr	1/Sr	$^{87}Rb/^{86}Sr$ (p)	$^{87}Sr/^{86}Sr$ (p)
Otaki Forks					
17843	190	64	.0157	8.638 (1.6)	.73324 (.048)
17844	182	79	.0127	6.673 (1.5)	.72766 (.100)
17845	169	121	.0083	4.044 (1.3)	.72109 (.054)
17846	178	125	.0080	4.126 (1.3)	.72192 (.078)
17847	43	272	.0037	.458 (1.9)	.71173 (.090)
Matata					
16020	75	229	.0044	.948 (1.5)	.70932 (.096)
16021	54	238	.0042	.657 (1.9)	.70864 (.065)
16022	84	298	.0034	.816 (1.3)	.70607 (.050)
16023	84	298	.0034	.816 (1.3)	.70723 (.073)
16024	54	349	.0029	.448 (1.8)	.70567 (.053)
Whakatane					
16038	118	186	.0054	1.837 (1.2)	.71090 (.042)
Broadlands					
16040#	113	185	.0054	1.769 (1.2)	.70963 (.058)
16042#	115	236	.0042	1.412 (1.2)	.71654 (.062)
Ureweras					
16010	91	300	.0033	.878 (1.2)	.70838 (.114)
16012	91	207	.0048	1.273 (1.9)	.70934 (.049)

NOTES: Errors (p) are for the 68% confidence interval, expressed as percentage. VUW numbers beginning with 160- refer to samples collected by Reid (1983).
hydrothermally altered samples.

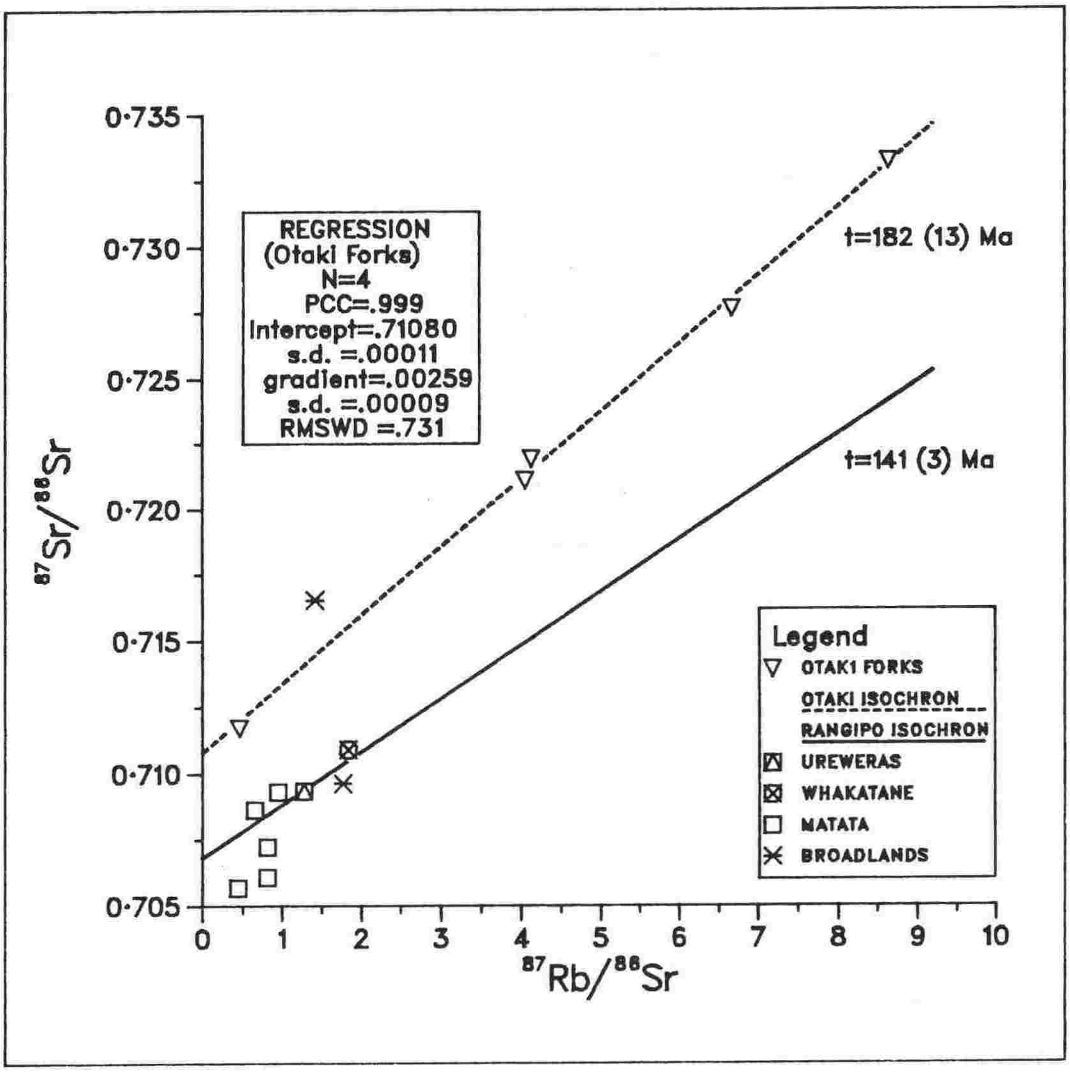

Fig.3.11: Rb-Sr whole-rock isochron plot of Torlesse terrane lithologies from various North Island localities. Regression data are for Otaki Forks argillites (182 Ma isochron). Rangipo Torlesse suite argillite isochron (141 Ma) is given for reference. N = number of samples; PCC = Pearson correlation coefficient; s.d. = standard deviation; RMSWD = root mean square of weighted deviations. Error on age (brackets) is for the 95% confidence interval.

The four Otaki Forks argillite samples (Appendix 2.1) were previously described by McKean (1976) who also dated them by the K-Ar method. Three of the samples were collected from the well-known fossil locality east of Pukehinau Stream, and the third from nearby in the Otaki River bed. Important zone fossils (Speden, 1976) from these localities include Monotis Richmondiana Zittel (Grant-Taylor and Waterhouse, 1963) which indicate a depositional age of Late Triassic. Using the revised time-scale of Harland et al. (1982), this corresponds to 219-225 Ma. K-Ar whole-rock ages for the rocks are younger, clustering around 200 Ma (McKean, 1976). Rb-Sr data (Fig.3.11) fall on an isochron (RMSWD=.73) giving an age of 182 (13) Ma and intercept of .7108 (11). This age is significantly greater than that of the Rangipo isochron, but much younger than the fossil (depositional) age, indicating that metamorphic resetting of Otaki Forks Torlesse sediments occurred some time after sedimentation, and at an earlier time than the Rangipo rocks. The significant difference in initial Sr isotopic ratios between the two isochrons may be best explained by lithological differences in the respective domains of equilibration. Members of the two rock suites are similar chemically and major differences in provenance are unlikely. Given that the source terrane for all Torlesse sediments is the same i.e. old granitic rocks with a significant pre-erosional isotopic history, then detrital material would be of two types (1) coarse-grained feldspar-rich detritus with relatively high Sr content and low $^{87}Sr/^{86}Sr$ and (2) fine-grained mica-rich detritus with lower Sr content and higher $^{87}Sr/^{86}Sr$. In crustal blocks (domains of equilibration) dominated by greywacke (e.g. Rangipo), the average isotopic ratio prior to equilibration would be much lower than those dominated by argillite (e.g. Otaki Forks).

Table 3.7: Average bulk-rock chemistry of Waipapa terrane metasediments.

LOC	Rangipo	Taumarunui	Karipiro	Taotaoro	Hendersons	Kawerau
SAMPLES	7	6	2	3	5	4
major elements (weight%)						
SiO_2	60.8	63.3	62.3	61.3	61.1	62.8
TiO_2	.9	.4	.8	.7	.8	.7
Al_2O_3	15.9	15.8	15.9	16.6	15.4	16.2
Fe_2O_3	6.9	5.9	6.4	6.0	6.6	5.2
MnO	.1	.1	.1	.1	.1	.1
MgO	2.5	2.2	2.5	2.4	2.9	1.6
CaO	3.7	2.7	3.3	3.3	3.7	2.9
Na_2O	3.8	4.3	4.2	4.1	3.6	3.4
K_2O	1.9	1.9	2.0	2.4	1.9	2.1
P_2O_5	.2	.2	.2	.2	.2	.2
LOI	3.0	3.0	2.1	2.7	3.5	4.6
Total	99.7	99.8	99.8	99.8	99.8	99.8
trace elements (ppm)						
Ba	491	460	527	616	529	474
Rb	55	57	60	68	60	71
Sr	472	454	447	664	454	432
V	154	120	136	136	147	114
Cr	32	46	38	46	40	53

NOTES: Sources: Rangipo - this work;
Taumarunui, Karapiro, Hendersons, Kawerau - Reid (1983).
Taotaoro - R.J.Korsch (unpublished data).

3.3 WAIPAPA TERRANE (RANGIPO WAIPAPA SUITE)

3.3.1 Introduction:

The Waipapa terrane of the North Island extends from west of Tongariro to north of Auckland (Fig.3.2) and consists mainly of poorly-fossiliferous, graded-bedded greywacke and argillite, probably derived from the Brook Street volcanic arc (Coombs et al., 1976). Transport was across the fore-arc basin, in submarine canyons to the trench floor (Korsch and Wellman, in press). Subsequently, complex deformation has occurred in an accretionary prism above a west-dipping subduction zone.

Bulk chemical composition of Waipapa terrane sediment (Reid, 1982; Roser, 1983) is significantly different from Torlesse and is closely related to provenance, as shown by alkali-silica discrimination (Roser, 1983). The rocks were probably deposited at a Pacific-type convergent margin whereas Torlesse sediments were deposited at a passive Andean-type margin or at an evolved continental margin against active oceanic lithosphere.

3.3.2 Petrography:

Lithologies range from medium greywackes to intra-formational breccias consisting of 50-100mm andesitic clasts in a sandy matrix. All are poorly-foliated but very well-indurated. Greywackes are poorly-sorted and contain a high proportion (20-50%) of severely altered volcanic lithics, identified by relict flow banding and porphyritic texture. Plagioclase ranges from albite to oligoclase and is the dominant detrital mineral occurring as subangular, partly sausuritised grains. Orthoclase comprises about 20% of total feldspar content. Subangular quartz, showing strain features and some recrystallisation, typically makes up 15-20% of the detrital mode. Less abundant detrital constituents are hornblende, augite, hypersthene, biotite, sphene, zircon and Fe-Ti oxides. Secondary minerals are chlorite and muscovite and both occur in the matrix as alteration products of

Table 3.8: Rb-Sr whole-rock isotopic data of Waipapa terrane metasediments.

VUW	Rb	Sr	1/Sr	$^{87}Rb/^{86}Sr$ (p)	$^{87}Sr/^{86}Sr$ (p)
Rangipo					
17833	49	380	.0026	.374 (1.9)	.70515 (.096)
17834	50	387	.0026	.374 (1.9)	.70523 (.079)
17835	66	526	.0019	.363 (1.4)	.70563 (.061)
17836	69	443	.0023	.454 (1.4)	.70548 (.097)
17838	51	567	.0018	.258 (1.7)	.70497 (.050)
17839*	47	419	.0024	.323 (2.0)	.70519 (.042)
17841*	88	343	.0029	.742 (1.2)	.70631 (.082)
17842	55	585	.0017	.272 (1.5)	.70528 (.071)
17837+	107	210	.0048	1.473 (1.2)	.70845 (.118)
17840*+	101	223	.0045	1.314 (1.2)	.70825 (.061)
Coromandel					
15968	100	303	.0033	.955 (1.1)	.70713 (.116)
Karapiro					
15969	67	415	.0024	.467 (1.5)	.70498 (.035)
15970	66	375	.0027	.509 (1.5)	.70503 (.026)
Hendersons					
15964	48	363	.0028	.383 (2.0)	.70708 (.044)
Kawerau					
15980#(116)	72	327	.0031	.637 (1.4)	.70622 (.036)
15981#(119)	70	388	.0026	.522 (1.4)	.70608 (.026)
15982#(122)	67	575	.0017	.337 (1.5)	.70574 (.061)
15984#(146)	77	443	.0023	.503 (1.3)	.70593 (.072)
. #(150)	72	515	.0019	.405 (1.3)	.70576 (.042)
. #(153)	54	363	.0028	.431 (1.7)	.70566 (.039)
16004#	51	580	.0017	.255 (1.8)	.70556 (.036)

NOTES: Errors (p) are for the 68% confidence interval, expressed as percentage. * samples from the same core; + volcanic clasts; # depth of origin of drill-core sample.

detrital minerals. Prehnite, epidote and calcite also occur as discrete authigenic grains and in veins with quartz. EPMA analyses of plagioclase, K-feldspar, hornblende, chlorite, muscovite, prehnite and epidote in 17833 are given in Appendix 3.

3.3.3 Bulk-rock chemistry:

The bulk-rock chemical compositions of Rangipo Waipapa suite sediments (Table 3.7; Fig.3.4) indicate that the greywackes are compositionally equivalent to intermediate calc-alkaline volcanic rocks, whereas breccia clasts have a more calcic and less alkalic composition (Appendix 2.1). There are no obvious chemical trends probably because of the variable abundance of volcanic-derived lithic clasts. Compared to the Rangipo Torlesse suite, the rocks are richer in MgO, CaO and Sr. Otherwise, apparent chemical differences can be explained by the lower proportion of modal quartz in the Waipapa sediments.

3.3.4 Rb-Sr Geochronology:

Whole-rock Rb-Sr isotopic data of Rangipo Waipapa suite metasediments (Table 3.8) yields an isochron (RMSWD=.36) which gives an age of 205 (17) Ma and intercept of .70428 (17) (Fig.3.12). The possibility that this age might represent the time of metamorphism was investigated through a comparative study of a similar sequence in northern N.S.W., Australia (Coffs Harbour Block; see PART 2). That study showed persuasively that re-homogenisation of Sr isotopes can occur in sediments made up mainly of acid to intermediate pyroclastics through the re-ordering of feldspar. In the Rangipo Torlesse suite, Sr isotopes were homogenised by albitisation of plagioclase and recrystallisation of matrix clays, both of which have occurred to some extent in the Rangipo Waipapa suite. Thus isotopic homogenisation is possible even in coarse-grained lithic-dominated rocks. The data could also be interpreted as a mixing line between greywacke matrix and lithic clasts, a possibility supported by the fair correlation

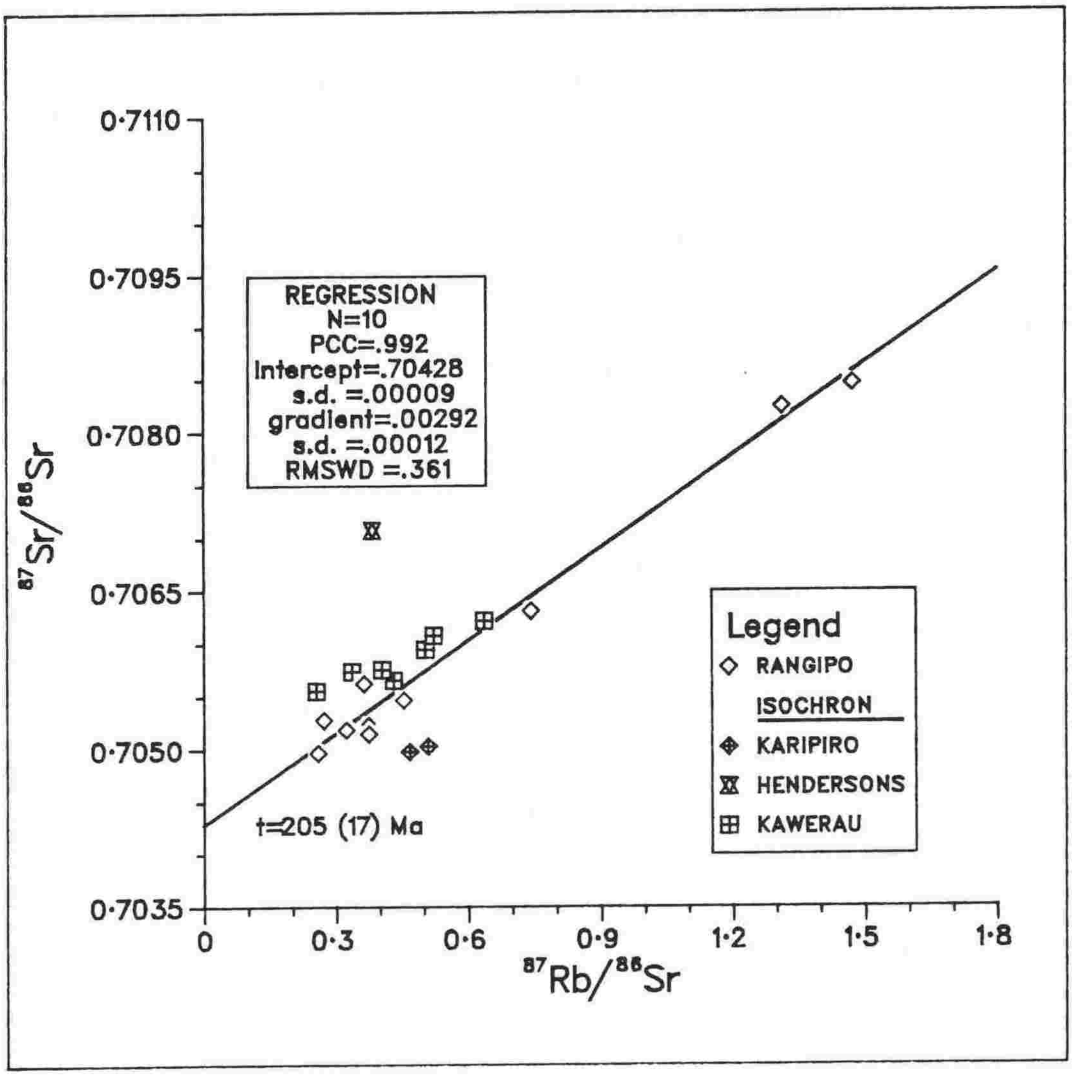

Fig.3.12: Rb-Sr whole-rock isochron plot of Waipapa terrane metasediments from various North Island localities. Regression data and isochron (205 Ma) are of Rangipo Waipapa suite. N = number of samples; PCC = Pearson correlation coefficient; s.d. = standard deviation; RMSWD = root mean square of weighted deviations. Error on age (brackets) is for the 95% confidence interval.

between $^{87}Sr/^{86}Sr$ and 1/Sr (PCC=.942). More analyses of Waipapa terrane lithologies are needed to investigate these two interpretations further, although the Coffs Harbour data would appear to favour metamorphic resetting age rather than binary mixing.

3.3.5 Regional variation:

Reid (1982) and Roser (1983) reported only small regional variations in the composition of Waipapa terrane rocks in the central North Island. The new data presented here support that observation although the data base is still relatively small. Some average analyses (Table 3.7) illustrate the the close similarity between the Rangipo Waipapa suite and samples from Hendersons Quarry, west of Kawerau. Both these suites occur near the Waipapa-Torlesse boundary (Fig.3.2) and a possible correlation is suggested. Drill-core samples from the Kawerau geothermal field show subtle differences in bulk-rock chemistry that probably result from hydrothermal alteration. Several samples described by Reid (1982) were analysed for Sr isotopic composition (Table 3.8) and most data plot close to the Rangipo 205 Ma isochron (including those from geothermal areas). The data indicate that Waipapa sediments have Sr isotopic ratios much lower than Torlesse sediments and that parameter is therefore useful for distinguishing between them.

3.4 TERTIARY SEDIMENTS (RANGIPO TERTIARY SUITE)

3.4.1 Introduction:

Lower Pliocene fossiliferous marine siltstones, sandstones and conglomerates occur to the NW, west and SW of the TVC (Fig.3.1). The oldest strata are near Hauhungatahi, where 200m of grey siltstone of Late Miocene (Taranaki Series) age underlies Quaternary andesitic flows and pyroclastics (Gregg, 1960). About 180m of yellow-brown micaceous sandstone containing bands of greywacke-conglomerate occur to the north in the Whakapapanui River and Waione Stream. In the Okupata stream valley, conglomerates of the Taranaki series overlie Landon series unconformably. Tongariro Power developement bore-hole "b2" (N111/999883) in the NW of the Centre, penetrated greywacke after passing through 25m of Taranaki Series sediments (Gregg, 1960). To the SE of Mount Ruapehu a thin cover of Pliocene (Wanganui Series) marine sediments consists of soft grey micaceous, fossiliferous sandstones and siltstones. These lack fresh volcanic detritus indicating that there was no contemporaneous volcanism (Fleming and Steiner, 1951). Similar sediments occur to the south at Horopito and Ohakune. In the Maowhango River valley, the Tertiary section includes over 350m of siltstone, sandstone and shell limestone with thin lenses of greywacke-conglomerate.

3.4.2 Petrography:

Lithologies of the Rangipo Tertiary suite are dominated by yellow-brown to green quartz-muscovite sandstones, fining into siltstones and muds. These show mineralogical and chemical trends dependent on grainsize, similar to those of the Rangipo Torlesse suite. The rocks are largely made up of well-rounded quartz grains (.05-.25mm) and muscovite flakes in preferred orientation in a muddy matrix. Feldspar lathes and clots of chlorite occur in some samples. In 17855, sandstone clasts (.2mm) are common but otherwise the rocks are lithic-free. Sandstones with fossils and calcareous cement

Table 3.9: Rb-Sr whole-rock isotopic data of Rangipo Tertiary suite sediments.

VUW	Rb	Sr	1/Sr	$^{87}Rb/^{86}Sr$ (p)	$^{87}Sr/^{86}Sr$ (p)
Calcareous siltstone					
17849	41	434	.0023	.271 (2.1)	.70753 (.053)
17856	74	293	.0034	.728 (1.4)	.70840 (.077)
17857	49	391	.0026	.366 (1.8)	.70830 (.147)
Micaceous sandstone					
17848	72	263	.0038	.792 (1.5)	.70765 (.086)
17850	105	242	.0041	1.259 (1.2)	.70881 (.066)
17851	97	211	.0047	1.335 (1.3)	.70861 (.065)
17852	115	152	.0066	2.189 (1.3)	.70983 (.065)
17853	96	242	.0041	1.152 (1.3)	.70910 (.078)
17854	82	263	.0038	.908 (1.3)	.70830 (.076)
17855	67	171	.0058	1.139 (1.7)	.70902 (.090)

NOTES: Errors (p) are for the 68% confidence interval, expressed as percentage.

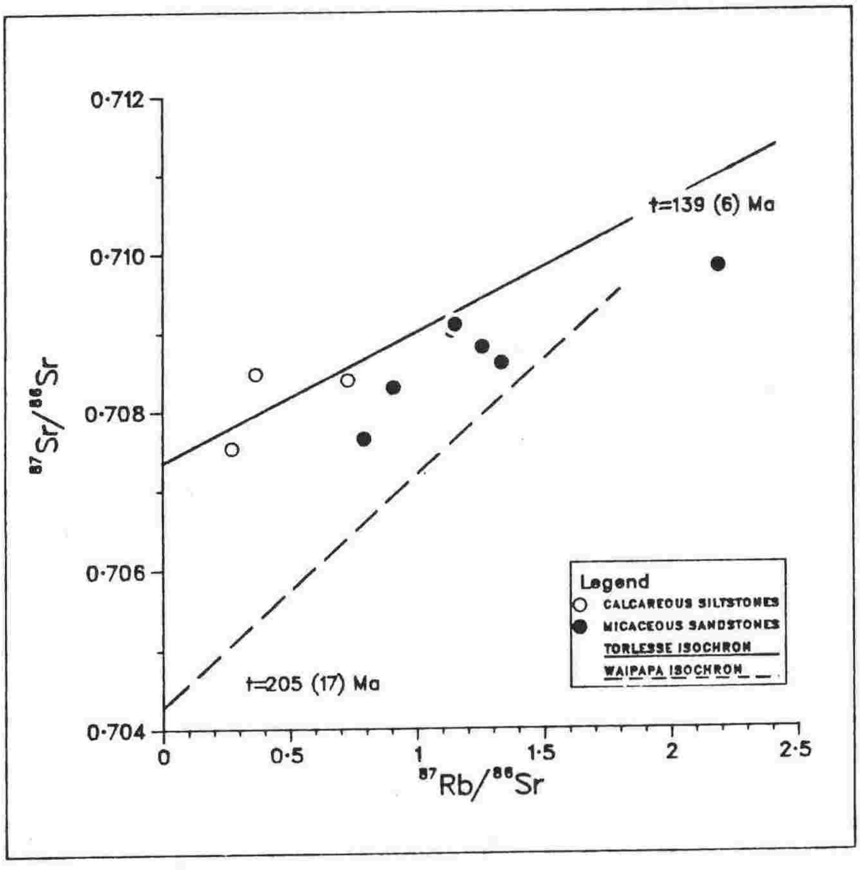

Fig.3.13: Rb-Sr whole-rock isochron plot of Rangipo Tertiary suite sediments. Reference isochrons are (i) Rangipo Torlesse suite (139 Ma) and (ii) Rangipo Waipapa suite (205 Ma).

occur both to the NW (e.g. 17849) and the SW (e.g.17857). Conglomerates occur in younger parts of the sequence particularly in the SW and contain well-rounded clasts of a variety of lithologies: for example, 17858 contains 5-10mm clasts of greywacke (of volcanogenic parentage from textural evidence), quartzite and chert, a 5mm clast of vesicular basalt and molluscan shell fragments. Therefore, there is petrographic evidence to suggest that Rangipo Tertiary suite sediments were derived from a variety of sources, including both Waipapa and Torlesse terranes.

3.4.3 Bulk-rock chemistry:

Bulk-rock chemical compositions of micaceous sandstones and siltstones (Appendix 2.1) exhibit trends which, for the most part, ressemble those of the Rangipo Torlesse suite (Fig.3.9). Differences can be largely explained by the higher volatile losses; for fine-grained rocks, 30% of LOI is absorbed water and the high combined total LOI results from the clay-dominated matrix retaining more water than the mica-dominated matrix of Torlesse greywacke. The CaO and Sr contents of the Tertiary sediments are similar to Rangipo Torlesse suite rocks but much lower than Rangipo Waipapa suite rocks; this indicates dominant input of detritus from the former. MgO and Cr both show trends which are not easily explained by differences in LOI and which, therefore, probably result from input from a separate, Cr-rich province (Dunn Mountain Ophiolite?).

3.4.4 Rb-Sr Geochronology:

Sr isotopic data of three calcareous siltstones and seven micaceous sandstones (Table 3.9) are plotted on an isochron diagram in (Fig.3.13). $^{87}Sr/^{86}Sr$ ratios range from .70753 to .70983 and most samples fall in the field between the Rangipo Torlesse isochron and the Rangipo Waipapa isochron.

3.5 SUMMARY

Sedimentary basement of the TVC consists of (1) Mesozoic Torlesse terrane greywacke and argillite forming the Kaimanawa mountains to the east (2) Mesozoic Waipapa terrane greywacke mainly underlying Tertiary sediments and volcanics to the west and (3) Late Tertiary sediments which are thin to the NW and thicken to the south.

Torlesse terrane metasediments range from micaceous argillite to quartzo-feldspathic greywacke. Bulk-rock chemistry suggests that detritus, derived from a dominantly granitic source, was hydraulically sorted during deposition, producing grainsize-dependent chemical trends. Rb-Sr isotopic data yield whole-rock isochrons giving ages of 139 (6) Ma (all samples) or 141 (3) Ma (argillites). These ages are interpreted as the time of low-grade metamorphism. However, argillites from Otaki Forks give a whole-rock age of 182 (13) Ma, which indicates resetting either during an earlier phase of the Rangitata orogeny or, more probably, during a separate tectonic event. Major differences in initial $^{87}Sr/^{86}Sr$ (.7068 for Rangipo; .7108 for Otaki Forks) are related to differences in the greywacke:argillite ratio in domains of isotopic equilibration.

Waipapa greywackes have an intermediate volcanic bulk-rock chemistry and contain detrital lithic material suggesting an origin at a Pacific - type continental margin. Rb-Sr isotopic data indicate that the rocks were metamorphosed (to prehnite-pumpellyite facies) at 205 (17) Ma and the low initial $^{87}Sr/^{86}Sr$ ratio of .7043 (2) confirms the original arc-type source for detritus.

Tertiary sediments include micaceous silstones and sandstones and minor calcareous siltstones and conglomerates. Mineralogical and chemical compositions are more closely similar to Torlesse terrane than Waipapa terrane sediments, but Sr isotopic compositions range between the two.

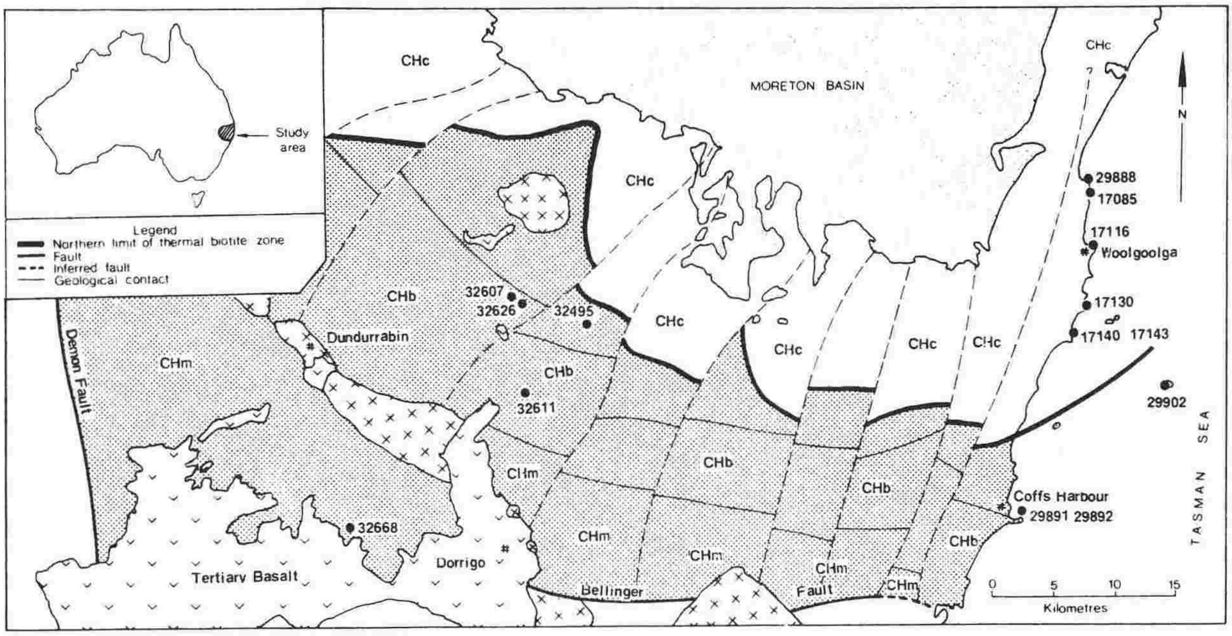

Fig.3.14: Geological map of southern Coffs Harbour block, eastern Australia showing sample locations.
CHm = Moombil beds; CHb = Brooklana beds; CHc = Coramba beds.
Crossed area = plutons of the Hillgrove and New England suite.
Shaded area is that affected by thermal biotite.

PART 2: Rb-Sr GEOCHRONOLOGY OF COARSE-GRAINED GREYWACKES AND ARGILLITES FROM THE COFFS HARBOUR BLOCK, EASTERN AUSTRALIA - A COMPARATIVE STUDY OF RESETTING OF Rb-Sr SYSTEMS IN GREYWACKE SEQUENCES

3.6 INTRODUCTION

In the New England Orogen of eastern Australia, the Coffs Harbour Block (Leitch, 1974; Korsch and Harrington, 1981) occupies an area of over 4500km^2 and consists of a very thick, monotonous suite of greywacke and argillite, intruded by several granitic plutons (Fig.3.14). The sedimentary sequence, informally referred to as the Coffs Harbour sequence, was deposited predominantly by turbidity currents, although there has been minor reworking by contour currents. A major problem in the Coffs Harbour Block has been to determine the age of the sedimentary sequence because no identifiable fossils have yet to be found. This Rb-Sr geochronological study is undertaken in an attempt to (at least) place an upper limit on the age of sedimentation of the Coffs Harbour sequence and, since most previous Rb-Sr studies on sediments and low-grade metasediments have focussed on fine-grained rocks such as argillites and pelites, to examine the Rb-Sr systematics of coarse-grained sedimentary rocks in relation to their fine-grained conterparts. That has important implications for the interpretation of Rb-Sr whole-rock isochrons of Torlesse and Waipapa terrane lithologies (c.f. Part 1).

3.7 PETROGRAPHY

The Coffs Harbour sequence has been subdivided into three lithostratigraphic units (Leitch et al., 1971; Korsch, 1978a) based on the proportion of argillite to greywacke. These are, in order of increasing

Table 3.10: Petrographic modes of greywackes from the Coffs Harbour sequence, eastern Australia.

CAT	UNIT	LITHOLOGY	qz	pl	ksp	hb	acc	mat	lv	l
A17116	Coramba D	f.sst	12.9	28.6	0.4	3.9	3.4	19.6	30.2	0.9
A17085	Coramba C	v.c.sst	10.4	51.8	5.4	8.8	0.6	10.2	8.2	4.2
A32493	Coramba B	v.c.sst	10.6	35.1	3.9	0.0	0.2	30.0	19.8	0.5
A17130	Coramba A	v.f.cgl	4.5	7.0	0.0	0.0	1.8	29.8	52.7	4.2
A17140	Coramba A	v.f.cgl	7.5	9.7	0.0	0.0	1.7	25.7	50.3	5.1
A17143	Coramba A	v.c.sst	9.9	16.4	0.2	0.0	4.5	21.2	45.9	1.9
A32626	Brooklana	c.sst	13.0	39.6	6.0	0.0	0.4	24.5	15.9	0.8
A32607	Brooklana	m.sst	22.9	12.5	4.5	0.0	0.1	34.4	22.1	3.7
A32668	Moombil	m.sst	22.3	10.1	1.7	0.0	0.2	46.0	18.5	1.3

NOTES: CAT = catalogue numbers of the Department of Geology, University of New England, Australia. c = coarse; m = medium; f = fine. cgl = conglomerate; sst = sandstone. qz = quartz; pl = plagioclase ksp = alkali feldspar; hb = detrital hornblende; acc = detrital accessory minerals; mat = matrix and secondary minerals; lv = volcanic lithics; l = plutonic, sedimentary, metamorphic lithics.

abundance of greywacke: Moombil, Brooklana and Coramba beds. In each unit there is a wide range of grainsize from fine granule-conglomerate to argillite (Table 3.10). Detailed petrography and detrital modes have been published elsewhere (Korsch, 1978b, 1981a) and only a summary is given here (Table 3.10). The rocks have a common provenance, being derived predominantly from a continental margin volcanic arc consisting mainly of dacite with minor rhyolite and andesite. They are all quartz-poor to quartz-intermediate, with a spectrum from lithic to feldspathic types. Within the Coramba beds, Korsch (1978b) recognised four sandstone petrofacies based on QFL proportions and the occurrence of detrital hornblende. Stratigraphically upwards, the petrofacies are: A = volcanolithic, B = feldspathic, C = hornblende-feldspathic, D = hornblende-volcanolithic. The feldspathic sandstones from units B and C are probably reworked crystal tuffs. Greywackes from the Moombil beds are similar to petrofacies A, and those from the Brooklana beds are similar to petrofacies A and B.

3.8 METAMORPHISM OF THE COFFS HARBOUR SEQUENCE

The Coffs Harbour sequence has undergone regional metamorphism (M1) of prehnite-pumpellyite to lower greenschist facies (Korsch, 1978c). A typical metamorphic assemblage at lower grades is quartz - albite - epidote - chlorite - white mica - prehnite - pumpellyite. With increasing metamorphism, prehnite and pumpellyite disappear at approximately the same grade and the metamorphic assemblage is quartz - albite - epidote - chlorite - white mica. In lower-grade rocks (zone I; Korsch, 1978c) there is little evidence of deformation or recrystallisation, no distinct preferred orientation of new mineral phases and only limited albitisation of plagioclase and alteration of hornblende to chlorite. With increasing grade (zone II) a schistosity develops and the matrix is coarser-grained. In the southern part of the Coffs Harbour Block (Fig.3.14), M1 has been

Table 3.11: Rb-Sr whole-rock isotopic data of metasediments from the Coffs Harbour sequence, eastern Australia.

CAT	UNIT	LITHOLOGY	Rb	Sr	1/Sr	$^{87}Rb/^{86}Sr$ (p)	$^{87}Sr/^{86}Sr$ (p)
i. ISOCHRON 1:							
A17085	Coramba C	v.c.sst	119	711	.0014	.484 (0.9)	.70708 (.067)
A17116	Coramba D	f.sst	121	439	.0023	.798 (1.0)	.70839 (.079)
A17143	Coramba A	v.c.sst	127	313	.0032	1.175 (1.0)	.71014 (.053)
A17140	Coramba A	v.c.cgl	127	266	.0038	1.379 (1.1)	.71111 (.090)
A17130	Coramba A	v.f.cgl	163	250	.0040	1.886 (1.0)	.71327 (.076)
N29888	Coramba D	arg	169	222	.0045	2.210 (1.0)	.71494 (.062)
ii. ISOCHRON 2							
N29891	Coramba A	arg	159	233	.0043	1.977 (1.0)	.71506 (.063)
N29892	Coramba A	arg	167	194	.0052	2.491 (1.1)	.71674 (.088)
A32611	Brooklana	arg	190	96	.0104	5.702 (1.3)	.72779 (.050)
N29902	S.S.I.	arg	303	139	.0072	6.314 (0.9)	.72958 (.072)
iii. Greywackes from thermal biotite zone							
A32493	Coramba B	v.c.sst	172	408	.0024	1.223 (0.8)	.70998 (.056)
A32626	Brooklana	c.sst	89	554	.0018	.462 (1.1)	.70700 (.063)
A32607	Brooklana	m.sst	94	316	.0032	.859 (1.2)	.70870 (.061)
A32668	Moombil	m.sst	81	334	.0030	.698 (1.3)	.70809 (.071)

NOTES: Catalogue numbers beginning with N- are VUW, with A- are of Department of Geology, University of New England, Australia. c = coarse; m = medium; f = fine. cgl = conglomerate; sst = sandstone; arg = argillite. S.S.I. = South Solitary Island. Errors (p) are for the 68% confidence interval, expressed as a percentage.

overprinted by static thermal metamorphism (M2). This is characterised by growth of randomly-orientated biotite which overprints the preferred orientation of M1 white mica.

3.9 Rb-Sr GEOCHRONOLOGY

3.9.1 Analytical results:

Rb-Sr whole-rock isotopic data of metasediments from the Coffs Harbour sequence (Table 3.11) are plotted on isochron diagrams in Fig.3.15. Six samples (A17085, A17116, A17143, A17140, A17130, N29888), from the eastern coastal region (see Fig.3.14 for localities) yield ISOCHRON 1 which gives an age of 318 (8) Ma and intercept of .70483 (32) (Fig.3.15a). These samples are all from Coramba beds and three of the four petrofacies (A, C and D) are represented. There is no evidence for thermal overprinting of rocks from this region of the Coffs Harbour Block (Korsch, 1978c).

Four greywacke samples (A32626, A32493, A32607, A32668) from within the thermal-biotite zone (Fig.3.14) plot close to ISOCHRON 1 (Fig.3.15b). If these are combined with the six coastal samples, there is little difference in the regression : age = 315 (13) Ma; intercept = .70484; RMSWD = .355. However, four argillite samples (N29891, N29892, A32611, N29902) from the same region fall on a second, younger isochron (ISOCHRON 2) giving an age of 238 (5) Ma and intercept of .70836 (68) (Fig.3.15b). Petrographic and stratigraphic information suggests that the thermal biotite zone extends offshore to include South Solitary Island (Fig.3.14), hence N29902 is included. However, if that is incorrect and N29902 is left off ISOCHRON 2, the resultant regression is almost unchanged: age = 241 (3) Ma; intercept=.70827 (26); RMSWD = .102.

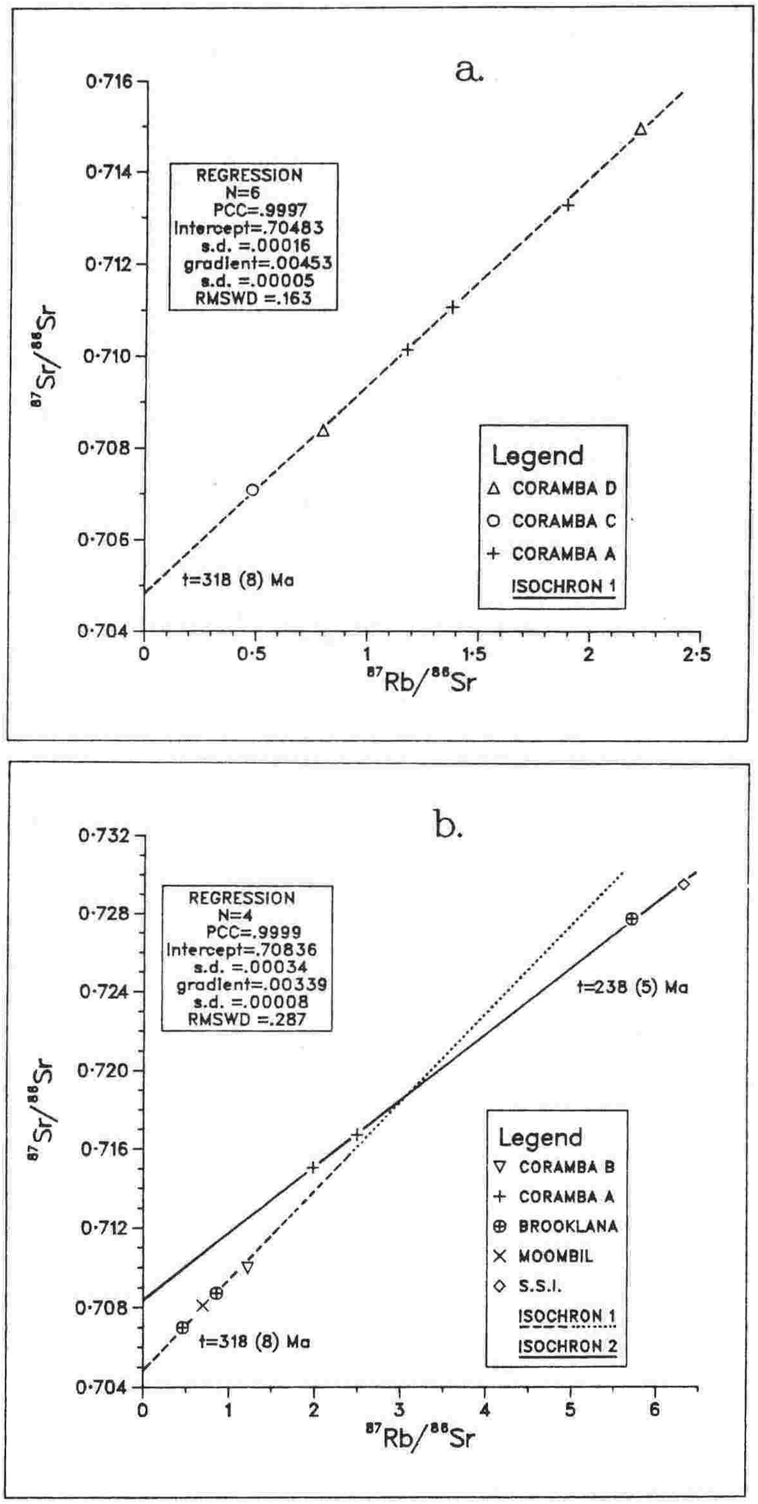

Fig.3.15: Rb-Sr whole-rock isochron plots of metasediments from the Coffs Harbour sequence.
a. ISOCHRON 1 for six metagreywackes
b. ISOCHRON 2 for four argillites from the thermal biotite zone - note different scale from a. Four greywackes from the thermal biotite zone plot close to ISOCHRON 1.
N = number of samples; PCC = Pearson correlation coefficient; s.d. = standard deviation; RMSWD = root mean square of weighted deviations. Error on age (brackets) is for the 95% confidence interval.

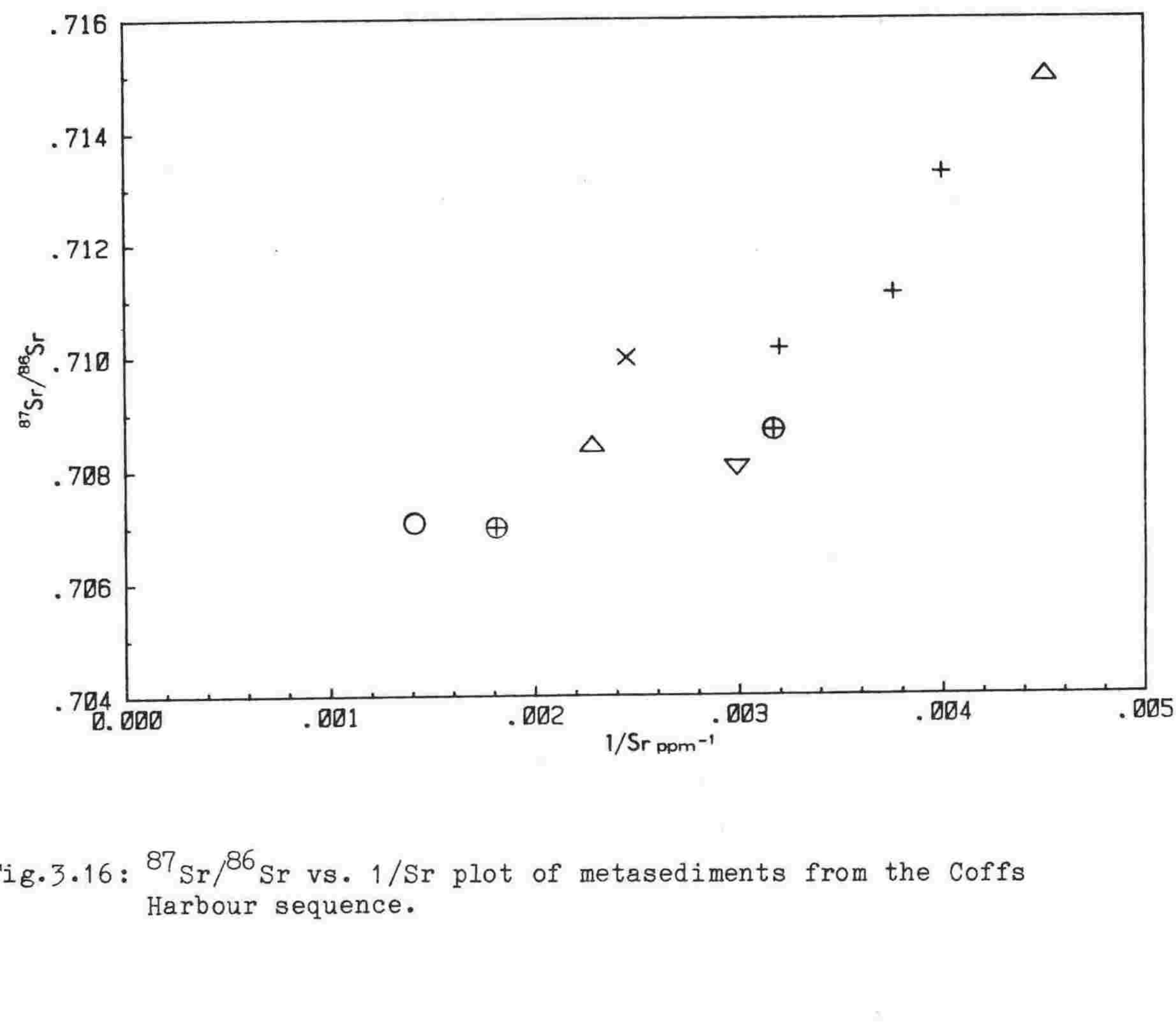

Fig.3.16: $^{87}Sr/^{86}Sr$ vs. 1/Sr plot of metasediments from the Coffs Harbour sequence.

3.9.2 Interpretation of ISOCHRON 1:

The linear array of a Rb-Sr whole-rock isochron may be produced in several ways including (i) binary mixing of detritus from isotopically different sources (ii) isotopic evolution of detritus from an isotopically uniform source and (iii) isotopic evolution after metamorphic re-equilibration. Each of these alternatives are now evaluated as possible explanations for ISOCHRON 1.

i. Binary mixing: The greywacke samples analysed contain up to 53% lithic fragments of various volcanic types (Table 3.11) which, though dominated by dacitic lithologies, testify to the diverse nature of the source region. In addition, they can be grouped into three petrofacies (Korsch, 1978b), each characterised by distinctive modal compositions (Table 3.10). Despite this, the six samples yield a well-defined isochron. It is difficult to postulate a suitable mixture of detrital materials from the proposed source region (calc-alkaline, continental margin volcanic arc (Korsch, 1978b)) to produce such a good correlation. To do so would require the mixing of only two Sr-bearing components, a situation unlikely for rocks from that tectonic setting. Thus, a binary mixing explanation for ISOCHRON 1 is not supported by the overall lithological characteristics of the rocks.

Faure (1977) showed that mixing of two components with differing Sr contents and isotopic ratios form a linear plot of $^{87}Sr/^{86}Sr$ vs. 1/Sr. When these variables are plotted for the Coffs Harbour samples (Fig.3.16), a linear relationship does emerge, but the correlation (PCC=.963) is inferior to that for the isochron (PCC=.9997). In rocks such as these where plagioclase is the dominant Sr-bearing phase, the range in Rb/Sr ratio will be largely controlled by the plagioclase content. Thus, the apparently significant correlation between $^{87}Sr/^{86}Sr$ and 1/Sr (Fig.3.16) for the six greywacke samples defining ISOCHRON 1 is a result of the mineralogical composition of the rocks and is not necessarily indicative of mixing.

ii. Derivation of detritus from an isotopically uniform source: If the Coffs Harbour volcanogenic sediments were derived from a volcanic source producing magma of uniform isotopic composition then the whole-rock age would correspond to the timing of the volcanism. This possibility is supported by the fact that the 318 Ma age (ISOCHRON 1) is consistent with the assumed time of arc volcanism in the Coffs Harbour region (Evernden and Richards, 1962; Roberts and Oversby, 1974). However, arc volcanics elsewhere do not usually have uniform isotopic compositions; lavas of Taupo Volcanic Zone, for example, range in $^{87}Sr/^{86}Sr$ from .704 to .706 (Ewart and Stipp, 1968; Chapter 4, this study). Even small variation in the Sr isotopic composition of the source volcanism should have a noticeable effect on the scatter about any resultant isochron since the range in Rb/Sr is relatively small (Fig.3.15a). Arguments against a binary mixing interpretation apply here also. The highly variable nature of the lithic component of the rocks and the variation in detrital mineral modes do not indicate a simple, uniform source with a uniform Sr isotopic composition.

iii. Regional low-grade metamorphism: The six samples defining ISOCHRON 1 include a wide spectrum of sedimentary lithologies (Table 3.12) yet, despite the overall coarse grainsize, they show a surprisingly strong correlation between Rb/Sr and $^{87}Sr/^{86}Sr$ (PCC=.9997). It has been shown above that this linear trend was probably not produced by mixing of detritus from isotopically different sources nor was it a result of evolution of originally isotopically uniform detritus. The most likely alternative explanation for ISOCHRON 1 is that it results from isotopic equilibration during regional low-grade metamorphism.

Equilibration of Sr isotopes in sedimentary rocks probably begins during the earliest stages of deposition and burial metamorphism. At this time, modification of matrix clays and detrital feldspars allow some interaction between bulk-rock Sr and that contained in pore-fluids (Dasch, 1969; Perry and Turekian, 1974; Chaudhuri, 1976). Gebauer and Grünenfelder

(1974) described Paleozoic sediments of Montagne Noire and showed that the more deformed rocks yielded ages corresponding to the known age of folding and anchimetamorphism. Clauer and Kröner (1979) reported Sr isotopic resetting in pelitic sediments of the Damara Group (Namibia) under zeolite to prehnite-pumpellyite metamorphic conditions. These, and most other similar studies concentrate on matrix-dominated pelitic sediments in which the porportion of Sr-bearing detrital minerals is low. However, Coffs Harbour sediments include coarse-grained volcanogenic greywackes in which detrital minerals and lithic fragments make up more than 50% of the mode (Table 3.11). Much of this detrital material is only partially altered and plagioclase is incompletely albitised and saussuritised. Priem et al. (1978) discussed Sr isotopic equilibration of broadly similar sediments (Megacryst Tuff Formation, Portugal), and suggested that Sr isotopic exchange in the rocks took place during disordering of feldspars under low greenschist facies metamorphic conditions. Farquarson and Richards (1975) suggested a similar mechanism to explain equilibration of Mount Isa tuff beds, Queensland, Austalia. They noted that the Rb-Sr age of the tuffs was 300 Ma younger than expected and the initial ratio was high. They interpreted this to indicate that Sr mobility and accompanying isotopic equilibration began during deposition, and continued during deep burial until the ambient temperature declined to a point where diffusion and structural re-ordering of feldspar ceased. Priem et al. (1978) pointed out that acid pyroclastic volcanics are often much less resistent to Sr re-equilibration than plutonic and high grade metamorphic rocks, and evidence of resetting in such rocks can be seen even where metamorphic effects are absent (Fairbairn et al., 1966; Lanphere, 1968).

The above studies indicate that metamorphic equilibration of coarse-grained rocks such as those of the Coffs Harbour sequence can occur under relatively low-grade conditions. Therefore, the preferred interpretation for ISOCHRON 1 is that it dates the earliest metamorphism of the Coffs

Harbour Block. Homogenisation of Sr isotopes must have occurred through progressive devitrification of volcanic glass in lithic fragments and changes in the structural state of detrital feldspar during cooling.

3.9.3 Interpretation of ISOCHRON 2:

The 238 Ma whole-rock age (ISOCHRON 2; Fig.3.15b) for argillites from the thermal biotite zone of the Coffs Harbour Block (Fig.3.14) is best interpreted as the time of thermal metamorphism associated with granite plutonism. Apparently, this metamorphism has only affected the Sr-isotopic systems of matrix-dominated argillites within the sequence because four biotite-bearing greywackes plot away from that array, falling close to ISOCHRON 1 (Fig.3.15b).

In a Rb-Sr geochronolical study of pelitic sediments from Namibia, Clauer and Kröner (1979) showed that Sr-isotopic equilibration occurred during two regional low-grade metamorphic events. However, the second equilibration was only evident in layers where the bulk-rock chemistry was suitable for the metamorphic crystallisation of stilpnomelane. In the Coffs Harbour Sequence, the growth of biotite is greatest in fine-grained rocks with high matrix contents. Since detrital clasts are uncommon in these rocks, it is likely that most of the Sr is contained in secondary minerals which exchange readily with Sr in pore fluids during metamorphism. In coarser-grained lithologies on the other hand, Sr would be contained largely in feldspar grains or lithic clasts and would be less susceptible to exchange. The absence of even partial equilibration of Sr isotopes in the biotite zone greywackes is surprising but may be the result of sampling bias (all four samples are coarse-sand grade and therefore likely to show the least evidence for isotopic exchange).

3.10 AGE CONSTRAINTS WITHIN THE COFFS HARBOUR BLOCK

Prior to 1970, the preferred age for the Coffs Harbour sequence was Silurian (e.g. Voisey, 1934; McElroy, 1962). Korsch (1971), however, suggested a Late Paleozoic age based on tentative correlation with rocks 180km to the south. From a comparative study of detrital modes of greywackes from the New England Orogen, Korsch (1984) concluded that the Coffs Harbour sequence correlated well with the Merlewood Formation of the Tamworth belt which, using conodonts, Mory (1981) showed to be predominantly middle to late Visean in age (corresponding to an age in range 320 to 352 Ma). The Merlwood Formation contains large amounts of tuffaceous material and at least one thick andesite flow (White, 1964). Several K-Ar ages on these rocks have been published but most are not in accord with known fossil ages and the samples have probably suffered loss of argon. Two K-Ar ages which are in agreement with the stratigraphic ages are 328 Ma (Evernden and Richards, 1962) and 326 (9) Ma (Roberts and Oversby, 1974).

Granitoids of the New England Batholith have been divided into several plutonic suites based on petrography, geochemistry and regional distribution (Korsch, 1977; Shaw and Flood, 1981; Hensel et al., 1982). Three distinct suites occur within the Coffs Harbour Block and currently accepted ages for them (based on plutons from elsewhere in the New England Orogen) are (1) Hillgrove plutonic suite - Rb-Sr whole-rock age = 289 (25) Ma (Shaw and Flood, 1977); Rb-Sr mineral age = 312 (10) Ma (Hensel et al., 1982) (2) New England plutonic supersuite - Rb-Sr mineral age = 260 (8) Ma (Hensel et al., 1982) (3) Stanthorpe plutonic suite - K-Ar biotite ages = 227 to 230 Ma (cited by Korsch, 1977); Rb-Sr mineral and whole-rock ages = 232 to 235 Ma (Hensel et al., 1982). Only one pluton from within the Coffs Harbour Block has been dated. The Dundurrabin Granodiorite (Hillgrove Plutonic Suite) intrudes the southern part of the Block and has a Rb-Sr whole-rock age of 308 (12) Ma (H.D.Hensel, pers. comm., 1982). Hence, the Coffs Harbour sequence, or at least the southern part of it, must be older than 308 (12) Ma.

The Coffs Harbour sequence is unconformably overlain by sediments of the Moreton basin in which the basal unit is the Nymboida Coal Measures containing an Anisian-Ladinian megaflora (Retallack et al., 1977). These give ages within the range 231 to 243 Ma (Harland et al., 1982).

The concordant relationship between the internal foliation of the Dundurrabin Granodiorite and the regional orientation of slaty cleavage in Coffs Harbour Block suggests that the development of cleavage was closely synchronous with intrusion of the pluton (Korsch, 1981b). The low-grade regional metamorphism (M1), dated here at 318 (8) Ma, agrees with the age of Dundurrabin Granodiorite (308 (12) Ma). In the Nambucca Slate Belt immediately to the south of the Bellinger Fault, (Fig.3.14), Leitch and McDougall (1979) inferred an age of orogenesis of 250-255 Ma, based on K-Ar ages of siltstones containing early Permian fossils. Deformation and metamorphism in the Nambucca slate belt appears to be absent in the adjacent Coffs Harbour Block which was therefore metamorphosed by M1 prior to deposition of those rocks.

Korsch (1978c) showed that the regional-scale metamorphism which produced the large zone of thermal biotite was post-tectonic and related to the intrusion of granitic batholiths. The age of the Stanthorpe plutonic suite (232-235 Ma, Hensel et al., 1982) agrees with that of argillite samples re-equilibrated at 238 (5) Ma. In the Nambucca Slate Belt, Leitch and McDougall (1979) reported K-Ar ages from the Stanthorpe plutonic suite in the range 226-231 Ma. However, none of the 17 K-Ar ages on siltstones reported from the slate belt were younger than 250 (4) Ma and hence the event which caused regional-scale thermal metamorphism of rocks in the Coffs Harbour Block did not accompany intrusion of the Stanthorpe plutons in the Nambucca Slate Belt.

3.11 SUMMARY AND CONCLUSIONS

Results of Rb-Sr dating of sediments from the Coffs Harbour sequence, eastern Australia have shown that low-grade metamorphism (prehnite-pumpellyite to lowest greenschist facies) can isotopically equilibrate sediments spanning grainsizes from argillite to fine-granule conglomerate. This re-setting occurred at 318 (8) Ma. A subsequent static metamorphic event at 238 (5) Ma, which produced thermal biotite on a regional scale, re-equilibrated only the finest-grained sediments and coarse-grained sediments remain unaffected. Comparison of metamorphic ages presented here from the Coffs Harbour Block, with K-Ar ages from the adjacent Nambucca Slate Belt (Leitch and McDougall, 1979) indicate that the New England Orogen has had a very complex tectonic history.

The study to some extent justifies the application of Rb-Sr whole-rock geochronology to Torlesse and Waipapa terrane metasediments. Hence the ages obtained for them reflect real geological events, although interpretation of their meaning is still equivocal.

****

CHAPTER 4: PETROGRAPHY, CHEMISTRY AND ISOTOPE COMPOSITION OF LAVAS FROM TONGARIRO VOLCANIC CENTRE, AND POTENTIAL PARENTAL MAGMAS

****

PART 1 reviews and discusses the petrography, bulk-rock chemistry and isotopic composition of lavas from Ruapehu and the nearby vents of Ohakune, Hauhungatahi, Pukeonake, Ngauruhoe, Pukekaikiore and Red Crater (Tongariro). This provides a framework within which to discuss the origin of meta-igneous xenoliths (Chapter 5.7) and also the data base to assess the viability of different petrogenetic models (Chapter 6).

PART 2 describes the petrology of all known basaltic lavas from Taupo Volcanic Zone, in order to find suitable parental magmas for petrogenetic modelling of TVC lavas.

PART 1: LAVAS OF RUAPEHU AND NEARBY VENTS

4.1 PREVIOUS WORK

Andesites of the TVC were first described petrographically by Clark (1960) who catagorised them in terms of phenocryst composition. Subsequently, Cole (1978) published a more definitive study, discussing bulk chemistry and probable petrogenesis. Cashman (1979) studied andesites of the Kakaramea-Tihia and Maungakatote massifs. She later collaborated with Cole and Rankin (Cole et al., 1983) to discuss rare-earth element constraints on crustal contamination models. Recent petrochemical investigations of lavas from Ruapehu and nearby vents have been made by W.R.Hackett. His detailed stratigraphy of Mount Ruapehu lavas provides a framework to chemically classify the lavas and to test petrogenetic models using Sr isotopic composition as an important constraint.

4.2 TECTONIC SETTING AND ERUPTIVE HISTORY

Tongariro Volcanic Centre is situated at the southern end of Taupo Volcanic Zone (Fig.1.3) and comprises four composite andesitic volcanoes: Ruapehu, Tongariro (including Ngauruhoe), Pihanga and Kakaramea-Tihia (Fig.3.1). Cole (1978) identified two main structural trends (1) an old NW-trending lineament defined by vents of Pihanga, Kakaramea-Tihia and older Tongariro (Mathews, 1967) and (2) a NNE-trending lineament which parallels the present-day regional trend of the Taupo Fault Belt (Grindley, 1960) and which is defined by the younger multiple vents of Tongariro and Ruapehu. This system of high-angle normal faults extends from the TVC to the Bay of Plenty (Fig.1.3) and is the main structural control on recent vent location.

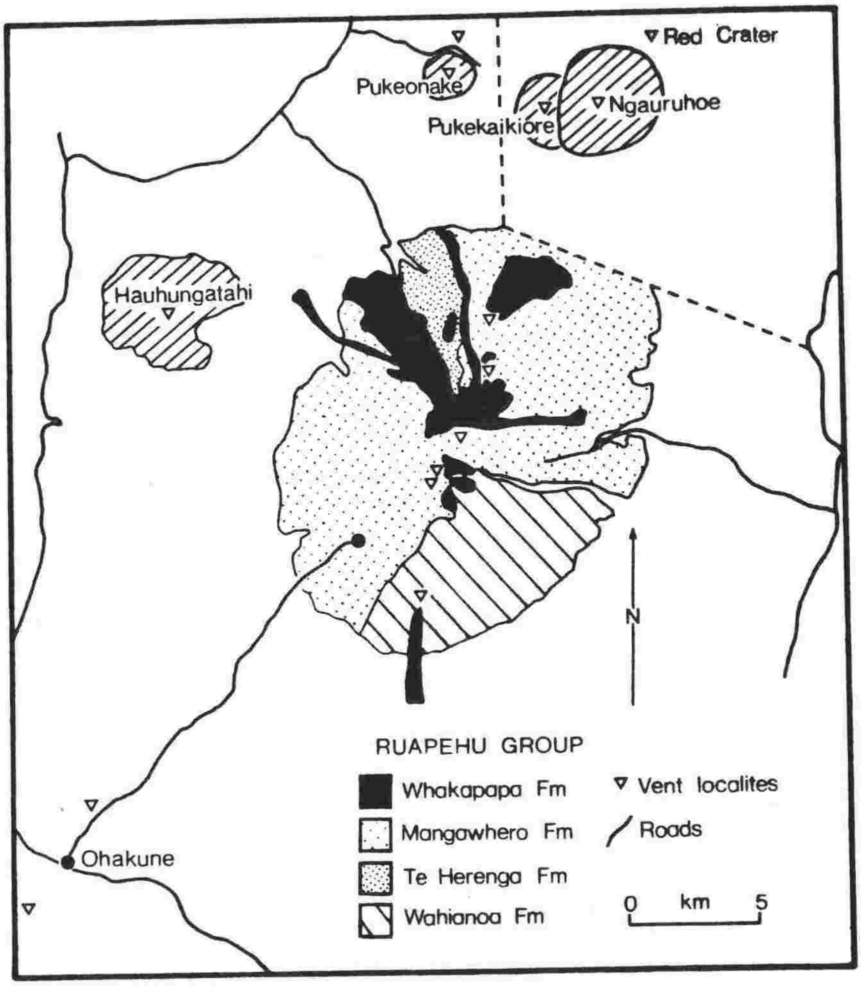

Fig.4.1: Distribution of Ruapehu Group Formations and location of nearby vents in the southern part of the TVC (used by permission, W.R.Hackett, 1985).

Mount Ruapehu is a stratovolcano which has produced voluminous lava, lahar and tephra over a period of at least 250 ka. Hackett (pers. comm., 1984) has proposed four new formation names for the Ruapehu Group which are (from oldest to youngest) Te Herenga, Wahianoa, Mangawhero and Whakapapa (Fig.4.1). The Te Herenga Formation, which forms the earliest Ruapehu cone, is now only poorly exposed on the mountain. The base rests on Tertiary sediments and a glacial unconformity marks a time break between this and younger formations. Stipp (1968) obtained a K-Ar age of 230 ka for a lava flow on Te Herenga Ridge and this probably dates the upper part of the Formation. Wahianoa Formation lavas are exposed mainly in the SE quadrant of Ruapehu (Fig.4.1). These are nowhere seen overlying those of the Te Herenga Formation and distinction is based on the greater degree of dissection and on petrographic criteria. No ages are available but the Wahianoa Formation is certainly older than the Mangawhero Formation which unconformably overlies it. Two K-Ar ages (24 ka and 36 ka) have been determined from the middle of the Mangawhero Formation (Stipp, 1968). These ages, the low degree of dissection and the presence of numerous intraformational unconformities, suggest that volcanism occurred between 15 ka and 50 ka ago. Young (post-glacial) lava flows and pyroclastics of the Whakapapa Formation were erupted from five discrete vents and are each given Member status by Hackett. These are Iwikau, Tama, Crater Lake, Rangataua and Pinnacle Ridge. Most Whakapapa Formation lavas are less than 10ka and all unconformably overlie deposits of older Formations.

Vents close to the Ruapehu massif include Red Crater, Pukekaikiore, Ngauruhoe, Pukeonake, Hauhungatahi and Ohakune (Fig.4.1). Red Crater lies within a small cone about 3km NNE of Ngauruhoe. Dark red and black basaltic scoria overlies old Tongariro lavas and the cone is intruded by radial dykes (Topping, 1973, 1974). The vent has remained active with ash eruptions up to 1926 (Thomson, 1926). Clasts of Taupo pumice occur in older

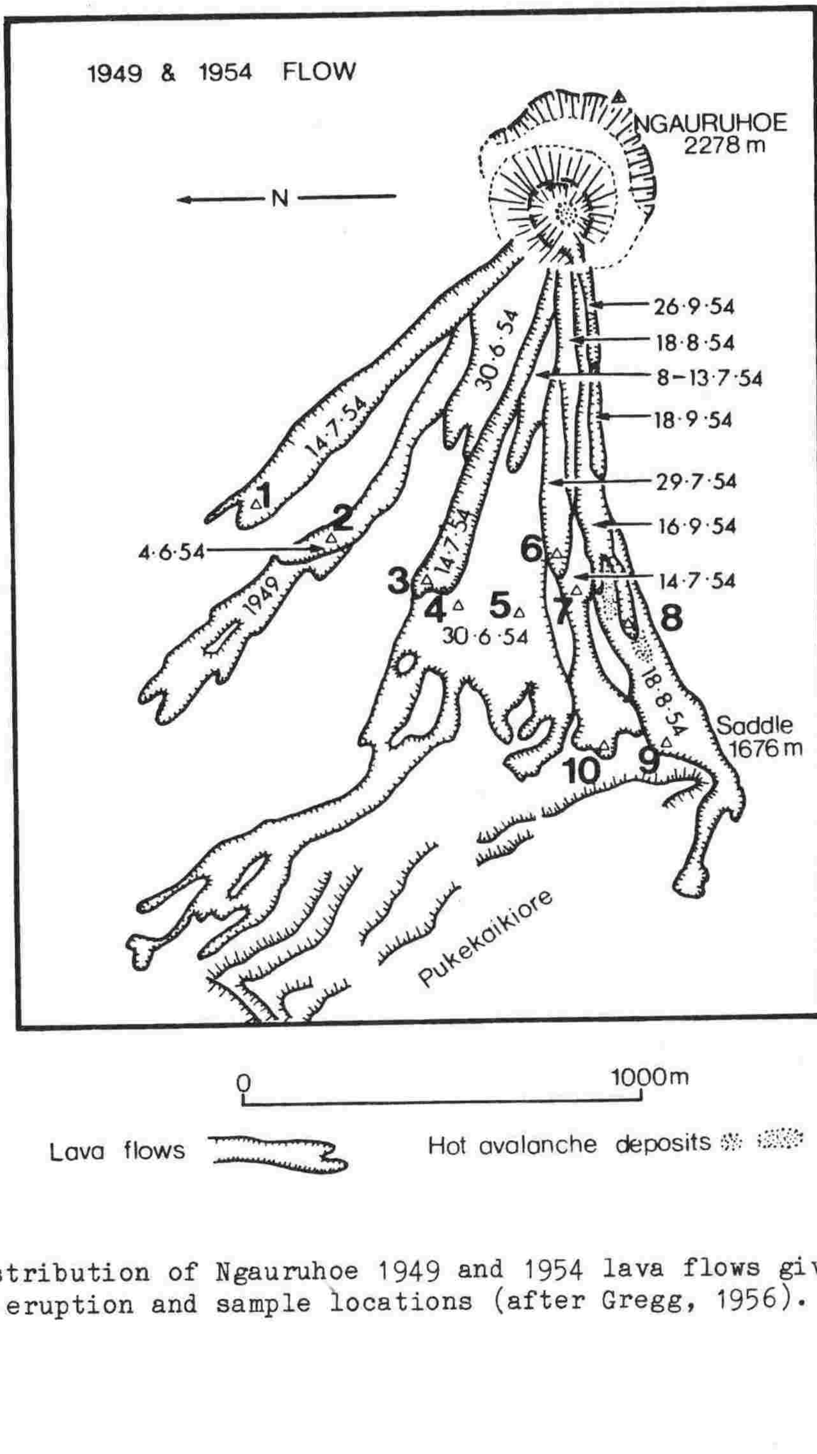

Fig.4.2: Distribution of Ngauruhoe 1949 and 1954 lava flows giving dates of eruption and sample locations (after Gregg, 1956).

Tongariro lavas, but not in the younger basaltic flows which are therefore regarded as younger than 1819 years BP (Topping, 1974). Pukekaikiore, 2km west of Ngauruhoe, is an old eroded outlier of the main Tongariro massif and is made up mainly of labradorite andesite flows (Cole, 1978). Several younger flows of olivine andesite from a vent near the summit overlie Rerewhakaaitu ash (14.7ka) and were probably erupted immediately after that tephra (Topping, 1974). Ngauruhoe is a composite cone which last erupted lava between June and September 1954 in thirteen separate flows of olivine andesite (Fig.4.2). The total volume of erupted material was about 5.8 x 10^6 m^3 (Gregg, 1956). Pukeonake scoria scoria cone is located 5.6 km WNW of Ngauruhoe and is overlain by Oruanui tephra (19.8 ka). The absence of a conspicuous paleosol suggests only a short time gap between formation the cone and deposition of the tephra (Napp, 1983). The Pukeonake Andesite Formation (Topping, 1973, 1974) consists of lava flows and pyroclastics distributed over a wide area and includes lava flows exposed on Highway 54 and at Mahuia Rapids. Hauhungatahi is a low eroded cone about 12km NW of Mount Ruapehu. It rests on Miocene marine siltstones and is overlain by Oruanui tephra and weathered andesitic ash of the Tongariro Subgroup (Topping, 1973, 1974). This suggests a minimum age of 19.8 ka for the formation, but the eroded morphology suggests that the cone is one of the oldest volcanic features in the region. / The southernmost vents of the TVC occur near Ohakune, 19km SW of the summit of Mount Ruapehu. Two explosion craters, 4.5km SW of Ohakune, are occupied by the Rangatau Lakes and at least five more craters occur 1km to the NW (Cole, 1978).

4.3 PETROGRAPHY:

The primary classification of Clark (1960) for TVZ andesites is used here with modifications to include a wider spectrum of lava types (i.e. basalt and dacite). Categories are defined on normalised volatile-free SiO_2 content:

< 53% SiO_2 = basalt,
53 to 57% SiO_2 = basic andesite,
57 to 63% SiO_2 = acid andesite,
> 63% SiO_2 = dacite.

and prefixes denote phenocryst content:

olivine > .5% = olivine-,
pyroxene > plagioclase = pyroxene-,
plagioclase > 2 x pyroxene = plagioclase-,
plagioclase < 2 x pyroxene = plagioclase-pyroxene-.

This scheme has general application in the field but is superceded in this study by a chemical classification scheme (section 4.5).

4.3.1 General features:

Lavas of Ruapehu and nearby vents are typically porphyritic with phenocrysts of plagioclase, orthopyroxene, clinopyroxene and sometimes olivine. Hornblende is absent except as minute traces in Wahianoa Formation acid andesite 16722. Groundmass consists mainly of microlites of plagioclase, pyroxene and Fe-Ti oxides and small amounts of acid-residuum. Few lavas are aphyric and none contain more than 10% glass. Glomerocrysts and mafic nodules, common in the more strongly porphyritic lavas (e.g.14913, 16713), are hypidiomorphic-granular aggregates ranging in size from a few mm to 8cm (Plate 4.1). They have feldspathic, websteritic or gabbroic compositions. Xenoliths of metasedimentary or volcanic material occur in many lavas (Plate 4.2)).

Plate 4.1: BEI (back-scattered electron image) photograph of Mangawhero Formation lava (host to xenolith 17434) showing pyroxene glomerocryst. Cluster consists of 10-15 pyroxene crystals (light grey), minor plagioclase (grey) and spinel (white). Scale bar = 1mm; field of view = 1.9mm.

Plate 4.2: BEI photograph of crustal xenoliths in Ngauruhoe 1954 lava. Quartz-rich xenolith (bottom) is surrounded by granitic melt; feldspathic xenolith (upper RHS) has plagioclase growth around its rim.
Scale bar = 1mm; field of view 1.9mm.

Plate 4.3: BEI photograph of olivine phenocrysts in Ngauruhoe 1954 lava. Crystals have forsteritic cores (darker) zoned to more Fe-rich outer margins. Hypersthene (dark grey) forms an enclosing reaction rim. Fine-grained mesostasis consists of plagioclase, pyroxene, spinel and dacitic glass.
Scale bar = .1mm; field of view = 1.2mm.

Plate 4.4: BEI photograph of plagioclase phenocryst in Ngauruhoe 1954 lava. The crystal is complexly zoned and has included pyroxene (white). The core (very dark grey) is Na-rich.
Scale bar = .1mm; field of view = .9mm.

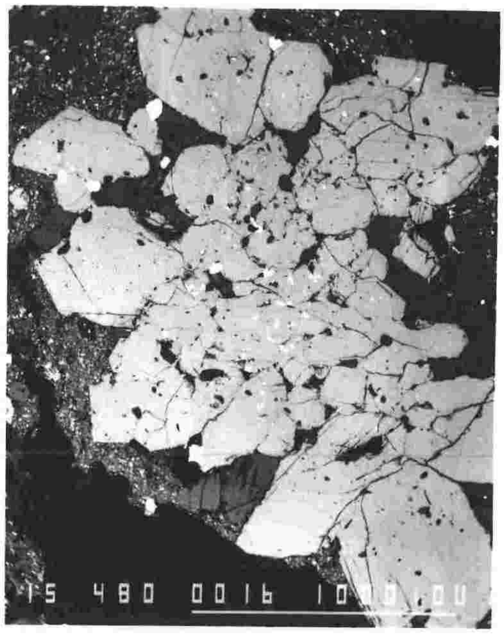

Plate 4-1

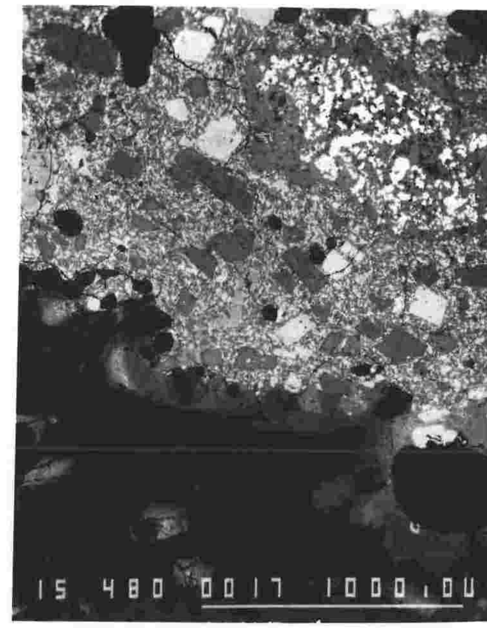

Plate 4-2

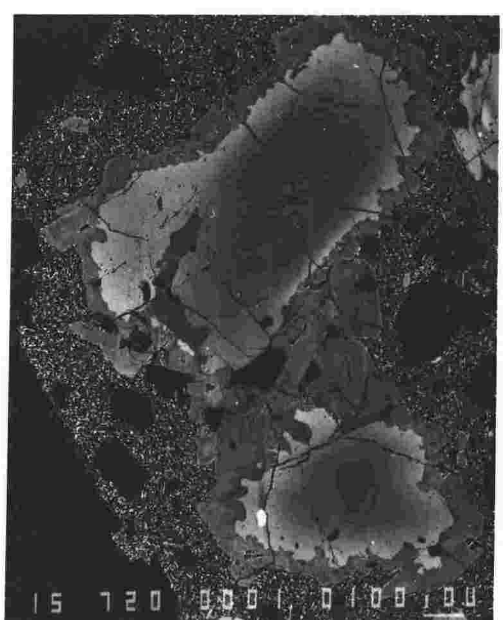

Plate 4-3

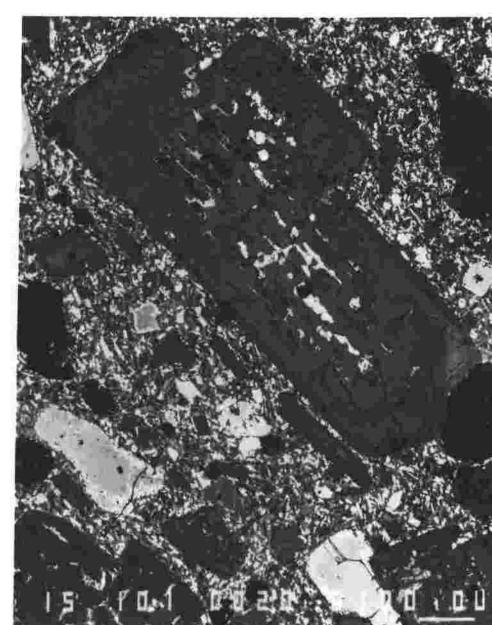

Plate 4-4

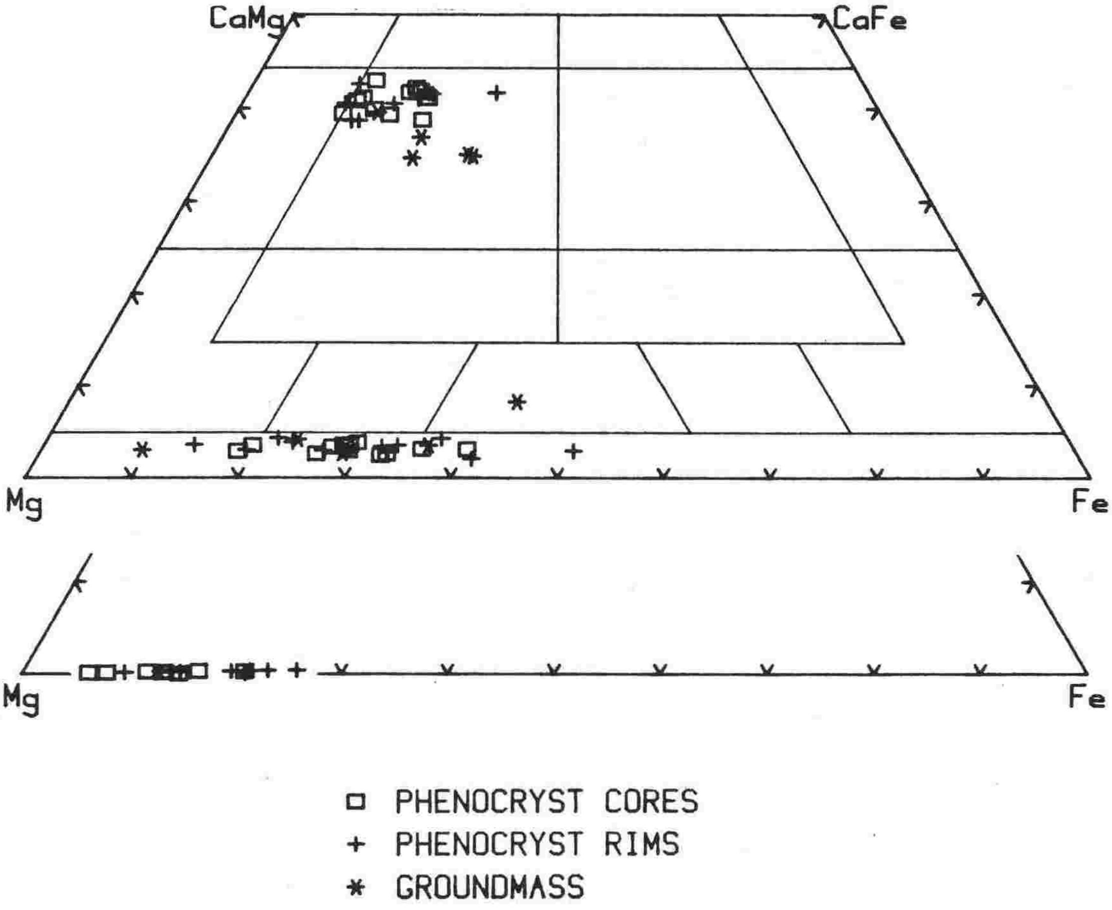

Fig.4.3: Compositions of mafic phenocrysts in selected lavas, plotted in terms of Ca, Mg and Fe; pyroxenes in upper quadrilateral, olivine in lower. Full analyses are given in Appendix 3. Fields as in Deer, Howie and Zussman (1978. p.3).

4.3.2 Mineralogy:

Olivine occurs in lavas spanning the entire compositional range from basalt (14855) to dacite (14829) but is present in amounts greater than 1% only in some basalts and basic andesites. It occurs as (1) primary phenocrysts or (2) as forsteritic xenocrysts in pyroxene-rich lavas which also contain glomerocrysts and/or mafic nodules (e.g. 16721). These are often mantled by orthopyroxene (Plate 4.3), or have resorbed cores containing chrome spinel inclusions (e.g.14871). Compositions range from Fo_{94} (resorbed phenocryst cores) to Fo_{74} (phenocryst rim) (Appendix 3; Fig.4.3), but most grains are normally zoned from Fo_{88} to Fo_{78} (14855). Olivine does not occur in the groundmass of any lava described.

Clinopyroxene is a phenocryst mineral in all lavas and decreases in proportion to orthopyroxene with increasing bulk-rock silica content. Most phenocrysts are normally zoned with rims similar in composition to groundmass microlites. However, in some lavas (e.g.14871), reverse zoning occurs and rims have overgrowths of orthopyroxene. Compositions show a restricted range from $Ca_{43}Mg_{47}Fe_{10}$ (11965) to $Ca_{34}Mg_{41}Fe_{25}$ (14867) (Fig.4.3). Non-quadrilateral components such as Ti, Al, Fe^{3+} and Na comprise less than 5% of total cations (see Appendix 3 for full EPMA analyses). In more-siliceous lavas, orthopyroxene gradually replaces olivine as the major Mg-rich ferromagnesian phenocryst. Grains are typically fresh, sub- to euhedral and normally zoned with compositions ranging from $Ca_3Mg_{79}Fe_{18}$ (14798) to $Ca_3Mg_{45}Fe_{52}$ (17887) (Fig.4.3).

Plagioclase phenocrysts are abundant in most lavas, are rarely subordinate to pyroxene and are absent only in olivine andesites from Ohakune, Pukekaikiore and Hauhungatahi. Compositions range from An_{89} (14855) to An_{40} (17871) (Appendix 3; Fig.4.4), in the labradorite-bytownite range. Most phenocrysts are oscillatorily zoned with an overall trend from calcic core to sodic rim (Plate 4.4). The latter are usually compositionally similar to groundmass microlites. Some crystals contain

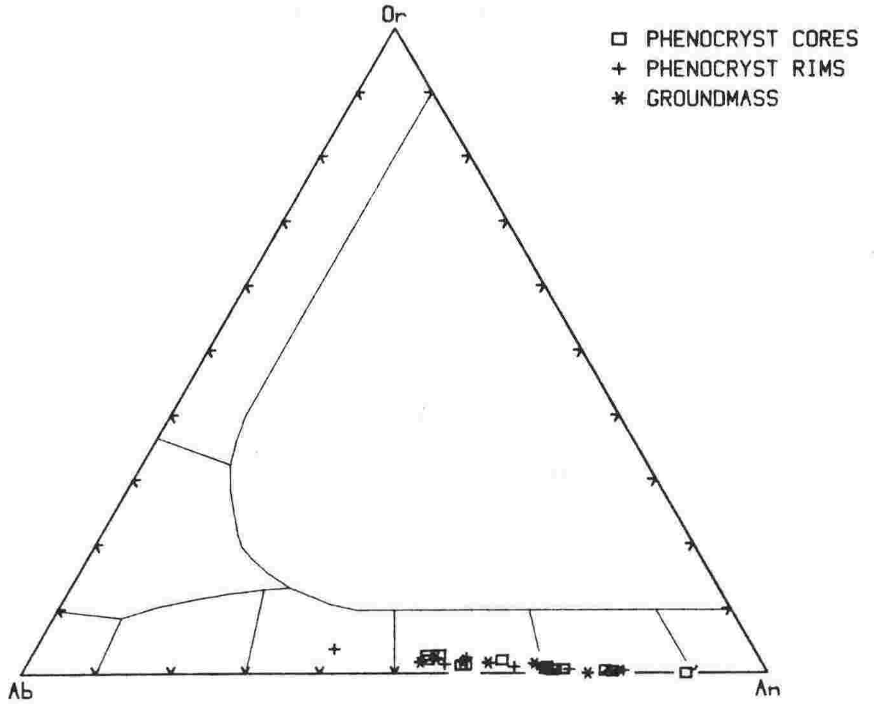

Fig.4.4: Compositions of plagioclase phenocrysts in selected lavas, plotted in terms of K, Na and Ca (Or, Ab and An). Full analyses are given in Appendix 3. Fields as in Deer, Howie and Zussman (1963, p.2).

Table 4.1: Modal composition of selected TVC lavas.

LOC	TH	WAH	WAH	WAH	WAH	WAH	WAH
VUW	14737	14925	14909	14867	14913	16721	16722
ol	-	1.9	-	-	-	.3	-
cpx	4.8	4.5	4.2	.2	.3	7.8	5.5
opx	5.9	7.7	1.7	2.1	1.7	6.6	4.1
pl	28.7	20.2	9.4	10.8	32.2	14.5	20.4
op	1.1	.1	-	.6	-	.1	1.4
phen	40.6	34.6	15.3	13.7	34.2	29.3	32.0
g/m	59.4	65.3	84.7	86.3	65.8	70.7	68.0
xen	-	.1	-	-	-	tr	tr

inclusions of glass, pyroxene, titanomagnetite or apatite and others have resorbed cores and Ca-rich rims. These and other reverse-zoned minerals exhibit petrographic features commonly associated with magma mixing (Eichelberger, 1975; Gill, 1981, p.287).

Oxide minerals occur as inclusions in phenocrysts, as microphenocrysts or as groundmass micolites. Chrome spinel forms inclusions in forsteritic olivine phenocrysts and rarely in associated magnesian clinopyroxenes. Compositions are poor in Ti and Fe and rich in Cr, Mg and Al. Discrete groundmass crystals are sometimes strongly zoned, with Fe-rich and Cr-poor outer mantles. Titanomagnetite is ubiquitous either as inclusions in pyroxene and plagioclase or as microphenocrysts. TiO_2 contents typically range from 6% to 20%. Ilmenite occurs sporadically and is rarely associated with titanomagnetite.

Apatite is an accessory mineral in acid andesites and dacites and occurs as stubby microphenocrysts (.1 to .3mm), inclusions in orthopyroxene and plagioclase, and in the groundmass. Alkali feldspar occurs only as rare microlites in hyalopilitic groundmasses. Tridymite is absent, though quartz-rich xenoliths and xenocrysts frequently occur (see Chapter 5.3).

4.3.3 Detailed description:

Mineral modes of selected lavas are given in Table 4.1.

Te Herenga Formation lavas are mainly plagioclase- and plagioclase-pyroxene andesites containing frequent pyroxene glomerocrysts. Olivine is rare. Wahianoa Formation lavas are similar to these but overall there is greater compositional diversity demonstrated by variable plagioclase:pyroxene and clinopyroxene:orthopyroxene ratios. Resorbed and mantled phenocrysts (e.g.16713), plagioclase-rich glomerocrysts (e.g.14900, 14913) and pyroxene-rich glomerocrysts (e.g.16713) occur in 85% of lavas examined (W.R.Hackett, pers. comm., 1984). Mangawhero Formation lavas range from basalt to dacite and most are similar to other Ruapehu lavas (Table 4.1). However, some (e.g.14883) contain a high proportion of xenoliths and

Table 4.1 cont:

LOC	MANG	MANG	MANG	MANG	MANG	MANG	MANG	MANG	MANG
VUW	14855	14859	14844	14889	14813	14811	14883	14882	14871
ol	7.0	3.8	.1	-	-	-	.6	.1	.5
cpx	7.3	4.0	6.1	.4	3.1	11.0	11.9	8.9	9.0
opx	2.1	2.7	7.6	1.5	5.9	7.8	7.8	6.9	10.5
pl	10.3	16.6	24.3	12.1	21.2	11.1	13.7	10.0	5.9
op	.2	-	.9	.7	.7	.2	-	-	-
phen	26.9	27.4	39.1	14.7	30.9	30.1	34.0	25.9	25.9
g/m	73.1	72.6	70.9	85.3	69.1	69.9	66.0	74.1	74.1
xen	-	.3	.1	-	-	-	-	-	-

LOC	WHAK	WHAK	WHAK	R-C	PUKE	PUK	N54	HAU	OH
VUW	14782	14828	17886	11965	24471	14848	29250	14816	14795
phen.	39.7	6.9	33.1	23.5	16.5	26.1	34.0	72.0#	9.6
ol	-	-	-	4.9	1.9	1.7	.2	1.0	.7
cpx	4.9	.4	1.8	7.2	9.8	9.4	2.6	14.3	7.6
opx	9.5	.3	5.8	.8	1.4	7.4	6.0	5.2	1.3
pl	24.5	6.2	25.0	10.6	.4	7.5	22.6	41.4	-
op	.8	-	.5	-	.1	-	-	.1	.7
g/m	60.1	93.1	66.1	76.5	83.5	73.9	66.0	28.0	90.4
xen.	tr	-	.8	-	.1	tr	2.6	-	tr

NOTES: TH = Te Herenga Formation; WAH = Wahianoa Formation;
MANG = Mangawhero Formation; WHAK = Whakapapa Formation;
RC = Red Crater; PUKE = Pukekaikiore; PUK = Pukeonake;
N54 = Ngauruhoe 1954; HAU = Hauhungatahi; OH = Ohakune.
ol = olivine; cpx = clinopyroxene; opx =orthopyroxene;
pl = plagioclase; op = opaques; phen = total phenocrysts;
g/m = groundmass; xen = xenoliths; tr = trace amounts.
microcrystalline with gradation to groundmass.

xenocrysts and others, (14871, 14879, 14880) contain abundant reversed-zoned phenocrysts indicative of magma mixing. Most Whakapapa Formation lavas are plagioclase-pyroxene acid andesites and dacites. Glomerocrysts and xenoliths are common in these and olivine is rare.

Red Crater basalt (11965) is petrographically similar to Ruapehu basalt (14855) having a high modal phenocryst content (23.5%). Olivine is present and plagioclase xenocrysts and pyroxene glomerocrysts with reaction rims are common. Groundmass is a black, intersertal texture of plagioclase, pyroxene and Fe-Ti oxide microlites in dacitic glass. Ngauruhoe 1954 andesite (29250) is a typical plagioclase-pyroxene lava containing abundant quartzose and vitrified xenoliths (Steiner, 1958). Olivine phenocrysts always have a reaction rim of hypersthene (Plate 4.3).

Pukeonake andesite has some features in common with the Mangawhero Formation lavas 14871, 14879, 14880, and may be coeval with them. Large forsteritic olivine crystals and dunite nodules occur with chrome spinel inclusions and hypersthene coronas. Clinopyroxene phenocrysts and glomerocrysts commonly have thin Mg-rich mantles. Embayed grains of hypersthene have spongey bronzite jackets and normally zoned microphenocrysts of bronzite occur in the groundmass. Plagioclase phenocrysts have clouded labradorite cores surrounded by clear bytownite jackets. Quartzose xenoliths and partially-melted xenoliths, similar to those in Ngauruhoe 1954 lava, are common.

The young Pukekaikiore lava described here is an olivine andesite with pyroxene and olivine phenocrysts in a felted groundmass. Plagioclase is only a minor phenocryst phase (Table 4.1). Hauhungatahi andesite is similar but more coarsely crystalline with augite and hypersthene phenocrysts (up to 6mm) and olivine microphenocrysts. These sometimes contain chrome spinel inclusions and are often rimmed by pyroxene. Xenoliths are absent. Ohakune lavas are also olivine andesites in which pyroxene and olivine are the major phenocryst phases and plagioclase occurs only as microphenocrysts or

Table 4.2: Crystallisation temperatures of lavas as determined by cation exchange equilibria.

Lava		Wood & Banno	Wells	Lindsley	Roeder et al
14855	c	1006	1030	1100	859
29250	c	1053	1106	1130	-
14850	c	971	1001	1040	795
14738#	c	973	1002	1020	-
14814*	c	967	1019	1050	-
14798	c	1091	1088	1100	-
14816	c	1121	1143	1170	797
14848	c	1028	1092	1115	518
14848	r	1100	1146	1165	-
14880	c	1017	1065	1130	740
14880	r	1166	1142	1180	-

NOTES: Methods - Wood & Banno (1973), Wells (1977), Lindsley (1983) (coexisting pyroxenes); Roeder et al., (1973) (coexisting olivine and chromian spinel) (Appendix 1.1 & 1.4).
# sample similar to 14737, * sample similar to 14813.
c = core, r = rim. Temperatures in degrees celcius.

in the groundmass. The latter consists of plagioclase, clino- and orthopyroxene, titanomagnetite and olivine microlites in brown, microvesicular, silicic glass. Porcellanitic and quartzose xenoliths are abundant in some flows.

4.3.4 Crystallisation conditions:

Crystallisation temperatures of TVC lavas, derived from coexisting ortho- and clinopyroxenes (c.f. Appendix 1.1) are given in Table 4.2. From basalt (14855) to dacite (14814), only a moderate decrease in temperature is inferred and most lavas range between 1000 °C and 1150 °C (Wells, 1977) or 1050 °C and 1200 °C (Lindsley, 1983). Hauhungatahi lavas give the highest temperatures and these are similar to estimates derived from basic rims of pyroxenes in hybrid lavas (e.g.14848). Coexisting olivine-spinel pairs (Roeder et al., 1979; Appendix 1.4) give variable and low results.

The phenocryst assemblages and compositions described constrain the temperatures, water contents and pressures which prevailed during crystallisation - temperatures of 1000 °C to 1100 °C, water contents less than 5 weight % and $P_{water} < P_{total}$ are typical of other orogenic andesite suites (Gill, 1981 p.203). Although quantitative estimates of crystallisation pressures are not available, low Na, Al and Ti contents in pyroxenes and high Ca contents in olivine suggest that these were less than about 8kb (Gill, 1981).

4.4 BULK-ROCK CHEMISTRY

4.4.1 General Features:

Bulk-rock chemistry and C.I.P.W norms of selected lavas are given in Table 4.3. Most are calc-alkaline rather than tholeiitic (Fig.4.5) and show only limited Fe-enrichment. Based on the Gill (1981) classification of intermediate volcanic rocks, most are medium-K orogenic andesites (Fig.4.6) with TiO_2 is less than 1.75 weight%. All compositions are quartz-hypersthene normative (Table 4.3).

Table 4.3: Bulk-rock chemistry and C.I.P.W. norms of selected lavas.

LOC	MANG	MANG	N54	TH	WHAK	MANG	WAH	MANG	WHAK
VUW	14855	14859	29250	14737	14782	14844	14867	14813	17886
major elements (weight%)									
SiO_2	52.7	53.9	56.2	56.5	58.1	58.8	61.2	64.3	66.9
TiO_2	.7	.7	.8	.7	.7	.7	.7	.8	.6
Al_2O_3	15.7	17.3	16.6	18.2	17.3	17.0	17.8	16.1	15.7
Fe_2O_3	1.5	1.5	1.4	1.4	1.2	1.1	1.1	.9	.7
FeO	7.5	7.3	7.0	6.8	5.9	5.6	5.2	4.3	3.3
MnO	.2	.1	.1	.1	.1	.1	.1	.1	.1
MgO	8.8	6.8	5.2	4.7	4.7	4.4	2.6	2.5	2.2
CaO	9.7	8.9	8.3	7.6	7.6	7.0	6.0	4.7	4.1
Na_2O	2.6	2.8	3.1	3.2	3.1	3.6	3.6	3.4	3.3
K_2O	.6	.7	1.2	.8	1.2	1.6	1.6	2.9	3.0
P_2O_5	.1	.1	.2	.1	.1	.1	.1	.1	.1
C.I.P.W. norm									
Qz	.2	3.2	6.4	8.1	10.0	8.6	14.5	18.0	22.4
Or	3.5	4.1	6.8	4.5	7.2	9.5	9.5	17.0	17.5
Ab	22.0	23.8	26.3	27.0	26.2	30.2	30.5	28.4	28.1
An	29.4	32.5	27.9	32.9	29.8	25.6	27.7	20.4	19.2
Di	14.7	9.0	10.1	3.6	5.9	6.7	1.0	1.7	.5
Hy	26.4	23.8	18.7	20.4	17.7	16.1	13.6	11.5	9.9
Mt	2.2	2.1	2.0	2.0	1.7	1.6	1.5	1.2	1.0
Il	1.3	1.3	1.4	1.3	1.3	1.3	1.4	1.6	1.2
Ap	.2	.2	.4	.2	.2	.3	.3	.3	.3
trace elements (ppm)									
Sr	201	224	247	248	250	285	248	228	207
Rb	11	17	38	20	37	60	56	115	122
Ba	185	231	214	260	310	358	389	530	502
Zr	50	60	95	63	93	117	119	199	176
V	251	267	220	210	195	177	173	136	93
Cr	380	128	100	38	92	69	10	69	50
Ni	142	57	29	25	35	35	17	32	22
Mg*	68	62	57	55	59	58	47	52	55
K/Rb	450	338	252	318	274	222	236	207	202
Al/Sr	413	409	355	388	367	316	381	374	401

Table 4.3 cont:

LOC	WAH	MANG	WAH	HAU	PUKE	OH	WAH	PUK	MANG
VUW	14913	14883	16721	14816	24471	14795	16722	14848	14871
major elements (weight%)									
SiO_2	58.2	57.8	60.9	56.4	57.3	57.4	61.6	57.3	59.2
TiO_2	.7	.7	.8	.6	.6	.5	.6	.7	.6
Al_2O_3	20.5	15.6	15.3	15.3	14.8	15.0	15.8	14.4	14.2
Fe_2O_3	.9	1.2	1.0	1.3	1.2	1.3	.9	1.2	1.1
FeO	4.3	5.8	5.0	6.5	6.2	6.6	4.7	6.0	5.3
MnO	.1	.1	.1	.1	.1	.2	.1	.2	.1
MgO	2.2	7.0	5.4	7.3	6.9	6.6	4.7	8.7	8.0
CaO	8.2	7.6	6.2	9.6	9.3	9.1	6.5	7.3	7.0
Na_2O	3.6	2.7	3.2	2.3	2.5	2.5	3.4	2.8	2.8
K_2O	1.3	1.4	2.0	.6	.9	.7	1.7	1.5	1.6
P_2O_5	.1	.1	.2	.1	.1	.1	.1	.1	.1
C.I.P.W. norm									
Qz	10.0	8.5	12.1	8.8	9.2	10.0	13.6	6.0	9.5
Or	7.4	8.3	11.9	3.7	5.2	4.1	9.8	8.6	9.3
Ab	30.4	23.2	27.4	19.1	21.2	21.2	28.6	23.4	23.5
An	36.2	26.1	21.3	29.7	26.5	27.7	23.0	22.5	21.7
Di	2.8	8.7	6.8	7.3	15.5	13.8	6.8	10.4	9.7
Hy	10.3	22.0	17.3	21.3	19.3	20.0	15.5	25.7	23.3
Mt	1.3	1.7	1.5	1.9	1.8	1.9	1.4	1.7	1.6
Il	1.3	1.3	1.5	1.1	1.1	1.0	1.1	1.3	1.2
Ap	.3	.3	.4	.2	.2	.1	.3	.3	.3
trace elements (ppm)									
Ba	316	331	455	177	214	144	353	355	327
Rb	38	54	87	14	30	16	59	49	59
Sr	341	250	244	463	640	390	351	277	283
Zr	94	114	163	60	90	65	108	115	117
V	168	189	177	226	201	226	138	181	173
Cr	36	286	212	234	276	192	106	507	426
Ni	26	110	68	39	38	39	54	237	132
Mg*	48	68	66	67	66	64	64	72	73
K/Rb	275	214	192	358	244	356	235	248	223
Al/Sr	319	330	332	174	122	204	237	274	266

NOTES: Major analyses normalised to 100% volatile-free and Fe_2O_3 / FeO =.2.
I is measured $^{87}Sr/^{86}Sr$. Abbreviations as for Table 4.1.
For fuller trace element analyses see Appendix 2.2.

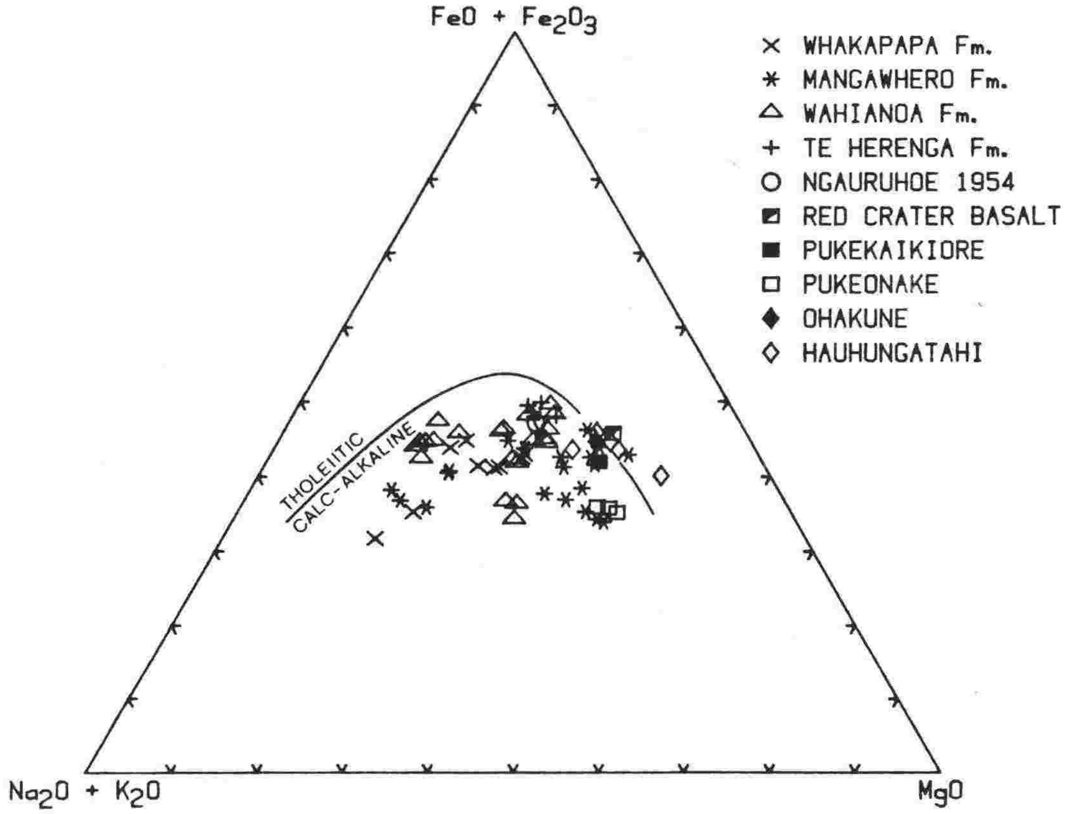

Fig.4.5: AFM diagram for lavas of Ruapehu and nearby vents. Curve sparates tholeiitic from calc-alkaline fields (Irvine and Baragar, 1971).

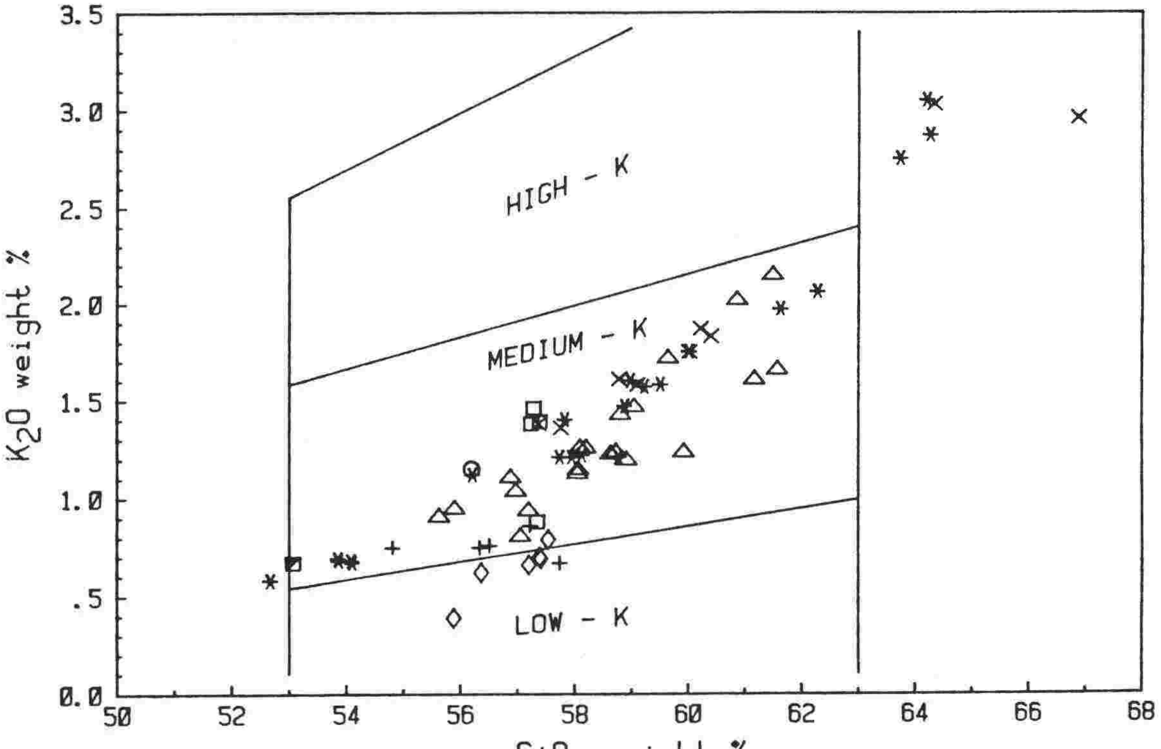

Fig.4.6: K_2O vs. SiO_2 Harker variation diagram for lavas of Ruapehu and nearby vents. Fields are for orogenic andesites (Gill, 1981; p.6). Symbols as in Fig.4.5.

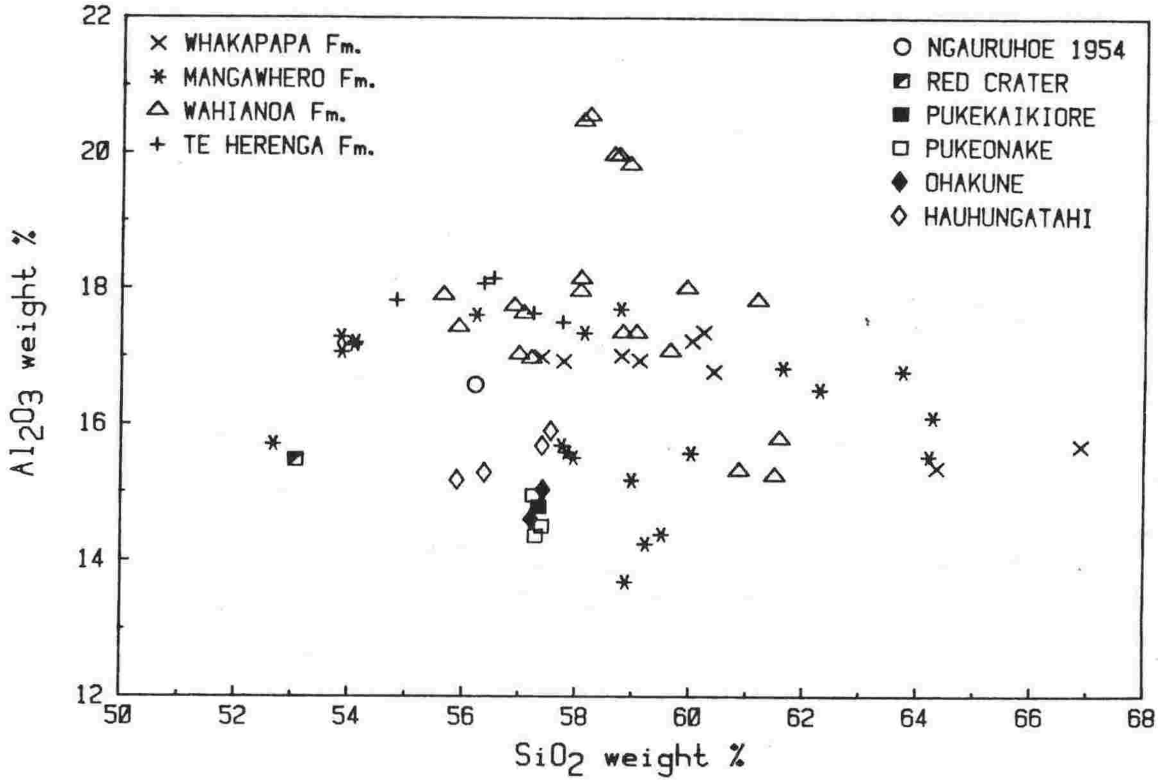

Fig.4.7: Al_2O_3 vs. SiO_2 Harker variation diagram for lavas of Ruapehu and nearby vents.

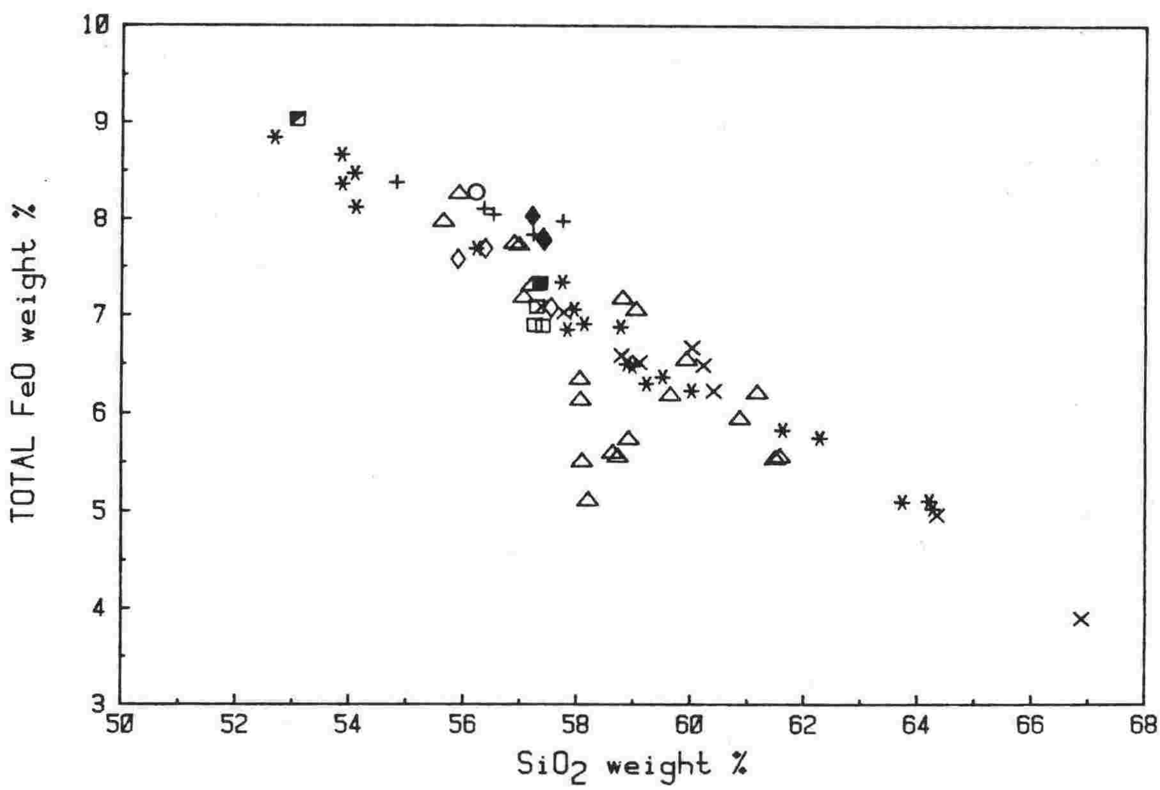

Fig.4.8: FeO vs. SiO_2 Harker variation diagram for lavas of Ruapehu and nearby vents. Symbols as in Fig.4.7.

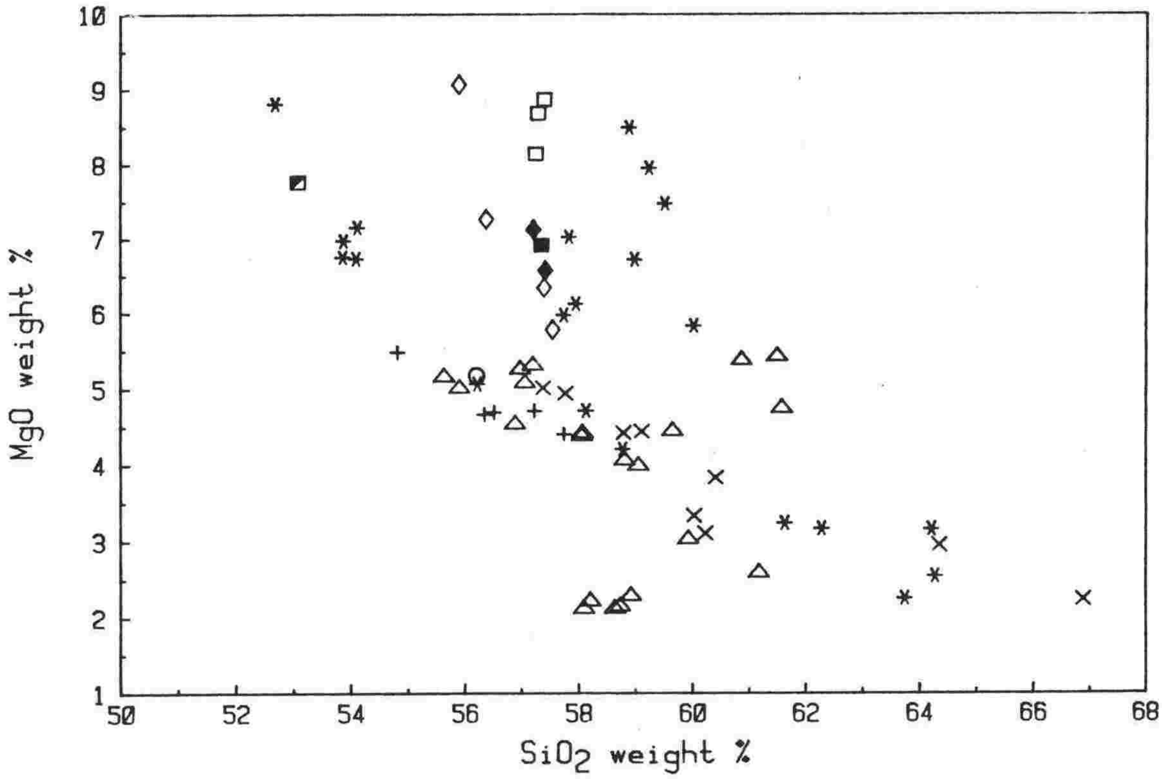

Fig.4.9: MgO vs. SiO_2 Harker variation diagram for lavas of Ruapehu and nearby vents.

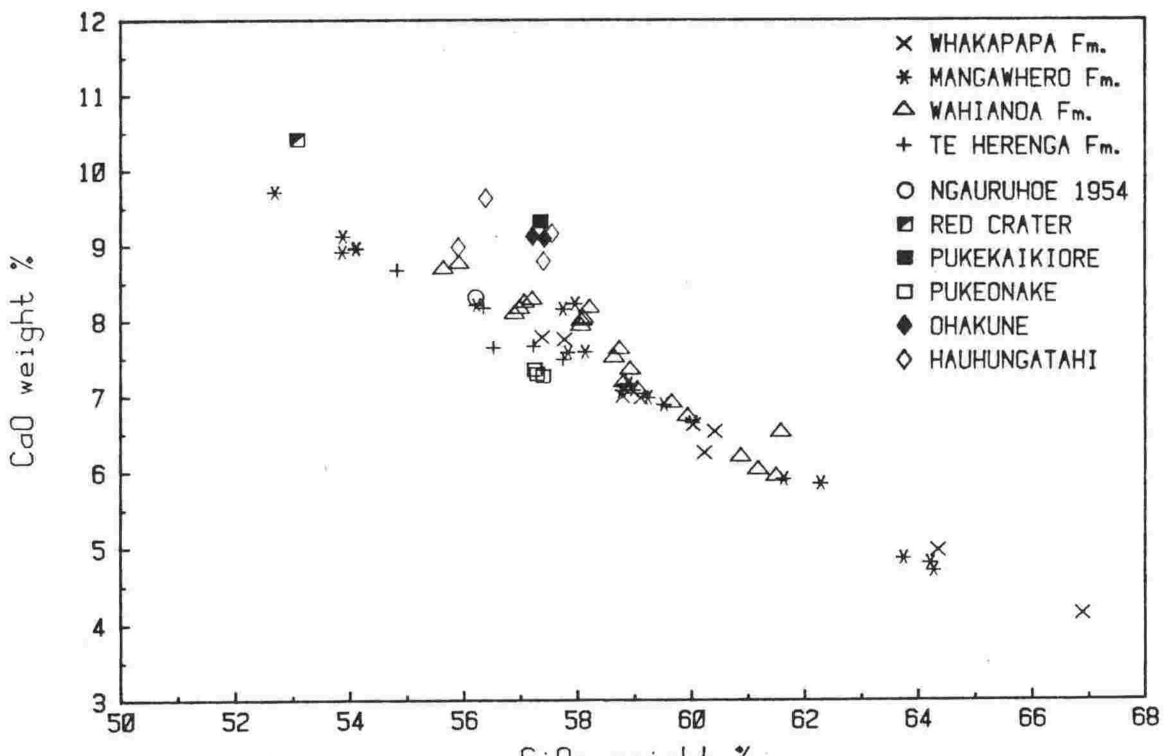

Fig.4.10: CaO vs. SiO_2 Harker variation diagram for lavas of Ruapehu and nearby vents.

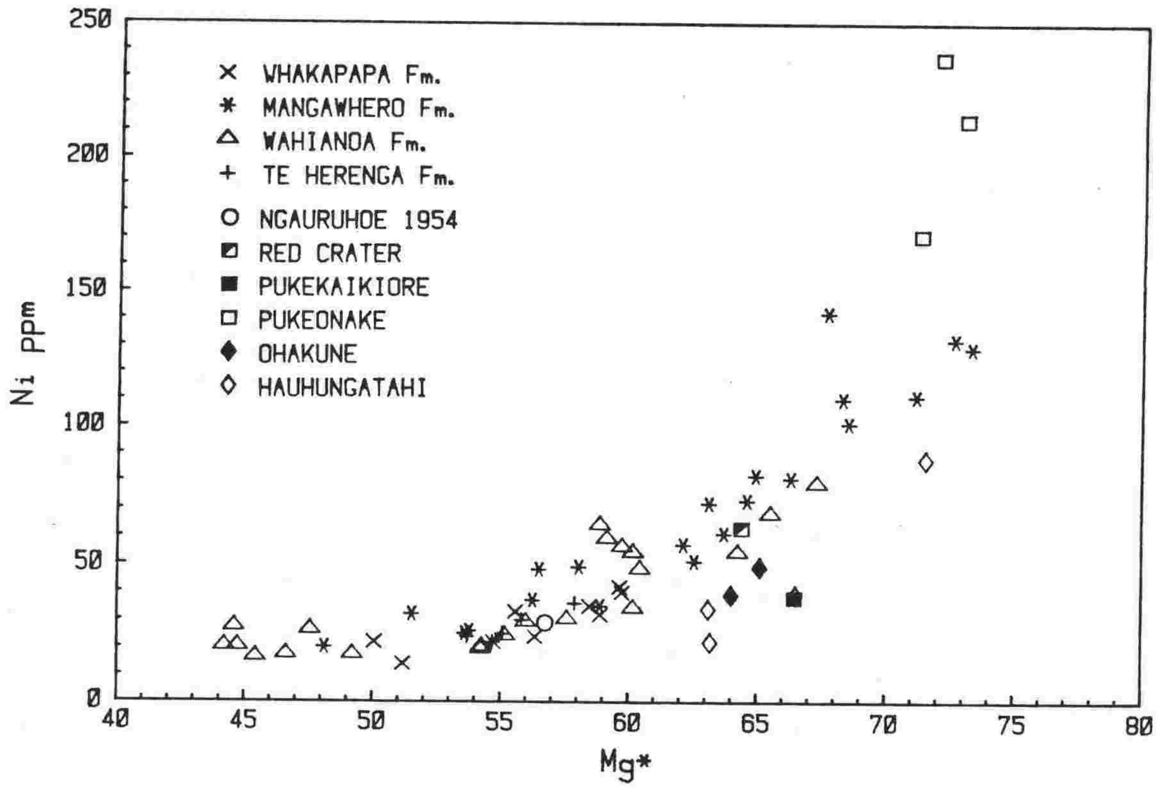

Fig.4.11: Ni vs. Mg* plot for lavas of Ruapehu and nearby vents.
$Mg^* = [\ Mg\ /\ (Mg+Fe^{2+})\ ]$, for $Fe_2O_3\ /\ FeO = .2$.

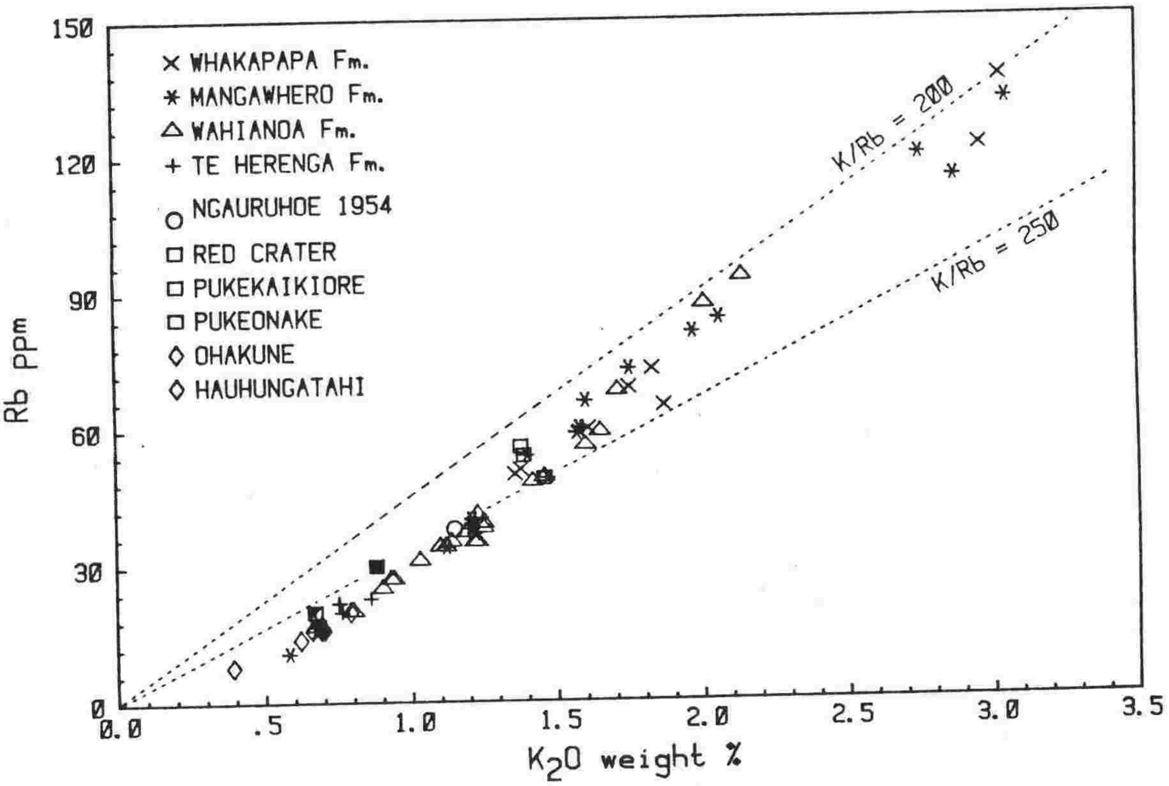

Fig.4.12: Rb vs. K_2O Harker variation diagram for lavas of Ruapehu and nearby vents.

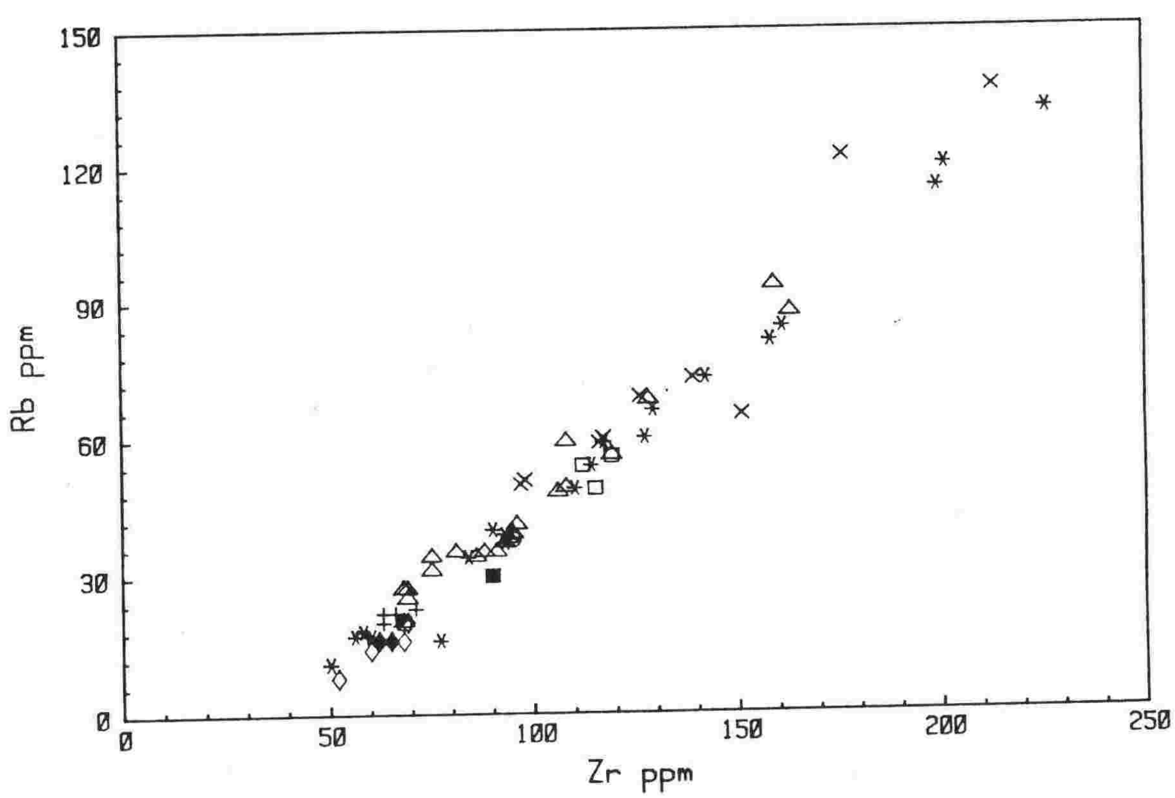

Fig.4.13: Rb vs. Zr Harker variation diagram for lavas of Ruapehu and nearby vents.

4.4.2 Compatible element contents:

Normally, magmatic evolution in calc-alkaline rocks leads towards silica enrichment and depletion in Ca, Fe and Mg (Gill, 1981). For this reason, silica content is used here as a measure of differentiation, against which concentrations of other elements can be compared.

SiO_2 contents range from 52.7% (14855) to 66.8% (17887). There is a small compositional gap between 61.5% and 63% which is interpreted as a result of sampling bias because of the consistent chemical and isotopic trends which link the lavas. Al_2O_3 shows a scatter on the Al_2O_3 vs. SiO_2 variation diagram (Fig.4.7) reflecting wide variation in modal plagioclase. Total FeO correlates negatively with silica (Fig.4.8) which is typical of many calc-alkaline volcanic suites (Gill, 1981, p.107) and is due to a decrease of mafic minerals with increasing silica content. The same trend is followed by Mn and V which are contained mainly in pyroxene, but not by Ti which shows a weak positive correlation with SiO_2, indicating that Fe-Ti oxide content is similar in all lavas. CaO shows a continuous and rapid decrease with increasing silica content (Fig.4.9) reflecting both a decrease in clinopyroxene content and plagioclase becoming more sodic. MgO contents vary from 9% to 2% (Fig.4.10) indicating substantial differences in modal olivine and pyroxene. Cr and Ni are strongly enriched in early-formed olivine, pyroxene and spinel and are most highly concentrated in the more basic lavas (Fig.4.11).

4.4.3 Incompatible element contents:

Incompatible elements, with bulk distribution coefficients (Kd) much less than 1, show substantial increases in concentration with increasing silica content of lavas. Since K-bearing minerals such as hornblende, biotite or K-feldspar are absent, K and Rb are strongly incompatible throughout the compositional range and correlate positively with SiO_2 (Fig.4.6). K/Rb ratios decrease continuously with increasing K_2O (Fig.4.12), mainly because of the increasing compatibility of K with respect to feldspar during

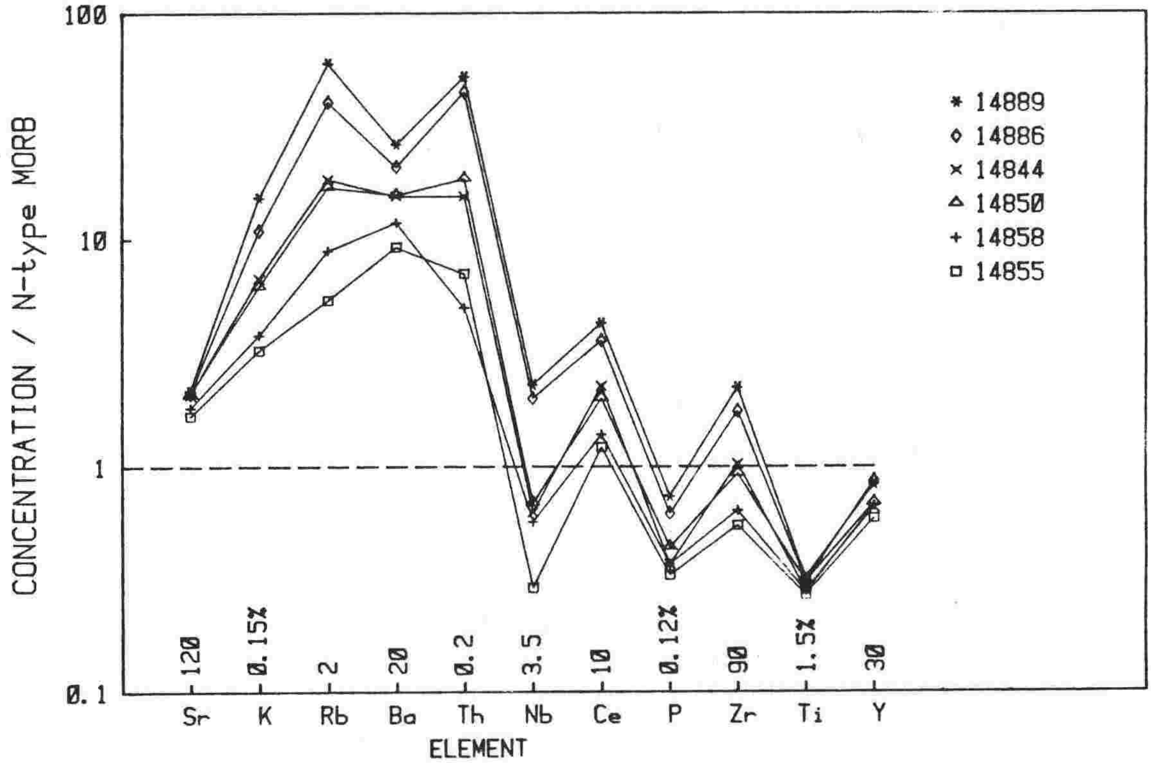

Fig.4.14: Spidergram of trace element concentrations in selected Mangawhero Formation lavas normalised to N-type MORB (Pearce, 1982). Normalisation constants are given along x-axis.

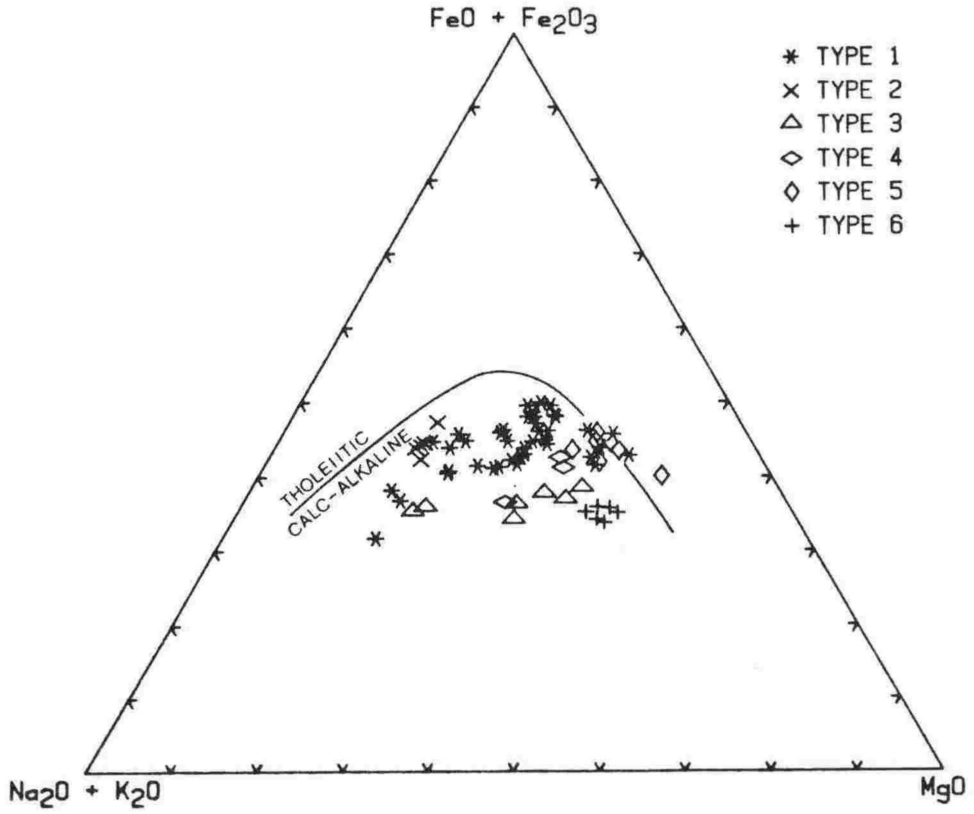

Fig.4.15: AFM diagram for lavas of Ruapehu and nearby vents plotted according to lava type (c.f.Fig.4.5).

differentiation (Rama Murthy and Griffin, 1970). Other incompatible elements such as Th, Nb, La, Ce and Zr also show progressive enrichment with increasing silica content although there are major differences in enrichment factors between some elements (e.g. 4-fold for Zr, 8-fold for Rb across the range 53 to 64% SiO_2). Some incompatible element correlations have non-zero intercepts (e.g.Fig.4.13) which could be explained by changes in bulk Kd during differentiation, but are more likely the result of variable enrichment due to crustal contamination. These processes are discussed more fully in Chapters 5 & 6.

Geochemical distribution patterns of trace elements (spidergrams) have recently been used to compare rocks (e.g. Wood, 1979; Sun, 1980; Thompson et al., 1984; Pearce, 1982, 1984). In the form used here, elements are normalised to their concentration in N-type MORB and ordered according to (i) their mobility in aqueous fluid i.e. ionic potential (ionic charge / ionic radius) and (ii) their incompatibility i.e. bulk Kd between garnet lherzolite and melt. They are so arranged that incompatibility increases from the outside to the centre of the pattern and relative mobility decreases from left to right (Pearce, 1984). Elements used in the pattern behave incompatibly during most partial melting and fractional crystallisation processes except when the following mineral species are present: plagioclase (Sr & Ba), Fe-Ti oxides (Ti), apatite (P & Ce), pyroxene (Y), alkali-feldspar (K, Rb & Ba).

Spidergrams show effectively the characteristic enrichment of large ion lithophile elements (LILE) K, Rb, Ba and Th in calc-alkaline lavas compared to N-type MORB (Fig.4.14). Lavas from Ruapehu and nearby vents show the following features: (1) Sr is only mildly enriched and shows little change from basalt to dacite (2) K, Rb and Th are greatly enriched and show progressive increase in concentration from basalt to dacite; Rb and Th show much greater relative enrichment than K (3) Ba is the most enriched element in the more basic lavas (showing a ten-fold enrichment in basalt 14855),

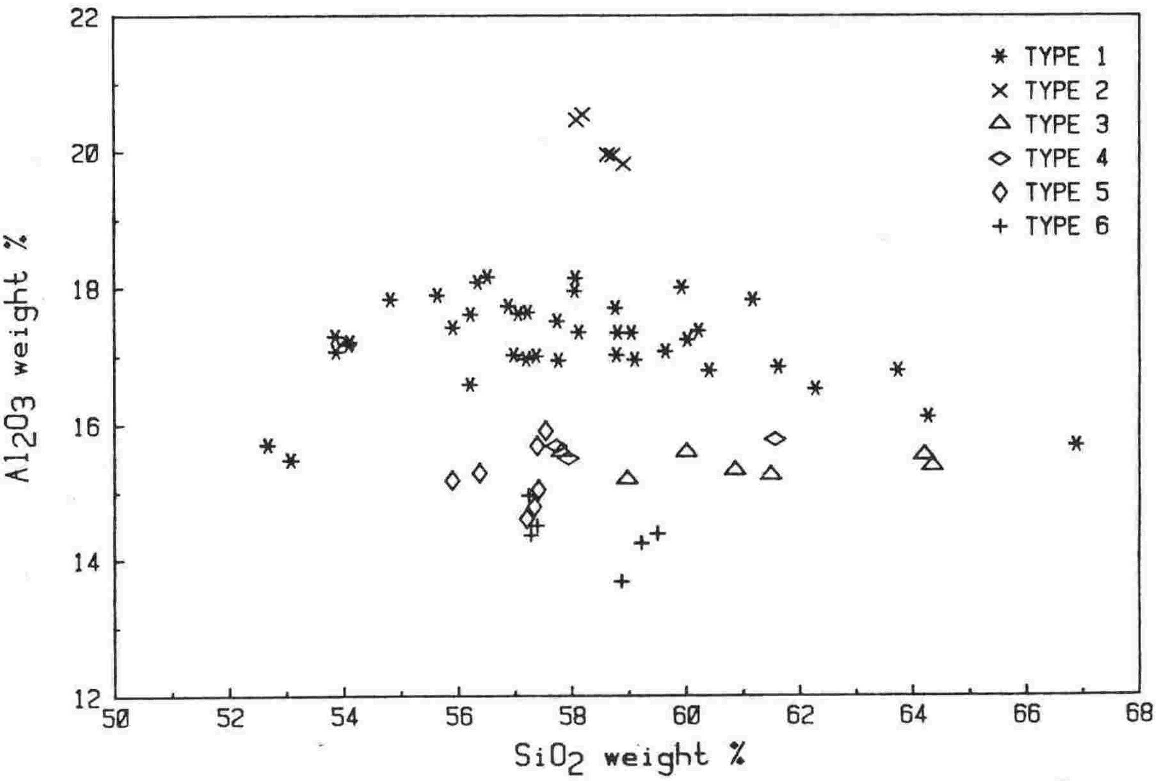

Fig.4.16: Al_2O_3 vs. SiO_2 Harker variation diagram for lavas of Ruapehu and nearby vents, plotted according to lava type (c.f.Fig.4.7).

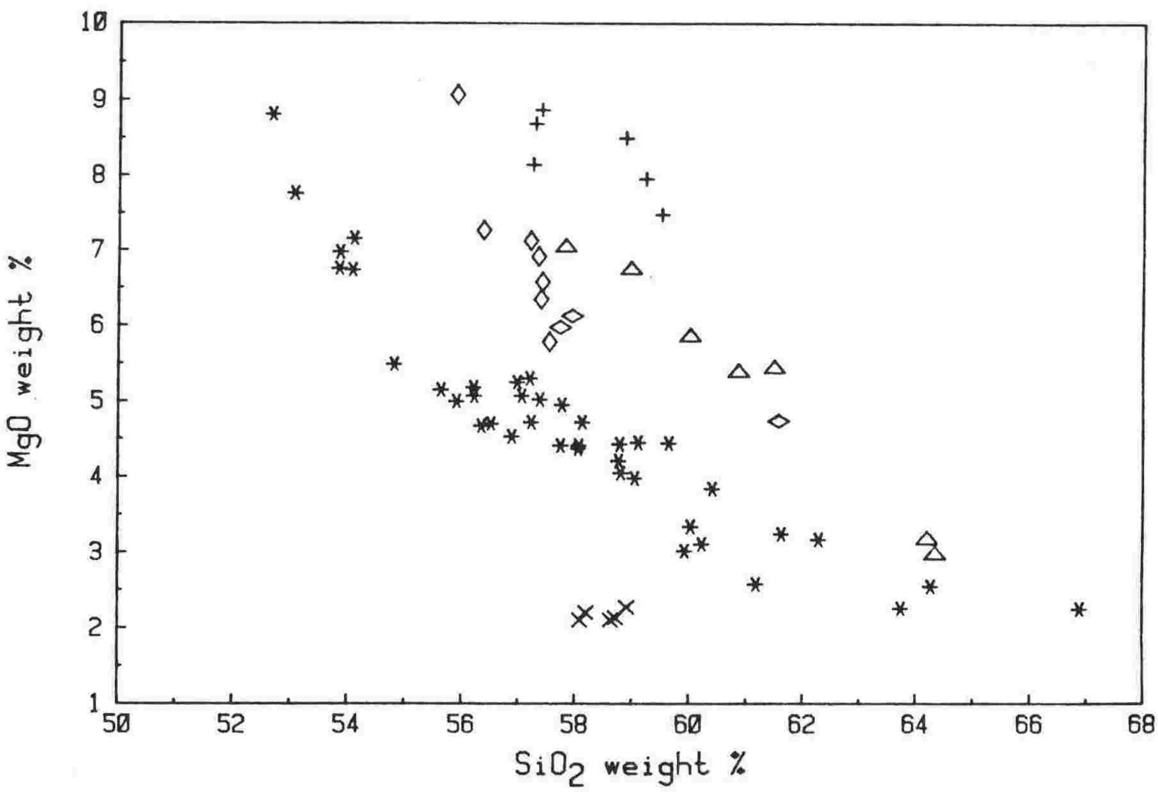

Fig.4.17: MgO vs. SiO_2 Harker variation diagram for lavas of Ruapehu and nearby vents, plotted according to lava type (c.f.Fig.4.9). Symbols as in Fig.4.16.

but shows only moderate increase from basalt to dacite, reflecting growing compatibility with sodic plagioclase (4) high field strength elements (HFSE), with the exception of Ce, are not greatly enriched; Ti and P are strongly depleted and show limited increase from basalt to dacite; Zr and Nb are enriched only in dacite; Y is depleted throughout.

4.5 LAVA CLASSIFICATION

Although lavas from Mount Ruapehu and nearby vents range from basalt to dacite, most are acid andesites. Since all are porphyritic and many contain glomerocrysts, xenoliths and/or disequilibrium phenocryst assemblages, none can be considered to truly represent a magmatic liquid and all may be accumulative to some extent. This limits the use of bulk-rock chemistry to classify and define petrogenetic trends or liquid lines of descent. Nevertheless, petrographic and chemical data suggest that it is possible to subdivide broadly the lavas into six distinct types and to constrain possible models of magma genesis for each type. These catagories are:

- TYPE 1 - Ruapehu Group lavas (from all four Formations), Ngauruhoe 1954 andesite and Red Crater basalt. These are plagioclase and plagioclase-pyroxene lavas ranging from basalt to dacite.
- TYPE 2 - Wahianoa Formation andesites (14900, 14901, 14911, 14913 & 14928). These have high modal plagioclase contents.
- TYPE 3 - Wahianoa Formation lavas (14886, 16721), Mangawhero Formation lavas (14882, 14883, 14884, 14839) and Whakapapa Formation lava (14839). These have moderately high modal pyroxene contents, except for two dacites (14829,14839) included because of bulk chemistry.
- TYPE 4 - Wahianoa Formation andesite (16722) and Mangawhero Formation andesites (14811 & 14812). These have moderately high pyroxene contents but are chemically distinct from TYPE 3.
- TYPE 5 - Hauhungatahi (14809, 14815, 14816, 14817), Ohakune (14795,

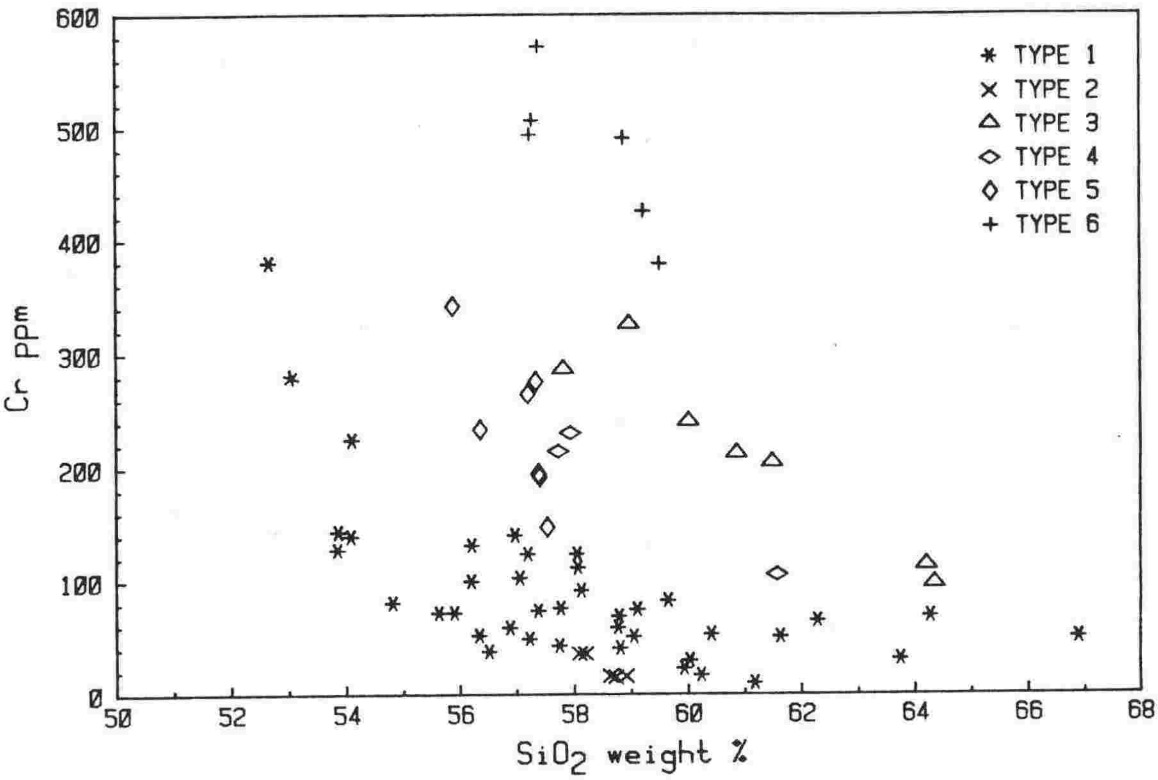

Fig.4.18: Cr vs. SiO_2 Harker variation diagram for lavas of Ruapehu and nearby vents, plotted according to lava type.

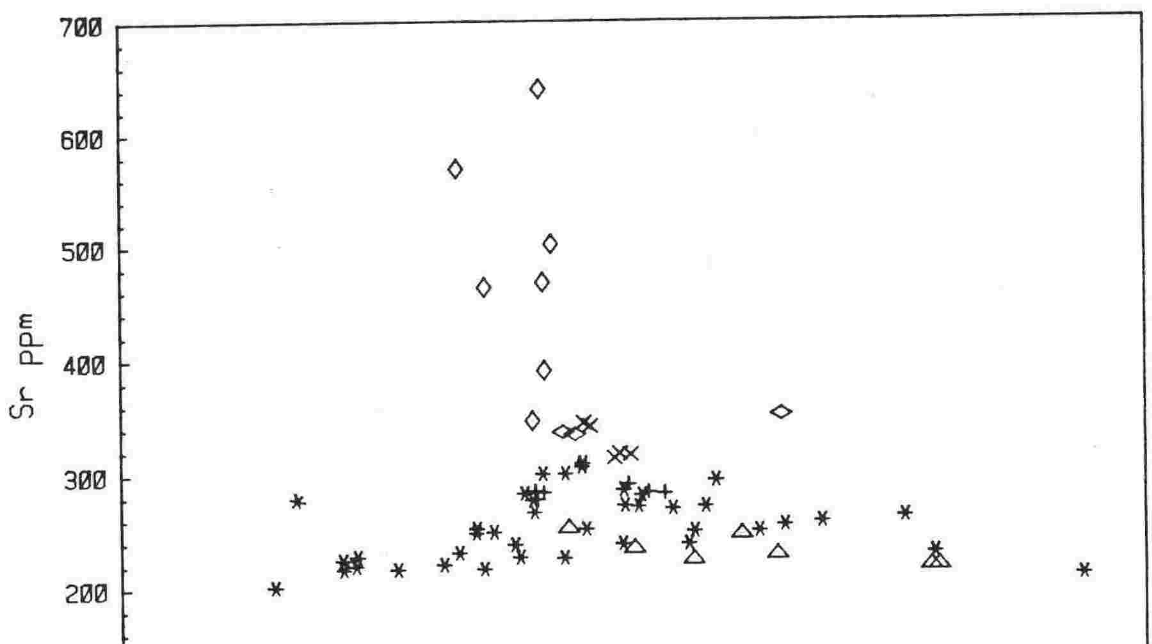

Fig.4.19: Sr vs. SiO_2 Harker variation diagram for lavas of Ruapehu and nearby vents, plotted according to lava type.
Symbols as in Fig.4.18.

14798) and Pukekaikiore (24471) olivine andesites. These have high modal pyroxene (and olivine) contents and very low plagioclase phenocryst contents.

- TYPE 6 - Pukeonake (14825, 14826, 14848) and Mangawhero Formation (14871, 14879, 14880) olivine andesites. These exhibit dis-equilibrium textures indicative of magma mixing.

Chemical compositions plotted with respect to lava type (Fig.4.15 to 4.19) illustrate the main characteristics of each: TYPE 1 lavas are relatively Fe-rich and follow closely a typical calc-alkaline trend (Fig.4.15); the oldest lavas (i.e. Te Herenga Formation) show the greatest Fe-enrichment (c.f.Fig.4.5). Between 52.5% and 57% SiO_2, there is an overall increase in Al_2O_3 (Fig.4.16) and rapid decrease in MgO (Fig.4.17) which might reflect early removal of olivine and pyroxene. Through the rest of the compositional range, Al_2O_3, FeO, CaO and MgO decrease smoothly with increasing silica. Cr and Ni follow trends similar to that of MgO (Fig.4.18) and concentrations are closely linked to Mg* (c.f.Fig.4.11). TYPE 2 lavas have high modal plagioclase and, as a consequence, have relatively high Al_2O_3 and Na_2O and low MgO and FeO contents. TYPE 3 lavas are pyroxene-rich and thus have high MgO, Cr and Ni and low Al_2O_3 contents. Incompatible elements have slightly higher concentrations than in other lavas of comparable silica content (Table 4.3). TYPE 4 lavas are also relatively MgO and Cr-rich but, although lower in Al_2O_3, they have higher Sr contents (Fig.4.19). TYPE 5 lavas are characteristically CaO-rich (c.f. Fig.4.9) and are depleted in alkalis (Fig.4.15; Fig.4.6) and LILE. They, like TYPE 4, have high Sr contents which, since Al_2O_3 is low, cannot be readily explained by higher modal plagioclase. TYPE 5 lavas are MgO- and Cr-rich but, despite having high Mg*, are low in Ni (Fig.4.11). TYPE 6 lavas have the highest MgO, Cr and Ni concentrations and the lowest Al_2O_3. Otherwise they are compositionally similar to TYPE 1 lavas.

Table 4.4a: Sr isotopic compositions of TVC lavas.

VUW	LOC	Rb	Sr	1/Sr	$^{87}Rb/^{86}Sr$	$^{87}Sr/^{86}Sr$	$^{87}Sr/^{86}Srm$	e
TYPE 1								
14765	TH	22	216	.0046	.289	.70509 64	.70507 29	4
						.70503 42		
						.70511 49		
14747	TH	22	216	.0046	.290	.70507 35	.70506 28	4
						.70505 44		
14737	TH	20	248	.0040	.232	.70518 38	.70518 19	2
						.70517 31		
						.70518 20		
14762	TH	23	265	.0038	.250	.70505 69	.70504 44	6
						.70503 50		
14741	TH	17	225	.0044	.218	.70483 43	.70483 38	3
						.70484 64		
						.70483 76		
14922	WAH	25	220	.0046	.324	.70522 56	.70518 25	2
						.70517 67		
14923	WAH	27	230	.0043	.341	.70518 38	.70518 37	4
						.70517 57		
						.70520 49		
14924	WAH	34	237	.0042	.414	.70526 19	.70526 19	4
14925	WAH	31	226	.0044	.403	.70523 52	.70523 52	8
14909	WAH	20	282	.0035	.206	.70491 60	.70491 60	9
14908	WAH	27	276	.0036	.284	.70496 34	.70496 34	6
14921	WAH	35	308	.0032	.324	.70512 39	.70512 39	8
14914	WAH	34	304	.0033	.320	.70500 49	.70500 49	9
14906	WAH	48	271	.0037	.518	.70566 80	.70566 80	14
14904	WAH	49	270	.0037	.529	.70567 42	.70567 42	6
14873	WAH	68	268	.0037	.734	.70561 76	.70561 76	12
16719	WAH	41	237	.0042	.504	.70548 50	.70548 50	9
14867	WAH	56	248	.0040	.659	.70554 70	.70554 70	8
14855	MANG	11	201	.0050	.155	.70476 32	.70490 32	3
						.70491 79		
						.70498 33		
						.70492 52		
14859	MANG	17	224	.0045	.219	.70501 51	.70502 31	4
						.70504 33		
14860	MANG	17	216	.0046	.228	.70505 36	.70505 45	8
14858	MANG	18	219	.0046	.235	.70508 45	.70508 45	6
14822	MANG	16	227	.0044	.203	.70503 37	.70503 37	7
14850	MANG	34	251	.0040	.392	.70529 42	.70529 42	7
14844	MANG	37	250	.0040	.426	.70555 53	.70554 27	3
						.70546 53		
						.70558 41		
14846	MANG	38	237	.0042	.461	.70574 66	.70578 40	5
						.70583 41		
						.70524 63		

Table 4.4 cont:

VUW	LOC	Rb	Sr	1/Sr	$^{87}Rb/^{86}Sr$	$^{87}Sr/^{86}Sr$	$^{87}Sr/^{86}Srm$	e
TYPE 1								
14886	MANG	81	253	.0039	.930	.70550 65	.70552 44	5
						.70557 54		
14885	MANG	84	256	.0039	.955	.70552 32	.70552 32	6
14889	MANG	120	260	.0039	1.342	.70574 65	.70574 38	4
						.70574 77		
						.70573 49		
14813	MANG	115	228	.0044				
14785	WHAK	51	299	.0033	.491	.70524 26	.70524 26	5
14784	WHAK	50	299	.0033	.486	.70523 38	.70523 38	7
14801	WHAK	69	248	.0040	.811	.70585 37	.70585 37	6
14782	WHAK	60	285	.0035	.611	.70536 39	.70536 39	6
14781	WHAK	59	280	.0036	.610	.70530 30	.70530 30	6
14804	WHAK	73	293	.0034	.719	.70586 32	.70584 26	3
						.70581 42		
17871	WHAK	122	207	.0048	1.700	.70615 57	.70620 50	6
						.70627 87		
11965	R-C	20	278	.0036	.203	.70462 25	.70462 25	5
29250	N54	37	249	.0040	.442	.70557 72	.70557 72	11
TYPE 2								
14911	WAH	39	344	.0029	.330	.70529 45	.70529 45	11
14913	WAH	38	341	.0029	.330	.70524 68	.70524 68	13
14900	WAH	35	313	.0032	.327	.70529 64	.70529 64	9
14901	WAH	35	317	.0032	.320	.70529 49	.70529 49	9
14928	WAH	37	316	.0032	.339	.70519 47	.70519 47	9
TYPE 3								
16721	WAH	87	244	.0041	1.030	.70549 54	.70549 54	9
14866	WAH	93	226	.0044	1.189	.70547 44	.70547 44	7
14883	MANG	54	250	.0040	.629	.70532 75	.70525 67	11
						.70519 107		
14884	MANG	66	232	.0043	.830	.70525 88	.70524 53	7
						.70524 63		
14882	MANG	73	222	.0045	.950	.70532 32	.70534 36	5
						.70537 70		
14829	MANG	132	215	.0046	1.779	.70544 43	.70545 27	3
						.70546 38		
14839	WHAK	137	215	.0046	1.839	.70540 22	.70542 16	2
						.70544 22		

Table 4.4 cont:

VUW	LOC	Rb	Sr	1/Sr	$^{87}Rb/^{86}Sr$	$^{87}Sr/^{86}Sr$	$^{87}Sr/^{86}Sr$	e
TYPE 4								
16722	WAH	59	351	.0028	.482	.70491 40	.70493 29	4
						.70493 42		
14812	MANG	39	336	.0030	.339	.70502 26	.70502 26	5
14811	MANG	39	336	.0030	.346	.70495 33	.70495 33	6
TYPE 5								
24471	PUKE	30	640	.0016	.136	.70440 46	.70440 46	8
14815	HAU	8	569	.0018	.039	.70419 50	.70419 50	12
14816	HAU	14	463	.0022	.090	.70423 22	.70424 21	2
						.70426 31		
14817	HAU	16	467	.0021	.098	.70421 64	.70421 64	12
14809	HAU	20	501	.0020	.113	.70420 52	.70420 52	10
14798	OH	16	346	.0029	.136	.70443 31	.70441 22	2
						.70437 52		
						.70441 49		
14795	OH	16	390	.0026	.120	.70436 41	.70436 41	7
TYPE 6								
14825	PUK	56	284	.0035	.572	.70479 33	.70479 33	7
14848	PUK	49	277	.0036	.509	.70481 74	.70481 41	4
						.70480 32		
14826	PUK	54	283	.0035	.555	.70483 32	.70483 32	6
14880	MANG	49	290	.0035	.490	.70480 33	.70482 25	3
						.70485 39		
14871	MANG	59	283	.0035	.597	.70489 55	.70489 55	8
14879	MANG	60	282	.0035	.616	.70484 72	.70484 72	11

NOTES: Abbreviations as for Table 4.1.
Individual $^{87}Sr/^{86}Sr$ ratios are given in column 7;
Mean $^{87}Sr/^{86}Sr$ ratios are given in column 8.
Errors (after each isotopic ratio) are one standard deviation.
e is the standard error of the mean (95% confidence interval).

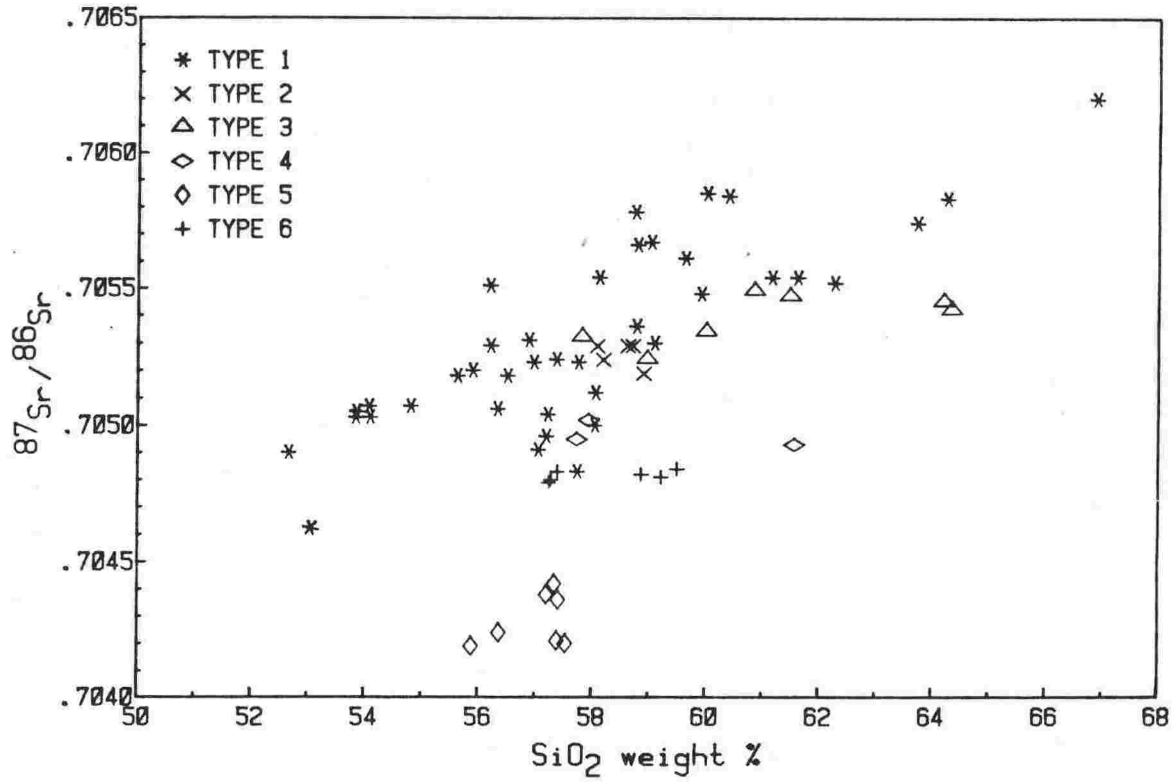

Fig.4.20: $^{87}Sr/^{86}Sr$ vs. SiO_2 diagram for lavas of Ruapehu and nearby vents, plotted according to lava type.

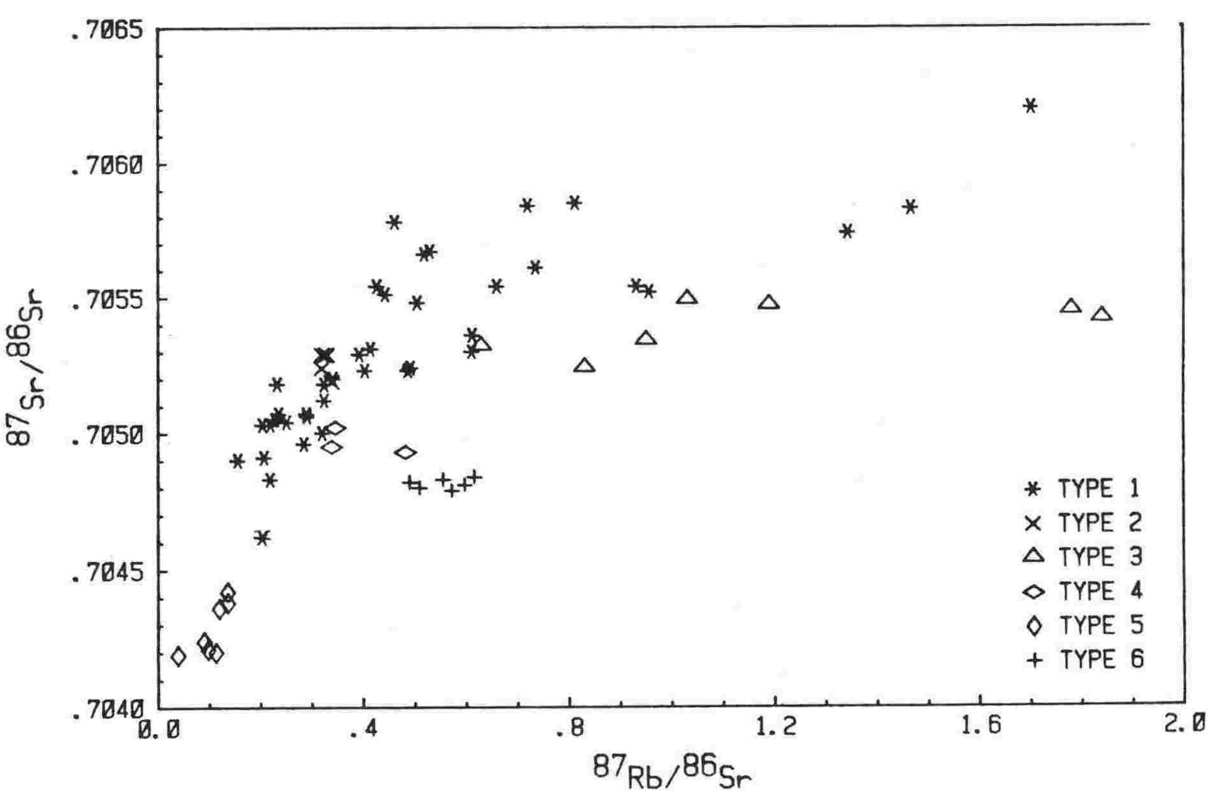

Fig.4.21: $^{87}Sr/^{86}Sr$ vs. $^{87}Rb/^{86}Sr$ diagram for lavas of Ruapehu and nearby vents, plotted according to lava type.

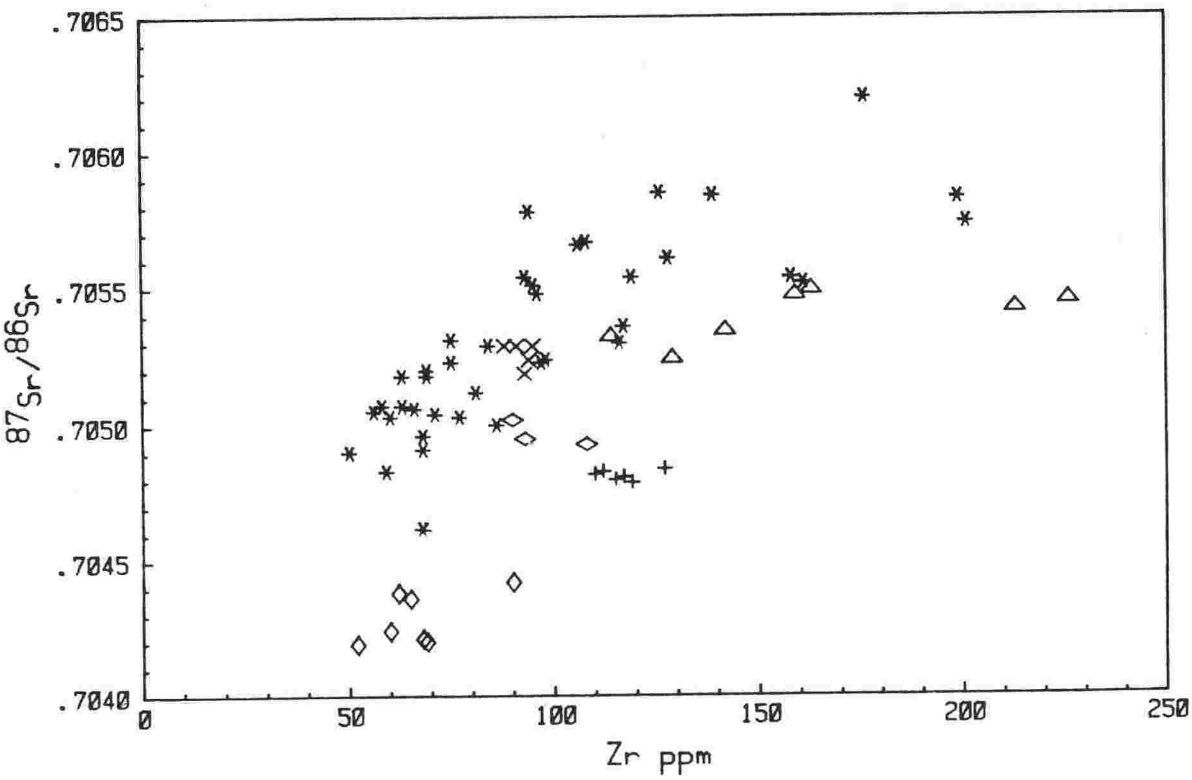

Fig.4.22: $^{87}Sr/^{86}Sr$ vs. Zr diagram for lavas of Ruapehu and nearby vents, plotted according to lava type.

4.6 Sr ISOTOPE CHEMISTRY

Sr isotope chemistry was first recognised to be a powerful tool in determining petrogenesis of volcanic rocks in the early 1960's (e.g. Faure and Hurley, 1963) and is now widely used, often in conjunction with other isotopes, to constrain potential source compositions or crustal contaminants in arc magmas (e.g. Hawkesworth et al., 1979; Francis et al., 1980; Thirlwall, 1982; Briqueu and Lancelot, 1979; Morris and Hart, 1983; also review by O'Nions, 1984).

Ewart and Stipp (1968) presented Sr isotopic data for a wide range of volcanic rocks from the TVZ and used them to develop various petrogenetic models. Since then, no other Sr isotopic analyses of TVZ lavas have been published. Recent improvement in analytical methods has yielded more precise data which, when applied to a stratigraphically controlled lava suite such as Ruapehu, can give a better understanding of the processes involved in their genesis. Sr isotopic data generated for this study are grouped according to lava type in Table 4.4, and show each type to have characteristic compositions (Fig.4.20). TYPE 1 lavas range from .70483 (14741) to .70620 (14813) and are weakly positively correlated with bulk-rock silica content (some scatter occurs between 56 and 60%). TYPE 2 lavas fall within the TYPE 1 field, suggesting a genetic link between the two (i.e. TYPE 2 might be TYPE 1 that have accumulated plagioclase?). TYPE 3 lavas show only limited increase in $^{87}Sr/^{86}Sr$ with increasing silica and, particularly at high silica content, have lower ratios than TYPE 1. TYPE 4 lavas have $^{87}Sr/^{86}Sr$ ratios much lower than TYPES 1 to 3 (for the same silica content). TYPE 5 lavas have the lowest $^{87}Sr/^{86}Sr$ ratios, ranging from .70420 (14809) to .70442 (24474). All TYPE 6 lavas have ratios close to .70480.

There is a broad temporal increase in the average SiO_2 contents and $^{87}Sr/^{86}Sr$ ratios of TYPE 1 lavas. The oldest lavas (Te Herenga Formation) are mostly basic andesites and have $^{87}Sr/^{86}Sr$ ratios of less than .70520, whereas the youngest lavas (Whakapapa Formation) are acid andesites and dacites and have $^{87}Sr/^{86}Sr$ ratios between .70520 and .70620. The most recent lava, Ngauruhoe 1954, is a basic andesite, but has the highest $^{87}Sr/^{86}Sr$ ratio of any lava of similar silica content (Fig.4.20). Plots of $^{87}Sr/^{86}Sr$ vs. $^{87}Rb/^{86}Sr$ (Fig.4.21) and $^{87}Sr/^{86}Sr$ vs. Zr (Fig.4.22) illustrate the broad positive correlations between Sr isotopic composition and incompatible element contents of TYPE 1 lavas. These could be the result of differences in mantle chemistry (e.g. Carter and Norry, 1976; Barberi et al., 1980), gradients in differentiated magma chambers (Hildreth, 1981) or, as seems more likely, crustal assimilation (e.g. Francis et al., 1980; Myers et al., 1984). Fuller discussion of these possibilities is given in Chapter 6.

4.7 SUMMARY

Lavas of Mount Ruapehu and nearby vents can be catagorised into six groups, each with distinctive chemical and isotopic characteristics. TYPE 1 represent the dominant lava type of Mount Ruapehu (Ngauruhoe 1954, the last major effusive, falls within this grouping). The lavas show strong negative correlations between silica and, particularly, FeO, MgO, CaO, Cr and Ni, and positive correlations between silica and LILE. Al_2O_3 and Sr are maximum between 56% and 58% SiO_2 and lower in lavas of other compositions. $^{87}Sr/^{86}Sr$ ratios are positively correlated with silica and LILE (Rb/Sr).

TYPE 2 lavas are strongly enriched in plagioclase and thus have high Al, Sr and Na contents, and low Mg and Fe contents. $^{87}Sr/^{86}Sr$ ratios are similar to those of TYPE 1 lavas.

TYPE 3 lavas are pyroxene-rich and have relatively high MgO, Cr, Ni and LILE and low Al_2O_3 . $^{87}Sr/^{86}Sr$ ratios are slightly lower than TYPE 1 lavas of the same silica content.

TYPE 4 lavas are pyroxene-rich and have high Sr, Mg and Cr and low Al_2O_3 and LILE. $^{87}Sr/^{86}Sr$ ratios are relatively low.

TYPE 5 lavas are olivine-pyroxene-rich and have high MgO, CaO, Sr and Cr and low Al_2O_3, Ni and LILE. $^{87}Sr/^{86}Sr$ ratios are much lower than those of other lava types.

TYPE 6 lavas show features normally associated with magma mixing and are thus considered to be hybrids. They have very high Mg*, Cr and Ni and $^{87}Sr/^{86}Sr$ ratios close to .70480.

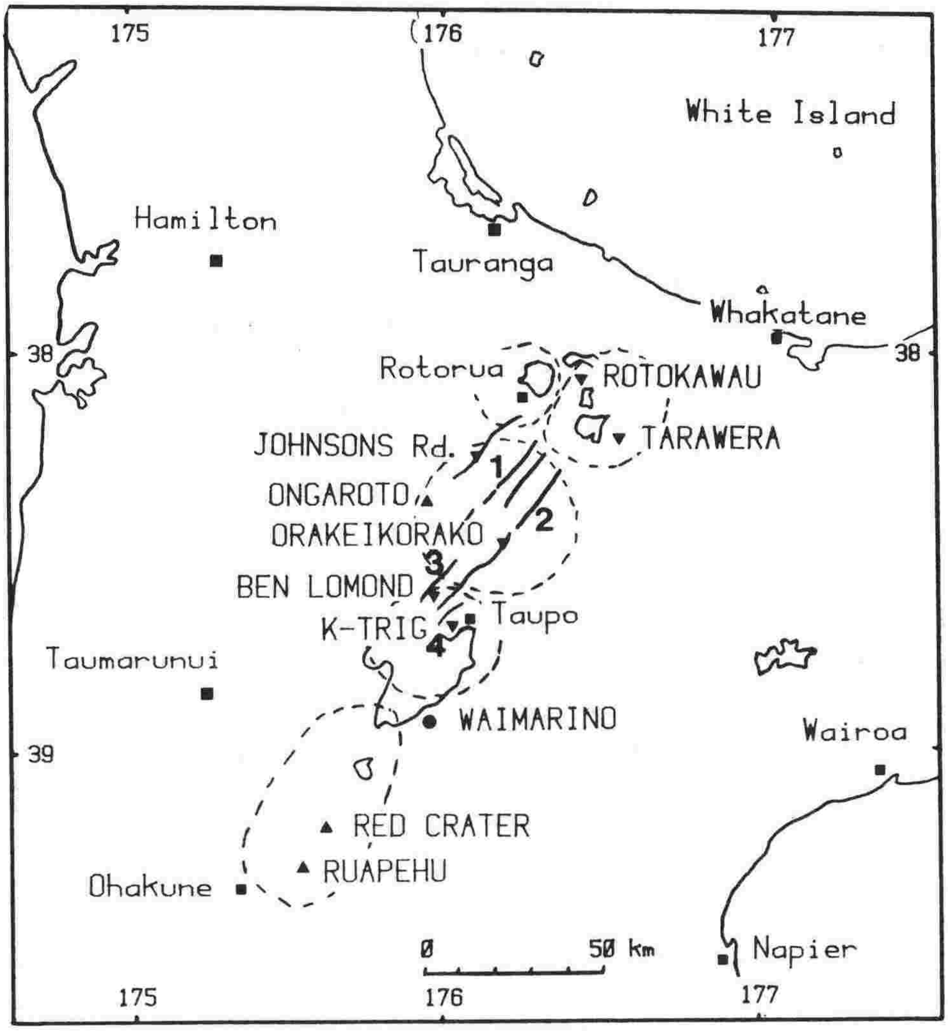

Fig.4.23: Generalised map of Taupo Volcanic Zone showing locations of basalts: triangles = low-alumina basalts, filled circle = Waimarino basalt; inverted triangles = high-alumina basalts. Volcanic Centres (dotted fields) are given in Fig.1.3. Faults: 1. Ngakuru, 2. Paeroa, 3. Whangamata, 4. Kaiapo.

PART 2: BASALTS OF TAUPO VOLCANIC ZONE

4.8 INTRODUCTION

Only two basalts are known from Tongariro Volcanic Centre, yet bulk-rock chemistry and petrography indicate that not all Ruapehu lavas nor those of nearby vents could be derived from magmas of that type. Hence, the following study of all known basalts from Taupo Volcanic Zone was undertaken in order to investigate the possibility that others exist which might also make suitable parental magma types. Cole (1973) described seven high-alumina basalts and one low-alumina-basalt, and references to these have since been made by Blattner and Reid (1982) (in an oxygen isotope study) and by Cole et al. (1983) (in a REE discussion). Hackett (in press) described an occurrence of magnesian quartz tholeiite at Waimarino, east of Lake Taupo.

4.9 TECTONIC SETTING AND ERUPTIVE HISTORY

Basaltic lavas are spatially and volumetrically restricted within the TVZ and probably amount to only about 4 km^3 (Cole, 1981), representing less than 0.1% of the total eruptives. They occur within each of the main Volcanic Centres (Fig.4.23); high-alumina basalts are particularly associated with the fault-bounded rhyolitic calderas of Okataina, Maroa and Taupo; low-alumina basalts are only found in or near Tongariro Volcanic Centre (Cole et al., 1983).

Rotokawau (22991), Johnson's Road (22997) and Ongaroto (22998) lie on a NNE-trending line near the western edge of the Taupo Graben and Tarawera (21717), Orakei korako (22993), Ben Lomond (22994) and K-Trig (22996) on a major fault of similar trend near the eastern side (Fig.4.23). As these two

Table 4.5: Chronology of basaltic eruptions within the TVZ.

VENT	TIME OF ERUPTION	BASIS OF ESTIMATION	SOURCE
Tarawera	10 June, 1886	Recorded History	Cole (1973)
Red Crater	<1.819ka	Taupo Pumice	Topping (1970)
Rotokawau	3ka	?	Cole (1973)
Waimarino	13.8 - 19.8ka	Tongariro Subgroup/ Oruanui Breccia	Hackett (1984)
Ruapehu	15 - 50ka	Mangawhero Formation	Hackett (p.c.)
K-Trig	137 +- .004ka	K-Ar date	Stipp (1968)
Ben Lomond	"	?	Cole (1973)
Orakeikorako	100 - 300ka	K-Ar dates	Stipp (1968)
Ongaroto	>100ka	?	Cole (1973)
Johnson's Road	>100ka	?	Cole (1973)

NOTES: Ruapehu basalt data from W.R.Hackett (pers comm., 1984).

lines are the inner graben boundaries it is probable that sites of eruption have been controlled by major regional faults, particularly where they intersect caldera structures (Cole, 1979). Waimarino basalt (17439), occurs on the eastern side of Lake Taupo in scattered exposure (Hackett, in press). Red Crater basalt (11965) was erupted from a recent crater of Tongariro, and Ruapehu basalt (14855) from a Mangawhero Formation vent. Neither eruption appear to be fault-controlled.

Table 4.5 summarises the eruptive history of basaltic volcanism in the TVZ. As shown, Johnson's Road and Ongaroto basalts are the oldest, being probably of late Pleistocene age, and Tarawera basalt, erupted on 10 June 1886, is the youngest. This indicates that lavas of basaltic composition have been erupted in minor amounts intermittently throughout the history of Taupo Volcanic Zone.

4.10 PETROGRAPHY AND MINERALOGY

Mineral modes of basalts are given in Table 4.6. Textures range from strongly porphyritic (Plates 4.5 & 4.6) to microcrystalline (Plate 4.7) or nearly aphyric (Plate 4.8). Olivine, augite, rare orthopyroxene and plagioclase occur as phenocrysts and no hydrous phases are present. Glomerocrysts of plagioclase and pyroxene occur particularly in 14855 and 11965 and are mostly xenocrystic in origin. Groundmass and interstitial glass often contain rapidly-grown silicates and oxides (Plate 4.11).

Compositional variations of phenocrysts in basalts are given in Table 4.7. Olivine is present in all basalts except 22994 and 22996 where it is replaced by spinel pseudomorphs (Plate 4.9), and 21717 where plagioclase is the only phenocryst phase. Olivine is usually the largest ferromagnesian phenocryst in high-alumina basalts, is subhedral to anhedral and frequently shows evidence of resorption. Crystals smaller than 1mm are commonly euhedral or skeletal (Cole, 1973).

Plate 4.5: BEI photograph of Waimarino basalt (magnesian quartz tholeiite) 17439. Olivine phenocrysts (centre LHS) have highly forsteritic cores (dark) and inclusions of chromian spinel. Rims are much more Fe-rich. The other phenocrysts are clinopyroxene (light grey). Groundmass is mainly plagioclase (grey) and pyroxene (white).

Scale bar = .1mm; field of view = .75mm.

Plate 4.6: BEI photograph of Red Crater low-alumina basalt 11965. Phenocrysts are olivine (upper centre, dark grey core), pyroxene (grey) and plagioclase (very dark grey).

Scale bar = .1mm; field of view = .75mm.

Plate 4.7: BEI photograph of Ongaroto low-alumina basalt 22998. Olivine phenocrysts (upper LHS) are less forsteritic than those of Waimarino basalt (Plate 4.5). Groundmass is microcrystalline with plagioclase (grey), interstitial pyroxene (white) and late-stage mesostasis containing spinel (bright white).

Scale bar = .1mm; field of view = .75mm.

Plate 4.8: BEI photograph of Tarawera high-alumina basalt 21717. Acicular plagioclase phenocrysts occur in a groundmass of pyroxene (white) and plagioclase (grey).

Scale bar = .1mm; field of view = .75mm.

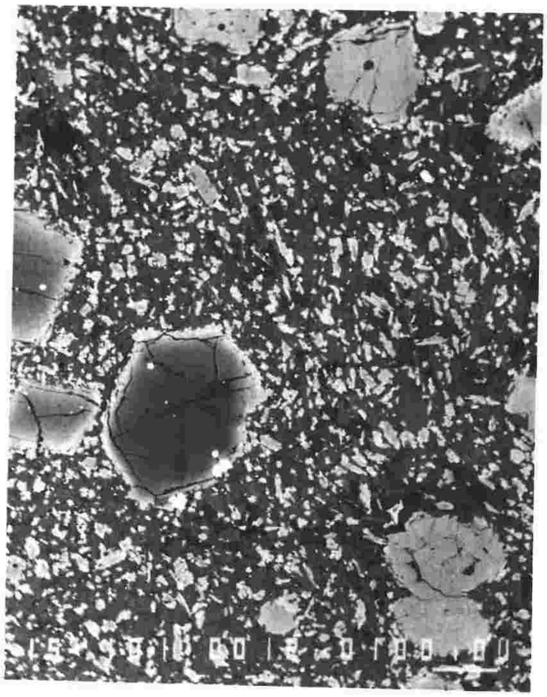

Plate 4-5

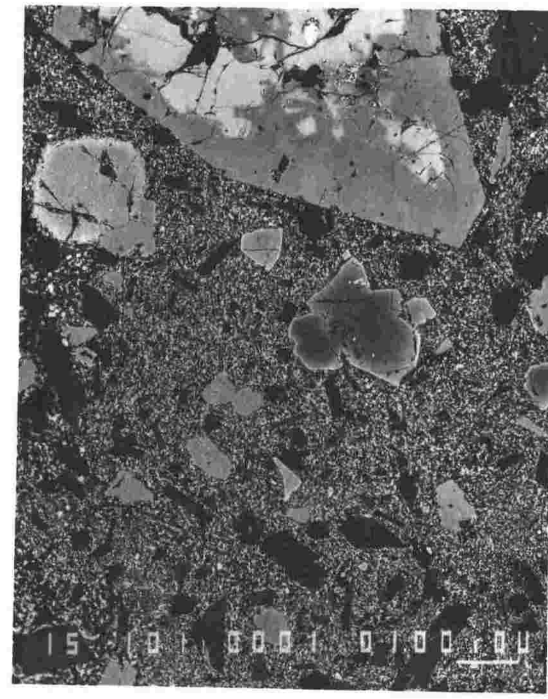

Plate 4-6

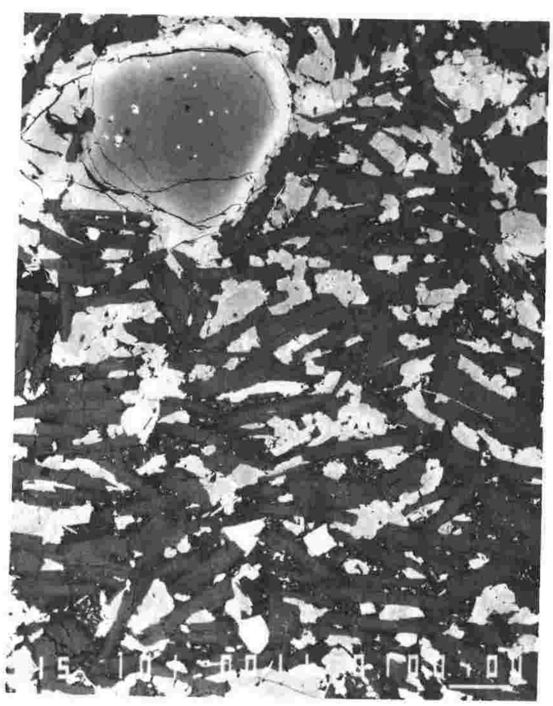

Plate 4-7

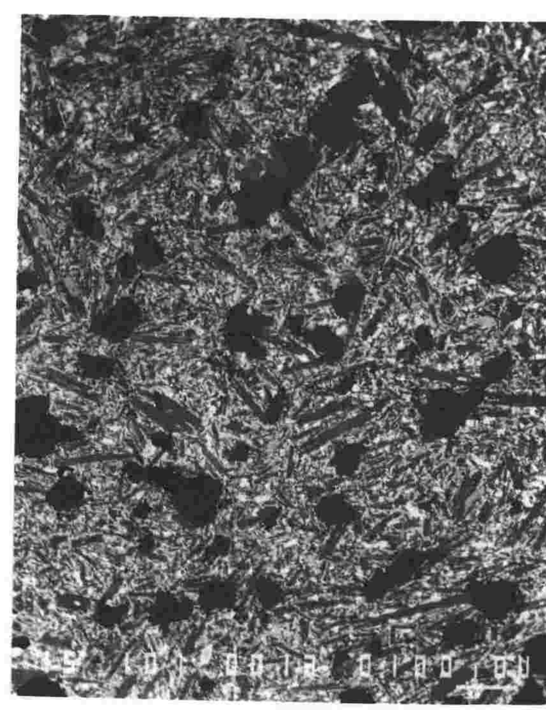

Plate 4-8

Plate 4.9: BEI photograph of K-Trig high-alumina basalt 22996. Euhedral plagioclase phenocrysts (grey) have interstitial pyroxene and mesostasis. Olivine phenocrysts (lower and centre LHS) are oxidised. Holes (black) indicate a high degree of vesicularity.

Scale bar = .1mm; field of view = .75mm.

Plate 4.10: BEI photograph of Orakeikorako high-alumina basalt 22993. Phenocrysts are olivine (white), augite (light grey) and plagioclase (grey).

Scale bar = .1mm; field of view = .75mm.

Plate 4.11: BEI photograph of interstitial assemblage in Orakeikorako high-alumina basalt 22993. Euhedral plagioclase phenocrysts (grey) have Na-rich rims in contact with acid residuum (light grey). Interstitial minerals are pyroxene, fayalitic olivine and spinel (white).

Scale bar = .01mm; field of view = .13mm.

Plate 4.12: BEI photograph of complexly zoned clinopyroxene phenocryst in Orakeikorako high-alumina basalt 22993. Dark zones indicate reduction in Ti, Al, Fe, Na and concomitant increase in Si, Mg, Ca - EPMA analyses of eight zones from core to rim are given in Appendix 3.

Scale bar = .01mm; field of view = .13mm.

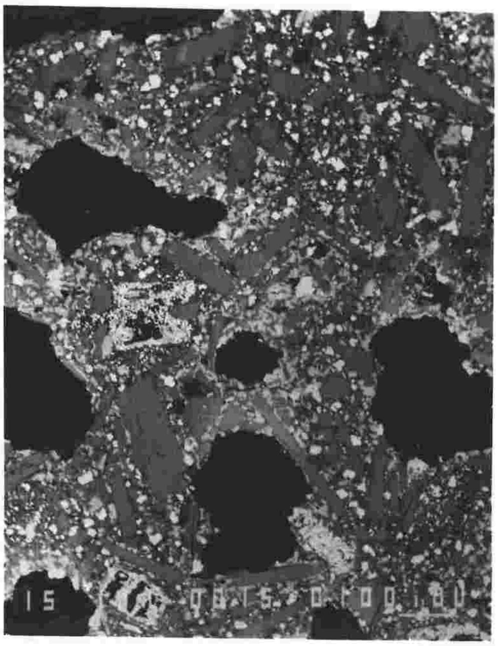

Plate 4-9

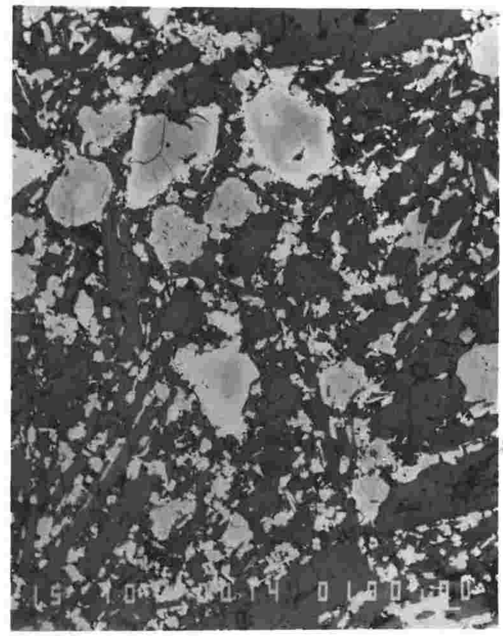

Plate 4-10

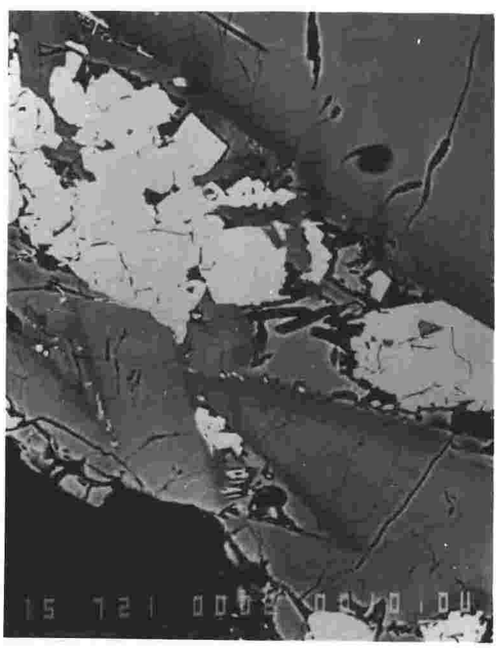

Plate 4-11

Plate 4-12

Table 4.6: Modal composition of basalts.

LOC	K-T	J-R	O-K	B-L	TAR	ROTO	ONG	RUAP	R-C	WAIM
VUW	22996	22997	22993	22994	21717	22769	22998	14855	11965	17439
pl	1.2	4.5	10.2	1.6	5.3	.3	.5	10.3	10.6	-
cpx	2.0	.8	3.4	g	.2	1.9	.2	7.3	7.2	7.4
opx	-	-	-	-	-	-	-	2.1	.8	-
ol	-	.6	3.8	.1	g	.7	7.9	7.0	4.9	16.1
phen	3.2	5.9	17.4	1.7	5.5	2.9	8.6#	26.7	23.5	23.7
g/m	96.8	93.5	78.8	94.5	93.5	89.4	91.4	73.3	76.5	75.8
xen	-	.6	3.8	3.8	1.0	7.7	-	-	-	.5

Notes: K-T = K-Trig; J-R = Johnson's Road; O-K = Orakeikorako;
B-L = Ben Lomond; TAR = Tarawera; ROT = Rotokawau; ONG = Ongaroto;
RUAP = Ruapehu; R-C = Red Crater; WAIM = Waimarino.
Abbreviations as for Table 4.1.
microcrystalline with gradation to groundmass.

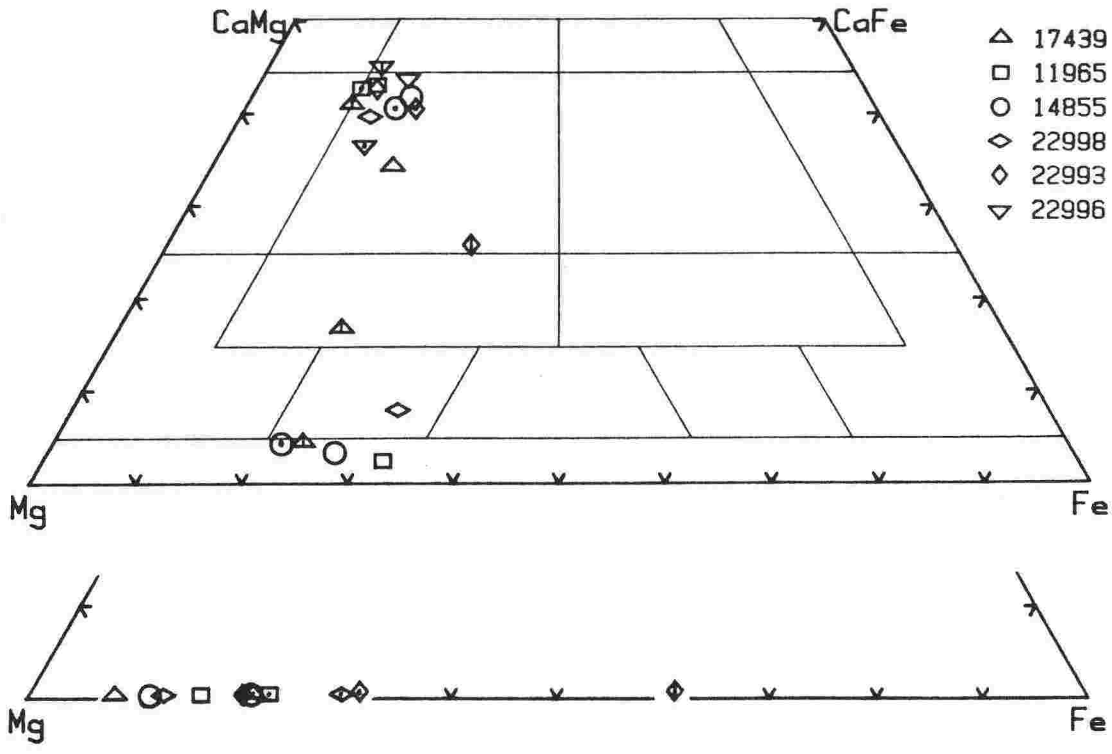

Fig.4.24: Compositions of mafic phenocrysts in selected basalts, plotted in terms of Ca, Mg and Fe; pyroxenes in upper quadrilateral, olivine in lower. Full analyses are given in Appendix 3. Rim compositions dotted, groundmass compositions vertical line. Fields as in Deer, Howie and Zussman (1978. p.3). Rims = dot, groundmass = vertical line.

Table 4.7: Compositional ranges of minerals in basalts.

VUW	ol (Fo)	cpx			opx			pl (An)	sp
		Ca	Mg	Fe+Mn	Ca	Mg	Fe+Mn		
22996	-	44-45	43-44	13-11	-	-	-	80-68	tmt
22993	80-38#	43-41	46-43	11-16	-	-	-	68	tmt
22998	87-70	40-36	48-53	12-23	-	-	-	70-28	*
14855	88-79	42-41	43-45	15-14	3-4	70-74	27-22	71	-
11965	85-70	43-33	46-53	11-14	3	65	32	70-76	-
17439	91-78	43-34	49-49	09-17	4	72	24	78	Crsp

NOTES: ol (Fo) refers to mole % forsterite; cpx refers to mole% Ca, Mg, and Fe respectively in clinpyroxene; opx refers to mole% Ca, Mg, and Fe respectively in orthopyroxene; pl (An) refers to mole% anorthite; tmt = titanomagnetite; Crsp = chromian spinel; * = tmt & Crsp; # = in groundmass; sp = spinel.

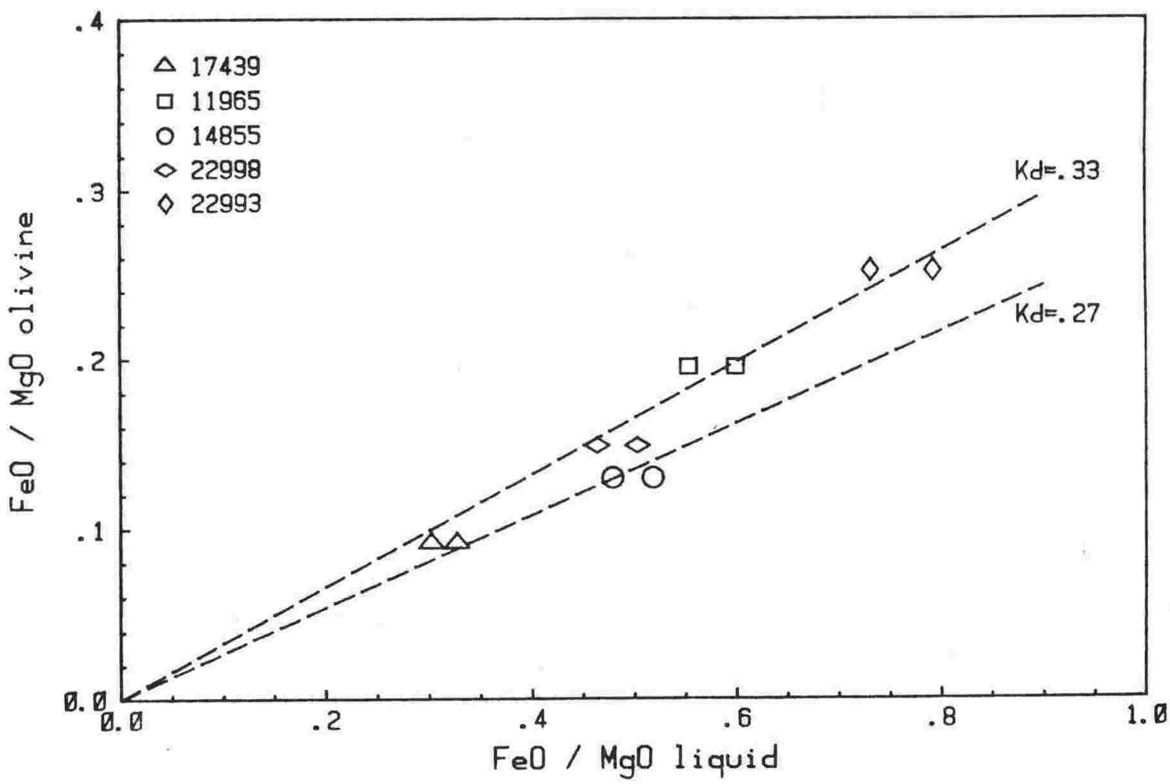

Fig.4.25: FeO/MgO (mole %) for coexisting olivine and liquid (bulk-rock) in selected basalts. For each pair of points, that to the right corresponds to a bulk-rock oxidation ratio of .1, to the left .2. For olivine, all iron is FeO. Distribution coefficients (Kd) from Roedder and Emslie (1970).

Waimarino basalt 17439 contains 16.1% modal olivine with highly magnesian cores (Fo_{91}) (Fig.4.24) zoned to more Fe-rich rims (Fo_{78}). In 22993, fayalitic olivine (Fo_{38}) occurs as .1mm microlites in late-stage acid residuum. Using the Roedder and Emslie (1970) distribution coefficient (Kd=.27-.33), compositions of early-formed phenocryst cores correspond to the appropriate Mg* of the bulk rock, indicating an approach to equilibrium (Fig.4.25).

Clinopyroxene occurs as small phenocrysts (<.5mm), as crystal aggregates or in the groundmass. In 22993 and 22998, phenocrysts are normally zoned (with respect to Mg-Fe substitution), but in other basalts, both normal and reverse zoning occurs. Most compositions fall in the augite field of the pyroxene quadrilateral (Fig.4.24). Complex zoning patterns are observed in some large (2mm) phenocrysts in high-alumina basalt (Plate 4.12). Chemical changes from core to rim (see Appendix 3) involve concommittant change in Si, Al, Ca and to a lesser extent Ti, Fe, Mg and Na suggesting that plagioclase removal from the melt was important in controlling chemical gradients.

Orthopyroxene is significantly absent as a phenocryst phase in all but the two low-alumina basalts (11965, 14855). However, it does occur in the groundmass of Waimarino basalt 17439 (with pigeonite) and in pyroxene-rich rims about large olivine grains in other lavas. Compositions range from bronzite to hypersthene (Fig.4.24). Glomerocrysts of two-pyroxenes are common to low-alumina basalts and, from the presence of resorbed cores, reverse zoning and reaction rims, these represent xenolithic material. One such cluster in 11965 contains grains of augite and hypersthene surrounded by a reaction rim of augite, the composition of which are similar to groundmass microlites (see Appendix 3).

Plagioclase phenocrysts occur in all basalts except 17439. Most contain a wide core of labradorite and a narrow rim which rapidly becomes more sodic towards the margin. Aggregates of xenocrystic origin sometimes occur

Table 4.8: EPMA analyses of mesostasis and acid residuum glass in selected basalts (and in Ngauruhoe 1954 lava).

TYPE	glass	glass	glass	mes#	mes
VUW	22993	22996	22998	22998	29250
SiO_2	69.82	79.58	76.37	65.09	65.94
TiO_2	.40	.60	1.20	1.00	2.03
Al_2O_3	11.37	10.31	13.19	13.28	12.25
FeO	2.83	.98	1.44	1.86	2.40
MnO	.18	.00	.00	.00	.00
MgO	.07	.08	.00	.09	.25
CaO	.74	.38	.45	.54	3.25
Na_2O	3.86	.86	1.05	3.05	2.82
K_2O	4.84	4.59	3.68	7.20	3.35
Cl	.54	.00	.38	.57	.25
TOTAL	94.64	97.38	97.76	92.68	96.58

NOTES: # contains microlites of feldspar.
Low totals indicate contained water.

and contain grains which are commonly oscillatory zoned with a midzone packed with clinopyroxene and glass inclusions. One example (from 11965) has an An_{52} core, a 10mm wide zone containing blebs of clinopyroxene (Ca_{39} Mg_{41} Fe_{20}) and an outer An_{72} rim, similar in composition to groundmass microlites.

The dominant oxide, titaniferous magnetite, occurs both as microphenocrysts and in the groundmass. TiO_2 contents in grains from some high-alumina basalts exceed 20% (e.g. 22993, Appendix 3). Alumina-rich chromian spinels occur as inclusions in olivine in 17439 (Plate 4.5) and 22998 (Plate 4.7); Cr/(Cr+Al) is higher in 17439 (.75) than in 22998 (.61) (Appendix 3) reflecting the different liquid compositions from which these earliest phases crystallised.

Groundmass glass compositions are typically SiO_2 and K_2O -rich (Table 4.8). 22993 has rhyolitic interstitial glass with about 70% SiO_2, 4.8% K_2O and 3.9% Na_2O, throughout which are small, anhedral grains of clinopyroxene, olivine and magnetite (Plate 4.11). Plagioclase phenocrysts in contact with the glass have an outer, .01mm wide, Na-rich zone. Orthoclase is a crystallising phase in late-stage residuum of 22998.

A variety of xenoliths and xenocrysts occur in most basalts. Only 22993 and 22998 are free of such inclusions, although 22996 and 22997 contain few per thin section. High-alumina basalts, in particular, contain xenocrysts of quartz, biotite and plagioclase (up to 3mm long) with the latter having a core of oligoclase and a rim of labradorite or bytownite and a cloudy zone in between (Cole, 1970)). These commonly occur in aggregates and are considered to represent fragments of devitrified rhyolite incorporated from an upper crustal source. Waimarino basalt 17439 contains quartz-rich xenoliths up to 5cm long which sometimes show a melt-reaction relationship with host lava (see Chapter 5.3).

Table 4.9: Bulk-rock chemistry and C.I.P.W. norms of basalts.

LOC	K-T	J-R	O-K	B-L	TAR	ROT	ONG	RUAP	R-C	WAIM
VUW	22996	22997	22993	22994	21717	22991	22998	14855	11965	17439
major elements (weight %).										
SiO_2	49.7	50.7	50.9	51.3	51.3	52.6	50.6	52.7	53.1	52.8
TiO_2	1.0	1.2	1.3	1.1	.8	.8	1.1	.7	.7	.5
Al_2O_3	17.5	17.7	17.1	17.5	17.4	17.5	15.7	15.7	15.5	12.8
Fe_2O_3	1.6	1.6	1.7	1.7	1.6	1.4	1.6	1.5	1.5	1.4
FeO	8.1	7.9	8.2	8.2	8.1	7.2	7.7	7.5	7.7	7.2
MnO	.2	.2	.2	.2	.2	.2	.2	.2	.2	.2
MgO	7.1	6.0	6.3	6.0	6.3	5.9	9.4	8.8	7.8	13.3
CaO	12.3	11.1	10.7	10.8	11.5	11.3	10.4	9.7	10.4	9.7
Na_2O	2.2	3.0	3.1	2.7	2.2	2.3	2.5	2.6	2.4	1.7
K_2O	.3	.6	.4	.5	.6	.7	.6	.6	.7	.4
P_2O_5	.1	.2	.2	.1	.1	.1	.2	.1	.1	.1
C.I.P.W. norm.										
Qz	-	-	-	.1	1.7	3.0	-	.2	.4	1.8
Or	2.0	3.8	2.4	3.1	3.3	4.3	3.2	3.5	4.1	2.6
Ab	18.9	25.3	26.4	23.2	18.2	19.4	21.3	22.1	22.0	14.0
An	36.6	32.4	31.5	34.0	36.2	35.4	30.0	29.4	28.7	26.3
Di	19.2	17.3	16.6	15.2	16.6	16.4	16.3	14.8	18.0	17.3
Hy	14.6	8.3	13.0	19.6	19.8	17.8	17.5	26.5	21.6	36.3
Ol	4.3	7.9	4.8	-	-	-	6.8	-	-	-
Mt	2.3	2.5	2.4	2.4	2.3	2.1	2.3	2.2	2.3	2.1
Il	1.9	2.2	2.5	2.1	1.6	1.5	2.1	1.3	1.4	.9
Ap	.3	.4	.5	.3	.2	.2	.6	.2	.3	.1
trace elements (ppm)										
Sr	344	370	347	348	318	359	330	199	278	342
Rb	8	14	8	14	15	19	9	12	20	15
Ba	95	171	145	131	.	.	.	190	137	122
Zr	56	102	147	84	70	71	107	50	68	48
La	8#	4	13#	6	7#	.	16#	6	6#	5
Ce	17#	19	27#	18	17#	.	34#	12	12#	11
V	244	315	286	252	305	262	282	260	271	226
Cr	120	66	37	44	63	81	634	371	281	1037
Ni	37	23	32	29	15	32	172	142	63	341
Mg*	61.0	54.9	57.7	56.3	58.0	59.4	68.3	67.7	62.8	76.8
K/Rb	373	375	442	304	311	312	469	445	287	242
K/Ba	29	31	23	32	-	-	-	38	41	29
Al/Sr	265	246	257	260	286	256	250	409	295	198
Ce/Y	.85	.68	.90	.72	.89	-	-	.67	.57	.85

NOTES: Major analyses normalised to 100% volatile-free and Fe_2O_3 / FeO =.2.
I is measured $^{87}Sr/^{86}Sr$. Abbreviations as for Table 4.6.
For fuller trace element analyses see Appendix 2.2.

4.11 BULK-ROCK CHEMISTRY

4.11.1 Major element composition:

Major element compositions and C.I.P.W. norms of basalts are given in Table 4.9. Using the alumina vs. total alkalis plot of Kuno (1960), compositions fall into three distinct fields, namely high-alumina basalt, tholeiite and intermediate between high-alumina basalt and tholeiite, termed here low-alumina basalt (after Cole et al., 1983). When plotted on an AFM diagram (Fig.4.27), the basalts show a trend towards Fe-enrichment. Tholeiite has high MgO, low FeO and low alkalis whereas high-alumina basalt has much lower MgO and higher FeO. Low-alumina basalt falls in the middle of a trend between the other compositions. Total alkalis increase only slightly from tholeiite to high-alumina basalt, suggesting that this trend may be caused by olivine removal rather than plagioclase accumulation.

TiO_2 contents vary from greater than 1% in basalts of Maroa and Taupo Volcanic Centres (22993, 22994, 22996, 22997) to less than 1% in basalts of Okataina and Tongariro Volcanic Centres (21717, 22991, 11965, 14855, 17439) P_2O_5 shows a similar variation pattern which is probably due to source heterogeneiity beneath Taupo Volcanic Zone.

Four of the basalts are olivine normative (22996, 22997, 22993, 22998) and all others are quartz normative, although only 22991 has more than 3% normative quartz (Table 4.9).

4.11.2 Trace element composition:

All compositions are enriched in LILE compared to N-type MORB (Fig.4.28). However, absolute concentrations of these elements and incompatible element ratios K/Rb (Fig.4.29), K/Ba and Ce/Y show a wide range (Table 4.9). Ti and Y are correlated (Fig.4.30) and, although possibly fortuitous, this could imply a fundamentally similar source for all basaltic magma types.

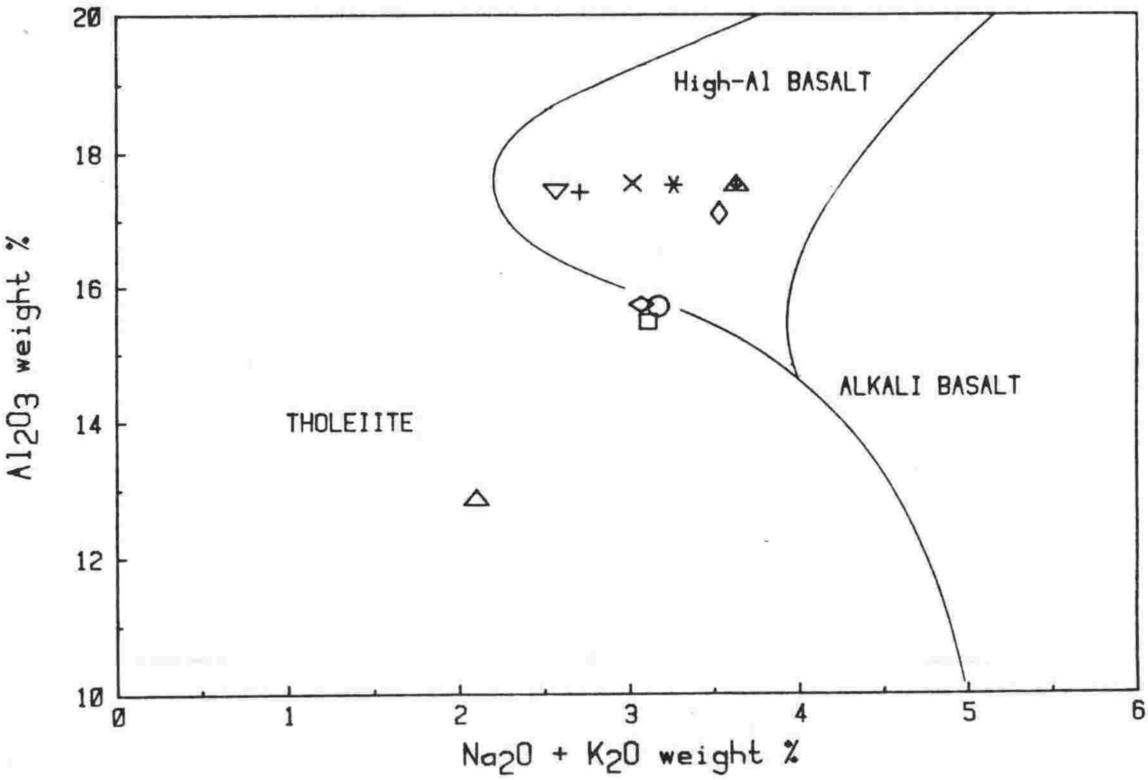

Fig.4.26: Al_2O_3 vs. $Na_2O + K_2O$ variation diagram for basalts. Fields from Kuno (1960), for basalts with 50% to 52.5% total silica.

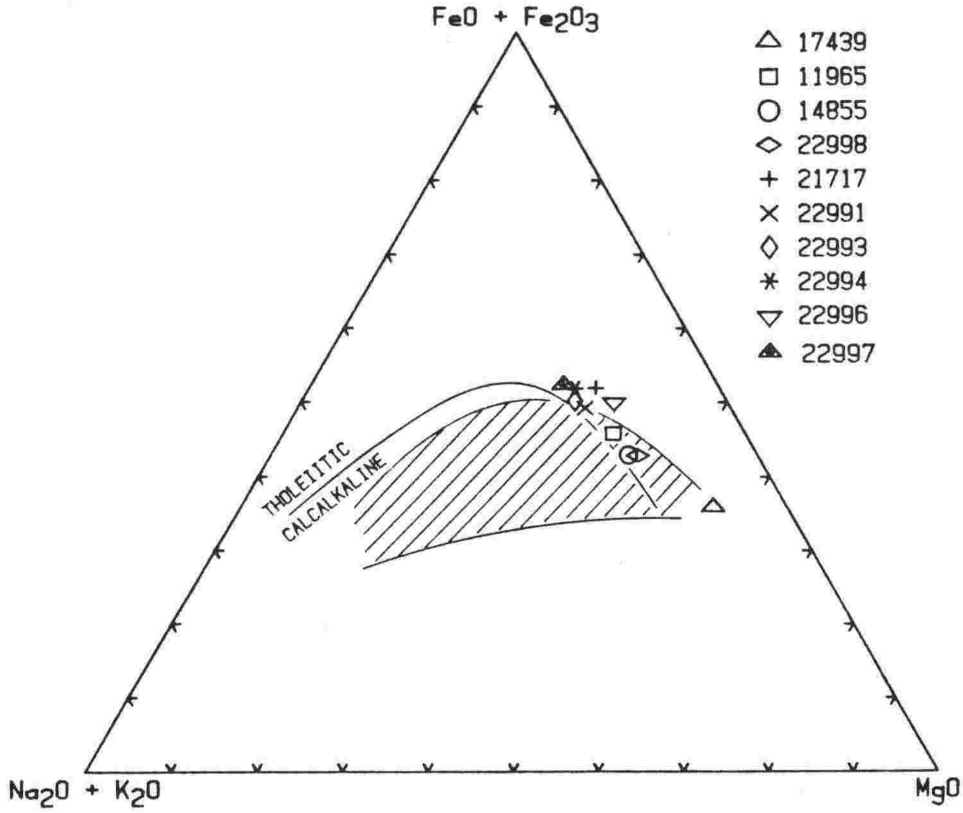

Fig.4.27: AFM diagram for basalts. Curve sparates tholeiitic from calc-alkaline lavas. Field is andesitic and dacitic lavas of Ruapehu and nearby vents.

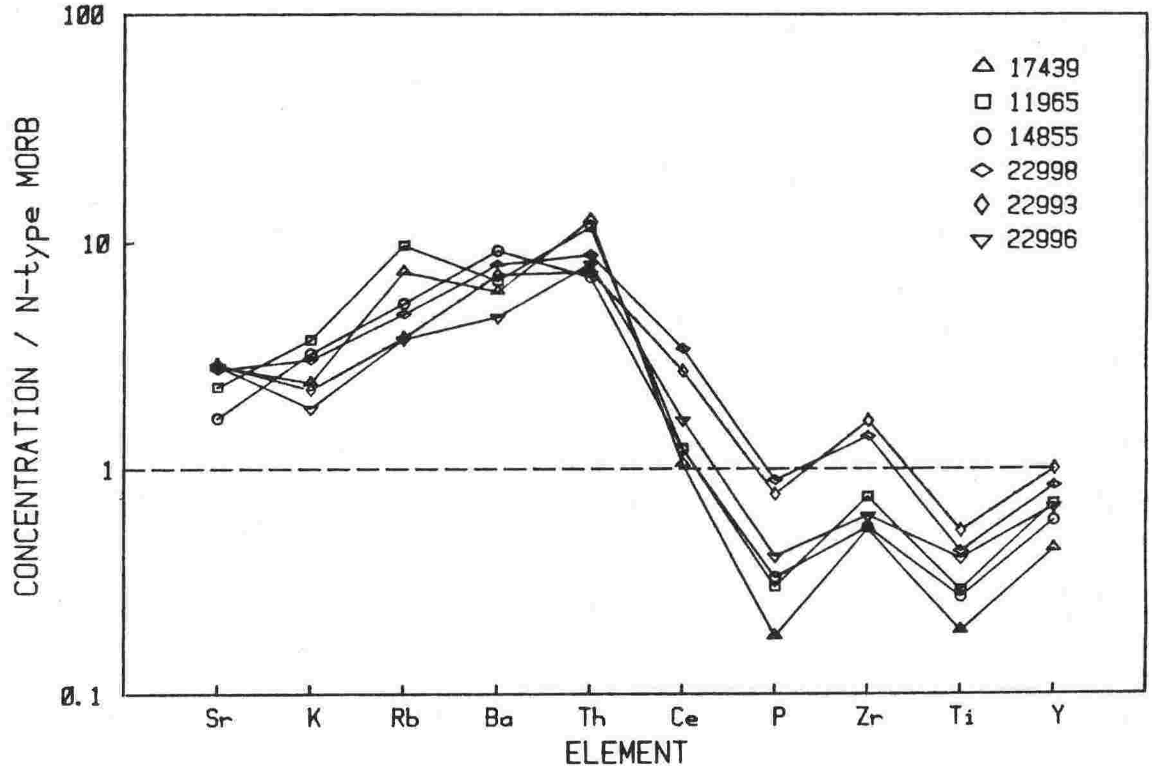

Fig.4.28: Spidergram of trace element concentrations of selected basalts normalised to N-type MORB (Pearce, 1982). For normalisation constants, see Fig.4.14.

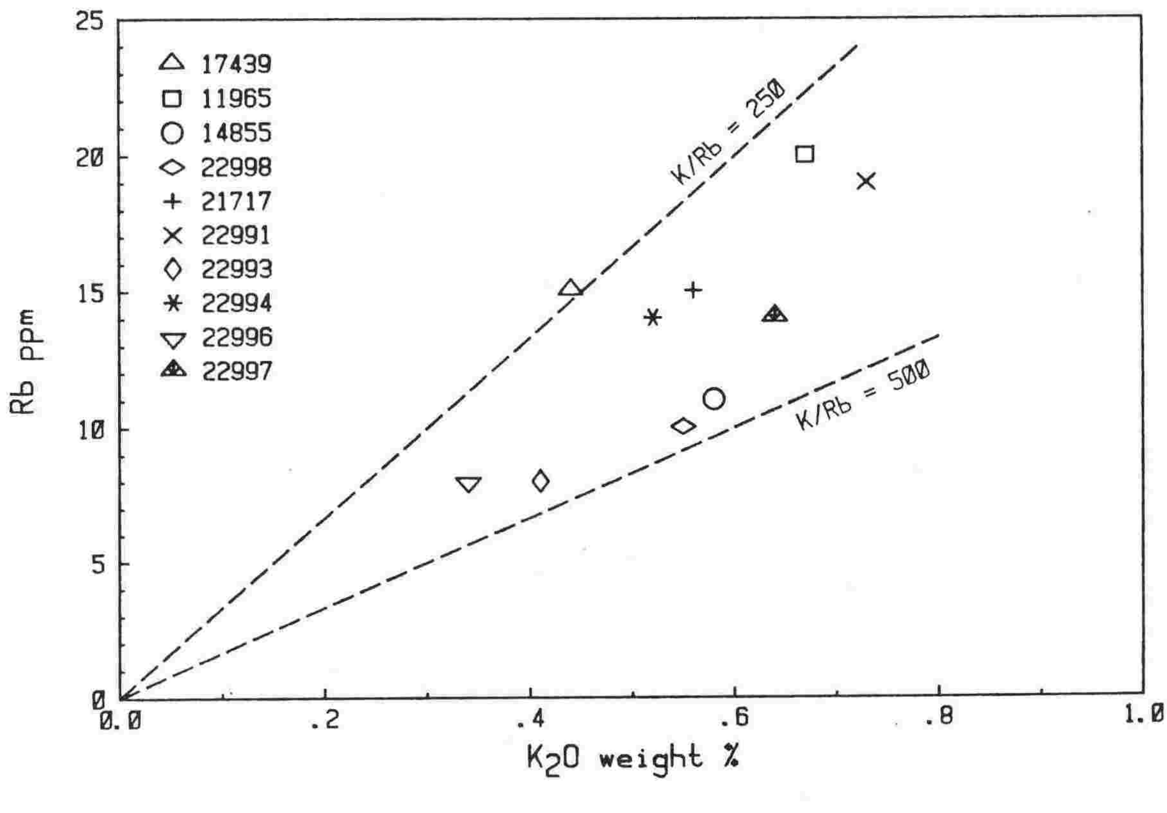

Fig.4.29: Rb vs. K_2O Harker variation diagram for basalts. Lines are for constant Rb/K ratios.

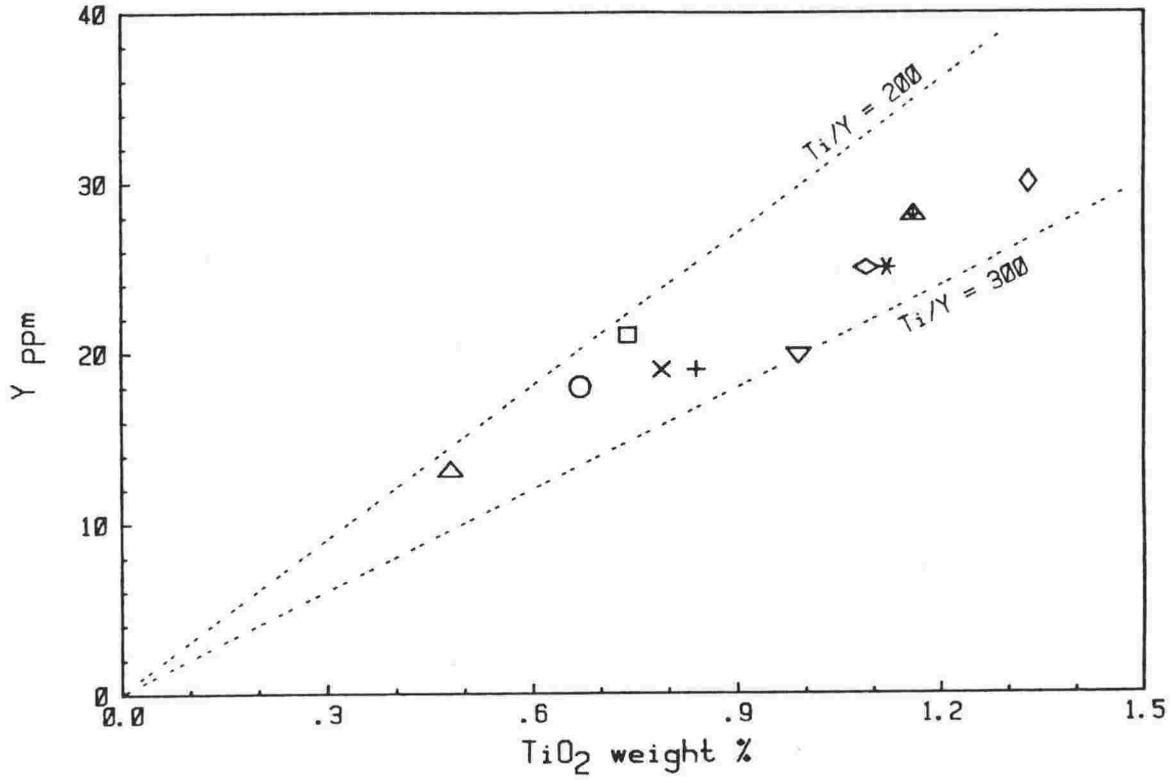

Fig.4.30: Y vs. TiO_2 Harker variation diagram for basalts. Lines are for constant Y/Ti ratios.

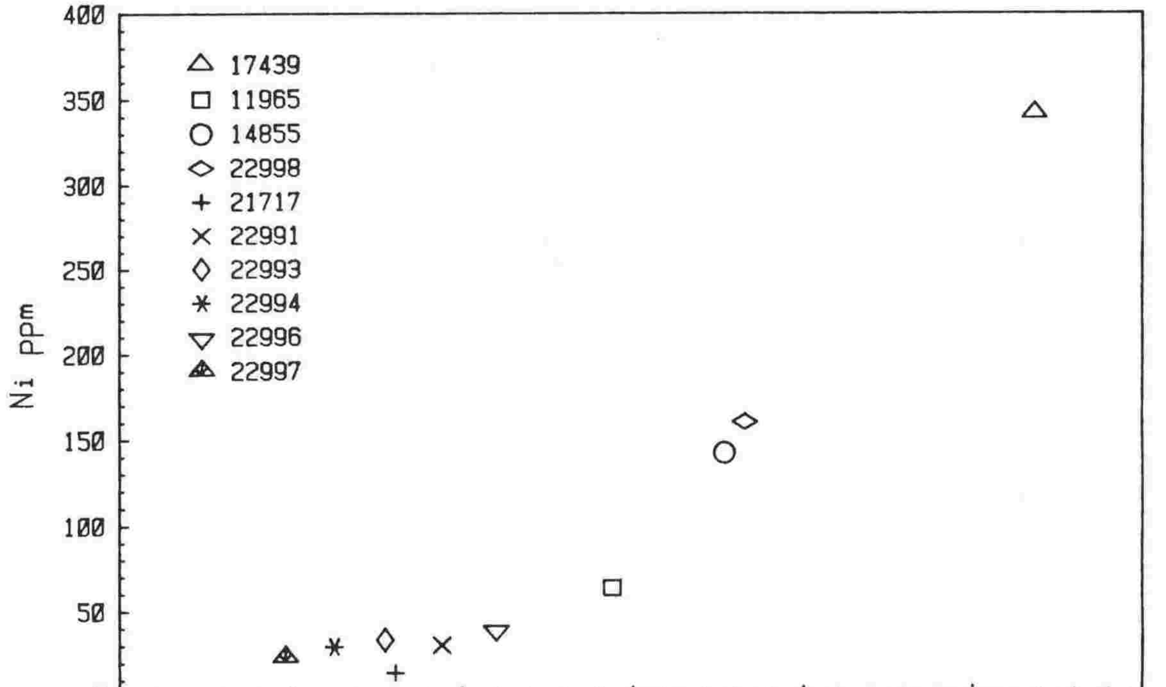

Fig.4.31: Ni vs. Mg* plot for basalts. Mg* = [Mg /(Mg+Fe^{2+})] for Fe_2O_3 / FeO = .2.

Rare-earth element compositions of three high-alumina basalts (21717, 22993 and 22996) and two low-alumina basalts (11965 and 22998) were reported by Cole et al. (1983). The data show these to be enriched in REE compared to chondritic values, and to show greater enrichment of light REE than heavy REE. Tarawera basalt (21717) is the least-enriched whilst Ongaroto basalt (22998) is the most-enriched. The patterns are typical of low-K orogenic basalts (Kay, 1980) which show negative or flat slopes and low total enrichments, and suggest they could originate from a garnet-free peridotite by fractionation of olivine and clinopyroxene (Cole et al., 1983). The flat heavy REE pattern argues against garnet involvement (Nicholls and Harris, 1980) and there is no evidence to indicate the involvement of amphibole i.e. no Ce anomaly (Jâkes and Gill, 1970).

Sr concentrations range from 200ppm (14855) to 373ppm (22997). For high-alumina basalts, there is a rough correlation between Sr and normative plagioclase contents (Table 4.9), but this is not apparent for other basalts. Cr and Ni contents are low (37-120ppm and 14-66ppm repectively) in high-alumina basalts and very high (1037ppm and 341ppm respectively in tholeiitic basalt 17439. There is a strong correlation between Ni (and Cr) content and bulk-rock Mg* (Fig.4.31) which is also consistent with the composition of olivine phenocryst cores (Fig.4.25). This indicates that all basalt types might be linked and major differences the result of olivine removal or addition. However, it should be stated that the high Cr and Ni contents of some lavas may be due to the occurrence of chromite microphenocrysts contained in olivine phenocrysts. V and Sc abundances are relatively uniform between the basalt types and show no correlation with Cr, Ni or Ti content.

Table 4.10: Isotopic compositions of basalts.

LOC	K-T	J-R	O-K	ONG	RUAP	R-C	WAIM
VUW	22996	22997	22993	22998	14855	11965	17439
$^{87}Rb/^{86}Sr$	.063	.110	.063	-	.054	.203	.126
$^{87}Sr/^{86}Sr$	.70442	.70446	.70392	-	.70492	.70462	.70455
$^{147}Sm/^{144}Nd$	.165	-	.157*	-	-	.153	-
$^{143}Nd/^{144}Nd$	.51205	-	.51215*	-	-	.51202	-
$^{206}Pb/^{204}Pb$	18.696	-	-	18.793	-	-	-
$^{207}Pb/^{204}Pb$	15.594	-	-	15.625	-	-	-
$^{208}Pb/^{204}Pb$	38.520	-	-	38.680	-	-	-
$^{0}/oo\ D^{18}Osmow$	6.3*	5.8	6.7	6.4	-	-	-

NOTES: Sr isotopic ratios calibrated against NBS987=.71025.
Nd isotopic ratios used by permission D.Froude, M.T.McCulloch.
Pb isotopic data from Armstrong and Cooper (1971).
Oxygen isotopic ratios from Blattner and Reid (1982).
Values denoted by * are different samples from the same locality.

4.12 ISOTOPE CHEMISTRY

Sr, Nd, Pb and O isotopic compositions of selected basalts are compiled in Table 4.10. $^{87}Sr/^{86}Sr$ ratios published by Ewart and Stipp (1968) range between .7042 and .7046 and are identical within the error limits given. However, re-analysis of some of their samples has revealed subtle but important differences in isotopic composition. Ratios are lowest in high-alumina basalts and range from .70392 (22993) to .70446 (22997). Waimarino basalt 17439 has a slightly higher ratio (.70455) while Red Crater basalt 11965 (.70462) and Ruapehu basalt 14855 (.70490) have the highest ratios. No clear correlation exists between $^{87}Sr/^{86}Sr$ and 1/Sr, but a crude correlation can be demonstrated between $^{87}Sr/^{86}Sr$ and $^{87}Rb/^{86}Sr$ (Fig.4.32). Linear regression of all points gives an "age" of 281 (50) Ma which might correspond to the time of a fractionation event in the source region (Carter and Norry, 1976). More likely, the correlation is an artifact of an isotopically heterogeneous mantle below the TVC or, alternatively, of crustal contamination during ascent.

$^{143}Nd/^{144}Nd$ ratios for three of the basalts (pers. comm. Dr.M.T.McCulloch and D.Froude, 1984) define a narrow range and correlate negatively with $^{87}Sr/^{86}Sr$ (Fig.4.33). The data plots away from the mantle array in the direction of $^{87}Sr/^{86}Sr$ enrichment which is normally interpreted to result from seawater contamination of subducted oceanic crust or crustal assimilation (Hawkesworth et al., 1979; Perfit et al., 1981). Nohda (1984) classified the lavas as B-2 type, similar to those found elsewhere in well-developed continental arcs where compressional stress conditions are observed in back-arc basins.

Lead isotopic ratios for two basalts are concordant within experimental error (Armstrong and Cooper, 1971). The ratios are substantially higher than for basalts of nearby Tonga-Kermadec arc (Ewart et al., 1977) or N-type MORB (Church and Tatsumoto, 1975) and therefore indicate some crustal contamination. Blattner and Reid (1982) presented oxygen isotopic data for

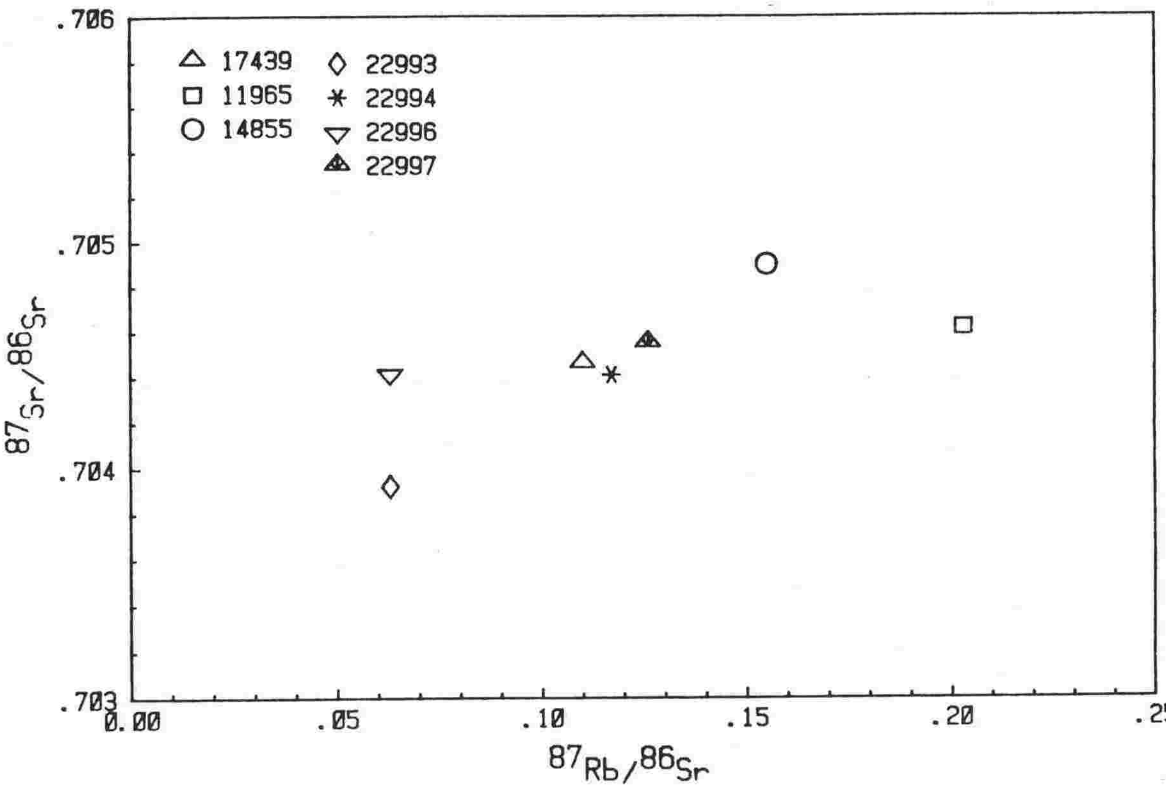

Fig.4.32: $^{87}Sr/^{86}Sr$ vs. $^{87}Rb/^{86}Sr$ diagram for basalts.

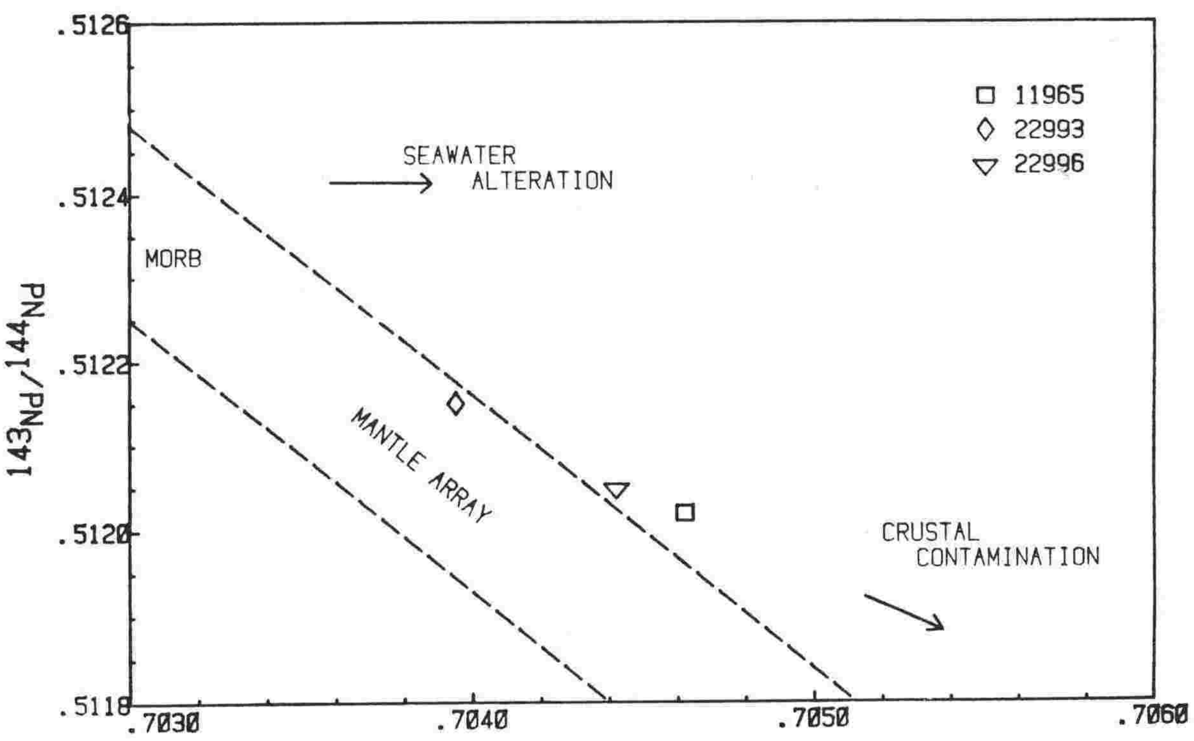

Fig.4.33: $^{143}Nd/^{144}Nd$ vs. $^{87}Sr/^{86}Sr$ diagram for basalts. Mantle array and MORB field from McCulloch and Perfit (1981).

some high-alumina basalts. Values given were significantly lower than for other lavas of the TVC (see Blattner and Reid, 1982, Fig 4).

4.13 PETROGENESIS OF BASALTS

4.13.1 General considerations:

Magma generation in a continental arc setting is a multi-stage process (Wilson and Davidson, 1984) which involves combination of a variety of components at several stages including (1) mantle wedge above subducted oceanic lithosphere (2) oceanic crust (consisting of a 10km thick slab of variably metamorphosed ocean floor basalt mantled by oceanic sediments, pelagic clays, carbonate oozes and terrigenous clastic sediments, which can be involved in both the upper parts of the subducted oceanic lithosphere and also in the base of the arc volcanic sequence) (3) seawater (which becomes indirectly involved as a result of hydrothermal alteration of subducted oceanic crust and circulation within the arc) (4) continental crust (which can contaminate magmas through fluid interaction or by assimilation of partial melts).

Evidence for non-mantle involvement in arc magma generation is found in trace element concentrations. Selective enrichment of LILE such as Sr, K, Rb, Ba, Th, LREE is observed when arc basalts are compared to N-type MORB. These elements are readily mobilised by a fluid phase and their enrichment has been attributed to metasomatism of the mantle wedge source region by hydrous fluids (IRS) derived from subducted oceanic crust (Nicholls and Ringwood, 1973). Kay (1980, 1984) showed that the trace element composition of Aleutian island arc basalts are consistent with a model involving mantle-derived magma contaminated by several percent of continent-derived sediment and partial melt of harzburgite from the subducted slab. Later this model was supported by McCulloch and Perfit (1981) who quantified the amounts of each component involved. However, Arculus and Johnson (1981) argued against this, claiming LILE enrichment in many non-arc basalts and pointing out that Sr enrichment is often uncorrelated or negatively correlated with $^{87}Sr/^{86}Sr$; such features were consistent with magma being contaminated by ^{87}Rb -poor lower crust. Most arc basalts have low abundances of HFS elements such as Nb, P, Zr, Ti, Y, Sc, Cr and HREE. This is usually attributed to high degrees of melting of the mantle source, stability of minor residual phases such as rutile, zircon or sphene in the source region or remelting of depleted mantle (Green, 1980, 1982; Pearce, 1982). Sr and Nd evidence (e.g. De Paolo and Johnson, 1979) indicates that most arc basalts are derived from sources with long-term depletion of LREE. Thus, high isotopic ratios are a powerful indication of involvement of crustal material in magma genesis.

4.13.2 Primary magmas in the Taupo Volcanic Zone?

At least three distinctive basaltic magma types occur in the TVZ. From their petrography, chemistry and isotopic compositions, each appears to have followed a separate genetic path and none truly represents unmodified primary liquid.

Wyllie (1984) reviewed constraints imposed by experimental petrology on possible and impossible magma sources and products, by using both the "forward" approach which defines the compositions of liquids generated by partial melting of source rocks at various depths, and the "reverse" approach which determines the conditions of multiple-mineral saturation at the liquidus of primitive magmas and correlates them with residual minerals of possible source rocks. Jaques and Green (1980) showed that magnesian quartz-tholeiite can be generated from 20-30% partial melting of pyrolite under water-saturated conditions, 10-15kb and 1200-1400 °C. The melts have Mg numbers close to 75 and contain Fo_{93} olivine. This olivine composition is similar to that predicted for upper mantle residual compositions after production of a basaltic melt (Sato, 1977), as required if equilibrium melting has taken place (Clarke and O'Hara, 1979). Primary magmas generated by hydrous melting of peridotite have, in addition to high Mg numbers and forsteritic olivine as a liquidus phase, high Ni (250-350ppm) and high Cr contents (500-600ppm) (Perfit et al., 1980). However, these characteristics are uncommon in arc basalts, most of which have Mg numbers less than 60 (mean=57.4; Ewart, 1976), Ni less than 50 and Cr less than 150.

Of those basalts described here, only Waimarino basalt 17439 could be primary. The bulk chemical composition and Mg number of 77 shows it capable of crystallising Fo_{92} olivine (in the range of residual mantle compositions) and Ni and Cr contents are suitably high. If shallow hydrous melting of the mantle wedge beneath the TVZ produced tholeiitic basalt, then it is probable that subducted oceanic crust provided volatile phases responsible both for initiating melting and enrichment in LILE and $^{87}Sr/^{86}Sr$. However, some interaction with continental crustal rocks during ascent is possible. Although Waimarino basalt exhibits the petrochemical criteria for primary status, other characteristics argue against this (1) such a highly porphyritic lava could have been modified compositionally by crystal accumulation or redistribution (Basaltic Volcanism Study Project, p.413) (2) olivine-liquid equilibria is dependent on the choice of suitable Kd values and the estimation of Mg number and might therefore be misleading (3) minor olivine + pyroxene accumulation could be an alternative explanation of the the high Cr and Ni concentrations (4) the lava contains small quartzose xenoliths similar to those found in other Ruapehu lavas which represent crustal material which is capable of melting and reacting with host lava (c.f. Chapter 5.3) - the occurrence of xenoliths may partly explain the relatively high $^{87}Sr/^{86}Sr$ ratio of this basalt type when compared to some others in the TVZ.

Ruapehu basalt 14855 has bulk composition which is only slightly out of equilibrium with first-formed olivine (Fig.4.25) and has lower Cr and Ni contents than Waimarino basalt. Plagioclase is an important liquidus phase and some mantled pyroxene and feldspar crystals suggest accidental accumulation from more evolved magmas. Relative to Waimarino basalt,

Table 4.11: Least squares model to generate Ruapehu basalt 14855 from Waimarino basalt 17439 (A5.1.1).

	P	D	MODEL	RESID.	PHASE	WGT%	%
SiO_2	53.0	52.9	53.0	+.08			
TiO_2	.5	.7	.7	-.02			
Al_2O_3	12.9	15.8	15.9	+.16			
FeO	8.5	8.9	9.0	+.09	Fo90	-6.37	67.01
MgO	13.3	8.8	8.9	+.08	CPX1	-3.14	32.99
CaO	9.7	9.8	9.8	+.07	An50	+15.88	0.00
Na_2O	1.7	2.6	2.3	-.27	MT10.0	+2.33	0.00
K_2O	.4	.6	.4	-.19			

CRYSTALS ADDED = 18.21%

SUM SQUARES RESID. = .1631 CRYSTALS REMOVED = 9.51%

	P	D	MODEL	BULK DC	% ERROR
Rb	15	11	13	.01	+ 18.2
Ba	122	185	112	.01	- 39.5
Zr	48	50	43	.09	- 10.4
Sr	342	201	415	.03	+106.5
V	226	251	338	.42	+ 34.7
Cr	1037	380	1356	3.97	+256.8
Ni	341	142	195	7.61	+ 37.3

NOTE: For methods, see Appendix 5.

Table 4.12: Least squares model to generate Ongaroto basalt 22998 from Waimarino basalt 17439 (A5.1.3).

	P	D	MODEL	RESID.	PHASE	WGT%	%
SiO_2	53.0	50.9	51.2	+.29			
TiO_2	.5	1.1	1.0	-.14			
Al_2O_3	12.9	15.8	16.1	+.26			
FeO	8.5	9.2	9.5	+.30	Fo90	-3.70	100.00
MgO	13.3	9.4	9.5	+.14	CPX1	+.37	0.00
CaO	9.7	10.5	10.6	+.08	An70	+20.89	0.00
Na_2O	1.7	2.5	1.8	-.71	MT17.5	+4.05	0.00
K_2O	.4	.6	.3	-.23			

CRYSTALS ADDED = 25.31%

SUM SQUARES RESID. = .8438 CRYSTALS REMOVED = 3.70%

	P	D	MODEL	BULK DC	% ERROR
Rb	15	10	12	.01	+ 20.0
Ba	122	197	96	.01	- 51.3
Zr	48	125	38	.01	- 69.6
Sr	342	330	407	.01	+ 23.3
V	226	220	386	.08	+ 75.5
Cr	1037	550	1869	1.00	+239.8
Ni	341	160	321	8.40	+100.6

Ruapehu basalt has higher concentrations of Ti, Al, Fe, P and alkalis, and lower concentrations of Mg, Cr, Ni and Sr. The two compositions cannot have been generated from the same source because they have significantly different Sr/Al (198 vs. 409) and K/Rb (224 vs. 445) (Table 4.9) - both these ratios should be unaltered by small degrees of crystal fractionation. These and other chemical differences are quantified by least squares mixing models (e.g. Table 4.11) which attempt to derive Ruapehu basalt from Waimarino basalt by fractionating olivine, clinopyroxene, plagioclase and magnetite (methods are outlined in Appendix 5). The models fail because, to obtain the best fit, both plagioclase and magnetite must be added, which is petrologically unreasonable and denied by the Sr and V contents. Alternatively, if olivine and clinopyroxene only are removed, predicted values for Rb, Sr and Cr are too high. Ruapehu basalt has the highest $^{87}Sr/^{86}Sr$ ratio of any basalt analysed but has a relatively low Rb content. This tends to reduce the importance of crustal contamination in its petrogenesis unless the contaminant is very old. It is probable, therefore, that Ruapehu basalt represents a second primitive magma type which could not have evolved from a primary composition similar to Waimarino basalt. Sr concentrations and incompatible element ratios indicate that the source regions for the two magmas were not identical and this may be the main explanation for the difference in Sr isotopic composition between them.

Red Crater basalt 11965 is similar in many respects to Ruapehu basalt having plagioclase and orthopyroxene phenocrysts and moderate Cr and Ni contents. Olivine is only slightly out of equilibrim with bulk-rock composition but is nevertheless often mantled by orthopyroxene. Pyroxene xenocrysts occur frequently and are rimmed by more Fe-rich compositions which are equilibrated with late-stage liquid. Red Crater basalt has higher incompatible element concentrations than either Waimarino or Ruapehu basalt. Although it has a relatively high Rb content (20ppm), its $^{87}Sr/^{86}Sr$ ratio (.70462) is less than Ruapehu basalt (.70490). Derivation of Red

Crater basalt from a Waimarino basalt-type parent by crystal fractionation (Model A5.1.2 in Appendix 5) yields a similar model, with similar difficulties, to that for Ruapehu basalt. Derivation of Red Crater basalt from Ruapehu basalt must imply accumulation of plagioclase to account for the higher Sr content. However, this is not predicted by the best-fit model (A5.1.3) which indicates clinopyroxene addition. It is concluded, therefore that Red Crater basalt represents a magma type which is similar in most respects to Ruapehu basalt but with higher Sr and LILE content and lower Sr isotopic ratio. These differences were inherited from an inhomogeneous mantle source and were not assumed from subsequent processes such as fractionation or contamination.

Ongaroto basalt 22998 is the third low-alumina basalt type described. Its origin was discussed by Cole (1973) who considered that the higher MgO, Ni and Cr contents relative to high-alumina basalt indicated that the rock was accumulative in olivine. However, this possibility is not supported by petrographic or chemical data presented here; olivine is in equilibrium with bulk-rock (Fig.4.25) and the Ni content is commensurate with Mg* (Fig.4.21). Cole et al. (1983) re-assessed the petrogenesis of Ongaroto basalt in the light of REE data and concluded that the lava was derived from a different mantle source or, alternatively, was contaminated. However, the high REE content cannot be easily explained by different restite phases in the source (e.g. apatite, garnet) since the overall pattern is similar to that of other basalts. Also they cannot be explained by crustal contamination because there is no evidence for this, either from the occurrence of xenoliths or high incompatible element contents. By comparison with the other low-alumina basalts (14855 and 11965), Ongaroto basalt has lower silica, K and Rb and higher Mg, Ni, Cr, Ti, Zr, Sr and REE and cannot, therefore, be derived from them by crystal fractionation. Some of these features also preclude derivation from a Waimarino basalt-type parent (Table 4.12), unless accumulation of plagioclase and magnetite occurs.

High-alumina basalts (HAB) constitute a chemically distinctive group of lavas which show petrographic, and some isotopic, diversity. Where present, olivine is in equilibrium with bulk-rock composition (Fig.4.25). Clinopyroxene, which sometimes occurs as large, complexly zoned phenocrysts is more commonly restricted to groundmass and is interstitial to plagioclase phenocrysts. Lavas are often highly vesicular but contain no hydrous minerals. LILE and HFS incompatible element contents are similar to other basalts but Cr and Ni concentrations are consistently low.

Cole (1973) proposed a model in which high-alumina basalt was generated by partial melting of mantle peridotite (Kuno, 1960) at depths of 30-35km (Green and Ringwood, 1967). He noted that "....the similarity in chemistry between the basalts shows that little fractionation occurred within the crust and suggests that the basalts which reached the surface came from a common source, probably at the base of the crust. The speed at which the magma rose is indicated by the texture, the aphyric Tarawera basalt rising more rapidly than the porphyritic basalts of the Maroa Caldera". Recent studies have shown that many high-alumina basalts which were formerly interpreted to be primary magmas (Shido et al., 1971) are plagioclase phyric with phenocrysts that are too calcic to have crystalised from the host magma. These do not reflect liquid compositions and derive their composition through phenocryst accumulation (Rhodes and Dungan, 1979). However, a few are aphyric with plagioclase on the liquidus and are unlikely to have aquired their composition through phenocryst accumulation. Kushiro (1979) suggested that such magmas may have crystallised along the olivine-plagioclase cotectic at high water pressures prior to eruption. The equilibrium constant for plagioclase-melt exchange reactions is strongly dependent on both temperature and water pressure (Drake, 1976), making calculations difficult. However, given T = 1100 °C and Pwater = 1kb, equilibrium plagioclase compositions should near An_{70}, and these are

Table 4.13: Least squares model to generate Ben Lomond Road basalt 22994 from Waimarino basalt 17439 (A5.1.5).

	P	D	MODEL	RESID.	PHASE	WGT%	%
SiO_2	53.0	51.4	51.5	+.12			
TiO_2	.5	1.1	1.3	+.14	PHASE	WGT%	%
Al_2O_3	12.9	17.6	17.7	+.13			
FeO	8.5	9.8	9.9	+.08	Fo90	-11.67	100.00
MgO	13.3	6.0	6.1	+.07	CPX1	+.20	0.00
CaO	9.7	10.8	10.9	+.05	An60	+31.55	0.00
Na_2O	1.7	2.8	2.4	-.37	MT17.5	+6.16	0.00
K_2O	.4	.5	.3	-.22			

CRYSTALS ADDED = 37.91%

SUM SQUARES RESID. = .2508 CRYSTALS REMOVED = 11.67%

	P	D	MODEL	BULK DC	% ERROR
Rb	15	14	9	.01	- 35.7
Ba	122	129	76	.01	- 41.1
Zr	48	84	30	.01	- 64.3
Sr	342	348	462	.01	+ 32.8
V	226	252	434	.08	+ 72.2
Cr	1037	44	2001	1.00	+4447.7
Ni	341	29	229	8.40	+689.7

Table 4.14: Least squares model to generate Orakeikorako basalt 22993 from Ongaroto basalt 22998 by olivine-clinopyroxene fractionation (A5.1.9).

	P	D	MODEL	RESID.	PHASE	WGT%	%
SiO_2	50.9	51.0	51.5	+.45			
TiO_2	1.1	1.3	1.2	-.11	PHASE	WGT%	%
Al_2O_3	15.8	17.2	17.4	+.20			
FeO	9.2	9.8	9.3	-.46	Fo90	-5.89	61.12
MgO	9.4	6.4	6.5	+.14	CPX1	-3.75	38.88
CaO	10.5	10.8	10.7	-.10			
Na_2O	2.5	3.1	2.8	-.30			
K_2O	.6	.4	.6	+.18			

SUM SQUARES RESID. = .6191 CRYSTALS REMOVED = 9.64%

	P	D	MODEL	BULK DC	% ERROR
Rb	10	8	11	.01	+ 37.5
Ba	197	145	218	.01	+ 50.3
Zr	125	147	137	.10	- 6.8
Sr	330	347	364	.04	+ 4.9
V	220	286	232	.48	- 18.9
Cr	550	37	386	4.50	+673.0
Ni	160	33	65	9.91	+ 97.0

observed (Table 4.7). The lack of plagioclase phenocrysts with highly calcic cores and the aphyric nature of some lavas (e.g.21717) indicate that the rocks crystallised under relatively anhydrous conditions at low pressures and have not accumulated significant amounts of plagioclase.

Primary magmas generated from peridotitic mantle invariably have high Mg numbers, Ni and Cr contents and forsteritic olivine on the liquidus (see above). High-alumina basalts of the TVZ exhibit none of these features and have plagioclase as a liquidus phase. This might suggest that the magmas were generated by fractionation (mainly of olivine) from a primary liquid. Attempts to model this using Waimarino basalt as the parent are unsuccessful (A5.1.5 & A5.1.6). Difficulties arise (Table 4.13) because, to achieve the high Al_2O_3 contents of HAB, large amounts of plagioclase must be added. This, for reasons given above is petrographically unreasonable and the different Al/Sr ratios (245-285 in HAB, 198 in 17439) produce unacceptably large Sr misfits. K/Rb ratios are also different (304-442 in HAB, 242 in 17439) but other incompatible element ratios are comparable (Table 4.9). From a low-alumina basalt parent, most HAB can only be generated by addition of plagioclase, magnetite and/or clinopyroxene (A5.1.7 & A5.1.8) and the models fit badly for Cr and Ni. If only olivine and clinopyroxene are fractionated (A5.1.9), there is a poor major element fit and still a Cr-Ni misfit (Table 4.14). Thus, it is considered that high-alumina basalt must represent a distinct magma type whose bulk-rock chemistry is not easily explained as resulting from modification of either primary tholeiite or low-alumina basalt.

4.14 SUMMARY AND CONCLUSIONS

It is likely that Taupo Volcanic Zone basalts represent several different primitive magma types, none of which is truly primary. All show chemical and isotopic evidence of contamination of source mantle by IRS fluids but only minor interaction with upper crustal material. Similarities of petrography and bulk-rock chemistry define three main magma types i.e. high-alumina basalt - low-alumina basalt - tholeiite. Within this spectrum there are subtle differences in incompatible element contents and isotopic composition which indicate heterogeneiity in the sub-continental source. Each basalt-type is spatially separated which suggests that they may not be directly related to each other by processes such as crystal fractionation or accumulation. Models which attempt to show such a relationship fail because of differences in incompatible element ratios, Al/Sr and Sr isotopic composition.

****

CHAPTER 5: PETROGRAPHY AND CHEMISTRY OF XENOLITHS

****

5.1 INTRODUCTION

5.1.1 Aims:

Few models of andesite petrogenesis which involve assimilation of continental crust properly define the nature of the crustal component. Xenoliths should be a particularly useful guide to the composition of potential assimilants and also, in some instances, the nature of the contamination process. These are abundant in lavas of Ruapehu and nearby vents, thus offering a rare opportunity to qualitatively assess the viability of using sedimentary basement lithologies, or partial melts of them, as endmembers in crustal assimilation mixing models.

In this chapter, a wide variety of xenolith types are described. These range from upper-crustal inclusions of largely unaltered volcanic and metasedimentary rocks to highly metamorphosed and/or partially melted equivalents of these rock types. Since the main purpose of the study is to investigate constraints on crustal contamination models for andesite petrogenesis, most emphasis is placed on description and interpretation of those xenolith types which are volumetrically and temporally significant and which show evidence of interaction with host lava. For completeness, however, xenoliths which are considered rare, are of unknown origin or seem to be of little importance as crustal contaminants are also described.

Most of the xenoliths are included in recent lavas of Ruapehu and Ngauruhoe. In some lavas (e.g. Ngauruhoe 1954) they make up more than 1% of the mode, but usually only a few mm to cm-sized fragments occur per cubic metre of lava (W.R.Hackett, pers.comm., 1984).

5.1.2 Previous studies:

Steiner (1958) described the petrography of vitrified, quartzose and feldspathic xenoliths from Ngauruhoe 1954 lava, providing a framework for the wider chemical study included here. The significance of those xenoliths to andesite petrogenesis was discussed by Ewart and Stipp (1968) in an isotopic and trace element study of TVZ volcanism, by Cole (1978) in a description of TVC andesites and by Blattner and Reid (1982) in an assessment of oxygen isotope data of TVZ lavas.

5.1.3 Xenolith lithologies:

Classification of xenoliths is, to some extent, arbitrary and has been attempted mainly to simplify description and chapter organisation:

TYPE UCX (upper crustal xenoliths) - these include several rare lithologies, many of which can be directly related to known sedimentary basement in the vicinity of the TVC on the basis of mineralogy, bulk-rock chemistry and isotopic composition.

TYPE VX (vitrified xenoliths) - these xenoliths occur only in Ngauruhoe and Pukeonake lavas and contain more than 50% glass representing partial melting of an original metagreywacke composition.

TYPE QX (quartzose xenoliths) - these include schists and gneisses which occur only in Iwikau Member pyroclastics on the northern slopes of Ruapehu, sacchoroidal quartz-rich xenoliths which are widespread and abundant and several other rare lithologies.

TYPE QPX (quartz-poor xenoliths) - these include rare biotite- and/or spinel-rich schists and more-abundant feldspar-rich xenoliths with granulitic textures and refractory chemistries.

TYPE IX (igneous xenoliths) - these include variably-altered blocks of surface volcanics, a natralunite-bearing nodule and cumulate nodules.

TYPE MIX (metaigneous xenoliths) - these xenoliths have basic to intermediate calc-alkaline chemistries and have strong metamorphic textures distinguishing them from TYPE IX xenoliths.

Table 5.1: Bulk-rock chemistry of TYPE UCX xenoliths 17452 (porcellanite) 17428, 17429, 17897 (metagreywacke); 17895, 17896 (calcsilicate). Tertiary siltstone 17856 is given for comparison.

VUW	17452	17856	17428	17429	17897	17895	17896
major elements (weight%)							
SiO_2	58.0	55.3	63.9	67.8	70.4	47.5	53.0
TiO_2	.7	.5	.8	.6	.4	.4	.4
Al_2O_3	15.5	11.6	16.7	17.0	11.9	10.1	11.5
Fe_2O_3	6.0	3.8	5.9	4.5	4.2	5.2	3.5
MnO	.2	.2	.1	.1	.1	.3	.2
MgO	2.1	1.5	1.7	1.3	1.3	1.2	.9
CaO	10.1	11.9	2.2	1.0	3.2	34.6	29.4
Na_2O	2.4	2.4	3.1	4.4	3.0	.1	.3
K_2O	2.4	1.9	2.7	3.1	1.4	.1	.1
P_2O_5	.2	.1	.2	.1	.1	.2	.3
LOI	2.2	10.6	3.1	.4	3.8	.2	.3
Total	99.8	99.8	99.4	99.3	99.8	99.9	99.9
trace elements (ppm)							
Ba	567	365	649	548	289	-	-
Ce	59	40	59	49	43	-	-
Cr	73	53	58	43	38	-	-
Rb	68	74	110	129	63	2	2
Sr	336	293	207	171	225	222	1158
Th	11	9	13	13	10	4	10
Y	26	20	27	25	19	23	27
Zr	169	150	186	242	119	-	-
Rb/Sr	.20	.25	.53	.75	.28	.01	.00
I	.70931	.70840	.71056	.71246	.70949	.70507	-

NOTES: All iron is Fe_2O_3 , I = $^{87}Sr/^{86}Sr$.

5.2 TYPE UCX - UPPER CRUSTAL XENOLITHS

TYPE UCX are inclusions of known sedimentary basement lithologies (i.e. Torlesse or Waipapa greywacke or Tertiary siltstone) which have undergone only minor mineralogical and chemical modification.

5.2.1 Porcellanite:

Yellow-brown 50x50x50mm porcellanitic blocks (e.g.17452) occur only in ejecta at Ohakune. In these blocks, sintering of original clays has produced a transluscent matrix surrounding scattered sub-rounded quartz and plagioclase grains. The latter have compositions ranging from $An_{29}Ab_{52}Or_{19}$ to $An_{53}Ab_{44}Or_{3}$. Minor amounts of aluminous ferrosalite ($Ca_{49}Mg_{15}Fe_{36}$) and rare zircon are also present. Bulk-rock chemistry and Sr isotopic composition of 17452 are similar to that of calcareous siltstone of Tertiary age from near Ohakune (Table 5.1). If such is the true source of porcellanitic xenoliths, then it indicates a near-surface origin. Incorporation has caused thermal reconstitution mainly by dehydration and alteration of calcite + mica to form pyroxene. However, the lack of reaction at the xenolith-host contact and the short time the xenolith was in the lava prior to eruption suggest that any chemical or isotopic exchange with host would have been small and effective within a small radius of the inclusion. Tertiary sediments form only a thin veneer above greywacke basement in the vicinity of the TVC and xenoliths which show clear petrographic and/or chemical similarities with Tertiary sediments are, significantly, found only in Ohakune lavas, which rise through the thickest part of that sequence.

5.2.2 Metagreywacke:

Rare inclusions of metagreywacke occur in some lavas of Ruapehu (17428, 17429) and Tongariro (17897, 17898 - these are float blocks from near the summit and are assumed to be xenoliths; pers. comm. Prof.R.H.Clark, 1984). Examples are well-indurated and foliated and show little effect of

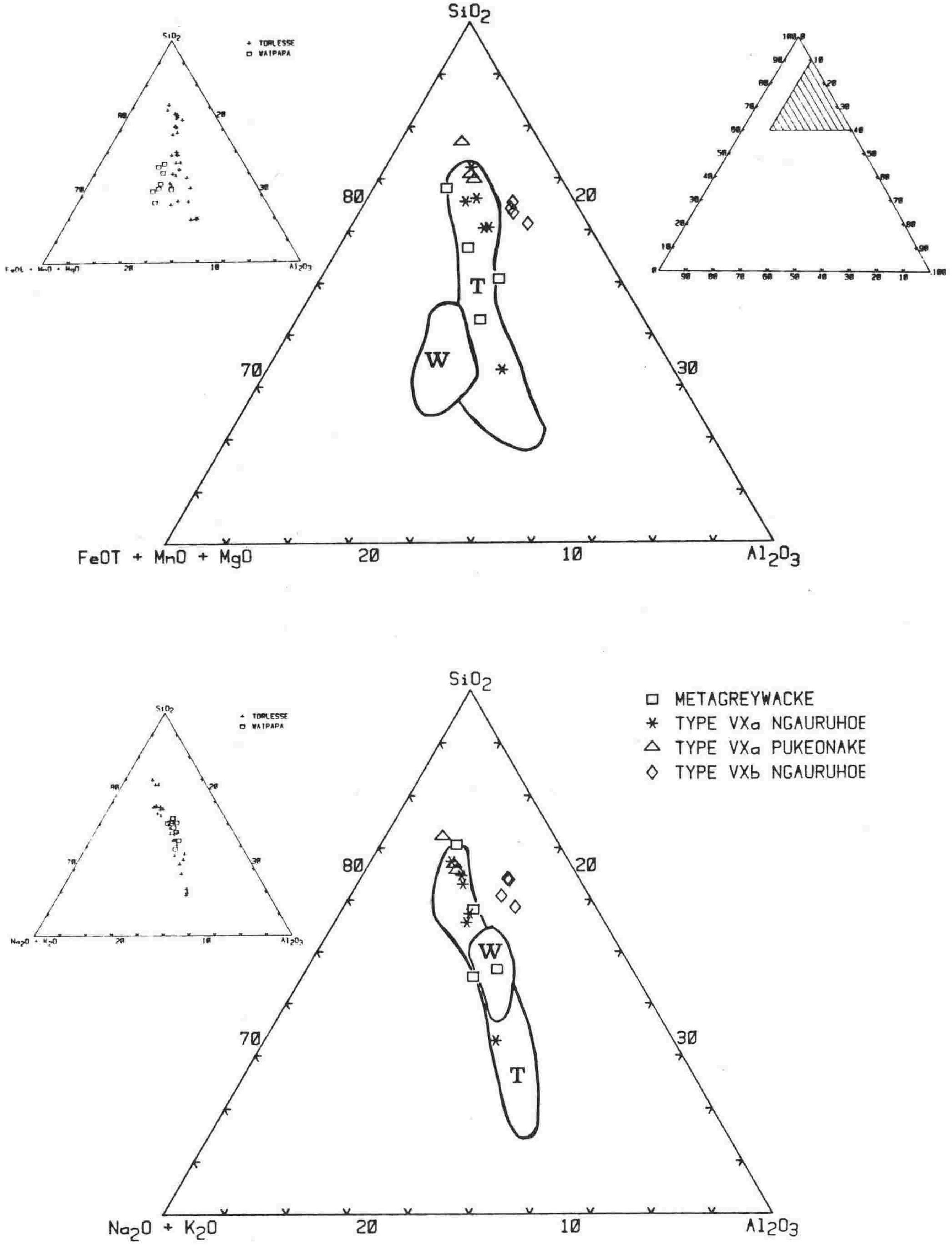

Fig.5.1: Triangular plot of metagreywacke and TYPE VX xenolith bulk-rock compositions (a) SiO_2 - FeO + MnO + MgO - Al_2O_3
(b) SiO_2 - Na_2O + K_2O - Al_2O_3
Fields are for Torlesse (T) and Waipapa (W) terrane metasediments (raw data are plotted on inset figure). Main plot is restricted in area (2nd inset).

pyrometamorphism except for variable degrees of dehydration. Textures and mineral assemblages are similar to Torlesse terrane metasediments; the assemblage (quartz) - albite - chlorite - muscovite - epidote (see Appendix 3 for EPMA analyses) is also found in Rangipo Torlesse suite lithologies (Chapter 3.2). Bulk-rock chemistry (Table 5.1; Fig.5.1) is consistent with such a link, as is Sr isotopic data (Fig.5.2) - three metagreywacke xenoliths plot close to the Rangipo Torlesse isochron. Blattner and Reid (1982) showed that 17897 (listed by them as sample 24013 and erroneously attributed to Ngauruhoe 1954 lava) has an oxygen isotopic ratio of 12.5 permil, close to that of average Torlesse terrane rocks (12.0 permil). These data indicate that metagreywacke xenoliths could be derived directly from Torlesse terrane metasediments having undergone little or no chemical change subsequent to inclusion. They are, moreover, rare occurrences with no significant influence on andesite petrogenesis.

5.2.3 Calcsilicate:

Two xenoliths from Ngauruhoe 1954 and Tongariro lavas, have mineral assemblages dominated by wollastonite. The first of these, 17895, is small (25x5mm), elongated and black-white flecked. It has coarse (.2-.5mm) interlobate wollastonite and anorthite with interstitial green-brown pleochroic ferrosilite (.1-.2mm) sometimes aggregating to form cm-wide layers. Apatite is a rare accessory. The second, 17896, is a brownish-white xenolith described by Steiner (1958, p.342) as "....a fragment of thermally metamorphosed schist". The rock has a xenoblastic to nematoblastic texture and fine grainsize (.05-.1mm), with frequent coarser patches (.2-.5mm) aligned parallel to a strong foliation. The mineral assemblage is wollastonite, anorthite, quartz and minor sphene (Appendix 3). Bulk-rock chemistries (Table 5.1) indicate very high Ca contents, consistent with high proportions of modal wollastonite.

Nicholls (1971) described similar xenoliths in lavas of Santorini Volcano, Greece. He considered these to represent fragments of basement

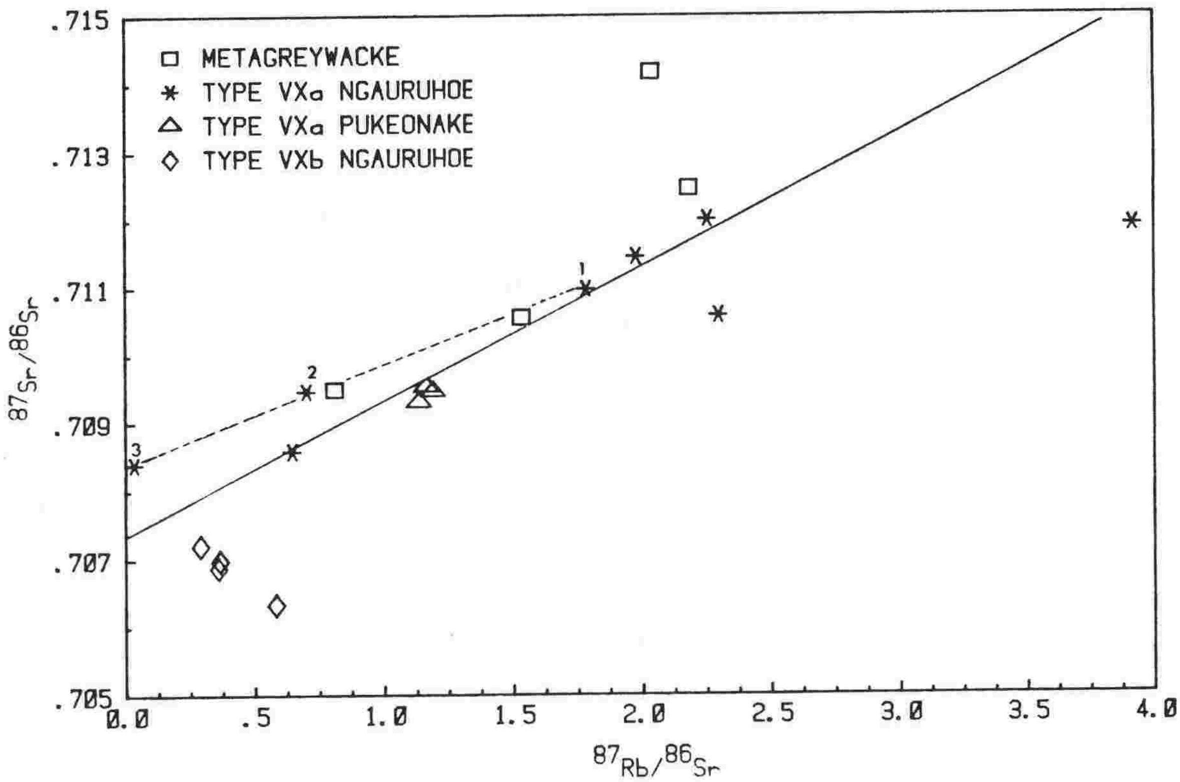

Fig.5.2: Rb-Sr whole-rock isochron plot of metagreywacke and TYPE VX xenoliths. Rangipo Torlesse suite 139 Ma isochron is given for comparison. Separates of TYPE VXa xenolith 17470 are linked (dotted line); 1 = vein-free 17471, 2 = bulk-rock 17470, 3 = quartz + plagioclase + wollastonite vein 17472.

marble, altered by thermal metamorphism and metasomatism at low fluid pressures and temperatures close to, or greater than 800 °C. A similar origin is suggested for 17895 and 17896 both of which could be derived from the Torlesse terrane, since limestones within it provide suitable source rocks. However, the low Sr isotopic ratio of 17895 (Table 5.1) is puzzling if the Torlesse terrane, with Sr isotopic ratios usually greater greater than .70700 (Chapter 3.2), is the source.

5.3 TYPE VX - VITRIFIED XENOLITHS

The occurrence of highly vitrified xenoliths in recent lava flows of Ngauruhoe was reported by Speight (1908), Grange and Williamson (1930), Battey (1949) and Cloud (1951). The 1954 flows, in particular, contain an abundance of xenoliths and some of these were described petrographically by Steiner (1958). Numerous vitrified xenoliths up to 1m in diameter occur in Ngauruhoe lava flows erupted on 18-8-54 and 16-9-54 (Fig.4.2), but are less common in earlier flows (Steiner, 1958). Similar xenoliths occur at Pukeonake as rare clasts. There are two chemically distinct types: TYPE VXa are compositionally similar to Torlesse terrane metasediments; TYPE VXb are dissimilar to either Torlesse or Waipapa terrane lithologies.

5.3.1 Petrography:

In hand-specimen, TYPE VXa display relict banding and lensoid structure (Steiner, 1958) of alternating light-coloured, quartz-rich layers and darker, quartz-poor layers (Plate 5.1B). The lamellae are often parallel, contorted and discontinuous over a few cm. Some examples (e.g.17470) have cross-cutting veins composed of quartz, wollastonite and plagioclase.

Plate 5.1: Petrographic features in hand-specimen of selected TYPE VX xenoliths; A - contact between 17474 and host lava (29250); B - layering of quartz-rich and quartz-poor segregations in 17469.

Plate 5.2: BEI photograph of TYPE VXa xenolith 17475. Sieved cordierite (dark grey) is surrounded by granitic glass (lighter grey). The grain has euhedral margins and is unzoned.
Scale bar = .01mm; field of view = .06mm

Plate 5.3: BEI photograph of quartz-rich association of TYPE VXa xenolith 17465. Minerals are quartz (dark grey, rounded), hypersthene (small, white quench crystals) and granitic glass (light grey, interstitial). Black areas are vesicles.
Scale bar = .1mm; field of view = .23mm.

Plate 5.4: BEI photograph of assemblage in TYPE VXb xenolith 17460. Cordierite (dark grey, middle & upper LHS) contains euhedral pleonaste (white). Plagioclase (light grey to dark grey) is marginal to the cordierite. Glass (very light grey, lower LHS) surrounds the both minerals.
Scale bar = .01mm; field of view = .13mm.

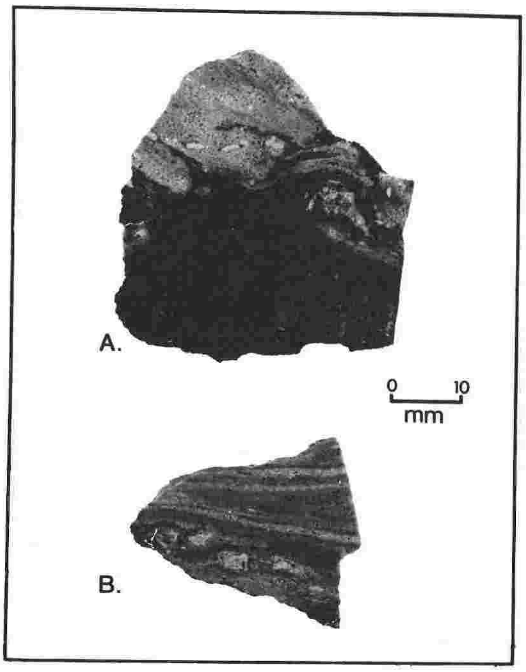

Plate 5-1

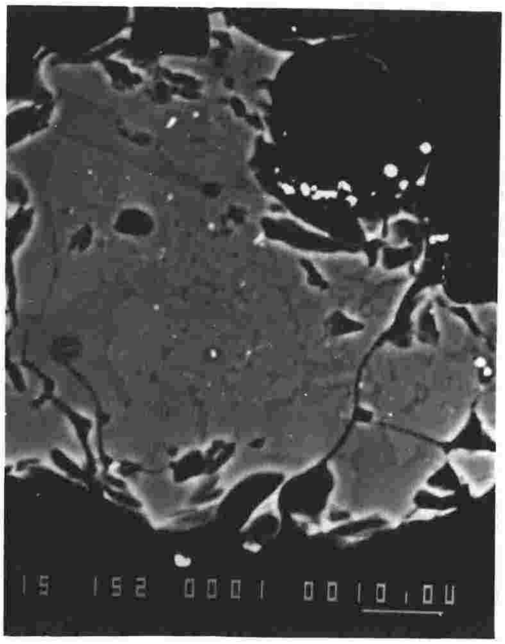

Plate 5-2

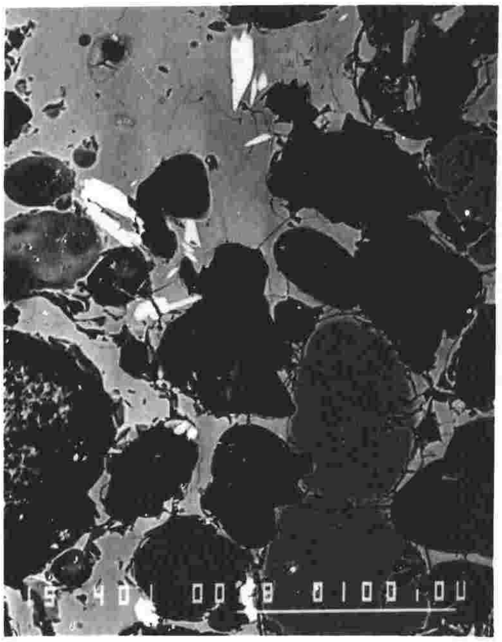

Plate 5-3

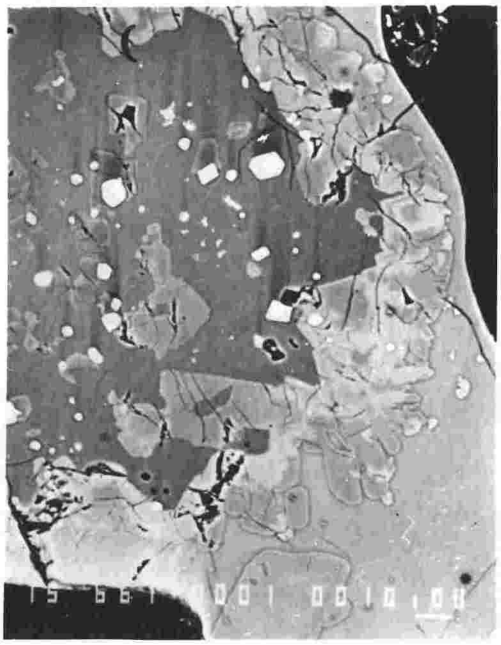

Plate 5-4

Table 5.2: Bulk-rock chemistry of selected TYPE VX xenoliths.

VUW	17465	17471	17469	17474	17461	17453	17475	17473	17464	17460
TYPE	VXa	VXa	VXa	VXa	VXa	VXa	VXa	VXb	VXb	VXb
LOC.	N54	N54	N54	N54	N54	PUK	PUK	N54	N54	N54
major elements (weight%)										
SiO_2	62.9	71.5	72.5	74.3	74.9	75.0	77.6	72.0	72.6	74.6
TiO_2	.8	.6	.5	.5	.4	.4	.4	.2	.2	.2
Al_2O_3	19.3	15.4	15.4	13.9	13.1	13.7	12.2	17.1	16.2	16.2
Fe_2O_3	.9	.5	.6	.6	.4	.5	.5	.3	.4	.3
FeOT	4.6	2.7	2.8	3.1	2.1	2.5	2.2	1.7	1.8	1.5
MnO	.1	.1	.0	.0	.1	.0	.0	.0	.1	.1
MgO	2.0	1.2	1.4	1.3	1.2	1.1	.9	.7	.8	.6
CaO	1.4	1.6	.6	.8	2.3	1.2	.8	4.1	3.7	3.0
Na_2O	2.6	3.4	3.2	2.6	3.3	3.2	3.0	2.0	2.2	1.7
K_2O	5.3	3.0	2.8	2.7	2.1	2.3	2.3	1.7	1.8	1.6
P_2O_5	.2	.1	.1	.1	.1	.1	.1	.1	.1	.1
LOI	.9	.3	.2	.2	.2	3.1	2.9	.1	.4	.3
C.I.P.W. norm										
Qz	19.3	33.8	38.2	43.3	40.0	42.1	47.2	43.2	42.7	50.1
Co	7.2	4.0	6.3	5.5	1.4	4.0	3.6	4.8	4.0	6.3
Or	31.5	17.8	16.6	16.1	12.5	13.4	13.5	9.9	10.9	9.6
Ab	21.7	28.3	27.2	22.3	27.9	27.2	25.2	17.0	18.4	14.4
An	5.6	7.2	2.2	3.2	5.8	5.4	3.5	19.8	18.1	14.6
Hy	11.3	6.8	7.5	7.6	5.8	6.2	5.4	4.2	4.9	4.0
Mt	1.3	.8	.8	.9	.6	.7	.7	.5	.5	.5
Il	1.6	1.1	1.0	.9	.8	.8	.8	.4	.4	.4
Ap	.4	.3	.3	.2	.2	.2	.2	.2	.2	.2
trace elements (ppm)										
Ba	678	470	536	414	449	405	307	268	268	368
Cr	55	45	40	35	37	32	27	7	9	6
Rb	181	130	124	115	77	85	71	55	74	60
Sr	134	211	159	146	347	207	180	554	369	479
V	113	73	72	72	56	56	46	18	19	14
Zr	212	241	222	171	187	197	200	114	102	103
Rb/Sr	1.352	.615	.778	.793	.223	.411	.392	.100	.201	.126
I	.71190	.71097	.71200	.71058	.70858	.70945	.70929	.70720	.70633	.70698

NOTES: N54 = Ngauruhoe 1954, PUK = Pukeonake. Major element analyses normalised to 100% volatile-free (volatile loss (LOI) is given for for comparison). Qz = quartz, Co = corundum, Or = orthoclase, Ab = albite, An = anorthite, Hy = hypersthene, Mt = magnetite, Il = ilmenite, Ap = apatite.

$I = {}^{87}Sr/{}^{86}Sr$, Fe_2O_3 / FeO = 0.2.

A small (5x5mm) vein separated from 17470 (=17472 in Appendix 2.3) is compositionally similar to calcsilicate xenoliths 17495 and 17496. Its Sr isotopic composition is relatively high (despite a low Rb/Sr ratio) and not in equilibrium with the rest of the xenolith (Fig.5.2). These data indicate that inclusion of similar vein material will have a strong effect on both chemical and isotopic characteristics of samples and, consequently, care was taken to exclude it.

TYPE VXa xenoliths are highly vesicular (25-50% vesicles); those from Pukeonake are similar to those from Ngauruhoe, despite having a much higher volatile content (Table 5.2). Contacts with host lava are usually sharp and megascopic evidence of inter-reaction is lacking. In some cases (e.g.17474) the contact is irregular and pieces of the xenolith are broken off and lodged in the lava 5-10cm away (Plate 5.1A). In others, lava has intruded along fractures or along the margins of veins.

Assemblages are dominated by light-brown, translucent silica-rich glass, making up 60% (17474) to 80% (17465) of the rock. Sieved cordierite frequently occurs within the glass (Plate 5.2), although in some quartz-rich segregations, it is replaced by hypersthene (Plate 5.3). Plagioclase is absent. Ilmenite (sometimes with exsolved rutile), pleonaste and (rarely) pyrite make up a few percent of the mode.

TYPE VXb xenoliths are well-indurated and variably vesicular. All examples are megascopically and microscopically similar, though 17466 has a reddish tinge due to oxidation near the contact. In thin-section, assemblages consist mainly of crystal aggregates of subhedral to anhedral cordierite (.05-.1mm) and plagioclase with small amounts of glass (Plate 5.4), and occasional larger (.2-.5mm) quartz and plagioclase grains.

5.3.2 Bulk-rock chemistry:

Bulk-rock chemical compositions of selected TYPE VX xenoliths (Table 5.2) show a range in silica content from 62% to 75%. Examples from Pukonake have higher volatile contents than those of Ngauruhoe but, when compared on an

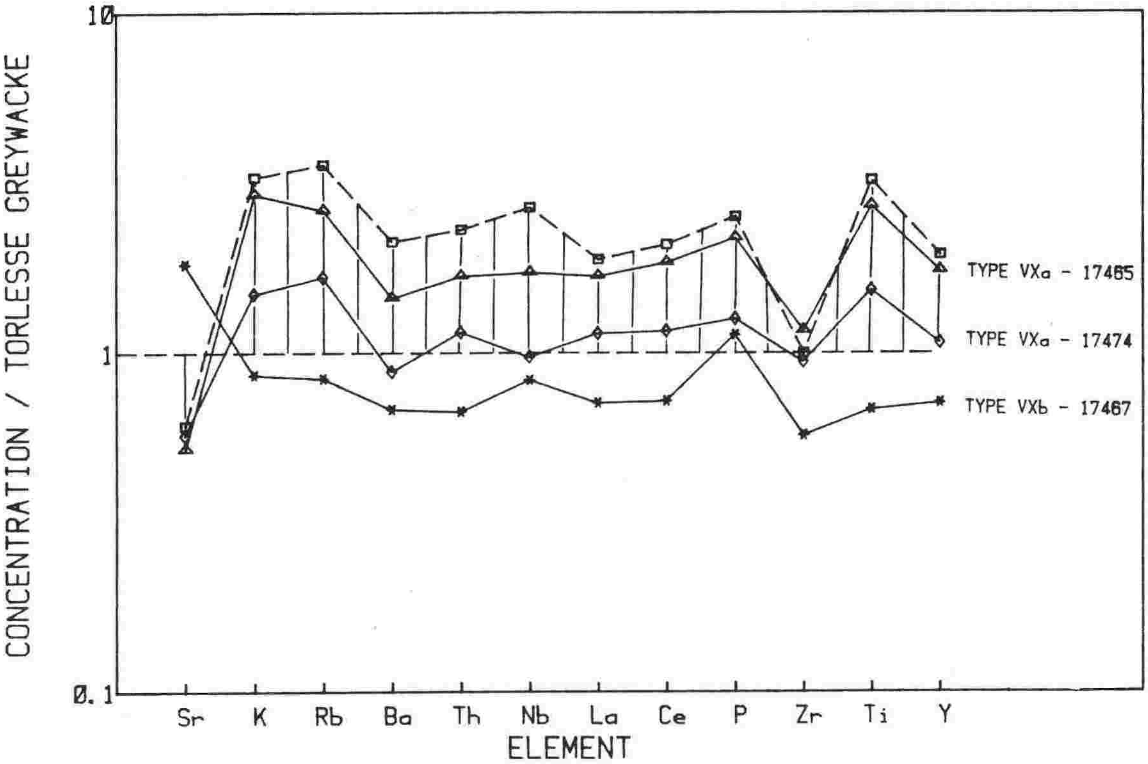

Fig.5.3: Spidergram of trace element concentrations in selected TYPE VX xenoliths, normalised to Torlesse greywacke (for normalisation constants see Table 3.3). Shaded area shows range in composition of Rangipo Torlesse suite metasediments.

anhydrous basis, are chemically identical. All are compositionally similar to Torlesse terrane metasediments (Fig.5.1 & Fig.5.3). This correlation indicates that most examples are greywacke analogues and only 17465 is an argillite equivalent (c.f. Chapter 3.2). Considering the advanced state of fusion and the probability of compositional variation within the Torlesse terrane, this close chemical correspondence is surprising; it has important implications for petrogenesis of host lavas and is further discussed in later sections. TYPE VXb xenoliths have significantly different bulk-rock chemistries from TYPE VXa (Table 5.2 & Fig.5.3). These differences, which include high CaO, Sr and Pb contents, rule out both Torlesse and Waipapa terranes as potential sources (Fig.5.1).

Sr isotopic compositions (Table 5.2 & Fig.5.2) support a genetic link between TYPE VXa xenoliths and Torlesse terrane metasediments: four examples, including all those from Pukeonake, fall on the Rangipo Torlesse suite isochron; three others fall close to it. Only the "argillite" xenolith 17465 shows significant departure. The reason for this is not clear but may be due to partial equilibration with host lava Sr, or may simply reflect regional variation in isotopic composition of the source terrane (such variations occur elsewhere - c.f. Chapter 3.7).

5.3.3 Glass chemistry:

EPMA analyses of glasses in selected TYPE VX xenoliths are given in Table 5.3. In TYPE VXa, all compositions are silica-rich and corundum normative but show much internal and external variation. In 17461, for example, compositions range from 72% SiO_2 in quartz-poor segregations to 81% SiO_2 in quartz-rich segregations near quartz grains. Glasses of "argillite" xenolith 17465 show the widest range in silica content (66% to 77%), are markedly higher in K_2O but are otherwise similar to glasses of "greywacke" xenoliths. TYPE VXb glasses range from 75% to 83% SiO_2 and are more CaO-rich than most TYPE VXa glasses.

Table 5.3: EPMA analyses of glasses in selected TYPE VX xenoliths.

VUW	17465	17465	17461	17461	17461	17475	17473	17460
TYPE	VXa	VXa	VXa	VXa	VXa	VXa	VXb	VXb
major elements (weight %)								
SiO_2	65.91	77.17	72.51	75.64	80.96	74.36	78.05	76.77
TiO_2	.72	.21	.43	.39	.27	.39	.30	.41
Al_2O_3	16.36	10.64	13.93	12.88	9.28	12.12	12.49	12.75
FeOT	3.32	1.55	3.00	2.11	1.30	2.74	1.77	2.33
MgO	.92	.30	.86	.61	.33	.55	.23	.26
CaO	1.13	.35	.85	.54	.34	.74	.95	1.17
Na_2O	3.06	1.87	4.44	3.84	3.15	3.09	2.57	2.70
K_2O	6.63	5.78	2.97	3.22	2.55	3.07	3.40	2.75
Total	98.05	98.00	99.15	99.21	98.18	97.06	99.76	99.14
C.I.P.W. norm								
Qz	17.0	42.7	30.3	37.7	51.7	41.5	46.6	46.4
Co	2.1	.7	1.9	2.1	.7	2.4	2.9	3.2
Or	40.0	34.9	17.7	19.2	15.4	18.7	20.1	16.4
Ab	26.4	16.2	38.0	32.8	27.2	26.9	21.8	23.1
An	5.7	1.8	4.3	2.7	1.7	3.8	4.7	5.9
Hy	7.3	3.3	7.0	4.8	2.8	5.9	3.3	5.9
Ilm	1.4	.4	.8	.8	.5	.8	.6	.8
Mg*	.33	.26	.34	.34	.31	.26	.19	.17
Fe/Mg	2.03	2.92	1.96	1.95	2.21	2.80	4.32	4.98

NOTES: Analyses by EPMA with beam diameter of 10 microns and reduced current; all iron as FeO; Mg* = [Mg/(Mg+Mn+Fe)].
Qz = quartz, Co = corundum, Or = orthoclase, Ab = albite, An = anorthite, Hy = hypersthene, Il = ilmenite.

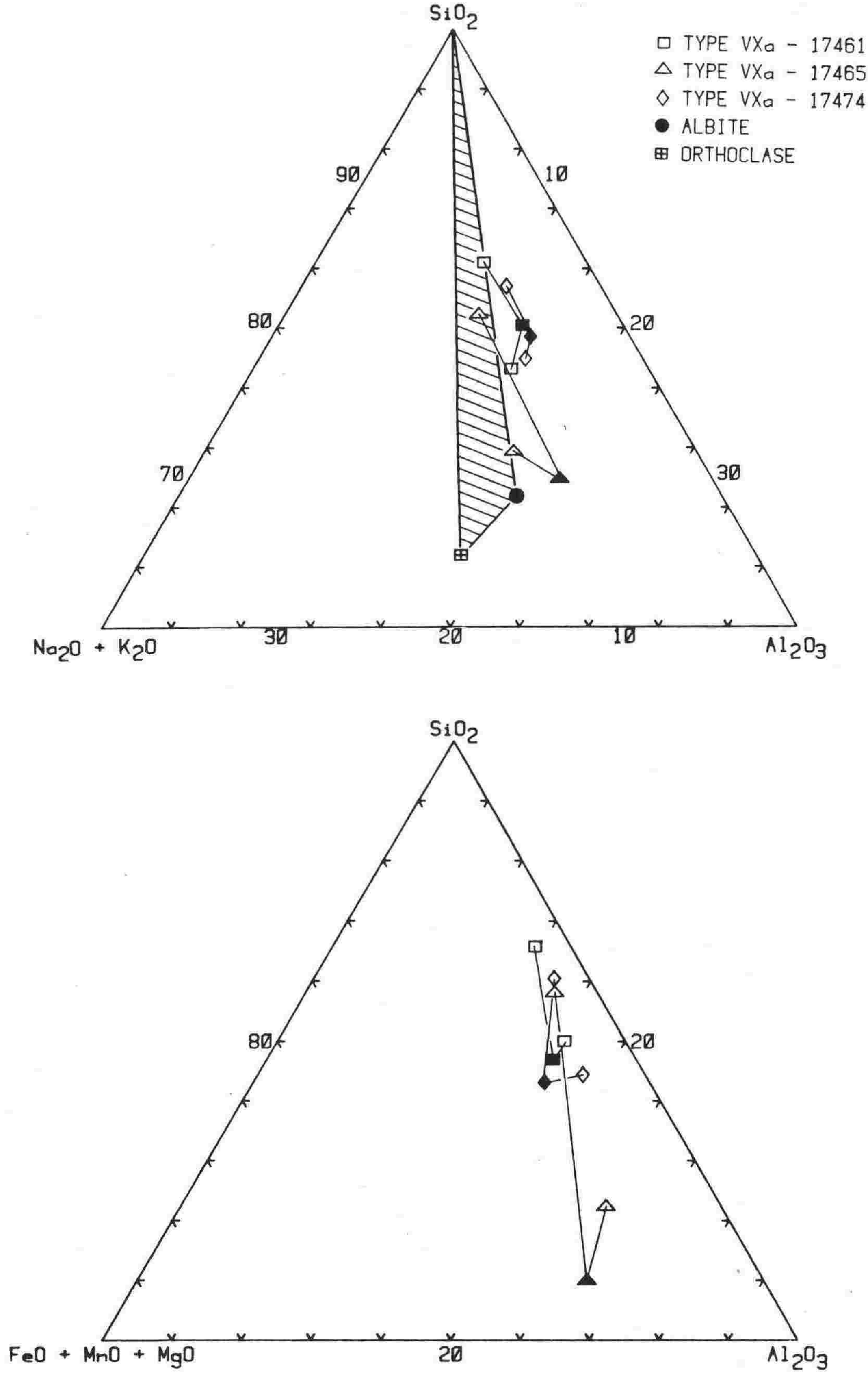

ig.5.4: Triangular plot of TYPE VXa bulk-rock and glass compositions.
(a) SiO_2 - FeO + MnO + MgO - Al_2O_3
(b) SiO_2 - Na_2O + K_2O - Al_2O_3
Field in (b) is for quartz + albite + orthoclase.
- Glasses are all more siliceous and less aluminous than bulk rocks, implying that restites formed by extraction of such glass will be the reverse i.e. less siliceous and more aluminous.

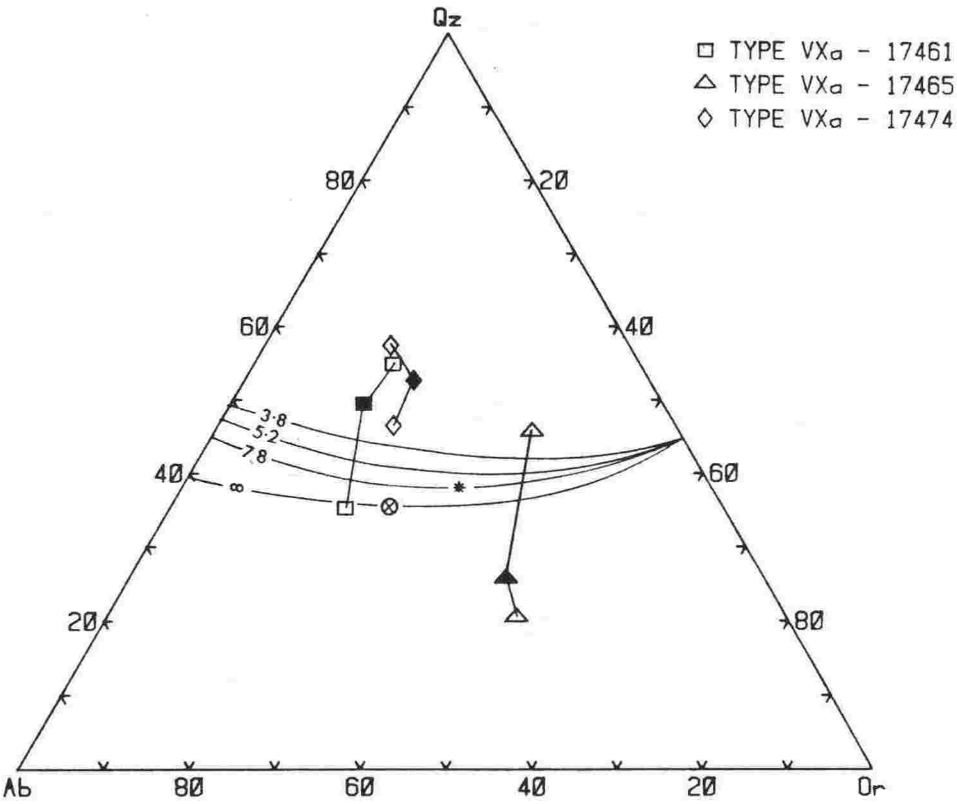

Fig.5.5: Normative glass compositions in selected TYPE VXa xenoliths plotted in the system quartz-albite-orthoclase (Tuttle and Bowen, 1958). Filled symbols are bulk rocks and tie-lines link silica-rich and silica-poor glasses in the same host. Asterisk = S-type granite minimum melt composition (White and Chappell, 1977); cotectic lines are for obsidian-anorthite mixtures with Ab/An ratios of 3.8, 5.2, 7.8 and infinity at P (H_2O) = 2kb von Platen, 1965 - circled cross is ternary minimum.

Selected glasses (open symbols) and corresponding bulk xenoliths (filled symbols) are plotted on ternary diagrams of SiO_2 - (FeO + MnO + MgO) - Al_2O_3 in Fig.5.4a and SiO_2 - Na_2O + K_2O) - Al_2O_3 in Fig.5.4b. These show that glasses are all more Na-, K, Si-rich and Al-, Fe-, Mg-poor than bulk xenoliths and plot in the region corresponding to Qz + Ab + Or. Normative compositions (Table 5.3) are plotted in the system quartz-albite-orthoclase in Fig.5.5. Glasses of 17461 and 17465 straddle the minimum granite melt curves at $P(H_2O)$=2kb (von Platen, 1965), whereas those from 17474, which has a more siliceous host xenolith composition, fall entirely in the quartz field. This diagram, however, poorly illustrates melting relationships in TYPE VXa xenoliths for two reasons: firstly, the range of glass compositions exhibited by each example reflects internal fine-scale inhomogeneity and therefore relates to local bulk compositions which would lie towards the quartz apex (quartz-rich segregations) and the albite-orthoclase join (quartz-poor segregations) respectively; secondly, the degree of melting is greater than 50% and has thus proceeded beyond the minimum for the compositions under consideration - average compositions, if they could be assessed, might be expected to fall close to the minimum melt curve (for quartzo-feldspathic assemblages) only in the initial stages of melting and, as higher percentages of melt form, will come progressively closer to bulk-rock compositions (Grapes, in press).

5.3.4 Mineral chemistry:

EPMA analyses of mafic minerals in TYPE VX xenoliths are given in Table 5.4. In cordierites, [Mg/(Mg+Fe+Mn)] ranges from .77 to .45 and is not directly related to changes in the composition of associated glass (i.e. cordierites of contrasting composition are often surrounded by homogeneous glass of the same composition). Overall, however, using 17465 as an example, the change in [Mg/(Mg+Fe+Mn)] between bulk-rock (.43), cordierite (.72 to .60) and "quartz-poor glass" (.33) implies a Kd (Fe/Mg (cord) / Mg/Fe (melt)) of .20 to .33. Schreyer and Shairer (1961) investigated the

Table 5.4: EPMA analyses of mafic minerals in selected TYPE VX xenoliths.

MINERAL	cord	cord	cord	cord	opx	opx	opx	pleon
VUW	17463	17474	17474	17460	17463	17465	17460	17460
TYPE	VXa	VXa	VXa	VXb	VXa	VXa	VXb	VXb
SiO_2	49.95	50.00	48.93	47.63	52.42	51.62	52.00	.00
TiO_2	.00	.00	.00	.00	.09	.45	.33	.35
Al_2O_3	33.50	32.84	33.39	33.33	2.01	2.17	1.42	60.10
Fe_2O_3	.00	.00	.00	.00	.00	.00	2.61	1.28
FeO	5.34	7.27	9.20	11.70	25.02	26.55	16.36	23.34
MnO	.00	.00	.00	.95	.35	.41	.44	.57
MgO	10.17	9.20	7.50	5.72	19.80	17.97	24.16	11.08
CaO	.10	.09	.00	.00	.06	.48	2.02	.12
Na_2O	.00	.00	.06	.12	.00	.00	.00	.00
K_2O	.00	.00	.00	.27	.00	.00	.00	.00
Total	99.88	99.40	99.28	99.72	99.75	99.65	99.34	96.93
oxygens	18	18	18	18	6	6	6	4
Si	5.02	5.06	5.00	4.94	1.97	1.97	1.91	.00
Ti	.00	.00	.00	.00	.00	.00	.01	.01
Al	3.97	3.91	4.02	4.07	.09	.10	.06	1.94
Fe	.00	.00	.00	.00	.00	.00	.07	.03
Fe	.45	.61	.80	1.01	.79	.85	.51	.54
Mn	.00	.00	.00	.08	.01	.01	.01	.01
Mg	1.52	1.39	1.14	.88	1.11	1.02	1.33	.46
Ca	.00	.01	.00	.00	.00	.02	.08	.00
Na	.00	.00	.01	.02	.00	.00	.00	.00
K	.00	.00	.00	.04	.00	.00	.00	.00
Total	10.96	10.98	10.97	11.04	3.97	3.98	4.00	3.00
Mg*	.77	.70	.59	.45	.58	.54	.69	.44
Fe/Mg	.30	.44	.70	1.15	.71	.83	.44	1.24

NOTES: cord = cordierite; opx = orthopyroxene; pleon = pleonaste.
All iron as FeO; Mg* = [Mg/(Mg+Mn+Fe)].

structural state of Mg-cordierite and showed that, using the distortion index (D) of Miyashiro (1957), cordierites can be described as being in a high, low or intermediate structural state. For 17465, D=.28 is consistent with a "high" structural state. this indicates little or no annealing subsequent to formation. However, distortion of the cordierite crystal lattice results from a complex set of conditions including temperature of crystallisation, bulk-rock chemistry, confining pressure, the presence of volatile components and the length of time that the mineral remains at high temperatures. It cannot therefore be used reliably as a geothermometer. However, the data for 17465 indicates that little time must have elapsed after crystallisation suggesting rapid incorporation and ascent to surface conditions.

In TYPE VXa xenoliths, orthopyroxene occurs only as rare subhedral grains in segregations associated with the most siliceous glasses. These typically contain 2-3% Al_2O_3 and less than 1% CaO (Table 5.4). [Mg/(Mg+Fe+Mn)] ranges from .58 to .54 and these values are lower than for cordierite in adjacent segregations, but are consistent with the correspondingly lower values for coexisting silica-rich glass (.26-.31). The data imply a Kd (Fe/Mg (opx) / Mg/Fe (melt)) of .24 to .38, a range similar to that for cordierite-melt equilibria. TYPE VXb orthopyroxenes are less aluminous and more Ca-rich than TYPE VXa (Table 5.4) and [Mg/(Mg+Fe+Mn)]=.69, implying a Kd of .25 (17460).

Pleonaste euhedra occur sporadically, often associated with cordierite and silica-poor glass. Compositions are typically Fe-rich, having [Mg/(Mg+Fe+Mn)] less than .5. The main Fe-Ti oxide, ilmenite, is a ubiquitous but minor component of all associations. EPMA analyses indicate an excess of TiO_2 for stochiometric ilmenite and the occurrence of exsolved rutile in 17462 suggests that most grains have been oxidised.

Plagioclase occurs only in TYPE VXb xenoliths as subhedral inclusions in cordierite or as crystal aggregates between cordierite and glass (Plate

5.4). Compositions range from An_{85} to An_{45} - rims in contact with glass are more sodic than cores.

5.3.5 Melting relationships:

The close chemical correspondence between TYPE VXa xenoliths and Torlesse terrane metasediments indicates that the original mineral assemblage was quartz + albite + chlorite + muscovite + minor Ca-rich secondary minerals such as epidote, prehnite, pumpellyite and calcite (see Chapter 3.2). During prograde metamorphism, this assemblage would have changed through gradual dehydroxylation of micas and formation of new minerals with high P-T stability fields. However, rapid heating of mica can cause melting without an initial dehydroxylation-oxidation stage, according to the reactions (Grapes, in press),

muscovite + quartz = aluminosilicate + peraluminous melt i.

biotite + albite +- quartz = Na-sanidine + pleonaste + Al-magnetite + peraluminous melt ii.

or (Wones and Eugster, 1964; von Platen, 1965),

biotite + quartz + O_2 = sanidine + Fe-Mg silicate + H_2O + melt iii.

The absence of any relict alumino-silicate phases in TYPE VX xenoliths suggest that melt may have formed directly without prior formation of sanidine, or that mineral was consumed at higher degrees of melting. Release of water during breakdown of mica promoted melting of quartz + feldspar, and this, in TYPE VXa xenoliths, continued until all feldspar was consumed. Arzi (1978) showed by experiment that melting of quartz and feldspar grains increases near biotite grains as a result of high local water pressure and that later glasses resulting from further melting, have lower K_2O contents, consistent with early elimination of sanidine. Textural relationships of cordierite (c.f. Plate 5.2) suggest that it grew directly from peraluminous melt, rather than from breakdown of biotite.

5.3.6 Origins:

Bulk-rock chemistry and Sr isotopic composition of vitrified xenoliths from Ngauruhoe and Pukeonake lavas indicate that they originated from shallow levels in the Torlesse basement. Prior to intense thermal metamorphism, they had undergone only low-grade metamorphic change. This conclusion differs from that of Steiner (1958) who considered the minor reaction observed at some xenolith-host contacts as evidence for a deep-seated origin (i.e. beneath the Torlesse basement). He considered the occurrence of quartz rather than tridymite to support this since, as shown by Moseman and Pitzer (1941), quartz is the stable form at moderately high pressures and elevated temperatures and can melt directly at pressures greater than 1kb. However, the close chemical correspondence between TYPE VXa xenoliths and Torlesse terrane metasediment argues against a deep-seated origin since processes of burial metamorphism would be expected to cause mineralogical and textural reconstitution and consequent disruption of bulk-rock chemistry and Sr isotopic systematics (on a hand-specimen scale at least). The absence of any relict high pressure minerals such as garnet supports this argument.

It is suggested therefore, that TYPE VXa xenoliths were incorporated into magma in high-level chambers and were thence rapidly transported to the surface. High magmatic temperatures of 1000 °C to 1100 °C (Table 4.4) caused almost total melting of the wall-rock; rapid ascent caused the xenolithic melt to quench and vesiculate as a result of a decrease in confining pressure, but allowed insufficient time to interact chemically and diffuse isotopically with the magma.

Plate 5.5: BEI photograph of assemblage (i) in TYPE QXa xenolith 17492. Minerals are quartz (dark grey), plagioclase (light grey) and pyroxene (white).

Scale bar = .1mm; field of view = .34mm.

Plate 5.6: BEI photograph of assemblage (ii) in TYPE QXa xenolith 17492. Minerals are quartz (dark grey), plagioclase (grey) and glass (light grey).

Scale bar = .1mm; field of view = .34mm.

Plate 5.7: BEI photograph of a garnet inclusion in TYPE QXa xenolith 17492. The assemblage of pleonaste (light-grey blebs), gedrite (darker grey) and ilmenite (white grain middle RHS) probably resulted from prograde alteration of cordierite.

Scale bar = .01mm; field of view = .17mm.

Plate 5.8: BEI photograph of reaction at the interface between TYPE QXb xenolith 17885 and host lava 14721. Zones are (from bottom to top): quartz (dark grey)- glass (light grey)-pyroxene (white)-host lava (plagioclase phenocrysts in dacitic mesostasis).

Scale bar = .1mm; field of view = .6mm.

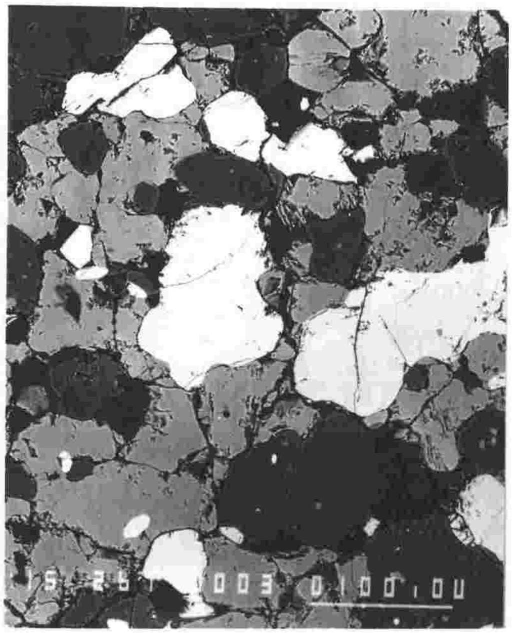

Plate 5-5

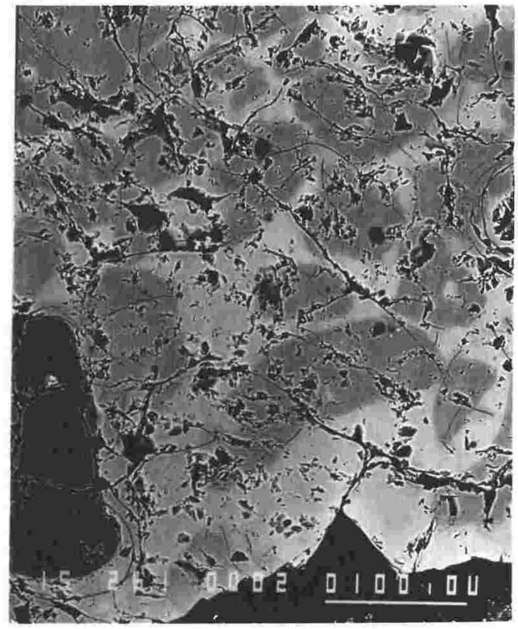

Plate 5-6

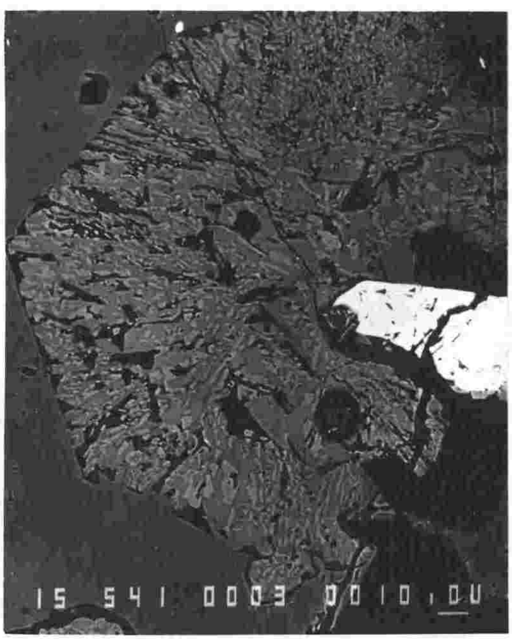

Plate 5-7

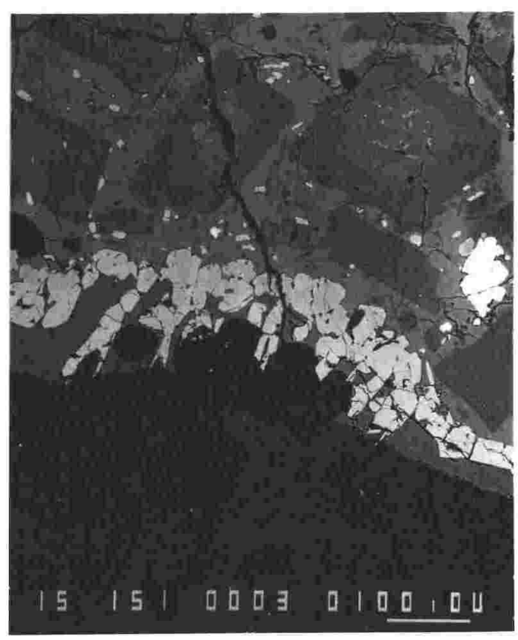

Plate 5-8

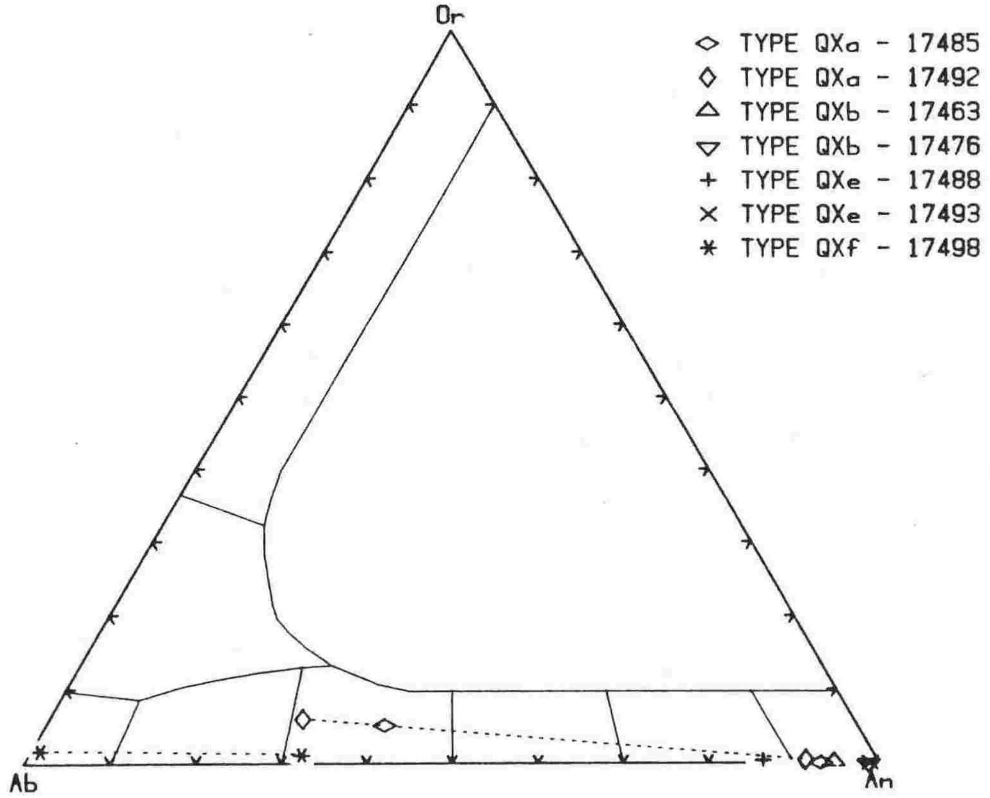

Fig.5.6: Plagioclase compositions in TYPE QX xenoliths plotted in terms Or - Ab - An (K - Na - Ca). Tie-lines link minerals in the same rock.

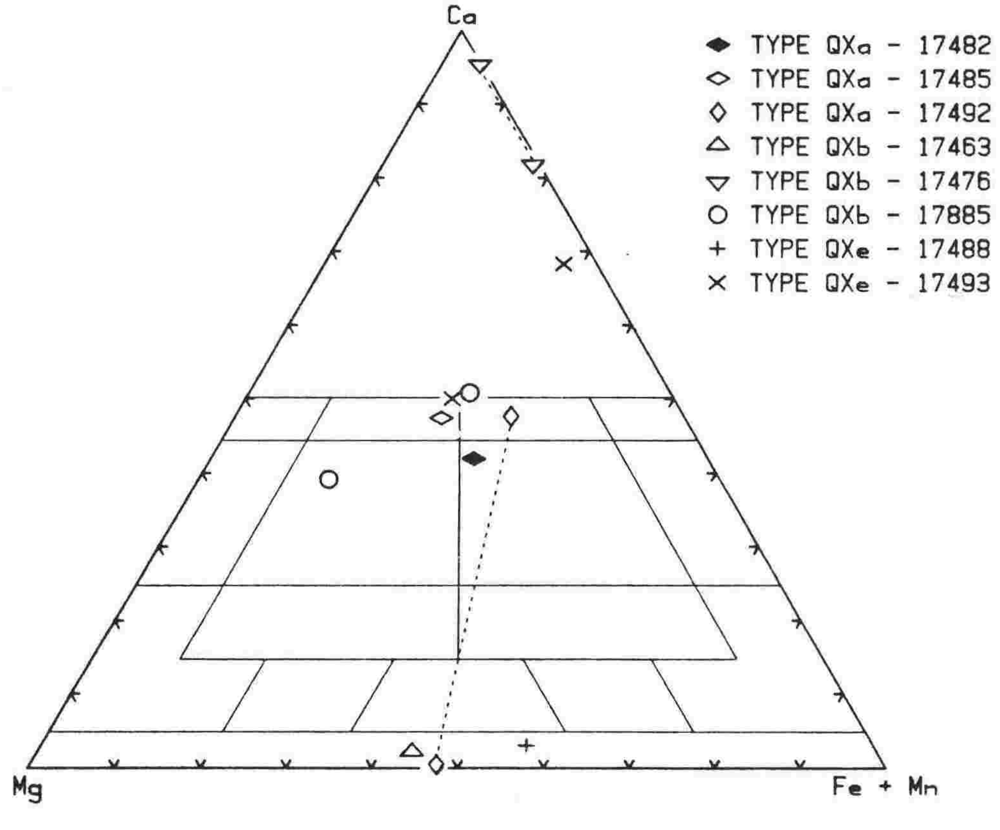

Fig.5.7: Pyroxene compositions in TYPE QX xenoliths plotted in terms of Ca - Mg - Fe. Tie-lines link minerals in the same rock.

5.4 TYPE QX - QUARTZ-RICH XENOLITHS

Quartz-rich xenoliths, many of which have high-grade metamorphic textures, are ubiquitous in lavas of Ruapehu and some nearby vents, and are locally abundant in Iwikau Member pyroclastics (W.R.Hackett, pers. comm., 1984). Quartzites, containing more than 90% modal quartz, occur in lavas of all ages and are the most abundant xenolith type. Other TYPE QX xenoliths are mineralogically and chemically diverse. These are classified using subscripts c-g.

Some TYPE QX xenoliths contain small amounts of partial melt, but are distinguished from TYPE VX xenoliths because their bulk-rock compositions (Table 5.5) are not directly comparable with known basement lithologies and because textures and mineral assemblages suggest a much more complex metamorphic history.

5.4.1 TYPE QXa:

These xenoliths have schistose or gneissic textures and exhibit cm-wide banding with contrasting mineral assemblages:

(i) quartz + calcic-plagioclase + clinopyroxene +- sphene +- ilmenite

(ii) quartz + sodic-plagioclase + garnet +- orthopyroxene +- biotite

EPMA analyses of phases in each assemblage are given in Appendix 3. In assemblage (i), plagioclase ranges in composition from bytownite to anorthite (Fig.5.6) and pyroxene from salite to ferroaugite (Fig.5.7). Sphene and ilmenite (commonly rimmed by hematite) are minor and textures are typically granoblastic (Plate 5.5). In assemblage (ii), plagioclase compositions are more sodic, ranging from An_{30} to An_{40} (Fig.5.6). In 17492, anhedral, unzoned plagioclase and quartz grains are surrounded by clear granitic glass (Plate 5.6). Occasional orthopyroxene (aluminous hypersthene) and almandine-rich garnet also occur. A 1mm hexagonal inclusion in one garnet grain (Plate 5.7) consists of a vermicular intergrowth of hercynite and gedrite (Hietanen, 1959). The hexagonal

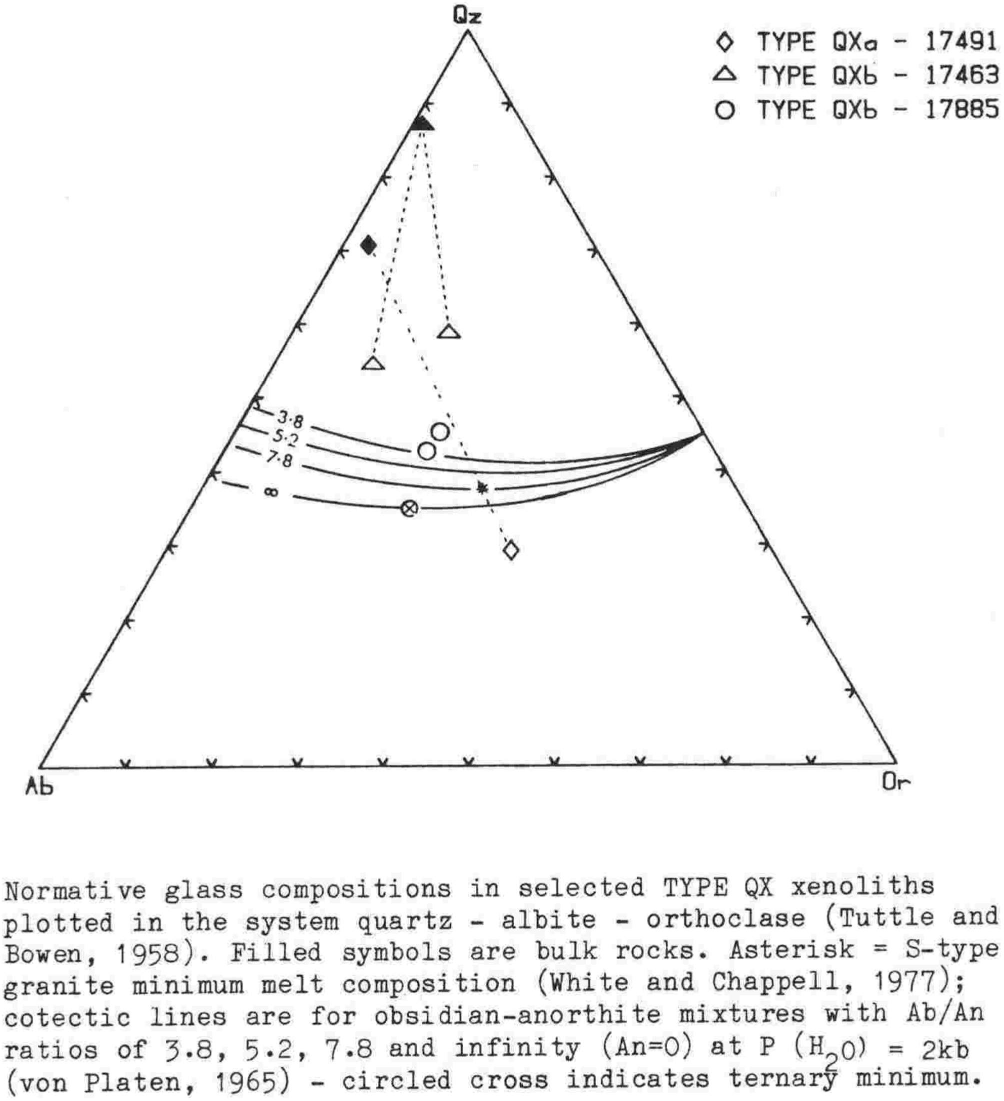

Fig.5.8: Normative glass compositions in selected TYPE QX xenoliths plotted in the system quartz - albite - orthoclase (Tuttle and Bowen, 1958). Filled symbols are bulk rocks. Asterisk = S-type granite minimum melt composition (White and Chappell, 1977); cotectic lines are for obsidian-anorthite mixtures with Ab/An ratios of 3.8, 5.2, 7.8 and infinity (An=0) at P (H_2O) = 2kb (von Platen, 1965) - circled cross indicates ternary minimum.

crystal shape and bulk composition of the constituent minerals (Appendix 3) suggest the inclusion was probably originally cordierite. Shreyer (1965) reported that at high temperatures and pressures of 10kb Fe-rich cordierite breaks down to assemblages containing an orthoamphibole (ferrogedrite). However, he was not certain whether these assemblages represent stable equilibrium, or whether they are metastable substitutes for other parageneses such as almandine + sillimanite + quartz. Grieve and Fawcett (1974) investigated the stability of chloritoid below 10 kb P (H_2O). They showed that the assemblage aluminous ferro-anthophyllite + staurolite + hercynite was stable with respect to chloritoid only at pressures greater than 5.5 kb and temperatures greater than 600 °C. They further showed that Fe-cordierite breaks down to ferro-anthophyllite + staurolite + quartz under similar P-T conditions. These studies suggest the breakdown of cordierite to gedrite + pleonaste was prograde and occurred in response to the increase in temperature following incorporation of the xenolith in host magma.

This sudden change in P-T conditions may also have triggered partial melting in 17492 which, from the K-rich, Ca-poor composition of the glass (Appendix 3), appears to have involved mainly the destruction of alkali-feldspar and biotite. In the normative Qz-Ab-Or system (Fig.5.8) the glass plots in the feldspar field and is not a minimum melt (note that the bulk-rock composition plots towards the quartz apex, being dominated by the melt-free quartz-anorthite assemblage).

No melt is present in 17485 where assemblage (ii) is quartz + biotite + plagioclase + garnet. Biotite-garnet exchange equilibria (Ferry and Spear, 1978; Appendix 1.6) gives a temperature for the garnet rim of 946 °C. This is higher than the temperature (808 °C at 10kb) for garnet-orthopyroxene equilibria in 17492 (Harley, 1984a; Appendix 1.7). Pressure estimates based on assemblage (i) (plagioclase + clinopyroxene + quartz) (Ellis, 1980; Appendix 1.3) give low or negative values, suggesting the equilibria is not

Table 5.5: Bulk-rock chemistry of selected TYPE QX xenoliths.

VUW	17482	17492	17485	17463	17436	17416	17468	17493	17488	17498
TYPE	QXa	QXa	QXa	QXb	QXb	QXc	QXd	QXe	QXe	QXf
major elements (weight%)										
SiO_2	65.6	70.9	72.5	85.3	98.0	61.7	99.3	88.4	95.4	79.7
TiO_2	.7	.5	.6	.0	.0	1.1	.0	.1	.1	.1
Al_2O_3	16.5	13.8	13.9	8.9	.8	19.1	.3	3.0	1.8	12.4
Fe_2O_3	.9	.6	.7	.1	.1	1.1	.0	.3	.3	.1
FeO	4.3	2.9	3.3	.5	.3	5.3	.1	1.7	1.3	.6
MnO	.1	.2	.1	.0	.0	.1	.0	1.3	.3	.0
MgO	1.8	1.1	1.3	.1	.2	2.2	.0	.7	.4	.2
CaO	6.0	9.3	4.5	3.8	.3	8.5	.2	4.5	.4	.5
Na_2O	3.2	.6	2.2	1.1	.2	.5	.1	.0	.1	6.3
K_2O	.6	.1	.9	.2	.1	.1	.1	.0	.1	.2
P_2O_5	.3	.2	.2	.0	.0	.3	.0	.1	.0	.0
LOI	.4	.9	1.5	.2	.0	4.4	.2	1.2	.9	.4
C.I.P.W. norm										
Qz	27.4	46.4	43.1	69.5	95.6	34.4	98.4	78.4	91.9	40.6
Co	.4	-	1.6	-	-	3.4	-	-	.8	1.0
Or	3.2	.4	5.2	1.0	.4	.6	.4	.2	.7	1.1
Ab	27.1	5.0	18.9	9.4	1.6	4.2	.4	.1	.8	53.5
An	28.0	34.8	21.1	18.7	1.1	40.5	.4	8.1	1.8	2.1
Di	-	8.7	-	.1	.2	-	.3	11.8	-	-
Hy	10.6	2.6	7.8	1.0	.9	12.8	-	.6	3.5	7.8
Other	3.3	2.1	2.3	.3	.2	4.3	.1	.8	.5	.3
trace elements (ppm)										
Ba	333	31	174	13	3	326	2	193	60	24
Cr	39	31	33	6	4	32	2	3	7	8
Rb	4	1	42	4	3	4	3	3	5	2
Sr	608	605	260	204	26	336	6	223	39	168
V	105	69	82	5	16	171	3	31	11	13
Zr	199	223	135	8	<2	290	3	31	25	29
Rb/Sr	.006	.002	.163	.018	.100	.013	-	.014	.137	.012
I	.70639	.70700	.70890	.70801	.70611	.70609	-	.70774	-	-

NOTES: I = $^{87}Sr/^{86}Sr$, Fe_2O_3 / FeO = 0.2.
Major element analyses normalised to 100% volatile-free (volatile loss (LOI) is given for comparison). Qz = quartz, Co corundum, Or = orthoclase, Ab = albite, An = anorthite, Hy = hypersthene, Other = magnetite, ilmenite, apatite.

appropriate to the compositions observed in these assemblages (the low alumina contents of clinopyroxene produce large errors in the estimation of the Ca-Tchermak's component). Garnet-orthopyroxene geobarometry (Harley, 1984b; Appendix 1.7) requires an alumino-silicate to be present in the assemblage and, since none were found, the calculated pressure of 7.75kb (at 800 °C) is suspect.

Bulk-rock chemical compositions of TYPE QXa xenoliths (Table 5.5) are strongly quartz-feldspar normative and slightly corundum normative. CaO contents are relatively high (4.5-9.3%) and alkalis are low (.7-3.8%). Sr contents are variable: 17482 (608ppm) and 17492 (605ppm) are much higher than 17485 (260). These data indicate that assemblage (i) dominates the bulk-rocks; partial melts, and minerals able to produce such melts, therefore constitute only a small percentage by volume.

5.4.2 TYPE QXb:

Nearly monomineralic quartzite xenoliths are abundant and widespread, particularly in Ohakune and Ngauruhoe 1954 lavas. Mineralogically, these consist either entirely of quartz (e.g.17436, 17468), or contain small pockets (less than 5% by volume) of plagioclase, pyroxene and/or spinel (e.g.17885, 17476, 17463). Textures are coarsely granoblastic (e.g.17885) although some examples have a directional fabric (17436). Quartz varies in grainsize from .05 to 1mm and usually shows undulose extinction. Rare plagioclase is anorthite (Fig.5.6) and pyroxene is typically salite or ferrosalite (Fig.5.7). A 5x5mm area in 17476 contains an intergrowth of anorthite and wollastonite with minute inclusions of a more Fe-rich wollastonite (Appendix 3); Mn-rich hypersthene occurs in 17463 (Appendix 3). Some examples contain small, irregular areas of plagioclase and pyroxene surrounded by silica-rich glass, but this association is by no means common (as was suggested by Steiner, 1958). Glass compositions are variable, but are more calcic and less potassic than 17492 (Appendix 3). Plotted in the Qz-Ab-Or system (Fig.5.8), glass from TYPE QXb xenolith

17463 falls within the quartz volume; those from 17885 are close to minimum melt compositions even though bulk-rock would plot close to the quartz apex.

Bulk-rock chemistry and C.I.P.W. norms of TYPE QXb xenoliths are included in Table 5.5. These show very high silica contents and relatively low K_2O contents which indicate that glass represents only a small proportion of total rock volume. Sr contents are high in proportion to feldspar content (e.g. 17463). Sr isotopic compositions (where these could be measured) are similar to TYPE QXa.

5.4.3 Origins:

The occurrence of quartz-rich segregations similar to TYPE QXb in some TYPE QXa xenoliths (e.g.17485) and the occurrence of Ca-rich assemblages (i.e. assemblage (i)) in both xenolith types suggests that these are linked by a common genesis. However, the widespread distribution of TYPE QXb and the relative rarity of TYPE QXa remains to be explained.

Battey (1949) suggested that quartzose xenoliths in Ngauruhoe 1949 lava were thermally altered Tertiary sandy limestones (interestingly, some large xenoliths of Tertiary grit have recently been described from Mount Egmont (Dr.J.Collen, pers.comm., 1984)). The abundance of quartzose xenoliths (to the exclusion of most other types) in Ohakune lava make a similar origin attractive since the Ohakune vents pass up through the thickest part of the Tertiary sequence in the vicinity of the TVC. However, there is evidence to suggest that TYPES QXa and QXb xenoliths were probably not derived from this near-surface source:

i) Luminescence petrography shows no differentiation of the quartz, as would be expected from diagenetic overgrowths on a detrital core derived from a metamorphic or igneous source; luminescence effects are those typical of high-temperature quartz (Dr.J.Collen, pers.comm., 1984).

ii) No significant quartz-sandstone or grit horizons occur in the North Island Tertiary sequence (Suggate, 1978).

Table 5.6: EPMA analysis of phases in 17885.

MINERAL	cpx	glass	glass	cpx	mes
ASSOC	xen	xen	rim	rim	lava
SiO_2	50.83	68.26	72.01	52.97	65.01
TiO_2	.17	.63	.63	.17	1.14
Al_2O_3	.68	10.64	10.01	.68	12.22
Fe_2O_3	.44	.00	.00	2.21	.00
FeO	14.22	4.64	4.04	7.44	7.33
MnO	.79	.00	.00	.33	.20
MgO	7.86	.74	.61	16.41	1.26
CaO	23.75	2.38	1.71	19.59	3.65
Na_2O	.26	2.91	2.89	.30	4.84
K_2O	.09	2.97	3.25	.00	1.36
Cl	.00	.09	.00	.10	.00
Total	99.08	93.24	95.14	99.91	97.11
oxygens	6	-	-	6	-
Si	1.984	-	-	1.964	-
Ti	.005	-	-	.005	-
Al	.031	-	-	.022	-
Fe^{3+}	.013	-	-	.062	-
Fe^{2+}	.465	-	-	.231	-
Mn	.026	-	-	.010	-
Mg	.458	-	-	.906	-
Ca	.994	-	-	.778	-
Na	.020	-	-	.022	-
K	.004	-	-	.000	-
Total	4.000	-	-	4.000	-

NOTES: cpx = clinopyroxene; mes = mesostasis.
xen = segregation in xenolith;
rim = reaction rim; lava = host lava.

iii) even if a suitable bed did exist beneath the TVC, it might be expected that the derivative metaquartzite xenoliths be accompanied by metasiltstones and metacalcarenites, both of which do occur.

An second possibity is that TYPES QXa and QXb xenoliths represent cherts from within the Mesozoic basement. Although difficult to deny on chemical or petrographic grounds (Roser, 1983), the relative abundance of these xenoliths is inconsistent with their rarity in the probable source terranes.

The most likely origin for quartz-rich xenoliths is that proposed by Steiner (1958) who considered them to represent relict bands of quartzo-feldspathic gneiss, separated from denser micaceous layers by thermal expansion during rapid increase in temperature. From this study, the parental gneiss might be equivalent to lower parts of the Mesozoic basement where greywacke has metamorphosed under high-grade conditions. Because of the likelihood of some chemical transfer resulting from gneissic segregation, it is not possible to directly relate these xenoliths to Torlesse greywacke - the high Ca and Sr contents and moderately low Sr isotopic ratios of 17482 and 17492 would require extensive mineralogical and chemical adjustment to be compatible with such a source. On the other hand, Sr isotopic ratios are too high for an origin as Waipapa terrane greywackes, unless some some isotopic enrichment has previously taken place (see section 5.8 for further discussion).

5.4.4 Contact relationships:

The interface between TYPE QXb xenoliths and host lava is of two types: Commonly, the xenolith edge meets host lava in a sharp regular line and mineral grains are smoothly broken across it (e.g.17476). In other cases, a narrow reaction zone surrounds the xenolith (Plate 5.8). This is made up of an irregular zone of clear, homogeneous, silica-rich glass and a zone next to host lava containing .5 to 1mm long clinopyroxene microlites. EPMA analyses of each phase is given in Table 5.6.

Holgate (1954) reviewed the facts relating to the behaviour of quartzose xenoliths immersed in basaltic magma, and concluded that the phenomena displayed are due to liquid immiscibility at the onset of crystallisation in the host. Diffusion into the xenolith margins of alkalis and water from the magma causes early production of a granitic melt at the contact. During cooling, the melt composition is progressively changed through further diffusion until finally it has a composition similar to that of late-stage residua of the host lava. Sato (1975) experimentally examined the phenomena of glass-clinopyroxene coronas around quartzose xenoliths and concluded that alkalis diffused against their concentration gradients. This behaviour was also reported by Watson and Jurewicz (1984) from experiments with oceanic tholeiite and granite at 1250 °C and 10kb. In the contact zone, interdiffusion of elements took place resulting in considerable uptake of potassium by the basaltic melt and eventual loss of Na from the basalt to the granite. Sato (1975) also explained the occurrence of clinopyroxene coronas; these result from high (Na+K)/Al ratios of corona glass which increases the effective CaO concentration causing clinopyroxene rather than orthopyroxene to crystallise.

Van Bergen and Barton (1984) described the interaction between aluminous metasedimentary xenoliths and siliceous magma from Mt. Amiata, Central Italy, and found similar reaction coronas which they interpreted as complex processes of magma-rock interaction. In some examples, the the zonation consisted of: xenolith core of sanidine + biotite + spinel + plagioclase + aluminosilicate - plagioclase - granitic glass - clinopyroxene - unmodified lava. They argued that melt from the xenolith accumulated around it, and diffusion gradients then led to impoverishment of the melt in Si, Na and K and enrichment in water, Fe, Mg and Ti. The instability of hercynitic spinel in the presence of siliceous liquid resulted in crystallisation of calcic plagioclase and a consequent positive Ca anomaly along the magma-xenolith contact. Although the interaction of

TYPE QXb xenoliths with basic magma does not directly parallel that situation, similar processes could apply - granitic partial melts produced under suitable conditions are sometimes extracted and thence interact with host lava. For 17885, host lava consists of plagioclase and pyroxene phenocrysts and mesostasis of dacitic composition (Table 5.6). The xenolithic melt is deficient in Fe and Mg compared to host lava and strong diffusive gradients might be set up resulting in crystallisation of pyroxene at the diffusive interface.

It is also possible that the xenolith acts merely as a reactive interface at which host mesostasis crystallises clinopyroxene, so being enriched in Si and K and depleted in Fe, Mg and Ca. However, there are difficulties with this interpretation. Firstly, both Al and Na are lower in the xenolithic melt than in the host mesostasis, yet these elements are also low in pyroxene. Concomitant crystallisation of plagioclase is a solution to this paradox but no plagioclase-rich zones occur. Secondly, there is no observed change in glass composition between the xenolith margin and the pyroxene zone, yet pyroxene is confined to that region immediately adjacent to the host lava. It is more likely, therefore, that zoned contact relationships between quartz-rich xenoliths and host lava result from extraction of partial melts from the xenolith which interact diffusively with host mesostasis.

5.4.5 Other TYPE QX xenoliths:

TYPE QXc xenolith 17416 is a pyroxene hornfels with some petrographic features suggestive of a metasedimentary origin. In hand-specimen it is brown to grey-black, elongated (30x10x5cm) and strongly foliated. Mineralogically, it consists mainly of granular aggregates of quartz + calcic plagioclase in a pseudo-opaque, fine-grained matrix of sieved quartz, plagioclase and orthopyroxene ($Ca_3Mg_{48}Fe_{49}$). Chemically, it is depleted in alkalis (.4%) and strongly corundum-normative (3.4%) (Table 5.5). The well-foliated, granoblastic texture and low alkali content suggest that this xenolith could have originated as a finely-laminated arkosic siltstone. However, its bulk-rock chemistry and low Sr isotopic ratio (.70608) preclude direct derivation from any known basement source.

TYPE QXd xenolith 17468 is a large (50x20x20cm), saccharoidal quartzite from Ngauruhoe 1954 lava. It consists entirely of a crumbly aggregate of clear quartz and so differs petrographically and chemically from other TYPE QX xenoliths (Table 5.5). This suggests a unique origin either as a pure quartz sandstone from an unknown source or, more likely, as a hydrothermal vein deposit.

TYPE QXe xenolith 17488 is a small, light brown sugary xenolith from the Iwikau Member pyroclastics. It has a granoblastic texture of unstrained, equidimentional (.2mm) quartz grains. Calcic plagioclase (An_{86}), orthopyroxene (manganoan ferrohypersthene) (Fig.5.7) and titanomagnetite occur interstitially as individual crystals and as crystal aggregates. Orthopyroxene has brown-green pleochroism, is partly oxidised and is high in Mn, similar to an orthopyroxene reported by Davidson and Mathison (1973) from a metamorphosed banded iron formation, North Dangin, Western Australia (see Deer, Howie and Zussman, 1978: p45, analysis 21). A second example, 17493 is from Whakapapa Formation lava near Bruce Road, Ruapehu, and has a coarse-grained (.5 to 1mm), granoblastic texture of unstrained quartz with interstitial plagioclase (An_{99}) (Fig.5.6), clinopyroxene (manganoan salite) and manganoan-ferroan wollastonite (Fig.5.7). Similar wollastonite compositions are recorded from Broken Hill (Stilwell, 1959) and from a calcareous zone of hornfels in Mn ore, Hijikuzu mine, Japan (Nambu et.al, 1971). Manganoan ferrosalite was reported by Tilley (1946) from Treburland manganese mine, Altarnun, Cornwall (see Deer, Howie and Zussman, 1978: p552, analyses 11 & 12; p216, analysis 10). Bulk-rock chemistry of 17493 (Table 5.5) shows relatively high concentrations of Mn, Ni, Cu and Zn (for a rock composed largely of quartz). The Sr isotopic ratio (.70773) is similar to that of other TYPE QX xenoliths.

The relatively high concentration of metals in TYPE QXe xenoliths suggests an origin distinct from the other quartz-rich xenoliths. One possible source would be Mn-enriched zones within the Waipapa terrane, such as those which are widespread in the Northland peninsula (Stanaway et al., 1978). However, this seems unlikely since xenoliths with petrographic or chemical characteristics of Waipapa terrane greywackes are absent and similar manganiferous zones are not described locally (Roser, 1983). Mn-enriched zones within the Torlesse terrane are more-attractive. A rare occurrence of rhodochrosite in chert associated with pillow lavas was described from a locality near Paraparaumu, north of Wellington, by Roser (1983). Piedmontite schists (Turner, 1946) occur within Chlorite IV rocks of the Haast schist terrane, also associated with metachert. The correlation between the Haast schist and Kaimanawa schist terranes (c.f. Fig.3.9) indicates that, although no surface expression occurs, such manganiferous horizons could be present in Torlesse terrane below the TVC.

TYPE QXf xenolith 17498 has a complex granoblastic texture and obscure mineralogy. Strained and sometimes broken, 2-3mm sized plagioclases occur in irregular crush zones containing veins rich in biotite and opaques. Quartzose segegations occur elsewhere. Plagioclase has mainly a sodic composition ($An_1Ab_{97}Or_2$) but contains irregular inclusions which are more Ca-rich (Fig.5.6). Mafic minerals including ferro-augite, olivine (Fo_{50}), ilmenite, titanomagnetite and pleonaste are locally abundant in small, interstitial enclosures. Similar assemblages to this occur frequently in quartzo-feldspathic segregations in gneiss, suggesting a possible source. However, this xenolith type is unique and a link to what should be a significant source type (since schist must comprise a substantial crustal thickness below the TVC) is considered unlikely. The assemblage is also compatible with that of a hydrothermal vein deposit. Given such an origin, then it must have acquired its present, granulated texture during inclusion as a xenolith.

Plate 5.9: BEI photograph of mineral assemblage in TYPE QPXa xenolith 17425. Phases are sillimanite (dark grey), plagioclase (grey), sanidine (light grey) and biotite (white). The rock has a strong foliation and sillimanite growth is in preferred orientation.
Scale bar = .1mm; field of view = 1.3mm.

Plate 5.10: Close-up of central area of Plate 5.9 showing sillimanite (dark grey) and sanidine (light grey) surrounded by plagioclase (grey) with biotite (white).
Scale bar = .1mm; field of view = .28mm.

Plate 5.11: BEI photograph of mineral assemblage in TYPE QPXa xenolith 17483. Sanidine (light grey) contains microlites of mullite and corundum (dark grey). Other minerals are plagioclase (grey, patchy) and biotite (white).
Scale bar = .01mm; field of view = .17mm.

Plate 5.12: BEI photograph of TYPE QPXa xenolith 17483. Glass (light grey) surrounds plagioclase (grey, patchy) and biotite (white).
Scale bar = .1mm; field of view = .23mm.

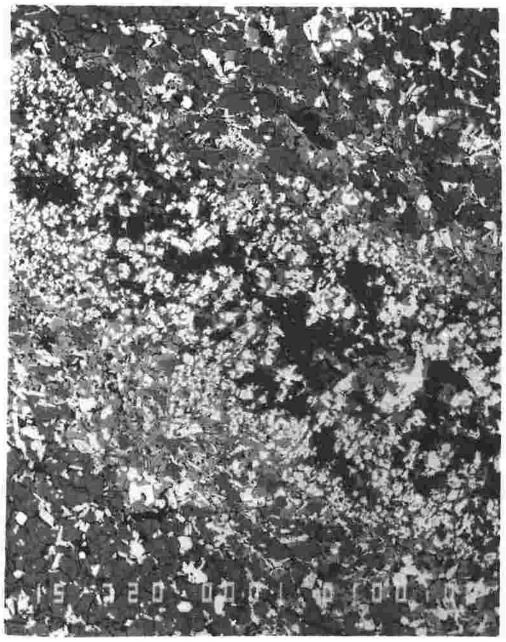

Plate 5-9

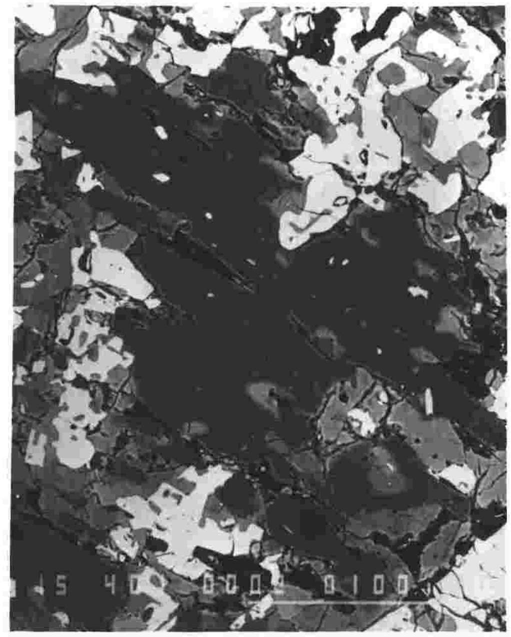

Plate 5-10

Plate 5-11

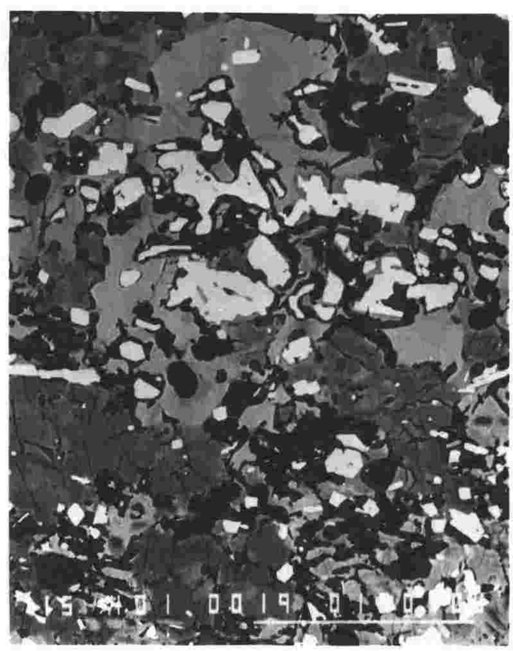

Plate 5-12

Table 5.7: Bulk-rock chemistry of selected TYPE QPX xenoliths.

VUW	17425	17484	17419	17443	17497	17423	17410	17489
TYPE	QPXa	QPXa	QPXb	QPXb	QPXb	QPXc	QPXd	QPXd
major elements (weight%)								
SiO_2	50.0	49.4	49.3	50.8	51.6	43.2	36.3	42.7
TiO_2	1.1	1.8	1.5	1.2	1.0	1.4	4.3	3.7
Al_2O_3	25.6	25.9	25.6	24.6	25.1	26.7	20.3	20.5
Fe_2O_3	3.7	3.5	3.9	4.2	3.5	5.9	10.8	5.5
FeO	3.7	3.5	3.9	4.2	3.5	5.9	10.8	5.5
MnO	.1	.1	.1	.1	.1	.3	.5	.2
MgO	3.0	2.7	2.5	2.9	2.5	4.0	9.0	8.2
CaO	4.3	7.7	8.9	6.7	8.6	5.7	5.7	9.3
Na_2O	4.6	3.6	3.6	4.4	3.6	2.7	1.3	1.7
K_2O	3.8	1.5	.6	.9	.2	4.2	.6	2.0
P_2O_5	.3	.4	.2	.2	.1	.1	.3	.8
LOI	.7	1.2	.8	.2	1.2	2.0	1.4	1.2
C.I.P.W. norm								
Qz	-	2.8	3.2	2.8	1.3	-	-	-
Co	6.9	5.1	3.4	4.8	3.2	7.6	7.8	.6
Or	22.3	8.9	3.4	5.4	1.4	24.8	3.7	11.7
Ab	34.0	30.7	30.6	37.1	32.2	13.2	11.0	14.4
An	19.4	35.9	42.6	31.5	41.9	27.5	26.4	40.9
Ne	2.6	-	-	-	-	5.3	-	-
Hy	-	7.5	8.0	9.7	11.2	-	25.1	4.9
Ol	6.9	-	-	-	-	10.1	1.5	10.8
Mt	5.4	5.1	5.1	6.0	5.1	8.5	15.6	7.5
Ilm	2.1	3.3	2.8	2.2	1.9	2.7	8.3	7.0
Ap	.6	.8	.5	.5	.2	.2	.7	1.8
trace elements (ppm)								
Ba	1709	587	783	878	292	991	360	590
Ce	78	76	nd	84	32	16	53	68
Cr	59	106	73	87	73	531	163	195
Rb	144	48	16	18	2	169	40	87
Sr	708	604	896	545	448	271	342	503
V	179	248	221	208	208	413	564	235
Zr	289	361	473	220	126	77	236	291
Rb/Sr	.203	.079	.050	.098	.014	.623	.115	.173
I	.70662	.70616	.70570	.70800	.70702	.71000	.70830	nd

NOTES: Major element analyses normalised to 100% volatile-free (volatile loss (LOI) is given for comparison). Qz = quartz, Co corundum, Or = orthoclase, Ab = albite, An = anorthite, Ne = nepheline, Hy = hypersthene, Ol = olivine, Mt = magnetite, Il = ilmenite, Ap = apatite. I = $^{87}Sr/^{86}Sr$, Fe_2O_3 / FeO = 0.2.

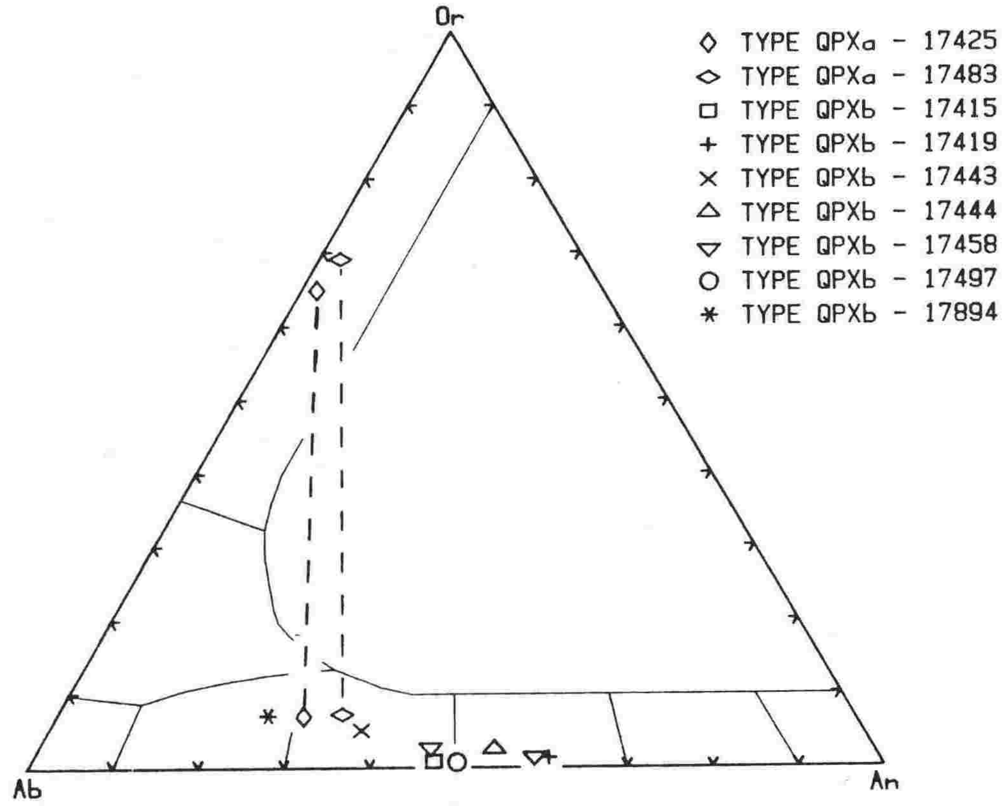

Fig.5.9: Composition of feldspars in selected TYPE QPX xenoliths, plotted in terms of K-Na-Ca. Tie-lines join coexisting phases in two TYPE QPXa xenoliths.

5.5 TYPE QPX - QUARTZ-POOR XENOLITHS

TYPE QPX xenoliths occur in most lavas but only TYPE QPXb (feldspar-rich assemblages) are abundant and these are ubiquitous as small grey-black inclusions. Bulk-rock chemistries are given in Table 5.7.

5.5.1 TYPE QPXa:

Several xenoliths with biotite-rich assemblages are described only from Iwikau Member pyroclastics. One unusually large (12x8x4cm) example, 17425, is strongly foliated and finely-segregated into layers of contrasting mineralogy. In the more felsic layers, plagioclase ($An_{33}Ab_{60}Or_{7}$) and sanidine (Or_{69}) coexist (Fig.5.9); in more mafic layers biotite, aluminous orthopyroxene (En_{49}), ilmenite and pleonaste occur. Sillimanite is frequently surrounded by sanidine and is orientated parallel to the foliation (Plates 5.9 & 5.10). In 17483, sanidine contains needles of mullite and larger anhedral crystals of corundum (Plate 5.11). Elsewhere, interstitial areas of syenitic glass (Appendix 3) occur (Plate 5.12). Bulk-rock chemistries are characterised by high concentrations of Al, alkalis, LILE and HFSE; mafic element concentrations are relatively low (Table 5.7). Sr isotopic compositions vary from .70616 (17484) to .71112 (17483).

Texture, mineralogy and bulk-rock chemistry suggest that TYPE QPXa xenoliths might represent micaceous segregations of greywacke, converted to gneiss by high-grade regional metamorphism (i.e. greywacke-gneiss). Because of a complex metamorphic history prior to incorporation, it is not possible to be equivocal about which of the basement terranes was the source; the high Sr content and low Sr isotopic ratio of 17425 are typical of Waipapa terrane greywackes whereas the higher Sr isotopic ratio of 17483 is more akin to Torlesse terrane rocks. Mineralogical relationships in 17425 and 17483 are of a slightly different type to those pertaining to TYPE VX xenoliths (c.f. section 5.3) (Brindley and Maroney, 1960):

muscovite + quartz = mullite + sanidine or peraluminous melt

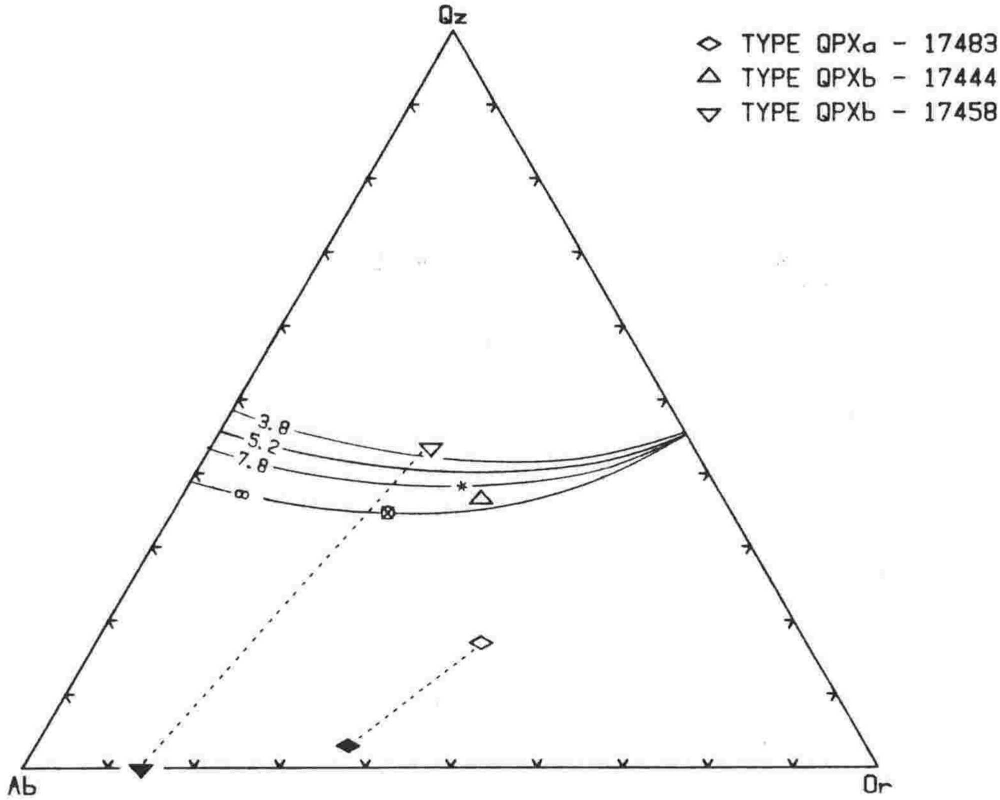

Fig.5.10: Normative glass compositions in selected TYPE QPX xenoliths plotted in the system quartz - albite - orthoclase (Tuttle and Bowen, 1958). Filled symbols are bulk rocks. Asterisk = S-type granite minimum melt composition (white and Chappell, 1977); cotectic lines are for obsidian-anorthite mixtures with Ab/An ratios of 3.8, 5.2, 7.8 and infinity (An=0) at P (H_2O) = 2kb (von Platen, 1965) - circled cross indicates ternary minimum.

In 17425, alteration of muscovite has produced sanidine with sillimanite; in 17483 this tranformation has proceeded further to produce a potassic melt which, in the Qz-Ab-Or system, plots towards the Ab-Or join and is not a minimum melt.

The bulk-rock composition of 17484 shows relative depletion in alkalis compared to other TYPE QPXa xenoliths which could result from removal of melt similar to that contained in 17483, although this is uncertain since original compositional similarities are obscured. Biotite is absent from the mineral assemblage of 17484 and orthopyroxene, sometimes as 1mm long porphyroblasts, occurs with plagioclase and pleonaste. This, therefore, probably represents a composition intermediate between biotite-rich TYPE QPXa and feldspar-rich TYPE QPXb (described below) and may provide a genetic link between them.

5.5.2 TYPE QPXb:

Feldspar-rich xenoliths are ubiquitous in lavas of the TVC. Steiner (1958), referred to dark grey feldspathic xenoliths in Ngauruhoe 1954 lava, which " ...represent re-melted, modified and recrystallised bands of quartzo-feldspathic gneiss.". Hackett (pers. comm., 1984) indicated such xenoliths were probably amongst the most abundant types in Ruapehu lavas but, because their grey colour matches that of host lavas they are less conspicuous than other types.

Most examples are elongated, angular and small (2-50mm x 1-10mm). All exhibit layering parallel to their long axis and many show partings in that direction. Textures range from hypidiomorphic granular (e.g.17497) to granoblastic (e.g.17419). Contacts are often sharp but irregular due to interpenetration of mineral grains (Plate 5.13) and margins are often intensely deformed and recrystallised.

Plate 5.13: BEI photograph of contact between TYPE QPXb xenolith 17419 (RHS) and host lava (LHS). Plagioclases in the xenolith are mildly zoned (darker shades indicate Na-rich compositions) giving a "clouded" appearance. Crystal edges penetrating host lava are euhedral and compositionally similar to microlites in the host lava. Near the contact, these, and accompanying pyroxenes, appear to be quench crystals.
Scale bar = .1mm; field of view = .3mm.

Plate 5.14: BEI photograph of TYPE QPXb xenolith 17443 showing layering and segregation of hypersthene (light grey), magnetite, ilmenite and pleonaste (all white) in a matrix of granoblastic plagioclase (grey).
Scale bar = 1mm; field of view = 1.9mm.

Plate 5.15: BEI photograph of a pleonaste porphyroblast in TYPE QPXb xenolith 17458. The core is corundum (sapphire) with inclusions of plagioclase (grey) and spinel. Granitic glass (light grey) is everywhere interstitial to plagioclase (see particularly top left).
Scale bar = .1mm; field of view = 1.1mm.

Plate 5.16: BEI photograph of vug assemblage in TYPE QPXb xenolith 17415. Minerals are plagioclase (grey, euhedral with sodic rims) and hypersthene (very light grey, euhedral with Fe-rich rims) in an interstitial glassy mesostasis. The assemblage may have grown in a volatile-rich pocket during metamorphism.
Scale bar = .1mm; field of view = 1.1mm.

Plate 5-13

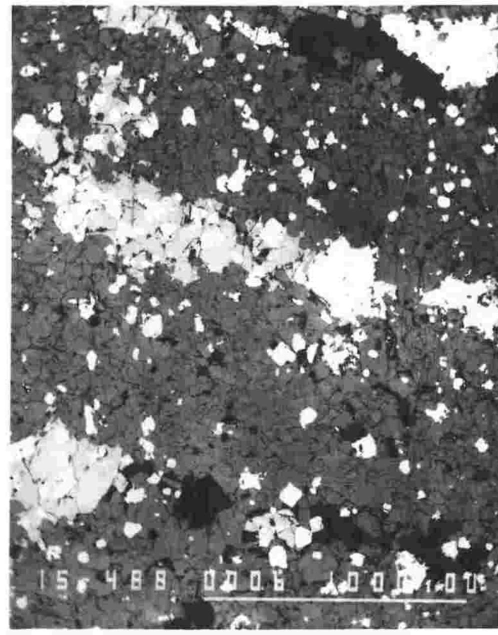

Plate 5-14

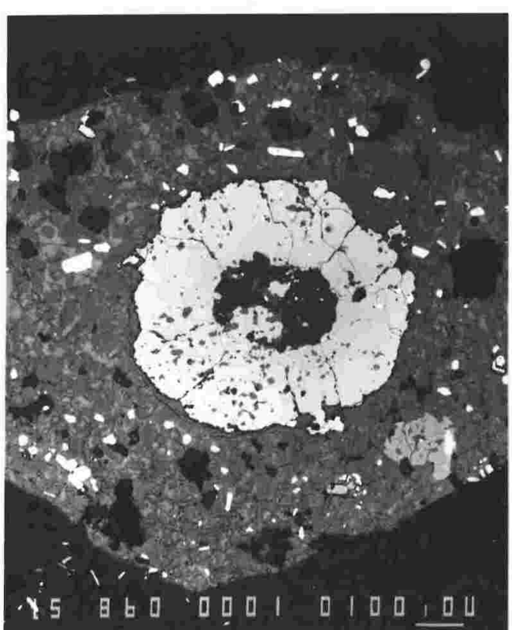

Plate 5-15

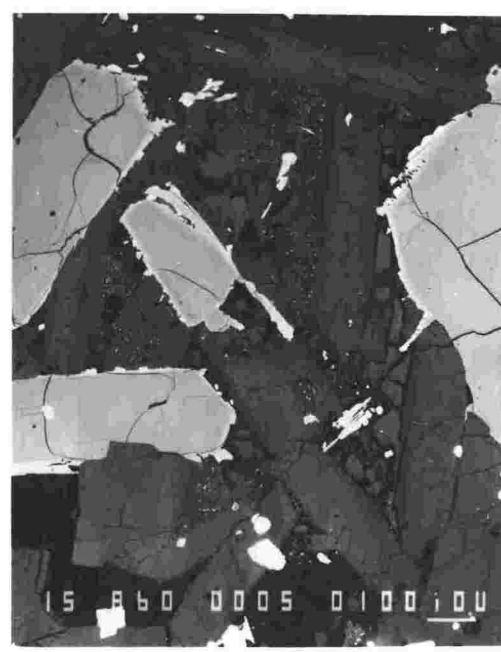

Plate 5-16

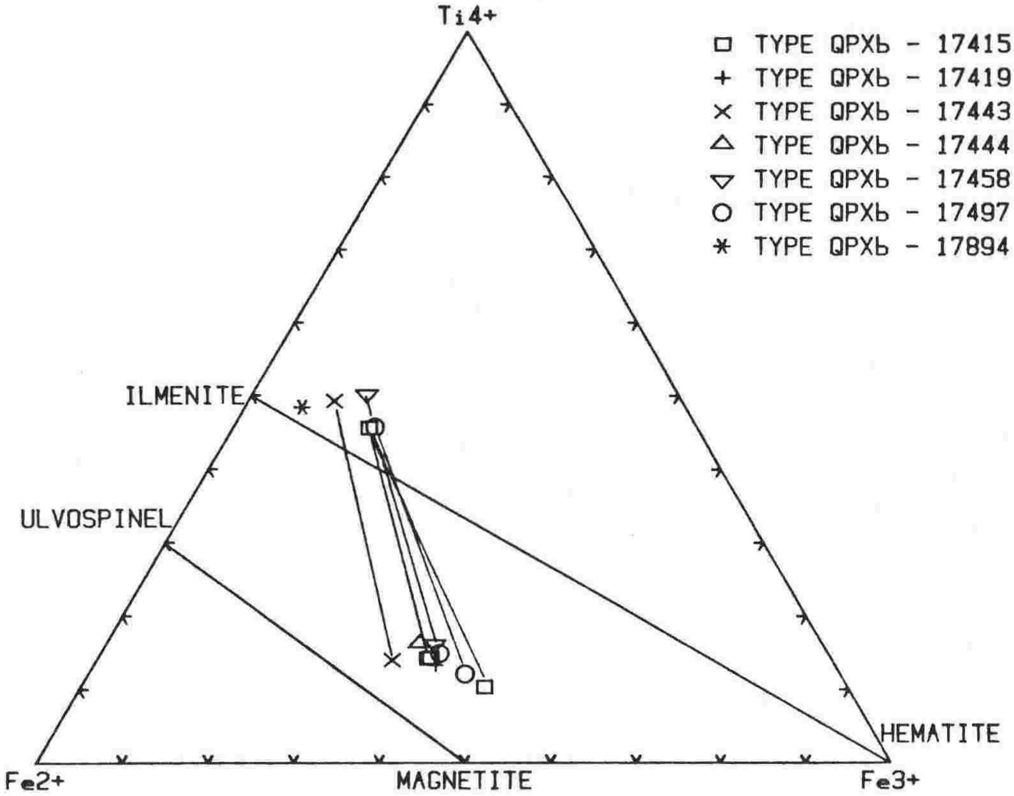

Fig.5.11: Ilmenite and magnetite analyses from selected TYPE QPXb xenoliths plotted in terms of Ti^{4+} - Fe^{2+} -Fe^{3+} (atoms). Tie-lines join coexisting phases in composite grains.

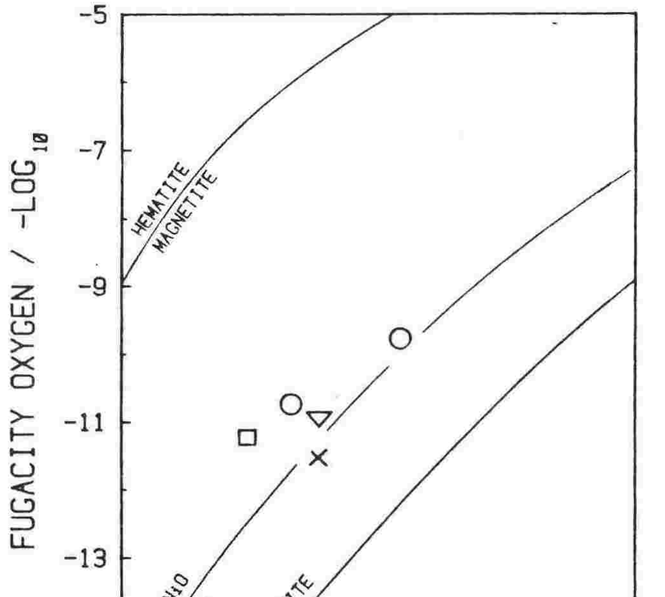

Fig.5.12: Temperature - oxygen fugacity conditions of metamorphism of selected TYPE QPXb xenoliths, based on determinations using the method of Stormer (1983). Key as for Fig.5.11.

Mineral assemblages are dominated by unzoned plagioclase, making up 60% to 80% by volume, whose compositions range from andesine to labradorite (Fig.5.9). In 17440 and 17419 (in particular) plagioclase becomes progressively more-clouded near the host-xenolith contact (Plate 5.13). Such clouding (Poldevaart and Gilkey, 1954) often results from diffusion of Fe into plagioclase through channels produced by unmixing and is most common in plagioclase of intermediate composition. It occurs when temperatures are held high for long periods of time in the presence of water (Smith, 1974). In 17419, clouding is probably related to thermal alteration near the contact caused by incorporation of the xenolith in the lava. EPMA analysis of the clouded marginal plagioclase reveals fine-scale variation in composition from An_{53} to An_{72} , but no significant change in FeO content.

Layering in TYPE QPXb xenoliths consists of 1-2mm wide segregations of subhedral, sub-ophitic, green-pink pleochroic hypersthene (En_{70}), titanomagnetite and ilmenite (Plate 5.14). Almandine garnet and cordierite occur in 17873, but not in other examples. Minor minerals are quartz, biotite (low-pressure alteration of hypersthene?) and zircon. Pleonaste is ubiquitous and occurs as rounded, .5-1mm diameter porphyroblasts sometimes with a corundum (sapphire) core (Plate 5.15). Ilmenite and titanomagnetite usually coexist (Fig.5.11) giving equilibration temperatures near 950 °C and equivalent oxygen fugacities of about -11, close to the Ni-NiO buffer (Fig.5.12).

Many TYPE QPXb xenoliths contain brown, interstitial glass which sometimes originates from host lava (Steiner, 1958); in 17458 the glass has a dacitic composition (Appendix 3) and contains numerous rounded micron-sized pyroxene microlites (inferred from chemistry); in 17415, brownish glass occurs in fractures and in small (10x10mm) vugs containing euhedral zoned plagioclase and hypersthene up to 1mm long (Plate 5.16). The plagioclases have cloudy, glass-filled interiors and orthopyroxenes are more Fe-rich than those of the surrounding xenolith (Appendix 3). This assemblage probably crystallised from a melt-rich pocket prior to incorporation of the xenolith in host lava and, subsequently, re-equilibrated with the last remaining liquid. Glass of a more siliceous composition (Appendix 3) pervades 17444 which, in the Qz-Ab-Or system (Fig.5.10), corresponds to a granitic minimum melt.

Textures, mineral habits and titanomagnetite-ilmenite equilibration temperatures suggest that TYPE QPXb xenoliths were recrystalised under granulite facies conditions. Cordierite and garnet in 17894 are probably relict from an original assemblage that pre-dates those changes but which suggests a pre-history as high-grade gneiss. Steiner (1958) noted that, occasionally, hypersthene phenocrysts protruded from host lava into xenolith interiors and that the crystal margins were markedly corroded, indicating that the xenolith was still liquid at the time the lava was crystallising. Such a relationship was rarely observed in the examples described here, although the presence of interstitial glass, granulitic textures and relict layering all suggest that these xenoliths were at some stage subjected to temperatures at or near the melting point of the assemblages observed.

Bulk-rock chemistries of TYPE QPXb xenoliths (Table 5.7) show high concentrations of Al_2O_3, Na_2O and CaO, reflecting high modal plagioclase contents. Sr concentrations are high, ranging from 448 to 896ppm; Rb concentrations are low, ranging from 2 to 26ppm. LILE and HFSE concentrations show consistent variation, being lowest in 17497 and highest in 17419. Normative mineralogy reflects well both modal compositions and mineral chemistries, indicating that assemblages are at or near equilibrium. This conclusion is supported by textural relationships. $^{87}Sr/^{86}Sr$ ratios range from .70570 to .70800 and are typically higher than host lavas (none of which exceed .70620 - c.f. Table 4.4).

5.5.3 Origins:

Feldspar-rich xenoliths (i.e. TYPE QPXb) could be fine-grained plagioclase cumulates resulting from fractional crystallisation of andesitic magma. However, the typically metamorphic textures, relict foliations, high P-T mineral assemblages and high Sr isotopic ratios do not support such an origin. Since most examples have higher $^{87}Sr/^{86}Sr$ ratios than their host lavas (or indeed of any recent lava of the TVZ) then they must be derived from a different source.

An alternative genesis linking both TYPES QPXa and QPXb into a crustal melting model seems more plausible and certainly more attractive. Read (1935) described feldspathic xenoliths ("orthonorites") in the Haddo House District of Aberdeenshire, Scotland. These were fine-grained plagioclase-rich rocks containing hypersthene as spongey, sometimes poikilitic masses, and were identical to "micronorite" xenoliths described by Read (1966) at Mill of Boddam, Insch, Aberdeenshire. There the host orthonorite contained bands and patches of micronorite which consisted of granular aggregations of feldspar and hypersthene with abundant opaques. In some bands, the hypersthene was "...packed in fairly continuous stripes and cemented by interstitial iron ore.". This description and published bulk-rock chemistries are strikingly similar to some TYPE QPXb xenoliths. Read interpreted the mineral assemblages as resulting from assimilation of pelitic country rock (andalusite-cordierite schist) by olivine gabbro. The pelitic rocks were first de-silicated and then the aluminous "restites" reacted with the contaminated magma to reprecipitate plagioclase and hypersthene (producing orthonorite zones). Micronorite zones were interpreted as relict aluminous restites which have re-equilibrated, in-situ, with the host lava.

Steiner (1958) considered that feldspathic xenoliths in Ngauruhoe 1949 and 1954 lavas represented re-melted feldspathic bands of gneiss. When such bands are broken up and scattered throughout a magma, they melt and interact with it. The resulting syntectic melt remains essentially feldspathic in composition and on crystallisation gives rise mainly to feldspar. Such an origin is supported by (1) granulitic texture (2) occurrence of relict high P-T minerals (garnet, cordierite) (3) high equilibration temperatures of coexisting Fe-Ti oxides (900 °C to 1000 °C). However, the dominantly metamorphic mineralogy and presence of relict metamorphic layering suggest a slightly different genesis, more in line with the interpretation of Read (1935, 1966) for Haddo House and Mill of Boddam orthonorites.

Chemical comparison (Table 5.7) between TYPES QPXa and QPXb shows that both are depleted in silica and high in alumina but that the latter is relatively alkali-depleted. This, and petrographic data suggest that these xenoliths might represent stages in the progressive alteration of dominantly feldspathic layers of gneiss (derived originally from basement greywacke). TYPE QPXb xenoliths are restites after extraction of granitic melt (similar to that of 17444), but are not totally remelted as suggested by Steiner (1958).

5.5.4 Other TYPE QPX xenoliths:

Two unusual xenolith types, both of which have silica-poor bulk-rock compositions (Table 5.7) occur rarely in some lavas but their origins and significance to crustal contamination of lavas remains obscure.

TYPE QPXc xenoliths 17423 & 17487 were both recovered from Iwikau Member pyroclastics and are very small (10x10x5mm), purple-grey in colour and weakly foliated. They have .25-.5mm wide discontinuous layers rich in spinel, and biotite forms a dense matted fabric with plagioclase (zoned from An_{85} to An_{56}, core to rim), pleonaste, titanomagnetite, ilmenite and hematite (Appendix 3). Ilmenite often forms an intergrowth with titanomagnetite and both are partially oxidised, as indicated by the coexistence of hematite, the low equilibration temperature (334 °C) and high oxygen fugacity (-38.86). Bulk-rock chemistry (Table 5.7) is unusual, particularly with respect to trace elements: alkali and LILE concentrations are high, as expected for a rock rich in biotite, but HFSE such as REE, Th, Nb, Y and Zr are all notably low; Cr, Ni and Cu concentrations are high. These features distinguish TYPE QPXc from the otherwise broadly-similar TYPE QPXa xenoliths. The unusual chemistry, though intriguing, does not immediately suggest a likely source from known basement lithologies.

TYPE QPXd xenoliths are small, strongly foliated and occur widely, sometimes being included in cumulate nodules (as in 17888). Mineral assemblages are characterised by high spinel contents. Narrow (mm-wide) layers rich in titaniferous biotite, poikilitic aluminous hypersthene and titanomagnetite or pleonaste alternate with layers rich in Ca-rich plagioclase (An_{74} to An_{96}). Olivine is a minor component in several examples, ranging in composition from Fo_{61} (17410) to Fo_{73} (17888). In 17489, coexisting titanomagnetite and ilmenite give an equilibration temperature of 979 °C. Overall grainsize of TYPE QPXd xenoliths is small (typically <.5mm) and textures are granoblastic. Xenolith-host contacts are sometimes marked by growth of clinopyroxene on the host side, but are otherwise regular and sharp. Bulk-rock chemistries are sometimes very silica-poor (17410) being typically olivine normative. TiO_2 is notably high.

The origin of TYPE QPXd xenoliths is unclear owing to their somewhat unusual compositions, small size and comparative rarity. A possible source are Torlesse terrane metabasites - these have similar mineralogies and bulk-rock chemistries (e.g. 17422 (this study); Roser, 1983). Alternatively, the xenoliths could be finely laminated mafic cumulates, but the high Sr isotopic ratios of some samples (e.g.17410 = .70800) preclude a cognate origin.

The presence of a strong foliation, granulitic texture and silica-poor bulk-rock chemistry strongly suggest that TYPE QPXd xenoliths represent restite assemblages, analogous to TYPE QPXb. The single high ilmenite-magnetite equilibration temperature (979 °C) indicates high-grade reconstitution but the occurrence of abundant biotite and the lack of any remnant partial melt is difficult to reconcile with such an interpretation. Tindle and Pearce (1983) presented a model for partial melting of greywacke in the upper crust based on mineralogy and chemistry of xenoliths within the Loch Doon granitic intrusion of Scotland. These were characterised by recrystallised biotite, actinolitic amphibole and green and brown spinel. Traces of brown glass occurred along cleavage planes of biotite. In this association, biotite is considered to be residual (with amphibole and plagioclase) after extraction of melt.

An origin as restites after extraction of melt from, and recrystallisation of, micaceous layers of greywacke-gneiss explains many petrographic and chemical features of TYPE QPXd xenoliths (e.g. high spinel content, high TiO_2 content, relict foliation). The presence of biotite may be due high Ti contents (6%-7%; Appendix 3) which tend to stabilise the mineral at progressively higher temperatures (Dr.R.H.Grapes, pers. comm., 1985); olivine will crystallise from silica-poor bulk chemistries under granulite facies conditions. The relative rarity of this xenolith type is due to two factors (1) micaceous layers of gneiss constitute only 10% to 20% of the bulk-rock (2) the xenoliths have relatively high specific gravity (compared to quartz-rich and feldspar-rich restites) causing them to sink preferentially - this may also explain the association of some TYPE QPXd xenoliths with cumulate nodules.

Table 5.8: Bulk-rock chemistry of TYPE IX xenoliths 17499, 17477, 17496 (volcanics); 17413 (pyroclastic); 17500 (pyroxenite); 17427 (norite); 17899 & 17412 (gabbro).

VUW	17499	17477	17496	17413	17500	17427	17899	17412
major elements (weight%)								
SiO_2	52.4	56.8	57.5	51.9	52.5	50.1	56.1	57.1
TiO_2	.7	.8	.7	.4	.6	.2	.5	.4
Al_2O_3	17.8	17.3	17.3	20.2	10.3	20.3	13.3	15.8
Fe_2O_3	1.4	1.3	1.3	1.3	1.8	1.2	1.3	1.3
FeO	7.1	6.4	6.6	6.7	9.3	6.0	6.4	6.7
MnO	.2	.1	.1	.1	.2	.1	.2	.1
MgO	7.9	4.7	4.7	7.7	14.3	8.2	10.5	9.0
CaO	9.9	8.0	7.8	9.1	9.2	11.8	9.1	5.9
Na_2O	2.2	2.8	3.1	2.4	1.3	1.5	1.9	2.6
K_2O	.2	1.4	.9	.2	.5	.3	.7	1.0
P_2O_5	.1	.1	.1	.0	.1	.0	.1	.1
LOI	.0	.1	.1	5.0	.5	.0	1.7	.9
C.I.P.W. norm								
Qz	3.0	8.9	9.7	1.6	.8	.4	6.8	7.8
Or	1.3	8.5	5.0	.9	2.9	1.7	4.4	5.6
Ab	19.0	23.4	26.1	20.4	10.6	12.8	15.9	21.8
An	38.0	30.7	30.8	43.9	21.0	47.8	25.7	28.6
Di	8.5	6.7	6.1	1.0	19.7	8.8	15.2	.0
Hy	26.6	18.1	19.0	29.5	41.2	26.2	29.1	33.2
Mt	2.1	1.9	1.9	1.9	2.7	1.8	1.9	2.0
Il	1.3	1.5	1.2	.7	1.1	.4	.9	.8
Ap	.2	.3	.2	.0	.1	.1	.1	.2
trace elements (ppm)								
Ba	160	300	202	89	129	80	176	254
Cr	259	38	55	142	1046	214	442	334
Ni	70	13	27	49	245	58	144	95
Rb	4	53	20	4	13	10	24	33
Sr	299	266	225	244	119	287	227	297
V	290	257	217	227	303	119	207	145
Zr	99	112	61	16	38	16	61	66
Rb/Sr	.013	.201	.087	.017	.111	.035	.107	.111
I	.	.70503	.	.70547	.70565	.70599	.70507	.70553

NOTES: Major element analyses normalised to 100% volatile-free (volatile loss (LOI) is given for comparison). Qz = quartz, Or = orthoclase, Ab = albite, An = anorthite, Di = diopside, Hy = hypersthene, Mt = magnetite, Il = ilmenite, Ap = apatite.
$I = {}^{87}Sr/{}^{86}Sr$ ...

5.6 TYPE IX - IGNEOUS XENOLITHS

Some xenoliths have petrographic features which are clearly igneous, indicating that they might have originated from a near-surface volcanic source (volcanic inclusions) or as cognate cumulates (cumulate nodules).

5.6.1 Volcanic inclusions:

Blocks of volcanic debris which have presumably been incorporated in advancing lava flows, are recognised by a marked colour contrast, a sharp, regular contact with their host and lack of textural modification. A typical example, 17496, is a pale-grey andesitic xenolith included in dark-grey Whakapapa Formation andesite from the northern slopes of Mount Ruapehu. The xenolith is porphyritic with 60% phenocrysts of plagioclase (75%), augite (15%) and hypersthene (10%) in a groundmass of plagioclase, pyroxene and spinel. Mineralogy and bulk-rock chemistry of this and similar xenoliths (Table 5.8) indicate that they have the same origins as their host lavas.

Xenoliths of hydrothermally altered andesite occur particularly in Mangawhero Formation lavas from the Girdlestone Peak section. They are typically yellow-brown cm-sized blocks with a brittle induration caused by sintering of the clay-rich matrix. In 17486, plagioclase and pyroxene phenocrysts are partly altered or completely replaced by clay and the originally glassy groundmass is thoroughly devitrified to a transluscent brown-matrix. However, a relict porphyritic texture is still easily recognisable. In other examples (e.g.17446) the xenolith is reduced to a structureless mass of greenish-brown clay containing minor disseminated white-mica and sulphides.

17413, a 5cm diameter nodule, contains bent and broken plagioclase and pyroxene crystals in a weakly mylonitised matrix. The wide variation in mineral chemistry (Appendix 3) and the texture suggest that it may be a pyroclastic bomb. Bulk-rock chemistry (Table 5.8), which shows a high

Table 5.9: X-ray powder diffraction data of natroalunite in 17426, compared to data published by Slansky (1975) (WI-4) and Parker (1962).

17426		WI-4		PARKER	
dA	I	dA	I	dA	I
5.693	25	5.688	17	5.69	12
5.610	14	-	-	5.58	12
4.918	>100	4.905	64	4.90	75
3.490	50	3.488	32	3.49	24
2.966	>100	2.973	100	2.97	70
2.965	>100	2.966	89	2.96	100
2.789	14	-	-	2.79	18
2.222	41	2.224	11	2.221	50
2.203	16	2.208	6	2.202	12
1.894	54	1.896	22	1.894	30
1.858	8	-	-	1.857	10
1.741	39	1.744	17	1.744	22
1.641	9	1.644	2	1.643	6
1.500	7	1.501	2	1.501	6
1.463	17	-	-	1.463	12
1.316	5	-	-	-	-
1.282	13	-	-	-	-

NOTES: CuKα radiation; Ni filter.

volatile loss, supports that interpretation.

5.6.2 Natroalunite-bearing nodule:

17426 was recovered as a small (5cm diameter) float block in the Whakapapanui Stream bed, northern Ruapehu and, though of uncertain derivation, was probably an inclusion in a recent Whakapapa Formation flow (W.R.Hackett, pers.comm., 1984). The xenolith is speckled orange-brown, is well-indurated and has a light-brown rind enclosing a fresh interior. Microscopic examination reveals a simple mineralogy of .1 to .2mm granular quartz grains (45%), fibrous, sometimes radiating clots of natroalunite (55%) and traces of rutile (see Frontispiece). Individual natroalunite crystals are less than .5mm wide and only a few microns thick. XRD analysis of the bulk-rock confirmed this mineralogy (Table 5.9) - all but two minor, high-angle peaks were assigned to either natroalunite, quartz or rutile and these are considered to be previously unreported peaks belonging to natroalunite.

Bulk-rock chemistry (Table 5.10) shows very low concentrations of Fe_2O_3, MnO, MgO and CaO. This is expected since quartz, natroalunite and rutile contain only trace amounts of these elements. Ignition losses confirm the DTA patterns reported previously for natroalunite (Kashkai and Babaev, 1969) and indicate de-watering at 500°C and partial thermal decomposition (2/3 S loss) at 900°C. The sulphur isotopic composition (courtesy of Dr.B.W.Robinson, INS) of +16.1 permil indicates significant low temperature fractionation. EPMA analysis of the natroalunite crystals was extremely difficult due to their high water content and thinness. Nevertheless, a partial analysis (Table 5.10) is similar to that derived after recalculating the bulk-rock analysis by removing from it SiO_2 (quartz) and TiO_2 (rutile). Individual natroalunite crystals are zoned having varying K/Na ratios (Frontispiece).

Alunite minerals have been reported previously from volcanic and hydrothermal associations in the TVZ (e.g. Steiner, 1953 (Wairakei); Wood,

Table 5.10: Chemistry of natroalunite-bearing nodule 17426.

	BULK-ROCK	N-ALUNITE1	N-ALUNITE2	RUTILE	RECALCULATED N-ALUNITE
SiO_2	44.09	.00	.00	.59	.00
TiO_2	.44	.00	.00	95.09	.00
Al_2O_3	20.99	36.70	37.31	.30	38.09
FeO	.21	.00	.00	3.21	.00
MnO	.00	.00	.00	.00	.00
MgO	.02	.00	.00	.00	.00
CaO	.09	.00	.00	.00	.00
Na_2O	2.98	4.70	6.02	.00	5.41
K_2O	1.52	4.80	2.66	.00	2.76
P_2O_5	.04	.00	.00	.00	.00
Cr_2O_3	.02	.00	.00	.88	.00
SO_3 #	(13.36)	37.40	37.40	.00	24.26
H_2O	26.29	-	-	.00	29.48
Total	96.67	83.59	83.39	100.06	100.00

NOTES: Natroalunite recalculated assuming only Al, Na, K, S and water included. # total S measured by Dr.B.W.Robinson (INS) 53490ppm. EPMA analyses of N-ALUNITE1 & N-ALUNITE2 with beam width of 10 micron and reduced current. Low totals indicate added volatiles.

1971 (Mt. Egmont)). Slansky (1975) reported an occurrence of natroalunite on White Island (Bay of Plenty); sample WI-4 appeared as a chalky-white, fine-grained fragment with petrographic features similar to altered andesitic lava. This suggested that the natroalunite in it formed by alteration of lava by hot acidic solutions, a process which has been demonstrated experimentally (Höller, 1967). For this to occur, temperatures must be in the range 90 °C to 180 °C and high concentrations of sulphuric acid are required (pH < 4.5). Wells et al. (1977) described a creamy-white deposit in the stream bed below Silica Springs outlet on Mount Ruapehu as hydrous, amorphous allophane. Bulk chemical analysis revealed high concentrations of Si, Al and S and low concentrations of K, Ca, Mn and Fe. Deposition was apparently influenced by a rise in pH downstream from the outlet consequent on loss of excess CO_2 . This occurrence suggests that natroalunite + quartz (sinter) might, under suitable conditions, precipitate from hydrothermal waters emanating from Mt. Ruapehu. This origin would best explain the simple mineralogy and bulk-rock chemistry. The indurated nature of the inclusion must therefore result from the thermal effect of brief immersion in the lava. In the light of this interpretation, it is interesting to note that the whole-rock $^{87}Sr/^{86}Sr$ ratio is .70535, close to an average for Ruapehu lavas (c.f. Table 4.4).

5.6.3 Cumulate nodules:

Glomerocrysts a few mm in diameter are important constituents of many TVC lavas (Chapter 4.2). Some of these are fragments of larger nodules with mineral compositions similar to host lava phenocrysts and are therefore cognate in origin. Others are not in equilibrium with host lava and are xenolithic in origin.

Ultramafic nodules of 5-20mm diameter occur in lava and scoria from Pukeonake. Lithologies include dunite (17887) and harzburgite (17888). Both contain forsteritic olivine (Fo88 to Fo92), bronzite (En84 to En87) and minor chrome spinel. Mineral compositions are similar to the rims of

Table 5.11: EPMA analyses of minerals in pyroxenite nodule 17500.

MINERAL	cpx	opx	hb	cpx	cpx	tmt	pl
ASSOC	core	core	rim	rim	rim	rim	rim
SiO_2	49.93	53.50	42.01	50.27	43.75	.10	50.14
TiO_2	.46	.00	1.81	1.46	2.38	2.38	.00
Al_2O_3	5.23	.74	13.12	3.67	9.61	3.93	31.18
Fe_2O_3	2.79	1.52	.00	3.51	5.74	.00	.00
FeO	6.14	17.05	10.70	2.71	3.20	76.15	.59
MnO	.18	.51	.00	.00	.00	.48	.00
MgO	14.85	25.69	14.50	15.95	12.53	5.36	.00
CaO	20.23	.47	11.02	21.85	20.20	.25	13.79
Na_2O	.30	.00	3.05	.50	.66	.00	3.65
K_2O	.00	.00	.50	.00	.00	.00	.17
Total	100.11	99.49	96.71	99.91	98.08	88.63	99.51
oxygens	6	6	22	6	6	4	8
Si	1.85	1.96	5.94	1.85	1.66	.004	2.30
Ti	.01	.00	.19	.04	.07	.068	.00
Al	.23	.03	2.19	.16	.43	.176	1.69
Fe^{3+}	.08	.04	.00	.10	.16	1.680	.00
Fe^{2+}	.19	.52	1.27	.08	.10	.742	.02
Mn	.01	.02	.00	.00	.00	.016	.00
Mg	.82	1.41	3.06	.87	.71	.304	.00
Ca	.80	.00	1.67	.86	.82	.010	.68
Na	.02	.00	.84	.04	.05	.000	.33
K	.00	.00	.09	.00	.00	.000	.01
Total	4.00	4.00	15.24	4.00	4.00	3.000	5.02

NOTES: cpx = clinopyroxene; opx = orthopyroxene; hb = hornblende; tmt = titanomagnetite; pl = plagioclase; Recalculations as in Appendix 3.

some phenocrysts in the lava and are therefore consistent with a cognate origin. They are probably derived from the parent basaltic magma involved magma mixing (c.f. description of TYPE 6 lavas, Chapter 4).

Large pyroxenite nodules are rare, though pyroxene-rich glomerocrysts are more common. One example, 17500, consists of a 10x20mm core of augite and hypersthene surrounded by a 5mm wide zone of partially altered hornblende. In the core, pale-green augite (up to 2mm) coexists with brown-green pleochroic hypersthene, which occurs both as discrete grains and as inclusions in augite and minor, interstitial zoned plagioclase (An_{70}) and spinel. The core is rimmed by sieved hornblende enclosed by patchy, opaque masses. These resolve into myriads of tiny titanomagnetite, augite and (minor) plagioclase crystals, an assemblage which reflects low-pressure alteration of hornblende to aluminous-clinopyroxene + plagioclase + titanomagnetite. Compositions of each of these phases are given in Table 5.11 (note that, although hornblende compositions are consistent throughout, compositions of the breakdown products vary somewhat). Thermal decomposition of hornblende is a useful indicator of P-T conditions. This was demonstrated by Spear (1981), who showed that hornblende alters to clinopyroxene on the hematite-magnetite buffer at between 695 °C and 738 °C (.5-3kb, Pf=Pt). The assemblage in 17500 thus represents the breakdown of hornblende, originally forming a reaction rim around the pyroxenite nodule, due to an increase in temperature following incorporation in the host magma.

Gabbroic nodules consisting of two pyroxenes, plagioclase and basaltic glass (e.g.17899, 17412) are widespread and occur frequently in the most phenocryst-rich lavas. Typical examples are 20-30cm in diameter, grey to greyish-white and variably vesicular. Contacts with host lava are irregular but sharp. Clinopyroxene normally dominates over orthopyroxene and both these minerals are larger (1-2mm) and more abundant than plagioclase. Pyroxene compositions are generally similar to those of host lava phenocrysts and yield similar equilibration temperatures (1000 °C to 1100 °C). Interstitial mesostasis consists of a dark-brown basaltic glass containing microlites of plagioclase and pyroxene. Plagioclase is rarely dominant (it is in 17412) and is often intensely clouded with exsolution of spinel from cores and outer zones.

Cumulus textures are thermally overprinted in two small, noritic nodules, 17427 and 17438. In the former, the mineral assemblage comprises 60% plagioclase (An_{88}), 25% bronzite (Mg_{75}), 10% augite (Mg_{80}), minor hornblende, Fe-oxide (pyrrhotite) and brown basaltic glass. Hornblende is present as .1-.3mm anhedral inclusions in bronzite or as sieved grains poikilitically enclosing plagioclase, bronzite and ilmenite. It is not clear whether such xenoliths are (1) cognate (2) related to an earlier magma or (3) TYPE MIX (see below). The metamorphic overprints might simply reflect a time-gap between formation and incorporation - this suggests that (2) is most likely.

5.7 TYPE MIX - METAIGNEOUS XENOLITHS

TYPE MIX xenoliths are predominantly small grey, fine-grained xenoliths with mafic mineral assemblages. They occur frequently and, though less conspicuous than most quartz-rich types, are probably volumetrically as important. All examples show evidence of varying degrees of thermal metamorphism ranging from overprinting of recognisable igneous textures to complete re-equilibration of pre-existing assemblages. Most have bulk-rock chemistries and Sr isotopic compositions different from surface lavas and that, together with textural evidence for recrystallisation at high metamorphic grade, suggests a deep-seated origin. Twenty TYPE MIX xenoliths are described, each having distinctive petrographic and/or chemical characteristics. Classification is therefore particularly difficult, and has been attempted only in a broad sense, being initially based mainly on grainsize:

Plate 5.17: BEI photograph of TYPE MIXa xenolith 17424 showing granoblastic texture with a strong directional orientation, :epresenting either an original igneous layering or a later schistosity. Mineral assemblage is plagioclase (grey), pyroxene (light grey, poikiloblastic) and ilmenite (white). Scale bar = 1mm; field of view = 1.9mm.

Plate 5.18: BEI photograph of TYPE MIXa xenolith 17441 showing typical granoblastic texture with coarse, poikilitic pyroxene and finer, interstitial plagioclase.
Scale bar = 1mm; field of view = 1.9mm.

Plate 5.19: BEI photograph of the contact between TYPE MIXa xenolith 17442 (RHS) and host lava. Crystals on the xenolith rim are in equilibrium with host lava and have euhedral terminations.
Scale bar = 1mm; field of view = 1.9mm.

Plate 5.20: BEI photograph of TYPE MIXc xenolith 17422. Plagioclases (grey, euhedral crystals have Na-rich rims in contact with granitic glass. Microlites of spinel occur near the contacts.
Scale bar = .01mm; field of view = .06mm.

Plate 5-17

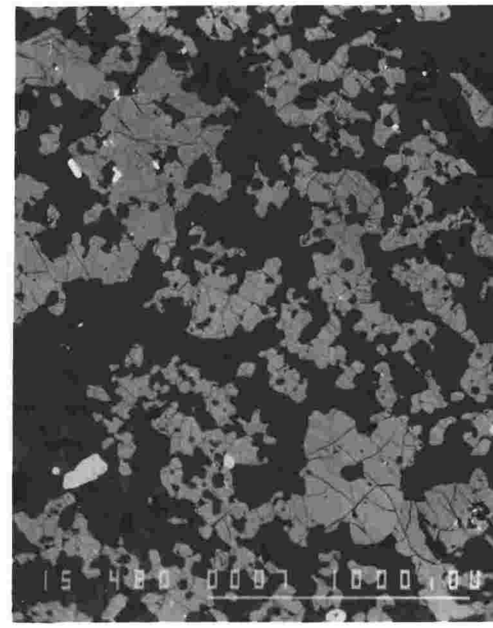

Plate 5-18

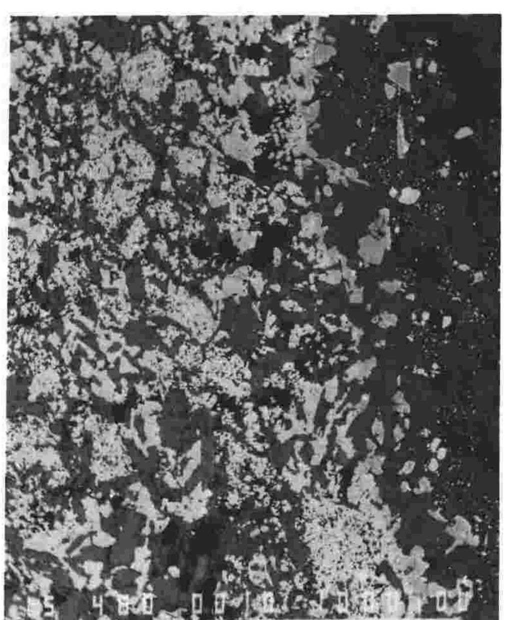

Plate 5-19

Plate 5-20

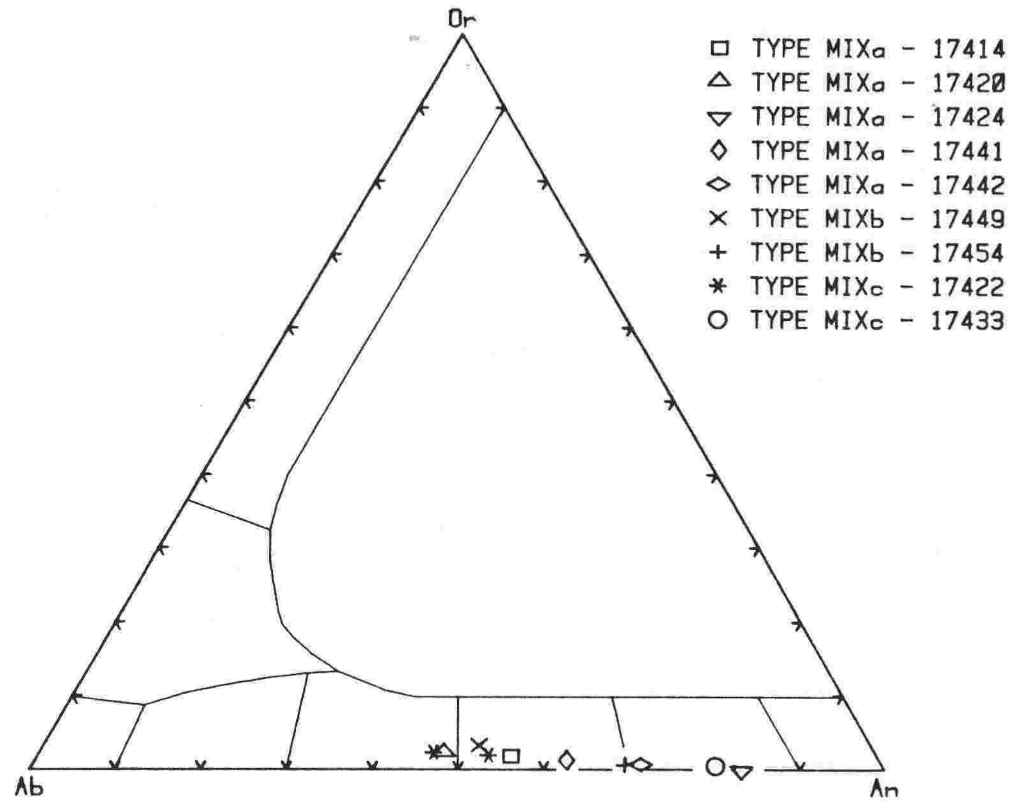

Fig.5.13: Plagioclase compositions of TYPE MIX xenoliths, plotted in terms of K - Na - Ca.

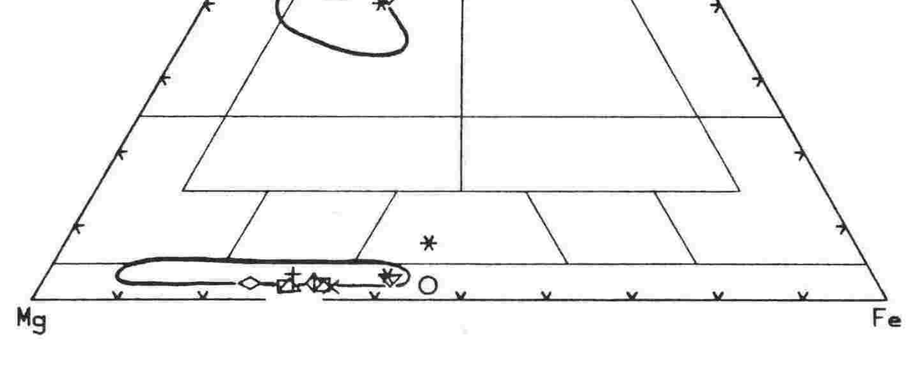

Fig.5.14: Pyroxene compositions of TYPE MIX xenoliths, plotted in terms of Ca - Mg - Fe. Fields are for host lavas (Fig.4.3). Key as for Fig.5.13.

TYPE MIXa = 2-5mm (poikilitic pyroxene) to .2-1mm (plagioclase);

TYPE MIXb = .2-1mm (average);

TYPE MIXc = less than .25mm.

5.7.1 Petrography:

Textures of most TYPE MIX xenoliths indicate a high degree of metamorphic equilibration. TYPE MIXa are typically poikiloblastic (Plate 5.17) and often show a directional fabric representing either relict igneous layering or a later schistosity. Some (e.g.17414) are cataclastised from severe shearing stress prior to inclusion. TYPES MIXb and MIXc are mostly xenomorphic granular, although one example (17450) has a relict igneous (porphyroblastic?) texture. Xenolith-host contacts are usually sharp and regular (Plates 5.19). In only a few cases is there a suggestion of reaction at this interface involving preferential growth of plagioclase.

TYPE MIX xenoliths have a restricted mineralogy of plagioclase, orthopyroxene, clinopyroxene and ilmenite. Chromian spinel occurs rarely (17414, 17442) and quartz is abundant only in some TYPE MIXc examples. Titanomagnetite, olivine and hydrous minerals are all typically absent. Plagioclase compositions range between An_{44} (17449) and An_{88} (17424) and are low in K (Fig.5.13). Zoning occurs only where igneous textures are still recognisable (e.g.17450 has a range from An_{58} to An_{88}).Orthopyroxene is bronzite or hypersthene and compositions are relatively Ca-poor compared to host lava phenocrysts (Fig.5.14). Clinopyroxenes are mainly augites containing less than 2% Al_2O_3, and are all more Ca-rich than host lava phenocrysts (Fig.5.14). Equilibration temperatures of coexisting pyroxene pairs range between 920 °C and 1014 °C (Wells, 1977) or 790 °C and 1020 °C (Lindsley, 1983 - Appendix 1.1). These are significantly lower than those of host lavas which range between 1000 °C and 1100 °C (c.f. Chapter 4.2). Ilmenites are low in alumina and contain 3-6 weight% MgO (Appendix 3).

Table 5.12: Bulk-rock chemistry of selected TYPE MIX xenoliths.

VUW	17424	17441	17442	17421	17420	17417	17414	17449
TYPE	MIXa	MIXa	MIXa	MIXa	MIXa	MIXb	MIXa	MIXb
major elements (weight%)								
SiO_2	48.8	52.6	53.4	53.7	54.8	54.9	55.0	57.3
TiO_2	1.5	.6	.6	.5	.4	.6	.5	.7
Al_2O_3	16.9	15.3	13.8	15.2	10.8	13.3	13.7	14.8
Fe_2O_3	2.2	1.6	1.4	1.4	1.4	1.7	1.3	1.3
FeO	10.8	7.8	6.9	6.9	6.8	8.4	6.7	6.5
MnO	.3	.2	.1	.2	.2	.2	.1	.2
MgO	8.7	9.7	12.9	10.3	12.9	10.2	13.1	7.9
CaO	9.3	10.0	8.9	8.9	10.3	7.9	6.8	8.5
Na_2O	1.5	1.8	1.6	2.6	2.1	2.1	1.8	2.6
K_2O	.1	.3	.3	.3	.3	.7	.8	.4
P_2O_5	.1	.1	.1	.1	.1	.1	.0	.1
(LOI)	1.4	.2	.2	.9	.8	1.3	1.9	.4
C.I.P.W. norm								
Qz	1.3	3.2	2.8	1.7	2.0	4.7	4.5	9.6
Or	.6	1.6	2.0	1.6	2.0	4.3	4.6	2.3
Ab	12.6	15.3	13.6	21.7	18.0	18.0	15.6	21.8
An	39.1	33.0	29.5	29.0	18.9	24.6	27.2	27.6
Di	5.5	13.4	11.2	11.6	25.3	11.7	5.3	11.3
Hy	34.9	30.0	37.6	31.2	31.0	33.2	40.0	24.2
Mt	3.1	2.3	2.0	2.0	2.0	2.4	1.8	1.9
Il	2.9	1.2	1.1	1.0	.8	1.0	1.0	1.2
Ap	.1	.1	.2	.2	.2	.1	.1	.4
trace elements (ppm)								
Ba	71	107	132	129	144	179	141	163
Cr	242	445	798	627	820	482	673	555
Ni	99	130	292	173	257	117	334	46
Rb	2	6	10	4	9	26	43	9
Sr	210	249	300	230	175	231	329	368
V	374	244	204	199	181	216	182	222
Zr	31	37	54	35	42	46	47	63
Rb/Sr	.008	.026	.032	.018	.050	.113	.131	.023
I	.70654	.70592	.70568	.70627	.70541	.70533	.70820	.70569

NOTES: I = $^{87}Sr/^{86}Sr$, Fe_2O_3 / FeO = 0.2.
Major element analyses normalised to 100% volatile-free (volatile loss (LOI) is given for comparison). Qz = quartz, Co = corundum, Or = orthoclase, Ab = albite, An = anorthite, Di = diopside, Hy = hypersthene, Mt = magnetite, Il = ilmenite, Ap = apatite.

Table 5.12 cont:

VUW	17479	17431	17422	17433	17432	17434
TYPE	MIXc	MIXc	MIXc	MIXc	MIXc	MIXc
major elements (weight %)						
SiO_2	50.8	54.5	55.1	57.6	58.9	62.7
TiO_2	.7	.6	.7	.6	.6	.5
Al_2O_3	19.7	19.3	17.2	17.1	19.0	18.8
Fe_2O_3	1.6	1.4	1.4	1.3	1.2	.9
FeO	8.2	7.2	6.7	6.5	5.9	4.5
MnO	.2	.1	.2	.2	.1	.1
MgO	8.0	5.6	5.1	5.4	3.9	2.1
CaO	7.9	7.3	9.2	10.1	7.5	6.2
Na_2O	2.4	3.4	3.6	1.2	2.3	3.8
K_2O	.3	.6	.7	.1	.5	.5
P_2O_5	.1	.1	.1	.1	.1	.1
LOI	.4	.7	1.0	1.2	1.8	.7
C.I.P.W. norm						
Qz	1.6	4.2	3.3	18.0	18.2	19.7
Co	1.5	.2	.0	.0	1.5	1.0
Or	1.6	3.2	4.0	.5	3.0	3.0
Ab	19.9	28.5	30.6	10.4	19.0	31.8
An	38.5	35.3	28.7	40.7	36.3	30.1
Di	.0	.0	13.5	7.0	.0	.0
Hy	32.9	25.1	16.5	20.2	18.9	12.1
Mt	2.4	2.1	2.0	1.9	1.7	1.3
Il	1.4	1.1	1.3	1.1	1.2	.7
Ap	.2	.3	.3	.2	.2	.2
trace elements						
Ba	280	173	97	54	353	.
Cr	311	43	84	99	25	.
Ni	73	12	19	35	7	2
Rb	5	16	17	<2	55	3
Sr	392	379	412	194	809	362
V	232	182	245	201	197	.
Zr	116	37	56	51	69	83
Rb/Sr	.012	.043	.041	.007	.067	.008
I	-	.70601	.70650	.70711	.70866	.70579

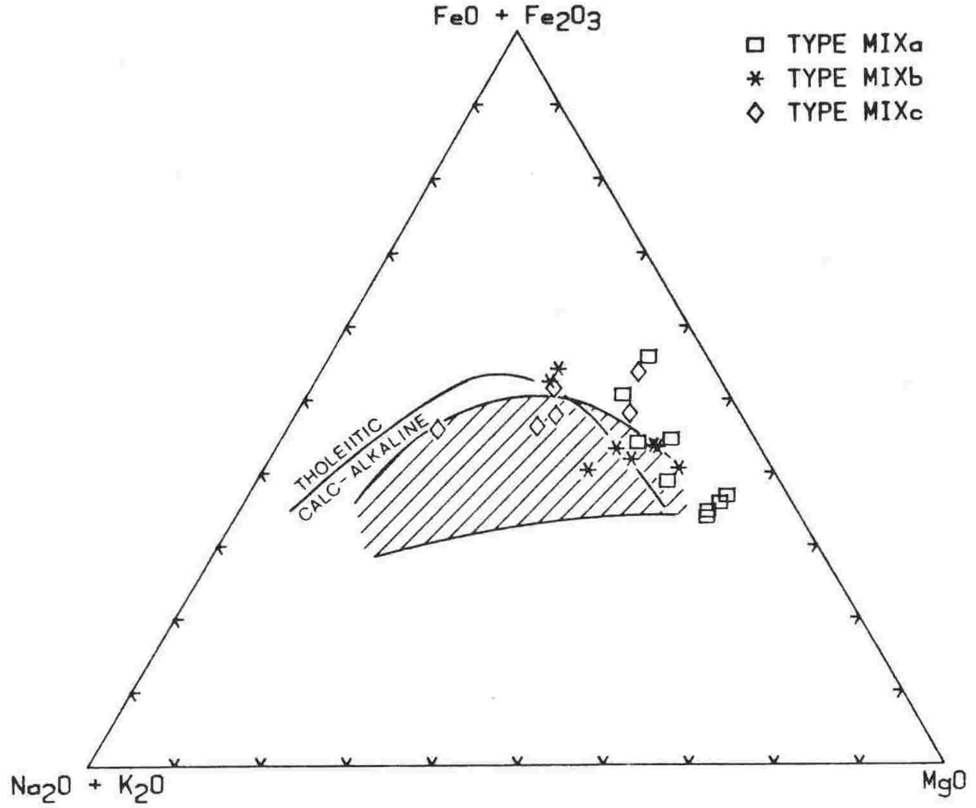

Fig.5.15: AFM plot of TYPE MIX xenoliths. Curve separates tholeiitic from calc-alkaline fields (Irvine and Baragar, 1971). Shaded area is for host lavas (Fig.4.5).

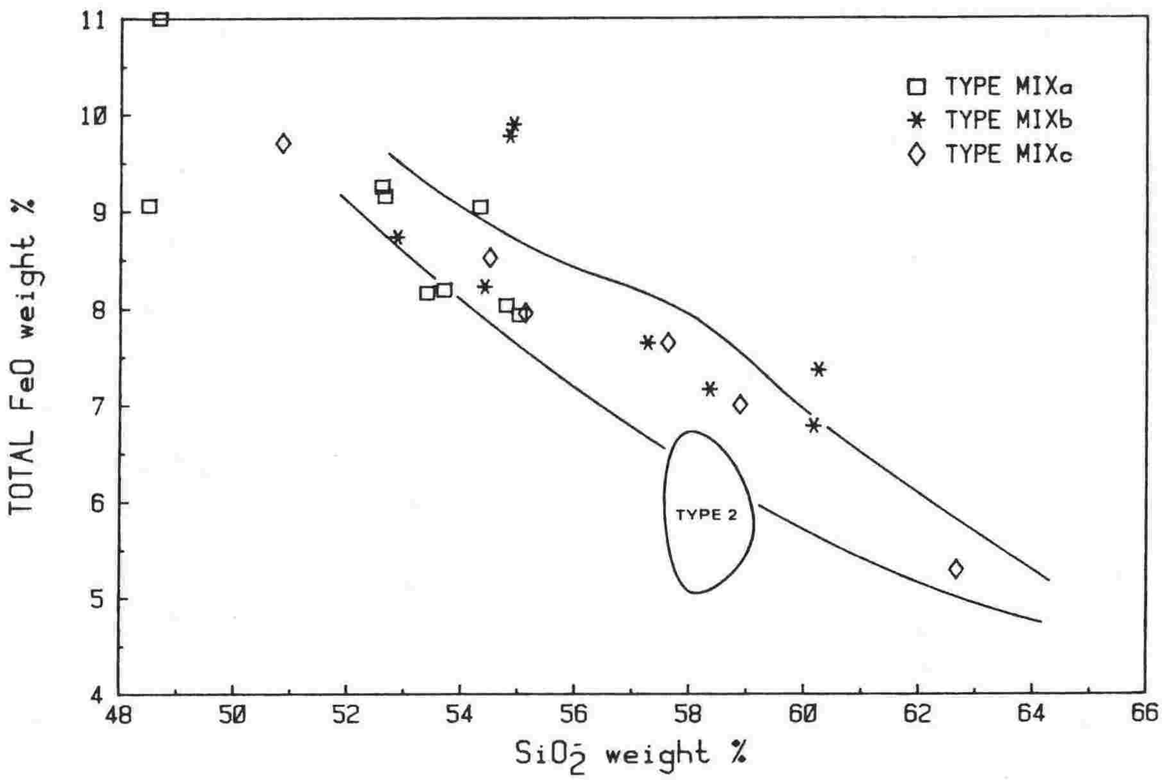

Fig.5.16: Total FeO vs. SiO_2 Harker variation diagram for TYPE MIX xenoliths. Field is that of host lavas (Fig.4.8).

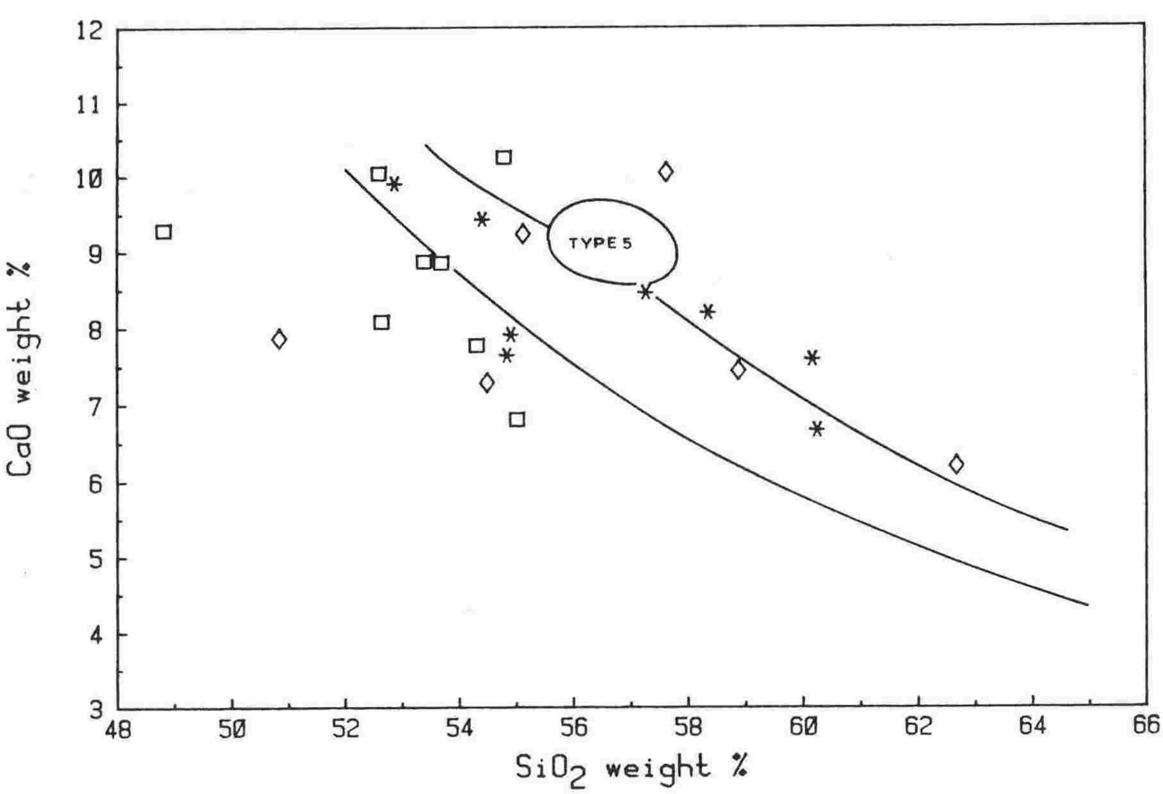

Fig.5.17: CaO vs. SiO_2 Harker variation diagram for TYPE MIX xenoliths. Field is that of host lavas (Fig.4.10). Key as for Fig.5.16.

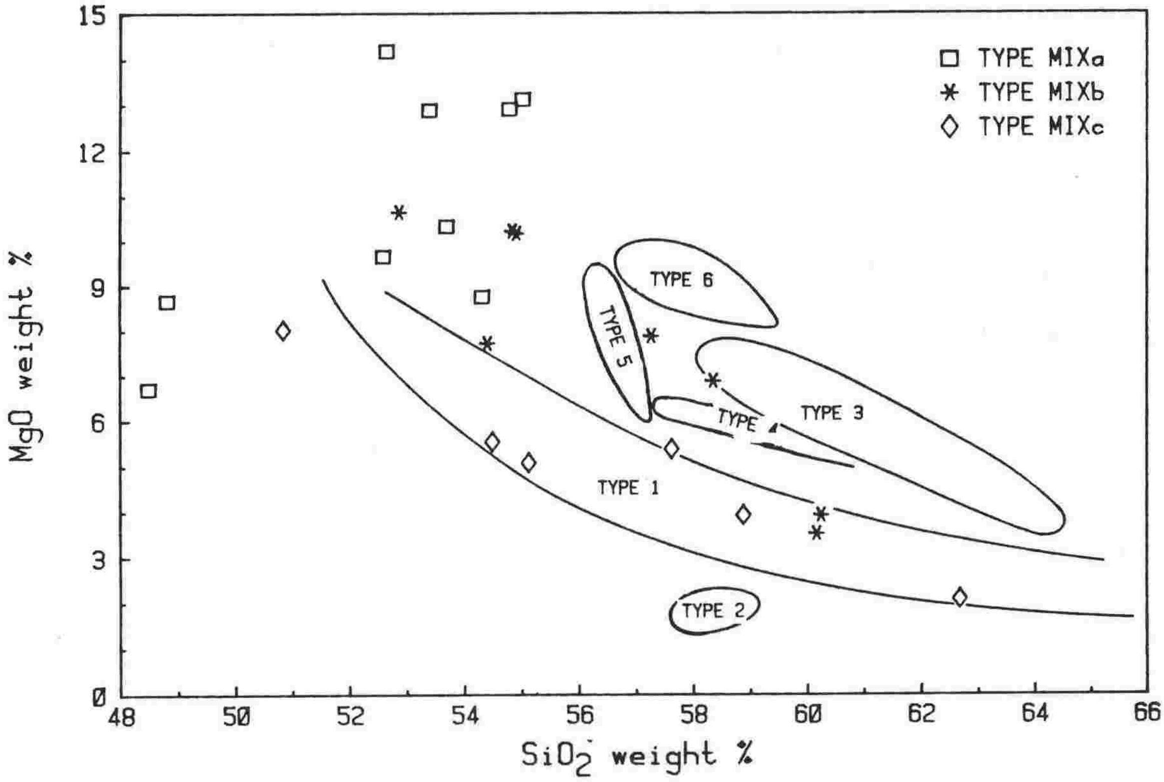

Fig.5.18: MgO vs. SiO_2 Harker variation diagram for TYPE MIX xenoliths. Fields are those of host lavas (Fig.4.9).

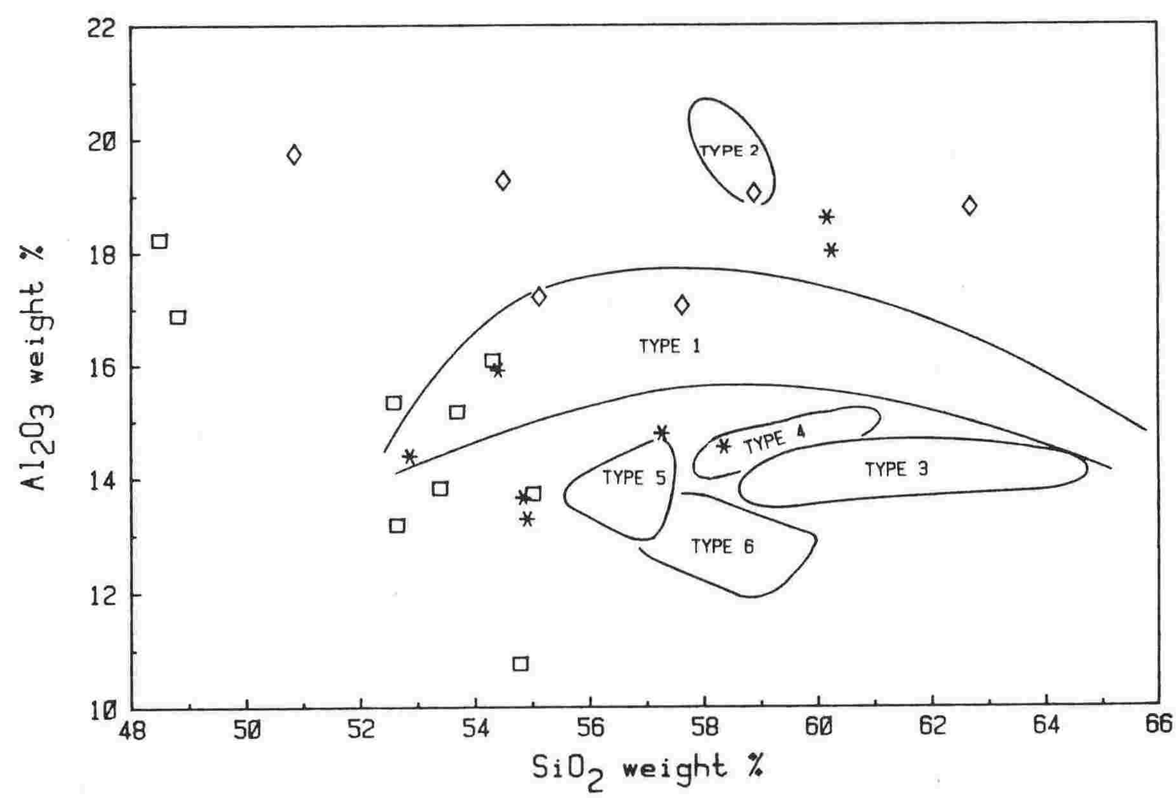

Fig.5.19: Al_2O_3 vs. SiO_2 Harker variation diagram for TYPE MIX xenoliths Fields are those of host lavas (Fig.4.7). Key as for Fig.5.18.

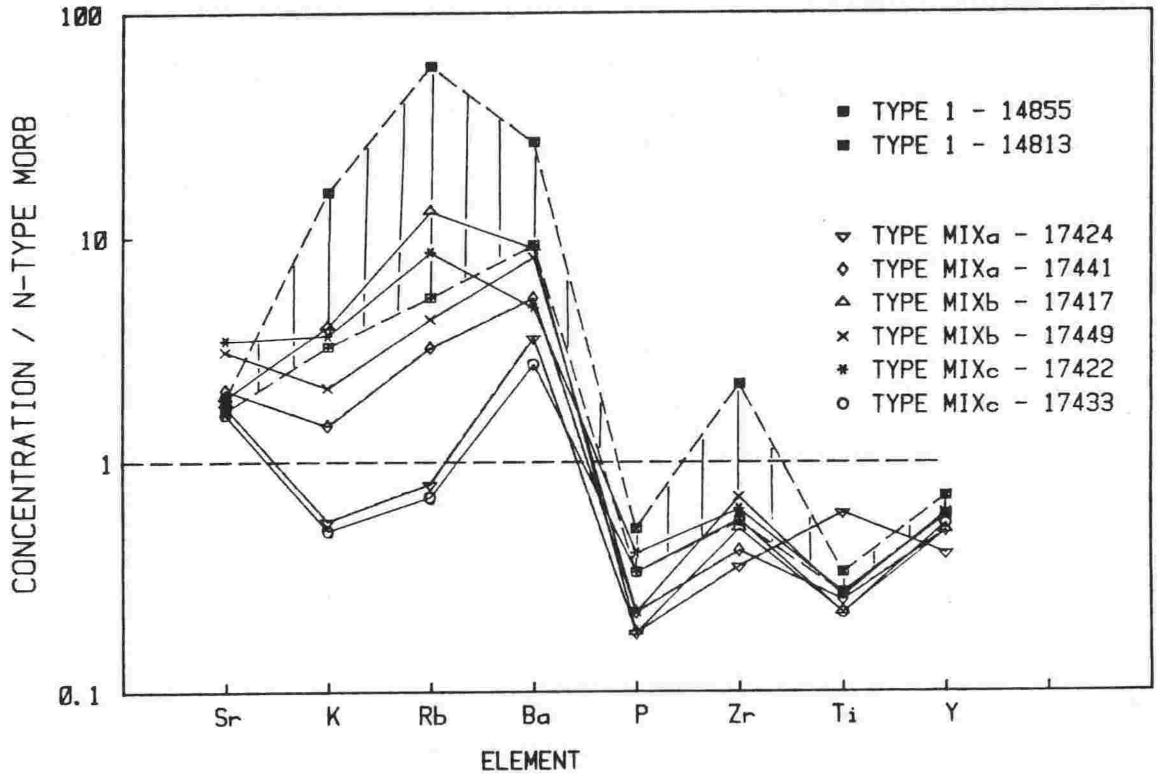

Fig.5.20: Spidergram of trace element concentrations in selected TYPE MIX xenoliths, normalised to N-type MORB values (Pearce, 1982). Normalisation constants are given in Fig.4.14. Field is for TYPE 1 host lavas (Fig.4.14).

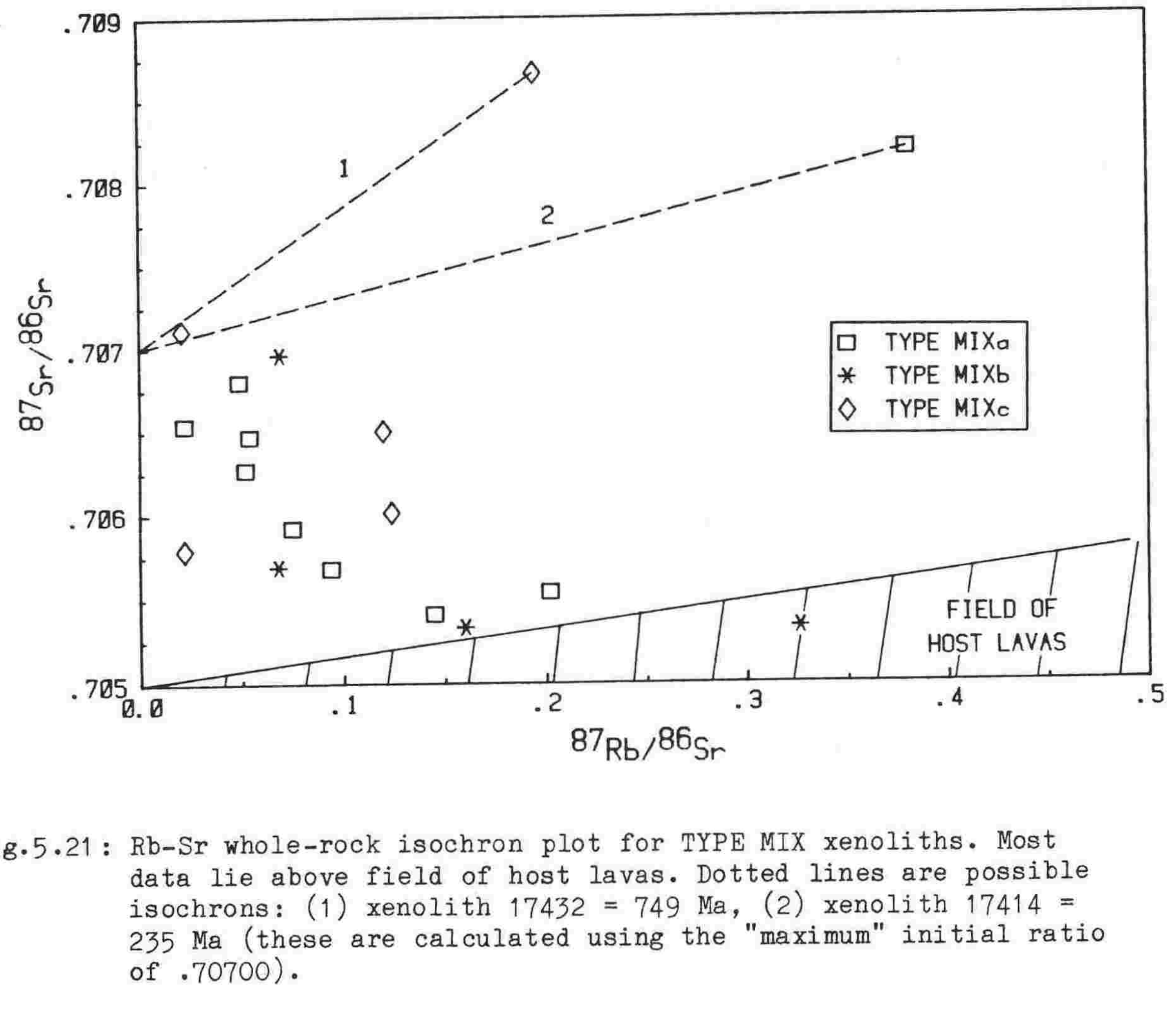

Fig.5.21 : Rb-Sr whole-rock isochron plot for TYPE MIX xenoliths. Most data lie above field of host lavas. Dotted lines are possible isochrons: (1) xenolith 17432 = 749 Ma, (2) xenolith 17414 = 235 Ma (these are calculated using the "maximum" initial ratio of .70700).

5.7.2 Bulk-rock chemistry:

In the following discussion, bulk-rock chemical compositions of TYPE MIX xenoliths are compared to those of surface (host) lavas, in order to assess whether both could have a common origin. To do this, silica-based Harker variation diagrams of some compatible elements, and spidergrams of incompatible elements are used.

SiO_2 contents (Table 5.12) range from 48% to 62% (i.e. from basalt to andesite). An AFM plot (Fig.5.15) shows that some compositions are depleted in alkalis compared to host lavas whereas others approximate to a calc-alkaline trend of limited iron enrichment. There is a close similarity in SiO_2 -FeO (Fig.5.16) and SiO_2 -CaO (Fig.5.17) trends with those of host lavas; significant departures occur mainly for TYPE MIXa with low silica contents. Many of these are also high in MgO (Fig.5.18) and low in Al_2O_3 (Fig.5.19). The presence of relict cumulate textures and high Cr (>500ppm) and Ni (>100ppm) contents suggest that these might represent metagabbroic cumulates. Most have Sr contents less than 250ppm, but three examples (17414, 17448, 17449) exceed 350ppm. Some MIXc xenoliths (e.g.17479, 17450) are Al_2O_3 -rich whereas others are relatively Ca-poor but Sr-rich (e.g.17432 has 809ppm Sr).

Incompatible element concentrations are characteristically low, even in more evolved compositions (Fig.5.20). Few xenoliths have K, Rb or Ba contents as high as host lavas and one example (17433) is extremely depleted. Concentrations of HFSE (P, Zr, Ti, Y) are also low relative to both N-MORB and host lavas. Although these spidergram patterns show broadly calc-alkaline affinities, they differ in detail from host lavas and have lower overall relative abundances.

$^{87}Sr/^{86}Sr$ ratios are relatively high, despite typically low $^{87}Rb/^{86}Sr$ ratios (Fig.5.21). Only 17417 falls in the range of host lava compositions. Because of the wide scatter of data and diverse petrography, no serious attempt was made to derive a model age for the suite. The three most radiogenic samples are petrographically and chemically dissimilar, and may not be genetically related. However, isochrons linking them (Fig.5.21) indicate that, for any reasonable assumed initial Sr isotopic ratio, model ages are in the order of several hundred million years.

5.7.3: Origins:

Textural, mineralogical, chemical and Sr isotopic data indicate that TYPE MIX xenoliths are not directly related to lavas now exposed in the TVC. Their origins must therefore lie either within known basement terranes or beneath them. One possibility is that they could be conglomerate clasts from Torlesse or Waipapa terranes. This is, however, unlikely since their basic chemistry is inconsistent with the predominance of granitic and dioritic clasts usually described from such conglomerates (Dr.R.J.Korsch, pers. comm., 1985). Alternatively, they could be Torlesse terrane metavolcanics. Roser (1983) described 81 metabasites from North Island localities, and showed that all have tholeiitic or calc-alkaline affinities similar to oceanic basalts. However, most have high Ti, Zr and Y contents, inconsistent with the relative depletion of these elements in TYPE MIX xenoliths, and widely differing incompatible element ratios. The one metabasite analysed here (17822) has a $^{87}Sr/^{86}Sr$ ratio of .70880, higher than any TYPE MIX xenolith. It is therefore considered unlikely than these xenoliths originated as metabasites which are, in any case, rare and volumetrically restricted within the Torlesse terrane.

Since there appears to be no likely source within known basement terranes, it is probable that TYPE MIX xenoliths originated from an unknown igneous source beneath the Mesozoic basement. The relatively high isotopic ratios but low incompatible element contents suggest an extended evolutionary history, and argue against the source volcanics being derived either from depleted mantle (since in that case the isotopic ratios should be relatively low) or by crustal contamination of basalt (since in this case the incompatible element concentrations should be high). The material now exposed as xenoliths may represent oceanic crust on which the first Torlesse terrane sediments were deposited. Some of the rocks are petrographically and chemically similar to those of the Marum Ophiolite Complex (Jaques, 1981; Jaques et al., 1983) and may therefore have formed in a similar environment (i.e. either Mid Ocean Ridge or back-arc basin).

The LILE-depleted chemistries of the rocks may be inherited from their source or, more likely, have resulted from volatile tranfer and/or partial melting of the rocks during granulite facies metamorphism. If the latter is correct, then this process has important implications for crustal contamination of TVC lavas. However, although one TYPE MIXc xenolith (17422) contains small amounts of siliceous glass (Plate 5.20), this is absent from other examples and uncertainty about genesis and original rock compositions make such speculations difficult to substantiate.

5.8 DISCUSSION

5.8.1 Summary description of dominant xenolith lithologies:

Although a wide range of xenolith types occur in lavas of Ruapehu and nearby vents, only a few are volumetrically significant and even fewer are considered important as crustal contaminants of andesitic magmas.

Vitrified xenoliths (TYPE VX) are of two kinds (1) TYPE VXa have bulk-rock chemistries and Sr isotopic compositions similar to Torlesse terrane greywacke. They typically contain more than 50% glass of granitic composition and a restite assemblage of quartz, cordierite (or hypersthene) and pleonaste. Glass compositions vary with bulk-rock chemistry and with the composition of internal fine-scale segregations. TYPE VXb are compositionally different, being richer in Al, Ca, Pb and Sr and poorer in Rb and Cr. They are less vitrified and, in addition to cordierite, quartz and pleonaste, have plagioclase in the restite. Both xenolith types were probably incorporated in host magma while in a high-level magma chamber and, consequently, show little alteration of bulk-rock composition or evidence for interaction with host lava.

Quartz-rich xenoliths, particularly those comprising more than 90% quartz (TYPE QXb) are the most abundant xenolith type. Quartzo-feldspathic gneisses (TYPE QXa) contain segregations of sodic plagioclase, garnet, biotite and/or granitic glass and segregations of quartz, calcic plagioclase and clinopyroxene. This latter assemblage also occurs in some TYPE QXb, suggesting that these may represent quartzose segregations of the gneiss. Some TYPE QX xenoliths are surrounded by a corona of silica-rich glass and clinopyroxene, a result of partial melting and diffusive interaction with host magma.

Small, foliated feldspathic xenoliths (TYPE QPXb) are widespread and probably as common as TYPE QXb xenoliths although, because of their dull grey colour, they are difficult to distinguish in outcrop. All display relict layering of hypersthene + spinel and have a xenomorphic granular or

Table 5.13: Metamorphic temperatures based on cation exchange equilibria.

VUW	TYPE	ASSEMBLAGE	TEMPERATURE (°C)	METHOD
17485	QXa	gnt-bio	946	Ferry & Spear (1978)
17492	QXa	gnt-opx	808	Harley (1984)
17498	QXe	tmt-ilm	913	Stormer (1983)
17425	QPXa	pl-ks	800	Brown & Parsons (1981)
17483	QPXa	pl-ks	825	"
17497	QPXb	tmt-ilm	932	Stormer (1983)
17415	QPXb	tmt-ilm	898	"
17443	QPXb	tmt-ilm	953	"
17458	QPXb	tmt-ilm	954	"
17489	QPXd	tmt-ilm	979	"
17427	IX	cpx-opx	972 / 1100	Wells (1977) /
17500	IX	cpx-opx	1022 / 1165	Lindsley (1983)
17424	MIXa	cpx-opx	985 / 890	"
17441	MIXa	cpx-opx	920 / 850	"
17438	MIXa	cpx-opx	938 / 830	"
17442	MIXa	cpx-opx	1003 / 920	"
17420	MIXa	cpx-opx	1007 / 1000	"
17454	MIXb	cpx-opx	983 / 1020	"
17449	MIXb	cpx-opx	947 / 790	"
17433	MIXc	cpx-opx	937 / 840	"
17422	MIXc	cpx-opx	1014 / 910	"

NOTES: QXa - quartz-rich garnet-bearing; QPXa - quartz-poor micaceous;
QXb - quartz-poor feldspathic; IX - cumulate nodules;
MIX - meta-igneous (coarse-intermediate-fine). gnt = garnet;
bio = biotite; opx = orthopyroxene; tmt = titanomagnetite;
ilm = ilmenite; pl = plagioclase; ks = alkali feldspar.
Methods described in Appendix 1.

granoblastic texture. These probably represent recrystallised restite assemblages resulting from extraction of granitic melt from dominantly feldspathic segregations of gneiss. Rare biotite-rich xenoliths (TYPE QPXa) containing sanidine + corundum, or sanidine + sillimanite + glass, are considered to be precursors of TYPE QPXb xenoliths. Small and uncommon spinel-rich xenoliths (TYPE QPXd) might represent restites after melt extraction from, and recrystallisation of, micaceous segregations of gneiss.

Because of the mineralogical and chemical transformations each of the "restite" xenolith types have undergone, their source remains equivocal. Torlesse terrane metasediments subjected to high-grade metamorphism at depth provide the most probable source types. There is no evidence for an underlying, ancient granite-gneiss terrane, and the moderately high $^{87}Sr/^{86}Sr$ ratios of some examples tend to exclude Waipapa terrane as a potential source. A preferred genetic model is as follows: the greywacke-gneiss precursor comprises quartz-rich, feldspar-rich and micaceous segregations. These are mutually incoherent when subjected to high temperatures and separate due to thermal expansion. Partial melts may be produced and extracted from them, causing contamination of host magmas and altering (slightly) the bulk-rock chemical compositions. Because of density contrasts, the quartz-rich and, to a lesser extent, feldspar-rich restites remain "floating" in the magma whereas the heavier micaceous restite "sinks".

Meta-igneous xenoliths (TYPE MIX) are relatively abundant, occurring in most lavas. They typically have re-equilibrated granoblastic textures and are petrographically of two main types: TYPE MIXa xenoliths are coarse-grained and consist of clino- and orthopyroxene poikilitically enclosing plagioclase and ilmenite. The presence of relict cumulus textures coupled with high MgO, Cr and Ni contents suggest that they originated as olivine/pyroxene-rich cumulates. TYPE MIXc xenoliths are finer-grained and

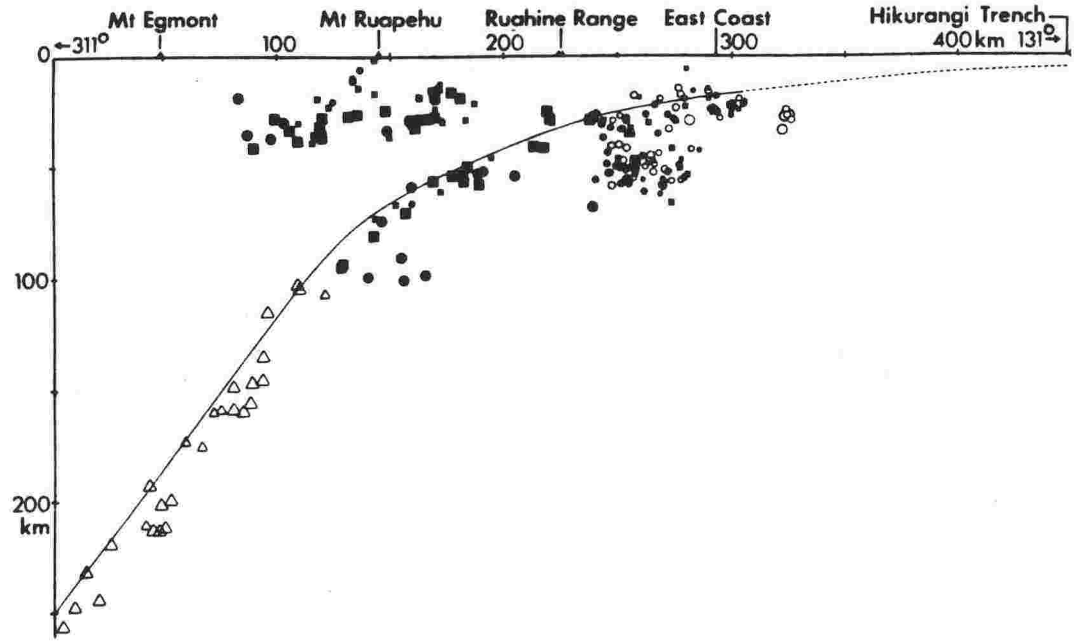

Fig.5.22: Vertical cross section along a microearthquake traverse showing inferred geometry of the upper surface of the subducted Pacific plate and possible crust-mantle boundary below Mount Ruapehu (after Reyners, 1980).

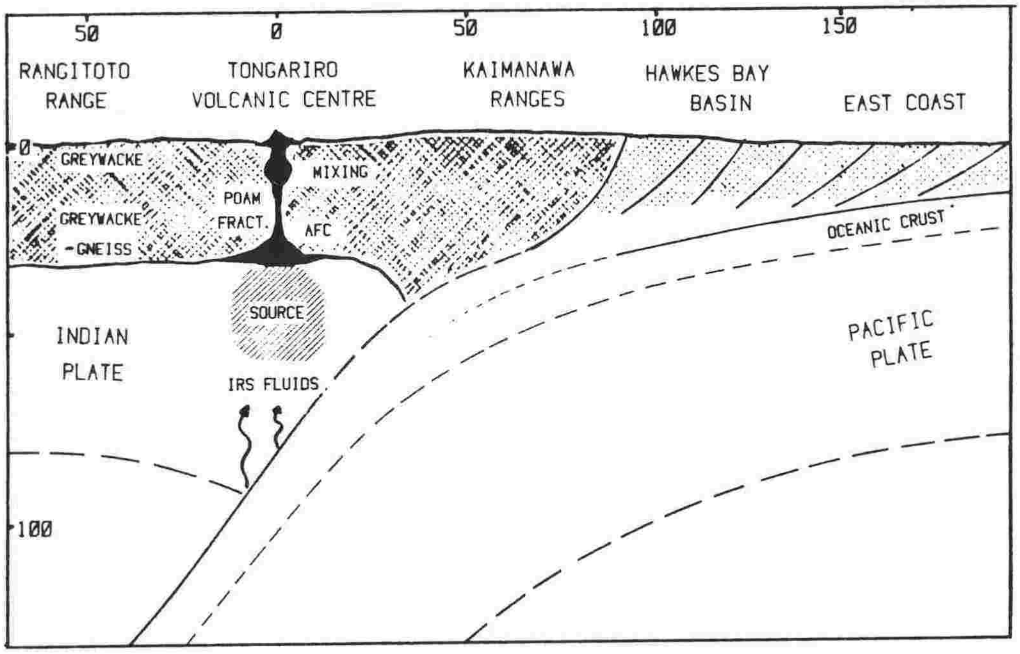

Fig.5.23: Illustration of the tectonic setting of lithosphere beneath Tongariro Volcanic Centre. Basalts are generated in the mantle wedge (source) which is metasomatised by fluids emanating from the subducted slab (IRS fluids). Crystal fractionation, contamination and/or mixing occurs at the crust/mantle boundary (modified after Pearce, 1983; Cole, 1979).

have broadly calc-alkaline chemistries and are lower in MgO, Cr and Ni. Intermediate compositions (TYPE MIXb) fall into both groups, although some are texturally distinct. Overall, mineralogies and bulk-rock chemistries of TYPE MIX xenoliths are different from host lavas and this, coupled with higher $^{87}Sr/^{86}Sr$ ratios, suggests a different origin. The most likely possibility is that these xenoliths represent oceanic crust on which Torlesse terrane rocks were originally deposited.

5.8.2 P-T conditions of metamorphism:

Some xenoliths contain mineral assemblages which allow temperature and pressure conditions of metamorphism to be estimated by several different, independent methods. The data, summarised in Table 5.13, indicate that most of the assemblages described recrystallised at temperatures of 800 °C to 1000 °C. Pressure estimates based on plagioclase + clinopyroxene + quartz assemblages are unreliable and range from reasonable values of about 8kb to negative values. However, the presence of garnet with orthopyroxene in 17470 indicates pressures close to 10kb (Wood, 1975). The absence of amphibole (except in two cumulate nodules) indicates largely anhydrous metamorphic conditions, and this is further supported by low volatile contents of partial granitic melts.

It is difficult to assess the depth of origin of many xenoliths because of the absence of suitable mineral assemblages from which to make accurate geobarometric estimates. Geophysical data pertaining to crustal thickness beneath the TVC is inconclusive; microearthquakes discontinue at 42km beneath Ruapehu (Fig.5.22), suggesting a major structural feature (Reyners, 1980), which may be interpreted as the crust-mantle boundary (J.Olsen, pers.comm., 1985). The coexistence of restite xenoliths and mafic granulites (TYPE MIX) suggest that these originate from a similar locality. The base of the continental crust would provide a suitable interface at which magma chambers might form and magma interact with already hot and highly metamorphosed wallrock. For a geothermal gradient of 25-30

Table 5.14: Illustration of the generation of feldspathic restites from micaceous assemblages by progressive removal of granitic melt.

VUW	-	28654	17425	17483	17484	17458	17483	17444
TYPE	ARG	SCHIST	QPXa	QPXa	QPXa	QPXb	MELT	MELT
major elements (weight%)								
SiO_2	58.3	63.9	50.3	49.2	49.8	50.5	65.7	73.8
TiO_2	1.0	.8	1.1	1.2	1.8	1.0	.3	.8
Al_2O_3	22.3	18.7	25.7	28.7	26.1	26.1	18.7	12.1
FeOT	6.9	5.9	7.2	9.0	6.8	6.9	4.1	3.3
MgO	2.4	2.2	3.0	3.0	2.7	2.9	.6	.5
CaO	1.4	2.0	4.3	2.5	7.8	8.1	.4	1.4
Na_2O	1.7	3.0	4.6	3.4	3.7	3.8	3.8	2.9
K_2O	6.0	3.6	3.8	3.0	1.5	.9	6.4	5.2
Ba	991	884	1709	1093	587	574	-	-
Cr	68	86	59	92	106	85	-	-
Rb	247	134	144	138	48	26	-	-
Sr	156	220	708	430	604	524	-	-
V	162	142	179	209	248	208	-	-
Zr	182	189	289	274	361	237	-	-

NOTES: ARG = argillite endmember composition as given in Table 3.3; SCHIST is from Grapes et al. (1980, analysis 24); MELT = partial melt. Major analyses normalised to 100% volatile-free.

degrees/km (Studt and Thompson, 1969), quartzo-felspathic and mafic basement would be metamorphosed to upper amphibolite to granulite facies assemblages at depths of 30-40km. It is suggested, therefore, that the crust beneath the TVC consists of about 40km of dominantly Torlesse terrane greywackes, progressively metamorphosed, from prehnite-pumpellyite facies at the surface to granulite facies at the base. At the crust-mantle interface, greywacke-gneiss (and mafic granulites?) are partially melted and interact with basaltic magmas generated in the mantle wedge below (Fig.5.23).

5.8.3 Partial melting of xenoliths:

Gribble and O'Hara (1967) discussed the interaction of pelitic materials with basic magma, particularly with reference to the Haddo House xenolith suite (Read 1935), and pointed out that the apparent enrichment in alumina and depletion in silica of residual xenoliths do not necessarily imply metasomatic interchange with the magma but are a natural result of the formation and separation of a partial melt fraction from an original schist at an appropriate temperature. This conclusion was also arrived at by McRae and Nesbitt (1980) who presented mass balance calculations documenting progressive bulk chemical changes in metagreywacke and metapelite after separation of increments of granite minimum melt. They noted that, during partial melting, enrichment of Fe relative to Mg and strong absorption of water in the melt leaves the restite with increasing proportions of Mg-rich minerals such as cordierite. Extraction of a granitic melt from metapelite results in an increase in the Al content of the restite, whereas for greywacke, extraction of an alkali granite melt is required to have the same effect. These results are similar to those predicted here. In Table 5.14, compositions are given which approximate those involved in partial melting of greywacke-gneiss. Biotite schist (28654) (Grapes et al., 1982) is a possible starting composition (an argillite composition is not strictly appropriate since it would be mineralogically and chemically

Table 5.15: Illustration of the generation of quartzose restites from quartz-rich assemblages by progressive removal of granitic melt.

VUW	-	28691	17485	17491	17463	17436	17463	17491
TYPE	GW	SCHIST	QXa	QXa	QXb	QXb	MELT	MELT
major elements (weight%)								
SiO_2	76.8	75.8	72.7	75.3	85.3	98.1	76.9	73.4
TiO_2	.3	.4	.6	.5	.0	.0	.2	.3
Al_2O_3	12.6	12.9	13.9	13.4	8.8	.8	12.5	13.7
FeOT	2.4	2.7	3.9	2.2	.6	.4	1.7	2.4
MgO	.8	1.0	1.3	.8	.1	.2	.6	.2
CaO	1.4	2.2	4.5	5.3	3.8	.3	3.6	.3
Na_2O	4.0	3.3	2.1	2.1	1.1	.2	2.6	3.3
K_2O	1.8	1.8	.9	.3	.2	.1	2.0	6.3
Ba	468	380	174	139	3	3	-	-
Cr	16	31	33	26	4	4	-	-
Rb	69	84	42	6	3	3	-	-
Sr	256	302	260	553	26	26	-	-
V	26	47	82	74	16	16	-	-
Zr	182	169	135	199	<2	<2	-	-

NOTES: GW = greywacke endmember composition as given in Table 3.3; SCHIST is from Grapes et al. (1980, analysis 30); MELT = partial melt. Major analyses normalised to 100% volatile-free; <2 = below detection limit.
17491 is a quartz-rich segregation of 17492.

modified (as a cm-sized xenolith) at the depths at which melting takes place - the McRae and Nesbitt model is thus unrealistic in that respect). TYPE QPXa xenoliths 17425 and 17484 represent stages of progressive extraction of melt from a biotite-schist-type parent and TYPE QPXb xenolith 17419 is the final restite after complete extraction and recrystallisation. Because the "real" starting compositions of each component in the model are unknown, it is not possible to mass balance the process. However, the data shows that predicted chemical changes i.e. increases in Al, Fe, Mg and Ca and decreases in Si and K have occurred between parent and restite. These changes indicate that about 20% to 30% removal of melt may have taken place. The restites (17425, 17483, 17484 & 17458) show a greater than expected enrichment of Ca and Sr (Table 5.14), perhaps as a result of back-diffusion during melt extraction. If so, then this should lead to at least partial equilibration of Sr isotopes in the process.

Gribble and O'Hara (1967) suggested that, simultaneous with the development of mullite- and spinel-bearing restite xenoliths from pelitic parts of a gneiss, quartz-rich restite xenoliths might also form. Table 5.15 gives a range of compositions from this study which might be appropriate to a model of partial melting and melt extraction from quartz-rich segregations of greywacke-gneiss. Again this model is difficult to mass-balance but supports the interpretation that the majority of quartzite xenoliths (TYPE QXb) are restite assemblages.

5.8.4 Processes of wall-rock assimilation:

Given that the majority of xenoliths (excluding TYPE MIX) are restites after extraction of partial granitic melts from segregations of greywacke-gneiss, then contamination processes involving interaction with and assimilation of that melt by the host magma become important in petrogenetic modelling. Kitchen (1984) described pyrometamorphism and contamination of basaltic magma at Tieveragh, County Antrim where a small dolerite plug cutting through tuffaceous sediments (Old Red Sandstone) contains glassy buchites which, at the contact, are variably hybridised with the basalt. The processes discussed by Kitchen, though relating to a more intimate situation, may be appropriate to the larger scale involved in andesite genesis in the TVC.

At Tieveragh, contamination of the basaltic magma by acid melt extracted from the buchites is apparently facilitated by mechanical mixing at the margins of the plug. This is probably caused by the instability and collapse of substantially melted wall-rock into an upward flowing magma column. Localised degassing and brecciation associated with the active conduit facilitates this process and the resulting lenses of contaminated melt become smeared the walls by the flow of the magma. Individual smears of basaltic and acid melt develop domains with contrasting melt structure, composition, temperature, and viscosity which are, at least initially, effectively immiscible. The size of each domain depends on the proportion of acid to basic melt and the vigour of mixing, although some are about 2-3mm in diameter. Heat transfer, mass transfer, and interchange of volatiles eventually allows the two melts of contrasting fluidity to mix. Yoder (1973) showed experimentally that water-saturated granitic and basaltic melts maintain an interface for short periods of time, but then hybridisation takes place between them. The similarity of concentration gradients of elements near the interface suggested to Yoder that element interactions play a dominant role in the diffusive transfer of material, but the extent of hybridisation depends mainly on the geometry of the interface, the degree of turbulence and the storage period. Watson and Jurewicz (1984) studied the behaviour of alkalis during diffusive interaction of granitic xenoliths with basaltic magma and concluded that selective transfer of Na and K is made possible by chemical diffusivities that are high in relation to that of the principle melt structure-controlling component, silica. Potassium was found to be effectively tranferred from felsic partial melt to basalt, while sodium migration was in the opposite sense, depleting the basalt in Na through diffusion up a concentration gradient. These results support previous suggestions by Watson (1982) that basaltic magmas originating in the subcontinental mantle are susceptible to selective contamination (see Chapter 6.4) - the relatively low diffusivity of K, however, indicates that selective uptake of that element is less efficient than previously supposed. Loss of sodium from magma to xenoliths or country rock is effective depending on the surface area of partially-molten crustal rock exposed to the basalt, the exposure time, and chemical parameters such as the Na_2O and SiO_2 contents of the felsic partial melt.

Bowen (1928) addressed the problem of wallrock assimilation by basaltic magma and showed that from heat-balance considerations, the process was only theoretically possible if the heat required for assimilation can be provided by the latent heat of crystallisation. Assimilation processes may result from nucleation and rapid growth of pyroxene and feldspar (Kitchen, 1984); the transfer of Si, Al, and alkalis from the acid melt domains causes crystallisation of Ca-poor pyroxene in addition to augite, and the early potassium enrichment in plagioclase feldspar. The diffusion of Ca, Mg and Fe in the reverse direction helps to break down the alumino-silicate network in the acid melt, reducing the kinetic barriers to diffusion and mechanical mixing. This done, the residual basaltic and acid melts, now much modified by diffusion and crystallisation, would merge, obscuring the original domain boundaries. The acid melt finally becomes interstitial, suggesting that for less than 20% contamination, basaltic magma is capable of completely assimilating acid melt and of removing any vestage of original domain structure.

Table 5.16: Bulk-rock chemistry of selected glasses from xenoliths.

VUW	17465	17461	17460	17492	17458	17463	17483	17444	17422
TYPE	VXa	VXa	VXb	QXa	QXb	QXb	QPXa	QPXb	MIX
major elements (weight%)									
SiO_2	67.2	76.2	77.4	73.4	75.7	76.9	65.7	73.8	76.8
TiO_2	.7	.4	.4	.3	.7	.2	.3	.8	.9
Al_2O_3	16.7	13.0	12.9	13.7	10.5	12.5	18.7	12.1	12.4
FeOT	3.4	2.1	2.4	2.4	4.3	1.7	4.1	3.3	.8
MgO	.9	.6	.3	.2	.6	.6	.6	.5	.1
CaO	1.2	.5	1.2	.3	1.8	3.6	.4	1.4	.5
Na_2O	3.1	3.9	2.7	3.3	3.0	2.6	3.8	2.9	2.6
K_2O	6.8	3.2	2.8	6.3	3.4	2.0	6.4	5.2	5.9
C.I.P.W. norm									
Qz	17.0	37.7	46.4	27.1	37.9	44.4	14.2	31.6	38.1
Co	2.1	2.1	3.2	.8	-	-	4.8	-	1.0
Or	40.0	19.2	16.4	37.5	20.2	12.0	37.8	30.7	34.6
Ab	26.4	32.8	23.1	28.2	25.7	22.3	32.0	24.7	22.1
An	5.7	2.7	5.9	1.6	5.0	16.2	2.0	4.4	2.3
Di	-	-	-	-	3.4	1.2	-	2.3	-
Hy	7.3	4.8	4.3	4.3	6.5	3.6	8.7	4.6	.2
Il	1.4	.8	.8	.6	1.3	.3	.5	1.6	1.7

NOTES: Major elements normalised to 100% volatile-free.
Qz = quartz, Co = corundum, Or = orthoclase, Ab = albite,
An = anorthite, Di = diopside, Hy = hypersthene, Il = ilmenite.

5.8.5 Conclusions:

This study of crustal xenoliths highlights two features of crustal contamination processes as they affect lavas of the TVC. Firstly, assimilation involves mainly granitic melts derived from partial melting of greywacke-gneiss. The melts are compositionally diverse (Table 5.16) having originated from mineralogically diverse segregations. This conclusion is based on the dominance of quartz-rich, feldspar-rich and (rare) spinel-rich xenoliths, all of which, by separate paths, are considered to be restite assemblages. Secondly, crustal interaction probably took place in magma chambers situated near the crust-mantle boundary. This is suggested by the close association of restite xenolith types with meta-igneous xenoliths which, for reasons outlined previously, must have been derived from a deep-seated source. The nature of the contaminating melt is difficult to define since only minor enclaves of what probably represent residual compositions are to be found in some xenoliths (Table 5.16). The significance of these and their application to crustal contamination models are considered further in Chapter 6 but it seems likely that no unique melt composition is involved. Although it is difficult to be certain which basement terrane is involved in melt extraction, the relatively high Sr isotopic ratios of many xenoliths favour Torlesse. Furthermore, it is unlikely that Waipapa terrane lithologies, with $^{87}Sr/^{86}Sr$ ratios between .70500 and .70700 could, by any reasonable crustal contamination process, account for the high ratios of most of the lavas (i.e. .70500 to .70600).

****

CHAPTER 6 : PETROGENETIC MODELLING OF TVC LAVAS

****

6.1 PETROGENETIC PROCESSES

The origin of calc-alkaline magmas erupted at plate margins (i.e. orogenic andesites) has received considerable attention in recent years (see Gill (1981) for a comprehensive summary). Petrogenetic processes fall into four broad catagories:

1. Partial melting of hydrated mantle or subducted oceanic crust.
2. Fractional crystallisation of primary basaltic magma.
3. Assimilation of a continental crust by parental magma.
4. Binary mixing of magmas of contrasting chemistry.

Each of the above are considered by some to be the most important process, but several studies indicate that more than one process may have operated to produce certain rock suites (e.g. Gerlach and Grove, 1982, Grove et al., 1982 - Medicine Lake; Myers et al, 1984 - Edgecumbe volcanic field; Thorpe et al., 1984 - Andes).

6.1.1 Partial melting:

In many volcanic arcs, basic and acid andesite are the most voluminous rocks sampled (Ewart, 1976), leading to the suggestion that most, if not all, are derived directly as primary melts (Kay, 1978; Tatsumi and Ishizaka, 1981; Aoki and Fukimaki, 1982). The reported occurrence of a high-magnesian andesite from Teraga-Ike in SW Japan by Tatsumi and Ishizaka (1981) supports this idea since the lava contains olivine phenocrysts which are in equilibrium both with bulk-rock Mg number and with presumed mantle peridotite compositions.

Recent experimental studies (Yoder, 1969; Kushiro, 1974; Ringwood, 1975) indicate that a wide range of magma types could be generated from peridotitic mantle above subduction zones under differing degrees of water saturation. However, the amount of silica-enrichment possible in a primary liquid derived from peridotite is still the subject of debate amongst experimentalists (e.g. Mysen and Boettcher (1975) vs Green (1976)). Although some island arc andesites may represent primary melts of the mantle wedge, most have compositions which differ greatly from those produced experimentally and, furthermore, do not represent liquids in equilibrium with peridotite. Such liquids should have the following characteristics (Perfit et al., 1980; Gill, 1981): (1) Mg numbers greater than 67 (2) Ni contents greater than 100ppm (3) high water and CO_2 contents (4) olivine and orthopyroxene as liquidus phases (at mantle pressures) (5) plagioclase not a liquidus phase (6) low LILE concentrations (unless there has been pre-enrichment of the mantle wedge). Those criteria apply to less than 5% of island arc andesites and to none from the TVC, except those which exhibit clear petrographic evidence of internal disequilibrium, indicating magma mixing (TYPE 6).

Wet melting of eclogite (or amphibolite) formed by subduction of oceanic crust has also been proposed as a mechanism for generating liquids of andesitic composition (Yoder and Tilley, 1962). Such liquids have been produced experimentally by 20-30% partial melting of eclogite at temperatures between 900 °C and 1000 °C, and pressures close to 30kb (Gill, 1974; Stern and Wyllie, 1978). However, at lower pressures, these would have lower formation temperatures than typical orogenic andesites (Gill, 1981). In addition, the experiments indicate 25% to 40% residual garnet which is at odds with observed HREE and Y concentration patterns in andesites. It has also been claimed that acid andesite could be derived as a near-eutectic melt of dry quartz eclogite (Green, 1972; Marsh and Carmichael, 1974). However, for a bulk composition similar to N-type MORB, the derived melt (at 30kb) has a [Ca/(Mg + Fe)] ratio higher than most orogenic andesites and is produced at unrealistically high temperatures

(Gill, 1981).

In summary then, most orogenic andesites are not likely to be primary melts of the mantle wedge above subduction zones, nor of subducted ocean floor basalts.

6.1.2 Fractional crystallisation:

Bowen (1928) proposed that orogenic andesites and their plutonic equivalents could result from crystal fractionation of basaltic magma, a petrogenetic process which still finds favour with many (e.g. Arculus and Wills, 1980; Hawkesworth and Powell, 1980). The main arguments to support it are (Gill, 1981, p.268): (1) the close spatial, temporal and mineralogical relationship observed between basalt, andesite and dacite, whose chemical compositions define smooth scatter in Harker-type variation diagrams and which, therefore, can be interpreted as representing liquid lines of descent (2) the occurrence of andesites in settings other than convergent plate margins which indicates that differentiation of basalt can be a mechanism for producing andesite either within or outside volcanic arcs (3) evidence for crustal-level magma reservoirs beneath active volcanoes and evidence from ejecta for compositional and mineralogical gradients within these reservoirs which both suggest that differentiation occurs during periods of repose (4) the occurrence of cognate mafic xenoliths and xenocrysts (5) trace element systematics, such as compatible-incompatible element ratios (6) isotopic similarity between andesites and associated basalts, which is necessary for magmatic differentiation by itself to be a viable mechanism (7) the low Mg numbers and Ni contents of orogenic andesites, which require differentiation if parental melts are derived from mantle peridotite.

Much of this evidence, however, is circumstantial and exceptions and contrary arguments abound (Gill, 1981, p.269) (1) some chemical variation diagrams contain scatter in excess of analytical error which, when allied to the high phenocryst content of many lavas, questions the validity of liquid lines of descent (2) mafic xenoliths can be alternatively interpreted as coagulated phenocrysts precipitated at low pressure subsequent to the development of diverse liquid compositions at greater depth (3) isotopic uniformity can result from other genetic processes such as partial melting of a homogeneous source and, indeed, does not occur in many orogenic andesite suites (4) the presumed parents and complementary crystal cumulates resulting from crystal fractionation processes often are missing or volumetrically minor.

The viability of crystal fractionation as an process of andesite petrogenesis may depend to some extent on the physics of magma storage and ascent (Marsh, 1978). The fluid dynamics of evolving magma chambers was discussed by Sparks et al. (1984) who noted that, in addition to thermal gradients, the forms of convection in magma chambers arise from compositional variations caused by processes such as fractional crystallisation, partial melting and contamination. These processes, together with phase changes such as volatile exsolution, generally cause much larger density changes than the thermal effects arising from associated temperature changes. When crystallisation occurs in multi-component systems, fluid immediately adjacent to growing crystals is generally either depleted or enriched in heavy components and can convect away from its point of origin. Sparks et al. consider this to be the dominant process involved in fractionation of magmas and further suggest that crystal settling is an inadequate and, in many situations, improbable mechanism for magmatic differentiatioin "....The convective motions in chambers are usually sufficiently vigorous to keep crystals in suspension, although settling can occur from thin fluid layers and within the boundary layers at the margins of a magma chamber". However, the process of convective fractionation "....enables compositional and thermal gradients to be formed in magma chambers both by closed system crystallisation and by repeated replenishment in open systems. During crystallisation along the

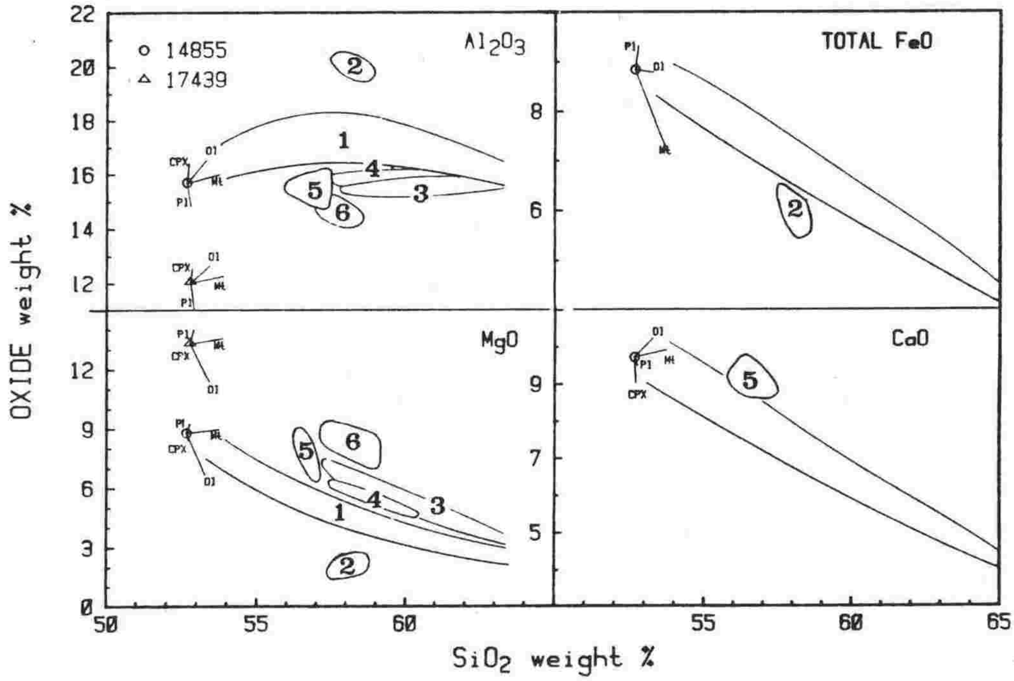

Fig.6.1: Silica variation diagrams for lavas of Ruapehu and nearby vents (c.f. Figs.4.8, 4.10, 4.16, 4.17) showing idealised fields of lava types 1 to 6 (in the FeO and CaO plots, outlying fields only are shown). Vectors predict trajectories of magmatic evolution relating to fractionation of the phase indicated. Ideal mineral compositions are used (olivine (Ol) = Fo90; clinopyroxene (CPX) = CPX1; plagioclase (Pl) = An80; magnetite (Mt) = MT10.0, c.f. Table A5.1). Vectors are proportional to 5% fractionation (Ol, CPX & Pl) or 2% fractionation (Mt). In the $FeO-SiO_2$ plot, CPX is coincident with Pl - note that the observed trend is possible only if magnetite is a fractionating phase.

margins of a chamber, highly fractionated magmas can be generated without requiring large amounts of crystallisation, because the removal and concentration of chemical components affects only a small fraction of the total magma".

Fractional crystallisation of orogenic andesites, if it occurs, will involve liquidus or near liquidus phases at low load and water pressures (Gill, 1981) which are represented by the dominant phenocryst minerals plagioclase, olivine (and/or orthopyroxene), augite and magnetite (POAM). "POAM fractionation" could explain many of the chemical trends observed in TVC lavas (Fig.6.1) (vectors indicate the chemical changes resulting from removal of each mineral phase). Quantitative modelling of these features are discussed in section 6.2.

6.1.3 Crustal contamination:

Involvement of crustal contamination in andesite genesis is suggested in many recent studies (e.g. Francis et al., 1980; Carlson et al., 1981; Thirlwall and Graham, 1984). Assimilation of continental crust by basaltic magma is often indicated by the presence of crustal xenoliths and usually results in higher SiO_2 contents, higher LILE concentrations, higher $^{87}Sr/^{86}Sr$ ratios and lower K/Rb (Gill, 1981). Such features are shown by many TVC lavas. Contamination processes are complex but are of three main types:

i. Bulk assimilation: Whole-sale melting and assimilation of continental crust in basaltic magma can explain the chemical and isotopic characteristics of some lava suites (e.g.Wood, 1980). However, for this to occur, the magma must be superheated otherwise only partial melting of the crustal component takes place. Superheated magmas are characteristically phenocryst-poor (Gill, 1981), unlike most TVC lavas which have typically more than 20% phenocrysts. Bulk assimilation is therefore not considered to be an important process in their genesis.

ii. Addition of a cotectic crustal melt: Partial melting of wallrock in the vicinity of a magma chamber can, depending on its bulk composition, produce melts enriched in silica, LILE and radiogenic Sr. These melts may, under certain conditions, integrate with surrounding magma, a process which, to maintain heat balance, must be accompanied by crystallisation (i.e. assimilation and fractional crystallisation (AFC), Taylor, 1980; De Paolo, 1981).

Melting of greywacke-gneiss basement beneath the TVC could be an important process of crustal contamination, as indicated by xenolith studies. As noted in Chapter 5, partial melting of crust and consequent "selective assimilation" is a more likely process than bulk assimilation. This is supported by Patchett (1980) who, from a study of the thermal effects of basaltic magma on adjacent wallrock, considered that "...total melting of the crust is possible only over a very short distance adjacent to the basalt, if at all". Consequently, the assimilant for those petrogenetic models which require one is assumed to be a granitic partial melt of greywacke-gneiss.

iii. Isotopic equilibration without addition of material: Selective contamination of magma by aqueous fluids enriched in radiogenic isotopes (and possibly also in LILE) has been considered important in certain circumstances (Briqueu and Lancelot, 1979b). However, it is a difficult process to model since the composition of the enriched fluids are unknown and hence is only applied here in an qualitative sense.

6.1.4 Magma mixing:

There is much petrographic evidence to indicate that magma mixing is an important petrogenetic process in calc-alkaline magmas. For example, phenocryst assemblages are commonly out of equilibrium with bulk-rock composition, as might result from mixing of mafic and silicic magmas (Kuno, 1950; Anderson, 1976; Eichelberger, 1975, 1978; McBirney, 1980). Models dealing with physical characteristics of magma chambers (e.g. Huppert and Turner, 1981) predict the existence of compositional zoning and density stratification, thus allowing the existence of a spectrum of compositions to be present in a single chamber and available for mixing. The significance claimed for magma mixing ranges from major, where it is seen as an alternative to crystal-liquid fractionation (Eichelberger, 1975), to minor, involving only back-mixing of liquids which are mutually related via crystal-liquid fractionation (McBirney, 1980). Its relative importance as a means of generating calc-alkaline lavas varies from being the dominant process (Anderson, 1976), to being merely a contributor in a group of processes acting at the same time (Grove et al., 1982).

In the following discussion magma mixing is considered as important in the petrogenesis of only those lavas which exhibit clear evidence of disequilibrium textures and which cannot be derived adequately by an alternative mechanism.

6.2 PETROGENETIC MODELS OF SELECTED TVC LAVAS

In this section, petrogenetic models of selected lavas from Ruapehu and nearby vents are described. These are designed to assess the feasibility of deriving liquids of intermediate composition from known basaltic parents by processes such as POAM crystal fractionation, combined crustal assimilation and fractional crystallisation (AFC) and magma mixing. In the models, ideal mineral compositions (Table A5.1) are used to simplify calculations and the following systematic guidelines are employed (see Appendix 5 for further discussion and justification):

1. Major elements are normalised volatile-free; all iron is FeO; MnO and P_2O_5 are excluded.
2. In crystal fractionation models, no more than four mineral phases are included, namely plagioclase, olivine or orthopyroxene, clinopyroxene and magnetite.
3. Best fit models are those for which the sum of the squares of the residuals (SSR) is minimised, providing the fractionating phases

are compositionally reasonable and the total amount of crystals removed is similar to, and in proportion to, the phenocryst content of the lava.

4. Calculated trace element abundances are considered acceptable if predicted values are within 20% of known values. (see Table A5.2 for Kd values used).

All petrogenetic models use individual lava compositions (rather than averages) and these are considered to be representative of the parent magma body. This concept was tested by chemically analysing twelve Ngauruhoe 1954 lava samples collected from different flows erupted at different times over a period of six months (localities and times of of eruption are given in Appendix 2 and Fig.4.2). The lava is highly porphyritic and contains a high proportion of xenoliths. Nevertheless, variation in bulk-rock chemistry (c.f. Appendix 2.2) is less than average analytical error indicating that individual samples do adequately reflect the bulk magma composition.

In the following discussion, models referred to are contained in Appendix 5 (e.g.A5.2.1), and some of these are also presented as tables.

6.2.1 Petrogenetic models of TYPE 1 lavas:

Major element variation diagrams (Fig.4.20 to Fig.4.25; Fig.6.1) show that most TYPE 1 lavas (i.e. plagioclase- and plagioclase-pyroxene - andesites and dacites) can be explained by POAM fractionation from a low-alumina basalt-type parent similar to Ruapehu basalt (14855) or Red Crater basalt (11965). However, TYPE 1 lavas also show a progressive increase in LILE concentration and $^{87}Sr/^{86}Sr$ ratio with increasing silica content, which might be interpreted in terms of crustal contamination. All models involving only POAM fractionation from a basaltic parent have large negative residuals for K_2O and similar disagreement (negative misfit) for LILE (Rb, Ba, Zr) (A5.2.1). The K_2O "anomaly" is removed by addition of a crustal component which, to be consistent with the findings of Chapter 5,

Table 6.1: Least squares model to generate Ngauruhoe 1954 TYPE 1 basic andesite 29250 from Mangawhero Formation TYPE 1 low-alumina basalt 14855 (Ruapehu basalt) by AFC (A5.2.2).

	P	D	MODEL	RESID.	PHASE	WGT%	%
SiO_2	52.9	56.5	56.5	+.02			
TiO_2	.7	.8	.8	-.00	PHASE	WGT%	%
Al_2O_3	15.8	16.7	16.7	+.01			
FeO	8.9	8.3	8.4	+.01	Fo90	-6.93	27.40
MgO	8.8	5.2	5.2	+.01	CPX1	-7.72	30.52
CaO	9.8	8.3	8.3	+.00	An80	-9.34	36.92
Na_2O	2.6	3.1	3.1	-.04	MT5.0	-1.31	5.16
K_2O	.6	1.2	1.1	-.02	MELT1	+5.46	0.00

SUM SQUARES RESID. = .0023 CRYSTALS REMOVED = 25.30%

	P	D	MODEL	BULK DC	% ERROR
Rb	11	38	15	.04	- 60.5
Ba	185	214	243	.07	+ 13.6
Zr	50	95	65	.10	- 31.6
Sr	201	247	219	.70	- 11.3
V	251	220	193	1.91	- 12.3
Cr	380	100	106	5.39	+ 6.0
Ni	142	29	33	5.97	+ 13.8

NOTES: P = parental magma; D = daughter magma.
MODEL = calculated daughter magma.
RESID.= residual (MODEL-D).
PHASE = phase removed (-) or added (+) (for compositions see Table A5.1).
WGT % = weight % of phases removed or added (relative to P).
% = percentage of total crystals removed.
BULK DC = bulk distribution coefficient (for individual distribution coefficients see Table A5.2).
% ERROR = % difference ((MODEL - D / D).

is assumed to be a granitic partial melt derived from greywacke-gneiss (i.e. K-rich melt).

Ngauruhoe 1954 lava is notable for its relatively high $^{87}Sr/^{86}Sr$ ratio in relation to its low silica content. The best-fit model (A5.2.2) indicates that it can be generated from a Ruapehu basalt-type parent by AFC, requiring 25% POAM fractionation plus addition of 5.5% K-rich melt. This gives an acceptable major element fit (SSR=.0023), and fails only to satisfy Rb and Zr requirements. However, both these elements will be enriched in the melt, a factor not considered in the trace element calculations. Insufficient data is available on the actual concentrations of Rb and Zr in the granitic melt but, if it is assumed the K/Rb ratio is the same as that of the original bulk-rock prior to melting (a reasonable assumption since no K-rich minerals occur in either quartz-rich (i.e TYPE QXb) or quartz-poor (i.e.QPXb) restite mineralogies, c.f. Chapter 5) then the melt should contain 200-400ppm Rb, so contributing some 10 to 20ppm to the lava (as required). If a K-poor melt composition (Table A5.1) is instead added in the model (A5.2.3), an inferior fit results, and the K_2O anomaly persists. With a Red Crater basalt-type parent (A5.2.4), the model gives a similar major element fit (SSR=.0043), but fails to satisfy Sr (too high) or Cr-Ni (too low). Red Crater basalt appeals as a parental magma type for Ngauruhoe 1954 lava because it is close geographically and was similarly erupted in relatively recent times. However, the older Ruapehu basalt is chemically more suitable (Table 6.1). Other possible parental basalt types yield inferior models: For Waimarino basalt, SSR is high (.4466) and both Sr and Cr fit poorly (A5.2.5); if this parental magma were to fractionate only olivine and clinopyroxene, which is possibly more realistic given the phenocryst mineralogy (Table 4.1), SSR is even greater (A5.2.6). For a high-alumina basalt-type parent (e.g.Ben Lomond Basalt 22994) (A5.2.7), the major element fit is good (SSR=.0039), but the model fails to satisfy most of the trace elements; a similar result is achieved if orthopyroxene rather than olivine is fractionated (A5.2.8).

From the above models, it is concluded that Ngauruhoe 1954 lava was most likely generated by AFC, involving 25% POAM fractionation of a low-alumina basalt (chemically intermediate to Ruapehu and Red Crater basalt-types) plus addition of 5% granitic partial melt. Proportions and types of mineral phases given by the best-fit model are similar to the lava mode (Table 4.1) and mineral compositions are realistic. The trace element fit is acceptable given the uncertain LILE contribution made by the melt.

Sr isotopic systematics are difficult to quantify since neither the Sr content nor the $^{87}Sr/^{86}Sr$ ratio of the proposed melt is known. In order to even attempt a quantitative isotopic model, certain questions must be addressed. Firstly, are segregations of greywacke-gneiss from which melt is extracted isotopically homogeneous (i.e. do the melts have the same isotopic ratio) ? The answer to this was to some extent given by a recent study (by the author) of quartzo-feldspathic schists from near the Alpine Fault (South Island, New Zealand). Feldspathic and micaceous layers of these rocks had the same $^{87}Sr/^{86}Sr$ ratios indicating that similar rocks drawn from depth (i.e. greywacke-gneiss) might be similarly equilibrated. Secondly, are melts from different crustal levels isotopically homogeneous? Indications from basement studies (Chapter 3) confirm that this may not be so, especially if isotopic equilibration is progressive with depth of burial. Thirdly, are contaminated magmas isotopically homogeneous? Laughlin et al. (1972) showed that initial $^{87}Sr/^{86}Sr$ ratios in individual flows of McCartys basalt (New Mexico, USA) varied considerably as a result of near surface crustal contamination. However, analysis of different flows from the same magma for this study (e.g.14859 & 14860, 14911 & 14913; Table 4.4) indicates that similar processes did not operate in the TVC.

The above data suggests, therefore, that assimilating melts are isotopically uniform and give rise to uniform contamination. Hence, semi-quantitative analysis of the Sr isotopic systematics of Ngauruhoe 1954 lava can be made, using the equations of mber during AFC (see 13a, P.192):

Sr isotopic composition of parent (14855) =	.70490	(Table 4.4)
Sr isotopic composition of daughter (29250) =	.70551	(Table 4.4)
Sr concentration of parent (14855) =	201	(Table 4.3)
Sr concentration of daughter (29250) =	247	(Table 4.3)
DSr =	.70	(Table 6.1)
mass assimilant / mass lava (Ma/Ml) =	.05	(Table 6.1)

If the Sr concentration in the contaminant = 100ppm (this value is considered appropriate since the original source, Torlesse metasediment, ranges between 156 and 256ppm (Table 3.3) and restite xenoliths are Sr - enriched (plagioclase-buffered), then the predicted $^{87}Sr/^{86}Sr$ ratio of the melt is .72960, a value which appears to be too high (by about .02000) for an average greywacke composition. However, if the amount of assimilation (Ma/Ml) is increased to 20% (higher than that given by the geochemical model) then the predicted ratio is .71122, a much more reasonable value. Alternatively, if the Sr concentration in the contaminant = 200ppm, then (using the original values for other variables) the predicted $^{87}Sr/^{86}Sr$ ratio would be .71755. These models indicate that a reasonable fit for the Sr isotopic composition of Ngauruhoe 1954 lava is possible but there are several unknowns in the equation for which a range of values can be used (i.e. only the composition of the daughter magma is known for sure).

Table 6.2: Partial bulk-rock chemistry of selected Mangawhero Formation TYPE 1 lavas.

	17855	17858	17850	17844	17886	17889
SiO_2	52.9	54.3	56.4	58.3	61.8	64.0
TiO_2	.7	.7	.8	.7	.8	.8
Al_2O_3	15.8	17.2	17.7	17.4	16.9	16.8
FeO	8.9	8.5	7.7	6.9	5.8	5.1
MgO	8.8	6.8	5.1	4.7	3.2	2.3
CaO	9.8	9.0	8.2	7.6	5.9	4.9
Na_2O	2.6	2.9	3.0	3.1	3.5	3.4
K_2O	.6	.7	1.1	1.2	2.0	2.8
Rb	11	18	34	37	81	120
Ba	185	237	313	310	418	527
Zr	50	58	84	93	158	201
Sr	201	219	251	250	253	260
V	251	258	216	195	162	115
Cr	380	140	132	92	51	31
Ni	142	51	49	35	26	20
I	.70490	.70507	.70529	.70554	.70554	.70574

Table 6.3: Least squares model to generate Mangawhero Formation TYPE 1 basic andesite 14858 from Mangawhero Formation TYPE 1 low-alumina basalt 14855 (Ruapehu basalt) by POAM fractionation.

	P	D	MODEL	RESID.	PHASE	WGT%	%
SiO_2	52.9	54.3	54.3	-.01			
TiO_2	.7	.7	.7	-.01			
Al_2O_3	15.8	17.2	17.2	-.02			
FeO	8.9	8.5	8.5	-.02	Fo90	-4.05	23.13
MgO	8.8	6.8	6.7	-.01	CPX1	-7.73	44.13
CaO	9.8	9.0	9.0	-.01	An60	-4.65	26.56
Na_2O	2.6	2.9	2.9	+.04	MT10.0	-1.08	6.18
K_2O	.6	.7	.7	+.02			

SUM SQUARES RESID. = .0027 CRYSTALS REMOVED = 17.51%

	P	D	MODEL	BULK DC	% ERROR
Rb	11	18	13	.03	- 27.8
Ba	185	237	222	.05	- 6.3
Zr	50	58	59	.14	+ 1.7
Sr	201	219	220	.52	+ 0.5
V	251	258	193	2.36	- 25.2
Cr	380	140	117	7.12	- 16.4
Ni	142	51	51	6.32	0.0

Table 6.4: Least squares model to generate Mangawhero Formation TYPE 1 basic andesite 14850 from Mangawhero Formation TYPE 1 low-alumina basalt 14855 (Ruapehu basalt) by AFC (A5.2.11).

	P	D	MODEL	RESID.	PHASE	WGT%	%
SiO_2	52.9	56.4	56.4	-.01			
TiO_2	.7	.8	.8	+.01			
Al_2O_3	15.8	17.7	17.7	+.01			
FeO	8.9	7.7	7.7	-.01	Fo90	-6.50	21.86
MgO	8.8	5.1	5.1	-.00	CPX1	-11.10	37.36
CaO	9.8	8.2	8.2	+.00	An50	-10.14	34.11
Na_2O	2.6	3.0	2.9	-.05	MT5.0	-1.98	6.67
K_2O	.6	1.1	1.2	+.04	MELT1	+5.11	0.00

SUM SQUARES RESID. = .0042 CRYSTALS REMOVED = 29.72%

	P	D	MODEL	BULK DC	% ERROR
Rb	11	34	16	.03	- 52.9
Ba	185	313	257	.06	- 17.9
Zr	50	84	68	.13	- 19.0
Sr	201	251	227	.66	- 9.6
V	251	216	152	2.43	- 29.6
Cr	380	132	52	6.63	- 60.6
Ni	142	49	26	5.80	- 46.9

Table 6.5: Least squares model to generate Mangawhero Formation TYPE 1 acid andesite 14844 from Mangawhero Formation TYPE 1 low-alumina basalt 14855 (Ruapehu basalt) by AFC (A5.2.13).

	P	D	MODEL	RESID.	PHASE	WGT%	%
SiO_2	52.9	58.3	58.3	+.00			
TiO_2	.7	.7	.7	-.04			
Al_2O_3	15.8	17.4	17.4	-.00			
FeO	8.9	6.9	6.9	+.01	Fo85	-8.69	19.30
MgO	8.8	4.7	4.7	+.00	CPX2	-14.44	32.06
CaO	9.8	7.6	7.6	+.00	An60	-19.33	42.91
Na_2O	2.6	3.1	3.1	+.03	MT12.5	-2.58	5.73
K_2O	.6	1.2	1.2	+.00	MELT1	+1.98	0.00

SUM SQUARES RESID. = .0024 CRYSTALS REMOVED = 45.02%

	P	D	MODEL	BULK DC	% ERROR
Rb	11	37	20	.04	- 45.9
Ba	185	310	321	.08	+ 3.5
Zr	50	93	85	.11	- 8.6
Sr	201	250	225	.81	- 10.0
V	251	195	131	2.09	- 32.8
Cr	380	92	23	5.70	- 75.0
Ni	142	35	13	5.05	- 62.9

Table 6.6: Least squares model to generate Mangawhero Formation TYPE 1 acid andesite 14886 from Mangawhero Formation TYPE 1 low-alumina basalt 14855 (Ruapehu basalt) by AFC (A5.2.16).

	P	D	MODEL	RESID.	PHASE	WGT%	%
SiO_2	52.9	61.8	61.8	-.03			
TiO_2	.7	.8	.8	+.01			
Al_2O_3	15.8	16.9	16.9	-.03			
FeO	8.9	5.8	5.8	-.03	Fo80	-10.74	22.15
MgO	8.8	3.2	3.2	-.01	CPX2	-15.48	31.91
CaO	9.8	5.9	5.9	-.01	An70	-20.05	41.33
Na_2O	2.6	3.5	3.6	+.07	MT10.0	-2.24	4.61
K_2O	.6	2.0	2.0	+.03	MELT1	+11.52	0.00

SUM SQUARES RESID. = .0081 CRYSTALS REMOVED = 48.51%

	P	D	MODEL	BULK DC	% ERROR
Rb	11	81	21	.04	- 74.1
Ba	185	418	342	.08	- 18.2
Zr	50	158	91	.10	- 42.4
Sr	201	253	232	.78	- 8.3
V	251	162	152	1.76	- 6.2
Cr	380	51	23	5.26	- 54.9
Ni	142	26	8	5.30	- 69.2

Table 6.7: Least squares model to generate Mangawhero Formation TYPE 1 dacite 14889 from Mangawhero Formation TYPE 1 low-alumina basalt 14855 (Ruapehu basalt) by AFC (A5.2.22).

	P	D	MODEL	RESID.	PHASE	WGT%	%
SiO_2	52.9	64.0	64.0	+.01			
TiO_2	.7	.8	.8	+.01	PHASE	WGT%	%
Al_2O_3	15.8	16.8	16.9	+.01			
FeO	8.9	5.1	5.1	+.01	Fo80	-11.38	19.76
MgO	8.8	2.3	2.3	+.01	CPX2	-18.30	31.78
CaO	9.8	4.9	4.9	+.00	An60	-25.24	43.83
Na_2O	2.6	3.4	3.4	-.04	MT10.0	-2.66	4.63
K_2O	.6	2.8	2.8	-.01	MELT1	+17.98	0.00

SUM SQUARES RESID. = .0020 CRYSTALS REMOVED = 57.59%

	P	D	MODEL	BULK DC	% ERROR
Rb	11	120	25	.04	- 79.2
Ba	185	527	408	.08	- 22.6
Zr	50	201	108	.10	- 46.3
Sr	201	260	233	.83	- 10.4
V	251	115	131	1.76	- 13.9
Cr	380	31	10	5.23	- 67.7
Ni	142	20	5	4.98	- 75.0

Table 6.8: Least squares model to generate Mangawhero Formation TYPE 1 acid andesite 14844 from Mangawhero Formation TYPE 1 basic andesite 14858 by AFC (A5.2.15).

	P	D	MODEL	RESID.	PHASE	WGT%	%
SiO_2	54.3	58.3	58.3	+.00			
TiO_2	.7	.7	.7	+.02	PHASE	WGT%	%
Al_2O_3	17.2	17.4	17.4	+.01			
FeO	8.5	6.9	6.9	-.00	Fo85	-4.85	16.50
MgO	6.8	4.7	4.7	+.00	CPX2	-6.88	23.39
CaO	9.0	7.6	7.6	+.00	An60	-15.43	52.49
Na_2O	2.9	3.1	3.1	-.03	MT7.5	-2.24	7.62
K_2O	.7	1.2	1.2	+.00	MELT1	+3.84	0.00

SUM SQUARES RESID. = .0016 CRYSTALS REMOVED = 29.40%

	P	D	MODEL	BULK DC	% ERROR
Rb	18	37	25	.04	- 32.4
Ba	237	310	325	.09	+ 4.8
Zr	58	93	80	.10	- 14.0
Sr	219	250	220	.98	- 12.0
V	258	195	150	2.56	- 23.1
Cr	140	92	29	5.56	- 68.5
Ni	51	35	16	4.35	- 54.3

Table 6.9: Least squares model to generate Mangawhero Formation TYPE 1 acid andesite 14886 from Mangawhero Formation TYPE 1 basic andesite 14850 by AFC (A5.2.20).

	P	D	MODEL	RESID.	PHASE	WGT%	%
SiO_2	56.4	61.8	61.8	-.00			
TiO_2	.8	.8	.8	+.01	PHASE	WGT%	%
Al_2O_3	17.7	16.9	16.9	-.00			
FeO	7.7	5.8	5.8	-.00	En80	-6.68	18.24
MgO	5.1	3.2	3.2	-.00	CPX2	-6.06	16.54
CaO	8.2	5.9	5.9	-.00	An70	-21.20	57.89
Na_2O	3.0	3.5	3.5	+.00	MT10.0	-2.68	7.33
K_2O	1.1	2.0	2.0	+.00	MELT1	+3.25	0.00

SUM SQUARES RESID. = .0001 CRYSTALS REMOVED = 36.62%

	P	D	MODEL	BULK DC	% ERROR
Rb	34	81	53	.05	- 34.6
Ba	313	418	472	.10	+ 12.9
Zr	84	158	127	.09	- 19.6
Sr	251	253	242	1.08	- 4.3
V	216	162	105	2.59	- 35.2
Cr	132	51	20	5.14	- 60.8
Ni	49	26	18	3.19	- 30.8

Table 6.10: Least squares model to generate Mangawhero Formation TYPE 1 dacite 14889 from Mangawhero Formation TYPE 1 acid andesite 14886 by AFC (A5.2.28)

	P	D	MODEL	RESID.	PHASE	WGT%	%
SiO_2	61.8	64.0	64.0	+.03			
TiO_2	.8	.8	.8	+.01	PHASE	WGT%	%
Al_2O_3	16.9	16.8	16.8	-.03			
FeO	5.8	5.1	5.1	+.01	En70	-2.34	18.92
MgO	3.2	2.3	2.2	-.02	CPX2	-3.17	25.92
CaO	5.9	4.9	4.9	+.01	An40	-6.42	52.00
Na_2O	3.5	3.4	3.5	+.06	MT5.0	-.41	3.36
K_2O	2.0	2.8	2.7	-.08	MELT1	+11.16	0.00

SUM SQUARES RESID. = .0124 CRYSTALS REMOVED = 12.34%

	P	D	MODEL	BULK DC	% ERROR
Rb	81	120	92	.05	- 23.3
Ba	418	527	471	.09	- 10.6
Zr	158	201	178	.10	- 11.4
Sr	253	260	254	.98	- 2.3
V	162	115	152	1.50	- 32.2
Cr	51	31	32	4.49	- 3.1
Ni	26	20	19	3.40	- 5.0

Mangawhero Formation lavas (Ruapehu) include a spectrum from basalt to dacite, providing an ideal suite with which to test AFC as a method of generating a range of evolved compositions from a single parent. The chemical trends exhibited by the suite are discussed in Chapter 4 and the salient features are included in Table 6.2. All the models attempted apply POAM fractionation with or without addition of a K-rich melt (those models using a K-poor melt (Appendix A5.2.12, A5.2.14, A5.2.17, A5.2.23) were never as successful suggesting that such a composition does not closely resemble the overall nature of the contaminant). The main features of the models are as follows:

i. Ruapehu basalt 14855 is the logical (same age and spatial distribution) and best fit parental magma for the suite.

ii. Simple POAM fractionation from basalt, or from any other member of the suite, to a more-evolved member nearly always produces a large negative residual for K_2O (and LILE misfit), indicating contamination. The exception to this is A5.2.9 which shows that basic andesite 14858 can be generated from basalt 14855 by POAM fractionation alone (Table 6.3); the negative misfit for Rb and increase in $^{87}Sr/^{86}Sr$ (Table 6.2) do suggest a small amount of contamination but the chemical similarity between parent and daughter has, in this case, rendered that indetectible - addition of K-rich melt to the model (A5.2.10) actually produces a large positive K_2O residual.

iii. Most models using Ruapehu basalt as parent are satisfactory (Table 6.4 to Table 6.7), but all show a persistent negative misfit for Cr and Ni. This is probably due to using too high Kd values for pyroxene, even though the lowest recommended values are used (Gill, 1981) - note that for some calc-alkaline suites (e.g. Santorini, Greece), values as low as 4.8 are considered appropriate (Mann, 1983). Incompatible trace elements (particularly Rb and Zr) show ever increasing negative misfits, which are compensated for by the increasing levels of contamination (5% in basic

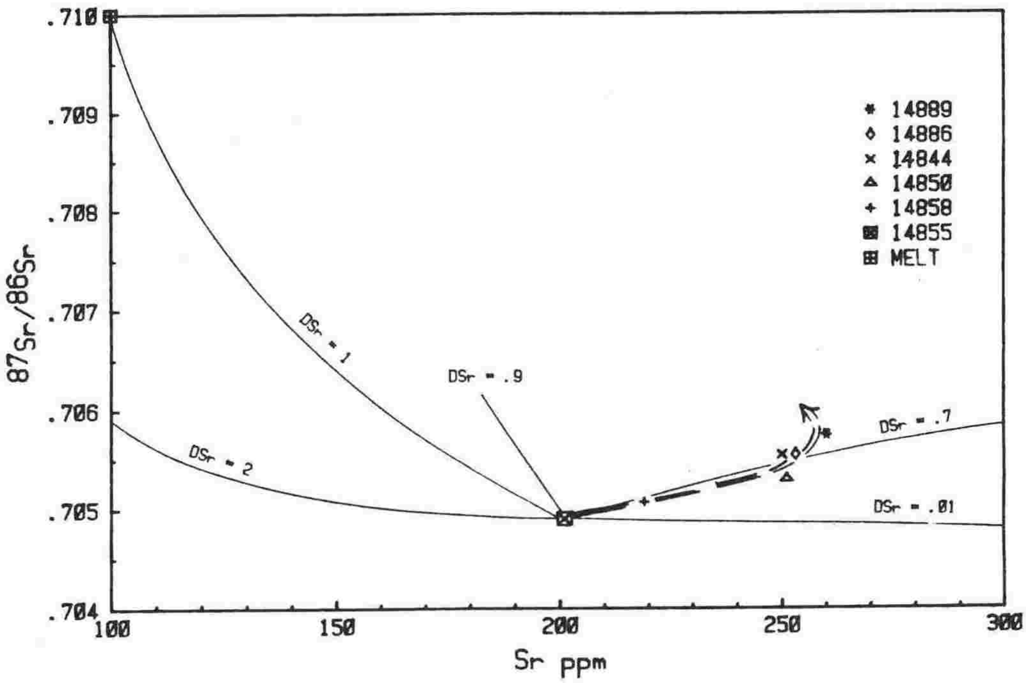

Fig.6.2: $^{87}Sr/^{86}Sr$ vs. Sr concentration for Mangawhero Formation magmas generated by AFC. Ma=.2Mc (i.e. the amount of assimilant added is 20% of the amount of crystals removed). DSr is the bulk distribution coefficient for Sr between fractionating phases and the magma and tie-lines are trajectories for the endmember compositions shown. The heavy dashed line represents a possible evolutionary path for DSr less than 1 (after De Paolo, 1981). A major uncertainty in the model is the composition of the assimilant which is here assumed to be a granitic melt of greywacke-gneiss.

andesite to 18% in dacite). Ba, Sr and V tend to fit most of the models well. There is an expected substantial increase in the total amount of crystals needed to be removed, from 30% for basic andesite to 58% for dacite. Of the total, plagioclase gradually increases in proportion from 34% to 44% whereas clinopyroxene decreases from 37 to 32% and olivine stays constant. Olivine is chosen for these models even though orthopyroxene probably replaces or accompanies it as a fractionating phase of more-evolved compositions; the effect of substitution would be to slightly change the Mg/Fe:silica ratio and to increase the total amount of fractionation required (and thus keep Cr, Ni contents constant). Addition of orthopyroxene as a fractionating mineral artificially improves the model fit, by increasing the degrees of freedom and is consequently resisted.

iv. Models employing an intermediate magma composition as parent give variable results (a) acid andesite 14844 can be generated from basic andesite 14858 by AFC (Table 6.8). The model is similar to that in which basalt 14855 is the parent (Table 6.5), but has a better overall fit (b) acid andesite 14886 can be generated from basic andesite 14850 by AFC if orthopyroxene is the Mg-rich fractionating phase (Table 6.9). An inferior result is achieved if olivine is fractionated (A5.2.19) or if acid andesite 14844 is the parent (A5.2.21) (c) dacite 14889 can be generated from acid andesite 14886 by AFC (Table 6.10). Other andesitic compositions also serve well as parents (A5.2.24 to A5.2.28) if large amounts of melt are added (20-25%). The good fits achieved by these models demonstrate that dacitic magmas of the TVC may not require special geneses such as partial melting of crust, but can be derived either directly from low-alumina basalt (c.f. Table 6.7) or from an evolved derivative of one.

v. Sr isotopic systematics of Mangawhero Formation TYPE 1 lavas are consistent with a model involving AFC of low-alumina basalt 14855. Using the De Paolo (1981) equations describing isotopic evolution during AFC, Fig.6.2 is constructed for the Mangawhero Formation lavas with Ma/Mc=.2 The

Table 6.11: Least squares model to generate Te Herenga Formation TYPE 1 basic andesite 14737 from Mangawhero Formation TYPE 1 low-alumina basalt 14855 (Ruapehu basalt) by POAM fractionation (A5.2.29).

	P	D	MODEL	RESID.	PHASE	WGT%	%
SiO_2	52.9	56.7	56.7	-.03			
TiO_2	.7	.7	.7	+.01	PHASE	WGT%	%
Al_2O_3	15.8	18.2	18.2	-.02			
FeO	8.9	8.1	8.0	-.03	Fo90	-7.24	19.03
MgO	8.8	4.7	4.7	-.02	CPX1	-14.39	37.82
CaO	9.8	7.7	7.7	-.02	An60	-13.91	36.56
Na_2O	2.6	3.2	3.2	-.00	MT10.0	-2.51	6.59
K_2O	.6	.8	.9	+.11			

SUM SQUARES RESID. = .0153   CRYSTALS REMOVED = 38.05%

	P	D	MODEL	BULK DC	% ERROR
Rb	11	20	17	.04	- 15.0
Ba	185	260	289	.07	+ 11.2
Zr	50	63	76	.13	+ 20.6
Sr	201	248	232	.70	- 6.5
V	251	210	128	2.41	- 39.0
Cr	380	38	26	6.61	- 31.6
Ni	142	25	17	5.44	- 32.0

Table 6.12: Least squares model to generate Whakapapa Formation TYPE 1 acid andesite 14804 from Red Crater TYPE 1 low-alumina basalt 11965 by AFC (A5.2.39).

	P	D	MODEL	RESID.	PHASE	WGT%	%
SiO_2	53.3	60.6	60.6	+.00			
TiO_2	.7	.7	.7	-.01	PHASE	WGT%	%
Al_2O_3	15.5	16.8	16.8	+.00			
FeO	9.1	6.3	6.3	+.00	Fo80	-6.13	13.87
MgO	7.8	3.8	3.8	+.00	CPX2	-18.37	41.54
CaO	10.5	6.6	6.6	+.00	An70	-17.09	38.64
Na_2O	2.5	3.3	3.3	+.00	MT12.5	-2.63	5.95
K_2O	.7	1.8	1.8	-.00	MELT1	+8.45	0.00

SUM SQUARES RESID. = .0002   CRYSTALS REMOVED = 44.22%

	P	D	MODEL	BULK DC	% ERROR
Rb	20	73	35	.04	- 52.1
Ba	137	413	235	.07	- 43.1
Zr	68	139	113	.13	- 18.7
Sr	278	293	323	.74	+ 10.2
V	271	164	130	2.26	- 20.7
Cr	281	53	10	6.68	- 81.1
Ni	63	24	6	5.19	- 75.0

data follow a trajectory indicating gradual increase in DSr with increasing fractionation. However, the relative scatter of the data suggests the assimilation process may not be well represented by a contaminant fixed with respect to trace element and Sr isotopic composition. Myers et al. (1984) were unable to model lavas of the Edgecumbe field, SE Alaska in terms of fixed endmember assimilation and so proposed the existence of a variable contaminant. Xenolith studies (Chapter 5), which show a wide range of possible melt compositions, support this idea, making quantitative isotopic modelling of contaminated lava series unrealistic.

Models for Te Herenga and Whakapapa Formation lavas present special difficulties because the suites contain no lavas of basaltic composition nor do they exhibit any clear chemical trends.

Te Herenga Formation andesites are characterised by relatively low K_2O contents so that fractionation models always yield positive residuals for that element. For example, basic andesite 14737 can be generated by POAM fractionation from a low-alumina basalt parent (such as 14855) (Table 6.11). The model has a good fit for most elements, but a K-rich melt (A5.2.38) or a K-poor melt (A5.2.39) must be removed rather than added if it is to be improved (this anomaly could be resolved if hornblende were an early fractionating phase but there is no evidence for its existence in these or other Ruapehu lavas). If the older and more closely coeval Ongaroto basalt-type is the parent (A5.2.40), an inferior major element fit results (SSR=.0605) and the amount of fractionation required (56%) is unreasonably large. It is therefore concluded that Te Herenga Formation magmas were probably generated from a low-alumina basalt parent by POAM fractionation alone. The lavas have variable but relatively low $^{87}Sr/^{86}Sr$ ratios which may have been inherited from their parent magmas or, alternatively, may indicate minor crustal contamination. However, this is difficult to model because of the uncertainty of the parental compositions (although Ruapehu basalt 14855 is a suitable parental type, it is much younger than Te Herenga Formation lavas and could not be the true parent of them).

Whakapapa Formation lavas are typically enriched in LILE and Sr compared to other TYPE 1 lavas, and some have relatively high Sr isotopic ratios (e.g.14804 = .70584). However, most can be adequately modelled from low-alumina basalt by AFC, with only relatively minor misfits. For example, acid andesite 14785 can be generated from Ruapehu basalt 14855 (A5.2.33) (Sr is low) or from Red Crater basalt 11965 (A5.2.34) (Sr fits but Ba and, to a lesser extent, Cr & Ni are too low). Similarly, acid andesite 17481 can be generated from Ruapehu basalt 14855 if olivine (A5.2.35) rather than orthopyroxene (A5.2.36) is the fractionating Mg-rich phase, or from Red Crater basalt 11965 (A5.2.37); model differences are the same as before. A near-perfect fit results when acid andesite 14804 is modelled from Red Crater basalt 11965 (Table 6.12). This model is better than that for a Ruapehu basalt-type (A5.2.38) for two reasons (1) Red Crater basalt is of a similar age to Whakapapa Formation lavas (2) the relatively high Sr content of those lavas requires a parent magma with higher Sr than that of Ruapehu basalt. Attempts to model acid andesite 14804 from acid andesite 14785 (A5.2.40) fail totally because, to balance the K_2O budget, a K-rich melt must be removed. This is impossible, and is also at odds with the relative $^{87}Sr/^{86}Sr$ ratios of these lavas (i.e. 14804 is much higher than 14785). The conclusion is, therefore, that these two lavas evolved separately, though probably from a similar parental magma type.

Table 6.13: Least squares model to generate Wahianoa Formation TYPE 2 acid andesite 14911 from Mangawhero Formation TYPE 1 low-alumina basalt 14855 (Ruapehu basalt) by AFC (A5.3.2).

	P	D	MODEL	RESID.	PHASE	WGT%	%
SiO_2	52.9	58.3	58.3	+.01			
TiO_2	.7	.7	.7	+.00	PHASE	WGT%	%
Al_2O_3	15.8	20.5	20.5	+.01			
FeO	8.9	5.5	5.5	+.00	Fo85	-10.72	30.22
MgO	8.8	2.1	2.1	+.00	CPX2	-16.53	46.61
CaO	9.8	8.0	8.0	+.00	An60	-6.01	16.96
Na_2O	2.6	3.6	3.6	-.03	MT10.0	-2.20	6.21
K_2O	.6	1.3	1.3	+.11	MELT1	+4.73	0.00

SUM SQUARES RESID. = .0009 CRYSTALS REMOVED = 35.47%

	P	D	MODEL	BULK DC	% ERROR
Rb	11	39	17	.02	- 56.4
Ba	185	317	282	.04	- 11.0
Zr	50	95	73	.15	- 23.2
Sr	201	344	267	.35	- 22.4
V	251	167	136	2.40	- 18.6
Cr	380	36	23	7.45	- 36.1
Ni	142	27	9	7.41	- 66.7

Table 6.14: Least squares model to generate Wahianoa Formation TYPE 2 acid andesite 14901 from Wahianoa Formation TYPE 1 acid andesite 16867 by plagioclase-magnetite addition (A5.3.10).

	P	D	MODEL	RESID.	PHASE	WGT%	%
SiO_2	61.4	58.9	59.1	+.15			
TiO_2	.7	.7	.7	-.02	PHASE	WGT%	%
Al_2O_3	17.9	20.0	20.3	+.33			
FeO	6.2	5.6	5.7	+.15			
MgO	2.6	2.1	2.0	-.16			
CaO	6.0	7.6	7.2	-.40	An60	+27.13	0.00
Na_2O	3.6	3.9	3.8	-.09	MT12.5	+1.23	0.00
K_2O	1.6	1.2	1.3	+.02			

SUM SQUARES RESID. = .3514 CRYSTALS ADDED = 28.46%

	P	D	MODEL	BULK DC	% ERROR
Rb	56	35	36	.07	+ 2.9
Ba	389	294	262	.15	- 10.9
Zr	119	91	63	.03	- 30.8
Sr	248	317	303	1.75	- 5.0
V	173	195	190	1.31	- 2.6
Cr	10	15	12	1.74	- 20.0
Ni	17	20	13	.44	- 35.0

6.2.2 Petrogenetic models of TYPE 2 lavas:

Wahianoa Formation TYPE 2 lavas are characterised mineralogically by high modal plagioclase and, chemically, by high Al and Sr contents and low Fe, Mg, Cr and Ni contents. They are interpreted (Chapter 4) to be TYPE 1 lavas which have accumulated plagioclase; this theory can be tested by least squares modelling, as follows.

Wahianoa Formation TYPE 1 acid andesite 14925 can be generated from Ruapehu basalt 14855 by AFC (A5.3.1), the results being similar to those for other TYPE 1 lavas (see previous section). This type of model is also appropriate for TYPE 2 acid andesite 14911 (Table 6.13) and is, therefore, one possible petrogenetic scheme for this lava type. In the model, clinopyroxene and olivine are the main fractionating phases and plagioclase is subordinate to them. The negative misfit for Sr (which is much less for 14901 (A5.3.3)) is reduced if the parental magma is Red Crater basalt 11965 (A5.3.4), but this yields an inferior fit otherwise. With high-alumina basalt 22994 as parent (A5.3.5), the model has a good major element fit (SSR=.0027), but fails to satisfy trace element requirements.

Attempts to model TYPE 2 lavas from other Wahianoa TYPE 1 lavas by POAM fractionation are unsuccessful. For example, acid andesite 14911 can be generated from basic andesite 14922 (A5.3.6) but the major element fit is poor (SSR=.0677). This is because, even if a very calcic plagioclase is fractionated (which is unreasonable), there remains a large negative residual for Na_2O . If magnetite is not a fractionating mineral, plagioclase of a sodic composition must be added while clinopyroxene and olivine (A5.3.7) or orthopyroxene (A5.3.8) are removed. Even though these models fit poorly for major elements, trace element requirements are well satisfied. The possibility that TYPE 2 lavas are variants of TYPE 1 lavas by accumulation of plagioclase is further supported by acid andesite 14901 which can be generated from acid andesite 16721 by 20% plagioclase addition (Table 6.14). Considering the small number of phases employed, the model

Table 6.15: Partial bulk-rock chemistry of selected Mangawhero Formation TYPE 3 lavas.

	14883	17884	17882	17829
SiO_2	58.0	59.2	60.2	64.4
TiO_2	.7	.7	.8	.9
Al_2O_3	15.6	15.2	15.6	15.6
FeO	6.9	6.5	6.3	5.1
MgO	7.0	6.7	5.8	3.2
CaO	7.6	7.1	6.7	4.8
Na_2O	2.7	3.0	2.9	3.1
K_2O	1.4	1.6	1.8	3.1
Rb	54	66	73	132
Ba	331	342	388	535
Zr	114	129	142	226
Sr	250	232	222	215
V	189	171	176	136
Cr	286	325	240	113
Ni	110	101	81	48
I	.70532	.70524	.70534	.70545

Table 6.16: Least squares model to generate Mangawhero Formation TYPE 3 acid andesite 14882 from Mangawhero Formation TYPE 3 acid andesite 14883 by POAM fractionation (A5.4.1).

	P	D	MODEL	RESID.	PHASE	WGT%	%
SiO_2	58.0	60.2	60.3	+.02			
TiO_2	.7	.8	.8	+.00			
Al_2O_3	15.6	15.6	15.6	+.02			
FeO	6.9	6.3	6.3	+.02	Fo85	-3.26	18.44
MgO	7.0	5.8	5.9	+.01	CPX2	-4.81	27.15
CaO	7.6	6.7	6.7	+.01	An60	-8.83	49.84
Na_2O	2.7	2.9	2.9	-.04	MT7.5	-.81	4.57
K_2O	1.4	1.8	1.7	-.04			

SUM SQUARES RESID. = .0044 CRYSTALS REMOVED = 17.71%

	P	D	MODEL	BULK DC	% ERROR
Rb	54	73	65	.04	- 12.3
Ba	331	388	395	.09	+ 1.8
Zr	114	142	136	.09	- 4.2
Sr	250	222	253	.94	+ 14.0
V	189	176	165	1.69	- 6.3
Cr	286	240	138	4.73	- 42.1
Ni	110	81	55	4.53	- 32.1

has an acceptable major element fit (SSR=.3265) and good trace element agreement. Addition of a small amount of magnetite greatly improves the fit for Ti and V (A5.3.10). It is concluded, therefore, that TYPE 2 lavas could be generated either from a low-alumina basalt parent by AFC or, alternatively, from TYPE 1 acid andesite by plagioclase (+ magnetite ?) accumulation.

Sr isotopic compositions of TYPE 2 lavas (Table 4.4) are similar to TYPE 1 which is consistent with the genetic link established between them by geochemical modelling. Therefore, the arguments on systematics are the same and are not re-iterated here.

6.2.3 Petrogenetic models of TYPE 3 lavas:

TYPE 3 lavas are characterised mineralogically by high pyroxene contents and, chemically, by relatively low Al and high Mg, Cr and Ni concentrations. These features might indicate (1) derivation from a more mafic parent than for TYPE 1 lavas (2) plagioclase fractionation or (3) accumulation of mafic minerals. Four Mangawhero Formation TYPE 3 lavas (Table 6.15) range from acid andesite to dacite and show little change in $^{87}Sr/^{86}Sr$ with increasing silica. This suggests that more evolved members of the suite could be derived from less evolved members by POAM fractionation alone; for andesites 14883, 14884 & 14882, that model is satisfactory, whether olivine (A5.4.1) or orthopyroxene (A5.4.2) is taken to be the Mg-rich fractionating phase (Table 6.16). However, dacite 14829 does not fit the model well (A5.4.3 & A5.4.4); for this, the best-fit requires addition of K-rich melt (A5.4.5), though the amount needed seems excessive given the small increase in $^{87}Sr/^{86}Sr$. If more-evolved lavas are considered as parents for 14829 (A5.4.6 & A5.4.7), this difficulty is accentuated so that for acid andesite 14882 (A5.4.8), the amount of melt addition is 22%. These models suggest that TYPE 3 dacite 14829 was not derived from another TYPE 3 lava but evolved separately.

One possible petrogenetic scheme for TYPE 3 lavas involves derivation

Table 6.17: Least squares model to generate Mangawhero Formation TYPE 3 acid andesite 14883 from Mangawhero Formation TYPE 1 low-alumina basalt 14855 (Ruapehu basalt) by AFC (A5.4.12).

	P	D	MODEL	RESID.	PHASE	WGT%	%
SiO_2	52.9	58.0	58.0	-.02			
TiO_2	.7	.7	.7	+.02			
Al_2O_3	15.8	15.6	15.6	-.03			
FeO	8.9	6.9	6.9	-.02	Fo85	-5.27	14.03
MgO	8.8	7.0	7.0	-.01	CPX2	-10.74	28.57
CaO	9.8	7.6	7.6	-.01	An60	-18.84	50.13
Na_2O	2.6	2.7	2.8	+.06	MT7.5	-2.73	7.27
K_2O	.6	1.4	1.4	-.00	MELT1	+6.39	0.00

SUM SQUARES RESID. = .0060 CRYSTALS REMOVED = 37.58%

	P	D	MODEL	BULK DC	% ERROR
Rb	11	54	17	.04	- 68.5
Ba	185	331	284	.09	- 14.2
Zr	50	114	76	.11	- 33.3
Sr	201	250	207	.94	- 17.2
V	251	189	123	2.51	- 34.9
Cr	380	286	38	5.91	- 85.3
Ni	142	110	30	4.30	- 72.7

Table 6.18: Least squares model to generate Mangawhero Formation TYPE 3 acid andesite 14882 from Mangawhero Formation TYPE 1 acid andesite 14886 by olivine-clinopyroxene addition (A5.4.19).

	P	D	MODEL	RESID.	PHASE	WGT%	%
SiO_2	61.8	60.2	60.4	+.22			
TiO_2	.8	.8	.7	-.06			
Al_2O_3	16.9	15.6	15.4	-.26			
FeO	5.8	6.3	6.0	-.22	Fo90	+4.59	0.00
MgO	3.2	5.8	5.9	+.04	CPX1	+6.08	0.00
CaO	5.9	6.7	6.6	-.06			
Na_2O	3.5	2.9	3.2	+.31			
K_2O	2.0	1.8	1.8	+.03			

SUM SQUARES RESID. = .2747 CRYSTALS ADDED = 10.67%

	P	D	MODEL	BULK DC	% ERROR
Rb	81	73	71	.02	- 2.7
Ba	418	388	369	.02	- 4.9
Zr	158	142	142	.15	+ 0.0
Sr	253	222	224	.05	+ .9
V	162	176	152	.66	- 13.6
Cr	51	240	218	6.13	- 9.2
Ni	26	81	113	9.37	- 39.5

from basalt by POAM fractionation. The high Mg number and high Cr and Ni contents of the lavas suggest a primitive parent, but models which have a Waimarino basalt-type parent are unsatisfactory (A5.4.9). Models using a low-alumina basalt-type parent, such as Red Crater basalt (A5.4.10) or Ongaroto basalt (A5.4.11) give much lower residuals, but fail to explain the high Cr and Ni contents. When acid andesite 14883 is modelled from Ruapehu basalt 14855 by AFC (Table 6.17) there is a good major element fit (SSR=.0060), but trace element requirements, particularly Sr, V, Cr and Ni, are not well satisfied. The model differs from that for TYPES 1 and 2 lavas because plagioclase comprises a higher proportion of phases fractionated. Trace element misfits persist with all TYPE 3 lavas modelled in this way, whether a low-alumina basaltic parent (A5.5.13, A5.5.14, A5.5.16) or a tholeiitic parent (A5.4.15) is assumed.

An alternative petrogenetic scheme involves accumulation of mafic minerals by TYPE 1 lavas. This process will better satisfy the requirement of higher Cr and Ni contents and is consistent with Sr isotopic constraints (the $^{87}Sr/^{86}Sr$ ratios of TYPE 1 are similar to TYPE 3). For example, TYPE 3 acid andesite 14883 can be generated from TYPE 1 acid andesite 14844 by 8.2% addition of olivine (4.5%) and augite (3.7%) (A5.4.17). However, a poor major element fit results unless 7% K-rich melt is added (A5.4.18). This is considered unlikely since the $^{87}Sr/^{86}Sr$ ratio of 14844 (.70554) is higher than that of 14883 (.70525). Better results are achieved for TYPE 3 acid andesite 14882 with TYPE 1 acid andesite 14886 as parent (A5.4.19) and for TYPE 3 dacite 14829 with TYPE 1 dacite 14813 as parent (A5.4.20). These show a good major element fit (given the small number of phases considered) and a very good trace element agreement (given the uncertainty of the Cr, Ni, V additions, made by assuming that 14855 is "donating" the additives (Table 6.18)).

It is concluded from these models that TYPE 3 lavas probably result from accumulation of olivine and clinopyroxene by TYPE 1 lavas, which

Table 6.19: Least squares model to generate Mangawhero Formation TYPE 4 acid andesite 14811 from Red Crater TYPE 1 basalt 11965 by POAM fractionation (A5.5.3).

	P	D	MODEL	RESID.	PHASE	WGT%	%
SiO_2	53.3	58.2	58.2	+.01			
TiO_2	.7	.7	.7	-.01			
Al_2O_3	15.5	15.6	15.6	-.00			
FeO	9.1	7.1	7.1	+.01	Fo80	-4.82	12.30
MgO	7.8	6.1	6.1	+.00	CPX2	-13.36	34.05
CaO	10.5	8.3	8.3	+.00	An70	-18.21	46.44
Na_2O	2.5	2.9	3.0	+.06	MT12.5	-2.83	7.21
K_2O	.7	1.2	1.1	-.07			

SUM SQUARES RESID. = .0083 CRYSTALS REMOVED = 39.22%

	P	D	MODEL	BULK DC	% ERROR
Rb	20	40	32	.04	- 20.0
Ba	137	294	216	.08	- 26.5
Zr	68	90	105	.12	+ 16.7
Sr	278	334	295	.88	- 11.7
V	271	207	125	2.55	- 39.6
Cr	281	231	19	6.42	- 91.8
Ni	63	73	10	4.63	- 86.3

Table 6.20: Least squares model to generate Wahianoa Formation TYPE 4 acid andesite 16722 from Mangawhero Formation TYPE 4 acid andesite by POAM fractionation (A5.5.9).

	P	D	MODEL	RESID.	PHASE	WGT%	%
SiO_2	58.2	61.7	61.7	+.01			
TiO_2	.7	.6	.6	+.02			
Al_2O_3	15.6	15.8	15.8	+.02			
FeO	7.1	5.6	5.5	-.01	En80	-4.64	17.37
MgO	6.1	4.7	4.7	-.00	CPX2	-8.36	31.28
CaO	8.3	6.5	6.5	-.01	An70	-11.96	44.75
Na_2O	2.9	3.4	3.4	+.02	MT12.5	-1.76	6.60
K_2O	1.2	1.7	1.7	+.00			

SUM SQUARES RESID. = .0011 CRYSTALS REMOVED = 26.72%

	P	D	MODEL	BULK DC	% ERROR
Rb	40	59	54	.04	- 8.5
Ba	294	353	391	.08	+ 10.8
Zr	90	108	118	.13	+ 9.3
Sr	334	351	350	.85	- .3
V	207	138	129	2.52	- 6.5
Cr	231	106	45	6.29	- 57.5
Ni	73	54	29	3.93	- 46.3

themselves were generated from low-alumina basalt by AFC.

6.2.4 Petrogenetic models of TYPE 4 lavas:

TYPE 4 lavas are distinguished from TYPES 1 and 2 lavas by high Mg, Ca, Cr and Ni contents and from these, and TYPE 3 lavas, by high Sr contents and low $^{87}Sr/^{86}Sr$ ratios.

Attempts to model TYPE 4 acid andesite 14811 from a Waimarino basalt-type parent by POAM fractionation (A5.5.1 & A5.5.5) are not successful. These give large residuals for K_2O and Na_2O (even if a very calcic plagioclase is fractionated) and fail to account for Rb and Sr contents. Better results are achieved with Ruapehu basalt as parent (A5.5.2) which produces a good major element fit (SSR=.0044), and only small misfits for Sr, V, Cr and Ni. With Red Crater basalt as parent (A5.5.3), some of these misfits are reduced (Table 6.19). The small but significant difference in $^{87}Sr/^{86}Sr$ between parent and daughter does not in this case imply crustal contamination since when that is modelled (A5.5.4), there is no improvement in the fit. Difficulties also arise in modelling acid andesite 16722 from Waimarino basalt 17439 (A5.5.5), even if a K-rich melt is added. In this case, none of the trace elements fit well and there are positive residuals for Na_2O and K_2O These, and the large Sr misfit are reduced if a low-alumina basalt parent of either a Ruapehu basalt-type (A5.5.6) or, partcularly, a Red Crater basalt-type (A5.5.7) is used.

Despite the difficulties of modelling TYPE 4 lavas from basaltic parents by POAM fractionation or AFC, there are close petrochemical similarities between them which suggest similar origins. As demonstrated by A5.5.8, acid andesite 16722 can be generated from the less-evolved acid andesite 14811 by POAM fractionation; if olivine is the Mg-rich fractionating phase (A5.5.8), about 23% crystals are removed and only Cr and Ni fit badly; if orthopyroxene is the Mg-rich fractionating phase (A5.5.9), the major element fit is greatly improved (SSR=.0011) but the Cr-Ni misfits persist (Table 6.20).

Table 6.21 : Partial bulk-rock chemistry of selected TYPE 5 lavas.

VUW	17439	17815	17816	17817	14798	24471
LOC	WAIM	HAU	HAU	HAU	OH	PUKE
SiO_2	53.0	56.1	56.6	57.6	57.4	57.5
TiO_2	.5	.6	.6	.6	.5	.6
Al_2O_3	12.9	15.2	15.3	15.7	14.7	14.8
FeO	8.5	7.6	7.7	7.8	8.1	7.4
MgO	13.3	9.1	7.3	6.4	7.1	6.9
CaO	9.7	9.0	9.7	8.8	9.2	9.4
Na_2O	1.6	2.1	2.3	2.3	2.3	2.5
K_2O	.4	.4	.6	.7	.7	.9
Rb	15	8	14	16	16	30
Ba	122	128	177	183	140	214
Zr	48	52	60	68	62	90
Sr	342	569	463	467	346	640
V	226	190	226	215	224	201
Cr	1037	342	234	195	265	276
Ni	341	88	39	34	49	38
I	.70455	.70419	.70424	.70421	.70438	.70442

Table 6.22: Least squares model to generate Hauhungatahi TYPE 5 acid andesite 14817 from magnesian quartz tholeiite 17439 (Waimarino basalt) by POAM fractionation (A5.6.1).

	P	D	MODEL	RESID.	PHASE	WGT%	%
SiO_2	53.0	57.6	57.6	-.00			
TiO_2	.5	.6	.6	-.01	PHASE	WGT%	%
Al_2O_3	12.9	15.7	15.7	-.00			
FeO	8.5	7.8	7.8	-.00	Fo90	-14.61	40.66
MgO	13.3	6.4	6.4	-.00	CPX1	-12.51	34.81
CaO	9.7	8.8	8.8	-.00	An80	-7.50	20.89
Na_2O	1.7	2.3	2.3	+.02	MT7.5	-1.31	3.64
K_2O	.4	.7	.7	-.01			

SUM SQUARES RESID. = .0007   CRYSTALS REMOVED = 35.93%

	P	D	MODEL	BULK DC	% ERROR
Rb	15	16	23	.03	+ 43.8
Ba	122	183	187	.04	+ 2.2
Zr	48	68	71	.11	+ 4.4
Sr	342	467	444	.41	- 4.9
V	226	215	180	1.51	- 16.3
Cr	1037	195	150	5.35	- 23.0
Ni	341	34	39	5.87	+ 14.7

6.2.5 Petrogenetic models of TYPE 5 lavas:

TYPE 5 olivine andesites were erupted mainly from vents at Hauhungatahi, Ohakune and Pukekaikiore and characteristically have high Sr and Cr concentrations, low LILE concentrations and low $^{87}Sr/^{86}Sr$ ratios (Table 6.21). These features suggest the lavas may not be strongly contaminated but may have been generated by simple crystal fractionation from suitable basaltic parents. Of the potential parental compositions, Waimarino basalt-type gives the best major element fit for most models. For example, Hauhungatahi basic andesite 14817 can be generated by 36% POAM fractionation of Waimarino basalt (SSR=.0007) and the model satisfies both K and Rb without without addition of a K-rich melt (Table 6.22). Models using low-alumina basalt-type parents give consistently poor results. Using Ruapehu basalt (A5.6.2) or Red Crater basalt (A5.6.3), there are large K_2O residuals, unsatisfactory trace element fits and unreasonable amounts of fractionation required (49%). Using Ongaroto basalt (A5.6.4), Sr is better satisfied but Zr is too high and V, Cr and Ni are all too low. For models using a high-alumina basalt-type parent (A5.6.5), more than 50% fractionation is required and the trace element fit is poor - Rb, Ba and Zr are too high and Sr, V, Cr and Ni are too low.

It is therefore concluded that Waimarino basalt is the most suitable basalt-type from which TYPE 5 lavas might be generated by POAM fractionation. This is further demonstrated by models A5.6.6 & A5.6.7 (Hauhungatahi basic andesite) and A5.6.8 (Ohakune acid andesite), and is supported by Sr isotopic systematics. TYPE 5 lavas have the lowest $^{87}Sr/^{86}Sr$ ratios, suggesting that contamination is a less important part of their genesis. However, they range widely in age and therefore differences in isotopic composition from the Waimarino basalt parent are difficult to assess (see further discussion in the next section).

It is difficult to model TYPE 5 lavas from other, less-evolved, TYPE 5

Table 6.23: Least squares model to generate Pukeonake TYPE 6 basic andesite 14826 by mixing magnesian quartz tholeiite 17439 (Waimarino basalt) with Mangawhero Formation TYPE 1 dacite 14889 (A5.7.7).

	P1	P2	D	MODEL	RESID.
SiO_2	53.0	64.0	57.6	57.6	-.02
TiO_2	.5	.8	.7	.6	-.07
Al_2O_3	12.9	16.8	14.5	14.5	-.00
FeO	8.5	5.1	6.9	7.0	+.13
MgO	13.3	2.3	8.9	8.6	-.26
CaO	9.7	4.9	7.3	7.7	+.38
Na_2O	1.7	3.4	2.7	2.4	-.27
K_2O	.4	2.8	1.4	1.4	+.02

SUM SQUARES RESID. = .3056 P1/P2 = 1.356

	P1	P2	D	MODEL	% ERROR
Rb	15	120	54	60	+ 11.1
Ba	122	527	320	294	- 8.1
Zr	48	201	112	113	+ 0.9
Sr	342	260	283	307	+ 8.5
V	226	115	182	179	- 1.6
Cr	1037	31	572	609	+ 6.4
Ni	341	20	214	205	- 4.2

NOTES: Abbreviations as for Table 6.1.
P1 = basic parent; P2 = acidic parent;
P1/P2 = ratio of parental endmembers mixed.

lavas. For example, Hauhungatahi acid andesite 14817 can be generated from Hauhungatahi basic andesite 14815 by POA fractionation (A5.6.9), but the fit is poor (SSR=.0607) and Rb and Sr requirements are not met. If the parent-daughter roles are reversed (A5.6.10) the more-basic lava can be generated by accumulation of olivine and clinopyroxene but again the major element fit is poor (SSR=1.1372). These models suggest that compositional variations in some TYPE 5 lavas are best explained in terms of different liquid lines of descent, rather than by crystal accumulation (an exception may be basic andesite (14815) which can be generated from Waimarino basalt-type by POAM fractionation (A5.6.6) but with an inferior major and trace element fit to other such models).

Pukekaikiore acid andesite is also classified TYPE 5, but has some chemical features which produce anomalies in the best-fit model (A5.6.11). The most important of these is a high Sr content which probably results from a higher concentration of this element in the "real" parental magma since the lava has the lowest normative plagioclase content (i.e. Al/Sr is highest ruling out plagioclase accumulation as an explanation). It also has a high alkali content suggesting a small degree of crustal contamination. However, this is not supported by the low $^{87}Sr/^{86}Sr$ ratio.

6.2.6 Petrogenetic modelling of TYPE 6 lavas:

Petrographic evidence of disequilibrium textures and reverse zoning in phenocrysts suggest that TYPE 6 lavas, which occur as Mangawhero Formation acid andesites and Pukeonake acid andesites, are hybrid lavas derived by mixing of two magmas with strongly contrasting chemistries (i.e basic and acidic). Of the possible basaltic magmas, only Waimarino basalt has sufficiently high Cr and Ni contents to produce a successful model; that magma type fits so well that all other potential parents can safely be ignored. There are, however, a number of possible acidic parents ranging from acid andesite to dacite which could be suitable. Some of these are evaluated below for selected TYPE 6 lavas:

Table 6.24: Least squares model to generate Mangawhero Formation TYPE 6 acid andesite 14871 by mixing magnesian quartz tholeiite 17439 (Waimarino basalt with Mangawhero Formation TYPE 1 dacite 14813 (A5.7.8).

	P1	P2	D	MODEL	RESID.
SiO_2	53.0	64.5	59.4	59.3	-.12
TiO_2	.5	.8	.6	.7	+.02
Al_2O_3	12.9	16.2	14.3	14.7	+.37
FeO	8.5	5.0	6.3	6.7	+.40
MgO	13.3	2.5	8.0	7.8	-.22
CaO	9.7	4.7	7.0	7.2	+.17
Na_2O	1.7	3.4	2.8	2.6	-.21
K_2O	.4	2.9	1.6	1.7	+.14

SUM SQUARES RESID. = .4576 P1/P2 = .917

	P1	P2	D	MODEL	% ERROR
Rb	15	115	59	68	+ 15.3
Ba	122	530	327	337	+ 3.1
Zr	48	199	117	128	+ 9.4
Sr	342	228	283	284	+ .4
V	226	136	173	180	+ 4.0
Cr	1037	69	426	535	+ 25.6
Ni	341	32	132	175	+ 32.6

Pukeonake basic andesite 14848 can be generated by mixing Waimarino basalt and TYPE 1 dacite 14813 in the ratio of 57:43 (A5.7.1). Given that two "potential" lava compositions are combined to produce an actual composition, the model fits remarkably well (SSR=.2651) and only Na and Cr show significant residuals. A very similar result is obtained with TYPE 1 dacite 14889 as the acidic endmember (A5.7.2), but not with TYPE 3 dacite 17439 (A5.7.3). In that model, there is an inferior major element fit (SSR=.5438) due to large residuals in Al_2O_3 and K_2O, and trace element requirements are poorly satisfied (particularly Rb). TYPE 1 acid andesites 14885 (A5.7.4) and 14886 (A5.7.5) also do not fit as well as TYPE 1 dacite; these models have large residuals for CaO and fit badly for Ba. It is concluded, therefore, that TYPE 6 Pukeonake andesite is best derived by binary mixing of a Waimarino basalt-type magma with TYPE 1 dacitic magma. This is further demonstrated with acid andesite 14826 (A5.7.6 & A5.7.7) for which the model fits both major and trace elements well (Table 6.23).

Mangawhero Formation TYPE 6 lavas are slightly more silica-rich than those from Pukeonake but can be modelled in the same way. For example, acid andesite 14872 can be generated by binary mixing of Waimarino basalt and TYPE 1 dacite 14813 (A5.7.8) in proportions of 48:52. This model (Table 6.24) fails only to satisfy the Cr and Ni requirements. If TYPE 1 dacite 14889 is the acidic parent (A5.7.9), there is an inferior major element fit (SSR=1.0875), but trace elements are well satisfied. If TYPE 3 dacite is the acidic parent (A5.7.10), the reverse is true and trace element requirements are only poorly satisfied.

Faure (1977, ch.7) showed that mixtures of two components with different Sr contents and $^{87}Sr/^{86}Sr$ ratios form straight lines on plots of 1/Sr and $^{87}Sr/^{86}Sr$. For TYPE 6 lavas (Fig.6.3), this relationship closely predicts the observed Sr isotopic systematics only if Waimarino basalt type is mixed with TYPE 3 dacite, a model which is chemically inferior to one using TYPE 1 dacite. However, it is possible that the preferred model fails

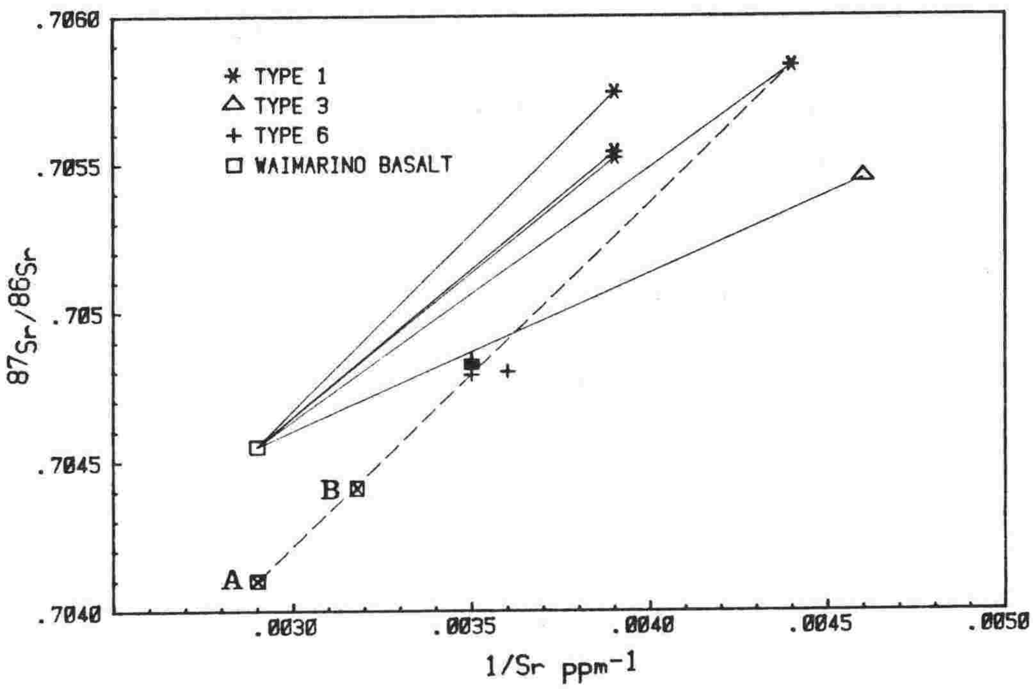

Fig.6.3: $^{87}Sr/^{86}Sr$ vs. 1/Sr for TYPE 6 lavas. Tie-lines join possible endmembers in binary mixing models; TYPE 3 dacite agrees best with Sr isotopic systematics but does not give good geochemical models. TYPE 1 dacite, which has the best geochemical fit, does not agree with Sr isotopic systematics unless the Waimarino basalt-type basic endmember is either less radiogenic (A) or both less radiogenic and less Sr-rich (B) than the composition observed. The latter produces a better fit for TYPE 5 Ohakune andesite generated from it by POAM fractionation.

to adequately explain the Sr isotopic systematics because the $^{87}Sr/^{86}Sr$ of Waimarino basalt is not the true value for the parental magma (though it represents a suitable parent-type, it is much younger than any TYPE 6 lava). To better satisfy the model, the basaltic parent must have a $^{87}Sr/^{86}Sr$ ratio, at the same Sr concentration, of .70410 (point A in Fig.6.3) or, at Sr=320ppm, of .70440 (point B).

The latter composition improves the model for Ohakune TYPE 5 acid andesite which is coeval with TYPE 6 (the original model, A5.6.8, has a positive Sr misfit which would be reduced by a lower Sr concentration in the basaltic parent. An interesting corollary of this is that if a Waimarino basalt-type is parental to TYPE 5 lavas, then there is an marked increase in the $^{87}Sr/^{86}Sr$ ratio with time, from .70420 (Hauhungatahi) to .70440 (Ohakune) to .70455 (Waimarino). A similar temporal change in Sr isotopic composition of TYPE 1 lavas has been previously mentioned (Chapter 4.5), and might indicate increased crustal involvement in the generation of the parental basaltic magmas.

6.3 SUMMARY AND CONCLUSIONS

The petrogenetic models discussed in this chapter investigate the viability of generating andesitic to dacitic lavas and suites of lavas in Tongariro Volcanic Centre by mechanisms such as POAM fractionation, crystal accumulation, AFC and magma mixing. All models use known magma compositions as potential parents, ideal mineral compositions as fractionating phases and an average melt composition as the (added) contaminating phase. The main results and conclusions from the study are as follows:

i. The majority of Ruapehu lavas (TYPE 1) can be generated from a low-alumina basalt-type parent (similar to Ruapehu or Red Crater basalt) by AFC, involving a combination of crystal fractionation and addition of a small amount of granitic partial melt. The melt, derived from greywacke-gneiss basement, is K-rich but variable in composition making accurate assessment of trace element and Sr isotopic systematics difficult.

ii. TYPE 2 lavas can be generated either from a TYPE 1 andesitic parent by plagioclase addition or, alternatively, from a Red Crater basalt-type parent by AFC (with restricted plagioclase fractionation).

iii. TYPE 3 lavas are best generated from TYPE 1 andesitic (or dacitic) parents by olivine + pyroxene addition. Alternatively, they can be generated from a Ruapehu basalt-type parent by AFC (with plagioclase fractionation dominant). However, that model fails to satisfy the high Cr an Ni contents and is not favoured.

iv. TYPE 4 lavas are distinguished from TYPES 1 to 3 by relatively higher Mg, Ca, Cr, Ni and Sr contents and lower $^{87}Sr/^{86}Sr$ ratios. They could be generated from a Red Crater basalt-type by POAM fractionation alone. However, there remain large misfits for Cr and Ni which might suggest some accumulation of olivine or pyroxene, or derivation from an as yet unknown parent (it is interesting to note that Wahianoa TYPE 4 acid andesite 16722 contains traces of resorbed hornblende and is the only Ruapehu lava to do so - hornblende acid andesite 24487 (Cole, 1978) has similar chemical characteristics and $^{87}Sr/^{86}Sr$ ratio (.70497) and may therefore have a similar petrogenetic history).

v. TYPE 5 lavas are best generated from a Waimarino basalt-type parent by POAM fractionation; low-alumina basalt-type parents are unsuitable because they are too low in both Sr and Cr and give much inferior major element fits.

vi. TYPE 6 lavas contain strong petrographic evidence of disequilibrium, and are probably produced by binary mixing of magnesian quartz tholeiite (similar to Waimarino basalt but slightly less Sr-rich and with a lower $^{87}Sr/^{86}Sr$ ratio) and Mangawhero Formation TYPE 1 dacite in a one to one ratio.

Sr isotopic systematics are consistent with these models and, indeed, were partly used to formulate them: TYPES 1, 2 and 3 lavas all have

$^{87}Sr/^{86}Sr$ ratios which are higher than the likely parental basalts and increase with increasing silica. This would be expected if the lava series were generated by AFC. TYPES 4 and 5 lavas do not show that correlation and the low Sr isotopic ratios suggest that crustal contamination is less important in their geneses. For TYPE 6 lavas, Sr isotopic compositions are satisfied by a simple binary mixing relationship. However, it is difficult to accurately model Sr isotopic systematics of contaminated lavas because most of the variables in the equation are unknown (i.e. Sr compositions of "true" parent and contaminant, $^{87}Sr/^{86}Sr$ ratios of "true" parent and contaminant, amount of contamination, bulk distribution coefficient). Though some of these variables can be reasonably well constrained, others cannot, making quantitative isotopic modelling impossible.

The main conclusion to be gained from the petrogenetic modelling study is that most Ruapehu lavas could have been derived from a low-alumina basaltic parent by AFC, or by AFC followed by crystal accumulation. Other rare lava types, including olivine andesites and hybrid lavas erupted from vents close to Ruapehu, appear to require a more tholeiitic parent. If the hybridisation theory for the genesis of TYPE 6 lavas is correct, then that would require initial generation of low-alumina basalt (Ruapehu basalt-type) from the mantle wedge, followed by extensive crystal fractionation and accompanying contamination (to produce the dacite) and then, finally, injection of tholeiitic basalt, mixing and eruption. This scenario clearly requires a complex set of events to take place but, despite that, is supported by compelling petrographic and chemical evidence.

****

CHAPTER 7 : MAIN FINDINGS AND SUGGESTIONS FOR FURTHER STUDY

****

The primary aim of this thesis has been to delineate constraints on petrogenesis of calc-alkaline magmas using lavas of Ruapehu volcano and nearby vents. Integral to this has been an assessment of the role of crustal contamination, a process which has been investigated through a detailed petrographic, chemical and isotopic study of local basement lithologies and of crustal xenoliths. The main results and conclusions are as follows:

Sedimentary basement lithologies in the vicinity of the TVC include (1) Waipapa terrane greywacke (2) Torlesse terrane greywacke and argillite (both of Mesozoic age) and (3) Late Tertiary marine sandstone, siltstone and conglomerate. Of these, only Torlesse terrane rocks appear to have sufficiently high Sr isotopic compositions (.70820 to .72455) to be important in terms of crustal contamination of TVC lavas.

Rb-Sr whole-rock geochronology indicates that Torlesse terrane metasediments were re-equilibrated during low-grade metamorphism at about 140 Ma BP, whereas those at Otaki Forks were re-equilibrated at 182 Ma. Further research is suggested to establish whether this age difference corresponds to separate major tectonic events (i.e. within the Rangitata Orogeny) or merely to local uplift.

Waipapa terrane greywackes are derived from andesitic volcanism and have much lower Sr isotopic ratios than Torlesse terrane lithologies (.70499 to .70845). The validity of a Rb-Sr metamorphic resetting age of 205 Ma is indicated by a complimentary analysis of similar rocks from the Coffs Harbour Block (Australia). However, additional analyses of Waipapa terrane rocks more suitable for Rb-Sr geochronology (i.e. with a wider range of Rb/Sr ratios) are necessary before the age obtained can be confirmed.

Crustal xenoliths contained in TVC lavas are mineralogically, chemically and genetically diverse. They include: upper crustal metasediments (porcellanite, metagreywacke & calcsilicate), igneous nodules (volcanics & cumulates) and vitrified metagreywacke. The latter occurs only in lava from Pukeonake and Ngauruhoe 1954 and is probably derived from high-crustal levels. This is suggested by the strong chemical and isotopic similarity with surface Torlesse terrane rocks which further indicates that such xenoliths have little influence on crustal contamination of host lavas. There are, however, three other, much more dominant xenolith types, all of which may be important in that respect:

Quartz-rich (TYPE QX) and quartz-poor (TYPE QPX) xenoliths are interpreted to be restites resulting from partial melting of the quartzose, feldspathic and micaceous parts of greywacke-gneiss (i.e. greywacke subjected to high-grade metamorphism at depth below the TVC). The frequency of occurrence of these restite assemblages implies that partial granitic melts are likely to be important in the genesis of many TVC lavas. Compositions of glasses trapped in some examples provides an insight into the nature of the contaminant and suggests that it is typically variable both chemically and isotopically. Experimental studies on the melting of Waipapa greywackes (Reid, 1982) and quartzo-feldspathic schists (Dr.R.H.Grapes, pers. comm., 1985) have suggested the validity of many of the above interpretations and similar studies of Torlesse terrane greywackes might confirm those results.

Meta-igneous xenoliths (TYPE MIX) comprise the third dominant type. These are chemically and mineralogically different from surface (host) lavas. Textures are granulitic, suggesting re-equilibration under high P-T conditions, and are therefore possibly derived from near the base of the crust. Most examples are depleted in alkalis and LILE but have relatively high $^{87}Sr/^{86}Sr$ ratios. Their importance in magma genesis is difficult to assess, requiring analysis of a much larger suite than is presently available to determine whether chemical trends are related to differentiation within the source or to removal of partial melts during granulite metamorphism.

Basalts of Taupo Volcanic Zone include high-alumina, low-alumina and tholeiitic types. These are spatially and chemically distinct and cannot be directly generated, one from the other. Of the three types, only low-alumina basalt and tholeiite are suitable parent types for TVC lavas since high-alumina basalt is too high in Sr, Zr and Ti and too low in Cr and Ni to satisfy most trace element requirements.

Ruapehu lavas and those of nearby vents are dominantly calc-alkaline, medium-K andesites. They are porphyritic containing plagioclase, augite, olivine (mainly in basalts and basic andesites), orthopyroxene (mainly in acid andesites and dacites) and titanomagnetite (also chromian spinel in basic lavas). Hydrous minerals are rare. The lavas can be categorised into six petrographically and chemically distinct groups (TYPES 1 to 6): TYPE 1 are plagioclase- and plagioclase-pyroxene lavas with coherent chemical trends and moderately high Sr isotopic ratios (.7048 to .7062); TYPE 2 are plagioclase andesites; TYPE 3 are pyroxene andesites; TYPE 4 are also pyroxene andesites, but differ from TYPE 3 by having higher Sr concentrations and lower $^{87}Sr/^{86}Sr$ ratios; TYPE 5 are olivine andesites with low modal plagioclase, high Sr and Cr concentrations and low $^{87}Sr/^{86}Sr$ ratios; TYPE 6 are mixed magmas (hybrids).

Petrogenetic modelling shows that it is possible to generate TYPES 1, 2, 3 and 4 lavas from low-alumina basalt by processes of POAM crystal fractionation or by combined fractionation and crustal assimilation (AFC). The spatially and volumetrically resticted TYPES 5 & 6 lavas are best derived from a more tholeiitic parent by crystal fractionation or by mixing with dacite (respectively). These models are consistent with petrographic, chemical and Sr isotopic constraints. Whether or not the above lava classification scheme might be applicable to a wider range of lavas in Tongariro Volcanic Centre (and elsewhere?) requires further analysis; this should be accompanied by a careful study of crustal xenoliths to determine the nature and extent of contamination for any petrogenetic scheme.

****

REFERENCES

****

Abbey, S., 1980. Studies in "standard samples" for use in the general analysis of silicate rocks and minerals. Part 6 : 1979 edition of "usable" values.
Geol. Surv. Can. Pap. 80-14. 30p.

Adams, C.J.D., 1975. New Zealand potassium-argon age list-2.
N.Z. J. Geol. Geophys., 18: 443-467.

Adams, C.J.D., 1980. Age and origin of the Southern Alps.
In: R.I.Walcott, M.M.Cresswell (Editors), The Origin of the Southern Alps, Bulletin 18-The Royal Society of New Zealand :73-78.

Anderson, A.T., 1968. Oxidation of the LaBlanche Lake titaniferous magnetite deposit, Quebec.
J. Geol., 76: 528-547.

Anderson, A.T., 1976. Magma mixing: petrological process and volcanological tool.
J. Volcan. Geotherm. Res., 1: 3-33.

Anderson, A.T., 1982. Parental basalts in subduction zones: Implications for continental evolution.
J. Geophys. Res., 87 (B8): 7047-7060.

Aoki, K.I. and Fujimaki, H., 1982. Petrology and geochemistry of calc-alkaline andesite of presumed upper mantle origin from Itinomi-gata, Japan.
Amer. Min., 67: 1-13.

Arculus, R.J. and Johnson, R.W., 1978. Critisism of generalised models for the magmatic evolution of arc-trench systems. Earth Planet. Sci. Lett., 39: 118-126.

Arculus, R.J. and Johnson, R.W., 1981. Island-arc magma sorces: a geochemical assessment of the roles of slab-derived components and crustal contamination. Geochem. Jour., 15: 109-133.

Arculus, R.J. and Wills, K.J.A., 1980. The petrology of plutonic blocks and inclusions from the lesser Antilles island arc. J. Pet., 21 (4): 743-799.

Armstrong, R.L. and Cooper, J.A., 1971. Lead isotopes in island arcs. Bull. Volcanologique 35: 27-63.

Aronson, J.L., 1965. Reconnaissance rubidium-strontium geochronology of New Zealand plutonic and metamorphic rocks. N.Z. J. Geol. Geophys., 8 (3): 401-423.

Arth, J.G., 1976. Behaviour of trace elements during magmatic processes - A summary of theoretical models and their applications. J. Res. U.S. Geol. Surv., 4 (1): 41-47.

Arzi, A.A., 1978. Fusion kinetics, water pressure, water diffusion and electrical conductivity in melting rocks, interrelated. J. Pet., 19: 153-159.

Banno, S. and Matsui, Y., 1973. On the formulation of partition coefficients for trace element distribution between minerals and magma. Chem. Geol., 11: 1-15.

Barberi, F., Civetta, L. and Varet, J., 1980. Sr isotopic composition of Afar volcanics and its implication for mantle evolution.

Earth Planet. Sci. Lett., 50: 247-259.

Barth, T.F.W., 1962. The feldspar geologic thermometer. Nor. Geol. Tidsskr., 42: 330-339.

Battey, M.H., 1949. The recent eruption of Ngauruhoe. Rec. Auck. (N.Z.) Inst., 3 (6): 387-395.

Bence, A.E. and Albee, A.L., 1968. Empirical correction factors for the electron microprobe analysis of silicates and oxides. J. Geol. 76: 382-403.

Bergen, M.J.V. and Barton, M., 1984. Complex interaction of aluminous metasedimentary xenoliths and siliceous magma; an example from Mt. Amiata (Central Italy). Contrib. Min. Pet., 86: 374-385.

Blattner, P. and Reid, F.W., 1982. The origin of lavas and ignimbrites of the Taupo Volcanic Zone, New Zealand in the light of oxygen isotope data. Geochim. Cosmochim. Acta, 46: 1417-1429.

Bowen, N.L., 1928. The evolution of igneous rocks. Princeton University Press (reprinted by Dover Press, 1956), 334p.

Bradshaw, J.D., Adams, C.J. and Andrews, P.B., 1980. Carboniferous to Cretaceous on the Pacific Margin of Gondwana: The Rangitata Phase of New Zealand. In: M.M. Cresswell and p. Vella (Editors), Gondwana Five. A.A. Balkema, Rotterdam,: 217-221.

Brindley, G.W. and Maroney, D.M., 1960. High temperature reactions of clay mineral mixtures and their ceramic properties, II. J. Amer. Ceram. Soc., 43: 511-516.

Briqueu, L and Lancelot, J.R., 1979a. Sr isotopes and K, Rb, Sr balance in sediments and igneous rocks from the subducted plate of the Vanuatu (New Hebrides) active margin.
Geochim. Cosmochim., Acta, 47: 191-200.

Briqueu, L and Lancelot, J.R., 1979b. Rb-Sr systematics and crustal contamination models for calc-alkaline igneous rocks.
Earth Planet. Sci. Lett., 43: 385-396.

Brooks, C., Hart, S.R. and Wendt, I., 1972. Realistic use of two-error regression treatments as applied to rubidium-strontium data.
Rev. Geophys. Space Phys., 10 (2): 551-577.

Brown, W.L. and Parsons, I., 1981. Towards a more practical two-feldspar geothermometer.
Contrib. Min. Pet., 76: 369-377.

Buddington, A.F. and Lindsley, D.H., 1964. Iron-titanium oxide minerals and synthetic equivalents.
J. Pet., 5: 310-357.

Butler, J.C., Artificial isochrons.
Lithos, 15: 207-214.

Carlson, R.W., Lugmair, G.W. and McDougall, J.D., 1981. Columbia River volcanism: the question of mantle heterogeneiity or crustal contamination.
Geochim. Cosmochim. Acta, 45: 2483-2499.

Carmichael, I.S.E., 1967. The iron-titanium oxides of salic volcanic rocks and their associated ferromagnesian silicates.
Contrib. Min. Pet., 14: 36-64.

Carter, S.R. and Norry, M.J., 1976. Genetic implications of Sr isotopic

data from the Eden volcano, South Arabia.
Earth Planet. Sci. Lett., 31: 161-166.

Cashman, K.V., 1979. Evolution of Kakaramea and Maungakatote Volcanoes, Tongariro Volcanic Centre, New Zealand.
Unpublished MSc (Hons.) thesis, Victoria University of Wellington.

Chaudhuri, S., 1976. The significance of rubidium-strontium age of sedimentary rock.
Contrib. Min. Pet. 59: 161-170.

Church, S.E. and Tatsumoto, M., 1975. Lead isotope relations in oceanic ridge basalts from the Juan de Fuca-Gorda Ridge area, NE Pacific Ocean.
Contrib. Min. Pet., 53: 253-279.

Clark, R.H., 1960. Andesite lavas of the North Island, New Zealand.
Proc. 21st Int. Geol. Cong., Norden, Pt.13: 123-131.

Clarke, D.B. and O'Hara, M.J., 1979. Nickel, and the existence of high-MgO liquids in nature.
Earth Planet. Sci. Lett., 44: 153-158.

Clauer, N., 1982. The rubidium-strontium method applied to sediments: certitudes and uncertainties.
In: G.S.Odin (Editor), Numerical dating in Stratigraphy.
J. Wiley and Sons, Chichester, New York, Brisbane, Toronto, Singapore: 245-275.

Clauer, N. and Kröner, A., 1979. Strontium and argon isotopic homogenisation of pelitic sediments during low-grade regional metamorphism: the Pan-African upper Damara sequence of Northern Namibia (South West Africa).
Earth Planet. Sci. Lett., 43: 117-131.

Cloud, P.E.Jr., 1951. The 1949 eruption of Ngauruhoe.
Sci. Mon. N.Y., 72: 241.

Cole, J.W., 1970. Petrology of the basic rocks of the Tarawera Volcanic Complex.
N.Z. J. Geol. Geophys. 13: 925-936.

Cole, J.W., 1973. High-alumina basalts of Taupo Volcanic Zone, New Zealand.
Lithos 6: 53-64

Cole, J.W., 1978. Andesites of the Tongariro Volcanic Centre, North Island, New Zealand.
J. Volcan. Geotherm. Res. 3: 121-153.

Cole, J.W., 1979. Structure, petrology, and genesis of Cenozoic volcanism Taupo Volcanic Zone, New Zealand - a review.
N.Z. J. Geol. Geophys. 22 (6): 631-657.

Cole, J.W., 1981. Genesis of lavas of the Taupo Volcanic Zone, North Island, New Zealand.
J. Volcan. Geotherm. Res. 10: 317-337.

Cole, J.W., 1982. Tonga - Kermadec - New Zealand.
In: R.S.Thorpe (Editor), Andesites. John Wiley & Sons, Chichester, New York, Brisbane, Toronto, Singapore,: 245-258.

Cole, J.W., 1984. Taupo - Rotorua depression: an ensialic marginal basin of North Island, New Zealand. In: B.P.Kokelaar and M.F.Howells (Editors), Marginal basin geology: volcanic and associated sedimentary and tectonic processes in modern and ancient marginal basins.
Spec. Pub. Geol. Soc. Lond.

Cole, J.W. and Lewis, K.B., 1981. Evolution of the Taupo - Hikurangi subduction system.
Tectonophysics, 72: 1-21.

Cole, J.W. and Nairn, I.A., 1975. Catalogue of the active volcanoes of the world including Solfatara fields, Part 22, New Zealand.
International Association of Volcanology and Chemistry of the Earth's Interior, Naples.

Cole, J.W., Cashman, K.V. and Rankin, P.C., 1983. Rare-earth element Geochemistry and the origin of andesites and basalts of the Taupo Volcanic Zone, New Zealand.
Chem. Geol. 38: 255-274.

Coombs, D.S., Landis, C.A., Norris, R.J., Sinton, J.M., Borns, D.J. and Craw, D., 1976. The Dun Mountain ophiolite belt, New Zealand, its tectonic setting, constitution, and origin, with special reference to the southern portion.
Amer. J. Sci., 276: 561-603.

Correns, C.W., 1978. Titanium.
In: K.H.Wedepohl (Editor), Handbook of Geochemistry.
Springer-Verlag, Berlin, Heidelberg, New York: 22B-220B.

Criscione, J.J., Davis, T.E. and Ehlig, P., 1978. The age of sedimentation/ diagenesis for the Bedford Canyon formation and the Santa Monica formation in Southern California : A Rb/Sr evaluation.
In: D.G. Howell and K.A. McDougall (Editors), Mesozoic Paleogeography of the Western United States, Symposium 2: Pacific Coast Paleogeography: 385-396.

Dahl, P.S., 1980. The thermal-compositional dependence of Fe^{2+}-Mg distributions between coexisting garnet and pyroxene: applications to geothermometry.

Amer. Min., 65: 854-866.

Dasch, E.J., 1969. Strontium isotopes in weathering profiles, deep-sea sediments, and sedimentary rocks.
Geochim. Cosmochim. Acta, 33: 1521-1552.

Davidson, L.R. and Mathison, C.I., 1973. Manganiferous orthopyroxenes and garnets from metamorphosed iron formations of the Quairading district, Western Australia.
Nues. Jahrb. Min. Mh.,: 47-57.

Davis, B.T.C. and Boyd, F.R., 1966. The join $Mg_2Si_2O_6$ - $CaMgSi_2O_6$ at 30 kilobars pressure and its application to pyroxenes from kimberlites.
J. Geophys. res., 71: 3567-3576.

Deer, W.A., Howie, R.A. and Zussman, J., 1963. Rock-forming minerals, Vol.4 : Framework silicates.
Longman, London: 435p.

Deer, W.A., Howie, R.A. and Zussman, J., 1978. Rock-forming minerals, Vol. 2A (2nd Ed.): Single-chain silicates.
Longman, London: 668p.

De Paolo, D.J., 1981. Trace element and isotopic effects of combined wallrock assimilation and fractional crystallisation.
Earth Planet. sci. Lett., 53: 189-202.

De Paolo, D.J. and Johnson, R.W., 1979. Magma genesis in the New Britain arc: constraints from Nd and Sr isotopes and trace element patterns.
Contrib. Min. Pet., 70: 367-379.

Drake, M.J., 1976. Plagioclase-melt equilibria.
Geochim. Cosmochim. Acta, 40: 457-465.

Eichelberger, J.C., 1975. Origin of andesite and dacite: evidence of mixing at Glass Mountain in California and at other circum-Pacific volcanoes.
Bull. Geol. Soc. Amer., 86: 1381-1391.

Eichelberger, J.C., 1978. Andesitic volcanism and crustal evolution.
Nature, 275: 21-27.

Ellis, D.J., 1980. Osumilite-sapphirine-quartz granulites from Enderby Land, Antarctica: P-T conditions of metamorphism, implications for garnet-cordierite equilibria and the evolution of the deep crust.
Contrib. Min. Pet., 74: 201-210.

Evans, B.W. and Wright, T.L., 1972. Composition of liquidus chromite from the 1959 (Kilauea Iki) and 1965 (Makaopuhii) eruptions of the Kilauea volcano.
Amer. Min., 57: 217-230.

Evernden, J.F. and Richards, J.R., 1962. Potassium-Argon ages in eastern Australia.
J. Geol. Soc. Aust., 9: 1-49.

Ewart, A., 1976. Mineralogy and chemistry of modern orogenic lavas - some statistics and implications.
Earth Planet. Sci. Lett., 31: 417-432.

Ewart, A. and Stipp, J.J., 1968. Petrogenesis of the volcanic rocks of the Central North Island, New Zealand, as indicated by a study of $^{87}Sr/^{86}Sr$ ratios, and Sr, Rb, K, U and Th abundances.
Geochim. Cosmochim. Acta, 32: 699-736.

Ewart, A., Brothers, R.N. and Mateen, A., 1977. An outline of the Geology and geochemistry and the possible petrogenetic evolution of the volcanic rocks of the Tonga-Kermadec-New Zealand island arc. J. Volcan. Geotherm. Res, 2: 205-250.

Fairbairn, H.W., Bottino, M.L., Pinson, W.H.Jr. and Hurley, P.M., 1966. Whole-rock and initial $^{87}Sr/^{86}Sr$ of volcanics underlying fossiliferous Lower Cambrian in the Atlantic provinces of Canada. Can. J. Earth Sci., 3: 509-521.

Farquharson, R.B. and Richards, J.R., 1975. Isotopic remobilisation in the Mount Isa tuff beds. Chem. Geol., 16: 73-88.

Faure, G., 1977. Isotope Geology (Chapters 6-8). John Wiley & sons, New York, 464p.

Faure, G. and Hurley, P.M., 1963. The isotopic composition of strontium in oceanic and continental basalts: applications to the origin of igneous rocks. J. Pet., 4 (1): 31-50.

Ferry, J.M. and Spear, F.S., 1978. Experimental calibration of the partitioning of Fe and Mg between biotite and garnet. Contrib. Min. Pet., 66: 113-117.

Fleming, C.A. and Steiner, A., 1951. Sediments beneath Ruapehu Volcano. N.Z. J. Sci. Tech., B32 (6): 31-2.

Francis, P.W., Thorpe, R.S., Moorbath, S., Kretzschmar, G.A. and Hammill, M., 1980. Strontium isotope evidence for crustal contamination of calc-alkaline volcanic rocks from Cerro Galan, northwest Argentina. Earth Planet. Sci. Lett., 48: 257-267.

Gebauer, D. and Grünenfelder, M., 1974. Rb-Sr whole-rock dating of late diagenetic to anchimetamorphic, Paleozoic sediments in Southern France

(Montagne Noire).
Contrib. Min. Pet., 47: 113-130.

Gebauer, D. and Grünenfelder, M., 1976. U-Pb zircon and Rb-Sr whole-rock dating of low-grade metasediments example : Montagne Noire (Southern France).
Contrib. Min. Pet., 59: 13-32.

Gerlach, D.C. and Grove, T.L. (1982). Petrology of Medicine Lake Highland volcanics: characterisation of endmembers of magma mixing.
Contrib. Min. Pet., 80: 147-159.

Gill, J.B., 1974. Role of underthrust oceanic crust in the genesis of a Fijian calc-alkaline suite.
Contrib. Min. Pet., 43: 29-45.

Gill, J.B., 1981. Orogenic andesites and plate tectonics.
Springer-Verlag, Berlin, Heidleberg, New York, 390pp.

Gladney, E.S. and Goode, W.E., 1981. Elemental concentrations in eight new United States Geological Survey rock standards - a review.
Geostandards Newsletter, 5 (1): 31-64.

Govindaraju, K., 1980. Report (1980) on three GIT-IWG rock reference samples anorthite from Greenland, AN-G; basalte d'Essey-la-cote, BE-N; granite de Beauvoir, MA-N.
Geostandards Newsletter 4 (1): 49-138.

Graham, I.J., 1983a. The Rb-Sr System. Manual 1: Chemical procedures.
N.Z. Dep. Sci. Ind. Res. Pub. INS-M-75.

Graham, I.J., 1983b. The Rb-Sr System. Manual 2: Mass Spectrometry.
N.Z. Dep. Sci. Ind. Res. Pub. INS-M-76.

Grange, L.I. and Williamson, J.H., 1930. Tongariro Subdivision.

N.Z. Geol. Surv. 24th Ann. Report, 1929-30: 10-13.

Grant-Taylor, T.L. and Waterhouse, J.B., 1963. Monotis from the Tararua range, Wellington.
N.Z. J. Geol. Geophys., 6: 623-627.

Grapes, R.H., (In Press). Melting and thermal reconstitution of pelitic xenoliths, Wehr volcano, East Eifel, West Germany.
J. Pet.

Grapes, R.H., Watanabe, T and Palmer, K, 1982. X.R.F. analyses of quartzo -feldspathic schists and metacherts, Franz Josef-Fox glacier area, Souther Alps, New Zealand.
Victoria University of Wellington Geol. Dept. Pub. No. 11.

Green, D.H., 1973. Experimental melting studies on a model upper mantle composition at high pressure under water-saturated and water-undersaturated conditions.
Earth Planet. Sci. Lett., 19: 37-53.

Green, D.H., 1976. Experimental testing of "equilibrium" partial melting of peridotite under water-saturated, high-pressure conditions.
Can. Min., 14: 255-268.

Green, D.H. and Ringwood, A.E., 1967. The genesis of basaltic magmas.
Contrib. Min. Pet., 15: 103-190.

Green, T.H., 1972. Crystallisation of calc-alkaline andesite under controlled high-pressure hydrous conditions.
Contrib. Min. Pet., 34: 150-166.

Green, T.H., 1980. Island-arc and continent-building magmatism - a review of key geochemical parameters and genetic processes.
Tectonophysics, 63: 367-385.

Green, T.H., 1982. Anatexis of mafic crust and high pressure crystallisation of andesite.
In: R.S.Thorpe (Editor), Andesites, J. Wiley and Sons, Chichester, New York, Brisbane, Toronto, Singapore: 465-487.

Gregg, D.R., 1956. Eruption of Ngauruhoe 1954-1955.
N.Z. J. Sci. Tech., B37: 675-688.

Gregg, D.R., 1960. The Geology of Tongariro Subdivision.
N.Z. Geol. Surv. Bull. n.s. 40.

Gribble, C.D. and O'Hara, M.J., 1967. Interaction of basic magma with pelitic materials.
Nature, 214 (5094): 1198-1201.

Grieve, R.A.F. and Fawcett, J.J., 1974. The stability of chloritoid below 10 kb P (H_2O).
J. Pet., 15 (1): 113-139.

Grindley, G.W., 1960. Geological map of New Zealand. Sheet 8 - Taupo.
N.Z. Dep. Sci. Ind. Res. Inf. Serv., 50: 79-86

Grove, T.L., Gerlach, D.C. and Sando, T.W. (1982). Origin of calc-alkaline series lavas at Medicine Lake volcano by fractionation, assimilation and mixing.
Contrib. Min. Pet., 80: 160-182.

Hackett, W.R., (In Press). The Waimarino basalt: a new basalt locality from the Taupo Volcanic Zone, New Zealand.
N.Z. J. Geol. Geophys.

Harland, W.B., Cox, A.V., Llewellyn, P.G., Pickton, C.A.G., Smith, A.G. and Walters, R., 1982. A Geologic Time Scale.
Cambridge: Cambridge University Press: xii + 131p.

Harley, S.L., 1984a. An experimental study of the partitioning of Fe and Mg between garnet and orthopyroxene.
Contrib. Min. Pet., 86: 359-373.

Harley, S.L., 1984b. The solubility of alumina in orthopyroxene coexisting with garnet in $FeO-MgO-Al_2O_3-SiO_2$ and $CaO-FeO-MgO-Al_2O_3-SiO_2$
J. Pet., 25 (3): 665-696.

Harley, S.L., 1984c. Comparison of the garnet-orthopyroxene geobarometer with recent experimental studies, and applications to natural assemblages.
J. Pet., 25 (3): 697-712.

Hart, S.R. and Davis, K.E., 1978. Nickel partitioning between olivine and silicate melt.
Earth Planet. Sci. Lett., 40: 203-219.

Hawkesworth, C.J., O'Nions, R.K. and Arculus, R.J., 1979. Nd and Sr isotope geochemistry of island arc volcanics, Granada, Lesser Antilles.
Earth Planet. Sci. Lett., 45: 237-248.

Hawkesworth, C.J. and Powell, M., 1980. Magma genesis in the lesser Antilles island arc.
Earth Planet. Sci. Lett., 51: 297-308.

Hensel, H.D., Chappell, B.W., Compston, W., McCulloch, M.T., 1982. A Neodymium and strontium isotopic investigation of granitoids and possible source rocks from New England, Eastern Australia.
In: P.G. Flood and B. Runnegar (Editors), New England Geology, Voisey Symposium Univ. New England, Dept. Geology: 193-200.

Hietanen, A., 1959. Kyanite-garnet gedritite near Orofino, Idaho.
Amer. Min., 44: 539-564.

Hildreth, Wes., 1981. Gradients in silicic magma chambers: Implications for lithospheric magmatism.
J. Geophys. Res., 86 (B11): 10153-10192.

Holgate, N., 1954. The role of liquid immiscibility in igneous petrogenesis.
J. Geol., 62: 439-480.

Höller, H., 1967. Experimentelle Bildung von Alunit-Jarosit durch die Einwirkung von Schwefelsaüre auf Mineralien und Gesteine.
Cont.trib. Min. Pet., 15: 309-329.

Huppert, H.E. and Turner, J.S., 1981. A laboratory model of a replenished magma chamber.
Earth Planet. Sci. Lett., 54: 144-152.

Irvine, T.N. and Baragar, W.R., 1971. A guide to the chemical classification of the common igneous rocks.
Can. J. Earth Sci., 8: 523-548.

Irving, A.J., 1973. A review of experimental studies of crystal/liquid trace element partitioning.
Geochim. Cosmochim. Acta., 42: 743-770.

Jackson, E.D., 1969. Chemical variation in coexisting chromite and olivine in chromitite zones of the Stillwater complex.
Econ. Geol. Mon., 4: 41-71.

Jâkes, P. and Gill, J.B., 1970. Rare earth elements and the island arc tholeiitic series.
Earth Planet. Sci. Lett., 9: 17-28.

Jaques, A.L., 1981. Petrology and petrogenesis of cumulate peridotites

and gabbros from the Marum Ophiolite Complex, northern Papua New Guinea
J. Pet., 22 (1): 1-40.

Jaques, A.L. and Green, D.H., 1980. Anhydrous melting of peridotite at 0-15kb pressure and the genesis of tholeiitic basalts.
Contrib. Min. Pet., 73: 287-310.

Jaques, A.L., Chappell, B.W. and Taylor, S.R., 1983. Geochemistry of cumulus peridotites and gabbros from the Marum Ophiolite Complex, northern Papua New guinea.
Contrib. Min. Pet., 82: 154-164.

Kashkai, M.A. and Babaev, I.A., 1969. Thermal investigations on alunite and its mixtures with quartz and dickite.
Min. Mag., 37 (285): 128-134.

Kay, R.W., 1978. Aleutian magnesian andesites: melts from subducted Pacific Ocean crust.
J. Volcan. Geotherm. Res., 4: 117-132.

Kay, R.W., 1980. Volcanic arc magmas: implications of a melting mixing model for element recycling in the crust-upper mantle system.
J. Geol., 88: 497-522.

Kay, R.W., 1984. Elemental abundances relevant to identification of magma sources.
Phil. Trans. Roy. Soc. Lond., A310: 535-547.

Kennedy, P.C., Roser, B.P. and Palmer, K, 1980. Analyses of the new A.N.R.T. / C.R.P.G. rock standards AN-G, BE-N and MA-N.
Victoria University of Wellington Geol. Dept. Pub. No. 16.

Kennedy, P.C., Palmer, K. and Roser, B.P., 1981. Chemical analysis of the eight U.S.G.S. rock standards: BHVO-1, MAG-1, QLO-1, RGM-1, SCo-1,

SDC-1, SGR-1, STM-1.
Victoria University of Wellington Geol. Dept. Pub. No. 21.

Kitchen, D., 1984. Pyrometamorphism and the contamination of basaltic magma at Tieveragh, Co. Antrim.
J. Geol. Soc. Lond., 141: 733-745

Korsch, R.J., 1971. Paleozoic sedimentology and igneous geology of the Woolgoolga district, North Coast, New South Wales.
J. Proc. R. Soc. N.S.W., 104: 63-75.

Korsch, R.J., 1977. A framework for the Palaeozoic geology of the southern part of the New England Geosyncline.
J. Geol. Soc. Aust., 25: 339-355.

Korsch, R.J., 1978a. Stratigraphic and igneous units in the Rockvale-Coffs Harbour region, northern New South Wales.
J. Proc. R. Soc. N.S.W., 111: 13-17.

Korsch, R.J., 1978b. Petrographic variations within thick turbidite sequences: an example from the late Paleozoic of eastern Australia.
Sedimentology, 25: 247-265.

Korsch, R.J., 1978c. Regional-scale thermal metamorphism overprinting low-grade regional metamorphism, Coffs Harbour Block, northern New South Wales.
J. Proc. R. Soc. N.S.W., 111: 89-96.

Korsch, R.J., 1981a. Some tectonic implications of sandstone petrofacies in the Coffs Harbour Association, New England Orogen, New South Wales.
J. Geol. Soc. Aust., 28: 261-269.

Korsch, R.J., 1981b. Deformational history of the Coffs Harbour Block.
J. Proc. R. Soc. NSW., 114: 17-22.

Korsch, R.J., 1984. Sandstone compositions from the New England Orogen, eastern Australia: Implications for tectonic setting. J. Sed. Pet. 54: 192-211.

Korsch, R.J. and Harrington, H.J., 1981. Stratigraphic and structural synthesis of the New England Orogen. J. Geol. Soc. Aust. 28: 205-226.

Korsch, R.W. and Wellman, H., (In Press). The geological evolution of New Zealand and the New Zealand region. In: A.E.M.Nairn, F.G.Stehli, S.Uyeda (Editors), The Ocean Basins and Margins, volume 7: the Pacific Ocean, Plenum Press, New York.

Kuno, H., 1950. Petrology of Hakone volcano and the adjacent areas Japan. Bull. Geol. Soc. Am., 61: 957-1019.

Kuno, H., 1960. High-alumina basalt. J. Pet., 1 (2): 121-145.

Kushiro, I., 1974. Melting of hydrous upper mantle and possible generation of andesitic magma: an approach from synthetic systems. Earth Planet. Sci. Lett., 22: 294-299.

Kushiro, I., 1979. Fractional crystallisation of basaltic magma. In: H.S.Yoder, Jr. (Editor), The evolution of igneous rocks. Princeton Univ. Press,: 171-203

Kushiro, I. and Nakamura, Y., 1970. Petrology of some lunar crystalline rocks. Proc. Apollo II Lunar Sci. Conf. 1: 607-626.

Lanphere, M.A., 1968. Geochronology of the Yavapai Series in central Arizona. Can. J. Earth Sci., 5: 757-762.

Laughlin, A.W., Brookins, D.G. and Garden, J.R., 1972. Variations in the initial strontium ratios of a single basalt flow.
Earth Planet. Sci. Lett., 14: 79-82.

Lindsley, D.H., 1983. Pyroxene thermometry.
Amer. Min., 68: 477-493.

Leitch, E.C., 1974. The geological development of the southern part of the New England Fold Belt.
J. Geol. Soc. Aust., 21: 133-156.

Leitch, E.C. and McDougall, I., 1979. The age of orogenesis in the Nambucca Slate Belt: A K-Ar study of low grade regional metamorphic rocks.
J. Geol. Soc. Aust., 26: 111-119.

Leitch, E.C., Neilson, M.J. and Hobson, E., 1971. 1:250000 geological sheet / SH56 10-11 Dorrigo-Coffs Harbour.
Geological Survey of N.S.W., Sydney.

Mann, A.C., 1983. Trace element geochemistry of high-alumin basalt - andesite - dacite - rhodacite lavas of the Main Volcanic Series of Santorini Volcano, Greece.
Contrib. Min. Pet., 84: 43-57.

MacKinnon, T.C., 1983. Origin of the Torlesse terrane and coeval rocks, South Island, New Zealand.
Bull. Geol. Soc. Amer., 94: 967-985.

Marsh, B.D., 1978. On the cooling of ascending andesitic magma.
Phil. Trans. Roy. Soc. Lond., A288: 611-625.

Marsh, B.D. and Carmichael, I.S.E, 1974. Benioff zone magmatism.

J. Geophys. Res., 79: 1196-1206.

Mathews, W.H., 1967. A contrbution to the geology of the Mount Tongariro Massif, North Island, New Zealand.
N.Z. J. Geol. Geophys. 10 (4): 1027-1038.

McBirney, A.R., 1980. Mixing and unmixing of magmas.
J. Volcan. Geophys. Res., 7: 357-371.

McCulloch, M.T. and Perfit, M.R., 1981. $^{143}Nd/^{144}Nd$, $^{87}Sr/^{86}Sr$ and trace element constraints on the petrogenesis of Aleutian island arc magmas.
Earth Planet. Sci. Lett., 56: 167-179.

McElroy, C.T., 1962. The geology of the Clarence-Moreton Basin. N.S.W.
N.S.W. Geol. Surv. Mem., 9.

McIntyre, G.A., Brooks, C., Compston, W. and Turek, A., 1966. The statistical assessment of Rb-Sr isochrons.
J. Geophys. Res., 71 (22): 5459-5468.

McKean, T.A.M., 1976. The petrology and K/Ar geochronology of the Wellington argillites-North Island, New Zealand.
Unpublished BSc (hons) thesis, Victoria University of Wellington.

McRae, N. and Nesbitt, H., 1980. Partial melting of common metasedimentary rocks: a mass balance approach.
Contrib. Min. Pet., 75: 21-26.

Miyashiro, A., 1957. Cordierite-indialite relations.
Amer. J. Sci., 255: 43-62.

Moorbath, S., 1969. Evidence for the age of deposition of the Torridonian sediments of northwest Scotland.
Scott. J. Geol., 5: 154-170.

Morris, J.D. and Hart, S.R., 1983. Isotopic and incompatible element constraints on the genesis of island arc volcanics from Cold Bay and Amak Island, Aleutians, and implications for mantle structure. Geochim. Cosmochim. Acta, 47: 2015-2030.

Mory, A.J.A., 1981. A review of Early Carboniferous stratigraphy in the Northern Tamworth Belt, New South Wales. Proc. Linn. Soc. N.S.W. 105: 213-236.

Moseman, M.A. and Pitzer, K.S., 1941. Thermodynamic properties of the crystalline forms of silica. J. Chem. Soc., 63: 2348-2356.

Myers, J.D., Sinha, A.K. and Marsh, B.D., 1984. Assimilation of crustal material by basaltic magma: strontium isotopic and trace element data from the Edgecumbe volcanic field, SE Alaska. J. Pet., 25 (1): 1-26.

Mysen, B.O. and Boettcher, A.L., 1975. Melting of hydrous mantle: II. Geochemistry of crystals and liquids formed by anatexis of mantle peridotite at high pressures and high temperature as a function of controlled activities of water, hydrogen and carbon dioxide. J. Pet., 16: 549-593.

Nairn, I.A., 1971. Studies of the Earthquake Flat Breccia Formation and other unwelded pyroclastic flow deposits of the Central Volcanic Region, New Zealand. Unpublished MSc thesis, Victoria University of Wellington.

Napp, J.B., 1983. Physical volcanology of Pukeonake scoria cone, Tongariro Volcanic Centre, central North Island, New Zealand. Unpublished BSc (hons) thesis, Victoria University of Wellington.

Nambu, M., Tanida, K. and Kitamura, T., 1971. Res. Inst. Min. Dress. Met.

Rept., 552, p.123 (quoted from M. Matsueda), 1973. Iron-wollastonite from the Sampo mine.
Min. J. Japan, 7: 180-201.

Nicholls, I.A., 1971. Calcareous inclusions in lavas and agglomerates of Santorini Volcano.
Contrib. Min. Pet., 30: 261-276.

Nicholls, I.A. and Harris, K.L., 1980. Experimental rare earth element partition coefficients for garnet, clinopyroxene and amphibole coexisting with andesitic and basaltic liquids.
Geochim. Cosmochim. Acta, 44: 287-308.

Nicholls, I.A. and Ringwood, A.E., 1973. Effect of water on olivine stability in tholeiites and the production of silica-saturated magmas in the island arc environment.
J. Geol., 81: 285-300.

Nohda, S., 1984. Classification of island arcs by Nd-Sr isotopic data.
Geochem. Jour., 18: 1-9.

Norrish, K. and Hutton, J.T., 1969. An accurate X-ray spectrographic method for the analysis of a wide range of geological samples.
Geochim. Cosmochim. Acta, 33: 431-453.

Norrish, K. and Chappell, B.W., 1977. X-ray fluorescence spectrometry.
In: J. Zussman (Editor), Physical Methods of Determinative Mineralogy (2nd.Ed.). Academic Press, London, New York, San Francisco: 201-272.

O'Nions, R.K., 1984. Isotopic abundances relevant to the identification of magma sources.
Phil. Trans. Roy. Soc. Lond., A310: 591-603.

Oxburgh, E.R. and McRae, T., 1984. Physical constraints on magma contamination in the continental crust: an example, the Adamello complex.
Phil. Trans. Roy. Soc. Lond., A310: 457-472.

Pankhurst, R.J. and O'Nions, R.K., 1973. Determination of Rb/Sr and $^{87}Sr/^{86}Sr$ ratios of some standard rocks; evaluation of X-ray fluorescence spectrometry in Rb-Sr geochemistry.
Chem. Geol., 12: 127-136.

Papanastassiou, D.A. and Wasserburg, G.J., 1969. Initial strontium isotopic abundances and the resolution of small time differences in the formation of planetary objects.
Earth Planet. Sci. Lett., 5: 361-376.

Papanastassiou, D.A. and Wasserburg, G.J., 1973. Rb-Sr ages and initial strontium in basalts from Appollo 15.
Earth Planet. Sci. Lett., 17: 324-337.

Papike, J.J., Cameron, K.L. and Baldwin, K., 1974. Amphiboles and pyroxenes: characterisation of other than quadrilateral components and estimates of ferric iron from microprobe data.
Geol. Soc. Amer. Abstr. Prog., 6: 1053-1054.

Patchett, P.J., 1980. Thermal effects of basalt on continental crust and crustal contamination of magmas.
Nature, 283: 559-561.

Pearce, J.A., 1982. Trace element characteristics of lavas from destructive plate boundaries.
In: R.S. Thorpe (Editor), Andesites. J.Wiley & Sons, Chichester, New York, Brisbane, Toronto, Singapore: 525-548.

Pearce, J.A., 1984. Role of the sub-continental lithosphere in magma

genesis at active continental margins.
In: C.J.Hawkesworth and M.J.Norry (Editors), Continental basalts and mantle xenoliths, Shiva, Cheshire: 230-249.

Pearce, J.A., Alabaster, T., Shelton, A.W. and Searle, M.P., 1981. The Oman ophiolite as a cretaceous arc-basin complex: evidence and implications.
Phil. Trans. Roy. Soc. Lond., A300: 299-317.

Perry, E.A. and Turekian, K.K., 1974. The effect of diagenesis on the redistibution of strontium isotopes in shales.
Geochim. Cosmochim. Acta, 38: 929-935.

Perfit, M.R., Gust, D.A., Bence, A.E., Arculus, R.J. and Taylor, S.R., 1980. Chemical characteristics of island-arc basalts: implications for mantle sources.
Chem. Geol., 30: 227-256.

Perfit, M.R., McCulloch, M.T. and Froude, D., (1981). Sr- and Nd isotopic variations in volcanic and plutonic rocks from the Aleutian islands and Taupo Volcanic Zone, New Zealand: Implications for island arc magma genesis.
Abstr. 1981 IAVCEI Symp. Arc Volc.: 292-293.

Platen, H.V., 1965. Experimental anatexis and genesis of migmatites.
In: W.S. Pitcher and G.W. Flinn (Editors), Controls of Metamorphism, Oliver and Boyd, Edinburgh, London: 203-216.

Plummer, J.W., 1980. Hal automation of Aldermaston Micromass 30
N.Z. Dep. Sci. Ind. Res. Pub. INS-M-57.

Powell, M. and Powell, R., 1977. Plagioclase - alkali feldspar geothermometry revisited.
Min. Mag., 41: 253-256.

Poldevaart, A. and Gilkey, A.K., 1954. On clouded plagioclase. Amer. Min., 39: 75-91.

Priem, H.N.A., Boelrijk, N.A.I.M., Hebeda, E.H., Schermerhorn, L.J.G., Verdurmen, E.A.Th. and Verschure, R.H., 1978. Sr isotopic homogenisation through whole-rock systems under low-greenschist facies metamorphism in carboniferous pyroclastics at Aljustrel (Southern Portugal).
Chem. Geol., 21: 307-314.

Rama Murthy, V. and Griffin, W.L., 1970. K/Rb fractionation by plagioclase feldspars.
Chem. Geol., 6: 265-271.

Read, H.H., 1935. The gabbros and associated xenolithic complexes of the Haddo House district, Aberdeenshire.
Quart. J. Geol. Soc. Lond., 91: 591-638.

Read, H.H., 1966. An orthonorite containing spinel xenoliths with late diaspore at Mill of Boddam, Insch, Aberdeenshire.
Proc. Geol. Ass., 77: 65-78.

Reed, J.J., 1957. Petrology of the Lower Mesozoic rocks of the Wellington region.
N.Z. Geol. Surv. Bull., n.s.57.

Reid, F.W., 1982. Geochemistry of Central North Island greywackes and genesis of silicic magmas.
Unpublished PhD thesis, Victoria University, Wellington, NZ. 329pp.

Rettallack, G., Gould, R.E. and Runnegar, B., 1977. Isotopic dating of a Middle Triassic megafossil flora from near Nymboida, northeastern New South Wales.

Proc. Linn. Soc. N.S.W., 101: 77-113.

Reyners, M., 1980. A microeathquake study of the plate boundary, North Island, New Zealand.
Geophys. J. Roy. Astr. Soc., 63: 1-22.

Rhodes, J.M. and Dungan, M.A., 1979. The evolution of ocean-floor basaltic magmas.
In: M.Talwani, C.G.Harrison and D.E.Hayes (Editors), Deep drilling results in the Atlantic Ocean: ocean crust, Amer. Geophys. Union, Washington D.C.: 262-272.

Ringwood, A.E., 1975. Composition and Petrology of the Earth's mantle. McCraw-Hill, New York: 618p.

Roberts, J. and Oversby, B.S., 1974. The lower Carboniferous Geology of the Rouchel District, New South Wales.
Aust. Bureau Min. Res. Geol. Geophys., Bull. 47.

Robie, R.A. and Waldbaum, D.R., 1968. Thermodynamic properties of minerals and related substances at 298.15 K (25.0 °C) and one atmosphere (1.1013 bars) pressure and at higher temperatures.
U.S. Geol. Surv. Bull. 1259.

Roddick, J.C. and Compston, W., 1977. Strontium isotopic equilibration: a solution to a paradox.
Earth Planet. Sci. Lett., 34: 238-246.

Roedder, P.L., Campbell, I.H. and Jamieson, H.E., 1979. A re-evaluation of the olivine-spinel geothermometer.
Contrib. Min. Pet., 68: 325-334.

Roeder, P.L. and Emslie, R.F., 1970. Olivine-liquid equilibrium.
Contrib. Min. Pet., 29: 275-289.

Roser, B.P., 1983. Comparative studies of copper and manganese mineralisation in the Torlesse, Waipapa and Haast Schist terranes, NZ. Unpublished PhD thesis, Victoria University, Wellington, NZ.

Ross, M. and Huebner, J.S., 1979. Temperature - composition relationships between naturally occurring augite, pigeonite and orthopyroxene at one bar pressure.
Amer. Min., 64: 1133-1155.

Rowe, G.H., 1980. Applied geology of Wellington rocks for aggregate and concrete.
Unpublished PhD thesis, Victoria University, Wellington, NZ.

Russell, R.D., 1977. A solution in closed form for the isotope dilution anlysis of strontium.
Chem. Geol. 20: 307-314.

Sarver, L.A., 1927. The determination of ferrous iron in silicates.
Amer. Chem. Soc. Jour., 49: 1472-1477.

Sato, H., 1975. Diffusion coronas around quartz xenocrysts in andesite and basalt from Tertiary Volcanic Region in northeastern Shikoku, Japan.
Contrib. Min. Pet., 50: 49-64.

Sato, H., 1977. Nickel content of basaltic magmas: indentification of primary magmas and a measure of the degree of olivine fractionation.
Lithos, 10: 113-120.

Schreyer, W. 1965. Zur stabilitat des ferrocordierits.
Contrib. Min. Pet., 11: 297-322.

Schreyer, W. and Schairer, J.F., 1961. Compositions and structural states of anhydrous Mg-cordierites: a re-investigation of the central part of

the system $MgO-Al_2O_3-SiO_2$.
J. Pet., 2 (3): 324-406.

Seck, H.A., 1971. Der einfluβ des drucks die zusammensetzung koexistierender alkalfeldspate und plagioclase im system $NaAlSi_3O_8$ - $KAlSi_3O_8$ - $CaAl_2Si_2O_8$ - H_2O
Contrib. Min. Pet., 31: 67-86.

Shaw, S.E. and Flood, R.H., 1977. Two "S-type" granite suites with low initial $^{87}Sr/^{86}Sr$ ratios from the New England Batholith, Australia.
Contrib. Min. Pet., 61: 163-173.

Shaw, S.E. and Flood, R.H., 1981. The New England Batholith, Eastern Australia: Geochemical variations in time and space.
J. Geophys. Res., 86: 10530-10544.

Sheppard, D.S., Adams, C.J., Bird, G.W., 1975. Age of metamorphism and uplift in the Alpine Schist belt, New Zealand.
Bull. Geol. Soc. Am., 86: 1147-1153.

Shido, F.A., Miyashiro, A. and Ewing, M., 1971. Crystallisation of abyssal tholeiites.
Contrib. Min. Pet., 31: 251-266.

Shipiro, L. and Brannock, W.W., 1962. Rapid analysis of silicates, carbonates and phosphate rocks.
Bull. U.S. Geol. Surv., 1144-A, 56p.

Slansky, Ervin, 1975. Natroalunite and alunite from White Island Volcano, Bay of Plenty, New Zealand.
N.Z. J. Geol. Geophys., 18 (2): 285-293.

Smith, J.V., 1974. Feldspar minerals. I. Crystal structure and physical properties.

Springer-Verlag, Heidelberg. 627p.

Smith, P. and Parsons, I., 1974. The alkali-feldspar solvus at 1 kilobar water-vapour pressure.
Min. Mag., 39: 747-767.

Sparks, R.S.J., Huppert, H.E. and Turner, J.S., 1984. The fluid dynamics of evolving magma chambers.
Phil. Trans. Roy. Soc. Lond., A310: 511-534.

Spear, F.S., 1981. An experimental study of hornblende stability and compositional variability in amphibolite.
Amer. J. Sci., 281: 697-734.

Spedding, N.B., 1981a. INS BASIC Interpreter - users manual.
N.Z. Dep. Sci. Ind. Res. Pub. INS-P-158.

Spedding, N.B., 1981b. INS HAL SYSTEM - users manual.
N.Z. Dep. Sci. Ind. Res. Pub. INS-P-159.

Speden, I.G., 1976. Fossil localities in the Torlesse rocks of the North Island, New Zealand.
J. Roy. Soc. N.Z., 6 (1): 73-91.

Speight, R., 1908. Geology of Tongariro National Park.
Dept. Lands. Rep., Parl. Pap., C-11: 7-13.

Spencer, K.J. and Lindsley, D.H., 1981. A solution model for coexisting iron-titanium oxides.
Amer. Min., 66: 1189-1201.

Sporli, K.B., 1978. Mesozoic tectonics, North Island, New Zealand.
Bull. Geol. Soc. Am., 89: 415-425.

Stanaway, K.J., Kobe, H.W. and Sekula, J., 1978. Manganese deposits and the associated rocks of Northland and Auckland, New Zealand. N.Z. J. Geol. Geophys., 21: 21-32.

Steiger, R.H. and Jager, E., 1977. Subcommission on geochronology: convention on the use of decay constants in geo- and cosmochronology. Earth Planet. Sci. Lett., 36: 359-362.

Steiner, A., 1953. Hydrothermal rock alteration at Warakei, New Zealand. Econ. Geol., 48: 1-13.

Steiner, A., 1958. Petrogenetic implications of the 1954 Ngauruhoe lava and its xenoliths. N.Z. J. Geol. Geophys. 1: 325-363.

Stern, C.R. and Wyllie, P.J., 1978. Phase compositions through crystallisation intervals in basalt-andesite-H_2O at 30 kb with implications for subduction zone magmas. Amer. Min., 63: 641-663.

Stevens, G.R., 1963. Jurassic belemnites in the Torlesse Group of the North Island. N.Z. J. Geol. Geophys., 6: 707-710.

Stille, P., 1981. The measurement of rubidium and strontium blanks in the geochronological laboratory. Chem. Geol., 32: 303-315.

Stilwell, F.L., 1959. Petrology of the Broken Hill lode and its bearing on ore genesis. Proc. Aust. Inst. Min. Metall., 190: 1084.

Stipp, J.J., 1968. The geochronology and petrogenesis of the Cenozoic volcanics of the North Island, New Zealand. Unpublished PhD thesis, ANU, Canberra, ACT, Australia.

Stormer, J.C. Jr., 1983. The effects of recalculation on estimates of temperature and oxygen fugacity from analyses of multicomponent iron-titanium oxides.
Amer. Min., 68: 586-594.

Studt, F.E. and Thompson, G.E.K., 1969. Geothermal heat flow in the North Island of New Zealand.
N.Z. J. Geol. Geophys., 12 (4): 673-683.

Suggate, R.P. (chief Editor), 1978. The Geology of New Zealand, Volume 1.
Government Printer, Wellington, 343p.

Sun, S., 1980. Lead isotopic study of young volcanic rocks from mid-ocean ridges, oceanic islands and island arcs.
Phil. Trans. Roy. Soc. Lond., A297: 409-445.

Tatsumi, Y and Ishizaka, K., 1981. Existence of andesitic primary magma: An example from southwest Japan.
Earth Planet. Sci. Lett., 53: 124-130.

Taylor, H.P. Jr., 1980. The effects of assimilation of country rocks by magmas on $^{18}O/^{16}O$ and $^{87}Sr/^{86}Sr$ systematics in igneous rocks.
Earth Planet. Sci. Lett., 47: 243-254.

Thirlwall., M.F., 1982. Systematic variation in chemistry and Nd-Sr isotopes across a Caledonian calc-alkaline volcanic arc: implications for source materials.
Earth Planet. Sci. Lett., 58: 27-50.

Thirlwall, M.F. and Graham, A.M., 1984. Evolution of high-Ca, high-Sr, C-series basalts from Grenada, lesser Antilles: the effects of intra-crustal contamination.
J. Geol. Soc. Lond., 141: 427-445.

Thompson, R.N., Morrison, M.A., Hendry, G.L. and Parry, S.J., 1984. An assessment of the relative roles of crust and mantle in magma genesis: an elemental approach.
Phil. Trans. Roy. Soc. Lond., A310: 549-590.

Thomson, J.A., 1926. Volcanoes of New Zealand - Tonga Volcanic Zone. A record of eruptions.
N.Z. J. Sci. Tech., 8: 354-371.

Thorpe, R.S., Francis, P.W. and O'Callaghan, L., 1984. Relative roles of source composition, fractional crystallisation and crustal contamination in the petrogenesis of Andean volcanic rocks.
Phil. Trans. Roy. Soc. Lond., A310: 675-692.

Tilley, C.E., 1946. Bustamite from Treburland manganese mine, Cornwall, and its paragenesis.
Min. Mag., 27: 236-241.

Tindle, A.G. and Pearce, J.A., 1983. Assimilation and partial melting of continental crust: evidence from the mineralogy and geochemistry of autoliths and xenoliths.
Lithos, 16: 185-202.

Topping, W.W., 1973. Tephrostratigraphy and chronology of Late Quaternary eruptives from the Tongariro Volcanic Centre, New Zealand.
N.Z. J. Geol. Geophys., 16 (3): 397-423.

Topping, W.W., 1974. Some aspects of Quaternary history of Tongariro Volcanic Centre.
Unpublished PhD thesis, Victoria University, Wellington, NZ.

Turner, F.J., 1946. Origin of piedmontite quartz-muscovite-schists of North-west Otago.

Trans. Roy. Soc. N.Z., 76: 246-249.

Voisey, A.H., 1934. A preliminary account of the geology of the middle North Coast district of New South Wales.
Proc. Linn. Soc. N.S.W., 54: 333-347.

Wass, S.Y. and Hollis, J.D., 1983. Crustal growth in south-eastern Australia - evidence from lower crustal eclogitic and granulitic xenoliths.
J. Met. Geol., 1: 25-45.

Watson, E.B., 1982. Basalt contamination by continental crust; some experiments and models.
Contrib. Min. Pet., 80: 73-87.

Watson, E.B. and Jurewicz, S.R., 1984. Behaviour of alkalies during diffusive interaction of granitic xenoliths with basaltic magma.
J. Geol., 92 (2): 121-131.

Wellman, H.W., 1952. The Permian-Jurassic stratified rocks of New Zealand
In: Symposium sur les series de Gondwana.
Proc. 19th Int. Geol. Congr.: 13-24

Wells, N., Childs, C.W. and Downes, C.J., 1977. Silica Springs, Tongariro National Park, New Zealand - analyses of the spring water and characterisation of the alumino-silicate deposit.
Geochim. Cosmochim. Acta., 41: 1497-1506.

Wells, P.R.A., 1977. Pyroxene thermometry in simple and complex systems.
Contrib. Min. Pet., 62: 129-139.

White, A.H., 1964. Geological Map of New England 1:100,000 Tamworth sheet No. 331, with marginal text.
Univ. New England.

Wilson, M. and Davidson, J.P., 1984. The relative roles of crust and upper mantle in the generation of oceanic island arc magmas. Phil. Trans. Roy. Soc. Lond., A310: 661-674.

Wones, D.R. and Eugster, H.P., 1964. Stability of biotite: experiment, theory and application. Amer. Min., 50: 1228-1272.

Wood, B.J., 1975. The influence of pressure, temperature and bulk composition on the appearance of garnet in ortho-gneisses - an example from South Harris, Scotland. Earth Planet. Sci. Lett., 26: 299-311.

Wood, B.J. and Banno, S., 1973. Garnet-orthopyroxene and orthopyroxene -clinopyroxene relationships in simple and complex systems. Contrib. Min. Pet., 42: 109-124.

Wood, C.P., 1971. Analysis of white powder found on Egmont summit collected by D.H.Rawson. Unpublished report held at the N.Z. Geol. Surv. (Lower Hutt).

Wood, D.A., 1979. A variably veined sub-oceanic upper mantle - genetic significance for mid-ocean ridge basalts from geochemical evidence. Geology, 7: 499-503.

Wood, D.A., 1980. THe application of a Th-Hf-Ta diagram to problems of tectonmagmatic classification and to establishing the nature of crustal contamination of basaltic lavas of the British Tertiary volcanic province. Earth Planet. Sci. Lett., 50: 11-30.

Wood, D.A, Joron, J.L., Marsh, N.G., Tarney, J. and Treuil, M., 1980. Major- and trace-element variations in basalts from the North

Philippine sea drilled during DSDP Leg 58: a comparative study of back-arc-basin basalts with lava series from Japan and mid-ocean ridges Init. Reports Deep Sea Drilling Project, 58: 873-894.

Wyllie, P.J., 1984. Constraints imposed by experimental petrology on possible and impossible magma sources and products. Phil. Trans. Roy. Soc. Lond., A310: 439-456.

Yoder, H.S. Jr., 1969. Calcalkalic andesites: experimental data bearing on the origin of their assumed characteristics. In: McBirney (Editor), Proc. Andesite Conf. Dep. Geol. Mineral Res. Oreg. Bull., 65: 43-64.

Yoder, H.S. Jr., 1973. Contemporaneous basaltic and rhyolitic magmas. Amer. Min., 58: 153-171.

Yoder, H.S. Jr. and Tilley, C.E., 1962. Origin of basaltic magmas: an experimental study of natural and synthetic rock systems. J. Pet., 3: 342-532.

York, D., 1966. Least-squares fitting of a straight line. Can. J. Phys., 44: 1079-1086.

York, D., 1967. The best isochron. Earth Planet. Sci. Lett., 2: 479-482.

York, D., 1969. Least-squares fitting of a straight line with correlated errors. Earth Planet. Sci. Lett., 5: 320-324.

Zen, E-an and Thompson, A.B., 1974. Low grade regional metamorphism : mineral equilibrium relations. Ann. Rev. Earth Planet. Sci., 2: 179-212.

$$T = -10202 / [\ln K - 7.65\, X_{Fe}^{opx} + 3.88\, (X_{Fe}^{opx})^2 - 4.6]$$

where $K = \dfrac{a^{cpx}_{Mg_2Si_2O_6}}{a^{opx}_{Mg_2Si_2O_6}}$; $X_{Fe}^{opx} = \left[\dfrac{Fe^{2+}}{Fe^{2+} + Mg^{2+}} \right]_{opx}$

and $a_{Mg_2Si_2O_6} = X^{M1}_{Mg} \cdot X^{M2}_{Mg}$

assuming Ca^{2+}, Na^{+}, Mn^{2+} occupy M2,

Al^{3+}, Cr^{3+}, Ti^{4+}, Fe^{3+} occupy M1

and Mg^{2+}, Fe^{2+} have a random distribution between the two sites. Eqn.2

$$T = 7341 / [\, 3.355 + 2.44\, X_{Fe}^{opx} - \ln K \,] \qquad \text{Eqn.3}$$

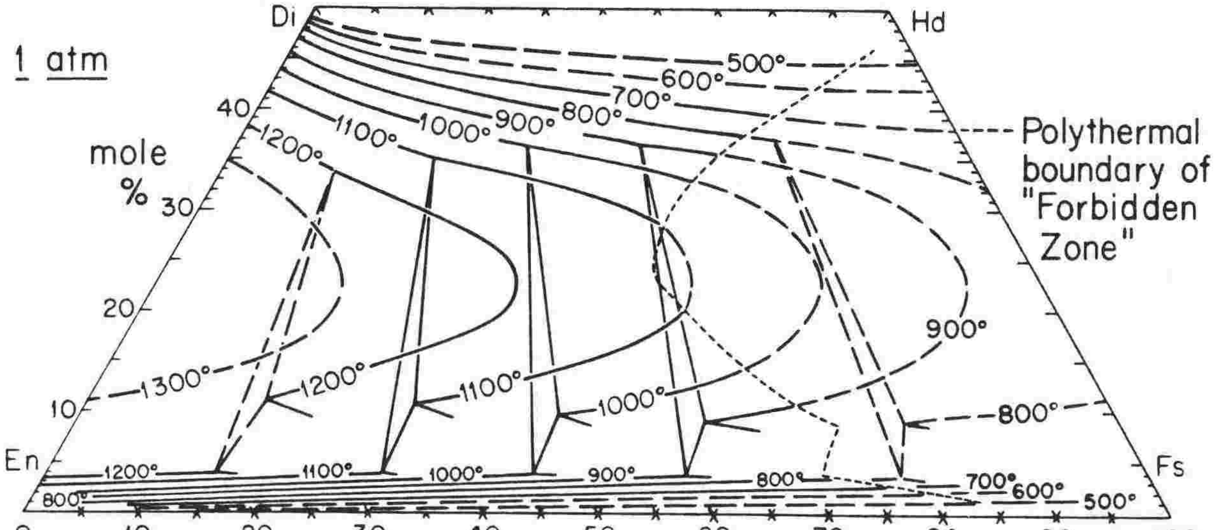

Fig.A1.1: Polythermal orthopyroxene - clinopyroxene - pigeonite relations contoured at 100 °C intervals for use in geothermometry. At various combinations of temperature and composition, the phase relations shown here may be metastable with respect to liquid, protopyroxene, ferrobustamite, olivine + silica, or combinations of these. Compositions of most natural pyroxene pairs must be projected according to the scheme outlined in the text before they are plotted.
Compositions in the "forbidden zone" are metastable with respect to augite + olivine + silica (after Lindsley, 1983).

****

APPENDIX 1: GEOTHERMOMETRY AND GEOBAROMETRY

****

Estimates of temperature and pressure based on mineral equilibria are meaningful only if there is accompanying petrographic evidence of equilibration i.e. smooth grain boundaries, lack of zoning in recrystallised minerals, lack of subsolidus exsolution and absence of retrograde alteration.

The following is a description of the chemographic requirements of various geothermometers and geobarometers which have been applied here (c.f. Chapter 4.3.4, Chapter 6).

A1.1 CLINOPYROXENE-ORTHOPYROXENE

Many attempts have been made to calibrate the temperature dependence of Mg-Fe partition between coexisting clino- and orthopyroxene:

$$MgSiO_3 \text{ (orthopyroxene)} = MgSiO_3 \text{ (clinopyroxene)} \qquad \text{Eqn.1}$$

Wood and Banno (1973) applied the diopside-enstatite miscibility gap data of Davis and Boyd (1966) to produce an empirical formula (Eqn.2) which assumes a random distribution of Fe^{2+} and Mg^{2+} between M1 and M2 sites. Calculation errors are in the order of 60 °C.

Wells (1977) revised the Wood and Banno geothermometer and produced a slightly different formula (Eqn.3). This gives satisfactory results over a temperature range of 785 °C to 1500 °C, for composition ranges of mole fraction Fe in opx = 0.0 to 1.0 and weight% Al_2O_3 in clinopyroxene = 0.0 to 10.0. Calculation errors are in the order of 70 °C.

Lindsley (1983) published graphical thermometers for coexisting clinopyroxene-orthopyroxene-(pigeonite) at different pressures, similar in

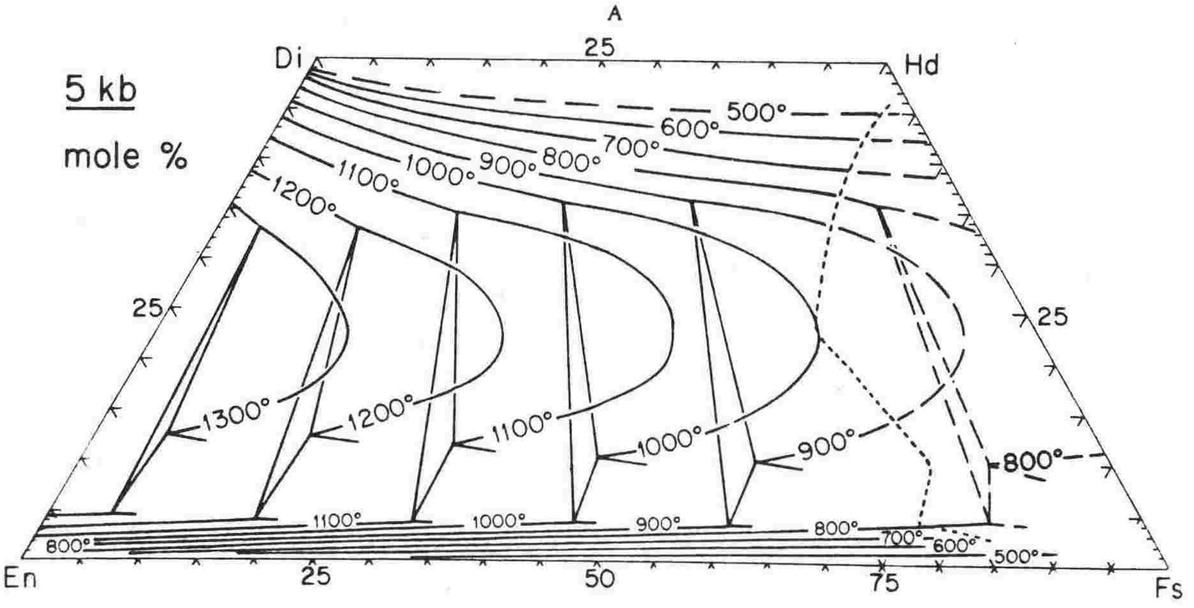

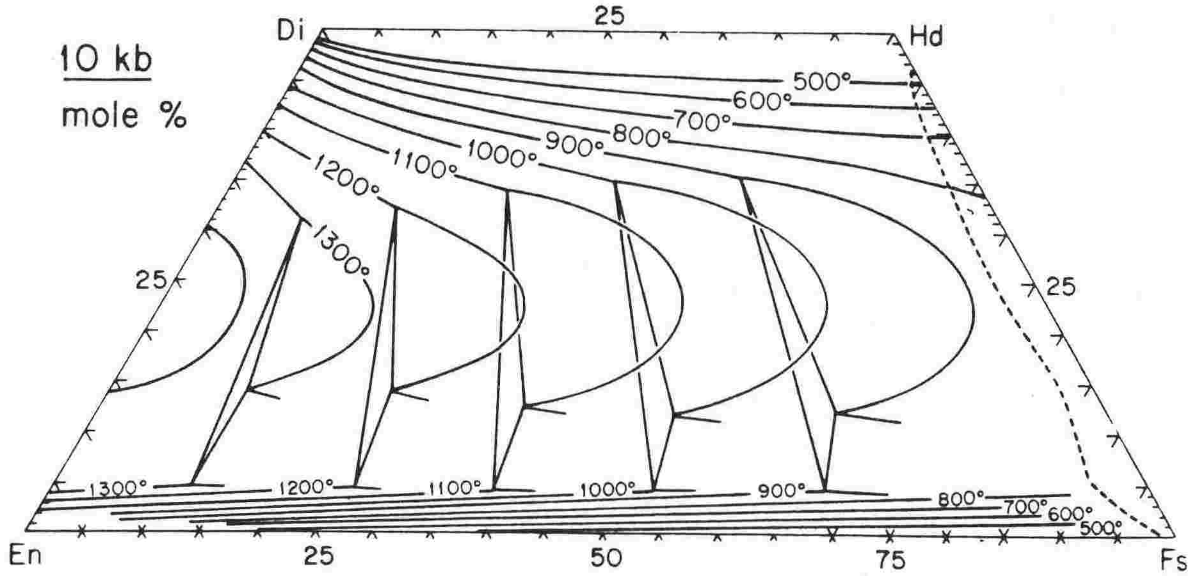

Fig.A1.1 (cont): Polythermal orthopyroxene - clinopyroxene - pigeonite relations at 5kb and 10kb.

form to those proposed by Ross and Huebner (1979). Lindsley critisised the use of both the Wood and Banno (1973) and the Wells (1977) geothermometers on the basis that their basic assumptions i.e. ideal mixing in clinopyroxene and large reaction enthalpy were seriously in in error (producing temperatures about 100 °C too high for metamorphic pyroxenes). Graphical solutions at 1, 5, 10 and 15 atm. for equilibration temperatures of coexisting pyroxenes (Fig.A1.1) are based on endmember components calculated as follows (after Lindsley, 1983):

<u>clinopyroxene</u>

- if ferric iron is known by measurement, both tetrahedral (1V) Al and octahedral (M1) Al may be inferred from charge balance considerations, through the relation (Papike et al., 1974):

$$Al(M1) + Fe^{3+}(M1) + Cr(M1) + 2\,Ti^{4+}(M1) = Al(IV) + Na(M2) \qquad (Eqn.4)$$

and from the requirement that Al(1V) + Al(M1) = Al(total). Where EPMA are used, Al(1V) = 2 - Si, remaining Al is assigned to the M1 site and ferric iron is calculated from charge balance (as in Eqn.4).

Pyroxene components can then be calculated in the sequence:

1. Ac = $NaFe^{3+}Si_2O_6$ = Na or Fe^{3+}, whichever is smaller
2. Jd = Al (M1) or remaining Na, whichever is smaller
3. TiCaTs = Ti
4. FeCaTs = remaining Fe^{3+}
5. AlCaTs = remaining Al(M1)

From this, Wo = (Ca + Ac - TiCaTs - FeCaTs - AlCaTs) / 2;

En = (1 - Wo) (1 - X)

Fs = (1 - Wo) (X)

where $X = Fe^{2+} / (Fe^{2+} + Mg)$.

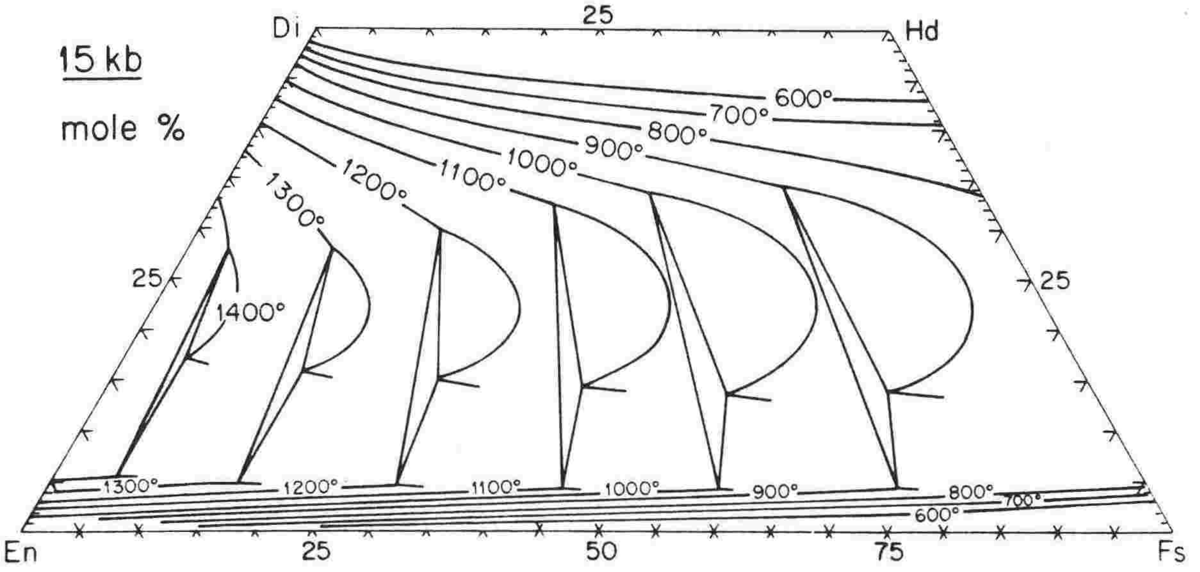

Fig.A1.1 (cont): Polythermal orthopyroxene - clinopyroxene - pigeonite relations at 15kb.

orthopyroxene

- Al(1V) = 2 - Si, Al(M1)

Al(M1) = Al(total) - Al(1V)

Fe^{3+} is estimated from Eqn.4.

$R^{3+} = [Al(M1) + Cr + Fe^{3+}]$

$R^{2+} = [Mg\ (1 - X) + Fe^{2+}\ (X)]$.

Pyroxene components can then be calculated in the sequence:

1. $NaR^{3+}Si_2O_6$ = Na or R^{3+}, whichever is smaller
2. $NaTiAlSiO_6$ = Ti or Al(1V) or remaining Na, whichever is smaller
3. $R^{2+}TiAl_2O_6$ = remaining Ti or [Al(1V)]/2, whichever is smaller
4. $R^{2+}R^{3+}AlSiO_6$ = remaining R^{3+} or [Al(1V)]/2

   (note that in a perfect analysis these should be equal).
5. Ca, and remaining Fe^{2+} and Mg are normalised to give

   Wo + En + Fs = 1.

The resulting compositions (i.e. ortthopyroxene and clinopyroxene) can be plotted on Fig.A1.1 to give the equilibration temperature.

The above scheme is only an approximation and ordering of Fe and Mg between M1 and M2 sites of pyroxenes may introduce additional complexities, especially at metamorphic temperatures. Recent data indicates that apparent temperatures yielded by the thermometer increase with increasing alumina content, suggesting that the removal of the Tschermak's components (steps 3 to 5) from the effective Wo content of clinopyroxene is an overcorrection resulting from an underestimation of the activity of Wo. Restriction of the thermometer to pyroxenes containing more than 90% Wo + En + Fs is therefore recommended (Lindsley, 1983).

$$X'_{Usp} = \frac{(n_{Ti,F})(x_{Fe^{2+},S2+})}{(0.5\ n_{Fe^{3+},F})(X_{Fe^{3+},S3+}) + (n_{Ti,F})(x_{Fe^{2+},S2+})}$$

(Eqn.5)

$$X'_{Ilm} = \frac{\sqrt{(n_{Fe^{2+},F})(n_{Ti,F})}}{(0.5\ n_{Fe^{3+},F}) + \sqrt{(n_{Fe^{2+},F})(n_{Ti,F})}}$$

(Eqn.6)

$$T(^{\circ}K) = \frac{(-A1 \cdot W_H^{Usp} - A2 \cdot W_H^{Mt} + A3 \cdot W_H^{Ilm} + A4 \cdot W_H^{Hem} + \Delta H^{\circ}_{exch})}{(-A1 \cdot W_S^{Usp} - A2 \cdot W_S^{Mt} + A3 \cdot W_S^{Ilm} + A4 \cdot W_S^{Hem} + \Delta S^{\circ}_{exch} - R \cdot \ln K^{exch})}$$

where $\Delta H^{\circ}_{exch} = 27799$ Joules/mole

$\Delta S^{\circ}_{exch} = 4.1920$ Joules/mole-degree

$A1 = -3X_{Usp}^2 + 4X_{Usp} - 1$

$A2 = 3X_{Usp}^2 - 2X_{Usp}$

$A3 = -3X_{Ilm}^2 + 4X_{Ilm} - 1$

$A4 = 3X_{Ilm}^2 - 2X_{Ilm}$

$K^{exch} = (X_{Usp} \cdot X_{Hem}^2)/(X_{Mt} \cdot X_{Ilm}^2)$

(Eqn.7)

$$\log_{10} f_{O_2} = MH + (12\ln(1 - X_{ilm}) - 4\ln(1 - X_{Usp}) + (1/RT)(8X_{Usp}^2(X_{Usp} - 1) \cdot W_G^{Usp} + 4X_{Usp}^2(1 - 2X_{Usp}) \cdot W_G^{Mt} + 12X_{Ilm}^2(1 - X_{Ilm}) \cdot W_G^{Ilm} - 6X_{Ilm}^2(1 - 2X_{Ilm}) \cdot W_G^{Hem}))/2.303$$

(Eqn.8)

A1.2 MAGNETITE-ILMENITE

The iron-titanium oxide geothermometer of Buddington and Lindsley (1964), recently re-formulated by Spencer and Lindsley (1981), shows that the temperature and oxygen fugacity of equilibrium between coexisting magnetite-ulvospinel (spinel phase) and ilmenite-hematite (rhombohedral phase) can be obtained from the compositions of the two phases. For this, a recalculation scheme is needed which best represents all elemental components, and many have been suggested (e.g. Buddington and Lindsley (1964), Carmichael (1967), Anderson (1968), Spencer and Lindsley (1981). Stormer (1983) proposed a new scheme based on models of ionic substitution which is consistent with thermodynamic models of the pure Fe-Ti system (Spencer and Lindsley, 1981) and provides a better basis for consideration of the effects of minor components. The recalculation procedure has the effect of normalising the cations to a stochiometric formula and of balancing the number of cation charges by varying the Fe^{2+}/Fe^{3+} ratio. A flow sheet of this procedure is as follows:

1. Calculate the molar proportions of all cations in the analyses for both the rhombohedral and spinel phases.
2. Normalise the cations in the spinel phase to a formula unit of three sites, and the cations in the rhombohedral phase to two sites.
3. Calculate the sum of the cationic charges per formula unit and subtract 8 for the spinel phase and 6 for the rhombohedral phase (the resulting numbers are the cation charge deficiency or excess).
4. Convert Fe^{2+} to Fe^{3+} to eliminate the charge, or the reverse to eliminate the excess (if it is not possible to balance the charges, the analysis cannot represent a stochiometric oxide phase).
5. The number of moles of each cation per formula unit is now known for both phases. For the spinel phase only, calculate the mole fraction of Fe^{2+} relative to the sum of all divalent cations, and the mole fraction of Fe^{3+} relative to all trivalent cations.

$$\Delta G^{o}_{P,T} = \Delta H - T\Delta S + (P-1)\ \Delta V = -RT\ln K \qquad \text{Eqn.10}$$

where G is standard Gibbs free energy

$$K = \frac{\alpha^{Cpx}_{CaTs} \cdot \alpha^{Qz}_{SiO_2}}{\alpha^{Pl}_{An}} = \frac{\alpha^{Cpx}_{Cats}}{\alpha^{Pl}_{An}} \qquad \text{Eqn.11}$$

$$-RT\ln K = 5359.8 + 2.9876T(K) - .349\ P\ (bars) \qquad \text{Eqn.12}$$

$$Kd = \left(\frac{X_{Mg}}{X_{Fe^{2+}}}\right)_{olivine} \left(\frac{X_{Fe^{2+}}}{X_{Mg}}\right)_{spinel} \qquad \text{Eqn.13}$$

$$t(K) = \frac{\alpha 3480 + \beta 1018 - \gamma 1720 + 2400}{\alpha 2.23 + \beta 2.56 - \gamma 3.08 - 1.47 + 1.987\ \ln K_D}$$

where $\alpha = \frac{Cr}{Cr+Al+Fe^{3+}}$ $\beta = \frac{Al}{Cr+Al+Fe^{3+}}$

$$\gamma = \frac{Fe^{3+}}{Cr+Al+Fe^{3+}} \qquad \text{Eqn.14}$$

6. Calculate X'(usp) using Eqn.5 and X'(ilm) using Eqn.6.

7. Determine T using Eqn.7 and oxygen fugacity using Eqn.8.

Minor components in Fe-Ti oxides can have a significant effect on calculated temperatures and oxygen fugacities. Inclusion of them in geothermometric calculations therefore can produce substantial differences from other methods.

A1.3 PLAGIOCLASE-CLINOPYROXENE-QUARTZ

The assemblage plagioclase-clinopyroxene-quartz, provides a useful geobarometer for crustal mafic granulites (Ellis, 1980), because of the large δV and small δS of the reaction

Anorthite = Ca Tschermaks Molecule + Quartz Eqn.9

$CaAl_2Si_2O_8$ $CaAl_2SiO_6$ SiO_2

The chemical equilibria for the above reaction in the $CaO-Al_2O_3-SiO_2$ system (Eqn.10) is simplified if the activity of SiO_2 in quartz is assumed to be unity (Eqn.11). The data of Robie and Waldbaum (1968) is used to estimate G^o , the standard Gibbs free energy of the reaction at temperature T (K) and 1 bar pressure, and the molar volume data is then used to derive the general formula (Eqn.12). This formula is applicable to clinopyroxenes with less than 0.35 Ca-Tschermak's component and adequately reproduces to within 1kb experimental data in the temperature range 700 °C to 1000 °C.

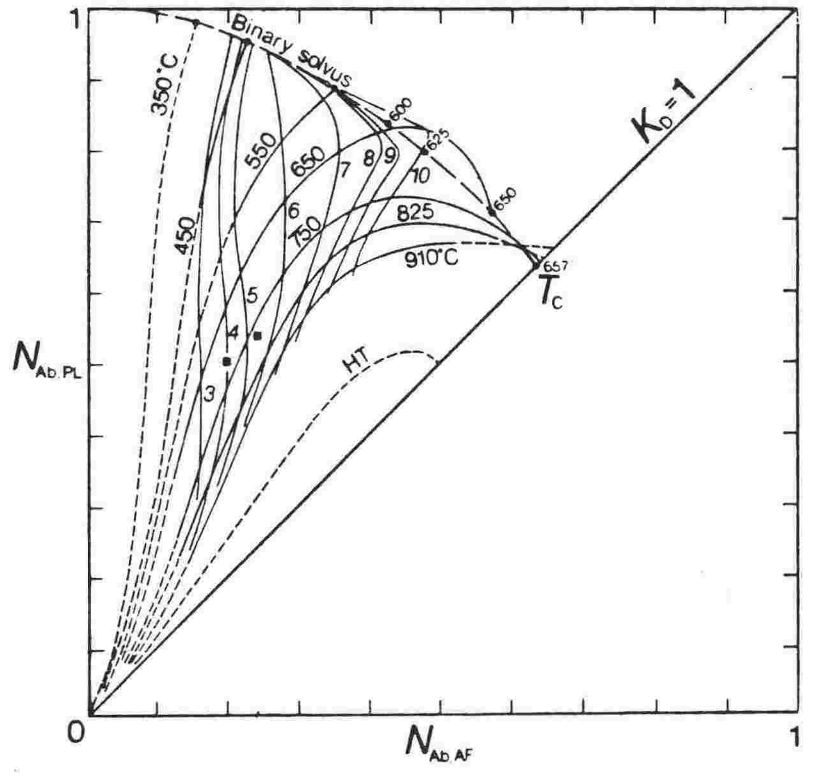

Fig.A1.2: Diagram illustrating the correct "form" of the two feldspar geothermometer based on the Seck (1971) (adjusted to 1kb) and the binary solvus data of Smith and Parsons (1974) (at 1kb). Isotherms for T > Tc (the critical temperature for An-free solid solutions) must terminate at the line for Kd=1. The composition at which they terminate depends on the curvature of the consolute line in the ternary system (it curves initially towards albite with increasing temperature but at very high pressures (in the absence of water) an isotherm such as HT is possible. At T < Tc isotherms immediately below Tc (e.g.650 °C) may cross the projected binary solvus curve before terminating. The thin numbered lines intersecting the isotherms are contoured in $N_{Or,PL}$. A feldspar pair is in equilibrium if, and only if, all the components are appropriately distributed between the two phases (after Brown and Parsons, 1981).

A1.4 OLIVINE-SPINEL

Olivine and spinel often coexist in primitive lavas and ultramafic rocks and the equilibrium distribution of Fe^{2+} and Mg between them (Eqn.13) provides a useful geothermometer. The formula derived by Jackson (1969) gives satisfactory results when applied to plutonic rocks but, as demonstrated by Evans and Wright (1972), gives temperatures in excess of 2000 °C when applied to volcanic assemblages. However, a re-evaluation by Roeder et al. (1979) shows that more realistic temperatures can be obtained for volcanic rocks by using a different free energy value for $FeCr_2O_4$ in the formulation (Eqn.14).

A1.5 TWO FELDSPARS

Many igneous and metamorphic rocks contain coexisting alkali and plagioclase feldspars whose compositions depend only on pressure and temperature, providing stable equilibrium between them is attained. Barth (1962) proposed a sem-impirical two-feldspar geothermometer based on the distribution of $NaAlSi_3O_8$. More recently, Powell and Powell (1977) attempted to improve on Bath's formulation using a temperature calibration based on experimental determinations of feldspar solvus relations and exchange reactions and on thermodynamic reasoning. Using the experimental data of Seck (1971) and Smith and Parsons (1974), Brown and Parsons (1981) constructed the general form of the thermometer at 1kb pressure (Fig.A1.2) (it may be applied at higher pressures by adding 18 °C per kb to the temperature obtained). However, this geothermometer is applicable only if the feldspar pairs are in equilibrium, as indicated by the following chemographic tests:

1. The alkali feldspar must lie on or outside the binary Ab-Or solvus when projected from An at the pressure of interest irrespective of the An content of the phases.
2. The alkali feldspar must lie on the K-rich side of the ternary

$$\ln K = -2109/T + .782 \quad \text{at } 2.07 \text{ kb}$$

where $K = (Mg/Fe)_{garnet}/(Mg/Fe)_{biotite}$

$$12454 = 4.662T - .057P - 3RT\ln K$$ Eqn.15

$$RT\ln K_D = 1391 + 1509\,(X_{Fe} - X_{Mg})^{GNT} + 2810\,(X_{Ca}^{GNT}) + 2855\,(X_{Mn}^{GNT})$$

where $K_D = (X_{Fe}/X_{Mg})^{GNT}/(X_{Fe}/X_{Mg})^{opx}$

X = mole fraction.

Eqn.16

critical point and ternary alkali feldspar compositions must project from An onto the Or-rich side of the binary solvus critical composition at Ab_{63} (Smith and Parsons, 1974).

3. Both feldspars must lie on the ternary feldspar solvus (Seck, 1971, Fig.5) when T is calculated for P=1kb.
4. Feldspar pairs lying on the ternary solvus are not necessarily in equilibrium, and to be so, must lie on the appropriate tie-line.

Petrographic evidence for equilibration must also be considered. In regional metamorphic rocks, because of the peristerite gap in sodic plagioclases, a two-feldspar geothermometer is only applicable to middle amphibolite and granulite facies rocks. While it is probable that sufficient time is available for Al/Si disorder to be approached in plagioclase this is not necessarily so in alkali feldspar.

The temperature range for which the two-feldspar geothermometer applies at low pressures is about 600 °C in metamorphic rocks to 1000 °C in alkali basalts; these temperatures are higher at higher pressures. Calculation errors are in the order of 50 °C (Brown and Parsons, 1981).

A1.6 BIOTITE-GARNET

Using experimentally-determined data on the partitioning of Fe and Mg between synthetic garnet $(Fe,Mg)_3Al_2Si_3O_{12}$ and synthetic biotite $K(Fe,Mg)_3AlSi_3O_{10}(OH)_2$, Ferry and Spear (1978) derived an equilibrium temperature at 2.07kb (Eqn.15). Their experiments indicate that Fe and Mg mix ideally in biotite and garnet solid solution at least in the composition interval 0.80 <= Fe/(Fe+Mg) <= 1.00, and that K is a function of Ca and Mn content of the garnet and the Ti and Al(V1) content of the biotite.

$$T(^\circ C)=\left\{\frac{3{,}740+1{,}400\,X_{gr}^{ga}+22.86\,P\,(\mathrm{kb})}{R\ln K_D+1.96}\right\}-273$$

with

$$K_D=\left\{\frac{\mathrm{Fe}}{\mathrm{Mg}}\right\}^{ga}\Big/\left\{\frac{\mathrm{Fe}}{\mathrm{Mg}}\right\}^{opx}$$

and

$$X_{gr}^{ga}=(\mathrm{Ca}/\mathrm{Ca}+\mathrm{Mg}+\mathrm{Fe})^{ga}.$$

Eqn.17

$$P\,(\mathrm{kb})=\frac{1}{206\cdot74}\left\{\begin{array}{l} RT\ln K_2+T[0\cdot15+0\cdot001507(T-970)]-2467 \\ -[2458(1000/T)-1261](2(X_{Fe}^{opx})^2) \\ -[3525(1000/T)-1667][1-2X_{Mg}^{opx}(1-X_{Al}^{M1}](1-X_{Mg}^{opx})(1-X_{Al}^{M1}) \\ -[4\cdot75T-6680][2(1-X_{Mg}^{opx})(1-X_{Al}^{M1})] \\ +920[(1-2X_{Al}^{M1})(1-X_{Al}^{M1})(1-X_{Mg}^{opx})] \\ +[5436-2\cdot45T][(1-X_{Mg}^{opx})[X_{Mg}^{opx}(1-X_{Al}^{M1})+X_{Al}^{M1}]] \\ +5700[X_{gr}^{ga}(X_{gr}^{ga}+X_{alm}^{ga})] \end{array}\right\}$$

where

$K_2 = (X_{py}^{ga})^3/(X_{Mg}^{opx})^3X_{Al}^{M1}(1-X_{Al}^{M1})$

X_{Mg}^{opx} = Mg/(Mg + Fe) in orthopyroxene,

X_{gr}^{ga} = Ca/(Ca + Mg + Fe) in garnet,

X_{py}^{ga} = Mg/(Ca + Mg + Fe) in garnet,

X_{Al}^{M1} = Al/2 in 6-oxygen unit orthopyroxene.

X_{Fe}^{opx} = Fe(/Mg + Fe) in orthopyroxene,

X_{alm}^{ga} = Fe/(Ca + Mg + Fe) in garnet.

Eqn.18

A1.7 GARNET-ORTHOPYROXENE

The temperature dependence of Fe^{2+} -Mg distribution between garnet and pyroxene was investigated by Dahl (1980) for metamorphic mineral pairs from the Ruby Range, SW Montana, USA. Using EPMA analyses and multiple linear regression techniques, Dahl calculated a formula which may be used as a relative but not absolute geothermometer (Eqn.16).

The pressure-temperature-compositional (P-T-X) dependence on the solubility of Al_2O_3 in orthopyroxene coexisting with garnet was experimentally determined in the P-T range 5-30kb and 800-1200 °C, in both FeO-MgO-Al_2O_3-SiO_2 and CaO-FeO-MgO-Al_2O_3-SiO_2 systems by Harley (1984a). The effects of Ca on Fe-Mg partitioning was attributed to non-ideal Ca-Mg interactions in the garnet. Reduction of the experimental data, combined with molar volume data from the endmember phases, yielded a formula (Eqn.17) applicable particularly to garnet peridotites and granulites. The accuracy and precision of the geothermometer are limited by the large relative errors of the experimental and natural-rock data and by the modest absolute variation in Kd with temperature.

Harley (1984b, 1984c) derived a garnet-orthopyroxene geobarometer applicable to the above systems for crustal granulites which also contain alumino-silicates (Eqn.18). The geobarometer is sensitive to relatively small changes in garnet composition but is independent of variations in the alumina content of coexisting orthopyroxene.

****

APPENDIX 2: LITHOLOGICAL DESCRIPTIONS & BULK CHEMICAL ANALYSES

****

Included here are brief lithological descriptions and bulk-rock chemical analyses of all samples referred to in the thesis.

Analytical methods are described and discussed in Chapter 2.

Samples are ordered according to rock type.

VUW = Catalogue number of Geology Dept., Victoria University.

CR = Cross reference - R (number) = Catalogue number, INS.

- P (number) = Catalogue number, NZGS.

LOC = Locality - N (grid reference) = NZMS 1 (thousand yard).

- S (grid reference) = NZMS 270 (metric).

FIELD = Field number; EPMA indicates that microprobe analyses are available (Appendix 3).

Major elements are normalised to 99.75 weight% oxides in order to facilitate cross-check comparisons (99.75% rather than 100% to allow for trace element content).

FeO was determined using the titrimetric dichromate method of Sarver (1927), as described in Shapiro and Brannock (1962).

LOI is loss on ignition at 1000°C.

Total* refers to original oxide total prior to normalisation.

I is measured $^{87}Sr/^{86}Sr$ ratio.

"." = not analysed; <2 = below detection limit (trace elements).

A2.1: SEDIMENTARY BASEMENT

GENERAL:

Drill-core and tunnel sample localities are plotted on Fig.3.1. Bracketted numbers are depths of origin for drill-core samples (m). Point counts for some greywacke samples are included (courtesy Dr.P.J. Barrett) e.g. "99.8% < .1mm; 500 counts" indicates 99.8% grains less than .1mm diameter and total grains counted = 500).
All iron is given as Fe_2O_3.

RANGIPO TORLESSE SUITE:

All samples contain detrital quartz, feldspar (80% to 90% plagioclase), lithic clasts of sedimentary, igneous and metamorphic origin, and minor amounts of magnetite, sphene, zircon, ilmenite and mica. Secondary minerals include muscovite, chlorite, prehnite, epidote and pumpellyite. Modal compositions are given in Table 3.2.

RANGIPO WAIPAPA SUITE:

Greywackes are made up of detrital feldspar, quartz and volcanic lithics with minor pyroxene, hornblende, epidote, sphene, zircon, magnetite and ilmenite. Secondary mineralogy includes muscovite, chlorite, prehnite and calcite.

RANGIPO TERTIARY SUITE:

Micaceous siltstones contain varying amounts of quartz, muscovite, biotite, feldspar and rare lithic material.

VUW	17515	17504	17505	17831	17820	17823	17518	17501	17507
FIELD	DM3-C	R7045A	R7045B	AM1-1	R7044	R7067B	R3-130	R7041B	R7062
SiO_2	56.32	64.54	61.73	66.68	58.74	63.09	59.00	55.82	58.81
TiO_2	0.90	0.65	0.71	0.65	0.80	0.70	0.83	0.92	0.82
Al_2O_3	21.43	16.98	17.50	16.45	19.70	16.82	18.68	21.09	18.22
Fe_2O_3T	5.76	4.60	6.48	5.02	5.64	5.66	6.85	5.70	7.47
MnO	0.06	0.11	0.15	0.06	0.11	0.16	0.07	0.08	0.08
MgO	1.91	1.68	2.04	1.23	1.97	2.00	1.84	2.08	2.19
CaO	0.20	1.44	1.14	0.12	1.60	2.06	1.66	1.95	1.73
Na_2O	0.89	0.83	1.68	2.06	2.83	1.85	2.29	2.16	1.74
K_2O	7.43	5.29	4.65	3.58	4.72	3.82	4.13	5.75	4.16
P_2O_5	0.08	0.11	0.13	0.01	0.17	0.14	0.16	0.19	0.17
LOI	4.78	3.53	3.53	3.89	3.47	3.44	4.24	4.03	4.37
Total*	99.90	99.96	99.47	99.27	99.11	99.07	99.41	99.48	99.80
Ba	1431	967	839	528	936	994	759	982	665
Ce	40	87	65	21	81	68	59	81	66
Cr	65	43	49	42	56	52	58	63	62
Cu	15	48	47	27	58	64	17	26	28
Ga	28	24	21	22	24	24	24	27	25
La	15	36	23	7	40	31	27	38	28
Mn	529	903	1303	389	770	1079	484	649	676
Nb	14	11	14	11	14	13	15	17	13
Ni	7	29	29	14	23	35	17	23	24
Pb	29	12	27	22	25	20	17	27	28
Rb	298	249	216	161	221	164	174	248	173
Sc	17	18	14	10	15	15	16	15	16
Sr	98	173	114	88	222	166	190	307	175
Th	20	18	19	14	22	18	21	24	19
Ti	5673	3859	4272	3945	4797	4141	4923	5570	5005
U	3.7	3.5	3.1	3.0	4.1	3.0	3.7	5.4	3.7
V	148	99	128	92	136	109	136	139	143
Y	20	32	29	14	35	31	33	39	31
Zn	54	108	133	124	106	102	95	100	115
Zr	197	135	132	173	158	148	203	147	152
K/Na	8.36	6.39	2.76	1.74	1.67	2.06	1.81	2.67	2.39
K/Rb	207	176	179	184	177	193	197	192	200
Rb/Sr	3.04	1.44	1.90	1.83	0.99	0.99	0.92	0.81	0.99
I	.72455	.71525	.71773	.71743	.71265	.71260	.71289	.71231	.71325

RANGIPO TORLESSE SUITE ARGILLITES

VUW 17515 LOC: Drill-Core DM3-119 (29.6m) T20 / 473 962
N122 / 240 505

Green-grey, poorly indurated argillite. 20% quartz veins (not included), minor surface alteration.

VUW 17504 CR: R7045 LOC: Moawhango Tunnel T20 / 498 056
N122 / 265 608

Green, foliated argillite (99.8% <.01mm; 500 counts).

VUW 17505 CR: R7045 LOC: Moawhango Tunnel T20 / 498 056
N122 / 265 608

Grey, foliated argillite (97.6% <.01mm; 500 counts). From same sample as 17504.

VUW 17831 LOC: Drill-Core AM1-1 (10.7m) T20 / 501 992
N122 / 270 538

Green-grey, poorly indurated argillite. Prominent cleavage.

VUW 17820 CR: R7044 LOC: Moawhango Tunnel T20 / 496 049
N122 / 263 600

Grey/green argillitic breccia. Quartz + calcite + prehnite veins; chlorite on shear plane.

VUW 17823 CR: R7067 LOC: Moawhango Tunnel T20 / 500 069
N122 / 267 622

Grey/green argillitic breccia. Similar to 17820, 17504 & 17505.

VUW 17518 LOC: Drill-Core R3 (39.6) T20 / 501 158
N112 / 265 720

Finely interlaminated fine-sand greywacke/grey argillite/green argillite. Prominent cleavage.

VUW 17501 CR: R7042 LOC: Moawhango Tunnel T20 / 494 039
N122 / 261 589

Finely laminated, argillite.

VUW 17507 CR: R7062 LOC: Moawhango Tunnel T20 / 515 154
N112 / 280 716

Dark grey, sheared argillite. 25% quartz + calcite veins parallel to foliation (not included).

VUW	17519	17506	17508	17510	17827	17503	17509	17514	17513	17511
FIELD	R206A	R7046	R7063	R7068	R209B	R7043	R7066	M2286	MS117	DM3A
SiO_2	63.18	62.38	60.99	69.18	61.67	55.93	63.48	64.73	66.62	65.47
TiO_2	0.72	0.68	0.67	0.48	0.68	0.90	0.68	0.65	0.64	0.61
Al_2O_3	17.37	17.19	19.34	14.78	18.24	20.72	17.22	16.60	15.93	16.26
Fe_2O_3T	5.84	6.47	4.99	4.03	4.73	6.22	5.08	5.28	5.34	4.76
MnO	0.06	0.18	0.05	0.05	0.06	0.08	0.07	0.06	0.07	0.08
MgO	1.72	2.05	1.76	1.49	1.72	2.13	1.76	1.54	1.54	1.43
CaO	1.26	1.41	1.04	1.07	1.65	1.62	1.45	1.10	0.88	1.26
Na_2O	2.75	1.60	3.08	2.31	2.53	2.62	3.19	3.32	2.80	3.02
K_2O	3.52	4.05	4.22	3.62	4.78	5.12	3.40	3.25	2.99	3.27
P_2O_5	0.19	0.20	0.14	0.13	0.14	0.30	0.18	0.16	0.12	0.16
LOI	3.13	3.53	3.48	2.60	3.56	4.11	3.24	3.06	2.81	3.43
Total*	99.37	99.62	99.72	99.41	99.35	99.87	99.43	98.87	99.32	99.72
Ba	556	919	721	555	767	997	688	572	382	665
Ce	62	69	77	55	57	77	58	59	45	57
Cr	53	48	43	29	46	67	43	45	42	40
Cu	22	73	17	12	22	26	23	18	13	15
Ga	23	23	23	18	23	27	21	22	18	18
La	26	28	37	27	26	34	29	26	17	22
Mn	546	1410	412	369	465	719	612	509	479	695
Nb	12	12	14	9	13	14	11	12	10	12
Ni	15	24	15	13	18	27	18	15	15	17
Pb	32	26	36	22	28	27	36	29	22	31
Rb	155	188	180	154	202	214	147	142	117	136
Sc	14	14	13	9	11	15	12	11	9	11
Sr	170	158	161	166	188	236	235	179	128	187
Th	19	21	23	14	17	21	17	18	14	16
Ti	4278	4173	3912	2703	4030	5531	3966	3862	3472	3663
U	2.5	4.5	5.8	3.6	3.5	4.2	3.7	4.7	2.5	4.2
V	120	111	91	62	100	173	104	101	100	94
Y	34	29	37	25	32	35	28	29	22	26
Zn	106	119	102	75	76	140	104	91	84	87
Zr	192	125	236	163	222	195	183	190	180	215
K/Na	1.28	2.52	1.37	1.57	1.89	1.96	1.07	0.98	1.07	1.08
K/Rb	189	179	195	195	197	199	192	190	213	200
Rb/Sr	0.91	1.19	1.11	0.93	1.07	0.90	0.62	0.79	0.91	0.73
I	.71287	.71415	.71425	.71246	.71332	.71281	.71095	.71220	.71350	.71153

RANGIPO TORLESSE SUITE INTERMEDIATES

VUW 17519 LOC: Drill-Core R206 (182.6m) T20 / 501 158
N112 / 265 720

Grey, foliated silty-argillite (82% <.01mm, 10% <.03mm, 4% <.065mm, 4% <.13mm 50 counts).

VUW 17506 CR: R7046 LOC: Moawhango Tunnel T20 / 502 058
N122 / 269 610

Grey, sheared silty-argillite (98.6% <.01mm; 500 counts). 5% quartz + calcite veins.

VUW 17508 CR: R7063 LOC: Moawhango Tunnel T20 / 515 140
N122 / 281 700

Grey, sheared silty-argillite.
Similar to 17506.

VUW 17510 CR: R7068 LOC: Rangipo Tunnel T19 / 536 293
N112 / 299 868

Dark grey, intensely sheared silty-argillite.

VUW 17527 LOC: Drill-Core R209 (198.4m) T20 / 501 158
N112 / 265 720

Dark grey, sheared argillite / fine-sand-greywacke tectonic mix.

VUW 17503 CR: R7043 LOC: Moawhango Tunnel T20 / 495 043
N122 / 262 594

Grey, sheared argillite / fine-sand-greywacke tectonic mix. (50% <.01mm, 36% <.03mm, 12% <.06mm, 2% <.13mm; 50 counts).

VUW 17509 CR: R7066 LOC: Moawhango Tunnel T20 / 500 069
N122 / 267 622

Grey argillite / fine-sand-greywacke tectonic mix.
Similar to 17503.

VUW 17514 LOC: Drill-Core M2-286 (87.2m) T19 / 492 241
N112 / 253 810

Grey argillite / fine-sand-greywacke tectonic mix.
Similar to 17503.

VUW 17513 LOC: Drill-Core MS-117 (32.6m) T19 / 492 241
N112 / 253 810

Grey argillite / fine-sand-greywacke tectonic mix.
20% quartz + calcite veins (not included).

VUW 17511 LOC: Drill-Core DM3-126 (29.6m) T20 / 473 962
N122 / 240 505

Grey argillite / medium-sand greywacke tectonic mix.

VUW	17828	17512	17826	17829	17830	17824	17517	17502	17516
FIELD	R214	AM2-8	R209A	R221A	R221B	R207A	R3-117	R7041C	P1
SiO_2	70.06	73.61	71.00	70.87	74.61	71.07	71.06	72.93	65.98
TiO_2	0.46	0.39	0.40	0.43	0.32	0.42	0.48	0.33	0.55
Al_2O_3	14.52	2.75	14.18	14.13	12.18	13.99	4.89	12.95	15.95
Fe_2O_3T	3.66	3.14	2.96	3.21	2.06	2.93	2.86	3.51	4.59
MnO	0.05	0.05	0.04	0.06	0.04	0.07	0.02	0.05	0.06
MgO	1.07	1.01	1.02	0.95	0.60	0.84	0.82	1.10	1.50
CaO	1.38	1.15	1.34	1.33	2.09	1.24	1.08	1.38	1.73
Na_2O	3.01	3.07	4.25	3.97	3.76	4.12	4.61	2.20	2.66
K_2O	3.15	2.37	2.50	2.62	1.74	2.88	1.86	2.80	3.57
P_2O_5	0.10	0.09	0.08	0.11	0.09	0.10	0.09	0.08	0.12
LOI	2.28	2.12	1.98	2.07	2.27	2.09	1.98	2.42	3.04
Total*	100.23	99.48	99.98	99.02	99.83	99.19	98.92	99.51	99.75
Ba	521	450	935	621	327	1356	347	452	624
Ce	45	36	35	40	33	57	32	36	54
Cr	30	24	22	25	19	22	28	23	37
Cu	9	6	6	6	5	6	8	9	13
Ga	16	13	17	14	10	17	16	13	20
La	19	17	13	20	16	27	17	14	25
Mn	374	251	324	454	284	518	272	428	502
Nb	8	7	7	8	5	9	8	7	11
Ni	12	5	7	8	5	5	9	11	19
Pb	23	22	24	25	19	25	19	26	36
Rb	129	96	94	104	71	97	80	120	150
Sc	7	6	4	7	5	6	6	5	10
Sr	209	240	247	314	293	231	282	217	248
Th	13	11	11	13	10	15	12	11	15
Ti	2547	2116	2172	2432	1758	2266	2506	22	3160
U	3.5	2.4	2.0	3.4	<2	4.4	4.7	3.4	4.3
V	62	45	48	50	34	45	60	42	78
Y	23	17	19	22	17	24	21	15	27
Zn	76	52	56	58	44	49	47	60	142
Zr	184	179	190	196	151	195	194	154	204
K/Na	1.05	0.77	0.59	0.66	0.46	0.70	0.40	1.27	1.34
K/Rb	203	205	222	208	204	246	192	194	198
Rb/Sr	0.62	0.40	0.38	0.33	0.24	0.42	0.29	0.55	0.60
I	.71058	.70962	.70922	.70908	.70867	.70921	.70924	.71074	.71086

RANGIPO TORLESSE SUITE INTERMEDIATES

VUW 17828 LOC: Drill-Core R214 (137.2m) T20 / 501 158
N112 / 265 720

Grey, sheared silty-greywacke.
20% quartz + calcite veins (not included).

VUW 17512 LOC: Drill-Core AM2-8 (37.2m) T20 / 501 992
N122 / 270 538

Grey, silty-greywacke. 1x1mm quartz +
calcite veins (not included). (EPMA).

RANGIPO TORLESSE SUITE GREYWACKES

VUW 17826 LOC: Drill-Core R209 (180.7m) T20 / 501 158
N112 / 265 720

Grey, foliated fine-greywacke (34% <.01mm,
2% <.03mm, 28% <.06mm, 14% <.13mm, 18% < .25mm,
4% <.5mm; 50 counts).

VUW 17829 LOC: Drill-Core R221 (89.9m) T20 / 501 158
N112 / 265 720

Grey, foliated fine-sand-greywacke.
20% quartz + calcite veins (not included).

VUW 17830 LOC: Drill-Core R221 (93.3m) T20 / 501 158
N112 / 265 720

Grey, foliated fine-sand-greywacke (28% <.01mm,
12% <.03mm, 22% <.06mm, 20% <.13mm, 14% <.25mm
4% <.5mm; 50 counts. Similar to 17826.

VUW 17824 LOC: Drill-Core R207 (46.3m) T20 / 501 158
N112 / 265 720

Grey-brown fine-medium-sand greywacke. Moderately
foliated. Brown oxychlorite is main secondary phase.

VUW 17517 LOC: Drill-Core R3 (35.7) T20 / 501 158
N112 / 265 720

Green, laminated fine/medium-sand-greywacke.
Prominent cleavage.

VUW 17502 CR: R7042 LOC: Moawhango Tunnel T20 / 494 039
N122 / 261 589

Grey, fine/medium-sand-greywacke.
10% qz-cc veins. From same sample as 17501.

VUW 17516 LOC: Drill-Core P1 (76.2m) T20 / 500 163
N112 / 264 725

Grey, massive fine/medium-sand-greywacke.

VUW	17825	17832	17821	17822	17843	17844	17845	17846	17847
FIELD	R207B	DM3B	R7064	R7064	R3853	R3855	R3855	R3857	N20
SiO_2	68.60	70.10	58.96	46.99	58.64	59.59	59.65	59.00	70.47
TiO_2	0.46	0.47	1.97	3.20	0.88	0.88	0.85	0.84	0.42
Al_2O_3	14.97	14.74	12.39	14.57	19.70	19.68	18.99	19.50	13.83
Fe_2O_3T	3.72	3.47	9.92	14.64	7.41	6.47	6.94	7.00	3.19
MnO	0.06	0.05	0.37	0.51	0.07	0.08	0.09	0.12	0.03
MgO	1.13	1.23	2.34	3.10	1.98	1.89	2.01	2.00	1.13
CaO	1.80	0.83	4.93	6.48	0.47	0.42	0.54	0.54	2.55
Na_2O	3.99	4.49	1.65	1.73	1.27	1.66	1.63	1.50	3.40
K_2O	2.61	2.44	2.36	2.27	3.72	3.72	3.38	3.60	1.11
P_2O_5	0.21	0.10	0.48	1.59	0.11	0.13	0.14	0.12	0.10
LOI	2.19	1.83	4.40	4.67	5.50	5.24	5.54	5.54	3.53
Total*	99.65	99.25	99.40	99.42	100.20	99.86	99.8	100.35	101.03
Ba	477	633	648	709	537	660	616	626	267
Ce	42	50	85	117	59	66	74	68	32
Cr	33	26	13	18	85	86	85	87	32
Cu	7	7	906	79	26	25	21	27	7
Ga	17	16	22	28	25	26	25	26	15
La	20	26	40	54	25	26	29	26	14
Mn	419	369	2791	3858	620	519	753	1055	342
Nb	7	7	65	68	14	14	14	14	6
Ni	10	15	19	28	34	34	35	36	13
Pb	26	21	12	12	19	24	29	28	18
Rb	106	79	94	88	190	182	169	178	43
Sc	7	8	17	24	17	16	15	16	10
Sr	294	303	289	301	64	79	121	125	272
Th	13	10	7	6	18	17	18	18	8
Ti	2608	2735	10873	17369	5411	5323	5261	5348	2455
U	1.6	2.0	1.3	3.7	3.2	3.2	2.9	2.7	1.1
V	62	66	161	140	176	176	181	181	58
Y	26	22	59	75	31	32	32	26	17
Zn	64	79	156	200	121	124	133	135	51
Zr	190	163	472	455	145	151	147	143	114
K/Na	0.65	0.54	1.43	1.31	2.92	2.24	2.07	2.40	.32
K/Rb	205	256	209	214	163	170	166	168	213
Rb/Sr	0.36	0.26	0.32	0.29	2.98	2.30	1.40	1.42	.16
I	.70930	.70820	.70877	.70880	.73324	.72766	.72109	.72192	.71173

RANGIPO TORLESSE SUITE GREYWACKES

VUW 17825 LOC: Drill-Core R207 (64.0m) T20 / 501 158
N112 / 265 720

Grey, massive medium/fine-sand-greywacke.

VUW 17832 LOC: Drill-Core DM3-119 (25.6m) T20 / 473 962
N122 / 240 505

Grey, massive medium-sand-greywacke.

RANGIPO TORLESSE SUITE METABASITES

VUW 17821 CR: R7064 LOC: Moawhango Tunnel T20 / 511 120
N122 / 277 678

Light green volcanoclastic sediment.
Clast from 17822.

VUW 17822 CR: R7064 LOC: Moawhango Tunnel T20 / 511 120
N122 / 277 678

Green, sheared metabasite with 10mm clasts.
Plagioclase + quartz + chlorite relicts in
indeterminable clay-rich matrix.

OTAKI FORKS TORLESSE SUITE

VUW 17843 CR: R3853 LOC: East of Pukehinau Stm. S26 / 969 384
N157 / 738 764

Dark grey, moderately-indurated argillite.

VUW 17844 CR: R3855 LOC: East of Pukehinau Stm. S26 / 969 384
N157 / 738 764

Dark grey, moderately-indurated argillite.
Similar to 17843.

VUW 17845 CR: R3856 LOC: East of Pukehinau Stm. S26 / 969 384
N157 / 738 764

Dark grey, moderately-indurated argillite.
Similar to 17843.

VUW 17846 CR: R3857 LOC: Otaki River S26 / 967 393
N157 / 736 773

Dark grey, moderately-indurated argillite.
Similar to 17843.

VUW 17847 CR: N20 LOC: Otaki River S26 / 967 393
N157 / 736 773

Speckled grey, moderately indurated feldspathic
greywacke.

VUW FIELD	17833 B4A	17834 B4B	17842 B2H	17838 B2D	17839 B2E	17835 B2A	17836 B2B	17841 B2G	17837 B2C	17840 B2F
SiO_2	63.13	60.63	60.12	58.75	60.26	60.09	62.80	61.56	62.14	60.99
TiO_2	0.91	0.92	0.86	1.03	0.94	0.99	0.80	0.84	0.72	0.76
Al_2O_3	15.11	15.82	17.25	16.42	15.59	15.93	15.05	15.49	15.70	16.09
Fe_2O_3T	5.68	6.75	6.07	8.32	7.96	7.10	6.55	6.38	5.25	5.50
MnO	0.09	0.12	0.09	0.12	0.11	0.10	0.10	0.10	0.08	0.09
MgO	2.12	2.54	2.56	2.70	2.65	2.69	2.44	2.19	1.90	1.94
CaO	3.70	3.89	3.22	3.91	3.52	4.02	3.71	4.70	6.02	6.78
Na_2O	4.20	4.19	4.69	3.63	3.84	3.20	2.86	2.40	1.44	1.16
K_2O	1.79	1.78	1.92	1.95	1.75	2.21	2.18	2.44	2.47	2.36
P_2O_5	0.20	0.21	0.18	0.22	0.22	0.23	0.18	0.19	0.13	0.12
LOI	2.81	2.88	2.78	2.71	2.92	3.20	3.07	3.46	3.90	3.95
Total*	99.73	99.25	99.34	99.34	99.03	99.05	99.40	99.35	99.28	99.51
Ba	384	351	484	651	430	568	567	556	340	316
Ce	37	37	35	44	44	42	38	50	45	47
Cr	25	24	26	36	32	44	34	36	39	41
Cu	26	27	34	33	29	33	30	27	31	31
Ga	16	19	18	18	16	18	19	20	23	22
La	14	16	16	19	20	19	17	22	21	22
Mn	749	906	835	957	959	992	842	787	701	715
Nb	6	6	5	5	6	5	6	7	8	7
Ni	9	10	13	15	13	18	13	15	15	14
Pb	15	17	17	16	13	20	15	14	22	29
Rb	49	50	55	51	47	66	69	88	107	101
Sc	16	17	17	18	17	19	15	17	17	18
Sr	380	387	585	567	419	526	443	343	210	223
Th	7.5	7.4	7.1	8.9	6.9	9.0	8.2	8.9	11.4	11.4
Ti	5288	5374	5081	6114	5587	5851	4766	8985	4404	4636
U	2.5	2.5	2.1	2.6	2.5	2.0	2.2	2.2	2.5	2.2
V	139	141	149	178	163	171	140	143	126	138
Y	22	24	20	25	24	25	21	25	25	25
Zn	84	90	83	98	87	94	82	83	92	91
Zr	158	172	145	183	158	169	163	156	183	187
K/Na	0.43	0.42	0.41	0.54	0.46	0.69	0.76	1.02	1.72	2.03
K/Rb	303	295	290	320	312	277	260	230	192	193
Rb/Sr	0.13	0.13	0.09	0.09	0.11	0.13	0.16	0.26	0.51	0.45
I	.70515	.70523	.70528	.70499	.70519	.70561	.70548	.70631	70845	.70825

==

RANGIPO WAIPAPA SUITE

==

VUW 17833 LOC: Drill-Core B4 (131.4m) S19 / 261 321
N111 / 998 890

Grey, massive, well-indurated medium-sand greywacke. 1-2mm volcanic clasts (EPMA).

VUW 17834 LOC: Drill-Core B4 (133.2m) S19 / 261 321
N111 / 998 890

Grey, massive, well-indurated medium-sand greywacke. Similar to 17833.

VUW 17842 LOC: Drill-Core B2 (96.6m) S19 / 244 303
N111 / 980 870

Grey, massive, well-indurated medium-sand greywacke. Similar to 17833.

VUW 17838 LOC: Drill-Core B2 (89.9m) S19 / 244 303
N111 / 980 870

Grey, massive well-indurated greywacke. Clasts > 2mm 15%.

VUW 17839 LOC: Drill-Core B2 (89.0m) S19 / 244 303
N111 / 980 870

Grey, massive well-indurated greywacke. Similar to 17838.

VUW 17835 LOC: Drill-Core B2 (53.0m) S19 / 244 303
N111 / 980 870

Grey, massive well-indurated greywacke-breccia. Clasts > 2mm 35%.

VUW 17836 LOC: Drill-Core B2 (58.2m) S19 / 244 303
N111 / 980 870

Grey, massive well-indurated greywacke-breccia. Similar to 17835.

VUW 17841 LOC: Drill-Core B2 (89.0m) S19 / 244 303
N111 / 980 870

Grey, massive well-indurated greywacke-breccia. Clasts > 2mm 60%.

VUW 17837 LOC: Drill-Core B2 (88.4m) S19 / 244 303
N111 / 980 870

Dark grey, massive well-indurated andesitic clast.

VUW 17840 LOC: Drill-Core B2 (89.0m) S19 / 244 303
N111 / 980 870

Dark grey, massive well-indurated andesitic clast.

VUW	17850	17853	17852	17851	17854	17848	17855	17857	17849	17856
FIELD	B9	D2	C9B	C9A	D21	A2A	DM3	AM4	A2B	FT-1
SiO_2	61.65	65.82	63.45	70.50	69.94	72.21	78.25	56.22	38.52	55.26
TiO_2	0.71	0.62	0.76	0.55	0.56	0.52	0.31	0.26	0.35	0.51
Al_2O_3	15.55	14.43	15.73	13.99	13.75	12.79	9.99	8.03	7.55	11.63
Fe_2O_3T	5.59	4.62	6.61	4.12	3.76	3.48	2.94	2.67	2.83	3.80
MnO	0.08	0.06	0.05	0.03	0.06	0.04	0.03	0.24	0.15	0.16
MgO	2.17	1.82	1.16	1.04	1.26	0.99	0.78	1.02	1.27	1.52
CaO	1.66	1.56	0.83	1.16	1.60	1.79	0.79	14.98	25.20	11.90
Na_2O	2.39	2.79	1.90	2.31	2.76	2.69	2.45	1.91	1.76	2.42
K_2O	2.64	2.39	2.73	2.30	2.17	1.93	1.84	1.37	1.08	1.89
P_2O_5	0.11	0.11	0.08	0.01	0.08	0.09	0.05	0.06	0.13	0.12
LOI	7.19	5.52	6.45	3.74	3.80	3.21	2.33	12.99	20.91	10.55
Total*	99.20	99.72	99.47	99.36	99.23	99.67	99.25	99.34	99.30	99.84
Ba	474	455	528	469	427	384	353	267	228	365
Ce	47	43	47	43	40	43	22	26	26	40
Cr	63	59	59	39	51	40	31	25	23	53
Cu	16	11	24	8	8	7	4	4	7	9
Ga	19	17	19	15	16	13	11	9	8	15
La	19	20	13	24	20	20	12	13	12	17
Mn	583	533	277	272	412	435	226	2102	1241	1437
Nb	9	8	9	6	7	6	4	4	3	7
Ni	25	23	16	14	15	14	10	13	8	20
Pb	21	18	46	16	15	11	16	8	9	12
Rb	105	96	115	97	82	72	67	49	41	74
Sc	14	10	14	9	10	9	5	12	18	15
Sr	242	242	152	211	263	263	171	391	434	293
Th	12	12	12	10	11	9	6	5	6	9
Ti	4183	3719	4924	3442	3355	3095	1911	1574	2087	2940
U	2.7	3.1	2.5	2.1	3.2	1.9	1.3	1.2	2.0	1.8
V	116	94	178	87	82	87	53	42	55	79
Y	25	23	19	23	21	18	12	11	11	20
Zn	80	71	66	59	54	51	47	32	32	53
Zr	192	200	184	188	195	148	77	67	142	150
K/Na	1.10	0.86	1.44	1.00	0.79	0.72	0.75	0.72	0.61	0.78
K/Rb	208	207	197	196	219	223	227	230	219	213
Rb/Sr	0.44	0.40	0.76	0.46	0.31	0.27	0.39	0.13	0.09	0.25
I	.70881	.70910	.70983	.70861	.70830	.70765	.70902	.70830	70753	.70840

RANGIPO TERTIARY SUITE

VUW 17850 LOC: Drill-Core B9 (124.1) T19 / 301 356
N112 / 040 930

Grey, massive, weakly-indurated micaceous fine-sandstone. Sparse foraminiferal fossils.

VUW 17853 LOC: Drill-Core D2 (48.5) T19 / 354 408
N112 / 097 989

Grey, massive, weakly-indurated micaceous fine-sandstone. Carbonaceous matter 5%.

VUW 17852 LOC: Drill-Core C9 (71.6) T19 / 348 400
N112 / 090 980

Brown/green, massive, poorly-indurated micaceous fine-sandstone.

VUW 17851 LOC: Drill-Core C9 (70.4) T19 / 348 400
N112 / 090 980

Grey/green, massive, poorly-indurated micaceous fine-sandstone.

VUW 17854 LOC: Drill-Core D21 (48.2) T19 / 354 408
N112 / 097 989

Grey, massive, poorly-indurated micaceous fine-medium sandstone.

VUW 17848 LOC: Drill-Core A2 (27.4) S19 / 233 291
N111 / 968 857

Brown, massive, poorly-indurated micaceous fine-medium sandstone.

VUW 17855 LOC: Drill-Core DM3-116 (11.9) T20 / 468 970
N122 / 235 513

Brown, massive, poorly-indurated micaceous medium sandstone.

VUW 17857 LOC: Drill-Core AM4-1 (57.0) T20 / 434 989
N122 / 197 533

Grey, massive, well-indurated fine-medium sandstone. Bryozoan, molluscan fossils 10%.

VUW 17849 LOC: Drill-Core A2 (30.5) S19 / 233 291
N111 / 968 857

Grey, massive, well-indurated fine-medium sandstone. Molluscan fossils 10-30%.

VUW 17856 LOC: OHAKUNE S20 / 180 975
N121 / 920 510

Grey, massive, weakly-indurated micaceous fine-medium sandstone. Foraminiferal fossils 10%.

RANGIPO TERTIARY SUITE

VUW 17858 LOC: Drill-Core AM4-1 (76.3) T20 / 434 989
N122 / 197 533

Fine-conglomerate with 5-15mm rounded greywacke and quartzite clasts.

VUW 17859 LOC: Drill-Core DM3-116 (16.8) T20 / 468 970
N122 / 235 513

Fine-conglomerate with 10-30mm angular greywacke clasts. Molluscan fossils 20%.

VUW 17860 LOC: Drill-Core DM2-2 (23.5) T20 / 500 992
N122 / 269 538

Medium-conglomerate with 20-50mm rounded sandstone clasts.

A2.2: LAVAS

Lavas of Ruapehu and nearby vents are listed by Formation, and described according to the classification in Chapter 4.5:

TYPE 1: plagioclase and plagioclase-pyroxene lavas.

TYPE 2: plagioclase accumulative lavas.

TYPE 3: pyroxene-plagioclase lavas.

TYPE 4: pyroxene-rich lavas.

TYPE 5: olivine-pyroxene lavas (olivine andesites).

TYPE 6: hybrid lavas (olivine andesites).

Most samples contain plagioclase and/or pyroxene glomerocrysts and crustal xenoliths.

Descriptions and major element analyses of Ruapehu, Waimarino, Pukeonake, Hauhungatahi and Ohakune lavas are by W.R.Hackett.

All trace elements and Sr isotopic compositions are new.

Mg* = Mg number.

Descriptions and major element analyses of high-alumina basalt and Red Crater basalt samples are by Dr.J.W.Cole.

VUW	14765	14747	14737	14762	14741	14922	14923	14924	14925
FIELD	A39	A20	A8	A36	A13	X13	X14	X15	X16
SiO_2	53.73	55.37	55.55	56.05	57.03	54.53	55.23	56.32	56.41
TiO_2	0.70	0.66	0.65	0.65	0.65	0.76	0.75	0.73	0.68
Al_2O_3	17.47	17.76	17.84	17.27	17.28	17.52	17.20	17.55	16.84
Fe_2O_3	3.45	2.63	2.51	4.12	2.91	3.49	1.98	2.21	2.14
FeO	5.11	5.61	5.65	3.98	5.27	4.66	6.37	5.66	5.70
MnO	0.14	0.12	0.12	0.11	0.13	0.13	0.14	0.12	0.11
MgO	5.37	4.58	4.61	4.61	4.35	5.04	4.93	4.48	5.19
CaO	8.50	8.03	7.51	7.51	7.38	8.50	8.64	7.99	8.06
Na_2O	2.94	2.83	3.14	3.00	3.17	2.61	2.59	2.86	2.84
K_2O	0.74	0.74	0.75	0.85	0.66	0.88	0.93	1.08	1.02
P_2O_5	0.10	0.09	0.09	0.11	0.09	0.10	0.10	0.10	0.10
LOI	1.51	1.34	1.33	1.51	0.83	1.51	0.89	0.63	0.64
Total*	99.89	99.54	100.34	100.33	99.55	99.33	99.75	99.32	99.69
Ba	227	206	260	258	188	243	230	292	268
Ce	17	17	.	19	14	.	23	.	.
Cr	81	52	38	49	43	72	72	59	141
Cu	71	53	72	58	35	57	55	53	62
Ga	20	18	21	18	19	20	22	22	17
La	10	11	.	13	9	.	15	.	.
Mn	1238	1017	1086	958	1027	.	1087	.	.
Nb	<2	2	<2	<2	2	<2	<2	<2	<2
Ni	36	22	25	30	24	30	29	24	64
Pb	2	5	10	5	5	7	7	7	7
Rb	22	22	20	23	17	25	27	34	31
Sc	32	24	22	27	26	.	33	.	.
Sr	216	216	248	265	225	220	230	237	226
Th	2	2	2	2	2	3	3	3	3
Ti	4191	3394	3841	3318	3821	.	4265	.	.
U	<2	<2	<2	<2	<2	<2	<2	<2	<2
V	253	186	210	186	210	242	240	226	225
Y	19	18	19	20	19	22	25	25	21
Zn	91	75	90	68	76	86	83	75	74
Zr	63	66	63	71	59	69	69	75	75
Mg*	58	55	55	56	54	58	56	55	59
K/Rb	285	285	313	306	323	298	285	266	270
Rb/Sr	0.100	0.100	0.080	0.086	0.075	0.112	0.118	0.143	0.139
I	.70507	.70506	.70518	.70504	.70483	.70518	.70520	.70531	.70523

TE HERENGA FORMATION LAVAS

VUW 14765 LOC: PINNACLE RIDGE (TALUS BLOCK) T20 / 317 148
N112 / 063 703

Intergranular, TYPE 1 basic andesite.
Sparse olivine phenocrysts altered to chlorite.

VUW 14747 LOC: WHAKAPAPANUI GORGE (LAVA FLOW) T20 / 312 154
N112 / 059 708

Porphyritic, TYPE 1 basic andesite.

VUW 14737 LOC: TE HERENGA RIDGE (LAVA FLOW) T20 / 307 161
N112 / 050 718

Porphyritic, TYPE 1 basic andesite.
Plagioclase glomerocrysts to 2mm (EPMA - 14738).

VUW 14762 LOC: PINNACLE RIDGE (LAVA FLOW) T20 / 318 136
N122 / 066 691

Finely porphyritic, TYPE 1 basic andesite.

VUW 14741 LOC: ARETE NORTH OF WHAKAPAPAIITI VALLEY (LAVA FLOW) S20 / 294 147
N112 / 038 704

Porphyritic, TYPE 1 2-pyroxene acid andesite.

WAHIANOA FORMATION LAVAS

VUW 14922 LOC: WHANGAEHU GORGE (THIN LAVA FLOW) T20 / 355 094
N122 / 106 644

Strongly porphyritic, TYPE 1 basic andesite.
Olivine phenocrysts.

VUW 14923 LOC: WHANGAEHU GORGE (BREADCRUSTED BOMB FROM TUFF BRECCIA) T20 / 356 094
N122 / 106 644

Porphyritic, TYPE 1 basic andesite.
Contains olivine and sparse plagioclase glomerocrysts.

VUW 14924 LOC: WHANGAEHU GORGE (LAVA FLOW) T20 / 357 094
N122 / 107 644

Strongly porphyritic, TYPE 1 basic andesite.
Abundant plagioclase & pyroxene-spinel
glomerocrysts to 3mm.

VUW 14925 LOC: WHANGAEHU GORGE (LAVA FLOW) T20 / 357 094
N122 / 107 644

Strongly porphyritic, TYPE 1 basic andesite.
Olivine to 2mm and olivine gabbro nodules to 3mm.

VUW	14909	14908	14914	14921	14911	14913	14900	14901	14928
FIELD	9	8	14	X12	11	13	1	2	X50
SiO_2	56.19	56.58	57.45	57.58	57.55	57.78	57.77	58.11	58.15
TiO_2	0.66	0.66	0.66	0.67	0.68	0.68	0.70	0.70	0.68
Al_2O_3	17.35	16.76	17.75	17.98	20.27	20.39	19.65	19.73	19.55
Fe_2O_3	2.37	2.51	2.49	1.63	2.30	1.68	3.51	1.81	2.06
FeO	4.93	4.95	4.02	4.60	3.37	3.54	2.34	3.86	3.80
MnO	0.11	0.13	0.09	0.10	0.08	0.06	0.08	0.07	0.08
MgO	4.98	5.24	4.31	4.36	2.08	2.18	2.07	2.11	2.24
CaO	8.09	8.17	7.83	7.92	7.93	8.09	7.38	7.52	7.23
Na_2O	3.04	3.05	3.29	3.14	3.59	3.57	3.95	3.80	3.74
K_2O	0.79	0.92	1.11	1.13	1.24	1.24	1.20	1.22	1.18
P_2O_5	0.09	0.09	0.12	0.12	0.11	0.13	0.13	0.12	0.12
LOI	1.14	0.70	0.64	0.51	0.55	0.40	0.96	0.71	0.92
Total*	99.47	100.02	100.18	99.52	100.08	99.65	100.54	100.13	99.83
Ba	279	256	320	306	317	316	302	294	296
Ce	.	.	.	27	.	.	26	22	.
Cr	103	124	124	112	36	36	16	15	16
Cu	55	66	73	41	59	60	60	64	36
Ga	18	19	17	19	18	20	21	21	19
La	.	.	.	13	.	.	13	12	.
Mn	.	.	.	856	.	.	764	740	.
Nb	<2	<2	3	<2	<2	<2	2	<2	4
Ni	56	48	59	54	27	26	20	20	16
Pb	5	6	13	9	7	6	6	7	8
Rb	20	27	34	35	39	38	35	35	37
Sc	.	.	.	26	.	.	22	22	.
Sr	282	276	305	308	344	341	313	317	316
Th	4	<2	3	4	5	3	4	5	5
Ti	.	.	.	4018	.	.	4073	3943	.
U	<2	<2	<2	<2	<2	<2	<2	<2	2.2
V	218	210	190	190	167	168	168	195	179
Y	18	20	19	21	20	20	17	21	22
Zn	79	73	68	64	63	61	67	43	65
Zr	68	68	86	81	95	94	88	91	93
Mg*	60	60	59	60	45	48	44	45	45
K/Rb	327	281	272	273	262	273	282	288	265
Rb/Sr	0.071	0.098	0.111	0.112	0.114	0.111	0.113	0.110	0.117
I	.70491	.70496	.70500	.70512	.70529	.70524	.70529	.70529	.70519

WAHIANOA FORMATION LAVAS

VUW 14909 LOC: WHANGAEHU GORGE (LAVA FLOW) T20 / 357 093
N122 / 107 643

Finely porphyritic, TYPE 1 basic andesite.

VUW 14908 LOC: WHANGAEHU GORGE (LAVA FLOW) T20 / 357 093
N122 / 107 643

Porphyritic, TYPE 1 2-pyroxene basic andesite.

VUW 14914 LOC: WHANGAEHU GORGE (LAVA FLOW) T20 / 358 093
N122 / 108 644

Strongly porphyritic, TYPE 1 acid andesite.
Abundant plagioclase / plagioclase-pyroxene
glomerocrysts to 2mm.

VUW 14921 LOC: WHANGAEHU GORGE (LAVA FLOW) T20 / 356 094
N122 / 106 644

Strongly porphyritic, TYPE 1 acid andesite.
Abundant plagioclase / plagioclase-pyroxene
glomerocrysts to 7mm.

VUW 14911 LOC: WHANGAEHU GORGE (LAVA FLOW) T20 / 357 094
N122 / 107 644

Strongly porphyritic, TYPE 2 acid andesite.
Abundant plagioclase glomerocrysts to 3mm.

VUW 14913 LOC: WHANGAEHU GORGE (LAVA FLOW) T20 / 358 094
N122 / 108 644

Strongly porphyritic, TYPE 2 acid andesite.
Abundant plagioclase glomerocrysts to 3mm.

VUW 14900 LOC: RIDGE BETWEEN WAHIANOA AND T20 / 344 094
WHANGAEHU VALLEYS (LAVA FLOW) N122 / 095 644
Porphyritic, TYPE 2 acid andesite.
Abundant plagioclase glomerocrysts to 4mm.

VUW 14901 LOC: RIDGE BETWEEN WAHIANOA AND T20 / 344 094
WHANGAEHU VALLEYS (LAVA FLOW) N122 / 095 644
Porphyritic, TYPE 2 acid andesite.

VUW 14928 LOC: RIDGE BETWEEN WAHIANOA AND T20 / 343 094
WHANGAEHU VALLEYS (LAVA FLOW) N122 / 094 644
Porphyritic, TYPE 2 acid andesite.
Abundant plagioclase glomerocrysts to 4mm.

VUW	14906	14904	14873	16719	16721	14867	14866	14722
FIELD	6	5A	M10	W1	W3	M5	M4	W4
SiO_2	57.94	58.25	58.61	59.47	60.34	60.75	61.07	61.02
TiO_2	0.74	0.75	0.70	0.65	0.77	0.72	0.70	0.57
Al_2O_3	17.07	17.10	16.77	17.86	15.17	17.69	15.13	15.63
Fe_2O_3	1.84	1.71	1.46	2.15	1.15	1.91	1.15	1.92
FeO	5.39	5.40	4.75	4.54	4.85	4.43	4.45	3.76
MnO	0.11	0.10	0.09	0.09	0.07	0.08	0.08	0.06
MgO	3.98	3.92	4.36	2.99	5.31	2.55	5.37	4.69
CaO	7.05	6.97	6.77	6.66	6.13	5.96	5.88	6.44
Na_2O	2.95	2.95	3.01	3.62	3.21	3.58	3.24	3.35
K_2O	1.40	1.44	1.68	1.22	1.99	1.59	2.12	1.64
P_2O_5	0.12	0.12	0.12	0.10	0.16	0.13	0.15	0.13
LOI	1.16	1.04	1.43	0.39	0.59	0.35	0.41	0.54
Total*	100.03	99.30	99.60	98.80	99.14	99.18	99.56	99.76
Ba	342	328	332	328	455	389	432	353
Ce	.	.	.	26	35	.	.	.
Cr	41	51	83	23	212	10	204	106
Cu	32	37	26	32	37	38	59	79
Ga	19	19	19	19	19	18	18	18
La	.	.	.	13	18	.	.	.
Mn	.	.	.	851	777	.	.	672
Nb	<2	2	5	5	7	5	6	5
Ni	19	20	34	17	68	17	79	17
Pb	11	10	13	7	13	13	11	8
Rb	48	49	68	41	87	56	93	59
Sc	.	.	.	25	23	.	.	17
Sr	271	270	268	237	244	248	226	351
Th	6	6	7	4	10	5	8	5
Ti	.	.	.	3558	4834	.	.	3333
U	<2	<2	3.1	<2	<2	<2	<2	2.0
V	204	196	173	153	177	173	140	138
Y	21	22	24	22	20	24	22	18
Zn	78	73	71	67	63	72	57	55
Zr	106	108	128	96	163	119	159	108
Mg*	54	54	60	49	66	47	67	60
K/Rb	239	242	205	246	191	234	191	233
Rb/Sr	0.179	0.183	0.254	0.174	0.356	0.228	0.411	0.166
I	.70566	.70567	.70561	.70548	.70549	.70554	.70547	.70490

WAHIANOA FORMATION LAVAS

VUW 14906 LOC: SW RIM WHANGAEHU GORGE (LAVA FLOW) (UNDERLIES 17904) — T20 / 346 093, N122 / 097 643

Porphyritic, TYPE 1 acid andesite.

VUW 14904 LOC: SW RIM WHANGAEHU GORGE (LAVA FLOW) — T20 / 346 093, N122 / 097 643

Porphyritic, TYPE 1 acid andesite.
Olivine phenocrysts.

VUW 14873 LOC: GIRDLESTONE PEAK (LAVA FLOW) — T20 / 311 086, N122 / 060 636

Porphyritic, TYPE 1 acid andesite.
Abundant feldspathic xenoliths.

VUW 16719 LOC: WAHIANOA VALLEY (LAVA FLOW) — T20 / 338 066, N122 / 089 622

Strongly porphyritic, TYPE 1 acid andesite.
Gabbroic nodules.

VUW 16721 LOC: WAHIANOA VALLEY (LAVA FLOW) — T20 / 335 067, N122 / 086 623

Strongly porphyritic, TYPE 3 acid andesite.
Olivine phenocrysts and abundant gabbroic nodules to 4mm.

VUW 14867 LOC: SOUTH RUAPEHU (LAVA FLOW) — T20 / 316 062, N122 / 063 611

Porphyritic, TYPE 1 acid andesite (EPMA).

VUW 14866 LOC: SOUTH RUAPEHU (LAVA FLOW) — T20 / 316 066, N122 / 063 615

Porphyritic, TYPE 3 acid andesite.

VUW 16722 LOC: WAHIANOA VALLEY (LAVA FLOW) — T20 / 327 068, N122 / 078 624

Porphyritic, TYPE 4 acid andesite.
Abundant gabbroic nodules.

VUW	14855	14859	14860	14858	14822	14850	14812	14883	14811
FIELD	L10	L21	L22	L20	E7	L6	E3	N3	E2
SiO_2	52.08	53.14	53.42	53.44	52.95	55.40	57.13	57.09	57.41
TiO_2	0.66	0.68	0.68	0.69	0.68	0.77	0.66	0.68	0.65
Al_2O_3	15.53	17.05	16.92	16.96	16.84	17.35	15.51	15.38	15.36
Fe_2O_3	2.69	3.27	2.55	2.82	2.95	2.30	2.70	1.62	2.21
FeO	6.32	5.60	6.00	5.84	5.30	5.50	4.84	5.30	5.01
MnO	0.16	0.13	0.14	0.12	0.13	0.12	0.16	0.11	0.17
MgO	8.71	6.66	6.92	6.65	6.99	4.99	5.91	6.93	6.07
CaO	9.60	8.79	9.05	8.85	8.77	8.09	8.07	7.48	8.15
Na_2O	2.58	2.77	2.88	2.83	2.67	2.92	2.83	2.70	2.87
K_2O	0.58	0.68	0.67	0.68	0.65	1.11	1.20	1.39	1.20
P_2O_5	0.09	0.10	0.09	0.10	0.10	0.12	0.10	0.11	0.10
LOI	0.75	0.88	0.44	0.79	1.72	1.09	0.65	0.96	0.56
Total*	100.03	99.76	99.80	100.47	100.53	100.04	99.91	100.06	100.62
Ba	185	231	220	237	404	313	298	331	294
Ce	12	.	.	14	21	20	.	26	.
Cr	380	128	144	140	225	132	215	286	231
Cu	77	50	61	49	48	54	59	34	60
Ga	16	16	16	18	20	19	19	18	17
La	6	.	.	11	13	8	.	14	.
Mn	1277	.	.	1212	1165	1001	1028	927	1052
Nb	<2	3	<2	2	4	2	4	4	3
Ni	142	57	61	51	82	49	72	110	73
Pb	2	3	6	3	7	8	8	8	7
Rb	11	17	17	18	16	34	39	54	40
Sc	35	.	.	32	30	26	26	26	25
Sr	201	224	216	219	227	251	336	250	334
Th	<2	<2	3	<2	4	4	4	7	5
Ti	4286	.	.	4159	4499	4298	4203	4318	4112
U	<2	<2	<2	<2	<2	<2	<2	<2	<2
V	251	267	263	258	236	216	209	189	207
Y	18	20	20	20	21	21	21	19	20
Zn	85	86	86	83	83	74	77	68	73
Zr	50	60	56	58	77	84	93	114	90
Mg*	68	62	64	63	65	58	63	68	65
K/Rb	445	334	327	315	342	270	253	211	250
Rb/Sr	0.054	0.076	0.079	0.081	0.070	0.136	0.117	0.217	0.119
I	.70490	.70503	.70505	.70507	.70503	.70529	.70495	.70532	.70502

MANGAWHERO FORMATION LAVAS

VUW 14855 LOC: EAST SIDE UNNAMED STREAM ABOVE FALLS (STEEPLY-DIPPING LAVA FLOW) — T20 / 330 166; N112 / 081 715

Light-grey TYPE 1 basalt.
Olivine and augite phenocrysts to 1mm + minor orthopyroxene phenocrysts (EPMA).

VUW 14859 LOC: BLUFF SOUTH OF TAMA MBR LAVA FIELD (LAVA FLOW) — T20 / 335 158; N112 / 083 715

Porphyritic TYPE 1 basic andesite.
Olivine and jacketted orthopyroxene phenocrysts + internally sieved plagioclase to 1mm.

VUW 14860 LOC: BLUFF SOUTH OF TAMA MBR LAVA FIELD (SAME LAVA FLOW AS 14859) — T20 / 335 158; N112 / 083 715

Porphyritic TYPE 1 basic andesite. Olivine + clinopyroxene phenocrysts + plagioclase-pyroxene glomerocrysts to 3mm.

VUW 14858 LOC: BLUFF SOUTH OF TAMA MBR LAVA FIELD (LAVA FLOW BELOW 14859) — T20 / 335 158; N112 / 083 715

Porphyritic TYPE 1 basic andesite. Olivine + clinopyroxene phenocrysts + plagioclase-pyroxene glomerocrysts to 5mm.

VUW 14822 LOC: PINNACLE RIDGE (LAVA FLOW) (UNCONFORMABLY OVERLIES TE HERENGA Fm.) — T20 / 321 164; N112 / 069 721

Porphyritic TYPE 1 basic andesite.
Olivine phenocrysts.

VUW 14850 LOC: NORTH RUAPEHU (LAVA FLOW) — T20 / 348 136; N122 / 099 690

Porphyritic TYPE 1 basic andesite (EPMA).
Minor plagioclase-pyroxene glomerocrysts to 4mm.

VUW 14812 LOC: NORTH RUAPEHU (LAVA FLOW) (UNDERLIES 14813) — T20 / 327 169; N122 / 078 718

Porphyritic TYPE 4 acid andesite.
Abundant plagioclase-pyroxene glomerocrysts to 3mm.

VUW 14883 LOC: MANGATURUTURU VALLEY (LAVA FLOW) — S20 / 274 101; N122 / 017 650

Porphyritic TYPE 3 acid andesite.
Olivine phenocrysts.

VUW 14811 LOC: NORTH RUAPEHU (LAVA FLOW) (UNDERLIES 14812) — T20 / 327 170; N122 / 079 719

Porphyritic TYPE 4 acid andesite.
Abundant plagioclase-pyroxene glomerocrysts.

VUW	14844	14846	14880	14884	14871	14879
FIELD	L1	L3	M17	N4	M8′	M16
SiO_2	57.03	57.86	58.13	58.35	58.60	58.70
TiO_2	0.69	0.68	0.58	0.68	0.63	0.63
Al_2O_3	17.01	17.42	13.51	15.02	14.09	14.19
Fe_2O_3	1.80	1.84	2.91	1.88	1.82	1.55
FeO	5.17	5.12	3.79	4.72	4.59	4.89
MnO	0.10	0.09	0.10	0.09	0.12	0.10
MgO	4.62	4.14	8.38	6.65	7.87	7.37
CaO	7.44	6.95	7.06	6.99	6.89	6.78
Na_2O	3.04	3.17	2.90	2.94	2.75	2.79
K_2O	1.19	1.19	1.45	1.59	1.55	1.56
P_2O_5	0.10	0.09	0.11	0.13	0.12	0.13
LOI	1.56	1.20	0.82	0.71	0.72	1.05
Total*	100.38	99.76	99.64	100.56	99.55	99.70
Ba	310	459	281	342	327	327
Ce	23	24	34	25	27	.
Cr	92	59	491	325	426	379
Cu	56	68	70	35	82	32
Ga	18	19	15	17	17	15
La	13	13	21	11	17	.
Mn	950	850	967	851	904	.
Nb	2	3	4	6	3	6
Ni	35	37	129	101	132	111
Pb	8	7	6	8	12	9
Rb	37	38	49	66	59	60
Sc	25	25	28	22	26	.
Sr	250	237	290	232	283	282
Th	3	3	6	6	6	8
Ti	3841	3794	3484	4055	3840	.
U	<2	<2	<2	2.0	<2	<2
V	195	186	168	171	173	169
Y	20	23	17	19	19	19
Zn	74	87	73	62	66	71
Zr	93	94	110	129	117	127
Mg*	59	56	73	69	73	71
K/Rb	269	262	246	198	220	216
Rb/Sr	0.147	0.159	0.169	0.287	0.206	0.213
I	.70554	.70578	.70482	.70524	.70481	.70484

MANGAWHERO FORMATION LAVAS

VUW 14844 LOC: NORTH RUAPEHU (LAVA FLOW) T20 / 346 134
N122 / 097 688

Porphyritic TYPE 1 acid andesite.
Abundant plagioclase / clinopyroxene glomerocrysts to 2mm + minor 2-pyroxene xenoliths.

VUW 14846 LOC: NORTH RUAPEHU (LAVA FLOW) T20 / 346 134
N122 / 097 688

Porphyritic TYPE 1 acid andesite. Olivine phenocrysts + pyroxene glomerocrysts to 3mm + minor jacketted orthopyroxene + spinel-rich xenoliths.

VUW 14880 LOC: NW SIDE GIRDLESTONE PEAK (PLUG-LIKE BODY) T20 / 314 089
N122 / 063 637

TYPE 6 acid andesite. Olivine, jacketed pyroxene, fritted plagioclase phenocrysts + dunite nodules to 3mm with orthopyroxene coronas (EPMA).

VUW 14884 LOC: MANGATURUTURU VALLEY (LAVA FLOW) S20 / 275 102
N122 / 018 650

Porphyritic TYPE 1 acid andesite.

VUW 14871 LOC: SADDLE BETWEEN GIRDLESTONE Pk. AND RUAPEHU SUMMIT (LAVA FLOW) T20 / 313 094
N122 / 062 642

TYPE 6 acid andesite. Olivine, jacketed pyroxene phenocrysts + minor dunite nodules to 6mm + olivine xenocrysts with orthopyroxene coronas.

VUW 14879 LOC: SADDLE BETWEEN GIRDLESTONE Pk. AND RUAPEHU SUMMIT (VERTICAL BRECCIA DYKE) T20 / 313 094
N122 / 062 642

TYPE 6 acid andesite. Olivine, jacketed pyroxene, fritted plagioclase phenocrysts + plagioclase-pyroxene glomerocrysts.

VUW	14882	14886	14885	14889	14829	14813
FIELD	N2	N6	N5	N8	J1	E4
SiO_2	59.32	61.02	61.80	63.14	63.34	63.46
TiO_2	0.75	0.78	0.79	0.80	0.84	0.81
Al_2O_3	15.39	16.66	16.39	16.62	15.31	15.89
Fe_2O_3	1.41	1.64	1.03	1.48	2.05	1.43
FeO	4.90	4.30	4.79	3.71	3.19	3.67
MnO	0.07	0.07	0.07	0.06	0.04	0.12
MgO	5.76	3.19	3.14	2.23	3.11	2.50
CaO	6.56	5.84	5.80	4.82	4.74	4.64
Na_2O	2.86	3.47	3.25	3.35	3.02	3.31
K_2O	1.73	1.95	2.04	2.73	3.01	2.83
P_2O_5	0.14	0.17	0.17	0.20	0.15	0.14
LOI	0.86	0.66	0.49	0.61	0.97	0.94
Total*	99.38	100.26	99.23	99.44	100.19	99.97
Ba	388	418	410	527	535	530
Ce	20	36	30	43	34	40
Cr	240	51	65	31	113	69
Cu	29	37	34	27	44	46
Ga	16	20	19	18	19	20
La	11	19	17	20	21	18
Mn	815	753	746	621	590	623
Nb	5	7	6	8	6	4
Ni	81	26	25	20	48	32
Pb	10	14	13	14	17	17
Rb	73	81	84	120	132	115
Sc	22	19	18	13	18	16
Sr	222	253	256	260	215	228
Th	7	9	9	11	13	12
Ti	4718	4726	4606	4363	4636	4607
U	<2	<2	2.0	2.5	4.1	3.0
V	176	162	161	115	151	136
Y	19	26	27	25	24	21
Zh	63	69	69	56	54	60
Zr	142	158	161	201	226	199
Mg*	66	54	54	48	56	52
K/Rb	197	199	201	188	189	204
Rb/Sr	0.328	0.321	0.330	0.464	0.615	0.506
I	.70534	.70554	.70552	.70574	.70545	.70583

MANGAWHERO FORMATION LAVAS

VUW 14882 LOC: MANGATURUTURU VALLEY (LAVA FLOW) S20 / 274 101
N122 / 017 649

Porphyritic TYPE 1 acid andesite.

VUW 14886 LOC: MANGATURUTURU VALLEY (LAVA FLOW) S20 / 275 103
N122 / 018 651

Porphyritic TYPE 1 acid andesite.
Minor two-pyroxene xenoliths.

VUW 14885 LOC: MANGATURUTURU VALLEY (LAVA FLOW) S20 / 275 102
N122 / 018 650

Porphyritic TYPE 1 acid andesite.
Pyroxenite nodules to 4mm.

VUW 14889 LOC: MANGATURUTURU VALLEY (LAVA FLOW) S20 / 273 105
N122 / 016 653

Porphyritic TYPE 1 dacite.

VUW 14829 LOC: RIDGE CREST SOUTH OF WHAKAPAPAIITI STREAM (LAVA FLOW) S20 / 277 139
N122 / 020 688

Porphyritic TYPE 3 dacite.
Quartzose xenoliths (TYPE QXa) to 4cm.

VUW 14813 LOC: NORTH RUAPEHU (LAVA FLOW) T20 / 325 166
N122 / 076 715

Porphyritic TYPE 1 dacite. Abundant plagioclase + pyroxene glomerocrysts to 4mm (EPMA - 14814).

VUW	14785	14784	14782	14781	14801	14828	14804	14839	17886
FIELD	B6	B5	B3	B2	G1	H8	G4	K1G	N112A
SiO_2	56.76	57.20	58.25	58.59	59.28	59.20	59.72	63.51	65.92
TiO_2	0.67	0.68	0.67	0.67	0.72	0.86	0.73	0.78	0.62
Al_2O_3	16.81	16.77	16.86	16.80	17.02	17.06	16.60	15.16	15.46
Fe_2O_3	1.68	2.12	1.76	1.69	2.03	2.22	1.37	1.41	0.21
FeO	5.51	5.06	4.95	4.94	4.75	4.39	4.93	3.63	3.65
MnO	0.12	0.11	0.11	0.10	0.16	0.13	0.09	0.06	0.06
MgO	4.95	4.90	4.38	4.41	3.29	3.05	3.78	2.92	2.21
CaO	7.69	7.67	6.93	6.91	6.54	6.14	6.46	4.91	4.08
Na_2O	3.31	3.15	3.54	3.39	3.23	3.41	3.26	3.24	3.27
K_2O	1.37	1.35	1.60	1.56	1.73	1.84	1.81	3.00	2.92
P_2O_5	0.12	0.13	0.13	0.14	0.11	0.13	0.17	0.16	0.12
LOI	0.77	0.62	0.58	0.55	0.89	1.32	0.83	0.99	1.23
Total*	100.48	99.82	100.04	100.29	100.50	100.53	100.19	99.57	99.01
Ba	343	334	358	367	374	442	413	534	502
Ce	22	27	.	.	.	.	33	42	37
Cr	74	76	69	75	30	17	53	97	50
Cu	47	61	44	56	23	47	22	29	49
Ga	19	18	21	19	20	20	19	19	18
La	12	15	.	.	.	.	17	22	21
Mn	925	938	877	878	885	866	803	576	499
Nb	<2	3	3	2	6	5	6	6	6
Ni	40	42	35	32	14	22	24	33	22
Pb	8	10	12	13	13	12	15	18	20
Rb	51	50	60	59	69	65	73	137	122
Sc	22	24	20	19	19	19	19	14	11
Sr	299	299	285	280	248	270	293	215	207
Th	5	6	6	5	5	7	10	14	11
Ti	4051	4057	3882	4015	4170	5235	4180	4373	2903
U	<2	<2	<2	<2	<2	2.3	2.3	3.7	2.4
V	192	196	177	177	170	193	164	132	93
Y	18	20	20	20	23	25	23	26	25
Zn	72	73	71	72	75	77	67	55	40
Zr	98	97	117	116	126	151	139	213	176
Mg*	60	60	58	59	51	50	56	56	55
K/Rb	224	223	220	219	207	234	206	182	199
Rb/Sr	0.170	0.168	0.211	0.211	0.280	0.241	0.248	0.635	0.587
I	.70524	.70523	.70536	.70530	.70585	.	.70584	.70542	.7062

WHAKAPAPA FORMATION LAVAS

VUW 14785 LOC: ROAD TO MEADS WALL ROPE TOW T20 / 311 154
(LAVA FLOW ABOVE 14784) N112 / 057 708

Porphyritic TYPE 1 acid andesite.
Clinopyroxene / pyroxene-plagioclase
glomerocrysts to 3mm.

VUW 14784 LOC: ROAD TO MEADS WALL ROPE TOW T20 / 309 155
(LAVA FLOW BELOW 14785) N112 / 055 709

Porphyritic TYPE 1 acid andesite.
Clinopyroxene / pyroxene-plagioclase
glomerocrysts to 1mm.

VUW 14782 LOC: WHAKAPAPAIITI TRAILHEAD (LAVA FLOW) S20 / 295 181
N112 / 038 717

Porphyritic TYPE 1 acid andesite.
abundant pyroxene / pyroxene-plagioclase
glomerocrysts to 3mm.

VUW 14781 LOC: QUARRY NEAR ROAD TO WHAKAPAPA S20 / 294 174
SKIFIELD (LOWEST LAVA FLOW) N112 / 039 730

Porphyritic TYPE 1 acid andesite.
abundant pyroxene / pyroxene-plagioclase
glomerocrysts to 2mm.

VUW 14801 LOC: SOUTH RUAPEHU (LAVA FLOW NEAR T20 / 301 064
VENT OF RANGATAUA MEMBER) N122 / 050 610

Porphyritic TYPE 1 acid andesite.

VUW 14828 LOC: TAWHAI FALLS (LAVA FLOW)
N112 / 013 787

Nearly aphyric TYPE 1 acid andesite.

VUW 14804 LOC: KARIOI (RANGATAUA MEMBER LAVA FLOW) S20 / 299 962
N122 / 034 485

Strongly porphyritic TYPE 1 acid andesite.
Abundant pyroxene-plagioclase glomerocrysts to 3mm.

VUW 14839 LOC: WHAKAPAPAITI SUSPENSION BRIDGE S20 / 261 172
(BLACK, GLASSY AUTOBRECCIATED LAVA FLOW) N112 / 002 728

Finely porphyritic TYPE 3 dacite.

VUW 17886 LOC: NORTH RUAPEHU (1m FLOAT BLOCK) T20 / 355 161
N112 / 106 719

Microperlitic TYPE 1 dacite. Abundant quartzose
xenoliths (TYPE QXa) to 2cm (EPMA - 17887).

VUW	14815	14816	14817	14809	14798	14795	24471	14825	14848	14826
FIELD	H4A	H5	H6	H4	F4	F1	24471	H7-1	H7	H7-2
SiO_2	54.36	55.50	55.93	56.98	56.60	56.72	57.08	56.34	56.64	56.99
TiO_2	0.54	0.56	0.59	0.60	0.53	0.54	0.59	0.71	0.69	0.68
Al_2O_3	14.75	15.04	15.28	15.75	14.45	14.85	14.72	14.72	14.20	14.40
Fe_2O_3	1.99	2.78	2.99	1.41	2.10	2.74	1.73	1.21	1.67	1.23
FeO	5.58	5.07	4.90	5.74	6.05	5.21	5.74	5.70	5.50	5.73
MnO	0.11	0.11	0.19	0.16	0.19	0.19	0.14	0.09	0.15	0.12
MgO	8.82	7.15	6.18	5.72	7.05	6.49	6.88	8.01	8.58	8.80
CaO	8.74	9.48	8.57	9.07	9.02	8.98	9.28	7.23	7.21	7.21
Na_2O	2.00	2.22	2.23	2.71	2.31	2.47	2.49	2.92	2.73	2.64
K_2O	0.38	0.61	0.68	0.78	0.66	0.69	0.87	1.36	1.44	1.38
P_2O_5	0.07	0.08	0.07	0.12	0.07	0.06	0.09	0.13	0.11	0.12
LOI	2.42	1.14	2.12	0.70	0.73	0.81	0.14	1.32	0.83	0.45
Total*	99.36	99.46	100.65	100.71	100.09	100.36	99.48	99.70	100.40	99.46
Ba	128	177	183	229	140	144	214	344	355	320
Ce	13	.	.	.	.	15	30	.	29	.
Cr	342	234	195	148	265	192	276	494	507	572
Cu	80	64	59	64	102	89	97	93	96	79
Ga	18	15	17	16	18	16	17	16	16	17
La	11	.	.	.	.	5	11	.	15	.
Mn	.	1074	1074	1008	1135	1121	1119	.	940	.
Nb	3	2	2	4	3	3	4	4	5	6
Ni	88	39	34	22	49	39	38	171	237	214
Pb	2	6	7	2	5	6	4	12	8	8
Rb	8	14	16	20	16	16	30	56	49	54
Sc	.	30	27	24	31	29	32	.	21	.
Sr	569	463	467	501	346	390	640	284	277	283
Th	3	2	3	3	3	3	5	8	6	6
Ti	.	3742	3693	3706	3277	3447	3720	.	4437	.
U	<2	<2	<2	<2	2.0	<2	<2	<2	2.2	<2
V	190	226	215	199	224	226	201	186	181	182
Y	13	17	20	18	17	15	15	21	18	21
Zn	61	72	73	61	74	76	78	68	71	68
Zr	52	60	68	69	62	65	90	119	115	112
Mg*	72	67	63	63	65	64	66	71	72	73
K/Rb	417	353	359	333	335	351	243	201	246	212
Rb/Sr	0.013	0.031	0.034	0.039	0.047	0.042	0.047	0.198	0.176	0.192
I	.70419	.70424	.70421	.70420	.70438	.70436	.70440	.70479	.70480	.70483

LAVAS OF NEARBY VENTS

VUW 14815 LOC: RAILWAY CUTTING 200m NE OF St.H/w.4 OVERPASS (ERUA) (BLOCK FROM TALUS) — S20 / 166 155; N111 / 898 706

Intergranular TYPE 5 basic andesite. Clinopyroxene glomerocrysts to 4mm, minor zeolite in groundmass.

VUW 14816 LOC: NEAR SUMMIT HAUHUNGATAHI (BELOW LAVA FLOW 14809) — S20 / 212 165; N111 / 947 718

Intergranular TYPE 5 basic andesite. Clinopyroxene glomerocrysts to 3mm + olivine phenocrysts (EPMA).

VUW 14817 LOC: SUMMIT HAUHUNGATAHI — S20 / 211 166; N111 / 947 719

Intergranular TYPE 5 acid andesite. Similar to 14816

VUW 14809 LOC: PEAK TO SE OF HAUHUNGATAHI (LAVA FLOW) — S20 / 212 165; N111 / 948 718

Intergranular TYPE 5 acid andesite. Similar to 14816

VUW 14798 LOC: CUTTING ON LOOP ROAD OF OHAKUNE LAKES SCENIC RESERVE (PYROCLASTIC) — S20 / 149 939; N121 / 887 468

Hyalopilitic TYPE 5 acid andesite. Olivine phenocrysts + pyroxene-olivine glomerocrysts to 4mm (EPMA).

VUW 14795 LOC: QUARRY NEAR RAILWAY YARDS OHAKUNE (DENSE, UNOXIDISED BLOCK) — S20 / 175 976; N121 / 915 511

Pilotaxitic TYPE 5 acid andesite. Olivine phenocrysts + pyroxene-olivine glomerocrysts to 4mm.

VUW 24471 LOC: SUMMIT OF PUKEKAIKIORE (LAVA FLOW) — T19 / 360 245; N112 / 108 810

Porphyritic TYPE 5 acid andesite. Olivine phenocrysts.

VUW 14825 LOC: CUTTING ON St.H/w.47 (PUKEONAKE LAVA FLOW) — T19 / 308 324; N112 / 049 895

Porphyritic TYPE 6 acid andesite. Similar to 14848.

UW 14848 LOC: MAHUIA RAPIDS NEAR St.H/w.47 (PUKEONAKE LAVA FLOW) — S19 / 268 255; N112 / 007 819

Porphyritic TYPE 6 acid andesite. Large forsteritic olivine xenocrysts + rare dunite nodules to 5mm + jacketed pyroxene phenocrysts (EPMA).

VUW 14826 LOC: CUTTING ON St.H/w.47 (PUKEONAKE LAVA FLOW) — S19 / 297 301; N112 / 038 870

Porphyritic TYPE 6 acid andesite. Similar to 14825.

The following twelve Ngauruhoe 1954 lava samples were collected from different flows erupted on different days. All are TYPE 1 basic andesites with jacketted olivine phenocrysts and abundant xenoliths (mainly vitrified and quartz-rich types; c.f. Chapter 5). sample localities are given in Fig.4.2 and the analyses are ordered temporally:

VUW	DATE	YARD	METRIC
29240	JUNE 4 1954	N112 / 119 820	T19 / 370 253
29242	JUNE 30 1954	N112 / 116 817	T19 / 367 251
29243	JUNE 30 1954	N112 / 115 816	T19 / 366 250
29249	JUNE 30 1954	N112 / 106 818	T19 / 358 252
29250	JUNE 30 1954	N112 / 103 818	T19 / 355 252
29239	JULY 14 1954	N112 / 120 821	T19 / 371 254
29241	JULY 14 1954	N112 / 116 818	T19 / 367 252
29245	JULY 14 1954	N112 / 114 813	T19 / 365 247
29248	JULY 14 1954	N112 / 109 812	T19 / 361 246
29244	JULY 29 1954	N112 / 115 814	T19 / 366 248
29247	AUGUST 18 1954	N112 / 109 812	T19 / 361 246
29246	SEPTEMBER 16 1954	N112 / 114 812	T19 / 365 246

VUW	29240	29242	29243	29249	29250	29239
FIELD	NC-2	NC-4	NC-5	NC-1	NC-11	NC-12
SiO_2	55.58	55.95	55.78	55.76	55.82	55.84
TiO_2	0.74	0.75	0.75	0.75	0.75	0.77
Al_2O_3	16.55	16.29	16.40	16.46	16.51	16.74
Fe_2O_3	3.29	2.63	2.13	2.87	2.35	1.72
FeO	5.27	6.02	6.51	5.61	6.10	6.58
MnO	0.15	0.15	0.15	0.15	0.15	0.15
MgO	5.21	5.12	5.15	5.26	5.20	5.22
CaO	8.27	8.42	8.32	8.25	8.25	8.27
Na_2O	3.12	3.03	3.15	3.10	3.12	3.04
K_2O	1.14	1.12	1.18	1.15	1.13	1.19
P_2O_5	0.17	0.17	0.16	0.16	0.17	0.16
LOI	0.28	0.09	0.06	0.24	0.19	0.05
Total*	100.77	99.66	99.66	100.50	100.46	98.62
Ba	217	207	209	221	208	208
Ce	28	24	24	24	29	25
Cr	109	104	103	93	89	99
Cu	38	43	41	39	41	39
Ga	18	19	18	19	20	20
La	15	10	11	11	10	16
Mn	1226	1199	1186	1183	1154	1216
Nb	5	5	5	3	2	5
Ni	28	30	30	28	28	27
Pb	8	6	6	8	8	10
Rb	37	37	37	38	37	37
Sc	29	28	28	29	26	28
Sr	245	250	251	246	249	243
Th	3	3	4	4	4	4
Ti	4609	4421	4385	4588	4342	4443
U	0.0	0.5	0.9	2.0	0.8	0.9
V	218	222	220	224	213	225
Y	24	24	24	23	24	22
Zn	88	90	88	89	89	92
Zr	94	93	94	96	95	93
Mg*	57	56	56	57	57	57
K/Rb	253	250	267	249	255	266
Rb/Sr	0.153	0.149	0.146	0.156	0.148	0.154
I	.	.	.	.	.70551	.

VUW	29241	29245	29248	29244	29247	29246
FIELD	NC-3	NC-7	NC-10	NC-6	NC-9	NC-8
SiO_2	56.09	55.92	56.04	56.09	56.18	56.07
TiO_2	0.74	0.74	0.74	0.75	0.74	0.74
Al_2O_3	16.49	16.53	16.59	16.55	16.41	16.45
Fe_2O_3	3.02	2.41	2.01	2.06	2.17	2.42
FeO	5.49	6.07	6.43	6.34	6.29	5.97
MnO	0.15	0.15	0.15	0.15	0.15	0.15
MgO	5.02	5.09	5.13	5.06	5.08	5.19
CaO	8.24	8.23	8.29	8.24	8.25	8.25
Na_2O	3.03	3.13	3.09	3.12	3.07	3.11
K_2O	1.15	1.17	1.11	1.12	1.16	1.12
P_2O_5	0.17	0.16	0.16	0.16	0.17	0.15
LOI	0.17	0.16	0.02	0.11	0.08	0.13
Total*	101.14	100.63	100.79	100.23	100.59	100.83
Ba	213	221	203	225	219	213
~~Ce~~	25	25	25	24	24	24
Cr	109	94	96	96	103	104
Cu	38	40	42	42	40	44
Ga	18	20	20	19	18	19
~~La~~	13	16	9	13	14	10
Mn	1191	1174	1187	1143	1182	1174
~~Nb~~	4	6	3	5	3	4
Ni	28	27	30	27	33	28
Pb	7	8	7	8	7	10
Rb	38	39	38	38	38	39
Sc	29	27	28	29	30	29
Sr	248	246	251	244	245	250
~~Th~~	4	5	5	3	5	5
~~Ti~~	4325	4474	4442	4581	4509	4474
~~U~~	0.6	1.0	1.0	0.5	0.9	2.0
V	218	220	222	216	221	222
Y	24	22	23	24	24	21
Zn	88	87	91	87	91	89
Zr	93	94	96	94	95	98
Mg*	56	57	57	56	56	57
K/Rb	253	251	242	246	251	239
Rb/Sr	0.153	0.157	0.151	0.155	0.156	0.156
I	.	.	.	.	.	.

VUW	22996	22997	22993	22994	21717	22991	22998	11965	17439
FIELD	K-T	AT	O-K	BL	TAR	ROTO	ONG	R-C	WAIM
SiO_2	48.92	49.46	50.11	50.00	50.63	51.98	50.15	52.45	52.26
TiO_2	0.97	1.15	1.31	1.10	0.83	0.78	1.08	0.73	0.47
Al_2O_3	17.20	17.23	16.88	17.11	17.17	17.35	15.58	15.29	12.70
Fe_2O_3	10.42	11.18	10.67	10.56	10.42	9.36	10.06	9.92	1.96
FeO	0.00	0.00	0.00	0.00	0.00	0.00	0.00	0.00	6.59
MnO	0.15	0.17	0.18	0.18	0.17	0.17	0.18	0.17	0.16
MgO	6.97	5.81	6.24	5.81	6.17	5.86	9.27	7.67	13.17
CaO	12.07	10.81	10.57	10.51	11.34	11.16	10.32	10.29	9.61
Na_2O	2.20	2.95	3.08	2.68	2.12	2.26	2.49	2.41	1.64
K_2O	0.33	0.63	0.40	0.50	0.55	0.72	0.54	0.67	0.43
P_2O_5	0.11	0.15	0.21	0.14	0.10	0.08	0.24	0.08	0.05
LOI	0.40	0.21	0.10	1.16	0.25	0.04	-0.17	0.08	0.70
Total*	99.30	100.03	99.76	100.86	100.86	100.06	99.15	98.79	99.60
Ba	94	171	145	129	.	.	.	137	122
Ce	17	19	27	18	17	.	34	12	11
Cr	120	66	37	44	55	70	550	281	1037
Cu	33	32	42	47	25	39	53	73	85
Ga	18	20	19	18	18	18	20	15	13
La	8	4	13	6	7	.	16	6	5
Mn	1395	1559	1505	1509	.	.	.	1373	.
Nb	<2	<2	4	<2	2	<2	5	<2	<2
Ni	39	23	33	29	14	30	160	63	341
Pb	3	3	2	4	4	3	<2	2	3
Rb	8	14	8	14	15	19	10	20	15
Sc	39	38	31	37	40	33	33	36	.
Sr	344	370	347	348	318	359	330	278	342
Th	2	2	<2	3	2	3	2	2	3
Ti	6244	7883	9199	7144	.	.	.	4494	.
U	<2	<2	<2	<2	<2	<2	<2	<2	<2
V	244	315	286	252	256	237	220	271	226
Y	20	28	30	25	19	19	25	21	13
Zn	76	95	90	84	94	82	83	84	76
Zr	56	102	147	84	82	83	125	68	48
Mg*	61	55	58	56	58	59	68	64	77
K/Rb	373	375	442	304	311	312	469	287	242
Rb/Sr	.022	0.038	0.022	0.041	0.047	0.054	0.029	0.070	0.044
I	.70442	.70446	.70392	.70441	.	.	.	.70462	.70455

BASALTS OF THE TAUPO VOLCANIC ZONE

VUW 22996 LOC: K-TRIG PUNATEKAHI TAUPO (LAVA FLOW) — U18 / 737 784, N94 / 504 412

Porphyritic, vesicular high-alumina basalt. Plagioclase + augite phenocrysts; olivine replaced (EPMA).

VUW 22997 LOC: JOHNSON'S ROAD NEAR ATIAMURI (LAVA FLOW) — U16 / 824 186, N85 / 586 854

Porphyritic, vesicular high-alumina basalt. Finer-grained but similar to 22996.

VUW 22993 LOC: TATUA ORAKEI KORAKO (LAVA FLOW) — U17 / 795 949, N94 / 562 594

Intergranular, highly vesicular high-alumina basalt. Olivine phenocrysts, augite xenocrysts (EPMA).

VUW 22994 LOC: BEN LOMOND ROAD TAUPO (LAVA FLOW) — T17 / 667 871, N93 / 425 505

Porphyritic, vesicular high-alumina basalt. Olivine replaced. Similar to 22996.

VUW 21717 LOC: SOUTH OF RUAWAHIA TARAWERA (DYKE) — V16 / 170 244, N77 / 963 928

Nearly aphyric high-alumina basalt. Plagioclase microphenocrysts, rare xenocrysts.

VUW 22991 LOC: ROTOKAWAU LAKE ROTOATUA — V16 / -, N76 / -

Porphyritic, vesicular high-alumina basalt. Similar to 22997.

VUW 22998 LOC: WATT'S QUARRY ONGAROTO — T17 / 663 079, N84 / 414 732

Intergranular low-alumina basalt. Olivine phenocrysts chromian spinel inclusions (EPMA).

VUW 11965 LOC: RED CRATER TONGARIRO — T19 / 395 272, N112 / 146 841

Porphyritic low-alumina basalt. Olivine + augite + labradorite phenocrysts, plagioclase + pyroxene glomerocrysts in black hyalopilitic matrix (EPMA).

VUW 17439 LOC: WAIMARINO RIVER SE TAUPO — T19 / 644 382, N112 / 414 969

Olivine quartz tholeiite. Forsteritic olivine with chromian spinel inclusions in hyalopilitic matrix of bytownite + hypersthene + augite (EPMA).

A2.3: XENOLITHS

HOST - host lavas are given in Appendix 2.2 or in Hackett (1985).
TH, WAH, MANG etc. indicates inclusion in unnamed lavas from Ruapehu (abbreviations are those given in Table 4.1).

FLOAT - xenolith not derived from outcrop lava (includes those collected from Iwikau Member pyroclastics).

Xenolith size is given in brackets after general description.

Classification and order of presentation is that followed in Chapter 5.

VUW	17452	17429	17428	17898	17897	17895	17896
FIELD	FXT-1	N112-C	ARGXEN	24013b	24013a	NX-1	NX-9
SiO_2	58.00	63.88	67.79	69.60	70.44	47.46	52.97
TiO_2	0.68	0.77	0.59	0.56	0.42	0.39	0.39
Al_2O_3	15.46	16.73	16.96	14.78	11.93	10.13	11.46
Fe_2O_3	5.95	1.01	0.80	4.71	4.15	5.22	3.45
FeO	0.00	4.41	3.29	0.00	0.00	0.00	0.00
MnO	0.19	0.07	0.06	0.05	0.07	0.31	0.24
MgO	2.11	1.69	1.30	1.58	1.32	1.17	0.87
CaO	10.13	2.16	0.96	0.27	3.16	34.62	29.42
Na_2O	2.39	3.08	4.39	3.75	3.00	0.07	0.33
K_2O	2.38	2.66	3.05	1.74	1.42	0.06	0.08
P_2O_5	0.18	0.16	0.13	0.14	0.08	0.15	0.28
LOI	2.30	3.14	0.44	2.56	3.76	0.17	0.25
Total*	100.36	100.81	98.92	99.73	99.30	99.46	99.45
Ba	567	649	548	296	289	.	.
Ce	59	59	49	50	43	.	.
Cr	73	58	43	48	38	.	.
Cu	236	19	8	18	17	11	7
Ga	17	18	22	17	14	12	11
La	26	26	26	26	23	.	.
Mn	1580	642	426	374	614	.	.
Nb	8	10	10	9	6	3	6
Ni	30	20	14	16	14	20	19
Pb	9	23	25	21	18	<2	4
Rb	68	110	129	82	63	2	2
Sc	26	14	8	9	8	.	.
Sr	336	207	171	116	225	222	1158
Th	11	13	13	11	10	4	10
Ti	4036	4406	3129	3376	2502	.	.
U	4.1	<2	2.3	2.1	2.6	<2	2
V	180	127	79	87	69	.	.
Y	26	27	25	18	19	23	27
Zn	150	75	58	85	79	42	70
Zr	169	186	242	184	119	100	188
K/Rb	292	201	196	177	187	295	318
Rb/Sr	0.201	0.530	0.754	0.703	0.280	0.008	0.002
I	.70931	.71056	.71246	.71417	.70949	.70507	.

UPPER CRUSTAL XENOLITHS (TYPE UCX)

VUW 17452 HOST: 14795 LOC: OHAKUNE S20 / 175 976
N121 / 920 510

Orange-brown porcellanite (70X70X70mm).
Rounded quartz + oligoclase-andesine + ferrosilite in altered matrix (of above) (EPMA).

VUW 17429 HOST: FLOAT LOC: IWIKAU MEMBER AIRFALL? T20 / 355 161
N112 / 106 719

Cataclastised semi-schist. Quartz + albite + chlorite + muscovite + epidote.

VUW 17428 HOST: FLOAT LOC: IWIKAU MEMBER AIRFALL? T20 / 364 147
N112 / 115 715

Grey, foliated semi-schist (150x120x50mm).
Relict graded bedding. Similar to 17429 (EPMA).

VUW 17898 HOST: FLOAT LOC: TONGARIRO T20 / -
N112 / -

Grey, foliated semi-schist (25x30x30mm).
Similar to 17429.

VUW 17897 HOST: FLOAT LOC: NORTH CRATER TONGARIRO T19 / 393 281
N112 / 143 851

Grey, foliated semi-schist (80x80x30mm). Similar to 17429. Quartz + calcite vein (1.5mm) (not included).

VUW 17895 HOST: FLOAT LOC: TONGARIRO T20 / -
CR 16865 N112 / -

Grey-brown calcsilicate schist (45x35x10mm).
Nematoblastic texture of ferro-salite + wollastonite (EPMA).

VUW 17896 HOST: 29250 LOC: NGAURUHOE T19 / 355 252
N112 / 103 818

White-black speckled calcsilicate schist (15x5x5mm). Nematoblastic texture of anorthite + wollastonite + sphene (EPMA). Contact sharp and regular.

VUW	17465	17470	17471	17472	17469	17462	17474	17461
FIELD	NX-7	NX-13a	NX-13b	NX-13c	NX-12	NX-4	NX-15	NX-3
SiO_2	61.90	70.85	70.82	63.95	71.90	73.73	73.77	74.37
TiO_2	0.82	0.44	0.55	0.06	0.50	0.46	0.47	0.43
Al_2O_3	18.95	12.09	15.23	2.67	15.27	14.20	13.83	12.97
Fe_2O_3	5.95	3.17	3.54	1.91	3.69	3.53	4.03	2.79
FeO	0.00	0.00	0.00	0.00	0.00	0.00	0.00	0.00
MnO	0.05	0.05	0.05	0.16	0.03	0.04	0.04	0.06
MgO	1.94	0.94	1.23	0.48	1.42	1.13	1.26	1.14
CaO	1.33	6.95	1.59	29.43	0.60	0.78	0.77	2.27
Na_2O	2.52	2.67	3.32	0.49	3.19	2.80	2.61	3.27
K_2O	5.25	2.28	2.98	0.28	2.78	2.72	2.70	2.10
P_2O_5	0.17	0.10	0.11	0.00	0.12	0.10	0.10	0.10
LOI	0.87	0.20	0.34	0.30	0.24	0.26	0.16	0.24
Total*	99.29	100.00	100.05	99.20	99.94	99.16	99.63	99.10
Ba	678	352	470	40	536	419	414	449
Ce	66	39	50	9	52	43	42	43
Cr	55	38	45	9	40	31	35	37
Cu	37	46	32	22	121	25	48	20
Ga	23	13	16	2	19	18	17	15
La	29	19	25	6	26	16	19	18
Mn	538	521	350	1284	383	276	311	423
Nb	10	7	8	<2	8	7	6	5
Ni	21	12	12	13	12	9	10	8
Pb	26	19	24	3	25	20	26	47
Rb	181	96	130	11	124	113	115	77
Sc	13	12	9	17	8	7	9	7
Sr	134	397	211	988	159	166	146	347
Th	17	10	13	3	12	11	12	10
Ti	4641	2551	3147	436	2947	2532	2836	2468
U	4.1	2.1	2.2	<2	<2	2.9	2.2	2.8
V	113	61	73	13	72	64	72	56
Y	31	19	23	10	23	19	19	17
Zn	88	54	60	34	81	58	67	85
Zr	212	203	241	36	222	171	171	187
K/Rb	241	198	191	211	187	200	194	226
Rb/Sr	1.352	0.242	0.615	0.011	0.778	0.682	0.793	0.223
I	.71190	.70946	.71097	.70839	.71200	.71145	.71058	.70858

VITRIFIED XENOLITHS - TYPE VXa NGAURUHOE 1954

VUW 17465 HOST: 29250 LOC: NGAURUHOE T19 / 355 252
N112 / 103 818

Grey pumice with contorted white banding (65x35x30mm). White segregations = quartz + hypersthene + silica-rich glass; dark segregations = cordierite + silica-poor glass +- quartz. Also pleonaste + ilmenite + pyrite (EPMA).

VUW 17470 HOST: 29250 LOC: NGAURUHOE T19 / 355 252
CR P16868 N112 / 103 818

Light-grey, banded pumice with large white vein (80x60x50mm). Composition of banding similar to 17465.

VUW 17471 HOST: 29250 LOC: NGAURUHOE T19 / 355 252
CR P16868 N112 / 103 818

Pumiceous part of 17470.

VUW 17472 HOST: 29250 LOC: NGAURUHOE T19 / 355 252
CR P16868 N112 / 103 871

Vein separate from 17470. Granoblastic quartz + wollastonite + anorthite.

VUW 17469 HOST: 29250 LOC: NGAURUHOE T19 / 355 252
CR P16867 N112 / 103 818

Light-grey, banded pumice (90x60x60mm). Composition of banding similar to 17465. Sharp, irregular contact.

VUW 17462 HOST: 29250 LOC: NGAURUHOE T19 / 355 252
N112 / 103 818

Light-grey, mostly homogeneous pumice (60x60x50mm). Quartz + cordierite + silica-rich glass + pleonaste (EPMA). Sharp, irregular contact.

VUW 17474 HOST: 29250 LOC: NGAURUHOE T19 / 355 252
CR P16874 N112 / 103 818

Light-grey, mostly homogeneous pumice (60x40x25mm). Similar to 17462. 1mm reaction zone at contact? (EPMA).

VUW 17461 HOST: 29250 LOC: NGAURUHOE T19 / 355 252
N112 / 103 818

Light-grey, banded pumice (40x30x30mm). Composition similar to 17462. Sharp, irregular contact (EPMA). Dark, contorted segregations (1mm). Minor veining.

VUW	17453	17435	17475	17473	17464	17466	17467	17460
FIELD	PPX-1	H7X-21	PPX-4	NX-14	NX-6	NX-8a	NX-8b	NX-2
SiO_2	72.25	72.80	74.94	71.64	72.02	73.54	73.55	74.05
TiO_2	0.42	0.41	0.38	0.22	0.21	0.21	0.21	0.19
Al_2O_3	13.17	12.94	11.80	17.04	16.05	16.17	16.14	16.11
Fe_2O_3	3.14	0.47	2.84	2.19	2.37	2.17	2.34	2.01
FeO	0.00	2.47	0.00	0.00	0.00	0.00	0.00	0.00
MnO	0.03	0.02	0.04	0.04	0.12	0.09	0.09	0.09
MgO	1.03	0.96	0.88	0.66	0.77	0.58	0.65	0.61
CaO	1.17	1.08	0.78	4.10	3.74	3.40	3.25	3.04
Na_2O	3.10	3.12	2.87	2.00	2.15	1.47	1.67	1.69
K_2O	2.19	2.14	2.21	1.67	1.82	1.73	1.56	1.62
P_2O_5	0.10	0.08	0.07	0.10	0.09	0.09	0.09	0.09
LOI	3.14	3.25	2.94	0.09	0.39	0.30	0.21	0.25
Total*	99.39	98.81	100.00	99.29	99.55	99.32	99.88	100.28
Ba	405	368	307	268	268	346	321	368
Ce	37	40	36	26	29	31	26	28
Cr	32	27	27	7	9	2	6	6
Cu	9	12	7	4	19	10	16	15
Ga	15	15	12	17	17	16	17	17
La	17	14	16	13	10	12	12	11
Mn	270	275	247	445	885	842	868	807
Nb	6	5	5	5	4	4	5	5
Ni	10	10	7	2	6	<2	3	<2
Pb	16	16	18	50	95	61	61	52
Rb	85	81	71	55	74	61	58	60
Sc	8	6	6	5	5	4	4	5
Sr	207	202	180	554	369	479	466	479
Th	10	9	9	7	6	7	7	7
Ti	2456	2322	21065	1211	1167	1198	1192	1139
U	2.5	<2	2.2	<2	<2	<2	<2	<2
V	56	53	46	18	19	15	15	14
Y	18	18	16	14	14	13	13	13
Zn	55	51	47	64	103	60	62	53
Zr	197	194	200	114	102	100	104	103
K/Rb	214	219	261	251	204	235	224	223
Rb/Sr	0.411	0.402	0.392	0.100	0.201	0.127	0.124	0.126
I	.70945	.70952	.70929	.70720	.70633	.70701	.70687	.70698

VITRIFIED XENOLITHS - TYPE VXa PUKEONAKE

VUW 17453 HOST: 14824 LOC: PUKEONAKE SCORIA CONE T19 / 318 256
N112 / 062 821

Light-grey, homogeneous pumice (20x20x20mm).
Quartz + glass + cordierite + pleonaste.

VUW 17435 HOST: 14824 LOC: PUKEONAKE SCORIA CONE T19 / 318 256
N112 / 062 821

Light-grey, homogeneous pumice (40x15x10mm).
Similar to 17453.

VUW 17475 HOST: 14824 LOC: PUKEONAKE SCORIA CONE T19 / 318 256
N112 / 062 821

Light-grey, homogeneous pumice (40x30x20mm).
Similar to 17453 (EPMA).

VITRIFIED XENOLITHS - TYPE VXb NGAURUHOE 1954

VUW 17473 HOST: 29250 LOC: NGAURUHOE T19 / 355 252
CR P16871 N112 / 103 818

Light-grey, saccharoidal pumice (50x40x40mm) with conspicuous blue-cordierites. Quartz + cordierite + labradorite + glass + pleonaste + titanomagnetite (EPMA).

VUW 17464 HOST: 29250 LOC: NGAURUHOE T19 / 355 252
N112 / 103 818

Light-grey, pumice (100x90x20mm). Similar to 17473. Contact sharp.

VUW 17466/67 HOST: 29250 LOC: NGAURUHOE T19 / 355 252
N112 / 103 818

Light-grey, brittle pumice (100x30x30mm).
Similar to 17473. 17466 is oxidised outer rind (3mm).

VUW 17460 HOST: 29250 LOC: NGAURUHOE T19 / 355 252
N112 / 103 818

Light-grey, brittle pumice (60x40x30mm).
Similar to 17473 (EPMA).

VUW	17480	17490	17491	17492	17482	17485	17463	17436
FIELD	B10Xa	BXGa	BXGb	BXGc	B10Xd	B10Xi	NX-5	FXQ
SiO_2	59.56	61.46	74.30	69.86	64.87	71.00	84.82	97.78
TiO_2	0.84	0.52	0.49	0.53	0.71	0.56	0.01	0.00
Al_2O_3	18.47	16.87	13.25	13.59	16.32	13.61	8.82	0.78
Fe_2O_3	5.16	4.66	2.28	3.71	5.59	4.19	0.63	0.10
FeO	0.00	0.00	0.00	0.00	0.00	0.00	0.00	0.30
MnO	0.17	0.25	0.10	0.18	0.12	0.06	0.01	0.01
MgO	1.84	1.12	0.83	1.07	1.73	1.24	0.10	0.16
CaO	8.75	13.30	5.18	9.16	5.97	4.40	3.81	0.31
Na_2O	2.90	0.33	2.07	0.58	3.17	2.18	1.11	0.19
K_2O	0.94	0.02	0.34	0.06	0.54	0.86	0.17	0.07
P_2O_5	0.29	0.24	0.10	0.15	0.30	0.18	0.04	0.00
LOI	0.84	0.98	0.82	0.85	0.43	1.46	0.23	0.00
Total*	99.83	99.63	99.45	99.43	99.22	99.57	100.29	98.63
Ba	611	10	139	31	333	174	13	3
Ce	54	41	32	45	52	38	4	5
Cr	48	28	26	31	39	33	6	4
Cu	72	33	30	31	13	46	16	56
Ga	22	20	13	15	20	15	4	<2
La	24	18	16	21	23	17	<2	<2
Mn	1275	1942	693	1273	950	534	98	132
Nb	11	8	5	7	9	7	<2	<2
Ni	20	8	3	6	13	8	<2	<2
Pb	13	3	13	4	20	10	6	9
Rb	47	<2	6	<2	4	42	4	3
Sc	18	12	10	12	14	11	<2	<2
Sr	714	666	553	605	608	260	204	26
Th	14	8	8	11	12	8	<2	<2
Ti	4922	3144	2426	2992	3902	3179	78	45
U	3.4	2.7	<2	2.0	3.2	2.0	<2	<2
V	115	70	74	69	105	82	5	16
Y	27	17	15	21	26	16	<2	<2
Zn	69	73	37	44	779	51	7	28
Zr	224	194	199	223	199	135	8	<2
K/Rb	166	208	488	416	1252	169	379	226
Rb/Sr	0.066	0.001	0.010	0.002	0.006	0.163	0.018	0.100
I	.	.70703	.70696	.	.70639	.70890	.70801	.70611

QUARTZ-RICH XENOLITHS (TYPE QX)

VUW 17480 HOST: FLOAT LOC: IWIKAU MEMBER AIRFALL T20 / 328 139
N122 / 079 688

Brown/white banded schist (25x25x25mm) (TYPE QXa). Assemblage 1: biotite + plagioclase; assemblage 2: quartz + plagioclase; clinopyroxene-rich zone between.

VUW 17490-92 HOST: FLOAT LOC: IWIKAU MEMBER AIRFALL T20 / 328 139
N122 / 079 688

Green/grey/white saccharoidal gneiss (50x50x50mm) (TYPE QXa). Assemblage 1 (17490): quartz + anorthite + ferrosalite + sphene; assemblage 2 (17491): andesine + orthopyroxene + almandine garnet + glass + ilmenite (EPMA). Whole rock = 17492.

VUW 17482 HOST: FLOAT LOC: IWIKAU MEMBER AIRFALL T20 / 328 139
N122 / 079 688

Red/green/white banded schist (45x20x10mm) (TYPE QXa). Similar to 17492 but less well-developed associations (EPMA).

VUW 17485 HOST: FLOAT LOC: IWIKAU MEMBER AIRFALL T20 / 328 139
N122 / 079 688

Brown/white contorted banded gneiss (60x50x40mm) (TYPE QXa). Assemblage 1: quartz + anorthite + salite + ilmenite + hematite + sphene; assemblage 2: andesine + biotite + almandine garnet; quartz-rich areas (EPMA).

VUW 17463 HOST: 29250 LOC: NGAURUHOE T19 / 355 252
N112 / 103 818

White coarse-grained quartzite (70x45x40mm). Unstrained granular quartz. Small areas of anorthite + hypersthene + glass. Oxidised contact (3mm) (EPMA).

VUW 17436 HOST: 14795 LOC: OHAKUNE RAILWAY QUARRY S20 / 171 981
N121 / 911 516

White coarse-grained quartzite (25x15x15mm) (TYPE QXb). Nematoblastic texture of strained, interlobate quartz. Reactive contact.

VUW 17455 HOST: FLOAT LOC: IWIKAU MEMBER AIRFALL T20 / 328 139
N121 / 911 516

White coarse-grained quartzite (TYPE QXb). Similar to 17436. Minor opaques.

VUW 17893 HOST: 14795 LOC: OHAKUNE RAILWAY QUARRY S20 / 171 981
N121 / 911 516

White fine-grained (.1-.5mm) quartzite (TYPE QXb). Strained, granular, cracked quartz with matted areas of anorthite + salite + glass.

VUW 17899 HOST: 29250 LOC: NGAURUHOE T19 / 355 252
N112 / 103 818

White coarse-grained quartzite (TYPE QXb). Unstrained granular quartz.

VUW	17468	17416	17493	17488	17498
FIELD	NX-11	A14-X	BX-20	B10XM	AX-WS
SiO_2	98.83	58.74	86.94	94.12	79.09
TiO_2	0.01	1.08	0.08	0.07	0.07
Al_2O_3	0.30	18.18	2.96	1.76	12.27
Fe_2O_3	0.13	2.53	2.13	1.68	0.74
FeO	0.00	3.72	0.00	0.00	0.00
MnO	0.01	0.14	1.28	0.26	0.03
MgO	0.01	2.08	0.65	0.37	0.20
CaO	0.15	8.11	4.40	0.38	0.45
Na_2O	0.05	0.47	0.01	0.09	6.27
K_2O	0.07	0.09	0.04	0.12	0.19
P_2O_5	0.00	0.26	0.06	0.01	0.02
LOI	0.19	4.36	1.20	0.90	0.42
Total*	100.35	100.72	100.30	99.99	100.05
Ba	2	326	193	60	24
Ce	5	55	39	21	9
Cr	2	32	3	7	8
Cu	3	230	61	16	18
Ga	<2	18	5	3	5
La	2	21	12	5	5
Mn	37	1186	11128	1941	80
Nb	<2	8	<2	2	<2
Ni	<2	15	57	24	3
Pb	<2	18	2	<2	12
Rb	3	4	3	5	2
Sc	<2	23	8	2	2
Sr	6	336	223	39	168
Th	<2	12	4	2	<2
Ti	92	6206	479	392	405
U	<2	<2	<2	<2	<2
V	3	171	31	11	13
Y	2	37	16	8	2
Zn	2	86	47	18	13
Zr	3	290	31	25	29
K/Rb	206	176	103	188	786
Rb/Sr	0.459	0.013	0.014	0.137	0.012
I	.	.70608	.70774	.	.

QUARTZ-RICH XENOLITHS (TYPE QX)

VUW 17885 HOST: 14824 LOC: PUKEONAKE SCORIA CONE T19 / 318 256
N112 / 062 821

White, coarse-grained quartzite (TYPE QXb). Unstrained granular quartz with areas of broken grains + anorthite + augite + glass. Reaction rim of silica-rich glass + augite (5mm) (EPMA).

VUW 17459 HOST: 14824 LOC: PUKEONAKE SCORIA CONE T19 / 318 256
N112 / 062 821

White, coarse-grained quartzite (TYPE QXb). Etched, clouded, strained granular quartz.

VUW 17476 HOST: 14785 LOC: ROAD TO MEADS WALL TOW T20 / 311 154
N112 / 057 708

White, coarse-grained quartzite (TYPE QXb). Mildly strained interlobate quartz with areas of anorthite + wollastonite intergrowth (2x5mm) (EPMA).

VUW 17468 HOST: 29250 LOC: NGAURUHOE T19 / 355 252
N112 / 103 818

White massive, saccharoidal quartzite (TYPE QXc) (120X80X60mm). Crumbly aggregation of rock crystal.

VUW 17416 HOST: TH LOC: WHAKAPAPAIITI VALLEY S20 / 292 148
N112 / 036 705

Dark-grey, fine-grained foliated metasiltstone (TYPE QXd) (140x50x20mm). Quartz + plagioclase segregations in microcrystalline groundmass (+ clinopyroxene) (EPMA). Sharp, regular contact.

VUW 17488 HOST: FLOAT LOC: IWIKAU MEMBER AIRFALL T20 / 328 139
N122 / 079 688

Light-brown, saccharoidal quartzite (TYPE QXe) (20x15x10mm). Unstrained, interlobate granular quartz with interstitial plagioclase + manganoan ferrohypersthene + titanomagnetite (EPMA).

VUW 17493 HOST: WHAK LOC: WHAKAPAPA SKIFIELD T20 / 310 150
N122 / 058 699

Grey / white saccharoidal schist (TYPE QXe) (25x15x5mm). Unstrained, granular quartz with interstitial anorthite + manganoan-ferroan-wollastonite + manganoan-ferrosalite + sphene (EPMA).

VUW 17498 HOST: FLOAT LOC: WHAKAPAPANUI STREAM T20 / 312 154
N112 / 059 708

White quartzite (40x40x30mm) (TYPE QXf). Partially mylonitised texture of strained quartz + albite. Minor ferro-augite + olivine + titanomagnetite + pleonaste (EPMA). Sharp, irregular contact.

VUW	17483	17484	17425
FIELD	B10XF	B10XG	B10XH
SiO_2	46.64	48.55	49.55
TiO_2	1.11	1.72	1.07
Al_2O_3	27.25	25.41	25.34
Fe_2O_3	9.35	7.25	2.97
FeO	0.00	0.00	4.29
MnO	0.11	0.06	0.12
MgO	2.87	2.64	2.98
CaO	2.39	7.56	4.22
Na_2O	3.24	3.56	4.53
K_2O	2.80	1.47	3.74
P_2O_5	0.22	0.34	0.26
LOI	3.75	1.19	0.68
Total*	99.62	99.02	99.11
Ba	1093	587	1709
Ce	83	76	78
Cr	92	106	59
Cu	47	15	30
Ga	41	36	38
La	36	34	32
Mn	869	554	754
Nb	18	20	15
Ni	33	23	24
Pb	43	12	25
Rb	138	48	144
Sc	23	26	19
Sr	430	604	708
Th	24	24	23
Ti	7053	10278	7111
U	5.3	4.7	4.8
V	209	248	179
Y	35	30	31
Zn	173	174	116
Zr	274	361	289
K/Rb	168	256	216
Rb/Sr	0.322	0.079	0.203
I	.71112	.70616	.70662

QUARTZ-POOR XENOLITHS - TYPE QPXa

VUW 17483 HOST: FLOAT LOC: IWIKAU MEMBER AIRFALL T20 / 328 139
N122 / 079 688

Grey gneiss (10x5x5mm). Finely segregated and foliated. Assemblage 1 = oligoclase + sanidine (+corundum); assemblage 2 = biotite + pleonaste titanomagnetite + glass (EPMA).

VUW 17484 HOST: FLOAT LOC: IWIKAU MEMBER AIRFALL T20 / 328 139
N122 / 079 688

Grey gneiss (25x10X10mm). Plagioclase + hypersthene + pleonaste. Similar to 17483.

VUW 17425 HOST: FLOAT LOC: IWIKAU MEMBER AIRFALL T20 / 328 139
N122 / 079 688

Grey gneiss (120X80X25mm). Finely segregated and foliated. Assemblage 1 = oligoclase + sanidine (+ sillimanite); assemblage 2 = biotite + aluminous hypersthene + pleonaste + ilmenite (EPMA). Quartz veins.

VUW	17419	17418	17458	17415	17443	17497	17440
FIELD	B6XA	B3XA	BGX-4	A11-X	TLX-8	AX-9	BRX-16
SiO_2	48.74	48.99	49.17	50.16	50.33	50.68	52.58
TiO_2	1.45	1.19	0.96	1.09	1.16	0.96	0.91
Al_2O_3	25.25	24.60	25.42	24.93	24.35	24.61	23.96
Fe_2O_3	4.96	4.71	7.33	1.30	8.67	7.34	5.84
FeO	2.90	2.90	0.00	5.71	0.00	0.00	0.00
MnO	0.07	0.06	0.09	0.07	0.09	0.06	0.07
MgO	2.49	2.55	2.79	2.41	2.89	2.42	2.49
CaO	8.75	9.72	7.93	8.48	6.59	8.43	9.34
Na_2O	3.57	2.87	3.66	4.22	4.34	3.74	3.60
K_2O	0.57	0.51	0.84	0.23	0.90	0.24	0.71
P_2O_5	0.20	0.21	0.17	0.12	0.22	0.10	0.12
LOI	0.81	1.44	1.39	1.03	0.20	1.18	0.13
Total*	100.03	99.99	99.83	99.57	98.79	98.96	99.84
Ba	783	234	574	319	878	292	310
Ce	.	.	50	41	84	32	37
Cr	73	94	85	80	87	73	61
Cu	38	28	42	96	74	87	58
Ga	36	37	35	34	41	31	27
La	.	.	25	19	41	17	16
Mn	628	553	589	535	726	586	460
Nb	13	7	7	8	16	6	6
Ni	26	36	32	23	32	22	21
Pb	13	4	7	3	17	4	6
Rb	16	16	26	<2	18	2	20
Sc	23	20	16	22	23	21	13
Sr	896	548	524	475	545	448	534
Th	24	9	10	10	16	6	8
Ti	7864	6821	573	6088	6904	5649	4911
U	4.0	2.4	2.2	<2	4.8	<2	<2
V	221	231	208	203	208	208	164
Y	30	19	18	16	28	13	14
Zn	92	124	144	121	188	113	62
Zr	473	187	237	147	220	126	129
Mg*	42	43	47	42	44	44	50
K/Rb	304	264	264	2125	405	956	289
Rb/Sr	0.017	0.029	0.050	0.002	0.034	0.005	0.038
I	.70570	.70647	.70755	.70723	.70800	.70702	.70633

==

QUARTZ-POOR XENOLITHS - TYPE QPXb

==

VUW 17419 HOST: 14785 LOC: ROAD TO MEADS WALL TOW T20 / 311 154
N112 / 057 708

Grey vesicular nematoblastic hornfels
(15x60x30mm). Labradorite (clouded near contact) +
hypersthene + pleonaste + titanomagnetite (EPMA).
Mafic minerals in subparallel layers.
Contact sharp, regular with clouding (1mm).

VUW 17418 HOST: 14782 LOC: WHAKAPAPAIITI TRAILHEAD S20 / 295 181
N112 / 038 717

Grey vesicular hornfels
Similar to 17419.

VUW 17458 HOST: WHAK LOC: SOUTH RUAPEHU? T20 / -
N122 / -

Grey vesicular hornfels (30x10x10mm). Pleonaste
with corundum core (EPMA). Similar to 17419.

VUW 17415 HOST: TH LOC: WHAKAPAPAIITI VALLEY S20 / 294 147
N112 / 038 704

Grey vesicular hornfels (10x10x10mm). Contains
Contains vugs with plagioclase (sodic rim) +
hypersthene + dacitic glass (EPMA).

VUW 17443 HOST: WHAK LOC: LOWER TAMA LAKE T20 / 345 195
N112 / 093 755

Grey, banded hornfels with 1mm mafic
segregations (35x20x10mm). Similar to 17419 (EPMA).

VUW 17497 HOST: TH LOC: WHAKAPAPAIITI VALLEY S20 / 294 147
N112 / 038 704

Light-grey vesicular hornfels
(30x25x15). Similar to 17415 (EPMA).

VUW 17440 HOST: WHAK LOC: BELOW "TOP O BRUCE" S20 / 293 161
N112 / 038 717

Light-grey vesicular hornfels (15x15x5mm).
Highly clouded plagioclase. Similar to 17419.

VUW 17444 HOST: WHAK LOC: SOUTH RUAPEHU T20 / 301 064
N122 / 050 610

Light-grey vesicular hornfels
Labradorite + hypersthene + titanomagnetite +
pale brown silica-rich glass (EPMA).

VUW 17894 HOST: WAH LOC: WHANGAEHU GORGE? T20 / -
N122 / -

Light-grey hornfels. Relict almandine garnet
garnet + cordierite. Similar to 17419 (EPMA).

VUW	17487	17423	17410	17489	17457	17447
FIELD	B10XL	B10XB	WX-4	B10XN	B3X-1	XXC
SiO_2	40.49	42.12	36.21	41.83	41.97	44.72
TiO_2	1.70	1.40	4.33	3.63	2.06	2.86
Al_2O_3	25.97	26.04	20.23	20.08	22.54	19.51
Fe_2O_3	13.24	8.15	6.40	11.37	15.86	11.92
FeO	0.00	3.54	13.75	0.00	0.00	0.00
MnO	0.26	0.26	0.54	0.16	0.27	0.36
MgO	4.49	3.90	8.96	8.01	5.89	8.12
CaO	5.21	5.53	5.70	9.08	8.91	9.60
Na_2O	2.15	2.66	1.30	1.67	1.55	1.52
K_2O	4.18	4.09	0.62	1.94	0.44	0.33
P_2O_5	0.11	0.09	0.30	0.77	0.11	0.45
LOI	1.94	1.97	1.43	1.22	0.15	0.37
Total*	99.14	100.00	100.00	99.07	100.00	99.16
Ba	881	991	360	590	162	291
Ce	15	16	53	68	17	54
Cr	625	531	163	195	852	202
Cu	169	132	269	38	487	26
Ga	27	26	30	24	26	24
La	6	3	17	33	8	21
Mn	2047	2036	4440	1404	1980	2769
Nb	3	3	18	58	4	32
Ni	122	107	79	128	81	95
Pb	31	31	32	8	4	5
Rb	184	169	40	87	19	15
Sc	51	51	73	32	62	44
Sr	284	271	342	503	233	223
Th	2	<2	<2	4	2	4
Ti	10105	9465	28303	23427	12554	17577
U	<2	<2	<2	<2	2.4	2.9
V	441	443	564	235	391	366
Y	22	18	60	34	30	34
Zn	237	202	286	102	196	116
Zr	93	77	236	291	79	201
K/Rb	189	201	130	185	197	181
Rb/Sr	0.646	0.623	0.115	0.173	0.079	0.068
I	.	.71000	.70830	.	.70701	.70722

QUARTZ-POOR XENOLITHS (TYPE QPX)

VUW 17487 HOST: FLOAT LOC: IWIKAU MEMBER AIRFALL T20 / 328 139
N122 / 079 688

Grey-purple gneiss (TYPE QPXc) (10X5X5mm).
Contorted bands and lenticular masses of plagioclase + biotite + pleonaste + minor titanomagnetite + ilmenite.

VUW 17423 HOST: FLOAT LOC: IWIKAU MEMBER AIRFALL T20 / 328 139
N122 / 079 688

Grey-purple gneiss (TYPE QPXc) (20X20X10mm).
Similar to 17487 (EPMA).

VUW 17410 HOST: WAH LOC: WAHIANOA VALLEY T20 / 335 072
N122 / 085 622

Grey, fine-grained spinel-rich schist (TYPE QPXd) (60x40x15mm). Bytownite-anorthite + pleonaste + hypersthene + minor biotite + olivine (EPMA).

VUW 17489 HOST: FLOAT LOC: IWIKAU MEMBER AIRFALL T20 / 328 139
N122 / 079 688

Grey, fine-grained spinel-rich schist (TYPE QPXd) (20x10x5). Zoned labradorite-bytownite + hypersthene + biotite + titanomagnetite + ilmenite (EPMA).

VUW 17457 HOST: 14782 LOC: WHAKAPAPAIITI TRAILHEAD S20 / 295 181
N112 / 038 717

Grey, fine-grained, inhomogeneous spinel-rich schist (TYPE QPXd) (30x30x30mm). Vesicular. Similar to 17410. Sharp, regular contact.

VUW 17447 HOST: WAH LOC: SW RIM WHANGAEHU GORGE T20 / 359 096
N122 / 109 646

Grey, fine-grained, vesicular spinel-rich schist (TYPE QPXd) (10x10x10mm). Similar to 17410. Sharp, regular contact.

VUW 17888 HOST: WAH LOC: SW RIM WHANGAEHU GORGE T20 / 359 096
N122 / 109 646

Grey, fine-grained, granular spinel-rich schist (TYPE QPXd) (25x10x5mm). Bytownite + olivine + hypersthene + titanomagnetite (EPMA).

VUW 17892 HOST: TH LOC: UNKNOWN -
-

Grey, fine-grained, granular spinel-rich schist (TYPE QPXd) (25x10x5mm). Plagioclase + olivine + hypersthene + titanomagnetite (EPMA).
Augite-rich reaction rim.

VUW	17499	17444	17496	17486	17446	17413
FIELD	MX-13	TLX-10	TLX-5	B10XJ	MX-1	XX
SiO_2	51.89	56.72	56.89	58.50	60.83	49.16
TiO_2	0.66	0.80	0.64	0.65	0.65	0.34
Al_2O_3	17.65	17.32	17.09	16.63	18.47	19.18
Fe_2O_3	9.20	1.28	8.62	4.78	6.27	1.04
FeO	0.00	6.39	0.00	0.00	0.00	6.54
MnO	0.21	0.13	0.14	0.07	0.05	0.11
MgO	7.79	4.69	4.64	6.67	6.06	7.31
CaO	9.78	7.98	7.71	5.32	3.29	8.63
Na_2O	2.22	2.76	3.05	4.15	2.25	2.29
K_2O	0.22	1.44	0.84	0.71	1.09	0.15
P_2O_5	0.10	0.14	0.08	0.11	0.05	0.01
LOI	0.02	0.07	0.05	2.17	0.74	4.99
Total*	99.70	98.46	99.67	98.91	99.43	99.82
Ba	160	300	202	274	332	89
Ce	19	.	17	20	19	9
Cr	259	38	55	103	65	142
Cu	14	16	40	16	24	33
Ga	20	19	20	19	14	19
La	5	.	8	7	6	3
Mn	1695	.	1126	613	345	1138
Nb	3	3	<2	3	<2	0
Ni	70	13	27	22	10	49
Pb	6	7	3	8	11	<2
Rb	4	53	20	31	39	4
Sc	31	25	29	24	27	29
Sr	299	266	225	272	111	244
Th	5	6	3	7	2	2
Ti	4048	.	3141	3829	3829	2001
U	2.6	3	<2	<2	<2	<2
V	290	257	217	178	231	227
Y	20	22	18	21	18	10
Zn	100	84	82	36	53	67
Zr	99	112	61	115	74	16
Mg*	66	57	56	77	69	67
K/Rb	469	224	356	187	231	296
Rb/Sr	0.013	0.201	0.087	0.115	0.354	0.017
I	.	.	.	.	.70529	.70547

IGNEOUS XENOLITHS (TYPE IX)

VUW 17499 HOST: MANG LOC: SOUTH RUAPEHU T20 / -
N122 / -

Grey porphyritic andesite (30x20x10mm). Relict plagioclase phenocrysts in pilotaxitic groundmass. Irregular, sharp contact.

VUW 17444 HOST: FLOAT LOC: LOWER TAMA LAKE T20 / 345 195
N112 / 093 755

Grey porphyritic andesite. Plagioclase + pyroxene phenocrysts in pilotaxitic groundmass.

VUW 17496 HOST: FLOAT LOC: LOWER TAMA LAKE T20 / 345 195
N112 / 093 755

Grey porphyritic andesite (150x150x50mm). Plagioclase + pyroxene phenocrysts in pilotaxitic groundmass.

VUW 17486 HOST: FLOAT LOC: IWIKAU MEMBER AIRFALL T20 / 328 139
N122 / 079 688

Brown, speckled highly altered andesite (25x15x10mm). Relict plagioclase phenocrysts in brown, transluscent matrix.

VUW 17446 HOST: MANG LOC: SOUTH RUAPEHU T20 / -
N122 / -

Brown, highly altered lava. No relict texture visible - may have been cumulate.

VUW 17413 HOST: WAH LOC: S RIM WHANGAEHU GORGE T20 / 359 096
N122 / 109 646

White, speckled nodule (15x15x10mm). Corroded, Corroded, bent and broken labradorite + augite + hypersthene + ilmenite + titanomagnetite (EPMA). Minor alteration - could be pyroclastic.

VUW 17426 HOST: FLOAT LOC: WHAKAPAPANUI STREAM T20 / 313 194
N112 / 059 733

Orange-white, speckled nodule (65x50x50mm). Fine-grained quartz sinter + radiating needles natroalunite + minor rutile (EPMA).

VUW	17426	17427	17500	17437	17412
FIELD	BXA	G1-X	15-X	WX-2	W4-X
SiO_2	45.01	50.01	51.91	54.60	56.38
TiO_2	0.46	0.20	0.56	0.45	0.42
Al_2O_3	21.44	20.26	10.16	12.95	15.65
Fe_2O_3	0.00	1.45	12.07	8.26	1.43
FeO	0.00	5.81	0.00	0.00	6.55
MnO	0.00	0.14	0.22	0.15	0.13
MgO	0.09	8.20	14.17	10.22	8.92
CaO	0.12	11.84	9.11	8.82	5.81
Na_2O	4.65	1.51	1.24	1.83	2.55
K_2O	1.70	0.29	0.48	0.72	0.94
P_2O_5	0.09	0.03	0.05	0.05	0.08
LOI	26.19	0.00	-0.23	1.71	0.90
Total*	98.55	98.50	99.03	99.56	99.90
Ba	114	80	129	176	254
Ce	10	.	14	12	15
Cr	128	214	1046	442	334
Cu	3	95	55	97	53
Ga	5	15	12	14	17
La	6	.	5	11	5
Mn	10	.	1789	1169	1159
Nb	<2	.	<2	<2	<2
Ni	2	58	245	144	95
Pb	3	6	6	9	7
Rb	10	10	13	24	33
Sc	6	.	56	36	22
Sr	134	287	119	227	297
Th	<2	.	2	4	5
Ti	2338	.	3613	2849	2562
U	<2	<2	<2	<2	2.6
V	90	119	303	207	145
Y	<2	9	16	14	9
Zn	3	80	106	75	74
Zr	39	16	38	61	66
Mg*	100	71	73	74	71
K/Rb	1453	244	306	247	238
Rb/Sr	0.072	0.035	0.111	0.107	0.111
I	.70535	.70599	.70565	.70507	.70553

IGNEOUS XENOLITHS (TYPE IX - CUMULATE NODULES)

VUW 17427 HOST: 14801 LOC: SOUTH RUAPEHU T20 / 301 064
N122 / 050 610

Norite nodule with hypidiomorphic granular texture (slight metamorphic overprint). Bytownite + augite + bronzite. Minor hornblende + basaltic glass + pyrrhotite (EPMA).

VUW 17438 HOST: 14824 LOC: PUKEONAKE SCORIA CONE T19 / 318 256
N112 / 062 821

Norite nodule with hypidiomorphic granular texture (slight metamorphic overprint). Labradorite + augite + hypersthene + pleonaste (replacement) + dacitic glass (EPMA).

VUW 17500 HOST: 14915 LOC: S RIM WHANGAEHU GORGE T20 / 358 095
N122 / 108 645

Pyroxenite nodule with reaction rim of decomposing hornblende (25x25x20mm). Core = hypersthene-bronzite + augite; rim = hornblende + augite + plagioclase + titanomagnetite (EPMA).

VUW 17451 HOST: WHAK LOC: WHAKAPAPA SKIFIELD T20 / 312 145
N122 / 058 699

Proxenite nodule similar to core of 17500

VUW 17456 HOST: WAH LOC: SW RIM WHANGAEHU GORGE T20 / 359 096
N122 / 109 646

Pyroxenite nodule. Augite + interstitial hypersthene + plagioclase + titanomagnetite + basaltic glass (EPMA). Contact sharp, regular.. Spinel-rich & feldspathic xenolith included.

VUW 17437 HOST: WAH LOC: WAHIANOA VALLEY T20 / 335 072
N122 / 085 622

Gabbroic nodule. Plagioclase + augite + bronzite + interstitial basaltic glass.

VUW 17412 HOST: 16722 LOC: WAHIANOA VALLEY T20 / 327 068
N122 / 078 624

Gabbroic nodule (30x20x20mm). Plagioclase + augite + bronzite + interstitial basaltic glass. Similar to 17899.

VUW 17890 HOST: 14824 LOC: PUKEONAKE SCORIA CONE T19 / 318 256
N112 / 062 821

Dunite nodules. Dominantly forsteritic olivine + minor chromian spinel + bronzite (EPMA).

VUW 17891 HOST: 14824 LOC: PUKEONAKE SCORIA CONE T19 / 318 256
N112 / 062 821

Harzburgite nodule. Forsteritic olivine + bronzite + minor plagioclase + augite + chromian spinel + basaltic glass.

VUW	17430	17424	17411	17441	17421	17442	17414	17481	17420
FIELD	BX-10	B10XE	WX-5	BRX-17	B6XD	TLX-1	AXA	B10XC	B6XC
SiO_2	47.61	48.02	51.58	51.92	53.08	52.74	53.83	53.45	54.23
TiO_2	1.36	1.50	0.57	0.62	0.52	0.55	0.50	0.68	0.43
Al_2O_3	17.90	16.61	12.91	15.15	15.00	13.66	13.43	15.82	10.66
Fe_2O_3	3.13	1.73	1.41	10.15	0.93	8.96	0.89	9.89	1.28
FeO	6.08	10.93	7.69	0.00	7.27	0.00	6.96	0.00	6.80
MnO	0.13	0.29	0.15	0.19	0.19	0.14	0.12	0.19	0.18
MgO	6.59	8.52	13.89	9.54	10.21	12.72	12.83	8.62	12.76
CaO	13.15	9.14	7.92	9.92	8.76	8.77	6.66	7.65	10.15
Na_2O	2.00	1.46	1.64	1.79	2.53	1.59	1.79	2.36	2.10
K_2O	0.23	0.10	0.13	0.26	0.26	0.34	0.76	0.49	0.33
P_2O_5	0.18	0.05	0.08	0.06	0.08	0.09	0.04	0.09	0.07
LOI	1.40	1.41	1.78	0.16	0.92	0.20	1.94	0.51	0.77
Total*	100.45	100.06	99.83	100.28	100.77	99.99	100.12	99.85	99.79
Ba	125	71	146	107	129	132	141	170	114
Ce	15	13	16	9	.	10	11	16	14
Cr	268	242	1046	445	627	798	673	460	820
Cu	67	14	28	24	24	23	42	63	35
Ga	18	15	15	16	17	13	13	16	12
La	11	3	4	2	.	3	7	7	11
Mn	1199	2154	1330	1433	1213	1068	1136	1558	1432
Nb	5	<2	3	2	<2	2	<2	3	<2
Ni	71	99	395	130	173	292	334	121	257
Pb	4	6	3	3	<2	7	9	7	<2
Rb	6	2	4	6	4	10	43	19	9
Sc	48	40	36	31	26	31	31	34	43
Sr	373	210	186	249	230	300	329	266	175
Th	<2	2	2	2	<2	2	2	3	<2
Ti	7861	8665	3369	3524	3108	3454	2955	4117	2561
U	<2	<2	<2	<2	<2	2.1	<2	<2	<2
V	273	374	196	244	199	204	182	236	181
Y	23	12	15	15	14	15	16	14	13
Zn	67	106	89	87	78	84	78	107	83
Zr	66	31	52	37	35	54	47	53	42
Mg*	61	59	77	69	73	77	78	67	77
K/Rb	301	517	308	335	521	290	146	218	311
Rb/Sr	0.017	0.008	0.019	0.026	0.018	0.032	0.131	0.070	0.050
I	.70680	.70654	.70647	.70592	.70627	.70568	.70820	.70554	.70541

META-IGNEOUS XENOLITHS - TYPE MIXa (coarse)

VUW 17430 HOST: WHAK LOC: WHAKAPAPA SKIFIELD T20 / 310 150
N122 / 058 699

Coarse-grained pyroxene hornfels with strong foliation (70x50x30mm). Labradorite + hypersthene + titanomagnetite + ilmenite + apatite + glass (crowded with <1 micron microlites of augite? (EPMA).

VUW 17424 HOST: FLOAT LOC: IWIKAU MEMBER AIRFALL T20 / 328 139
N122 / 079 688

Strongly nematoblastic pyroxene hornfels (40X20X20mm). Bytownite + hypersthene + augite + ilmenite (EPMA).

VUW 17411 HOST: WAH LOC: WAHIANOA VALLEY T20 / 334 066
N122 / 085 622

Coarse-grained pyroxene hornfels (15x15x10mm). Plagioclase + coarsely poikiloblastic pyroxene. Slightly altered?

VUW 17441 HOST: WHAK LOC: BRUCE ROAD S20 / 293 161
N112 / 038 717

Coarse-grained pyroxene hornfels (15x15x10mm). Labradorite + coarsely poikiloblastic hypersthene + augite + ilmenite (EPMA).

VUW 17421 HOST: 14785 LOC: ROAD TO MEADS WALL TOW T20 / 311 154
N112 / 057 708

Coarse-grained pyroxene hornfels (55x45x35mm). Labradorite-bytownite + coarsely poikiloblastic hypersthene + augite + ilmenite (EPMA). Similar to 17441. Sharp, regular contact.

VUW 17442 HOST: WHAK LOC: TAMA LAKES T20 / 345 195
N112 / 093 755

Coarse-grained pyroxene hornfels (20x30x15mm). Bytownite + coarsely poikiloblastic bronzite + augite + chromian spinel + ilmenite (EPMA). Plagioclase has a relict trachytic texture? Sharp, regular contact.

VUW 17414 HOST: FLOAT LOC: WHAKAPAPANUI STREAM T20 / 300 184
N112 / 043 743

Coarse-grained, mortared textured pyroxene hornfels (100x100x100mm). Highly bent and altered labradorite + coarsely poikiloblastic hypersthene + augite + chromian spinel + ilmenite + minor quartz (EPMA).

VUW 17481 HOST: FLOAT LOC: IWIKAU MEMBER AIRFALL T20 / 328 139
N122 / 079 688

Coarse-grained pyroxene hornfels (20x10x5mm). Plagioclase + poikiloblastic pyroxene. Similar to 17441.

VUW	17494	17454	17417	17478	17449	17448	17495	17450
FIELD	BXKX-1	BGX-2	B5X-A	B5X-1	MX-2	MX-3	BXKX-2	MX-11
SiO_2	52.10	53.85	54.05	54.28	56.50	57.65	58.98	59.15
TiO_2	0.69	0.64	0.54	0.46	0.64	0.54	0.62	0.65
Al_2O_3	14.17	15.74	13.08	13.51	14.58	14.37	17.63	18.29
Fe_2O_3	9.56	9.04	2.17	10.75	8.37	7.86	8.01	7.40
FeO	0.00	0.00	7.78	0.00	0.00	0.00	0.00	0.00
MnO	0.15	0.18	0.21	0.20	0.16	0.18	0.11	0.14
MgO	10.48	7.64	10.01	10.34	7.77	6.81	3.86	3.47
CaO	9.76	9.34	7.79	7.58	8.35	8.11	6.53	7.47
Na_2O	2.15	2.72	2.09	2.12	2.54	3.19	2.58	2.05
K_2O	0.22	0.51	0.72	0.60	0.38	0.67	0.23	0.22
P_2O_5	0.08	0.10	0.05	0.06	0.06	0.10	0.03	0.10
LOI	0.38	0.00	1.25	-0.16	0.38	0.27	1.17	0.80
Total*	99.24	100.11	99.71	98.99	99.58	99.64	99.84	99.69
Ba	110	149	179	162	163	251	228	90
Ce	8	7	.	12	26	17	12	14
Cr	558	206	482	503	555	367	25	18
Cu	80	44	80	88	20	18	29	7
Ga	16	18	.	13	18	17	20	17
La	4	2	.	0	10	4	6	<2
Mn	1368	1266	.	1700	1182	1162	985	1084
Nb	2	<2	<2	2	2	2	2	2
Ni	147	89	117	116	46	80	15	12
Pb	6	9	10	3	8	6	11	8
Rb	5	14	26	20	9	14	2	6
Sc	36	31	.	33	28	26	24	21
Sr	242	249	231	248	368	372	259	245
Th	2	3	.	2	7	2	3	5
Ti	4207	3877	.	2913	3693	3002	3826	3853
U	<2	<2	.	<2	3.5	<2	2	<2
V	266	236	216	203	222	197	204	207
Y	18	18	15	12	18	14	12	19
Zn	77	84	97	104	81	83	93	86
Zr	59	50	46	38	63	57	66	61
Mg*	72	66	68	69	68	67	53	52
K/Rb	367	306	230	247	367	406	908	315
Rb/Sr	0.021	0.055	0.113	0.082	0.023	0.037	0.008	0.024
I	.	.70533	.70533	.	.70569	.70564	.	.70696

META-IGNEOUS XENOLITHS - TYPE MIXa (coarse)

VUW 17420 HOST: 14785 LOC: ROAD TO MEADS WALL TOW T20 / 311 154
N112 / 057 708

Coarse-grained pyroxene hornfels (55x45x35mm). Andesine + coarsely poikiloblastic hypersthene + augite + ilmenite (EPMA). Similar to 17441.

META-IGNEOUS XENOLITHS - TYPE MIXb (intermediate)

VUW 17494 HOST: WHAK LOC: WHAKAPAPA SKIFIELD T20 / 310 150
N122 / 058 699

Coarse/medium-grained pyroxene hornfels (15x15x10mm). Plagioclase + poikiloblastic pyroxene + ilmenite.

VUW 17454 HOST: WHAK LOC: SOUTH RUAPEHU T20 / -
N122 / -

Pyroxene hornfels. Labradorite-bytownite + sieved hypersthene + augite (EPMA).

VUW 17417 HOST: 14784 LOC: ROAD TO MEADS WALL TOW T20 / 309 155
N112 / 055 709

Medium-grained pyroxene hornfels (25x20x20mm). Hypidiomorphic-granular texture with plagioclase + pyroxene. Contact sharp, irregular.

VUW 17478 HOST: 14784 LOC: ROAD TO MEADS WALL TOW T20 / 309 155
N112 / 055 709

Medium-grained pyroxene hornfels (25x20x20mm). Similar to 17417.

VUW 17449 HOST: MANG LOC: UNKNOWN -
-

Medium-grained pyroxene hornfels (25x20x20mm). Andesine-labradorite + poikiloblastic hypersthene + augite + ilmenite + minor apatite + quartz (EPMA).

VUW 17448 HOST: MANG LOC: UNKNOWN -
-

Medium-grained pyroxene hornfels (25x20x20mm). Similar to 17449.

VUW 17495 HOST: WHAK LOC: WHAKAPAPA SKIFIELD T20 / 310 150
N122 / 058 699

Brown, poorly foliated fine-grained hornfels. Plagioclase + pyroxene + quartz.

VUW 17450 HOST: MANG LOC: UNKNOWN -
-

Grey, fine-grained hornfels with relict porphyritic texture. Labradorite-anorthite + hypersthene + ilmenite (EPMA).

VUW	17479	17431	17422	17433	17432	17434
FIELD	B5X-B	BX-22	BXWS	M7X-1	BX-24	T5-X
SiO_2	50.05	53.94	54.41	56.82	57.64	62.10
TiO_2	0.72	0.59	0.69	0.55	0.61	0.45
Al_2O_3	19.43	19.06	16.98	16.81	18.64	18.61
Fe_2O_3	10.61	1.73	2.05	0.57	1.31	0.94
FeO	0.00	6.87	6.00	7.02	5.67	4.39
MnO	0.21	0.12	0.17	0.15	0.10	0.08
MgO	7.90	5.49	5.02	5.32	3.86	2.06
CaO	7.75	7.21	9.12	9.91	7.29	6.14
Na_2O	2.32	3.33	3.57	1.21	2.20	3.72
K_2O	0.27	0.54	0.66	0.09	0.50	0.50
P_2O_5	0.09	0.13	0.11	0.09	0.10	0.10
LOI	0.40	0.73	0.98	1.21	1.83	0.65
TOTAL*	98.88	99.57	100.14	100.02	100.27	99.89
Ba	280	173	97	54	353	.
Ce	24	14	.	.	.	.
Cr	311	43	84	99	25	.
Cu	67	77	52	33	30	25
Ga	21	19	19	20	23	19
La	8	6	.	.	.	.
Mn	1615	1145	1223	1204	917	.
Nb	5	1	1	0	2	0
Ni	73	12	19	35	7	2
Pb	5	6	9	6	12	12
Rb	5	16	17	<2	55	3
Sc	32	20	27	24	21	.
Sr	392	379	412	194	809	362
Th	3	2	3	<2	<2	4
Ti	4353	3363	1193	3060	3498	.
U	<2	<2	<2	<2	<2	<2
V	232	182	245	201	197	.
Y	14	11	18	16	14	16
Zn	226	79	82	73	74	59
Zr	116	37	56	51	69	83
Mg*	63	58	57	60	54	45
K/Rb	492	277	319	532	76	1480
Rb/Sr	0.012	0.043	0.041	0.007	0.067	0.008
I	.	.70601	.70650	.70711	.70866	.70579

META-IGNEOUS XENOLITHS - TYPE MIXc (fine)

VUW 17479 HOST: 14784 LOC: ROAD TO MEADS WALL TOW T20 / 309 155
N112 / 055 709

Grey, homogeneous fine-grained pyroxene hornfels.
Dominantly plagioclase + pyroxene.

VUW 17431 HOST: WHAK LOC: WHAKAPAPA SKIFIELD T20 / 312 145
N122 / 058 699

Grey, homogeneous fine-grained hornfels
(30x30x10mm). Dominantly plagioclase + pyroxene.

VUW 17422 HOST: FLOAT LOC: WHAKAPAPANUI STREAM T20 / 300 184
N112 / 043 743

Grey, homogeneous fine-grained hornfels
(70x45x35mm). Andesine-labradorite + hypersthene +
pigeonite (overgrowth on hypersthene) + augite +
titanomagnetite + minor apatite + interstitial
glass (EPMA).

VUW 17433 HOST: MANG LOC: SOUTH RUAPEHU T20 / 306 092
N122 / 055 640

Grey, homogeneous fine-grained hornfels
(70x45x35mm). Bytownite-anorthite + hypersthene +
augite + ilmenite + quartz (EPMA).
Sharp, regular contact.

VUW 17432 HOST: WHAK LOC: WHAKAPAPA SKIFIELD T20 / 312 145
N122 / 058 699

Brown, poorly foliated fine-grained hornfels
(100x60x50mm). Labradorite + hypersthene + quartz (EPMA).

VUW 17434 HOST: MANG LOC: SW RIM CRATER LAKE T20 / 306 100
N122 / 055 648

Light-brown-grey, homogeneous fine-grained
hornfels (70x45x35mm). Graphic texture of
plagioclase + pyroxene + quartz.
Sharp, regular contact.

****

APPENDIX 3: ELECTRON PROBE MICROANALYSES

****

Analytical methods are detailed in Chapter 2.3.

Analyses are ordered according to VUW catalogue number.

ol	- olivine	bio	- biotite	cord	- cordierite
cpx	- clinopyroxene	chl	- chlorite	sill	- sillimanite
woll	- wollastonite	mus	- muscovite	cor	- corundum
pig	- pigeonite	hb	- hornblende	gnt	- garnet
opx	- orthopyroxene	ged	- gedrite	ilm	- ilmenite
pl	- plagioclase	preh	- prehnite	rut	- rutile
ks	- alkali feldspar	epid	- epidote	hem	- hematite
glass	- glass	ap	- apatite	tmt	- titanomagnetite
mes	- mesostasis	hal	- halite	crsp	- chromian spinel
		sph	- sphene	pleon	- pleonaste

LOC: c=core; r=rim; g=groundmass

ASSOC: mineral associations described in analysis notes.

ANAL: number of analyses i.e. 1= single analysis; m2= mean of two similar analyses etc.

All pyroxene analyses recalculated for Fe^{3+} stochiometrically.

- indicates not analysed; .00 indicates below detection limit.

$Fe^{*} = Fe^{3+} + Fe^{2+} + Mn$.

VUW: 11965 FIELD: R-C
FORMATION: RED CRATER (TONGARIRO)
LITHOLOGY: LOW-ALUMINA BASALT

MINERAL	ol	ol	cpx	cpx	cpx	opx	pl	pl	pl
LOC	c	r	c	r	c	c	c	r	g
ASSOC	-	-	-	-	1	1	-	-	-
ANAL	m2	1	m2	1	1	1	1	1	1
SiO_2	39.65	38.78	51.50	51.99	53.51	53.45	51.34	50.81	49.04
TiO_2	.00	.00	.50	.23	.15	.14	.00	.00	.00
Al_2O_3	.00	.00	3.77	2.25	1.54	1.03	29.99	30.44	31.48
Cr_2O_3	.00	.00	.23	.00	.00	.00	.00	.00	.00
Fe_2O_3	.00	.00	1.23	1.97	.94	.00	.00	.00	.00
FeO	15.57	20.78	5.56	4.18	7.90	19.69	.72	.94	.83
MnO	.13	.64	.23	.35	.27	.49	.00	.00	.00
MgO	44.76	40.45	16.03	16.79	18.97	23.07	.20	.20	.20
NiO	.10	.00	.00	.00	.00	.00	.00	.00	.00
CaO	.18	.21	21.05	21.10	16.73	1.21	14.26	14.22	15.71
Na_2O	.00	.00	.16	.20	.15	.00	3.36	3.25	2.82
K_2O	.00	.00	.00	.00	.00	.00	.17	.09	.00
Total	100.39	100.86	100.26	99.06	100.16	99.08	100.04	99.95	100.08
oxygens	4	4	6	6	6	6	8	8	8
Si	.995	.994	1.89	1.91	1.95	1.99	2.34	2.32	2.25
Ti	.000	.000	.01	.01	.00	.00	.00	.00	.00
Al	.000	.000	.16	.10	.07	.05	1.61	1.64	1.70
Cr	.000	.000	.01	.00	.00	.00	.00	.00	.00
Fe^{3+}	.000	.000	.03	.06	.03	.00	.00	.00	.00
Fe^{2+}	.327	.446	.17	.13	.24	.61	.03	.04	.03
Mn	.003	.014	.01	.01	.01	.02	.00	.00	.00
Mg	1.674	1.546	.88	.93	1.03	1.28	.01	.01	.01
Ni	.002	.000	.00	.00	.00	.00	.00	.00	.00
Ca	.005	.006	.83	.84	.66	.05	.70	.70	.77
Na	.000	.000	.01	.01	.01	.00	.30	.29	.25
K	.000	.000	.00	.00	.00	.00	.01	.01	.00
Total	3.006	3.006	4.00	4.00	4.00	4.00	5.00	5.01	5.01
endmember units									
An	-	-	-	-	-	-	69.84	70.82	75.82
Ab	-	-	-	-	-	-	29.17	28.69	24.18
Or	-	-	-	-	-	-	.99	.49	.00
Ca	.25	.30	43.08	42.71	33.35	2.46	-	-	-
Mg	83.34	76.84	45.58	47.32	52.60	65.42	-	-	-
Fe*	16.41	22.86	11.34	9.97	14.05	32.12	-	-	-
% Ilm	-	-	-	-	-	-	-	-	-
% Usp	-	-	-	-	-	-	-	-	-

VUW: 11965 FIELD: R-C
FORMATION: RED CRATER (TONGARIRO)
LITHOLOGY: LOW-ALUMINA BASALT

MINERAL	cpx#	pl	pl	cpx	opx	cpx+
LOC	c	c	r	c	c	c
ASSOC	1/pl	1	1	2	2	3
ANAL	1	1	1	1	1	1
SiO_2	50.15	55.25	50.53	52.05	52.66	49.67
TiO_2	1.10	.00	.00	.21	.00	.61
Al_2O_3	3.30	28.24	30.26	1.37	.77	4.76
Cr_2O_3	.00	.00	.00	.00	.00	.32
Fe_2O_3	3.35	.00	.00	1.37	.00	4.15
FeO	9.02	.40	.60	10.40	22.31	3.38
MnO	.48	.00	.00	.44	.59	.00
MgO	13.99	.00	.19	13.51	21.11	15.56
NiO	.00	.00	.00	.00	.00	.00
CaO	18.27	11.03	14.73	20.24	1.05	21.76
Na_2O	.67	5.39	3.05	.34	.00	.21
K_2O	.00	.23	.17	.00	.00	.00
Total	100.33	100.54	99.53	99.93	98.49	100.42
oxygens	6	8	8	6	6	6
Si	1.87	2.48	2.32	1.95	1.99	1.81
Ti	.03	.00	.00	.01	.00	.02
Al	.15	1.50	1.64	.06	.03	.21
Cr	.00	.00	.00	.00	.00	.01
Fe^{3+}	.09	.00	.00	.04	.00	.12
Fe^{2+}	.28	.02	.02	.33	.71	.10
Mn	.02	.00	.00	.01	.02	.00
Mg	.78	.00	.01	.76	1.19	.85
Ni	.00	.00	.00	.00	.00	.00
Ca	.73	.53	.73	.81	.04	.85
Na	.05	.47	.27	.03	.00	.02
K	.00	.01	.01	.00	.00	.00
Total	4.00	5.01	5.00	4.00	3.98	4.00
endmember units						
An	-	52.37	72.35	-	-	-
Ab	-	46.35	26.67	-	-	-
Or	-	1.28	.98	-	-	-
Ca	38.49	-	-	41.75	2.19	44.24
Mg	40.96	-	-	38.78	60.79	43.99
Fe*	20.55	-	-	19.47	37.02	11.77
% Ilm	-	-	-	-	-	-
% Usp	-	-	-	-	-	-

NOTES: Xenocrysts in basalt.
exsolution from pl; + rim around glomerocryst.

VUW: 14738 FIELD: A9 #
FORMATION: TE HERENGA (RUAPEHU)
LITHOLOGY: TYPE 1 BASIC ANDESITE

MINERAL	cpx	cpx	cpx	opx	opx	pl	pl	pl	tmt
LOC	c	r	g	c	r	c	r	g	g
ASSOC	-	-	-	-	-	-	-	-	-
ANAL	1	1	1	1	1	1	1	1	1
SiO_2	51.56	50.70	51.12	52.75	53.76	48.86	48.23	55.59	.00
TiO_2	.34	.47	.42	.20	.29	.00	.00	.00	12.09
Al_2O_3	2.37	3.70	1.45	1.67	1.15	31.78	31.76	27.52	2.37
Cr_2O_3	.00	.00	.00	.00	.00	.00	.00	.00	.90
Fe_2O_3	.88	3.24	1.85	.00	.29	.00	.00	.00	41.08
FeO	8.82	7.60	12.76	17.56	16.53	.81	.76	1.21	39.67
MnO	.23	.27	.41	.32	.37	.00	.00	.00	.21
MgO	14.35	14.27	14.16	24.21	25.66	.00	.00	.00	1.37
NiO	.00	.00	.00	.00	.00	.00	.00	.00	.00
CaO	19.95	20.19	16.90	1.68	1.51	16.09	16.17	10.98	.00
Na_2O	.38	.40	.31	.00	.00	2.32	2.13	5.28	.00
K_2O	.00	.00	.00	.00	.00	.05	.07	.29	.00
Total	98.88	100.84	99.38	98.39	99.56	99.91	99.12	100.87	97.69
oxygens	6	6	6	6	6	8	8	8	4
Si	1.93	1.87	1.94	1.95	1.95	2.25	2.23	2.50	.000
Ti	.01	.01	.01	.01	.01	.00	.00	.00	.346
Al	.11	.16	.07	.07	.05	1.72	1.73	1.46	.106
Cr	.00	.00	.00	.00	.00	.00	.00	.00	.027
Fe^{3+}	.03	.09	.05	.00	.01	.00	.00	.00	1.175
Fe^{2+}	.28	.24	.41	.55	.51	.03	.03	.05	1.261
Mn	.01	.01	.01	.01	.01	.00	.00	.00	.007
Mg	.80	.79	.80	1.34	1.40	.00	.00	.00	.078
Ni	.00	.00	.00	.00	.00	.00	.00	.00	.000
Ca	.80	.80	.69	.07	.06	.79	.80	.53	.000
Na	.03	.03	.02	.00	.00	.21	.19	.46	.000
K	.00	.00	.00	.00	.00	.00	.00	.02	.000
Total	4.00	4.00	4.00	4.00	4.00	5.00	4.98	5.02	3.000
endmember units									
An	-	-	-	-	-	79.04	80.46	52.58	-
Ab	-	-	-	-	-	20.66	19.14	45.73	-
Or	-	-	-	-	-	.30	.40	1.69	-
Ca	41.94	41.64	35.05	3.41	2.98	-	-	-	-
Mg	41.94	40.97	40.92	68.30	70.54	-	-	-	-
Fe*	16.12	17.39	24.03	28.29	26.48	-	-	-	-
% Ilm	-	-	-	-	-	-	-	-	-
% Usp	-	-	-	-	-	-	-	-	.380

NOTES: Analysis by W.R.Hackett; # sample similar to 17437.

VUW: 14798 FIELD: F4
FORMATION: OHAKUNE
LITHOLOGY: TYPE 5 ACID ANDESITE

MINERAL	ol	ol	cpx	cpx	cpx	opx	opx	opx	pl	pl
LOC	c	r	c	r	g	c	r	g	c	g
ASSOC	-	-	-	-	-	-	-	-	-	-
ANAL	1	1	1	1	1	1	1	1	1	1
SiO_2	40.75	40.63	53.88	53.98	50.66	55.75	55.66	52.51	49.55	51.25
TiO_2	.00	.00	.15	.11	.46	.14	.14	.23	.00	.00
Al_2O_3	.00	.00	1.51	1.11	3.16	1.38	.74	1.71	31.72	29.81
Cr_2O_3	.00	.00	.17	.28	.23	.27	.00	.00	.00	.00
Fe_2O_3	.00	.00	.00	.36	.42	.00	.64	2.97	.00	.00
FeO	12.48	13.85	6.43	5.69	10.81	12.00	12.16	12.47	.82	.95
MnO	.17	.17	.26	.16	.25	.21	.22	.30	.00	.00
MgO	47.29	45.58	17.13	17.86	15.74	29.13	29.31	26.63	.13	.13
NiO	.00	.09	.00	.00	.00	.00	.00	.00	.00	.00
CaO	.11	.15	20.11	20.27	16.38	1.51	1.60	2.15	15.27	13.79
Na_2O	.00	.00	.19	.21	.19	.00	.00	.00	2.37	3.19
K_2O	.00	.00	.00	.00	.00	.00	.00	.00	.07	.10
Total	100.80	100.47	99.83	100.03	98.30	100.39	100.47	98.97	99.93	99.02
oxygens	4	4	6	6	6	6	6	6	8	8
Si	1.002	1.009	1.98	1.97	1.92	1.97	1.97	1.92	2.27	2.25
Ti	.000	.000	.00	.00	.01	.00	.00	.01	.00	.00
Al	.000	.000	.07	.05	.14	.06	.03	.07	1.71	1.61
Cr	.000	.000	.01	.01	.01	.00	.00	.00	.00	.00
Fe^{3+}	.000	.000	.00	.01	.01	.00	.02	.08	.00	.00
Fe^{2+}	.257	.288	.20	.17	.34	.36	.36	.38	.03	.04
Mn	.004	.004	.01	.01	.01	.01	.01	.01	.00	.00
Mg	1.733	1.686	.94	.97	.89	1.54	1.55	1.45	.01	.01
Ni	.000	.002	.00	.00	.00	.00	.00	.00	.00	.00
Ca	.003	.004	.79	.79	.66	.06	.06	.08	.75	.68
Na	.000	.000	.01	.02	.01	.01	.00	.00	.21	.28
K	.000	.000	.00	.00	.00	.00	.00	.00	.00	.01
Total	2.999	2.993	4.01	4.00	4.00	4.01	4.00	4.00	4.98	4.98
endmember units										
An	-	-	-	-	-	-	-	-	77.98	70.35
Ab	-	-	-	-	-	-	-	-	21.60	29.04
Or	-	-	-	-	-	-	-	-	.42	.61
Ca	.15	.20	40.91	40.58	34.69	2.92	3.06	4.19	-	-
Mg	86.78	85.07	48.47	49.74	46.36	78.60	77.67	72.31	-	-
Fe*	13.07	14.73	10.62	9.68	18.95	18.48	19.27	23.50	-	-
% Ilm	-	-	-	-	-	-	-	-	-	-
% Usp	-	-	-	-	-	-	-	-	-	-

NOTE: Analysis by W.R.Hackett.

VUW: 14814 FIELD: E5 #
FORMATION: MANGAWHERO (RUAPEHU)
LITHOLOGY: TYPE 1 DACITE

MINERAL	cpx	cpx	cpx	opx	opx	pl	pl	tmt
LOC	c	r	g	c	r	c	g	g
ASSOC	–	–	–	–	–	–	–	–
ANAL	1	1	1	1	1	1	1	1
SiO_2	52.20	52.11	51.40	53.72	53.23	53.31	51.62	.14
TiO_2	.63	.50	.70	.28	.21	.00	.00	19.42
Al_2O_3	2.44	1.82	2.96	.87	.95	29.30	30.00	1.44
Cr_2O_3	.00	.00	.00	.00	.00	.00	.00	.00
Fe_2O_3	.00	.00	.00	.00	.83	.00	.00	28.35
FeO	10.22	10.14	10.87	20.60	19.72	.56	.93	45.90
MnO	.23	.31	.37	.47	.50	.00	.00	.40
MgO	14.11	14.43	15.03	23.47	23.45	.00	.00	1.46
NiO	.00	.00	.00	.00	.00	.00	.00	.00
CaO	19.42	20.44	17.36	1.33	1.43	11.76	13.11	.10
Na_2O	.33	.29	.24	.00	.00	4.40	3.51	.00
K_2O	.00	.00	.00	.00	.00	.21	.25	.00
Total	99.58	100.04	98.93	100.74	100.32	99.54	99.42	97.21
oxygens	6	6	6	6	6	8	8	4
Si	1.95	1.96	1.93	1.97	1.95	2.43	2.35	.005
Ti	.02	.01	.02	.01	.01	.00	.00	.556
Al	.11	.08	.13	.04	.04	1.57	1.61	.065
Cr	.00	.00	.00	.00	.00	.00	.00	.000
Fe^{3+}	.00	.00	.00	.00	.02	.00	.00	.812
Fe^{2+}	.32	.31	.34	.63	.61	.02	.04	1.462
Mn	.01	.01	.01	.02	.02	.00	.00	.013
Mg	.79	.79	.84	1.28	1.29	.00	.00	.083
Ni	.00	.00	.00	.00	.00	.00	.00	.000
Ca	.78	.81	.70	.05	.06	.57	.69	.004
Na	.02	.02	.02	.00	.00	.39	.31	.000
K	.00	.00	.00	.00	.00	.01	.02	.000
Total	4.00	3.99	3.99	4.00	4.00	4.99	5.02	3.000
endmember units								
An	–	–	–	–	–	58.89	67.92	–
Ab	–	–	–	–	–	39.88	30.60	–
Or	–	–	–	–	–	1.23	1.48	–
Ca	41.13	42.02	36.89	2.62	2.86	–	–	–
Mg	41.61	41.24	44.43	64.75	64.64	–	–	–
Fe*	17.26	16.74	18.68	32.63	32.50	–	–	–
% Ilm	–	–	–	–	–	–	–	–
% Usp	–	–	–	–	–	–	–	.580

NOTES: Analysis by W.R.Hackett; # sample similar to 14813.

VUW: 14816 FIELD: H5
FORMATION: HAUHUNGATAHI
LITHOLOGY: TYPE 5 BASIC ANDESITE

MINERAL	ol	ol	cpx	opx	pl	pl	pl	crsp#
LOC	c	r	c	c	c	r	g	c
ASSOC	-	-	-	-	-	-	-	ol
ANAL	1	1	1	m2	1	1	1	1
SiO_2	40.85	40.47	52.60	55.58	46.83	49.15	51.60	.00
TiO_2	.00	.00	.18	.15	.00	.00	.00	.51
Al_2O_3	.00	.00	2.14	1.45	33.46	32.17	30.22	11.03
Cr_2O_3	.00	.00	.31	.22	.00	.00	.00	47.28
Fe_2O_3	.00	.00	1.30	.00	.00	.00	.00	9.71
FeO	12.62	18.15	4.93	12.40	.67	.74	1.01	18.76
MnO	.20	.27	.22	.27	.00	.00	.00	.00
MgO	46.86	42.62	17.97	27.86	.13	.00	.17	9.34
NiO	.11	.00	.00	.00	.00	.00	.00	.00
CaO	.10	.14	19.53	1.77	17.71	15.84	14.01	.00
Na_2O	.00	.00	.18	.00	1.21	2.34	3.41	.00
K_2O	.00	.00	.00	.00	.00	.05	.12	.00
Total	100.74	101.65	99.36	99.70	100.01	100.29	100.54	96.63
oxygens	4	4	6	6	8	8	8	4
Si	1.006	1.012	1.93	1.98	2.16	2.25	2.34	.000
Ti	.000	.000	.01	.00	.00	.00	.00	.013
Al	.000	.000	.09	.06	1.82	1.73	1.62	.445
Cr	.000	.000	.01	.01	.00	.00	.00	1.279
Fe^{3+}	.000	.000	.04	.00	.00	.00	.00	.250
Fe^{2+}	.260	.379	.15	.37	.03	.03	.04	.537
Mn	.004	.006	.01	.01	.00	.00	.00	.000
Mg	1.720	1.588	.98	1.48	.01	.00	.01	.476
Ni	.002	.000	.00	.00	.00	.00	.00	.000
Ca	.003	.004	.77	.07	.87	.78	.68	.000
Na	.000	.000	.01	.00	.11	.21	.30	.000
K	.000	.000	.00	.00	.00	.00	.01	.000
Total	2.995	2.989	4.00	3.98	5.00	5.00	5.00	3.000
endmember units								
An	-	-	-	-	89.10	78.70	69.33	-
Ab	-	-	-	-	10.90	20.99	29.97	-
Or	-	-	-	-	-	.31	.70	-
Ca	.15	.21	39.48	3.53	-	-	-	-
Mg	86.56	80.32	50.51	76.85	-	-	-	-
Fe*	13.29	19.47	10.01	19.62	-	-	-	-
% Ilm	-	-	-	-	-	-	-	-
% Usp	-	-	-	-	-	-	-	.305

NOTE: Analysis by W.R.Hackett; # inclusion in olivine.

VUW: 14829 FIELD: J1
FORMATION: MANGAWHERO (RUAPEHU)
LITHOLOGY: TYPE 3 DACITE

MINERAL	ol	ol	cpx	cpx	opx	opx	opx	pl	pl	pl
LOC	c	r	c	r	c	r	g	c	r	g
ASSOC	-	-	-	-	-	-	-	-	-	-
ANAL	1	1	1	1	1	1	1	1	1	1
SiO_2	39.92	39.62	52.95	52.10	48.76	50.92	52.64	55.09	53.71	55.22
TiO_2	.00	.00	.62	.64	.27	.13	.35	.00	.00	.00
Al_2O_3	.00	.00	2.19	2.36	5.54	1.13	3.30	27.53	28.99	28.16
Cr_2O_3	.00	.00	.45	.00	.00	.00	.00	.00	.00	.00
Fe_2O_3	.00	.00	.00	.00	1.47	.97	.00	.00	.00	.00
FeO	13.96	19.23	6.63	9.16	21.75	23.76	17.24	.54	.55	.56
MnO	.14	.23	.21	.27	.00	.64	.42	.00	.00	.00
MgO	45.83	41.39	16.58	14.78	20.55	19.80	24.05	.00	.00	.00
NiO	.55	.33	.00	.00	.00	.00	.00	.00	.00	.00
CaO	.00	.00	19.90	19.83	.15	1.03	1.28	10.70	11.91	11.25
Na_2O	.00	.00	.40	.30	.00	.00	.00	5.00	4.52	4.96
K_2O	.00	.00	.00	.00	.00	.00	.00	.47	.35	.42
Total	100.40	100.80	99.93	99.44	98.49	98.38	99.28	99.33	100.03	100.67

oxygens	4	4	6	6	6	6	6	8	8	8
Si	.995	1.005	1.94	1.94	1.84	1.97	1.94	2.52	2.43	2.48
Ti	.000	.000	.02	.02	.01	.00	.01	.00	.00	.00
Al	.000	.000	.10	.10	.25	.05	.13	1.46	1.55	1.49
Cr	.000	.000	.01	.00	.00	.00	.00	.00	.00	.00
Fe^{3+}	.000	.000	.00	.29	.04	.03	.00	.00	.00	.00
Fe^{2+}	.291	.408	.20	.01	.69	.76	.53	.02	.02	.03
Mn	.003	.005	.01	.82	.00	.02	.01	.00	.00	.00
Mg	1.702	1.566	.91	.79	1.16	1.13	1.32	.00	.00	.00
Ni	.011	.007	.00	.00	.00	.00	.00	.00	.00	.00
Ca	.000	.000	.78	.02	.01	.04	.05	.52	.58	.54
Na	.000	.000	.03	.00	.00	.00	.00	.44	.40	.43
K	.000	.000	.00	.00	.00	.00	.00	.03	.02	.02
Total	3.002	2.991	4.00	3.99	4.00	4.00	3.99	4.99	5.00	4.99

endmember units										
An	-	-	-	-	-	-	-	52.90	58.09	54.26
Ab	-	-	-	-	-	-	-	44.35	39.90	43.33
Or	-	-	-	-	-	-	-	2.75	2.01	2.41
Ca	-	-	41.19	41.08	3.16	2.11	2.67	-	-	-
Mg	85.27	79.13	47.76	42.58	61.15	57.01	68.93	-	-	-
Fe*	14.73	20.87	11.05	16.34	35.69	40.88	28.40	-	-	-
% Ilm	-	-	-	-	-	-	-	-	-	-
% Usp	-	-	-	-	-	-	-	-	-	-

NOTE: Analysis by W.R.Hackett.

VUW: 14848 FIELD: H7
FORMATION: PUKEONAKE
LITHOLOGY: TYPE 6 ACID ANDESITE

MINERAL	ol	ol	cpx	cpx	cpx	opx	opx	pl	pl	pl
LOC	c	r	c	r	g	c	r	c	r	g
ASSOC	-	-	-	-	-	-	-	-	-	-
ANAL	1	1	m2	m2	m2	m3	m2	m3	1	1
SiO_2	41.22	40.40	53.01	53.44	52.63	53.76	55.08	57.17	51.58	53.47
TiO_2	.00	.00	.43	.46	.60	.25	.29	.00	.00	.00
Al_2O_3	.00	.00	2.24	2.00	2.19	1.56	1.61	27.42	30.63	28.39
Cr_2O_3	.00	.00	.24	.36	.18	.11	.06	.00	.00	.00
Fe_2O_3	.00	.00	.07	.00	1.08	.00	.00	.00	.00	.00
FeO	6.05	12.32	8.82	6.87	7.03	18.21	14.57	.49	.48	.69
MnO	.00	.14	.16	.19	.19	.28	.30	.00	.00	.00
MgO	51.38	46.71	16.04	17.29	16.77	23.82	26.35	.06	.15	.19
NiO	.62	.43	.00	.00	.00	.04	.00	.00	.00	.00
CaO	.08	.14	19.16	18.85	19.54	1.91	1.96	10.95	13.70	12.28
Na_2O	.00	.00	.35	.25	.29	.04	.00	4.74	3.40	4.12
K_2O	.00	.00	.00	.00	.00	.00	.00	.48	.20	.27
Total	99.35	100.14	100.52	99.71	100.50	99.98	100.22	101.31	100.14	99.41
oxygens	4	4	6	6	6	6	6	8	8	8
Si	1.001	1.002	1.94	1.96	1.93	1.97	1.98	2.54	2.34	2.44
Ti	.000	.000	.01	.01	.02	.01	.01	.00	.00	.00
Al	.000	.000	.10	.09	.10	.07	.07	1.44	1.64	1.53
Cr	.000	.000	.01	.01	.01	.00	.00	.00	.00	.00
Fe^{3+}	.000	.000	.00	.00	.03	.00	.00	.00	.00	.00
Fe^{2+}	.123	.255	.27	.21	.22	.56	.44	.02	.02	.03
Mn	.000	.003	.01	.01	.01	.01	.01	.00	.00	.00
Mg	1.860	1.726	.87	.95	.92	1.30	1.41	.00	.01	.01
Ni	.012	.009	.00	.00	.00	.00	.00	.00	.00	.00
Ca	.002	.004	.76	.74	.77	.08	.08	.52	.67	.60
Na	.000	.000	.03	.02	.02	.00	.00	.41	.30	.37
K	.000	.000	.00	.00	.00	.00	.00	.03	.01	.02
Total	2.998	2.999	4.00	4.00	4.00	4.00	4.00	4.96	4.99	5.00
endmember units										
An	-	-	-	-	-	-	-	54.56	68.45	61.67
Ab	-	-	-	-	-	-	-	42.52	30.33	36.72
Or	-	-	-	-	-	-	-	2.81	1.22	1.61
Ca	.10	.20	39.34	38.73	39.58	3.85	3.88	-	-	-
Mg	93.74	86.88	46.17	49.40	47.21	66.86	72.92	-	-	-
Fe*	6.16	12.92	14.49	11.87	13.21	29.29	23.20	-	-	-
% Ilm	-	-	-	-	-	-	-	-	-	-
% Usp	-	-	-	-	-	-	-	-	-	-

NOTES: Analysis by W.R.Hackett.

VUW: 14848 FIELD: H7
FORMATION: PUKEONAKE
LITHOLOGY: TYPE 6 ACID ANDESITE

MINERAL	tmt	crsp	crsp
LOC	c	c	c
ASSOC	-	-	-
ANAL	1	1	1
SiO_2	.28	.24	.00
TiO_2	13.48	1.62	.44
Al_2O_3	.81	6.52	9.95
Cr_2O_3	.00	49.78	51.58
Fe_2O_3	38.93	8.82	7.01
FeO	41.51	29.59	19.81
MnO	.31	.00	.00
MgO	.55	3.37	8.78
NiO	.00	.00	.00
CaO	.15	.00	.00
Na_2O	.00	.00	.00
K_2O	.00	.00	.00
Total	96.02	99.94	97.57
oxygens	4	4	4
Si	.011	.009	.000
Ti	.397	.043	.011
Al	.037	.272	.401
Cr	.000	1.389	1.394
Fe^{3+}	1.147	.235	.183
Fe^{2+}	1.360	.874	.564
Mn	.010	.000	.000
Mg	.032	.178	.447
Ni	.000	.000	.000
Ca	.006	.000	.000
Na	.000	.000	.000
K	.000	.000	.000
Total	3.000	3.000	3.000
endmember units			
An	-	-	-
Ab	-	-	-
Or	-	-	-
Ca	-	-	-
Mg	-	-	-
Fe*	-	-	-
% Ilm	-	-	-
% Usp	.408	.711	.428

VUW: 14850 FIELD: L6
FORMATION: MANGAWHERO (RUAPEHU)
LITHOLOGY: TYPE 1 BASIC ANDESITE

MINERAL	ol	ol	cpx	cpx	opx	opx	pl	pl	tmt#	crsp+
LOC	c	r	c	r	c	r	c	r	c	c
ASSOC	-	-	-	-	-	-	-	-	opx	ol
ANAL	1	1	m2	1	m2	1	1	1	m2	1
SiO_2	40.78	40.63	51.72	51.41	53.35	53.20	51.56	50.89	.06	.00
TiO_2	.00	.00	.54	.57	.21	.29	.00	.00	9.68	.55
Al_2O_3	.00	.00	2.96	2.95	1.96	1.69	30.54	31.04	4.71	16.91
Cr_2O_3	.00	.00	.00	.00	.00	.00	.00	.00	.50	45.71
Fe_2O_3	.00	.00	.46	.00	.00	.00	.00	.00	44.46	6.62
FeO	12.47	12.97	8.82	10.06	18.18	19.60	.48	.62	35.42	19.53
MnO	.14	.13	.21	.25	.38	.50	.00	.00	.33	.00
MgO	46.67	45.52	14.44	14.04	24.53	22.99	.00	.00	3.02	10.08
NiO	.35	.25	.00	.00	.00	.00	.00	.00	.06	.00
CaO	.12	.17	20.13	19.72	1.48	1.70	14.20	14.83	.00	.00
Na_2O	.00	.00	.38	.28	.00	.00	3.11	2.95	.00	.00
K_2O	.00	.00	.00	.00	.00	.00	.11	.10	.00	.00
Total	100.53	99.67	99.66	99.28	100.09	99.97	100.00	100.43	98.24	99.40
oxygens	4	4	6	6	6	6	8	8	4	4
Si	1.005	1.012	1.92	1.92	1.94	1.97	2.34	2.31	.002	.000
Ti	.000	.000	.02	.02	.01	.01	.00	.00	.269	.013
Al	.000	.000	.13	.13	.09	.07	1.64	1.66	.205	.644
Cr	.000	.000	.00	.00	.00	.00	.00	.00	.115	1.168
Fe^{3+}	.000	.000	.01	.00	.00	.00	.00	.00	1.238	.161
Fe^{2+}	.257	.270	.28	.32	.56	.60	.02	.02	1.093	.528
Mn	.003	.003	.01	.01	.01	.02	.00	.00	.010	.000
Mg	1.715	1.690	.80	.79	1.34	1.26	.00	.00	.002	.000
Ni	.007	.005	.00	.00	.00	.00	.00	.00	.166	.486
Ca	.003	.005	.80	.79	.06	.07	.69	.72	.000	.000
Na	.000	.000	.03	.02	.00	.00	.27	.26	.000	.000
K	.000	.000	.00	.00	.00	.00	.01	.01	.000	.000
Total	2.990	2.985	4.00	4.00	4.00	4.00	4.97	4.98	3.000	3.000
endmember units										
An	-	-	-	-	-	-	71.16	73.08	-	-
Ab	-	-	-	-	-	-	28.22	26.32	-	-
Or	-	-	-	-	-	-	.62	.60	-	-
Ca	.15	.25	42.29	41.69	2.96	3.44	-	-	-	-
Mg	86.75	85.91	42.18	41.27	68.13	64.77	-	-	-	-
Fe*	13.10	13.84	15.53	17.04	28.91	31.79	-	-	-	-
% Ilm	-	-	-	-	-	-	-	-	-	-
% Usp	-	-	-	-	-	-	-	-	.306	.514

NOTES: Analysis by W.R.Hackett.
inclusion in opx; + inclusion in ol.

VUW: 14855 FIELD: L10
FORMATION: MANGAWHERO (RUAPEHU)
LITHOLOGY: LOW-ALUMINA BASALT

MINERAL	ol	ol	cpx	cpx	opx	opx	pl	pl	tmt	crsp#
LOC	c	r	c	r	c	r	c	r	g	c
ASSOC	-	-	-	-	-	-	-	-	-	ol
ANAL	m2	1	m3	m2	m4	1	1	1	1	m2
SiO_2	40.90	39.53	51.14	52.55	53.21	55.24	50.67	48.70	.10	.06
TiO_2	.00	.00	.45	.31	.21	.21	.00	.00	12.83	.55
Al_2O_3	.06	.00	3.67	2.25	1.82	1.03	29.86	31.82	.86	10.68
Cr_2O_3	.00	.00	.22	.27	.03	.13	.00	.00	.10	49.36
Fe_2O_3	.00	.00	1.00	.32	1.27	.00	.00	.00	40.04	10.00
FeO	10.91	19.33	7.99	8.21	16.11	13.89	.66	.66	40.25	18.01
MnO	.13	.28	.18	.17	.33	.29	.00	.00	.38	.00
MgO	46.97	40.84	14.77	15.82	25.34	27.56	.11	.14	.60	10.31
NiO	.34	.00	.00	.06	.03	.00	.00	.00	.10	.13
CaO	.15	.17	19.93	19.83	1.70	.24	14.34	16.28	.22	.00
Na_2O	.00	.00	.33	.24	.00	.00	3.24	2.28	.00	.00
K_2O	.00	.00	.00	.00	.00	.00	.09	.06	.00	.00
Total	99.46	100.15	99.68	100.04	100.05	100.59	98.97	99.94	95.50	99.10
oxygens	4	4	6	6	6	6	8	8	4	4
Si	1.013	1.010	1.90	1.93	1.93	1.96	2.34	2.24	.004	.000
Ti	.000	.000	.01	.01	.01	.01	.00	.00	.380	.014
Al	.000	.000	.16	.10	.08	.04	1.62	1.72	.040	.419
Cr	.000	.000	.01	.01	.00	.00	.00	.00	.003	1.298
Fe^{3+}	.000	.000	.03	.01	.04	.00	.00	.00	1.189	.254
Fe^{2+}	.226	.413	.25	.25	.49	.42	.03	.03	1.324	.499
Mn	.003	.006	.01	.01	.01	.01	.00	.00	.013	.000
Mg	1.733	1.556	.82	.87	1.37	1.47	.01	.01	.035	.512
Ni	.007	.000	.00	.00	.00	.00	.00	.00	.003	.004
Ca	.004	.005	.79	.79	.07	.09	.71	.80	.009	.000
Na	.000	.000	.02	.02	.00	.00	.29	.20	.000	.000
K	.000	.000	.00	.00	.00	.00	.01	.00	.000	.000
Total	2.986	2.990	4.00	4.00	4.00	4.00	5.01	5.00	3.000	3.000
endmember units										
An	-	-	-	-	-	-	70.85	79.67	-	-
Ab	-	-	-	-	-	-	28.66	19.94	-	-
Or	-	-	-	-	-	-	.49	.39	-	-
Ca	.20	.25	41.79	40.59	3.38	4.34	-	-	-	-
Mg	88.19	78.59	43.05	45.14	69.49	74.04	-	-	-	-
Fe*	11.61	21.16	15.16	14.27	27.13	21.62	-	-	-	-
% Ilm	-	-	-	-	-	-	-	-	-	-
% Usp	-	-	-	-	-	-	-	-	.388	.294

NOTE: Analysis by W.R.Hackett; # inclusion in ol.

VUW: 14867 FIELD: M5
FORMATION: WAHIANOA (RUAPEHU)
LITHOLOGY: TYPE 1 ACID ANDESITE

MINERAL	cpx	pig	opx	opx	opx	pl	pl	tmt
LOC	g	g	c	r	g	c	r	g
ASSOC	-	-	-	-	-	-	-	-
ANAL	1	1	1	1	m2	1	1	1
SiO_2	51.67	51.25	53.39	52.00	52.12	53.41	53.79	.10
TiO_2	.43	.29	.16	.35	.27	.00	.00	15.74
Al_2O_3	1.05	.55	1.31	1.02	.97	28.28	28.86	1.65
Cr_2O_3	.00	.00	.00	.00	.00	.00	.00	.36
Fe_2O_3	1.61	.93	.00	.00	1.77	.00	.00	35.35
FeO	13.35	24.65	16.30	22.47	21.05	.64	.88	43.72
MnO	.49	.77	.31	.58	.52	.00	.00	.44
MgO	14.22	17.40	25.59	20.65	21.72	.00	.00	.91
NiO	.00	.00	.00	.00	.00	.00	.00	.00
CaO	17.00	4.01	1.31	1.59	1.76	12.21	11.57	.00
Na_2O	.26	.00	.00	.00	.00	4.69	4.86	.00
K_2O	.00	.00	.00	.00	.00	.21	.23	.00
Total	100.08	99.85	98.37	98.66	100.18	100.44	100.19	98.27
oxygens	6	6	6	6	6	8	8	4
Si	1.94	1.96	1.97	1.96	1.94	2.41	2.43	.004
Ti	.01	.01	.00	.01	.01	.00	.00	.449
Al	.05	.03	.06	.05	.04	1.56	1.54	.074
Cr	.00	.00	.00	.00	.00	.00	.00	.011
Fe^{3+}	.05	.03	.00	.00	.05	.00	.00	1.010
Fe^{2+}	.42	.79	.50	.71	.66	.02	.03	1.386
Mn	.02	.03	.01	.02	.02	.00	.00	.014
Mg	.80	.98	1.41	1.17	1.21	.00	.00	.052
Ni	.00	.00	.00	.00	.00	.00	.00	.000
Ca	.69	.17	.05	.09	.07	.59	.56	.000
Na	.02	.00	.00	.00	.00	.41	.43	.000
K	.00	.00	.00	.00	.00	.01	.01	.000
Total	4.00	4.00	4.00	4.00	4.00	5.01	5.00	3.000
endmember units								
An	-	-	-	-	-	58.28	56.00	-
Ab	-	-	-	-	-	40.53	42.60	-
Or	-	-	-	-	-	1.19	1.40	-
Ca	34.89	8.25	2.64	4.28	3.54	-	-	-
Mg	40.57	49.68	71.37	58.84	60.33	-	-	-
Fe*	24.54	42.07	25.99	36.88	36.13	-	-	-
% Ilm	-	-	-	-	-	-	-	.479
% Usp	-	-	-	-	-	-	-	-

NOTES: Analysis by W.R.Hackett.

VUW: 14880 FIELD: M17
FORMATION: MANGAWHERO (RUAPEHU)
LITHOLOGY: TYPE 6 ACID ANDESITE

MINERAL	ol	ol	cpx	cpx	opx	opx	opx	pl	pl	crsp
LOC	c	r	c	r	c	r	g	c	r	c
ASSOC	-	-	-	-	-	-	-	-	-	-
ANAL	1	1	1	1	1	m2	1	1	1	1
SiO_2	41.56	40.80	51.00	52.64	53.43	56.45	56.94	52.80	53.84	.00
TiO_2	.00	.00	.83	.28	.12	.14	.10	.00	.00	.15
Al_2O_3	.00	.00	2.27	1.51	1.46	1.41	1.23	28.90	28.21	4.57
Cr_2O_3	.00	.00	.14	.00	.20	.30	.81	.00	.00	55.68
Fe_2O_3	.00	.00	1.44	1.94	.30	.00	.12	.00	.00	10.40
FeO	7.67	9.23	9.25	5.20	17.72	9.08	6.26	.72	.70	16.95
MnO	.00	.20	.25	.23	.31	.17	.14	.00	.00	.00
MgO	50.40	49.97	14.88	17.96	24.52	31.03	33.49	.00	.00	9.84
NiO	.24	.19	.00	.00	.00	.06	.00	.00	.00	.11
CaO	.07	.13	18.52	19.32	1.77	1.90	1.62	12.76	11.82	.00
Na_2O	.00	.00	.42	.22	.00	.00	.00	3.86	4.39	.00
K_2O	.00	.00	.00	.00	.00	.00	.00	.35	.41	.00
Total	99.94	100.52	99.00	99.30	99.83	100.54	100.71	99.39	99.37	97.70
oxygens	4	4	6	6	6	6	6	8	8	4
Si	1.008	.994	1.92	1.93	1.96	1.97	1.96	2.41	2.46	.000
Ti	.000	.000	.02	.01	.00	.00	.00	.00	.00	.004
Al	.000	.000	.10	.07	.06	.06	.05	1.56	1.52	.187
Cr	.000	.000	.00	.00	.01	.01	.02	.00	.00	1.531
Fe^{3+}	.000	.000	.04	.05	.01	.00	.00	.00	.00	.274
Fe^{2+}	.156	.188	.29	.16	.54	.27	.18	.03	.03	.491
Mn	.000	.004	.01	.01	.01	.01	.01	.00	.00	.000
Mg	1.822	1.814	.84	.99	1.34	1.61	1.72	.00	.00	.510
Ni	.005	.004	.00	.00	.00	.00	.00	.00	.00	.003
Ca	.002	.003	.75	.76	.07	.07	.06	.63	.58	.000
Na	.000	.000	.03	.02	.00	.00	.00	.34	.39	.000
K	.000	.000	.00	.00	.00	.00	.00	.02	.02	.000
Total	2.993	3.007	4.00	4.00	4.00	4.00	4.00	5.00	4.99	3.000
endmember units										
An	-	-	-	-	-	-	-	63.32	58.38	-
Ab	-	-	-	-	-	-	-	34.65	39.19	-
Or	-	-	-	-	-	-	-	2.03	2.43	-
Ca	.10	.15	38.79	38.71	3.54	3.62	3.05	-	-	-
Mg	92.04	90.31	43.35	50.08	67.73	82.23	87.43	-	-	-
Fe*	7.86	9.54	17.86	11.21	28.73	14.15	9.52	-	-	-
% Ilm	-	-	-	-	-	-	-	-	-	-
% Usp	-	-	-	-	-	-	-	-	-	.092

NOTES: Analysis by W.R.Hackett.

VUW: 17410 FIELD: WX-4
FORMATION: WAHIANOA (RUAPEHU)
LITHOLOGY: TYPE QPXd XENOLITH

MINERAL	ol	opx	pl	pl	bio	pleon	cpx	opx
LOC	c	c	c	c	c	c	c	c
ASSOC	-	-	-	-	-	-	1	1
ANAL	m3	m3	1	1	m3	m5	1	1
SiO_2	35.84	50.09	44.38	48.71	38.14	.08	50.93	51.54
TiO_2	.00	.42	.00	.00	6.99	1.24	.38	.31
Al_2O_3	.00	3.60	35.77	31.87	13.68	51.39	1.33	.60
Cr_2O_3	.00	.00	.00	.00	.00	.00	.00	.00
Fe_2O_3	.00	.67	.00	.00	.00	10.99	.00	.00
FeO	32.91	23.19	.20	.43	8.67	25.03	15.33	25.90
MnO	1.16	1.09	.00	.00	.00	.66	.98	1.08
MgO	29.61	19.78	.06	.00	18.01	10.04	11.47	17.89
CaO	.00	.56	19.26	15.16	.00	.00	18.59	1.69
Na_2O	.00	.00	.49	2.76	.85	.00	.13	.00
K_2O	.00	.00	.00	.27	9.34	.00	.00	.00
Total	99.52	99.40	100.16	99.20	95.68	99.43	99.14	99.01
oxygens	4	6	8	8	22	4	6	6
Si	.991	1.89	2.05	2.25	5.53	.002	1.96	1.99
Ti	.000	.01	.00	.00	.76	.026	.01	.01
Al	.000	.16	1.94	1.73	2.34	1.710	.06	.03
Cr	.000	.00	.00	.00	.00	.000	.00	.00
Fe^{3+}	.000	.02	.00	.00	.00	.233	.00	.00
Fe^{2+}	.761	.74	.01	.02	1.05	.591	.49	.84
Mn	.027	.04	.00	.00	.00	.016	.03	.04
Mg	1.220	1.12	.01	.00	3.89	.422	.66	1.03
Ca	.000	.02	.95	.75	.00	.000	.77	.07
Na	.000	.00	.04	.25	.24	.000	.01	.00
K	.000	.00	.00	.02	1.73	.000	.00	.00
Total	2.999	4.01	5.00	5.02	15.54	3.000	3.99	4.01
endmember units								
An	-	-	95.60	74.01	-	-	-	-
Ab	-	-	4.40	24.41	-	-	-	-
Or	-	-	.00	1.58	-	-	-	-
Ca	.00	1.19	-	-	.00	-	39.32	3.56
Mg	60.76	57.91	-	-	78.74	-	33.74	52.21
Fe*	39.24	40.90	-	-	2.26	-	26.92	44.23
% Ilm	-	-	-	-	-	-	-	-
% Usp	-	-	-	-	-	.519	-	-

NOTES: Association 1: coexisting pyroxenes at edge of xenolith (probably host).

VUW: 17413   FIELD: XX
FORMATION: WAHIANOA (RUAPEHU)
LITHOLOGY: TYPE IX XENOLITH (PYROCLASTIC?)

MINERAL	cpx	opx	opx#	pl	pl	ilm	tmt
LOC	c	c	c	c	c	c	c
ASSOC	1	-	1	-	-	-	-
ANAL	1	M5	1	1	1	1	1
SiO_2	52.09	52.21	52.63	54.37	53.65	.00	.13
TiO_2	.54	.29	.31	.00	.00	46.26	15.31
Al_2O_3	1.73	.96	.91	27.66	29.36	.31	3.07
Cr_2O_3	.00	.00	.00	.00	.00	.00	1.53
Fe_2O_3	1.71	1.74	.68	.00	.00	13.17	32.22
FeO	9.05	19.94	20.47	.38	.38	34.81	40.61
MnO	.31	.54	.40	.00	.00	.30	.28
MgO	14.72	22.55	22.55	.10	.08	3.64	2.43
CaO	20.22	1.57	1.67	11.20	12.13	.00	.00
Na_2O	.27	.00	.00	5.09	4.59	.00	.00
K_2O	.00	.00	.00	.22	.18	.00	.00
Total	100.64	99.80	99.62	99.02	100.37	98.49	95.58
oxygens	6	6	6	8	8	3	4
Si	1.91	1.95	1.96	2.48	2.41	.000	.005
Ti	.02	.01	.01	.00	.00	.871	.440
Al	.08	.04	.04	1.49	1.56	.009	.138
Cr	.00	.00	.00	.00	.00	.000	.046
Fe^{3+}	.05	.05	.02	.00	.00	.249	.926
Fe^{2+}	.28	.62	.64	.01	.02	.729	1.297
Mn	.01	.02	.01	.00	.00	.006	.009
Mg	.81	1.25	1.25	.01	.01	.136	.138
Ca	.80	.06	.07	.55	.59	.000	.000
Na	.02	.00	.00	.45	.40	.000	.000
K	.00	.00	.00	.01	.01	.000	.000
Total	4.00	4.00	4.00	5.00	5.00	2.000	3.000
endmember units							
An	-	-	-	54.55	58.96	-	-
Ab	-	-	-	44.17	40.04	-	-
Or	-	-	-	1.28	1.00	-	-
Ca	41.05	3.14	3.37	-	-	-	-
Mg	41.62	62.52	62.95	-	-	-	-
Fe*	17.33	34.34	33.68	-	-	-	-
% Ilm	-	-	-	-	-	.865	-
% Usp	-	-	-	-	-	-	.506

NOTE: # exsolution blebs in cpx (association 1).

VUW: 17414 FIELD: AXA
FORMATION: TE HERENGA (RUAPEHU)
LITHOLOGY: TYPE MIXa XENOLITH

MINERAL	cpx	cpx	opx	opx	pl	ilm	crsp
LOC	c	c	c	c	c	c	c
ASSOC	-	-	-	-	-	-	-
ANAL	1	1	1	1	m3	1	1
SiO_2	52.88	53.24	53.34	53.65	53.89	.07	.09
TiO_2	.17	.31	.19	.23	.00	50.66	.35
Al_2O_3	.62	.69	.76	.73	28.80	.11	9.88
Cr_2O_3	.00	.00	.00	.00	.00	1.18	52.87
Fe_2O_3	1.03	1.00	.22	1.16	.00	3.95	6.26
FeO	7.27	5.78	20.33	17.43	.21	39.15	23.38
MnO	.25	.17	.53	.32	.00	.32	.00
MgO	15.53	15.87	23.44	25.50	.05	3.46	6.51
NiO	.00	.00	.00	.00	.00	.00	.55
CaO	21.54	22.50	1.00	.90	11.31	.00	.08
Na_2O	.13	.19	.00	.00	4.88	.00	.00
K_2O	.00	.00	.00	.00	.31	.00	.00
Total	99.42	99.75	99.81	99.92	99.45	98.90	99.97
oxygens	6	6	6	6	8	3	4
Si	1.96	1.96	1.97	1.96	2.45	.002	.003
Ti	.01	.01	.01	.01	.00	.948	.009
Al	.03	.03	.03	.03	1.54	.003	.396
Cr	.00	.00	.00	.00	.00	.023	1.420
Fe^{3+}	.03	.03	.01	.03	.00	.074	.160
Fe^{2+}	.23	.18	.63	.53	.01	.815	.664
Mn	.01	.01	.02	.01	.00	.007	.000
Mg	.86	.88	1.29	1.39	.00	.128	.330
Ni	.00	.00	.00	.00	.00	.000	.015
Ca	.86	.89	.04	.04	.55	.000	.003
Na	.01	.01	.00	.00	.43	.000	.000
K	.00	.00	.00	.00	.02	.000	.000
Total	4.00	4.00	4.00	4.00	5.00	2.000	3.000
endmember units							
An	-	-	-	-	55.29	-	-
Ab	-	-	-	-	42.91	-	-
Or	-	-	-	-	1.80	-	-
Ca	43.28	45.07	2.01	1.75	-	-	-
Mg	43.43	44.37	65.12	69.50	-	-	-
Fe*	13.29	10.56	32.87	28.75	-	-	-
% Ilm	-	-	-	-	-	.960	-
% Usp	-	-	-	-	-	-	.475

VUW: 17415 FIELD: A11-X
FORMATION: TE HERENGA (RUAPEHU)
LITHOLOGY: TYPE QPXb XENOLITH

MINERAL	opx	opx	pl	tmt	tmt	pleon
LOC	c	c	c	c	c	c
ASSOC	1	1	1	1	1	1
ANAL	m3	m3	m9	1	1	m4
SiO_2	52.17	49.57	56.24	.10	.06	.05
TiO_2	.28	.43	.09	12.29	13.23	.97
Al_2O_3	3.11	6.19	27.45	11.15	6.80	52.12
Cr_2O_3	.00	.00	.00	.00	.00	.00
Fe_2O_3	1.74	3.47	.00	33.36	35.90	12.28
FeO	16.21	14.87	.35	36.87	38.99	21.56
MnO	.42	.51	.00	.32	.38	.27
MgO	25.61	24.69	.00	4.50	3.09	12.51
CaO	.27	.23	9.80	.00	.00	.00
Na_2O	.00	.00	5.99	.00	.00	.00
K_2O	.00	.00	.13	.00	.00	.00
Total	99.81	99.96	100.05	98.59	98.45	99.76
oxygens	6	6	8	4	4	4
Si	1.90	1.81	2.53	.004	.002	.001
Ti	.01	.01	.00	.325	.362	.020
Al	.13	.27	1.46	.462	.291	1.701
Cr	.00	.00	.00	.000	.000	.000
Fe^{3+}	.05	.10	.00	.881	.982	.256
Fe^{2+}	.49	.45	.01	1.082	1.185	.499
Mn	.01	.02	.00	.010	.012	.006
Mg	1.39	1.34	.00	.236	.167	.516
Ca	.01	.01	.47	.000	.000	.000
Na	.00	.00	.52	.000	.000	.000
K	.00	.00	.01	.000	.000	.000
Total	4.00	4.00	5.00	3.000	3.000	3.000
endmember units						
An	-	-	47.11	-	-	-
Ab	-	-	52.10	-	-	-
Or	-	-	.79	-	-	-
Ca	.46	.47	-	-	-	-
Mg	71.15	70.06	-	-	-	-
Fe*	28.39	29.47	-	-	-	-
% Ilm	-	-	-	-	-	-
% Usp	-	-	-	.478	.453	.371

NOTES: Association 1: main area of xenolith.

VUW: 17415 FIELD: A11-X
FORMATION: TE HERENGA (RUAPEHU)
LITHOLOGY: TYPE QPXb XENOLITH

MINERAL	opx	opx	opx	pl	pl	pl	glass	ilm	tmt
LOC	c	r	c	c	c	r	c	c	c
ASSOC	2	2	2	2	2	2	2	2	2
ANAL	1	1	1	1	1	1	1	1	1
SiO_2	53.15	50.30	49.34	55.43	56.51	63.14	75.05	.00	.10
TiO_2	.21	.48	.56	.00	.00	.00	.95	44.74	9.99
Al_2O_3	.89	5.15	6.98	27.53	27.17	22.26	13.20	.30	3.80
Cr_2O_3	.00	.00	.00	.00	.00	.00	.00	.00	.46
Fe_2O_3	1.22	2.64	3.20	.00	.00	.00	.00	15.66	44.11
FeO	18.16	15.11	14.97	.45	.37	.38	.85	33.84	36.98
MnO	.46	.50	.36	.00	.00	.00	.00	.61	.47
MgO	24.07	25.02	24.57	.07	.00	.00	.20	3.24	1.96
CaO	1.75	.29	.27	10.48	9.63	4.23	.33	.00	.00
Na_2O	.00	.00	.00	5.74	6.14	8.70	.99	.00	.00
K_2O	.00	.00	.00	.27	.23	.76	2.12	.00	.00
Total	99.91	99.49	100.25	99.97	100.05	99.47	93.69	98.39	97.87
oxygens	6	6	6	8	8	8	-	3	4
Si	1.96	1.84	1.79	2.50	2.54	2.82	-	.000	.004
Ti	.01	.01	.02	.00	.00	.00	-	.846	.282
Al	.04	.22	.30	1.46	1.44	1.17	-	.009	.168
Cr	.00	.00	.00	.00	.00	.00	-	.000	.014
Fe^{3+}	.03	.07	.09	.00	.00	.00	-	.297	1.246
Fe^{2+}	.56	.46	.46	.02	.01	.01	-	.713	1.161
Mn	.01	.02	.01	.00	.00	.00	-	.013	.015
Mg	1.32	1.36	1.33	.01	.00	.00	-	.122	.110
Ca	.07	.01	.01	.51	.46	.20	-	.000	.000
Na	.00	.00	.00	.50	.54	.75	-	.000	.000
K	.00	.00	.00	.02	.01	.04	-	.000	.000
Total	4.00	4.00	4.00	5.02	5.00	4.99	-	2.000	3.000
endmember units									
An	-	-	-	49.71	45.80	20.26	-	-	-
Ab	-	-	-	48.74	52.91	75.43	-	-	-
Or	-	-	-	1.55	1.29	4.31	-	-	-
Ca	3.46	.57	.58	-	-	-	-	-	-
Mg	66.15	70.82	70.22	-	-	-	-	-	-
Fe*	30.39	28.61	29.20	-	-	-	-	-	-
% Ilm	-	-	-	-	-	-	-	.840	-
% Usp	-	-	-	-	-	-	-	-	.319

NOTE: Association 2: vug containing euhedral minerals and glass.

VUW: 17416 FIELD: A14X
FORMATION: TE HERENGA (RUAPEHU)
LITHOLOGY: TYPE QXd XENOLITH

MINERAL	opx	pl	pl
LOC	c	c	c
ASSOC	-	-	-
ANAL	1	1	1
SiO_2	50.70	49.24	46.66
TiO_2	.20	.00	.00
Al_2O_3	.53	31.70	33.95
Cr_2O_3	.00	.00	.00
Fe_2O_3	.61	.00	.00
FeO	28.84	.44	.43
MnO	.93	.00	.00
MgO	16.53	.06	.00
CaO	1.23	14.83	17.62
Na_2O	.00	2.73	1.84
K_2O	.00	.17	.00
Total	99.57	99.17	100.50
oxygens	6	8	8
Si	1.97	2.27	2.14
Ti	.01	.00	.00
Al	.02	1.72	1.84
Cr	.00	.00	.00
Fe^{3+}	.02	.00	.00
Fe^{2+}	.94	.02	.02
Mn	.03	.00	.00
Mg	.96	.00	.00
Ca	.05	.73	.87
Na	.00	.24	.16
K	.00	.01	.00
Total	4.00	4.99	5.03
endmember units			
An	-	74.24	84.08
Ab	-	24.75	15.92
Or	-	1.01	.00
Ca	2.55	-	-
Mg	48.00	-	-
Fe*	49.45	-	-
% Ilm	-	-	-
% Usp	-	-	-

VUW: 17419 FIELD: B6X-A
FORMATION: WHAKAPAPA (RUAPEHU)
LITHOLOGY: TYPE QPXb XENOLITH

MINERAL	opx	pl	pl	pl	tmt	pleon
LOC	c	c	c	c	c	c
ASSOC	-	-	1	1	-	-
ANAL	m3	m3	1	1	m2	m2
SiO_2	49.08	52.59	49.70	55.15	.05	.14
TiO_2	.65	.00	.00	.13	11.65	1.35
Al_2O_3	7.22	29.44	32.16	28.24	11.40	49.86
Cr_2O_3	.00	.00	.00	.00	.00	.00
Fe_2O_3	3.42	.00	.00	.00	34.80	14.18
FeO	13.21	.43	.48	.32	36.69	22.16
MnO	.42	.00	.00	.00	.00	.32
MgO	25.32	.08	.07	.00	4.53	12.20
CaO	.41	12.33	15.02	11.22	.00	.05
Na_2O	.00	4.39	3.14	5.27	.00	.00
K_2O	.00	.23	.14	.37	.00	.00
Total	99.73	99.49	100.71	100.70	100.22	99.12
oxygens	6	8	8	8	4	4
Si	1.78	2.40	2.26	2.48	.002	.004
Ti	.02	.00	.00	.00	.306	.028
Al	.31	1.58	1.72	1.50	.470	1.638
Cr	.00	.00	.00	.00	.000	.000
Fe^{3+}	.09	.00	.00	.00	.915	.297
Fe^{2+}	.40	.02	.02	.01	1.072	.516
Mn	.01	.00	.00	.00	.000	.008
Mg	1.37	.01	.01	.00	.236	.508
Ca	.02	.60	.73	.54	.000	.000
Na	.00	.39	.28	.46	.000	.002
K	.00	.01	.01	.02	.000	.000
Total	4.00	5.01	5.03	5.01	3.000	3.000
endmember units						
An	-	60.26	72.11	52.94	-	-
Ab	-	38.45	27.10	45.00	-	-
Or	-	1.29	.79	2.06	-	-
Ca	.85	-	-	-	-	-
Mg	72.35	-	-	-	-	-
Fe*	26.90	-	-	-	-	-
% Ilm	-	-	-	-	-	-
% Usp	-	-	-	-	.383	.454

NOTES: Association 1: light/dark areas in clouded grain.

VUW: 17420 FIELD: B6XC
FORMATION: WHAKAPAPA (RUAPEHU)
LITHOLOGY: TYPE MIXa XENOLITH

MINERAL	cpx	opx	pl
LOC	c	c	c
ASSOC	-	-	-
ANAL	1	1	1
SiO_2	52.60	53.88	56.79
TiO_2	.61	.00	.00
Al_2O_3	1.81	.37	27.04
Cr_2O_3	.17	.10	.00
Fe_2O_3	1.29	.76	.00
FeO	6.70	17.87	.41
MnO	.19	.55	.00
MgO	15.76	25.25	.00
CaO	20.71	.79	9.88
Na_2O	.42	.00	5.84
K_2O	.00	.00	.39
Total	100.25	99.57	100.35
oxygens	6	6	8
Si	1.93	1.98	2.55
Ti	.02	.00	.00
Al	.08	.02	1.43
Cr	.01	.00	.00
Fe^{3+}	.04	.02	.00
Fe^{2+}	.21	.55	.02
Mn	.01	.02	.00
Mg	.86	1.38	.00
Ca	.81	.03	.48
Na	.03	.00	.51
K	.00	.00	.02
Total	4.00	4.00	5.01
endmember units			
An	-	-	47.26
Ab	-	-	50.55
Or	-	-	2.19
Ca	42.36	1.55	-
Mg	44.80	69.12	-
Fe*	14.84	29.33	-
% Ilm	-	-	-
% Usp	-	-	-

NOTES: Analysis by W.R.Hackett.

VUW: 17421 FIELD: B6XD
FORMATION: WHAKAPAPA (RUAPEHU)
LITHOLOGY: TYPE MIXa XENOLITH

MINERAL	cpx	cpx	opx	pl	pl	pl	ilm
LOC	c	c	c	c	c	c	c
ASSOC	-	-	-	-	-	-	-
ANAL	m6	1	1	1	1	m12	m4
SiO_2	52.83	51.02	52.62	55.49	48.99	53.00	.08
TiO_2	.40	.60	.30	.00	.00	.00	50.18
Al_2O_3	1.43	2.57	1.50	27.68	32.11	29.68	.24
Cr_2O_3	.41	.00	.00	.00	.00	.00	1.26
Fe_2O_3	1.04	2.69	.68	.00	.00	.00	5.87
FeO	6.56	9.94	20.88	.57	.63	.55	38.13
MnO	.14	.33	.50	.00	.00	.00	.31
MgO	15.10	13.74	22.24	.08	.00	.08	3.80
CaO	22.18	19.40	1.66	10.75	15.74	12.86	.00
Na_2O	.31	.41	.00	5.31	2.59	4.29	.00
K_2O	.00	.00	.00	.31	.07	.16	.00
Total	100.39	100.70	100.39	100.17	100.12	100.63	99.87
oxygens	6	6	6	8	8	8	3
Si	1.96	1.90	1.94	2.50	2.24	2.39	.002
Ti	.01	.02	.01	.00	.00	.00	.927
Al	.06	.11	.07	1.47	1.73	1.58	.007
Cr	.01	.00	.00	.00	.00	.00	.025
Fe^{3+}	.03	.08	.02	.00	.00	.00	.109
Fe^{2+}	.20	.31	.65	.02	.02	.02	.784
Mn	.00	.01	.02	.00	.00	.00	.007
Mg	.83	.76	1.22	.01	.00	.01	.139
Ca	.88	.78	.07	.52	.77	.62	.000
Na	.02	.03	.00	.46	.23	.38	.000
K	.00	.00	.00	.02	.00	.01	.000
Total	4.00	4.00	4.00	5.00	4.99	5.01	2.000
endmember units							
An	-	-	-	52.08	76.74	61.96	-
Ab	-	-	-	46.12	22.86	37.15	-
Or	-	-	-	1.80	.40	.89	-
Ca	45.14	40.08	3.34	-	-	-	-
Mg	42.12	39.46	62.15	-	-	-	-
Fe*	12.74	20.46	34.51	-	-	-	-
% Ilm	-	-	-	-	-	-	.940
% Usp	-	-	-	-	-	-	-

VUW: 17422 FIELD: BXWS
FORMATION: WHAKAPAPA (RUAPEHU)
LITHOLOGY: TYPE MIXc XENOLITH

MINERAL	cpx	opx	pig	pl	pl	glass	tmt
LOC	c	c	c	c	c	c	c
ASSOC	-	-	-	-	-	-	-
ANAL	1	1	m2	1	1	1	1
SiO_2	51.83	52.16	51.64	55.50	57.02	75.49	.14
TiO_2	.36	.23	.27	.00	.00	.90	16.75
Al_2O_3	1.48	.76	.44	27.38	26.37	12.23	1.41
Cr_2O_3	.00	.00	.00	.00	.00	.00	.36
Fe_2O_3	1.16	.21	.59	.00	.00	.00	34.21
FeO	11.37	24.34	25.21	.69	.89	.83	43.86
MnO	.21	.48	.64	.00	.00	.00	.41
MgO	13.66	20.04	17.43	.00	.00	.06	1.54
CaO	19.27	1.58	3.71	10.94	9.77	.46	.00
Na_2O	.36	.00	.07	5.22	6.07	2.57	.00
K_2O	.00	.00	.00	.35	.40	5.76	.00
Total	99.70	99.80	100.00	100.08	100.52	98.30	98.68
oxygens	6	6	6	8	8	-	4
Si	1.94	1.97	1.97	2.51	2.56	-	.005
Ti	.01	.01	.01	1.40	.00	-	.474
Al	.07	.03	.02	1.46	1.40	-	.063
Cr	.00	.00	.00	.00	.00	-	.011
Fe^{3+}	.03	.01	.02	.00	.00	-	.969
Fe^{2+}	.36	.77	.81	.03	.03	-	1.379
Mn	.01	.02	.02	.00	.00	-	.013
Mg	.77	1.13	.99	.00	.00	-	.086
Ca	.78	.06	.15	.53	.47	-	.000
Na	.03	.00	.01	.46	.53	-	.000
K	.00	.00	.00	.02	.02	-	.000
Total	4.00	4.00	4.00	5.01	5.01	-	3.000
endmember units							
An	-	-	-	52.63	45.99	-	-
Ab	-	-	-	45.56	51.76	-	-
Or	-	-	-	1.91	2.25	-	-
Ca	40.05	3.22	7.63	-	-	-	-
Mg	39.48	56.94	49.95	-	-	-	-
Fe*	20.47	39.84	42.42	-	-	-	-
% Ilm	-	-	-	-	-	-	-
% Usp	-	-	-	-	-	-	.495

VUW: 17423 FIELD: B10XB
FORMATION: WHAKAPAPA (RUAPEHU)
LITHOLOGY: TYPE QPXc XENOLITH

MINERAL	pl	pl	bio	ilm	hem	ilm#	tmt	pleon
LOC	c	r	c	c	c	c	c	c
ASSOC	-	-	-	1	1	1	1	-
ANAL	1	1	m3	m2	1	1	m3	m2
SiO_2	53.47	45.61	33.09	.27	.27	.11	.18	.39
TiO_2	.00	.00	4.52	51.93	.41	45.85	11.83	.34
Al_2O_3	30.19	34.64	18.20	.15	1.42	5.66	7.09	55.38
Cr_2O_3	.00	.00	.00	.00	.00	.28	.00	.79
Fe_2O_3	.00	.00	.00	.47	95.00	.00	37.22	3.49
FeO	.38	.23	21.80	41.00	.00	39.59	40.74	32.63
MnO	.00	.00	.65	3.38	.29	2.93	.48	.98
MgO	.00	.00	8.40	1.79	.20	2.88	1.25	4.99
CaO	12.17	17.74	.00	.00	.13	.00	.00	.00
Na_2O	4.97	1.56	.54	.00	.00	.00	.00	.00
K_2O	.56	.16	9.27	.00	.00	.00	.00	.00
Total	101.74	99.94	96.47	98.99	97.72	97.30	98.79	98.99
oxygens	8	8	22	3	3	3	4	4
Si	2.39	2.10	5.09	.007	.007	-	.007	.011
Ti	.00	.00	.52	.986	.008	-	.326	.007
Al	1.59	1.88	3.30	.005	.045	-	.307	1.870
Cr	.00	.00	.00	.000	.000	-	.000	.018
Fe^{3+}	.00	.00	.00	.009	1.922	-	1.028	.075
Fe^{2+}	.01	.01	2.81	.854	.000	-	1.249	.782
Mn	.00	.00	.09	.072	.007	-	.015	.024
Mg	.00	.00	1.93	.067	.008	-	.068	.213
Ca	.58	.88	.00	.000	.004	-	.000	.000
Na	.43	.14	.16	.000	.000	-	.000	.000
K	.03	.01	1.82	.000	.000	-	.000	.000
Total	5.03	5.02	15.72	2.000	2.000	-	3.000	3.000
endmember units								
An	55.74	85.39	-	-	-	-	-	-
Ab	41.20	13.63	-	-	-	-	-	-
Or	3.06	.98	-	-	-	-	-	-
Ca	-	-	.00	-	-	-	-	-
Mg	-	-	39.99	-	-	-	-	-
Fe*	-	-	60.01	-	-	-	-	-
% Ilm	-	-	-	.995	-	-	-	-
% Usp	-	-	-	-	-	-	.436	.796

NOTES: # interface between coexisting ilmenite and titanomagnetite.

VUW: 17424 FIELD: B1OXE
FORMATION: WHAKAPAPA (RUAPEHU)
LITHOLOGY: TYPE MIXa XENOLITH

MINERAL	cpx	cpx	opx	opx	pl	pl	pl	ilm
LOC	c	c	c	c	c	c	c	c
ASSOC	-	-	-	-	-	-	-	-
ANAL	1	1	1	1	1	1	1	1
SiO_2	51.15	51.17	51.79	51.68	48.28	46.31	46.19	.00
TiO_2	.38	.42	.26	.28	.00	.00	.00	48.30
Al_2O_3	1.74	1.67	1.10	1.26	33.11	33.50	34.28	.16
Cr_2O_3	.00	.00	.00	.00	.00	.00	.00	.24
Fe_2O_3	1.22	.91	.25	.84	.00	.00	.00	8.33
FeO	11.10	12.09	24.53	23.80	.37	.22	.32	36.30
MnO	.31	.28	.59	.53	.00	.00	.00	.57
MgO	13.20	12.84	19.63	20.20	.00	.00	.00	3.68
CaO	19.99	19.60	1.61	1.33	16.28	16.73	17.46	.00
Na_2O	.20	.26	.00	.00	2.30	1.89	1.29	.00
K_2O	.00	.00	.00	.00	.06	.00	.00	.00
Total	99.29	99.24	99.76	99.92	100.40	98.65	99.54	97.58
oxygens	6	6	6	6	8	8	8	3
Si	1.93	1.94	1.96	1.95	2.20	2.16	2.13	.000
Ti	.01	.01	.01	.01	.00	.00	.00	.916
Al	.08	.08	.05	.06	1.78	1.84	1.87	.005
Cr	.00	.00	.00	.00	.00	.00	.00	.005
Fe^{3+}	.04	.03	.01	.02	.00	.00	.00	.158
Fe^{2+}	.35	.39	.78	.75	.01	.01	.01	.766
Mn	.01	.01	.02	.02	.00	.00	.00	.012
Mg	.75	.73	1.10	1.14	.00	.00	.00	.138
Ca	.81	.79	.07	.05	.80	.83	.86	.000
Na	.02	.02	.00	.00	.20	.17	.12	.000
K	.00	.00	.00	.00	.00	.00	.00	.000
Total	4.00	4.00	4.00	4.00	4.99	5.01	4.99	2.000
endmember units								
An	-	-	-	-	79.36	83.07	88.25	-
Ab	-	-	-	-	20.34	16.93	11.75	-
Or	-	-	-	-	.30	.00	.00	-
Ca	3.28	2.72	41.51	41.04	-	-	-	-
Mg	56.09	57.31	38.19	37.39	-	-	-	-
Fe*	40.63	39.97	20.30	21.57	-	-	-	-
% Ilm	-	-	-	-	-	-	-	.914
% Usp	-	-	-	-	-	-	-	-

VUW: 17425 FIELD: B10XH
FORMATION: WHAKAPAPA (RUAPEHU)
LITHOLOGY: TYPE QPXa XENOLITH

MINERAL	opx	pl	pl	pl	ks	biot	sill	ilm	pleon
LOC	c	c	c	c	c	c	c	c	c
ASSOC	-	-	-	-	1	-	1	-	-
ANAL	m3	1	1	m10	m9	m3	1	m3	1
SiO_2	45.74	60.92	58.18	59.97	64.69	34.72	34.55	.11	.07
TiO_2	.20	.00	.00	.00	.00	5.08	.00	51.42	.29
Al_2O_3	8.06	24.46	26.81	25.40	19.41	17.83	65.43	.15	55.63
Cr_2O_3	.00	.00	.00	.00	.00	.00	.00	.00	.00
Fe_2O_3	1.05	.00	.00	.00	.00	.00	.50	1.95	6.09
FeO	28.24	.00	.00	.15	.00	17.13	.00	41.31	30.02
MnO	.93	.00	.00	.00	.00	.16	.00	1.34	.34
MgO	14.31	.00	.00	.00	.00	11.21	.07	2.08	6.55
CaO	.15	6.05	8.35	7.01	.50	.00	.00	.00	.00
Na_2O	.00	7.24	6.13	6.92	3.12	.64	.13	.00	.00
K_2O	.00	1.51	.83	1.26	11.69	9.04	.00	.00	.00
Total	98.68	100.18	100.30	100.71	99.41	95.81	100.68	98.36	99.99
oxygens	6	8	8	8	8	22	5	3	4
Si	1.78	2.71	2.60	2.67	2.96	5.22	.93	.003	.002
Ti	.01	.00	.00	.00	.00	.58	.00	.976	.006
Al	.37	1.28	1.41	1.33	1.05	3.16	2.08	.005	1.854
Cr	.00	.00	.00	.00	.00	.00	.00	.000	.000
Fe^{3+}	.03	.00	.00	.00	.00	.00	.00	.037	.130
Fe^{2+}	.93	.00	.00	.01	.00	2.16	.01	.872	.724
Mn	.03	.00	.00	.00	.00	.02	.00	.029	.008
Mg	.84	.00	.00	.00	.00	2.51	.00	.078	.276
Ca	.01	.29	.40	.33	.03	.00	.00	.000	.000
Na	.00	.63	.53	.60	.28	.19	.01	.000	.000
K	.00	.09	.05	.07	.68	1.74	.00	.000	.000
Total	4.00	5.00	4.99	5.00	5.00	15.58	3.03	2.000	3.000
endmember units									
An	-	28.87	40.87	33.32	2.49	-	-	-	-
Ab	-	62.57	54.28	59.54	28.15	-	-	-	-
Or	-	8.56	4.85	7.14	69.36	-	-	-	-
Ca	.33	-	-	-	-	.00	-	-	-
Mg	45.68	-	-	-	-	53.63	-	-	-
Fe*	53.99	-	-	-	-	46.37	-	-	-
% Ilm	-	-	-	-	-	-	-	.980	-
% Usp	-	-	-	-	-	-	-	-	.511

NOTES: Association 1: sillimanite needles in sanidine.

VUW: 17427 FIELD: G1X
FORMATION: WHAKAPAPA (RUAPEHU)
LITHOLOGY: TYPE IX XENOLITH

MINERAL	cpx	opx	pl
LOC	c	c	c
ASSOC	-	-	-
ANAL	m3	m2	m3
SiO_2	50.98	52.70	45.93
TiO_2	.53	.24	.00
Al_2O_3	3.04	1.83	33.93
Cr_2O_3	.00	.00	.00
Fe_2O_3	2.81	2.21	.00
FeO	4.70	15.03	.20
MnO	.29	.82	.00
MgO	15.27	25.89	.00
CaO	21.41	.97	17.78
Na_2O	.39	.00	1.44
K_2O	.00	.00	.00
Total	99.42	99.69	99.28
oxygens	6	6	8
Si	1.88	1.91	2.13
Ti	.02	.01	.00
Al	.13	.08	1.85
Cr	.00	.00	.00
Fe^{3+}	.08	.06	.00
Fe^{2+}	.15	.46	.01
Mn	.01	.03	.00
Mg	.85	1.41	.00
Ca	.85	.04	.88
Na	.03	.00	.13
K	.00	.00	.00
Total	4.00	4.00	5.00
endmember units			
An	-	-	87.25
Ab	-	-	12.75
Or	-	-	.00
Ca	44.15	1.91	-
Mg	43.78	70.73	-
Fe*	12.07	27.36	-
% Ilm	-	-	-
% Usp	-	-	-

VUW: 17428 FIELD: ARGXEN
FORMATION: WHAKAPAPA (RUAPEHU)
LITHOLOGY: TYPE UCX XENOLITH

MINERAL	pl	chl	hal
LOC	c	c	c
ASSOC	-	-	-
ANAL	1	1	1
SiO_2	69.01	24.81	1.37
TiO_2	.22	.00	.00
Al_2O_3	19.01	20.03	.24
Cr_2O_3	.00	.00	.00
Fe_2O_3	.00	.00	.00
FeO	.38	32.00	.25
MnO	.00	.59	.00
MgO	.00	9.20	.16
CaO	.34	.00	.00
Na_2O	11.87	.00	63.32#
K_2O	3.07	.00	.11
Cl	.00	.00	59.02
Total	100.80	86.63	124.47#
oxygens	8	28	-
Si	2.99	5.51	-
Ti	.01	.00	-
Al	.97	5.25	-
Cr	.00	.00	-
Fe^{3+}	.00	.00	-
Fe^{2+}	.01	5.95	-
Mn	.00	.11	-
Mg	.00	3.05	-
Ca	.02	.00	-
Na	1.00	.00	-
K	.00	.00	-
Cl	.00	.00	-
Total	5.00	19.87	-
endmember units			
An	1.57	-	-
Ab	98.43	-	-
Or	.00	-	-
Ca	-	.00	-
Mg	-	33.47	-
Fe*	-	66.53	-
% Ilm	-	-	-
% Usp	-	-	-

NOTE: # Na as oxide.

VUW: 17430 FIELD: BX10
FORMATION: WHAKAPAPA (RUAPEHU)
LITHOLOGY: TYPE MIXa XENOLITH

MINERAL	opx	pl	pl	glass#	ilm	tmt
LOC	c	r	c	c	c	c
ASSOC	-	-	-	-	-	-
ANAL	1	1	1	1	1	1
SiO_2	53.11	48.61	52.87	63.00	.00	.10
TiO_2	.32	.00	.00	1.90	40.11	13.20
Al_2O_3	.98	31.66	28.94	11.66	.57	3.57
Cr_2O_3	.00	.00	.00	.00	.00	.70
Fe_2O_3	.00	.00	.00	.00	24.95	39.02
FeO	18.38	.67	.72	9.36	30.83	37.82
MnO	.57	.00	.00	.00	.21	.39
MgO	24.17	.08	.10	1.11	2.82	3.46
CaO	1.68	15.73	12.15	3.71	.00	.00
Na_2O	.00	2.86	4.42	4.04	.00	.00
K_2O	.00	.15	.27	2.72	.00	.00
Cl	.00	.00	.00	.21	.00	.00
Total	99.21	99.76	99.47	97.71	99.49	98.26
oxygens	6	8	8	-	3	4
Si	1.96	2.24	2.41	-	.000	.004
Ti	.01	.00	.00	-	.756	.367
Al	.04	1.72	1.56	-	.017	.155
Cr	.00	.00	.00	-	.000	.020
Fe^{3+}	.00	.00	.00	-	.471	1.084
Fe^{2+}	.57	.03	.03	-	.646	1.168
Mn	.02	.00	.00	-	.005	.012
Mg	1.33	.01	.01	-	.105	.190
Ca	.07	.78	.60	-	.000	.000
Na	.00	.26	.39	-	.000	.000
K	.00	.01	.02	-	.000	.000
Total	4.00	5.05	5.02	-	2.000	4.000
endmember units						
An	-	74.76	59.62	-	-	-
Ab	-	24.39	38.79	-	-	-
Or	-	.85	1.59	-	-	-
Ca	3.38	-	-	-	-	-
Mg	67.17	-	-	-	-	-
Fe*	29.45	-	-	-	-	-
% Ilm	-	-	-	-	.708	-
% Usp	-	-	-	-	-	.401

NOTES: # glass crowded with <1 micron cpx?

VUW: 17433 FIELD: M7X-1
FORMATION: MANGAWHERO (RUAPEHU)
LITHOLOGY: TYPE MIXc XENOLITH

MINERAL	cpx	opx	pl	ilm
LOC	c	c	c	c
ASSOC	-	-	-	-
ANAL	m4	m4	m7	1
SiO_2	51.63	50.88	47.90	.00
TiO_2	.36	.32	.00	50.14
Al_2O_3	1.67	.80	32.55	.10
Cr_2O_3	.00	.00	.00	.00
Fe_2O_3	.18	.14	.00	6.75
FeO	11.10	26.80	.24	37.62
MnO	.28	.75	.00	.64
MgO	12.90	18.15	.00	3.83
CaO	20.95	.94	16.53	.00
Na_2O	.18	.00	2.26	.00
K_2O	.00	.00	.09	.00
Total	99.25	98.78	99.57	99.08
oxygens	6	6	8	3
Si	1.95	1.96	2.21	.000
Ti	.01	.01	.00	.935
Al	.08	.04	1.77	.003
Cr	.00	.00	.00	.000
Fe^{3+}	.01	.00	.00	.126
Fe^{2+}	.35	.87	.01	.781
Mn	.01	.03	.00	.013
Mg	.73	1.05	.00	.142
Ca	.85	.04	.82	.000
Na	.01	.00	.20	.000
K	.00	.00	.01	.000
Total	4.00	4.00	5.02	2.000
endmember units				
An	-	-	79.79	-
Ab	-	-	19.73	-
Or	-	-	.48	-
Ca	43.73	1.97	-	-
Mg	37.46	52.82	-	-
Fe*	18.81	45.21	-	-
% Ilm	-	-	-	-
% Usp	-	-	-	.931

VUW: 17432 FIELD: BX-24
FORMATION: WHAKAPAPA (RUAPEHU)
LITHOLOGY: TYPE MIXc XENOLITH

MINERAL	opx	pl
LOC	c	c
ASSOC	-	-
ANAL	m5	m5
SiO_2	51.37	51.26
TiO_2	.20	.00
Al_2O_3	.94	30.38
Cr_2O_3	.00	.00
Fe_2O_3	1.01	.00
FeO	25.39	.36
MnO	.53	.00
MgO	19.56	.00
CaO	.64	13.92
Na_2O	.00	3.54
K_2O	.00	.28
Total	99.64	99.74
oxygens	6	8
Si	1.95	2.34
Ti	.01	.00
Al	.04	1.64
Cr	.00	.00
Fe^{3+}	.03	.00
Fe^{2+}	.81	.01
Mn	.02	.00
Mg	1.11	.00
Ca	.03	.68
Na	.00	.31
K	.00	.02
Total	4.00	5.00
endmember units		
An	-	67.42
Ab	-	30.99
Or	-	1.59
Ca	1.30	-
Mg	55.77	-
Fe*	42.93	-
% Ilm	-	-
% Usp	-	-

VUW: 17438 FIELD: H7X-14
FORMATION: PUKEONAKE
LITHOLOGY: TYPE IX XENOLITH (CUMULATE)

MINERAL	cpx	opx	pl	glass	pleon
LOC	c	c	c	c	c
ASSOC	-	-	-	-	-
ANAL	1	1	1	1	1
SiO_2	51.45	52.72	54.23	62.03	.00
TiO_2	.65	.40	.00	.97	1.02
Al_2O_3	2.51	1.69	27.99	13.99	51.58
Cr_2O_3	.00	.11	.00	.00	.13
Fe_2O_3	.95	.00	.00	.00	11.37
FeO	11.04	18.87	.46	4.95	22.70
MnO	.28	.35	.00	.12	.16
MgO	15.13	23.32	.10	2.27	11.32
NiO	.00	.00	.00	.00	.26
CaO	16.89	2.07	11.40	4.96	.00
Na_2O	.47	.00	4.36	3.09	.00
K_2O	.00	.00	.36	2.30	.00
Total	99.36	99.53	98.90	94.68	98.54
oxygens	6	6	8	-	4
Si	1.92	1.95	2.48	-	.000
Ti	.02	.01	.00	-	.022
Al	.11	.07	1.51	-	1.713
Cr	.00	.00	.00	-	.003
Fe^{3+}	.03	.00	.00	-	.241
Fe^{2+}	.35	.58	.02	-	.535
Mn	.01	.01	.00	-	.004
Mg	.85	1.28	.00	-	.475
Ni	.00	.00	.00	-	.006
Ca	.68	.08	.56	-	.000
Na	.03	.00	.39	-	.000
K	.00	.00	.02	-	.000
Total	4.00	3.98	4.98	-	3.000
endmember units					
An	-	-	57.78	-	-
Ab	-	-	40.04	-	-
Or	-	-	2.18	-	-
Ca	22.74	4.10	-	-	-
Mg	44.27	65.64	-	-	-
Fe*	32.99	30.26	-	-	-
% Ilm	-	-	-	-	-
% Usp	-	-	-	-	.432

NOTES: Analysis by W.R.Hackett.

VUW: 17439   FIELD: WAIM
FORMATION: WAIMARINO
LITHOLOGY: QUARTZ THOLEIITE

MINERAL	ol	ol	cpx	cpx	cpx	cpx	opx	pl	crsp#
LOC	c	r	g	c	r	g	g	g	c
ASSOC	-	-	-	-	-	-	-	-	ol
ANAL	1	1	1	1	1	1	1	1	1
SiO_2	41.61	39.50	54.90	51.73	53.27	53.17	54.65	50.32	.06
TiO_2	.00	.00	.18	.42	.19	.21	.15	.00	.21
Al_2O_3	.00	.00	.92	2.50	2.51	2.61	.90	31.30	12.86
Cr_2O_3	.00	.04	.00	.13	.51	.30	.00	.00	56.44
Fe_2O_3	.00	.00	.00	.68	.00	.04	.00	.00	4.20
FeO	8.07	19.61	13.07	9.74	5.50	5.97	14.97	.83	11.64
MnO	.05	.30	.31	.24	.15	.10	.35	.00	.00
MgO	49.79	40.94	22.09	16.98	16.61	17.44	26.20	.19	14.81
NiO	.36	.17	.00	.00	.00	.00	.00	.00	.13
CaO	.14	.19	8.25	16.58	21.02	20.21	2.23	15.09	.00
Na_2O	.00	.00	.00	.17	.19	.15	.00	2.42	.00
K_2O	.00	.00	.00	.00	.00	.00	.00	.04	.00
Total	100.02	100.75	99.72	99.17	99.95	100.20	99.45	100.19	100.35
oxygens	4	4	6	6	6	6	6	8	4
Si	1.011	1.006	2.00	1.94	1.95	1.95	1.98	2.29	.002
Ti	.000	.000	.01	.01	.01	.01	.00	.00	.005
Al	.000	.000	.04	.11	.11	.11	.04	1.68	.478
Cr	.000	.000	.00	.00	.00	.00	.00	.00	1.408
Fe^{3+}	.000	.000	.00	.02	.00	.00	.00	.00	.100
Fe^{2+}	.164	.418	.40	.30	.17	.18	.45	.03	.307
Mn	.001	.006	.01	.01	.00	.00	.01	.00	.000
Mg	1.803	1.554	1.20	.94	.91	.95	1.42	.01	.697
Ni	.007	.003	.00	.00	.00	.00	.00	.00	.003
Ca	.004	.005	.32	.66	.82	.79	.09	.74	.000
Na	.000	.000	.00	.01	.01	.01	.00	.21	.000
K	.000	.000	.00	.00	.00	.00	.00	.00	.000
Total	2.990	2.992	3.98	4.00	3.98	4.00	3.99	4.96	3.000
endmember units									
An	-	-	-	-	-	-	-	77.64	-
Ab	-	-	-	-	-	-	-	22.15	-
Or	-	-	-	-	-	-	-	.21	-
Ca	.20	.25	16.68	34.16	43.01	40.89	4.42	-	-
Mg	91.46	78.40	62.18	48.61	47.23	49.07	71.97	-	-
Fe*	8.34	21.35	21.14	17.23	9.76	10.04	23.61	-	-
% Ilm	-	-	-	-	-	-	-	-	-
% Usp	-	-	-	-	-	-	-	-	.377

NOTES: Analysis by W.R.Hackett; # inclusion in olivine.

VUW: 17441 FIELD: BRX-17
FORMATION: WHAKAPAPA (RUAPEHU)
LITHOLOGY: TYPE MIXa XENOLITH

MINERAL	cpx	opx	pl	ilm
LOC	c	c	c	c
ASSOC	-	-	-	-
ANAL	m2	m3	m4	1
SiO_2	53.12	52.90	51.97	.16
TiO_2	.24	.13	.00	49.24
Al_2O_3	1.23	.55	29.23	.00
Cr_2O_3	.36	.00	.00	.32
Fe_2O_3	.57	1.25	.00	7.81
FeO	7.42	19.02	.46	37.18
MnO	.00	.38	.00	.42
MgO	14.72	23.87	.00	3.85
CaO	22.03	1.13	12.81	.00
Na_2O	.40	.00	4.18	.00
K_2O	.00	.00	.23	.00
Total	100.09	99.23	98.88	98.98
oxygens	6	6	8	3
Si	1.97	1.98	2.39	.004
Ti	.01	.00	.00	.919
Al	.05	1.59	.02	.000
Cr	.01	.00	.00	.006
Fe^{3+}	.02	.00	.04	.146
Fe^{2+}	.23	.02	.59	.773
Mn	.00	.00	.01	.009
Mg	.81	.00	1.32	.143
Ca	.87	.63	.05	.000
Na	.03	.37	.00	.000
K	.00	.01	.00	.000
Total	4.00	4.00	5.01	2.000
endmember units				
An	-	-	62.05	-
Ab	-	-	36.68	-
Or	-	-	1.27	-
Ca	45.21	2.24	-	-
Mg	42.06	65.94	-	-
Fe*	12.73	31.82	-	-
% Ilm	-	-	-	.920
% Usp	-	-	-	-

VUW: 17442 FIELD: TLX-1
FORMATION: WHAKAPAPA (RUAPEHU)
LITHOLOGY: TYPE MIXa XENOLITH

MINERAL	cpx	opx	pl	ilm	crsp	crsp
LOC	c	c	c	c	c	c
ASSOC	-	-	-	-	-	-
ANAL	m4	m8	m12	1	1	1
SiO_2	53.08	53.93	50.06	.07	.09	.07
TiO_2	.36	.33	.00	49.34	7.98	3.28
Al_2O_3	1.08	.91	31.09	.14	6.61	8.08
Cr_2O_3	.17	.00	.00	.66	35.21	44.46
Fe_2O_3	1.10	1.10	.00	5.95	11.10	10.20
FeO	5.10	14.85	.40	33.83	30.47	26.97
MnO	.00	.23	.00	.24	.00	.00
MgO	16.72	27.08	.08	5.74	5.69	5.83
CaO	21.84	1.13	14.49	.12	.20	.00
Na_2O	.21	.00	3.22	.00	.00	.00
K_2O	.00	.00	.12	.00	.00	.00
Total	99.66	99.56	99.46	96.09	97.35	98.89
oxygens	6	6	8	3	4	4
Si	1.96	1.96	2.30	.002	.003	.002
Ti	.01	.01	.00	.993	.214	.086
Al	.05	.04	1.68	.004	.278	.332
Cr	.00	.00	.00	.013	.990	1.224
Fe^{3+}	.03	.03	.00	.113	.298	.267
Fe^{2+}	.16	.45	.02	.712	.907	.786
Mn	.00	.01	.00	.005	.000	.000
Mg	.92	1.46	.01	.215	.302	.303
Ca	.86	.04	.71	.003	.008	.000
Na	.02	.00	.29	.000	.000	.000
K	.00	.00	.01	.000	.000	.000
Total	4.00	4.00	5.02	2.000	3.000	2.000
endmember units						
An	-	-	70.99	-	-	-
Ab	-	-	28.32	-	-	-
Or	-	-	.69	-	-	-
Ca	43.85	2.21	-	-	-	-
Mg	46.69	73.38	-	-	-	-
Fe*	9.46	24.41	-	-	-	-
% Ilm	-	-	-	.935	-	-
% Usp	-	-	-	-	.849	.760

VUW: 17443 FIELD: TLX-8
FORMATION: WHAKAPAPA (RUAPEHU)
LITHOLOGY: TYPE QPXb XENOLITH

MINERAL	opx	opx	pl	pl	ilm	tmt	pleon
LOC	c	c	c	c	c	c	c
ASSOC	-	-	-	-	-	-	-
ANAL	m2	1	1	1	1	1	m2
SiO_2	51.00	47.99	56.67	59.34	.00	.00	.00
TiO_2	.18	.39	.00	.00	48.69	15.59	.36
Al_2O_3	3.23	6.46	26.96	25.33	.40	8.04	58.41
Cr_2O_3	.00	.00	.00	.00	.00	.00	.00
Fe_2O_3	1.99	2.49	.00	.00	9.97	30.96	4.48
FeO	18.92	19.22	.37	.29	36.11	41.61	25.69
MnO	.55	.52	.00	.00	.54	.37	.46
MgO	23.20	21.18	.00	.00	4.00	3.17	9.92
CaO	.26	.18	9.44	7.54	.00	.00	.00
Na_2O	.00	.00	5.84	6.60	.00	.00	.00
K_2O	.00	.00	.52	.85	.00	.00	.00
Total	99.93	98.43	99.80	99.95	99.71	99.74	99.32
oxygens	6	6	8	8	3	4	4
Si	1.90	1.81	2.55	2.65	.000	.000	.000
Ti	.01	.01	.00	.00	.902	.417	.008
Al	.14	.29	1.43	1.33	.012	.337	1.892
Cr	.00	.00	.00	.00	.000	.000	.000
Fe^{3+}	.06	.07	.00	.00	.185	.829	.093
Fe^{2+}	.59	.61	.01	.01	.744	1.238	.590
Mn	.02	.02	.00	.00	.010	.011	.011
Mg	1.29	1.19	.00	.00	.147	.168	.406
Ca	.01	.01	.46	.36	.000	.000	.000
Na	.00	.00	.51	.58	.000	.000	.000
K	.00	.00	.03	.05	.000	.000	.000
Total	4.00	4.00	4.99	4.98	2.000	3.000	3.000
endmember units							
An	-	-	45.78	36.61	-	-	-
Ab	-	-	51.20	58.42	-	-	-
Or	-	-	3.02	4.97	-	-	-
Ca	.51	.37	-	-	-	-	-
Mg	65.71	63.28	-	-	-	-	-
Fe*	33.78	36.35	-	-	-	-	-
% Ilm	-	-	-	-	-	-	-
% Usp	-	-	-	-	-	.899	.553

VUW: 17444 FIELD: GX
FORMATION: WHAKAPAPA (RUAPEHU)
LITHOLOGY: TYPE QPXb XENOLITH

MINERAL	opx	pl	glass	ap	tmt
LOC	c	c	c	c	c
ASSOC	-	-	-	-	-
ANAL	1	1	1	1	1
SiO_2	52.50	56.25	70.95	.51	.11
TiO_2	.26	.00	.80	.00	15.60
Al_2O_3	1.66	27.56	11.59	.14	1.89
Cr_2O_3	.00	.00	.00	.00	.29
Fe_2O_3	.90	.00	.00	.00	35.37
FeO	21.02	.51	3.16	1.33	40.97
MnO	.48	.00	.00	.13	.27
MgO	22.85	.00	.43	.32	2.45
CaO	.60	10.81	1.37	53.96	.07
Na_2O	.00	4.95	2.81	.00	.00
K_2O	.00	.38	5.00	.00	.00
P_2O_5	.00	.00	.18	40.95	.00
Total	100.27	100.46	96.29	97.34	97.02
oxygens	6	8	-	12	4
Si	1.94	2.52	-	.04	.004
Ti	.01	.00	-	.00	.445
Al	.07	1.46	-	.01	.085
Cr	.00	.00	-	.00	.009
Fe^{3+}	.03	.00	-	.00	1.009
Fe^{2+}	.65	.02	-	.09	1.299
Mn	.02	.00	-	.00	.009
Mg	1.26	.00	-	.04	.138
Ca	.02	.52	-	4.70	.003
Na	.00	.43	-	.00	.000
K	.00	.02	-	.00	.000
P	.00	.00	-	2.82	.000
Total	4.00	4.97	-	7.70	3.000
endmember units					
An	-	53.45	-	-	-
Ab	-	44.28	-	-	-
Or	-	2.27	-	-	-
Ca	1.21	-	-	-	-
Mg	63.82	-	-	-	-
Fe*	34.97	-	-	-	-
% Ilm	-	-	-	-	-
% Usp	-	-	-	-	.463

NOTES: Analysis by W.R.Hackett.

VUW: 17449 FIELD: MX-2
FORMATION: MANGAWHERO (RUAPEHU)
LITHOLOGY: TYPE MIXb XENOLITH

MINERAL	cpx	opx	pl	ilm	opx	pl
LOC	c	c	c	c	c	c
ASSOC	-	-	-	-	1	1
ANAL	1	1	1	1	1	1
SiO_2	53.90	52.97	55.94	.10	51.49	58.52
TiO_2	.17	.00	.00	52.56	.19	.00
Al_2O_3	1.02	.68	27.97	.07	.98	27.15
Cr_2O_3	.00	.00	.00	.61	.00	.00
Fe_2O_3	.00	1.54	.00	.40	1.75	.00
FeO	9.58	20.02	.11	38.90	22.73	.20
MnO	.23	.65	.00	.53	.69	.00
MgO	14.14	23.33	.00	4.36	21.12	.00
CaO	21.62	.86	10.34	.14	.51	9.15
Na_2O	.22	.00	5.16	.00	.00	6.12
K_2O	.00	.00	.56	.00	.00	.60
Total	100.88	100.05	100.08	97.67	99.47	101.74
oxygens	6	6	8	3	6	8
Si	1.98	1.97	2.51	.003	1.95	2.58
Ti	.01	.00	.00	.988	.01	.00
Al	.04	.03	1.48	.002	.04	1.41
Cr	.00	.00	.00	.000	.00	.00
Fe^{3+}	.00	.04	.00	.008	.05	.00
Fe^{2+}	.30	.62	.00	.812	.72	.01
Mn	.01	.02	.00	.011	.02	.00
Mg	.78	1.29	.00	.162	1.19	.00
Ca	.86	.03	.50	.004	.02	.43
Na	.02	.00	.45	.000	.00	.52
K	.00	.00	.03	.000	.00	.03
Total	4.00	4.00	4.97	2.000	4.00	4.98
endmember units						
An	-	-	50.81	-	-	43.69
Ab	-	-	45.91	-	-	52.88
Or	-	-	3.28	-	-	3.43
Ca	44.16	1.69	-	-	1.05	-
Mg	40.19	64.23	-	-	59.46	-
Fe*	15.65	34.08	-	-	39.49	-
% Ilm	-	-	-	.996	-	-
% Usp	-	-	-	-	-	-

NOTES: Association 1: in contact zone (probably=host).

VUW: 17450   FIELD: MX-11
FORMATION: MANGAWHERO (RUAPEHU)
LITHOLOGY: TYPE MIXb XENOLITH

MINERAL	opx	pl	pl	pl	pl	ilm
LOC	c	c	c	c	c	c
ASSOC	-	-	-	-	-	-
ANAL	m6	1	1	1	1	1
SiO_2	50.56	53.67	52.42	48.69	45.52	.09
TiO_2	.25	.00	.00	.00	.00	51.15
Al_2O_3	1.38	28.68	29.39	32.02	34.38	.25
Cr_2O_3	.00	.00	.00	.00	.00	.00
Fe_2O_3	1.07	.00	.00	.00	.00	4.50
FeO	27.31	.48	.25	.20	.14	39.91
MnO	.53	.00	.00	.00	.00	.61
MgO	18.09	.00	.00	.00	.00	3.13
CaO	.47	11.80	12.75	15.68	17.92	.00
Na_2O	.00	4.66	4.29	2.42	1.23	.00
K_2O	.00	.29	.32	.20	.08	.00
Total	99.66	99.58	99.42	99.21	99.27	99.39
oxygens	6	8	8	8	8	3
Si	1.94	2.44	2.39	2.25	2.11	.002
Ti	.01	.00	.00	.00	.00	.952
Al	.06	1.54	1.58	1.74	1.88	.007
Cr	.00	.00	.00	.00	.00	.000
Fe^{3+}	.03	.00	.00	.00	.00	.084
Fe^{2+}	.88	.02	.01	.01	.01	.826
Mn	.02	.00	.00	.00	.00	.013
Mg	1.04	.00	.00	.00	.00	.116
Ca	.02	.58	.62	.78	.89	.000
Na	.00	.41	.38	.22	.11	.000
K	.00	.02	.02	.01	.01	.000
Total	4.00	5.01	5.00	5.01	5.01	2.000
endmember units						
An	-	57.38	61.00	77.27	88.57	-
Ab	-	41.02	37.15	21.54	10.93	-
Or	-	1.60	1.85	1.19	.50	-
Ca	.96	-	-	-	-	-
Mg	52.32	-	-	-	-	-
Fe*	46.72	-	-	-	-	-
% Ilm	-	-	-	-	-	.955
% Usp	-	-	-	-	-	-

VUW: 17452 FIELD: FXT-1
FORMATION: OHAKUNE
LITHOLOGY: TYPE UCX XENOLITH (PORCELLANITE)

MINERAL	pl	pl	pl	cpx	cpx
LOC	c	c	c	c	c
ASSOC	-	-	-	-	-
ANAL	1	1	1	m2	1
SiO_2	64.56	55.32	60.74	45.23	41.79
TiO_2	.00	.00	.00	.32	.47
Al_2O_3	22.36	27.37	23.61	2.69	7.20
Cr_2O_3	.00	.00	.00	.00	.00
Fe_2O_3	.00	.00	.00	.00	.00
FeO	.24	1.07	.00	21.18	17.70
MnO	.00	.00	.00	.66	.40
MgO	.00	.00	.00	4.45	5.24
CaO	5.46	10.73	7.60	21.38	22.11
Na_2O	5.37	4.92	5.38	.47	.29
K_2O	3.08	.58	2.01	.00	.00
Total	101.07	99.99	99.34	96.38	95.20
oxygens	8	8	8	6	6
Si	2.84	2.51	2.73	1.89	1.74
Ti	.00	.00	.00	.01	.02
Al	1.16	1.46	1.25	.13	.35
Cr	.00	.00	.00	.00	.00
Fe^{3+}	.00	.00	.00	.00	.00
Fe^{2+}	.01	.04	.00	.74	.62
Mn	.00	.00	.00	.02	.01
Mg	.00	.00	.00	.28	.33
Ca	.26	.52	.37	.96	.99
Na	.46	.43	.47	.04	.02
K	.17	.03	.12	.00	.00
Total	4.90	4.98	4.94	4.07	4.08
endmember units					
An	28.94	52.79	38.53	-	-
Ab	51.58	43.77	49.37	-	-
Or	19.48	3.44	12.10	-	-
Ca	-	-	-	47.92	50.83
Mg	-	-	-	13.87	16.76
Fe*	-	-	-	38.21	32.41
% Ilm	-	-	-	-	-
% Usp	-	-	-	-	-

VUW: 17454 FIELD: BGX-2
FORMATION: WHAKAPAPA (RUAPEHU)
LITHOLOGY: TYPE MIXb XENOLITH

MINERAL	cpx	opx	pl
LOC	c	c	c
ASSOC	-	-	-
ANAL	1	1	1
SiO_2	51.39	52.70	50.65
TiO_2	.41	.22	.00
Al_2O_3	2.06	.96	30.23
Cr_2O_3	.27	.00	.00
Fe_2O_3	3.52	2.91	.00
FeO	5.45	15.90	.75
MnO	.25	.43	.00
MgO	15.19	25.05	.09
CaO	21.46	1.78	14.00
Na_2O	.33	.00	3.40
K_2O	.00	.00	.11
Total	100.33	99.95	99.23
oxygens	6	6	8
Si	1.90	1.92	2.33
Ti	.01	.01	.00
Al	.09	.04	1.64
Cr	.01	.00	.00
Fe^{3+}	.10	.08	.00
Fe^{2+}	.17	.49	.03
Mn	.01	.01	.00
Mg	.84	1.37	.01
Ca	.85	.07	.69
Na	.02	.00	.30
K	.00	.00	.01
Total	4.00	4.00	5.01
endmember units			
An	-	-	69.15
Ab	-	-	30.25
Or	-	-	.60
Ca	43.32	3.47	-
Mg	42.67	67.77	-
Fe*	14.01	28.76	-
% Ilm	-	-	-
% Usp	-	-	-

VUW: 17456 FIELD: XXB
FORMATION: WAHIANOA (RUAPEHU)
LITHOLOGY: TYPE IX XENOLITH (CUMULATE)

MINERAL	cpx	pl	pl	pl	tmt
LOC	c	c	c	c	c
ASSOC	-	-	-	-	-
ANAL	1	1	1	1	1
SiO_2	50.76	50.86	49.79	54.52	.10
TiO_2	.43	.00	.00	.00	11.26
Al_2O_3	3.36	31.41	33.09	29.58	2.57
Cr_2O_3	.00	.00	.00	.00	.61
Fe_2O_3	3.49	.00	.00	.00	41.79
FeO	6.11	.53	.58	.61	36.38
MnO	.32	.00	.00	.00	.43
MgO	14.60	.00	.06	.06	2.57
CaO	20.74	13.54	15.12	11.64	.00
Na_2O	.44	3.70	2.89	5.10	.00
K_2O	.00	.17	.05	.18	.00
Total	100.25	100.21	101.52	101.69	95.71
oxygens	6	8	8	8	4
Si	1.88	2.31	2.24	2.43	.004
Ti	.01	.00	.00	.00	.325
Al	.15	1.68	1.76	1.55	.116
Cr	.00	.00	.00	.00	.019
Fe^{3+}	.10	.00	.00	.00	1.207
Fe^{2+}	.19	.02	.02	.02	1.168
Mn	.01	.00	.00	.00	.014
Mg	.81	.00	.00	.00	.147
Ca	.82	.66	.73	.56	.000
Na	.03	.33	.25	.44	.000
K	.00	.01	.00	.01	.000
Total	4.00	5.01	5.00	5.01	3.000
endmember units					
An	-	66.27	74.22	55.34	-
Ab	-	32.73	25.48	43.57	-
Or	-	1.00	.30	1.09	-
Ca	42.74	-	-	-	-
Mg	41.86	-	-	-	-
Fe*	15.40	-	-	-	-
% Ilm	-	-	-	-	-
% Usp	-	-	-	-	.3

VUW: 17458 FIELD: BGX-4
FORMATION: WHAKAPAPA (RUAPEHU)
LITHOLOGY: TYPE QPXb XENOLITH

MINERAL	opx	pl	pl	glass	glass#	ilm	tmt	pleon	corund
LOC	c	r	c	c	c	c	c	c	c
ASSOC	-	-	-	-	-	-	-	1	1
ANAL	1	m2	m2	1	1	1	1	1	1
SiO_2	52.52	56.15	52.75	65.85	57.82	.00	.15	.00	.00
TiO_2	.30	.00	.00	1.38	2.81	48.82	15.46	.62	.89
Al_2O_3	3.18	27.49	29.20	13.53	10.74	.39	3.73	56.78	99.39
Cr_2O_3	.00	.00	.00	.00	.00	.00	.47	.00	.00
Fe_2O_3	3.43	.00	.00	.00	.00	12.94	36.16	8.43	.00
FeO	12.54	.36	.24	6.40	12.92	31.68	38.58	24.18	.39
MnO	.38	.00	.00	.00	.20	.46	.38	.27	.00
MgO	27.76	.08	.07	2.00	5.15	6.52	4.67	11.49	.00
CaO	.53	9.46	12.35	1.56	2.53	.11	.00	.00	.00
Na_2O	.00	5.95	4.71	2.46	2.50	.00	.00	.00	.00
K_2O	.00	.48	.27	2.96	2.00	.00	.00	.00	.00
Total	100.64	99.97	99.59	96.30	96.67	100.92	99.60	101.77	100.67
oxygens	6	8	8	-	-	3	4	4	-
Si	1.88	2.53	2.40	-	-	.000	.005	.000	-
Ti	.01	.00	.00	-	-	.878	.419	.013	-
Al	.13	1.46	1.57	-	-	.011	.158	1.803	-
Cr	.00	.00	.00	-	-	.000	.013	.000	-
Fe^{3+}	.09	.00	.00	-	-	.233	.980	.171	-
Fe^{2+}	.38	.01	.01	-	-	.634	1.162	.545	-
Mn	.01	.00	.00	-	-	.009	.012	.006	-
Mg	1.48	.01	.01	-	-	.232	.251	.462	-
Ca	.02	.46	.60	-	-	.003	.000	.000	-
Na	.00	.52	.42	-	-	.000	.000	.000	-
K	.00	.03	.02	-	-	.000	.000	.000	-
Total	4.00	5.02	5.03	-	-	2.000	3.000	3.000	-
endmember units									
An	-	45.79	58.46	-	-	-	-	-	-
Ab	-	51.44	40.00	-	-	-	-	-	-
Or	-	2.77	1.54	-	-	-	-	-	-
Ca	1.01	-	-	-	-	-	-	-	-
Mg	74.78	-	-	-	-	-	-	-	-
Fe*	24.21	-	-	-	-	-	-	-	-
% Ilm	-	-	-	-	-	.865	-	-	-
% Usp	-	-	-	-	-	-	.450	.478	-

NOTE: Association 1: corundum core in pleonaste.
Contains microlites of pyroxene.

VUW: 17460 FIELD: NX2
FORMATION: NGAURUHOE 1954
LITHOLOGY: TYPE VXb XENOLITH

MINERAL	opx	pl	pl	glass	glass	glass#	cord	tmt	pleon
LOC	c	c	r	c	c	c	c	c	c
ASSOC	-	-	-	-	-	-	-	-	-
ANAL	1	1	1	1	1	1	1	1	1
SiO_2	52.00	51.97	51.00	75.03	76.77	83.44	47.63	.20	.00
TiO_2	.33	.00	.00	.28	.41	.32	.00	17.71	.35
Al_2O_3	1.42	29.56	31.00	13.14	12.75	8.66	33.33	7.42	60.10
Cr_2O_3	.00	.00	.00	.00	.00	.00	.00	.00	.23
Fe_2O_3	2.61	.00	.00	.00	.00	.00	.00	25.93	1.28
FeO	16.36	.38	.33	2.17	2.33	1.74	11.70	41.68	23.34
MnO	.44	.00	.00	.12	.00	.00	.95	.57	.43
MgO	24.16	.07	.05	.60	.26	.28	5.72	3.83	11.08
CaO	2.02	13.41	13.98	1.77	1.17	.82	.00	.11	.12
Na_2O	.00	3.61	3.09	3.08	2.70	1.20	.12	.00	.00
K_2O	.00	.33	.19	3.10	2.75	2.35	.27	.00	.00
Total	99.34	99.33	99.64	99.29	99.14	98.81	99.72	97.45	96.93
oxygens	6	8	8	-	-	-	18	4	4
Si	1.92	2.38	2.33	-	-	-	4.94	.007	.000
Ti	.01	.00	.00	-	-	-	.00	.482	.007
Al	.06	1.60	1.67	-	-	-	4.07	.316	1.954
Cr	.00	.00	.00	-	-	-	.00	.00	.005
Fe^{3+}	.07	.00	.00	-	-	-	.00	.706	.027
Fe^{2+}	.51	.02	.01	-	-	-	1.01	1.261	.538
Mn	.01	.00	.00	-	-	-	.08	.018	.010
Mg	1.33	.01	.00	-	-	-	.88	.206	.455
Ca	.08	.66	.68	-	-	-	.00	.004	.004
Na	.00	.32	.27	-	-	-	.02	.000	.000
K	.00	.02	.01	-	-	-	.04	.000	.000
Total	4.00	5.01	4.97	-	-	-	11.04	3.000	3.000
endmember units									
An	-	66.10	70.75	-	-	-	-	-	-
Ab	-	32.00	28.11	-	-	-	-	-	-
Or	-	1.90	1.14	-	-	-	-	-	-
Ca	4.04	-	-	-	-	-	-	-	-
Mg	66.40	-	-	-	-	-	44.60	-	-
Fe*	29.56	-	-	-	-	-	55.40	-	-
% Ilm	-	-	-	-	-	-	-	-	-
% Usp	-	-	-	-	-	-	-	.626	.956

NOTES: # near quartz grain.

VUW: 17461 FIELD: NX-3
FORMATION: NGAURUHOE 1954
LITHOLOGY: TYPE VXa XENOLITH

MINERAL	opx	pl	glass	glass	glass#	cord+	cord	ilm
LOC	c	c	c	c	c	c	r	c
ASSOC	-	-	1	-	qz	1	-	-
ANAL	m2	1	1	1	1	1	1	1
SiO_2	52.42	62.29	72.51	75.64	80.96	48.98	49.95	.00
TiO_2	.09	.00	.43	.39	.27	.00	.00	52.22
Al_2O_3	2.01	22.75	13.93	12.88	9.28	34.00	33.50	.41
Cr_2O_3	.00	.00	.00	.00	.00	.00	.00	.88
Fe_2O_3	.00	.00	.00	.00	.00	.00	.00	3.17
FeO	25.02	.21	3.00	2.11	1.30	6.53	5.34	36.15
MnO	.35	.00	.00	.00	.00	.00	.00	.38
MgO	19.80	.00	.86	.61	.33	9.94	10.17	5.85
CaO	.06	4.79	.85	.54	.34	.00	.10	.00
Na_2O	.00	9.14	4.44	3.84	3.15	.21	.00	.00
K_2O	.00	.81	2.97	3.22	2.55	.22	.00	.00
Total	99.75	99.99	98.99	99.23	98.18	99.88	99.06	99.06
oxygens	6	8	-	-	-	18	18	3
Si	1.96	2.79	-	-	-	4.93	5.02	.000
Ti	.00	.00	-	-	-	.00	.00	.957
Al	.09	1.21	-	-	-	4.03	3.97	.012
Cr	.00	.00	-	-	-	.00	.00	.017
Fe^{3+}	.00	.00	-	-	-	.00	.00	.058
Fe^{2+}	.79	.01	-	-	-	.55	.45	.736
Mn	.01	.00	-	-	-	.00	.00	.008
Mg	1.11	.00	-	-	-	1.49	1.52	.212
Ca	.00	.23	-	-	-	.00	.00	.000
Na	.00	.79	-	-	-	.04	.00	.000
K	.00	.05	-	-	-	.03	.00	.000
Total	3.98	5.04	-	-	-	11.07	10.96	2.000
endmember units								
An	-	21.50	-	-	-	-	-	-
Ab	-	74.18	-	-	-	-	-	-
Or	-	4.32	-	-	-	-	-	-
Ca	.10	-	-	-	-	.00	.05	-
Mg	58.11	-	-	-	-	73.08	22.77	-
Fe*	41.79	-	-	-	-	26.92	77.18	-
% Ilm	-	-	-	-	-	-	-	.967
% Usp	-	-	-	-	-	-	-	-

NOTE: # glass near qz grain; + sieved cordierite in glass (association 1)

VUW: 17462 FIELD: NX-4
FORMATION: NGAURUHOE 1954
LITHOLOGY: TYPE VXa XENOLITH

MINERAL	glass	glass	glass	cord	ilm	rut
LOC	c	c	c	c	c	c
ASSOC	-	-	-	-	-	-
ANAL	1	1	1	1	m2	1
SiO_2	75.86	77.65	79.57	48.18	.10	.80
TiO_2	.10	.34	.36	.10	52.09	96.90
Al_2O_3	13.99	11.90	11.94	33.80	.32	.33
Cr_2O_3	.00	.00	.00	.00	.96	.34
Fe_2O_3	.00	.00	.00	.00	.00	.00
FeO	2.44	1.77	1.91	10.76	41.48	.93
MnO	.00	.00	.00	.16	.10	.00
MgO	.57	.21	.22	6.66	2.80	.10
CaO	.12	.21	.18	.00	.06	.00
Na_2O	2.91	3.07	3.03	.15	.00	.00
K_2O	1.86	3.38	1.99	.18	.00	.00
Total	97.85	98.53	99.20	99.99	96.91	99.40
oxygens	-	-	-	18	3	2
Si	-	-	-	4.94	.003	.011
Ti	-	-	-	.01	.987	.976
Al	-	-	-	4.08	.010	.005
Cr	-	-	-	.00	.019	.004
Fe^{3+}	-	-	-	.00	.000	.000
Fe^{2+}	-	-	-	.92	.887	.010
Mn	-	-	-	.01	.002	.000
Mg	-	-	-	1.02	.105	.002
Ca	-	-	-	.00	.002	.000
Na	-	-	-	.03	.000	.000
K	-	-	-	.02	.000	.000
Total	-	-	-	11.04	2.015	1.008
endmember units						
An	-	-	-	-	-	-
Ab	-	-	-	-	-	-
Or	-	-	-	-	-	-
Ca	-	-	-	.00	-	-
Mg	-	-	-	52.07	-	-
Fe*	-	-	-	47.93	-	-
% Ilm	-	-	-	-	-	-
% Usp	-	-	-	-	-	-

VUW: 17463 FIELD: NX-5
FORMATION: NGAURUHOE 1954
LITHOLOGY: TYPE QXb XENOLITH

MINERAL	opx	pl	glass	glass
LOC	c	c	c	c
ASSOC	-	-	-	-
ANAL	1	1	1	1
SiO_2	52.02	44.82	75.61	77.12
TiO_2	.00	.00	.15	.15
Al_2O_3	1.06	35.85	12.88	11.90
Cr_2O_3	.00	.00	.00	.00
Fe_2O_3	.00	.00	.00	.00
FeO	26.02	.00	1.60	1.70
MnO	1.07	.00	.00	.00
MgO	18.91	.00	.61	.50
CaO	1.01	18.20	3.71	3.33
Na_2O	.00	.56	3.10	2.14
K_2O	.00	.00	1.54	2.47
Total	100.09	99.43	99.20	99.31
oxygens	6	8	-	-
Si	1.97	2.07	-	-
Ti	.00	.00	-	-
Al	.05	1.95	-	-
Cr	.00	.00	-	-
Fe^{3+}	.00	.00	-	-
Fe^{2+}	.83	.00	-	-
Mn	.03	.00	-	-
Mg	1.07	.00	-	-
Ca	.04	.90	-	-
Na	.00	.05	-	-
K	.00	.00	-	-
Total	3.99	4.97	-	-
endmember units				
An	-	94.74	-	-
Ab	-	5.26	-	-
Or	-	.00	-	-
Ca	2.08	-	-	-
Mg	54.26	-	-	-
Fe*	43.66	-	-	-
% Ilm	-	-	-	-
% Usp	-	-	-	-

VUW: 17465 FIELD: NX-7
FORMATION: NGAURUHOE 1954
LITHOLOGY: TYPE VXa XENOLITH

MINERAL	opx	glass	glass	glass	cord	cord	cord	ilm	pleon
LOC	c	c	c	c	c	c	c	c	c
ASSOC	1	1	2	2	2	2	2	2	2
ANAL	m2	m2	m4	m3	1	1	1	1	m4
SiO_2	51.62	77.17	65.91	65.04	48.33	50.20	49.99	.00	.07
TiO_2	.45	.21	.72	1.05	.00	.00	.00	53.80	.47
Al_2O_3	2.17	10.64	16.36	17.68	33.33	32.67	32.54	.00	61.78
Cr_2O_3	.00	.00	.00	.00	.00	.00	.00	.00	.66
Fe_2O_3	.00	.00	.00	.00	.00	.00	.00	.00	1.25
FeO	26.55	1.55	3.32	3.96	9.18	6.51	6.58	38.16	23.16
MnO	.41	.00	.00	.00	.23	.00	.00	.55	.00
MgO	17.97	.30	.92	1.22	7.80	9.20	9.87	4.65	12.50
CaO	.48	.35	1.13	1.06	.00	.00	.00	.00	.00
Na_2O	.00	1.87	3.06	2.22	.00	.08	.12	.00	.00
K_2O	.00	5.78	6.63	4.95	.15	.61	.36	.00	.00
Total	99.65	97.87	98.05	97.18	99.02	99.27	98.46	97.16	99.89
oxygens	6	-	-	-	18	18	18	3	4
Si	1.97	-	-	-	4.97	5.08	5.05	-	.002
Ti	.01	-	-	-	.00	.00	.00	-	.009
Al	.10	-	-	-	4.04	3.90	3.88	-	1.939
Cr	.00	-	-	-	.00	.00	.00	-	.014
Fe^{3+}	.00	-	-	-	.00	.00	.00	-	.025
Fe^{2+}	.85	-	-	-	.79	.55	.56	-	.515
Mn	.00	-	-	-	.02	.00	.00	-	.000
Mg	1.02	-	-	-	1.19	1.39	1.49	-	.496
Ca	.02	-	-	-	.00	.00	.00	-	.000
Na	.00	-	-	-	.00	.02	.02	-	.000
K	.00	-	-	-	.02	.08	.05	-	.000
Total	3.97	-	-	-	11.03	11.02	11.05	-	3.000
endmember units									
An	-	-	-	-	-	-	-	-	-
Ab	-	-	-	-	-	-	-	-	-
Or	-	-	-	-	-	-	-	-	-
Ca	1.05	-	-	-	.00	.00	.00	-	-
Mg	53.74	-	-	-	59.61	71.58	72.79	-	-
Fe*	45.21	-	-	-	40.39	28.42	27.21	-	-
% Ilm	-	-	-	-	-	-	-	-	-
% Usp	-	-	-	-	-	-	-	-	.958

NOTE: Association 1: quartz-rich segregation; 2: quartz-poor segregation.

VUW: 17473 FIELD: NX-14
FORMATION: NGAURUHOE 1954
LITHOLOGY: TYPE VXb XENOLITH

MINERAL	glass	cord
LOC	c	c
ASSOC	-	-
ANAL	m3	1
SiO_2	78.05	48.51
TiO_2	.00	.00
Al_2O_3	12.49	34.43
Cr_2O_3	.00	.00
Fe_2O_3	.00	.00
FeO	1.77	9.08
MnO	.00	.23
MgO	.23	7.18
CaO	.95	.00
Na_2O	2.57	.00
K_2O	3.40	.00
Total	99.46	99.43
oxygens	-	18
Si	-	4.95
Ti	-	.00
Al	-	4.14
Cr	-	.00
Fe^{3+}	-	.00
Fe^{2+}	-	.78
Mn	-	.02
Mg	-	1.09
Ca	-	.00
Na	-	.00
K	-	.00
Total	-	10.98
endmember units		
An	-	-
Ab	-	-
Or	-	-
Ca	-	.00
Mg	-	57.87
Fe*	-	42.13
% Ilm	-	-
% Usp	-	-

VUW: 17474 FIELD: NX-15
FORMATION: NGAURUHOE 1954
LITHOLOGY: TYPE VXa XENOLITH

MINERAL	glass	glass	cord	cord
LOC	c	c	c	c
ASSOC	-	-	-	-
ANAL	m2	m2	1	m2
SiO_2	74.02	79.85	50.00	48.93
TiO_2	.87	.00	.00	.00
Al_2O_3	14.56	11.27	32.84	33.39
Cr_2O_3	.00	.00	.00	.00
Fe_2O_3	.00	.00	.00	.00
FeO	2.57	1.42	7.27	9.40
MnO	.00	.00	.00	.00
MgO	.24	.27	9.20	7.50
CaO	.36	.18	.09	.00
Na_2O	3.37	3.04	.00	.06
K_2O	3.03	2.35	.00	.00
Total	99.02	98.38	99.40	99.28
oxygens	-	-	18	18
Si	-	-	5.06	5.00
Ti	-	-	.00	.00
Al	-	-	3.91	4.02
Cr	-	-	.00	.00
Fe^{3+}	-	-	.00	.00
Fe^{2+}	-	-	.61	.80
Mn	-	-	.00	.00
Mg	-	-	1.39	1.14
Ca	-	-	.01	.00
Na	-	-	.00	.01
K	-	-	.00	.00
Total	-	-	10.98	10.97
endmember units				
An	-	-	-	-
Ab	-	-	-	-
Or	-	-	-	-
Ca	-	-	.49	.00
Mg	-	-	68.96	58.72
Fe*	-	-	30.55	41.28
% Ilm	-	-	-	-
% Usp	-	-	-	-

VUW: 17475 FIELD: PPX-4
FORMATION: PUKEONAKE
LITHOLOGY: TYPE VXa XENOLITH

MINERAL	glass	cord	cord
LOC	c	c	c
ASSOC	-	-	-
ANAL	1	1	1
SiO_2	74.36	49.65	49.14
TiO_2	.39	.00	.00
Al_2O_3	12.12	33.01	33.97
Cr_2O_3	.00	.00	.00
Fe_2O_3	.00	.00	.00
FeO	2.74	6.42	7.29
MnO	.00	.00	.00
MgO	.55	9.79	9.22
CaO	.74	.09	.08
Na_2O	3.09	.14	.11
K_2O	3.07	.00	.11
Total	97.06	99.10	99.99
oxygens	-	18	18
Si	-	5.03	4.96
Ti	-	.00	.00
Al	-	3.94	4.04
Cr	-	.00	.00
Fe^{3+}	-	.00	.00
Fe^{2+}	-	.54	.62
Mn	-	.00	.00
Mg	-	1.48	1.39
Ca	-	.01	.01
Na	-	.03	.02
K	-	.00	.01
Total	-	11.03	11.05
endmember units			
An	-	-	-
Ab	-	-	-
Or	-	-	-
Ca	-	.44	.40
Mg	-	72.78	68.99
Fe*	-	26.78	30.61
% Ilm	-	-	-
% Usp	-	-	-

VUW: 17476 FIELD: B6XQ
FORMATION: WHAKAPAPA (RUAPEHU)
LITHOLOGY: TYPE QXb XENOLITH

MINERAL	pl	woll	woll
LOC	c	c	c
ASSOC	-	-	-
ANAL	1	m2	m2
SiO_2	43.57	50.49	52.01
TiO_2	.00	.00	.00
Al_2O_3	35.12	.00	.38
Cr_2O_3	.00	.00	.00
Fe_2O_3	.00	.00	.00
FeO	.33	9.62	2.22
MnO	.00	.83	.44
MgO	.00	.23	.04
CaO	20.35	38.36	45.27
Na_2O	.13	.00	.00
K_2O	.00	.00	.00
Total	99.50	99.53	100.36
oxygens	8	6	6
Si	2.03	2.00	2.01
Ti	.00	.00	.00
Al	1.93	.00	.02
Cr	.00	.00	.00
Fe^{3+}	.00	.00	.00
Fe^{2+}	.01	.32	.07
Mn	.00	.03	.01
Mg	.00	.01	.00
Ca	1.02	1.63	1.87
Na	.01	.00	.00
K	.00	.00	.00
Total	5.00	3.99	3.98
endmember units			
An	98.83	-	-
Ab	1.17	-	-
Or	.00	-	-
Ca	-	81.88	95.51
Mg	-	.70	.10
Fe*	-	17.42	4.39
% Ilm	-	-	-
% Usp	-	-	-

VUW: 17482 FIELD: B1OXD
FORMATION: WHAKAPAPA (RUAPEHU)
LITHOLOGY: TYPE QXa XENOLITH

MINERAL	cpx	pl	pl	pl	ilm	hem
LOC	c	c	c	c	c	c
ASSOC	-	-	-	-	-	-
ANAL	m6	1	1	m3	m4	1
SiO_2	50.69	46.00	47.91	54.86	.00	.25
TiO_2	.17	.00	.00	.00	52.71	.96
Al_2O_3	.82	34.21	31.80	27.85	.15	.24
Cr_2O_3	.00	.00	.00	.00	.00	.00
Fe_2O_3	.03	.00	.00	.00	1.90	94.42
FeO	17.81	.31	.28	.16	41.78	.97
MnO	.85	.00	.00	.00	.95	.00
MgO	9.32	.00	.00	.00	2.54	.11
CaO	19.89	18.07	16.40	11.21	.10	.00
Na_2O	.00	1.23	2.15	4.52	.00	.00
K_2O	.00	.09	.18	.52	.00	.00
Total	99.58	99.91	98.72	99.12	100.13	96.95
oxygens	6	8	8	8	3	3
Si	1.97	2.12	2.23	2.48	.000	.007
Ti	.01	.00	.00	.00	.981	.020
Al	.04	1.86	1.74	1.50	.004	.008
Cr	.00	.00	.00	.00	.000	.000
Fe^{3+}	.00	.00	.00	.00	.034	1.938
Fe^{2+}	.58	.01	.01	.01	.864	.022
Mn	.03	.00	.00	.00	.020	.000
Mg	.54	.00	.00	.00	.094	.005
Ca	.83	.89	.82	.55	.003	.000
Na	.00	.11	.19	.40	.000	.000
K	.00	.01	.01	.03	.000	.000
Total	4.00	5.00	5.00	4.97	2.000	2.000
endmember units						
An	-	88.59	79.92	56.02	-	-
Ab	-	10.91	19.00	40.92	-	-
Or	-	.50	1.08	3.06	-	-
Ca	41.95	-	-	-	-	-
Mg	27.31	-	-	-	-	-
Fe*	30.74	-	-	-	-	-
% Ilm	-	-	-	-	.982	.021
% Usp	-	-	-	-	-	-

VUW: 17483 FIELD: B10XF
FORMATION: WHAKAPAPA (RUAPEHU)
LITHOLOGY: TYPE QPXa XENOLITH

MINERAL	pl	ks	glass	ks#	cor	bio	tmt	pleon
LOC	c	c	c	c	c	c	c	c
ASSOC	-	1	-	-	1	-	-	-
ANAL	1	1	1	1	1	1	1	1
SiO_2	61.66	65.88	64.41	43.88	.00	34.07	.14	.00
TiO_2	.00	.00	.25	.00	.00	3.47	8.55	.20
Al_2O_3	25.10	19.49	18.32	52.34	102.13	18.91	8.83	56.06
Cr_2O_3	.00	.00	.00	.00	.00	.00	.00	.00
Fe_2O_3	.00	.00	.00	.00	.00	.00	42.04	4.87
FeO	.19	.19	4.05	.18	.20	19.32	38.37	31.51
MnO	.00	.00	.00	.00	.00	.00	.62	.60
MgO	.00	.00	.61	.00	.00	9.29	1.04	5.58
CaO	6.02	.36	.39	.15	.00	.10	.00	.00
Na_2O	7.38	3.69	3.70	2.08	.00	.83	.00	.00
K_2O	1.19	10.92	6.27	6.94	.00	8.60	.00	.00
Total	101.54	100.53	98.00	105.57	102.33	94.59	99.59	98.82
oxygens	8	8	-	-	-	22	4	4
Si	2.71	2.97	-	-	-	5.23	.005	.000
Ti	.00	.00	-	-	-	.40	.233	.004
Al	1.30	1.04	-	-	-	3.43	.377	1.887
Cr	.00	.00	-	-	-	.00	.000	.000
Fe^{3+}	.00	.00	-	-	-	.00	1.147	.105
Fe^{2+}	.01	.01	-	-	-	2.48	1.163	.752
Mn	.00	.00	-	-	-	.00	.019	.015
Mg	.00	.00	-	-	-	2.13	.056	.237
Ca	.28	.02	-	-	-	.02	.000	.000
Na	.63	.32	-	-	-	.25	.000	.000
K	.07	.63	-	-	-	1.69	.000	.000
Total	5.00	4.99	-	-	-	15.63	2.000	3.000
endmember units								
An	28.94	1.86	-	-	-	-	-	-
Ab	64.21	33.26	-	-	-	-	-	-
Or	6.85	64.88	-	-	-	-	-	-
Ca	-	-	-	-	-	.34	-	-
Mg	-	-	-	-	-	45.99	-	-
Fe*	-	-	-	-	-	53.67	-	-
% Ilm	-	-	-	-	-	-	-	-
% Usp	-	-	-	-	-	-	.337	.539

NOTES: Association 1: corundum replacing sanidine.
corundum inclusions in sanidine?

VUW: 17485 FIELD: B1OXI
FORMATION: WHAKAPAPA (RUAPEHU)
LITHOLOGY: TYPE QXa XENOLITH

MINERAL	cpx	cpx	pl	sph	ilm#	hem	pl	bio	gnt	gnt
LOC	c	c	c	c	c	c	c	c	c	r
ASSOC	1	1	1	1	1/sph	1	2	2	2	2
ANAL	1	1	1	1	1	1	1	1	1	1
SiO_2	51.94	51.46	45.32	30.79	.00	1.09	58.32	34.92	37.96	39.35
TiO_2	.14	.14	.00	36.47	53.60	.00	.00	6.27	.00	.00
Al_2O_3	.63	.60	35.25	2.41	.09	.13	26.29	17.10	21.12	21.15
Cr_2O_3	.00	.00	.00	.00	.00	.00	.00	.00	.00	.00
Fe_2O_3	.35	.00	.00	.00	.00	98.09	.00	.00	.00	.00
FeO	13.41	14.68	.21	.53	41.58	.84	.00	17.18	27.98	27.87
MnO	1.25	.92	.00	.00	1.22	.00	.00	.00	5.32	2.98
MgO	9.84	9.18	.00	.00	2.48	.16	.00	10.94	5.84	6.85
CaO	22.90	22.72	19.33	27.41	.00	.14	8.23	.00	1.90	1.73
Na_2O	.15	.11	.78	.00	.00	.00	6.36	.53	.00	.00
K_2O	.00	.00	.00	.00	.00	.00	.89	9.21	.00	.00
Total	100.61	99.81	100.89	97.61	98.97	100.45	100.09	96.15	100.12	99.93
oxygens	6	6	8	20	-	3	8	22	12	12
Si	1.98	1.99	2.07	4.09	-	.029	2.61	5.23	3.00	3.06
Ti	.00	.00	.00	3.65	-	.000	.00	.71	.00	.00
Al	.03	.03	1.90	.38	-	.004	1.39	3.04	1.97	1.94
Cr	.00	.00	.00	.00	-	.000	.00	.00	.00	.00
Fe^{3+}	.01	.00	.00	.00	-	1.939	.00	.00	.00	.00
Fe^{2+}	.43	.48	.01	.06	-	.018	.00	2.15	1.85	1.82
Mn	.04	.03	.00	.00	-	.000	.00	.00	.36	.20
Mg	.56	.53	.00	.00	-	.006	.00	2.44	.69	.80
Ca	.94	.94	.95	3.90	-	.004	.39	.00	.16	.14
Na	.01	.01	.07	.00	-	.000	.55	.15	.00	.00
K	.00	.00	.00	.00	-	.000	.05	1.76	.00	.00
Total	4.00	4.01	5.00	12.08	-	2.000	4.99	15.48	8.03	7.96
endmember units										
An	-	-	93.21	-	-	-	39.56	-	-	-
Ab	-	-	6.79	-	-	-	55.32	-	-	-
Or	-	-	.00	-	-	-	5.12	-	-	-
Ca	47.42	47.64	-	-	-	-	-	.00	5.28	4.88
Mg	28.37	26.76	-	-	-	-	-	53.16	22.49	26.94
Fe*	24.21	25.60	-	-	-	-	-	46.84	72.26	68.18
% Ilm	-	-	-	-	-	-	-	-	-	-
% Usp	-	-	-	-	-	-	-	-	-	-

NOTES: Association 1: qz + cpx + pl; association 2: qz + pl + bio + gnt.
ilmenite blebs in sphene.

VUW: 17488 FIELD: B10XM
FORMATION: WHAKAPAPA (RUAPEHU)
LITHOLOGY: TYPE QXe XENOLITH

MINERAL	opx	pl	tmt
LOC	c	c	c
ASSOC	-	-	-
ANAL	1	1	1
SiO_2	49.33	45.96	.25
TiO_2	.12	.00	12.44
Al_2O_3	.75	34.31	1.77
Cr_2O_3	.00	.00	.00
Fe_2O_3	1.40	.00	42.26
FeO	25.36	.46	38.92
MnO	7.35	.00	3.01
MgO	13.72	.00	.59
NiO	.00	.00	.22
CaO	1.44	17.74	.00
Na_2O	.00	1.52	.00
K_2O	.00	.07	.00
Total	99.47	100.06	99.46
oxygens	6	8	4
Si	1.96	2.12	.009
Ti	.00	.00	.352
Al	.04	1.86	.079
Cr	.00	.00	.000
Fe^{3+}	.04	.00	1.198
Fe^{2+}	.84	.02	1.226
Mn	.25	.00	.096
Mg	.81	.00	.033
Ni	.00	.00	.007
Ca	.06	.88	.000
Na	.00	.14	.000
K	.00	.00	.000
Total	4.00	5.02	3.000
endmember units			
An	-	86.22	-
Ab	-	13.39	-
Or	-	.39	-
Ca	3.04	-	-
Mg	40.52	-	-
Fe*	56.44	-	-
% Ilm	-	-	-
% Usp	-	-	.361

VUW: 17489 FIELD: B1OXN
FORMATION: WHAKAPAPA (RUAPEHU)
LITHOLOGY: TYPE QPXd XENOLITH

MINERAL	opx	pl	pl	bio	ilm	tmt
LOC	c	c	r	c	c	c
ASSOC	-	-	-	-	-	-
ANAL	m2	1	1	m2	1	1
SiO_2	52.94	46.68	54.60	36.12	.00	.14
TiO_2	.27	.00	.00	6.94	46.39	13.07
Al_2O_3	2.77	33.62	28.50	16.03	.37	6.92
Cr_2O_3	.00	.00	.00	.00	.00	.00
Fe_2O_3	.62	.00	.00	.00	14.69	36.34
FeO	15.69	.42	.31	12.13	32.35	38.21
MnO	.74	.00	.00	.00	.49	.51
MgO	26.11	.00	.00	15.48	4.98	3.56
CaO	.43	17.27	10.80	.12	.00	.00
Na_2O	.00	1.66	5.03	.93	.00	.00
K_2O	.00	.15	.45	8.88	.00	.00
Total	99.57	99.80	99.69	96.63	99.27	98.75
oxygens	6	8	8	22	3	4
Si	1.92	2.15	2.47	5.26	.000	.005
Ti	.01	.00	.00	.75	.858	.355
Al	.12	1.83	1.52	2.76	.011	.294
Cr	.00	.00	.00	.00	.000	.000
Fe^{3+}	.02	.00	.00	.00	.272	.986
Fe^{2+}	.48	.02	.01	1.48	.666	1.153
Mn	.02	.00	.00	.00	.010	.016
Mg	1.411	.00	.00	3.36	.183	.191
Ca	.02	.85	.52	.02	.000	.000
Na	.00	.15	.44	.26	.000	.000
K	.00	.01	.03	1.65	.000	.000
Total	4.00	5.01	4.99	15.54	2.000	3.000
endmember units						
An	-	84.46	52.88	-	-	-
Ab	-	14.65	44.50	-	-	-
Or	-	.89	2.62	-	-	-
Ca	.87	-	-	.41	-	-
Mg	72.60	-	-	69.14	-	-
Fe*	26.53	-	-	30.45	-	-
% Ilm	-	-	-	-	.848	-
% Usp	-	-	-	-	-	.442

VUW: 17490 FIELD: BXGa
FORMATION: WHAKAPAPA (RUAPEHU)
LITHOLOGY: TYPE QXa XENOLITH

MINERAL	cpx	cpx	cpx	pl	pl	sph	ilm#
LOC	c	c	c	c	c	c	c
ASSOC	1	1	1	1	1	1	1
ANAL	m9	1	1	m9	1	1	1
SiO_2	50.28	49.90	51.58	44.82	45.37	30.63	.30
TiO_2	.13	.00	.00	.00	.00	35.98	46.02
Al_2O_3	.63	.40	.58	35.58	34.29	1.09	.15
Cr_2O_3	.00	.00	.20	.00	.00	.00	.00
Fe_2O_3	.17	.53	.21	.00	.00	.00	4.83
FeO	16.06	18.37	14.63	.28	.25	.34	36.93
MnO	1.11	1.20	.86	.00	.00	.00	2.13
MgO	6.77	5.29	9.27	.00	.00	.00	.96
CaO	22.25	23.93	23.16	18.68	17.57	27.80	.74
Na_2O	.10	.00	.00	.94	1.58	.00	.00
K_2O	.00	.00	.00	.07	.06	.00	.00
Total	99.50	99.62	100.49	100.37	99.12	95.84	92.06
oxygens	6	6	6	8	8	20	3
Si	1.97	1.98	1.97	2.06	2.11	4.16	.008
Ti	.00	.00	.00	.00	.00	3.67	.939
Al	.03	.02	.03	1.93	1.88	.17	.005
Cr	.00	.00	.01	.00	.00	.00	.000
Fe^{3+}	.01	.02	.01	.00	.00	.00	.099
Fe^{2+}	.60	.61	.47	.01	.01	.04	.839
Mn	.04	.04	.03	.00	.00	.00	.049
Mg	.40	.31	.53	.00	.00	.00	.039
Ca	.94	1.02	.95	.92	.88	4.04	.022
Na	.01	.00	.00	.08	.14	.00	.000
K	.00	.00	.00	.00	.00	.00	.000
Total	4.00	4.00	4.00	5.00	5.02	12.08	2.000
endmember units							
An	-	-	-	91.25	85.70	-	-
Ab	-	-	-	8.35	13.91	-	-
Or	-	-	-	.40	.39	-	-
Ca	47.60	50.93	47.79	-	-	-	-
Mg	20.13	15.71	26.63	-	-	-	-
Fe*	32.17	33.36	25.58	-	-	-	-
% Ilm	-	-	-	-	-	-	.947
% Usp	-	-	-	-	-	-	-

NOTES: Association 1: qz + pl + cpx; # inclusion in sphene.

VUW: 17491 FIELD: BXGb
FORMATION: WHAKAPAPA (RUAPEHU)
LITHOLOGY: TYPE QXa XENOLITH

MINERAL	opx	pl	glass	gnt	ilm	pleon#	ged#
LOC	c	c	c	c	c	c	c
ASSOC	2	2	3	3	3	3	3
ANAL	1	1	1	1	1	1	1
SiO_2	49.45	61.01	73.21	37.76	.00	.11	43.77
TiO_2	.18	.00	.31	.00	50.73	.34	.00
Al_2O_3	4.52	24.86	13.67	21.87	.15	52.01	9.56
Cr_2O_3	.00	.00	.00	.00	.00	.00	.00
Fe_2O_3	.00	.00	.00	.00	2.61	7.43	.00
FeO	27.59	.26	2.40	29.90	41.37	33.86	32.37
MnO	.28	.00	.00	.84	.50	.36	.92
MgO	17.27	.00	.16	7.78	2.10	3.73	11.77
CaO	.22	6.20	.32	.90	.00	.00	.20
Na_2O	.00	7.47	3.32	.00	.00	.00	.00
K_2O	.00	1.05	6.32	.00	.00	.00	.00
Cl	.00	.00	.09	.00	.00	.00	.00
Total	99.51	100.85	99.80	99.05	97.46	97.84	98.59
oxygens	6	8	-	12	3	4	22
Si	1.90	2.70	-	5.94	.000	.003	7.00
Ti	.01	.00	-	.00	.972	.008	.00
Al	.20	1.30	-	4.06	.005	1.813	1.80
Cr	.00	.00	-	.00	.000	.000	.00
Fe^{3+}	.00	.00	-	.00	.050	.165	.00
Fe^{2+}	.89	.01	-	3.94	.882	.837	4.33
Mn	.01	.00	-	.11	.011	.009	.13
Mg	.99	.00	-	1.83	.080	.164	2.81
Ca	.01	.29	-	.15	.000	.000	.03
Na	.00	.64	-	.00	.000	.000	.00
K	.00	.06	-	.00	.000	.000	.00
Total	4.01	5.00	-	16.03	2.000	3.000	16.10
endmember units							
An	-	29.58	-	-	-	-	-
Ab	-	64.49	-	-	-	-	-
Or	-	5.93	-	-	-	-	-
Ca	.48	-	-	2.52	-	-	.47
Mg	52.22	-	-	30.29	-	-	38.46
Fe*	47.30	-	-	67.19	-	-	61.07
% Ilm	-	-	-	-	.974	-	-
% Usp	-	-	-	-	-	.476	-

NOTES: Association 2: qz + pl + opx + gnt + glass.
breakdown of cordierite inclusion in garnet.

VUW: 17493 FIELD: BX-20
FORMATION: WHAKAPAPA (RUAPEHU)
LITHOLOGY: TYPE QXe XENOLITH

MINERAL	pl	cpx	woll	sph
LOC	c	c	c	c
ASSOC	-	-	-	-
ANAL	m2	m2	m3	1
SiO_2	42.84	51.00	49.30	30.17
TiO_2	.00	.15	.00	36.13
Al_2O_3	35.96	.61	.00	2.05
Cr_2O_3	.00	.00	.00	.00
Fe_2O_3	.00	.17	1.77	.00
FeO	.33	11.12	6.87	.57
MnO	.00	3.46	8.30	.66
MgO	.00	8.89	1.31	.00
CaO	20.00	23.92	32.27	27.07
Na_2O	.11	.00	.00	.00
K_2O	.00	.00	.00	.00
Total	99.24	99.32	99.82	96.65
oxygens	8	6	6	20
Si	2.00	1.98	1.97	4.07
Ti	.00	.00	.00	3.66
Al	1.98	.03	.00	.33
Cr	.00	.00	.00	.00
Fe^{3+}	.00	.01	.05	.00
Fe^{2+}	.01	.36	.23	.06
Mn	.00	.11	.28	.08
Mg	.00	.51	.08	.00
Ca	1.00	1.00	1.39	3.91
Na	.01	.00	.00	.00
K	.00	.00	.00	.00
Total	5.00	4.00	4.00	12.11
endmember units				
An	99.01	-	-	-
Ab	.99	-	-	-
Or	.00	-	-	-
Ca	-	50.03	68.28	-
Mg	-	25.84	3.85	-
Fe*	-	24.13	27.87	-
% Ilm	-	-	-	-
% Usp	-	-	-	-

VUW: 17497 FIELD: AX-9
FORMATION: TE HERENGA (RUAPEHU)
LITHOLOGY: TYPE QPXb XENOLITH

MINERAL	opx	pl	pl	pl	ilm	tmt	tmt
LOC	c	c	c	c	c	c	c
ASSOC	-	-	-	-	-	-	-
ANAL	m3	1	1	m19	1	1	1
SiO_2	52.04	51.64	56.97	55.41	.08	.13	.09
TiO_2	.37	.00	.00	.00	44.74	11.90	12.80
Al_2O_3	3.09	29.95	26.61	27.82	.47	2.41	10.56
Cr_2O_3	.00	.00	.00	.00	.00	.22	.00
Fe_2O_3	.54	.00	.00	.00	16.24	43.11	33.93
FeO	18.07	.57	.33	.46	33.14	38.75	35.03
MnO	.40	.00	.00	.00	.53	.47	.34
MgO	24.53	.06	.05	.00	3.67	2.07	5.93
CaO	.30	13.57	8.94	10.47	.09	.00	.00
Na_2O	.00	3.98	6.35	5.74	.00	.00	.00
K_2O	.00	.10	.21	.11	.00	.00	.00
Total	99.34	99.87	99.46	100.01	98.96	99.06	98.68
oxygens	6	8	8	8	3	4	4
Si	1.91	2.36	2.57	2.50	.002	.005	.003
Ti	.01	.00	.00	.00	.839	.334	.335
Al	.13	1.61	1.42	1.48	.014	.106	.434
Cr	.00	.00	.00	.00	.000	.007	.000
Fe^{3+}	.02	.00	.00	.00	.305	1.209	.889
Fe^{2+}	.56	.02	.01	.02	.691	1.209	1.021
Mn	.01	.00	.00	.00	.011	.015	.010
Mg	1.35	.00	.00	.00	.136	.115	.308
Ca	.01	.66	.43	.51	.002	.000	.000
Na	.00	.35	.56	.50	.000	.000	.000
K	.00	.01	.01	.01	.000	.000	.000
Total	4.00	5.01	5.00	5.01	2.000	3.000	3.000
endmember units							
An	-	65.07	43.26	49.85	-	-	-
Ab	-	34.34	55.54	49.46	-	-	-
Or	-	.59	1.20	.69	-	-	-
Ca	.62	-	-	-	-	-	-
Mg	69.33	-	-	-	-	-	-
Fe*	30.05	-	-	-	-	-	-
% Ilm	-	-	-	-	.833	-	-
% Usp	-	-	-	-	-	.353	.461

VUW: 17498 FIELD: AXWS
FORMATION: TE HERENGA (RUAPEHU)
LITHOLOGY: TYPE QXf XENOLITH

MINERAL	ol	cpx	pl	pl#	ilm	tmt	?	pleon
LOC	c	c	c	c	c	c	c	c
ASSOC	-	-	-	-	-	-	1	1
ANAL	1	1	1	1	1	1	1	1
SiO_2	35.14	51.94	68.29	59.45	.00	.00	25.82	.12
TiO_2	.00	.21	.00	.00	33.84	7.33	.00	.00
Al_2O_3	.00	.24	19.45	25.16	4.10	1.82	17.17	54.94
Cr_2O_3	.00	.84	.00	.00	.00	.00	.00	.00
Fe_2O_3	.00	1.15	.00	.00	.00	47.14	.00	7.83
FeO	40.75	13.05	.00	.00	47.82	34.16	41.51	28.49
MnO	.62	.31	.00	.00	.00	.00	.47	.35
MgO	23.38	12.55	.00	.00	.65	.85	14.60	7.68
CaO	.00	18.35	.24	6.87	.00	.00	.00	.00
Na_2O	.00	.66	11.52	8.02	.00	.00	.00	.00
K_2O	.00	.00	.31	.19	.00	.00	.00	.00
Total	99.89	99.28	99.81	99.69	88.48	91.30	99.57	99.47
oxygens	4	6	8	8	3	4	?	4
Si	1.006	1.98	2.99	2.66	.000	.000	.00	.003
Ti	.000	.01	.00	.00	.714	.227	.00	.000
Al	.000	.01	1.01	1.33	.136	.088	.00	1.827
Cr	.000	.03	.00	.00	.000	.000	.00	.000
Fe^{3+}	.000	.03	.00	.00	.436	1.458	.00	.166
Fe^{2+}	.976	.42	.00	.00	.687	1.175	.00	.672
Mn	.015	.01	.00	.00	.000	.000	.00	.008
Mg	.997	.71	.00	.00	.027	.052	.00	.323
Ca	.000	.75	.01	.33	.000	.000	.00	.000
Na	.000	.05	.98	.70	.000	.000	.00	.000
K	.000	.00	.02	.01	.000	.000	.00	.000
Total	2.994	4.00	5.01	5.03	2.000	3.000	.00	3.000
endmember units								
An	-	-	1.09	31.82	-	-	-	-
Ab	-	-	97.22	67.12	-	-	-	-
Or	-	-	1.69	1.06	-	-	-	-
Ca	.00	38.51	-	-	-	-	-	-
Mg	50.15	36.62	-	-	-	-	-	-
Fe*	49.85	24.87	-	-	-	-	-	-
% Ilm	-	-	-	-	.763	-	-	-
% Usp	-	-	-	-	-	.240	-	-

NOTES: Association 1: breakdown products; # blebs in plagioclse.

VUW: 17500 FIELD: 15X
FORMATION: WAHIANOA (RUAPEHU)
LITHOLOGY: TYPE IX XENOLITH (CUMULATE)

MINERAL	cpx	cpx	opx	hb	pl	cpx	cpx	tmt
LOC	c	r	c	c	c	r	g	c
ASSOC	1	1	1	2	2	2	2	2
ANAL	1	1	1	m2	1	1	1	1
SiO_2	49.93	51.97	53.50	42.01	50.14	50.27	43.75	.10
TiO_2	.46	.31	.00	1.81	.00	1.46	2.38	2.38
Al_2O_3	5.23	3.08	.74	13.12	31.18	3.67	9.61	3.93
Cr_2O_3	.00	.00	.00	.00	.00	.00	.00	.00
Fe_2O_3	2.79	2.09	1.52	.00	.00	3.51	5.74	58.69
FeO	6.14	6.60	17.05	10.70	.59	2.71	3.20	23.34
MnO	.18	.22	.51	.00	.00	.00	.00	.48
MgO	14.85	14.50	25.69	14.50	.00	15.95	12.53	5.36
CaO	20.23	21.57	.47	11.02	13.79	21.85	20.20	.25
Na_2O	.30	.46	.00	3.05	3.65	.50	.66	.00
K_2O	.00	.00	.00	.50	.17	.00	.00	.00
Total	100.11	100.80	99.49	96.71	99.51	99.91	98.08	94.53
oxygens	6	6	6	22	8	6	6	4
Si	1.85	1.91	1.96	5.94	2.30	1.85	1.66	.004
Ti	.01	.01	.00	.19	.00	.04	.07	.068
Al	.23	.13	.03	2.19	1.69	.16	.43	.176
Cr	.00	.00	.00	.00	.00	.00	.00	.000
Fe^{3+}	.08	.06	.04	.00	.00	.10	.16	1.680
Fe^{2+}	.19	.20	.52	1.27	.02	.08	.10	.742
Mn	.01	.01	.02	.00	.00	.00	.00	.016
Mg	.82	.80	1.41	3.06	.00	.87	.71	.304
Ca	.80	.85	.02	1.67	.68	.86	.82	.010
Na	.02	.03	.00	.84	.33	.04	.05	.000
K	.00	.00	.00	.09	.01	.00	.00	.000
Total	4.00	4.00	4.00	15.24	5.02	4.00	4.00	3.000
endmember units								
An	-	-	-	-	66.93	-	-	-
Ab	-	-	-	-	32.08	-	-	-
Or	-	-	-	-	.99	-	-	-
Ca	42.31	44.43	.95	27.87	-	44.96	45.75	-
Mg	43.21	41.56	70.07	51.01	-	45.64	39.46	-
Fe*	14.48	14.01	28.98	21.12	-	19.40	14.79	-
% Ilm	-	-	-	-	-	-	-	-
% Usp	-	-	-	-	-	-	-	.058

NOTES: Association 1: core of xenolith; 2: reaction rim.

VUW: 17512   FIELD: AM2-8
FORMATION: RANGIPO TORLESSE SUITE
LITHOLOGY: GREYWACKE

MINERAL	pl	pl	mus
LOC	c	c	c
ASSOC	-	-	-
ANAL	1	m6	1
SiO_2	68.88	68.75	50.43
TiO_2	.00	.00	.88
Al_2O_3	19.93	20.14	33.13
Cr_2O_3	.00	.00	.00
Fe_2O_3	.00	.00	.00
FeO	.00	.00	3.90
MnO	.00	.00	.12
MgO	.00	.00	1.93
CaO	.00	.34	.00
Na_2O	11.84	11.72	.18
K_2O	.00	.00	5.37
Total	100.65	100.95	95.94
oxygens	8	8	22
Si	2.99	2.97	6.50
Ti	.00	.00	.09
Al	1.02	1.03	5.04
Cr	.00	.00	.00
Fe^{3+}	.00	.00	.00
Fe^{2+}	.00	.00	.42
Mn	.00	.00	.01
Mg	.00	.00	.37
Ca	.00	.02	.00
Na	.99	.98	.05
K	.00	.00	.88
Total	5.00	5.00	13.36
endmember units			
An	100.00	98.40	-
Ab	0.00	1.60	-
Or	0.00	0.00	-
Ca	-	-	-
Mg	-	-	-
Fe*	-	-	-
% Ilm	-	-	-
% Usp	-	-	-

VUW: 17833 FIELD: B4A
FORMATION: RANGIPO WAIPAPA SUITE
LITHOLOGY: GREYWACKE

MINERAL	pl	pl	pl	pl	ks	chl	mus	hb	preh	epid
LOC	c	c	c	c	c	c	c	c	c	c
ASSOC	-	-	-	-	-	-	-	-	-	-
ANAL	m6	1	1	m3	m4	m3	m2	m3	m2	1
SiO_2	68.72	66.58	64.78	63.91	64.90	28.09	51.97	48.48	42.68	37.54
TiO_2	.00	.00	.00	.00	.00	2.40	.08	.45	.00	.00
Al_2O_3	19.28	20.21	21.64	22.26	17.99	14.86	26.77	7.29	22.23	23.54
Cr_2O_3	.00	.00	.00	.00	.00	.00	.00	.00	.00	.00
Fe_2O_3	.00	.00	.00	.00	.00	.00	.00	.00	.00	.00
FeO	.00	.26	.15	.26	.22	27.92	3.48	10.75	2.50	11.61
MnO	.00	.00	.00	.00	.00	.50	.08	.22	.00	.00
MgO	.00	.00	.00	.00	.00	10.65	1.24	15.45	.10	.00
CaO	.06	.90	2.77	4.07	.01	.90	1.37	12.28	26.35	23.39
Na_2O	12.15	11.10	9.82	9.01	.48	.00	.51	1.03	.00	.00
K_2O	.00	.35	.27	.84	15.76	1.16	8.91	.15	.00	.00
Total	100.21	99.40	99.43	100.35	99.36	86.48	94.41	96.10	93.86	96.08
oxygens	8	8	8	8	8	28	22	22	22	12
Si	3.00	2.94	2.87	2.83	3.01	6.17	6.98	6.79	6.05	2.97
Ti	.00	.00	.00	.00	.00	.40	.01	.05	.00	.00
Al	.99	1.05	1.13	1.16	.99	3.85	4.24	1.20	3.72	2.20
Cr	.00	.00	.00	.00	.00	.00	.00	.00	.00	.00
Fe^{3+}	.00	.00	.00	.00	.00	.00	.00	.00	.00	.00
Fe^{2+}	.00	.01	.01	.01	.01	5.13	.39	1.26	.30	.77
Mn	.00	.00	.00	.00	.00	.09	.01	.03	.00	.00
Mg	.00	.00	.00	.00	.00	3.49	.25	3.23	.02	.00
Ca	.00	.04	.13	.19	.00	.21	.20	1.84	4.00	1.99
Na	1.03	.95	.84	.77	.06	.00	.13	.28	.00	.00
K	.00	.02	.02	.05	.94	.33	1.53	.03	.00	.00
Total	5.02	5.01	5.00	5.01	5.01	19.67	13.74	14.71	14.09	7.93
endmember units										
An	.29	3.96	13.13	19.05	.00	-	-	-	-	-
Ab	99.71	94.06	84.85	76.21	4.41	-	-	-	-	-
Or	.00	1.98	2.02	4.74	95.59	-	-	-	-	-
Ca	-	-	-	-	-	2.38	-	29.01	92.66	72.08
Mg	-	-	-	-	-	39.09	-	50.76	6.85	.00
Fe*	-	-	-	-	-	58.53	-	20.24	.49	27.92
% Ilm	-	-	-	-	-	-	-	-	-	-
% Usp	-	-	-	-	-	-	-	-	-	-

VUW: 17885 FIELD: PQX-1
FORMATION: PUKEONAKE
LITHOLOGY: TYPE QXb XENOLITH

MINERAL	cpx	pl	glass	glass	cpx	mes
LOC	c	c	c	c	c	c
ASSOC	1	1	1	2	3	4
ANAL	1	1	1	m3	m2	m2
SiO_2	50.83	44.58	68.26	72.01	52.97	65.01
TiO_2	.17	.00	.63	.63	.17	1.14
Al_2O_3	.68	35.95	10.64	10.01	.51	12.22
Cr_2O_3	.00	.00	.00	.00	.00	.00
Fe_2O_3	.44	.00	.00	.00	2.21	.00
FeO	14.22	.00	4.64	4.04	7.44	7.33
MnO	.79	.00	.00	.00	.33	.20
MgO	7.86	.00	.74	.61	16.41	1.26
CaO	23.75	19.11	2.38	1.71	19.59	3.65
Na_2O	.26	.68	2.91	2.89	.30	4.84
K_2O	.09	.00	2.97	3.25	.00	1.36
Cl	.00	.00	.09	.00	.00	.10
Total	99.09	100.32	93.26	95.14	99.31	97.11
oxygens	6	8	-	-	6	-
Si	1.98	2.05	-	-	1.96	-
Ti	.01	.00	-	-	.01	-
Al	.03	1.95	-	-	.02	-
Cr	.00	.00	-	-	.00	-
Fe^{3+}	.01	.00	-	-	.06	-
Fe^{2+}	.47	.00	-	-	.23	-
Mn	.03	.00	-	-	.01	-
Mg	.46	.00	-	-	.91	-
Ca	.99	.94	-	-	.78	-
Na	.02	.06	-	-	.02	-
K	.00	.00	-	-	.00	-
Total	4.00	5.00	-	-	4.00	-
endmember units						
An	-	93.92	-	-	-	-
Ab	-	6.08	-	-	-	-
Or	-	.00	-	-	-	-
Ca	50.82	-	-	-	39.15	-
Mg	23.39	-	-	-	45.60	-
Fe*	25.79	-	-	-	15.25	-
% Ilm	-	-	-	-	-	-
% Usp	-	-	-	-	-	-

NOTES: Association 1: broken area of xenolith;
2: contact zone; 3: cpx reaction rim;
4: host lava.

VUW: 17887 FIELD: N112B #
FORMATION: WHAKAPAPA (RUAPEHU)
LITHOLOGY: TYPE 1 DACITE

MINERAL	cpx	opx	opx	pl	pl	ilm+
LOC	r	c	r	c	r	c
ASSOC	-	-	-	-	-	pl
ANAL	1	m2	m2	1	1	1
SiO_2	51.25	51.38	50.73	54.80	58.59	.00
TiO_2	.40	.31	.24	.00	.00	48.83
Al_2O_3	1.26	1.18	.94	28.36	25.49	.14
Cr_2O_3	.00	.00	.00	.00	.00	.00
Fe_2O_3	.83	1.22	.00	.00	.00	5.13
FeO	13.23	23.50	29.57	.40	.34	41.88
MnO	.32	.50	.60	.00	.00	.47
MgO	11.98	20.08	15.89	.00	.00	2.05
NiO	.00	.00	.00	.00	.00	.00
CaO	19.91	1.53	1.38	11.27	8.23	.16
Na_2O	.27	.00	.00	5.18	6.36	.00
K_2O	.00	.00	.00	.37	.64	.00
Total	99.45	99.70	99.35	100.38	99.65	98.66
oxygens	6	6	6	8	8	3
Si	1.96	1.94	1.98	2.47	2.63	.000
Ti	.01	.01	.01	.00	.00	.925
Al	.06	.05	.04	1.51	1.35	.004
Cr	.00	.00	.00	.00	.00	.000
Fe^{3+}	.02	.04	.00	.00	.00	.146
Fe^{2+}	.42	.75	.96	.02	.01	.834
Mn	.01	.02	.02	.00	.00	.010
Mg	.68	1.13	.92	.00	.00	.077
Ni	.00	.00	.00	.00	.00	.000
Ca	.82	.06	.06	.54	.40	.004
Na	.02	.00	.00	.45	.55	.000
K	.00	.00	.00	.02	.04	.000
Total	4.00	4.00	3.99	5.01	4.98	2.000
endmember units						
An	-	-	-	53.49	40.12	-
Ab	-	-	-	44.44	56.13	-
Or	-	-	-	2.07	3.75	-
Ca	41.73	3.11	2.95	-	-	-
Mg	34.92	56.93	47.00	-	-	-
Fe*	23.35	39.96	50.05	-	-	-
% Ilm	-	-	-	-	-	.923
% Usp	-	-	-	-	-	-

NOTES: Analysis by W.R.Hackett.
sample similar to 17886 ; + inclusion in pl.

VUW: 17888 FIELD: XXA#
FORMATION: WAHIANOA (RUAPEHU)
LITHOLOGY: TYPE QPXd XENOLITH

MINERAL	ol	opx	pl	tmt
LOC	c	c	c	c
ASSOC	-	-	-	-
ANAL	1	m7	m3	m4
SiO_2	37.35	51.70	45.27	.18
TiO_2	.00	.28	.00	11.07
Al_2O_3	.00	2.33	35.01	4.04
Cr_2O_3	.00	.00	.00	.62
Fe_2O_3	.00	1.71	.00	41.93
FeO	23.99	18.03	.57	38.40
MnO	.35	.59	.00	.30
MgO	37.44	23.59	.00	2.04
CaO	.07	1.09	18.14	.00
Na_2O	.00	.00	1.38	.00
K_2O	.00	.00	.00	.00
Total	99.34	99.32	100.37	98.58
oxygens	4	6	8	4
Si	.989	1.92	2.08	.007
Ti	.000	.01	.00	.309
Al	.000	.10	1.90	.177
Cr	.000	.00	.00	.018
Fe^{3+}	.000	.05	.00	1.173
Fe^{2+}	.531	.56	.02	1.194
Mn	.008	.02	.00	.009
Mg	1.478	1.30	.00	.113
Ca	.002	.04	.90	.000
Na	.000	.00	.12	.000
K	.000	.00	.00	.000
Total	3.011	4.00	5.02	3.000
endmember units				
An	-	-	87.83	-
Ab	-	-	12.17	-
Or	-	-	.00	-
Ca	.10	2.23	-	-
Mg	73.24	66.09	-	-
Fe*	26.66	31.68	-	-
% Ilm	-	-	-	-
% Usp	-	-	-	.358

NOTES: # inclusion in cumulate nodule.

VUW: 17890 FIELD: H7X-6#
FORMATION: PUKEONAKE
LITHOLOGY: TYPE IX XENOLITH

MINERAL	ol	glass	crsp
LOC	c	c	c
ASSOC	-	-	-
ANAL	1	1	1
SiO_2	41.15	53.56	.00
TiO_2	.00	.97	.51
Al_2O_3	.00	18.14	11.03
Cr_2O_3	.00	.00	53.32
Fe_2O_3	.00	.00	6.74
FeO	10.26	6.12	16.33
MnO	.00	.12	.00
MgO	47.58	4.40	11.44
NiO	.31	.00	.22
CaO	.12	8.82	.00
Na_2O	.00	4.46	.00
K_2O	.00	2.04	.00
Total	99.42	98.63	99.59
oxygens	4	-	4
Si	1.015	-	.000
Ti	.000	-	.013
Al	.000	-	.426
Cr	.000	-	1.382
Fe^{3+}	.000	-	.166
Fe^{2+}	.212	-	.448
Mn	.000	-	.000
Mg	1.749	-	.560
Ni	.006	-	.006
Ca	.003	-	.000
Na	.000	-	.000
K	.000	-	.000
Total	2.985	-	3.000
endmember units			
An	-	-	-
Ab	-	-	-
Or	-	-	-
Ca	.15	-	-
Mg	89.09	-	-
Fe*	10.76	-	-
% Ilm	-	-	-
% Usp	-	-	.443

NOTES: Analysis by W.R.Hackett.
similar to PDX-1

VUW: 17894 FIELD: Xc
FORMATION: WAHIANOA (RUAPEHU)
LITHOLOGY: TYPE QPXb XENOLITH

MINERAL	opx	opx	pl	cord	gnt	gnt	ilm	pleon
LOC	c	r	c	c	c	r	c	c
ASSOC	-	-	-	-	-	-	1	1
ANAL	1	1	1	1	1	1	1	1
SiO_2	47.79	46.55	61.31	48.09	37.90	37.69	.00	.00
TiO_2	.21	.26	.00	.00	.11	.10	48.56	.74
Al_2O_3	3.60	6.14	23.65	32.76	21.33	21.34	.16	51.35
Cr_2O_3	.00	.00	.00	.00	.40	.00	.41	2.94
Fe_2O_3	1.44	1.44	.00	.00	.00	.00	6.80	5.98
FeO	32.36	28.22	.14	9.77	32.00	31.39	40.54	30.04
MnO	.48	.30	.00	.11	.79	.88	.31	.12
MgO	13.59	14.60	.00	8.16	7.23	7.13	1.58	6.42
CaO	.21	.16	5.27	.10	.74	.77	.00	.00
Na_2O	.00	.25	8.05	.00	.00	.00	.00	.00
K_2O	.00	.00	1.25	.00	.00	.00	.00	.00
Total	99.68	97.92	99.67	98.99	100.50	99.30	98.36	97.59
oxygens	6	6	8	18	12	12	3	4
Si	1.88	1.83	2.74	4.96	2.97	2.98	.000	.000
Ti	.01	.01	.00	.00	.01	.01	.929	.016
Al	.17	.29	1.25	3.98	1.97	1.99	.005	1.768
Cr	.00	.00	.00	.00	.03	.00	.008	.068
Fe^{3+}	.04	.04	.00	.00	.00	.00	.130	.131
Fe^{2+}	1.07	.93	.01	.84	2.10	2.08	.861	.734
Mn	.02	.01	.00	.01	.05	.06	.007	.003
Mg	.80	.86	.00	1.25	.84	.84	.060	.280
Ca	.01	.01	.25	.01	.06	.07	.000	.000
Na	.00	.02	.70	.00	.00	.00	.000	.000
K	.00	.00	.07	.00	.00	.00	.000	.000
Total	4.00	4.00	5.02	11.05	8.03	8.03	2.000	3.000
endmember units								
An	-	-	24.76	-	-	-	-	-
Ab	-	-	68.30	-	-	-	-	-
Or	-	-	6.94	-	-	-	-	-
Ca	.49	.38	-	.52	3.07	3.14	-	-
Mg	41.28	46.41	-	59.23	27.64	27.64	-	-
Fe*	58.23	53.21	-	40.25	70.33	70.22	-	-
% Ilm	-	-	-	-	-	-	.932	-
% Usp	-	-	-	-	-	-	-	.728

NOTES: Analysis by W.R.Hackett.

VUW: 17895 FIELD: NX-1
FORMATION: TONGARIRO
LITHOLOGY: TYPE UCX XENOLITH (CALCSILICATE)

MINERAL	cpx	woll
LOC	c	c
ASSOC	-	-
ANAL	1	1
SiO_2	50.04	51.05
TiO_2	.00	.00
Al_2O_3	.50	.00
Cr_2O_3	.00	.00
Fe_2O_3	1.14	1.33
FeO	18.36	.84
MnO	.81	.44
MgO	5.59	.23
CaO	23.44	46.31
Na_2O	.14	.00
K_2O	.00	.00
Total	100.02	100.20
oxygens	6	6
Si	1.98	1.97
Ti	.00	.00
Al	.02	.00
Cr	.00	.00
Fe^{3+}	.03	.04
Fe^{2+}	.61	.03
Mn	.03	.02
Mg	.33	.01
Ca	.99	1.93
Na	.01	.00
K	.00	.00
Total	4.00	4.00
endmember units		
An	-	-
Ab	-	-
Or	-	-
Ca	49.87	95.34
Mg	16.54	.64
Fe*	33.69	4.02
% Ilm	-	-
% Usp	-	-

VUW: 17896 FIELD: NX-9
FORMATION: NGAURUHOE 1954
LITHOLOGY: TYPE UCX XENOLITH (CALCSILICATE)

MINERAL	woll	pl	pl	sph
LOC	c	c	c	c
ASSOC	-	-	-	-
ANAL	1	1	1	1
SiO_2	51.49	42.46	43.82	29.83
TiO_2	.00	.00	.00	37.28
Al_2O_3	.06	36.24	34.44	.85
Cr_2O_3	.00	.00	.00	.00
Fe_2O_3	.34	.00	.00	.00
FeO	2.16	.21	.87	1.16
MnO	.40	.00	.00	.00
MgO	.40	.00	.00	.00
CaO	45.50	20.14	19.07	26.95
Na_2O	.00	.00	.54	.00
K_2O	.00	.00	.00	.00
Total	100.35	99.05	98.74	96.07
oxygens	6	8	8	20
Si	2.00	1.99	2.06	4.06
Ti	.00	.00	.00	3.81
Al	.00	2.00	1.91	.14
Cr	.00	.00	.00	.00
Fe^{3+}	.01	.00	.00	.00
Fe^{2+}	.07	.01	.03	.13
Mn	.01	.00	.00	.00
Mg	.02	.00	.00	.00
Ca	1.89	1.01	.96	3.93
Na	.00	.00	.05	.00
K	.00	.00	.00	.00
Total	4.00	5.01	5.01	12.07
endmember units				
An	-	100.00	95.14	-
Ab	-	.00	4.86	-
Or	-	.00	.00	-
Ca	94.21	-	-	-
Mg	1.15	-	-	-
Fe*	4.64	-	-	-
% Ilm	-	-	-	-
% Usp	-	-	-	-

VUW: 22993 FIELD: O-K
FORMATION: ORAKEI KORAKO
LITHOLOGY: HIGH-ALUMINA BASALT

MINERAL	cpx	cpx	cpx	cpx	cpx	cpx	cpx	cpx
LOC	1	2	3	4	5	6	7	8
ASSOC	-	-	-	-	-	-	-	-
ANAL	1	1	1	1	1	1	1	1
SiO_2	49.10	51.15	49.04	50.67	48.38	51.27	51.45	50.11
TiO_2	1.33	.83	1.11	.75	1.47	.83	1.07	1.36
Al_2O_3	6.06	4.40	5.94	4.30	6.39	3.77	2.32	2.05
Cr_2O_3	.00	.00	.00	.00	.00	.17	.00	.00
Fe_2O_3	2.11	1.60	3.18	1.61	3.65	2.25	1.39	1.85
FeO	5.38	5.09	5.25	5.71	5.24	5.02	9.17	13.88
MnO	.00	.00	.32	.00	.29	.23	.32	.46
MgO	15.23	15.76	14.81	15.22	14.30	15.75	14.90	12.59
NiO	.00	.00	.00	.00	.00	.00	.00	.00
CaO	19.95	21.26	20.25	21.04	20.62	21.42	19.38	17.49
Na_2O	.39	.32	.37	.32	.37	.28	.35	.42
K_2O	.00	.00	.00	.00	.00	.00	.00	.00
Total	99.55	100.41	100.27	99.62	100.71	100.99	100.35	100.21
oxygens	6	6	6	6	6	6	6	6
Si	1.81	1.88	1.81	1.87	1.78	1.87	1.90	1.91
Ti	.04	.02	.03	.02	.04	.02	.03	.04
Al	.26	.19	.26	.19	.28	.16	.10	.09
Cr	.00	.00	.00	.00	.00	.01	.00	.00
Fe^{3+}	.06	.04	.09	.05	.10	.06	.04	.05
Fe^{2+}	.17	.16	.16	.18	.16	.15	.29	.44
Mn	.00	.00	.01	.00	.01	.01	.01	.02
Mg	.84	.86	.81	.84	.79	.86	.83	.71
Ni	.00	.00	.00	.00	.00	.00	.00	.00
Ca	.79	.83	.80	.83	.81	.84	.77	.71
Na	.03	.02	.03	.02	.03	.02	.03	.03
K	.00	.00	.00	.00	.00	.00	.00	.00
Total	4.00	4.00	4.00	4.00	4.00	4.00	4.00	4.00
endmember units								
An	-	-	-	-	-	-	-	-
Ab	-	-	-	-	-	-	-	-
Or	-	-	-	-	-	-	-	-
Ca	42.62	44.06	42.69	44.01	43.48	43.60	39.96	36.81
Mg	45.20	45.38	43.44	44.27	41.99	44.59	42.75	36.90
Fe*	12.18	10.56	13.87	11.72	14.53	11.81	17.29	26.29
% Ilm	-	-	-	-	-	-	-	-
% Usp	-	-	-	-	-	-	-	-

NOTES: Zoned clinopyroxene phenocryst - analysis localities given in accompanying figure.

VUW: 22993 FIELD: O-K
FORMATION: ORAKEI KORAKO
LITHOLOGY: HIGH-ALUMINA BASALT

MINERAL	ol	ol	cpx	cpx	pl	pl#	ol	cpx	glass	tmt
LOC	c	r	c	r	c	r	g	g	g	c
ASSOC	-	-	-	-	-	-	-	-	-	-
ANAL	1	1	1	1	m2	1	1	1	1	1
SiO_2	38.88	37.12	50.44	51.60	50.40	55.99	33.76	51.25	69.82	.21
TiO_2	.00	.00	.75	.90	.00	.00	.00	.66	.40	20.10
Al_2O_3	.00	.00	5.45	2.28	30.27	27.34	.25	1.17	11.37	.90
Cr_2O_3	.00	.00	.59	.00	.00	.00	.00	.00	.00	.00
Fe_2O_3	.00	.00	1.52	.50	.00	.00	.00	1.89	.00	26.06
FeO	18.67	27.24	5.15	9.23	.54	.86	47.51	15.61	2.83	46.56
MnO	.26	.54	.00	.26	.00	.00	.72	.58	.18	.55
MgO	41.53	33.94	15.77	14.83	.15	.12	17.13	15.84	.07	.87
NiO	.00	.00	.00	.00	.00	.00	.00	.00	.00	.00
CaO	.19	.34	20.41	19.34	14.31	10.84	.50	12.53	.74	.27
Na_2O	.00	.00	.35	.39	3.72	5.52	.00	.30	3.86	.00
K_2O	.00	.00	.00	.00	.10	.20	.00	.00	4.84	.00
Cl	.00	.00	.00	.00	.00	.00	.00	.00	.53	.00
Total	99.53	99.18	100.43	99.33	99.34	100.78	99.87	99.83	94.64	95.52
oxygens	4	4	6	6	8	8	4	6	-	4
Si	.998	.999	1.84	1.92	2.32	2.51	1.005	1.95	-	.008
Ti	.000	.000	.02	.03	.00	.00	.000	.02	-	.589
Al	.000	.000	.24	.10	1.64	1.45	.009	.05	-	.041
Cr	.000	.000	.02	.00	.00	.00	.000	.00	-	.000
Fe^{3+}	.000	.000	.04	.01	.00	.00	.000	.05	-	.764
Fe^{2+}	.401	.613	.16	.29	.02	.03	1.183	.49	-	1.518
Mn	.006	.012	.00	.01	.00	.00	.018	.02	-	.018
Mg	1.590	1.362	.85	.83	.01	.01	.760	.89	-	.051
Ni	.000	.000	.00	.00	.00	.00	.000	.00	-	.000
Ca	.005	.010	.80	.78	.71	.52	.016	.51	-	.011
Na	.000	.000	.03	.03	.33	.48	.000	.02	-	.000
K	.000	.000	.00	.00	.01	.01	.000	.00	-	.000
Total	3.000	2.996	4.00	4.00	5.04	5.01	2.991	4.00	-	3.000
endmember units										
An	-	-	-	-	67.90	51.81	-	-	-	-
Ab	-	-	-	-	31.53	47.01	-	-	-	-
Or	-	-	-	-	.57	1.18	-	-	-	-
Ca	.25	.50	42.63	40.52	-	-	.82	25.81	-	-
Mg	79.41	68.20	45.83	43.24	-	-	38.44	45.38	-	-
Fe*	20.34	31.30	11.54	16.24	-	-	60.74	28.81	-	-
% Ilm	-	-	-	-	-	-	-	-	-	-
% Usp	-	-	-	-	-	-	-	-	-	.607

NOTES: # rim in contact with acid-residuum glass.

VUW: 22996 FIELD: K-T
FORMATION: K-TRIG
LITHOLOGY: HIGH-ALUMINA BASALT

MINERAL	ol#	cpx	cpx	cpx	pl	pl	pl	glass	tmt
LOC	c	c	r	g	c	r	g	g	g
ASSOC	-	-	-	-	-	-	-	-	-
ANAL	1	1	1	1	1	1	1	1	1
SiO_2	38.10	48.72	52.62	51.25	48.04	52.57	51.24	79.58	.00
TiO_2	.00	1.32	.36	.89	.00	.00	.00	.60	7.86
Al_2O_3	1.18	6.03	2.40	2.23	32.61	29.47	30.77	10.31	.88
Cr_2O_3	.00	.36	.00	.00	.00	.00	.00	.00	.00
Fe_2O_3	.00	1.64	1.27	1.53	.00	.00	.00	.00	50.60
FeO	24.16	6.31	7.07	4.90	.73	.91	1.18	.98	29.37
MnO	.56	.19	.25	.47	.00	.00	.00	.00	.73
MgO	30.48	14.29	17.88	15.71	.12	.09	.09	.08	3.98
NiO	.00	.00	.00	.00	.00	.00	.00	.00	.00
CaO	.50	20.63	18.23	22.41	16.33	12.85	14.44	.38	.25
Na_2O	.00	.22	.16	.00	2.34	4.18	3.55	.86	.00
K_2O	.00	.00	.00	.00	.00	.31	.27	4.59	.00
Total	94.98	99.71	100.24	99.39	100.17	100.38	101.54	97.38	93.67
oxygens	-	6	6	6	8	8	8	-	4
Si	-	1.80	1.92	1.90	2.21	2.39	2.32	-	.000
Ti	-	.04	.01	.03	.00	.00	.00	-	.232
Al	-	.26	.10	.10	1.76	1.58	1.64	-	.041
Cr	-	.01	.00	.00	.00	.00	.00	-	.000
Fe^{3+}	-	.05	.04	.04	.00	.00	.00	-	1.493
Fe^{2+}	-	.20	.22	.15	.03	.04	.05	-	.962
Mn	-	.01	.01	.02	.00	.00	.00	-	.024
Mg	-	.79	.97	.87	.01	.01	.01	-	.233
Ni	-	.00	.00	.00	.00	.00	.00	-	.000
Ca	-	.82	.72	.89	.80	.63	.70	-	.105
Na	-	.02	.01	.00	.21	.37	.31	-	.000
K	-	.00	.00	.00	.00	.02	.02	-	.000
Total	-	4.00	4.00	4.00	5.02	5.04	5.05	-	3.000
endmember units									
An	-	-	-	-	79.59	62.05	68.31	-	-
Ab	-	-	-	-	20.41	36.18	30.14	-	-
Or	-	-	-	-	-	1.77	1.55	-	-
Ca	-	43.89	36.69	45.26	-	-	-	-	-
Mg	-	42.29	50.03	44.10	-	-	-	-	-
Fe*	-	13.82	13.28	10.64	-	-	-	-	-
% Ilm	-	-	-	-	-	-	-	-	-
% Usp	-	-	-	-	-	-	-	-	.200

NOTES: # olivine severely corroded (partial analysis only).

VUW: 22998 FIELD: ONG
FORMATION: ONGAROTO
LITHOLOGY: HIGH-ALUMINA BASALT

MINERAL	ol	ol	cpx	cpx	cpx	cpx	opx
LOC	c	r	c	c	c	c	c
ASSOC	1	-	-	-	-	-	-
ANAL	1	1	1	1	1	1	m2
SiO_2	40.31	37.67	50.74	52.61	50.63	52.00	52.72
TiO_2	.00	.00	1.00	.43	1.43	.66	.50
Al_2O_3	.00	.00	4.11	1.87	1.14	2.08	.77
Cr_2O_3	.00	.00	.50	.41	.00	.36	.00
Fe_2O_3	.00	.00	2.35	1.19	1.22	2.85	.68
FeO	12.32	26.62	6.35	6.88	12.30	5.02	18.58
MnO	.00	.49	.26	.32	.43	.27	.51
MgO	46.51	35.88	17.07	18.81	14.33	17.13	21.95
NiO	.00	.00	.00	.00	.00	.00	.00
CaO	.19	.16	18.34	16.95	17.16	19.72	3.97
Na_2O	.00	.00	.23	.18	.34	.36	.04
K_2O	.00	.00	.00	.00	.00	.00	.00
Total	99.33	100.82	100.95	99.65	98.98	100.45	99.72
oxygens	4	4	6	6	6	6	6
Si	1.001	.994	1.85	1.94	1.93	1.91	1.96
Ti	.000	.000	.03	.01	.04	.02	.01
Al	.000	.000	.18	.08	.05	.09	.03
Cr	.000	.000	.02	.01	.00	.00	.00
Fe^{3+}	.000	.000	.07	.03	.04	.08	.02
Fe^{2+}	.258	.587	.19	.21	.39	.15	.58
Mn	.000	.011	.01	.01	.01	.01	.02
Mg	1.735	1.410	.93	1.03	.81	.94	1.22
Ni	.000	.000	.00	.00	.00	.00	.00
Ca	.005	.005	.72	.67	.70	.77	.16
Na	.000	.000	.02	.01	.03	.03	.00
K	.000	.000	.00	.00	.00	.00	.00
Total	2.999	3.007	4.00	4.00	4.00	4.00	4.00
endmember units							
An	-	-	-	-	-	-	-
Ab	-	-	-	-	-	-	-
Or	-	-	-	-	-	-	-
Ca	.25	.25	37.19	34.00	35.81	39.67	7.95
Mg	86.84	70.04	48.18	52.45	41.64	47.98	61.22
Fe*	12.91	29.71	14.63	13.55	22.55	12.35	30.83
% Ilm	-	-	-	-	-	-	-
% Usp	-	-	-	-	-	-	-

NOTES: Association 1: olivine with chromian spinel.

VUW: 22998 FIELD: ONG
FORMATION: ONGAROTO
LITHOLOGY: HIGH ALUMINA BASALT

MINERAL	pl	pl	glass	mes#	tmt	crsp
LOC	c	r	g	g	g	c
ASSOC	-	-	-	-	-	1
ANAL	1	1	1	1	m2	1
SiO_2	50.13	61.10	76.37	65.09	.10	.09
TiO_2	.00	.00	1.20	1.00	18.46	.72
Al_2O_3	30.77	23.62	13.19	13.28	2.02	17.59
Cr_2O_3	.00	.00	.00	.00	.00	41.24
Fe_2O_3	.00	.00	.00	.00	30.17	8.72
FeO	.90	.69	1.44	1.86	46.51	20.98
MnO	.00	.00	.00	.00	.46	.14
MgO	.09	.00	.00	.09	.82	9.09
NiO	.00	.00	.00	.00	.00	.00
CaO	14.36	5.69	.45	.54	.00	.00
Na_2O	3.43	7.53	1.05	3.05	.00	.00
K_2O	.00	.92	3.68	7.20	.00	.00
Cl	.00	.00	.38	.57	.00	.00
Total	99.68	99.55	97.76	92.68	98.54	98.57
oxygens	8	8	-	-	4	4
Si	2.30	2.74	-	-	.004	.003
Ti	.00	.00	-	-	.523	.018
Al	1.67	1.25	-	-	.090	.678
Cr	.00	.00	-	-	.000	1.065
Fe^{3+}	.00	.00	-	-	.856	.215
Fe^{2+}	.04	.03	-	-	1.466	.574
Mn	.00	.00	-	-	.015	.004
Mg	.01	.00	-	-	.046	.443
Ni	.00	.00	-	-	.000	.000
Ca	.71	.27	-	-	.000	.000
Na	.31	.65	-	-	.000	.000
K	.00	.05	-	-	.000	.000
Total	5.04	4.99	-	-	3.000	3.000
endmember units						
An	70.01	27.86	-	-	-	-
Ab	29.99	66.73	-	-	-	-
Or	.00	5.41	-	-	-	-
Ca	-	-	-	-	-	-
Mg	-	-	-	-	-	-
Fe*	-	-	-	-	-	-
% Ilm	-	-	-	-	-	-
% Usp	-	-	-	-	.565	.459

NOTES: # contains orthoclase microlites.

VUW: 29250 FIELD: N54
FORMATION: NGAURUHOE 1954
LITHOLOGY: TYPE 1 BASIC ANDESITE

MINERAL	ol	ol	cpx	cpx	opx	opx	pl	pl	mes
LOC	c	r	c	c	c	r	c	r	c
ASSOC	-	-	-	-	-	-	-	-	-
ANAL	1	1	1	m3	m4	m2	m4	m3	1
SiO_2	38.70	37.97	52.10	51.91	52.85	52.36	50.05	51.83	65.94
TiO_2	.00	.00	.47	.32	.20	.23	.00	.00	2.03
Al_2O_3	.00	.00	3.85	2.64	1.47	1.14	31.23	29.89	12.25
Cr_2O_3	.00	.00	.00	.22	.00	.00	.00	.00	.00
Fe_2O_3	.00	.00	.00	.82	1.51	1.07	.00	.00	.00
FeO	19.40	23.01	19.34	6.85	16.38	19.76	.60	.74	6.47
MnO	.22	.55	.44	.14	.43	.45	.00	.00	.00
MgO	42.01	37.92	15.29	16.51	24.82	22.63	.08	.11	.25
NiO	.00	.00	.00	.00	.00	.00	.00	.00	.00
CaO	.15	.21	5.64	19.37	1.82	1.78	14.54	13.07	3.23
Na_2O	.00	.00	.65	.25	.00	.00	3.02	3.73	2.82
K_2O	.00	.00	.19	.00	.00	.00	.12	.18	3.35
Total	100.48	99.66	97.97	99.03	99.48	99.42	99.62	99.55	96.34
oxygens	4	4	6	6	6	6	8	8	-
Si	.987	.997	1.98	1.93	1.95	1.95	2.29	2.37	-
Ti	.000	.000	.01	.01	.01	.01	.00	.00	-
Al	.000	.000	.17	.12	.06	.05	1.69	1.61	-
Cr	.000	.000	.00	.01	.00	.00	.00	.00	-
Fe^{3+}	.000	.000	.00	.02	.04	.03	.00	.00	-
Fe^{2+}	.414	.505	.62	.21	.50	.62	.02	.03	-
Mn	.005	.007	.01	.00	.01	.01	.00	.00	-
Mg	1.595	1.484	.87	.91	1.36	1.26	.01	.01	-
Ni	.000	.000	.00	.00	.00	.00	.00	.00	-
Ca	.004	.006	.23	.77	.07	.07	.71	.64	-
Na	.000	.000	.05	.02	.00	.00	.27	.33	-
K	.000	.000	.01	.00	.00	.00	.01	.01	-
Total	3.005	2.999	3.95	4.00	4.00	4.00	5.00	5.00	-
endmember units									
An	-	-	-	-	-	-	72.33	65.49	-
Ab	-	-	-	-	-	-	27.06	33.50	-
Or	-	-	-	-	-	-	.61	1.01	-
Ca	.20	.30	13.33	39.95	3.62	3.57	-	-	-
Mg	79.04	74.13	50.20	47.31	68.33	63.22	-	-	-
Fe*	20.76	25.57	36.47	12.74	28.05	33.21	-	-	-
% Ilm	-	-	-	-	-	-	-	-	-
% Usp	-	-	-	-	-	-	-	-	-

****

APPENDIX 4: COMPUTER PROGRAMS

****

Computer programs written for Rb-Sr isotopic analysis are listed here in full with accompanying explanatory notes.

A4.1: CALCULATION OF $^{87}Rb/^{86}Sr$ FROM Rb/Sr AND $^{87}Sr/^{86}Sr$

The program is written for SAS (Statistical Analysis Systems).

Variables are from Handbook of Physics and Chemistry (55th Ed.).

```
DATA RBSR.CHEM;
     SET DATA.CHEM;
     A1=.0068;
     A2=.1194;
     A3=I*A2;
     S1=A1+A2+A3+1;
     N1=A1/S1*83.9134;
     N2=A2/S1*85.9094;
     N3=A3/S1*86.9089;
     N4= 1/S1*87.9056;
     M1=A2/S1;
     M2=N1+N2+N3+N4;
     M3=85.4678;
     M4=.2785;
     RB_SR=RB/SR;
     R87_86=RB_SR*M4/M1*M2/M3;
     I_SR=1/SR;
     DROP A1 A2 A3 S1 M1 N1 N2 N3 N4 M2 M3 M4;
     FORMAT RB_SR R87_86 6.3 I_SR 6.4;
     LABEL RB=Rb;
     LABEL SR=Sr;
     LABEL RB_SR=Rb/Sr;
     LABEL R87_86=87Rb/86Sr;
     LABEL I_SR=1/Sr;
     LABEL I=87Sr/86Sr;
PROC SORT;
     BY LOC VUW;
PROC PRINT ;
     BY LOC;
     TITLE RATIOS FOR SR ISOTOPIC ANALYSIS;
     VAR VUW LOC RB SR RB_SR R87_86 I_SR I;
```

Table A4.1: FMU settings for Rb and Sr isotopic analysis.

CHANNEL	Sr IA MASS	Sr IA GAUSS	Sr ID MASS	Sr ID GAUSS	Rb ID MASS	Rb ID GAUSS
1	84.5	841.5	84.5	841.5	84.5	841.5
2	85	858.8	85	858.8	85	858.8
3	86	887.5	86	887.5	87	916.0
4	87	916.0	87	916.0	88	944.5
5	88	944.5	88	944.5	84.5	841.5
6	89	974.5	84	830.0	-	-
7	84.5	841.5	84.5	841.5	-	-
MEASURE TIME	2.5s		3.0s		2.5s	
DELAY TIME	2.5s		3.0s		3.0s	

NOTES: Sr IA = Sr isotopic composition analysis;
Sr ID = Sr isotope dilution analysis;
Rb ID = Rb isotope dilution analysis.
GAUSS = FMU magnetic field reading (+ 2kG).
MEASURE TIME = time to make 27 readings of IBC
DELAY TIME = time to switch channels (i.e. to new MASS) and to perform required calculations.

Table A4.2: KEY options - listed are the expected responses for each of the three Rb-Sr HAL programs.

COMMAND	Sr IA	Sr ID	Rb ID
Carry On	0	0	0
Enter KEY Loop	1	1	1
Print Running Mean	2	2/5	2
Edit	3	3	3
Calculate & Print Grand mean	4	4	4
Print Blocks of Ten Scans	5	-	5
Print Final Headings	6	6	6
Restart	7	7	7
Go to end of Program	8	8	8
Calculate Sr (Rb) concentration	-	9	9

A4.2: SEMI-AUTOMATIC DATA ACQUISITION FROM MM30B

Programs in INS BASIC (Spedding, 1981a, 1981b) for semi-automatic data acquisition from MM30B (INS solid-source mass spectrometer) are based on an original version designed by E.H.Duckworth and Dr.C.J.D.Adams. The program listed here is for Sr IA analysis (c.f. Chapter 2.4) and is similar in form to two other programs for Sr ID and Rb ID analysis respectively. The main features are discussed in Chapter 2.4.2 and further expanded on in Graham (1983b).

s = statement; FMU = field memory unit; IBC = ion beam current

FMU settings are given in Table A4.1 and KEY options in Table A4.2.

Comments in the program are prefaced by REM or follow a colon.

```
 50 REM LAST MODIFIED ON 15-12-83
100 REM Rb-Sr HAL PROGRAM, VERSION 2
150 REM STRONTIUM ISOTOPIC COMPOSITION (SR IA) ANALYSIS
200 REM CREATE HEADINGS
300 DIM X(15),Y(15),G$(50),A$(50),          : DIMENSION ARRAYS & STRINGS
400 DATA 1,1,80,4                           : CREATE UPPER BOX
410 RESTORE 400
420 GOSUB 5040
430 GOSUB 4030
440 DATA 11,1,3,6,6,6,6,6,6,10,10,10,11,2  : CREATE LOWER BOX
450 RESTORE 440
460 PRINT CHR$(27);"Y&";                    : CURSOR TO ROW 6
470 GOSUB 5040
480 GOSUB 4100
490 DIM A(27),B(650),C(6),D(500)
495 LET Y2=0                                : SET TOTAL NUMBER OF SCANS
500 PRINT CHR$(27);"H";                     : CURSOR TO HOME
510 FOR M=1 TO 10                           : PRINT SCREEN HEADINGS
520 PRINT CHR$(27);"K"                      :     ON TELETYPE
530 NEXT M                                  :
550 PRINT CHR$(27);"G"                      : CLEAR SCREEN
580 REM BEGIN ANALYSIS
590 PRINT "READY TO START? - THEN TYPE GO"
600 INPUT F$                                : CHECK CORRECT START
610 IF F$="GO" THEN 620                     :   (s590-s615)
615 GOTO 590
620 PRINT CHR$(27);"Y*";                    : CURSOR TO ROW 11
630 PRINT CHR$(27);"G";                     : CLEAR SCREEN BELOW ROW 11
640 REM NORMALISE FLAGS
650 LET F1=0                                : AUTO START
660 LET F3=0                                : BLOCKS OF 10 SCANS
```

```
 670 LET F4=0                            : KEY
 700 LETPUT(163)=155                     : INITIALISE 8255 CHIPS
 710 LETPUT(171)=146                     :          "
 720 LETPUT(171)=7                       : PUT HOLD SIGNAL LOW
 730 LETPUT(171)=15                      : START FMU
 740 LETPUT(171)=14                      :      "
 730 LETPUT(171)=11                      : PROGRAM CONTROL ON
 760 IF F1=2 THEN 840                    : CHECK AUTO START
 770 LET F1=2                            :  (s760-s790)
 780 IF GET(169)>128 THEN 730
 790 GOTO 780
 840 KEY G1                              : INITIALISE KEY REGISTER
 850 GET BPOKE(32846)=48                 : ZERO IN SPACE ABOVE DATA
 860 LET X1=6                            : NUMBER OF CHANNELS
 870 LET X2=7                            : NUMBER OF CHANNELS + DUMMY
 880 LET Y1=102                          : MAX. NUMBER SUCCESSIVE SCANS
 890 LET V=27                            : NUMBER OF IBC MEASUREMENTS
 900 LET S1=0
 910 LET S2=0
 920 LET S3=0                            : INITIALISE VARIABLES FOR
 930 LET T1=0                            : SUMS IN MEAN CALCULATION
 940 LET T2=0                            :   (s900-s950)
 950 LET T3=0
 955 REM BEGIN DATA GENERATION
 960 LET Y=1                             : INITIALISE SCAN NUMBER
 970 LET X=0                             : INITIALISE CHANNEL NUMBER
1000 CALL(81,H)                          : OBTAIN FMU CHANNEL NUMBER
1010 IF F4=0 GOSUB 2500                  : CHECK FOR PROGRAM HALT
1015 REM CHECK FMU CHANNEL NUMBER = X
1020 IF H<>X THEN 1000
1030 LET A=0                             : INITIALISE SUM FOR IBC MEAN
1040 FOR M=1 TO V
1050 CALL(82,A(M))                       : OBTAIN AND SUM IBC READINGS
1060 LET A=A+A(M)                        : (s1040-s1070)
1070 NEXT M
1100 LET F2=0
1110 CALL(83,H)
1120 IF H=X THEN 1150                    : CHECK THAT NEXT X AGREES
1130 LET F2=1                            : WITH FMU CHANNEL NUMBER
1140 GOTO 1110                           : (s1100-s1150)
1150 IF F2=1 THEN 1000
1200 LET X=X+1                           : NEW CHANNEL NUMBER
1210 LET I=X+(X1*(Y-1))                  : ARGUMENT FOR ARRAY B(I)
1220 LET B(I)=INT(A/V)                   : STORE IBC MEAN IN ARRAY B(I)
1230 IF H2=1 THEN 1230                   : CHECK FOR PRINT & PROCEED
1240 GOSUB 6000                          : PRINT IBC MEAN
1250 IF X<X1 THEN 1000                   : COMPLETE THE SCAN
1260 IF Y=1 THEN 1800                    : SKIP INTERPOLATION ON SCAN 1
1290 REM CALCULATE INTERPOLATED VALUES
1300 FOR X=1 TO X1
1310 LET I=X+(X1*(Y-1))                  : ADD DIFFERENCE BETWEEN IBC
1320 LET K=B(I)-B(I-X1)                  :  MEANS OF SUCCESSIVE SCANS
1330 LET C(X)=B(I-X1)+(K*(X1-X)/X2)      :  TO THE FIRST IBC MEAN
1335 REM SUBTRACT BACKGROUND (CHANNEL 1)
1340 IF X=1 THEN 1380
1350 LET C(X)=C(X)-C(1)
1360 IF C(X)>0 THEN 1380
1370 LET C(X)=1                          : AVOID DIVISION BY ZERO
1375 NEXT X
1385 REM RB CONTAMINATION
```

```
1385 IF C(2)<2 THEN 1400                              : INSIGNIFICANT READING
1390 LET C(4)=C(4)-(C(2)*.3857)
1395 REM CALCULATE RATIOS
1400 LET R=C(3)/C(5)                                  : 86Sr/88Sr
1410 LET S=C(4)/C(3)                                  : 87Sr/86Sr
1420 LET T=S*((R+.1194)/.2388)                        : NORMALISE 87Sr/86Sr
1470 REM CALCULATE RUNNING MEAN AND STANDARD
1475 REM DEVIATION OF RATIOS BY SUMMING
1480 REM THE DIFFERENCE BETWEEN THE FIRST
1480 REM RATIO AND EACH SUCCESSIVE RATIO
1500 IF Y<>2 THEN 1540                                : SKIP AFTER IST RATIO
1510 LET Q1=R
1520 LET Q2=S
1530 LET Q3=T
1540 LET R1=R-Q1
1550 LET R2=S-Q2
1560 LET R3=T-Q3
1570 LET S1=S1+R1
1580 LET S2=S2+R2
1590 LET S3=S3+R3
1600 LET R6=S1/(Y-1)+Q1                               : RUNNING MEAN 86Sr/88Sr
1610 LET R7=S2/(Y-1)+Q2                               : RUNNING MEAN 87Sr/86Sr
1620 LET R8=S3/(Y-1)+Q3                               : RUNNING MEAN 87Sr/86Sr(N)
1640 LET T1=T1+(R1*R1)
1650 LET T2=T2+(R2*R2)
1660 LET T2=T2+(R2*R2)
1665 REM RUNNING STANDARD ERRORS OF THE MEAN
1670 LET V1=INT(1E05/(Y-1)*SQR(((Y-1)*T1-(S1*S1))/(Y-1)))
1680 LET V2=INT(1E05/(Y-1)*SQR(((Y-1)*T2-(S2*S2))/(Y-1)))
1690 LET V3=INT(1E05/(Y-1)*SQR(((Y-1)*T3-(S3*S3))/(Y-1)))
1700 IF H5=1 THEN 1700                                : PRINT AND PROCEED
1710 GOSUB 6210                                       : PRINT RUNNING MEAN AND S.E.
1720 LET Y2=Y2+1                                      : INCREMENT TOTAL-SCAN NUMBER
1730 REM STORE CURRENT 87Sr/86Sr NORM. IN ARRAY D
1740 LET D(Y2)=T
1800 ON F4-47 GOTO 1810, 1900                         : KEY OPTIONS
1810 LET Y=Y+1                                        : INCREMENT SCAN NUMBER
1815 LETPUT(171)=11                                   : PROGRAM CONTROL OF MM30B ON
1820 LET F4=0                                         : RESET KEY TO CONTINUE
1830 LET BPOKE(32846)=48                              : ZERO IN SPACE ABOVE DATE
1840 IF Y2>500 THEN 1860                              : ABORT IF EXCEED TOTAL SCANS
1850 IF Y<Y1 THEN 970                                 : CONTINUE ANALYSIS
1860 GOTO 6300                                        : PRINT RUNNING MEAN TO END
1890 REM KEY OPTIONS LOOP
1891 REM 0 = CONTINUE THE ANALYSIS
1892 REM 1 = NO CHANGE
1893 REM 2 = PRINT RUNNING MEAN AND S.E.
1894 REM 3 = EDIT
1895 REM 4 = CALCULATE AND PRINT GRAND MEAN AND S.E.
1896 REM 5 = CALCULATE AND PRINT BLOCKS OF TEN SUCCESSIVE RATIOS
1897 REM 6 = PRINT SAMPLE INFORMATION
1898 REM 7 = START NEW BLOCK OF SCANS
1899 REM 8 = END PROGRAM
1900 LETPUT(171)=10                                   : PROGRAM CONTROL OF MM30B OFF
1905 GOSUB 2500                                       : CHECK KEY
1910 ON F4-47 GOTO 1810,1920,6300,7000,8000,8500,9300,500,1950
1920 GOTO 1905
1950 LETPUT(171)=10                                   : PROGRAM CONTROL OFF
1960 LETPUT(171)=6                                    : PUT HOLD SIGNAL HIGH
1980 STOP                                             : PROGRAM END
```

```
2490 REM SUBROUTINE 1: KEY CHECK
2500 KEY F4                                    : SCRUTINISE KEY
2510 IF F4=0 THEN 2530                         : CARRY ON IF KEY=0
2520 LET BPOKE(32846)=F4                       : KEY IN SPACE ABOVE DATE
2530 RETURN

3900 REM SUBROUTINE 2: SAMPLE INFORMATION
4000 DATA 1,1,"Rb-Sr PROJECT",25,1,"STRONTIUM ISOTOPE ASSAY"
4005 DATA 60,1,"DATE : ",1,2,"SAMPLE NO. : ",60,2,"ANALYST : "
4010 DATA 1,3,"LOCALITY : ",1,4,"ROCK TYPE : "
4015 DATA 1,7,"CHANNEL 1       2       3       4       5       6"
4020 DATA 1,8,"MASS  84.5      85      86      87      88    84.5"
4025 DATA 60,7,"RATIOS",50,8,"86/88",61,8,"87/86",72,8,"87/86N"
4029 REM PRINT HEADINGS FOR UPPER BOX
4030 RESTORE 4000
4035 FOR M=1 TO 2
4040 GOSUB 4500
4045 NEXT M
4049 REM INPUT SAMPLE INFORMATION
4050 RESTORE 4005
4055 FOR M=1 TO 5
4060 GOSUB 4500
4065 PRINT CHR$(27);"T";                       : REMEMBER CURSOR POSITION
4070 PRINT CHR$(27);"X!";CHR$(27);"Y'";G$      : PRINT STRING FROM (1,12)
4075 PRINT CHR$(27);"F";                       : ERASE CURRENT ROW ON SCREEN
4080 INPUT A$
4085 PRINT CHR$(27);"U";A$                     : REMEMBER CURRENT POSITION &
4090 NEXT M                                    :  RESTORE FORMER POSITION
4095 RETURN
4099 REM PRINT HEADINGS IN LOWER BOX
4100 RESTORE 4015
4110 FOR M=1 TO 4
4120 GOSUB 4500
4130 NEXT M
4490 REM TRANSFER HEADINGS TO SCREEN
4500 READ X,Y,G$
4505 REM PRINT STRING FROM INPUT POSITIONS
4510 PRINT CHR$(27);"X";CHR$(32+X);CHR$(27);"Y";CHR$(32+Y);G$;
4520 RETURN

4990 REM SUBROUTINE 3: BOXES FOR SAMPLE INFORMATION
5000 DATA !,A,1,%                              : GRAPHIC SYMBOLS
5010 DATA E," ",E,E                            :  (s5000-s5030)
5020 DATA 9,A,I,5
5030 DATA ),A,=,-
5040 READ P,Q
5050 FOR M=1 TO P
5060 READ X(M)
5070 NEXT M
5080 FOR M=1 TO Q
5090 READ Y(M)
5100 NEXT M
5110 RESTORE 5000
5120 GOSUB 5500
5130 FOR M=1 TO Q
5140 FOR N=1 TO Y(M)
5150 RESTORE 5010
5160 GOSUB 5500
5170 NEXT N
```

```
5180 IF M=Q EXIT 5210
5190 GOSUB 5500
5200 NEXT M
5210 RESTORE 5030
5220 GOSUB 5500
5230 RETURN
5500 READ A$,B$,C$,D$,
5510 PRINT A$
5520 FOR O=1 TO P
5530 FOR R=1 TO X(O)
5540 PRINT B$
5550 NEXT R
5560 IF O=P THEN 5590
5570 PRINT C$
5580 GOTO 5600
5590 PRINT D$
5600 NEXT O
5610 RETURN

5990 REM SUBROUTINE 4: DATA PRINT
6000 IF X>1 THEN 6015
6005 LET H1=1
6010 PRINT[H1] "E";Y AS 3I;                      : SCAN NUMBER
6015 LET H2=1
6020 PRINT[H2] "E";B(I) AS 6I;                   : IBC MEAN
6030 IF Y>1 THEN 6060
6040 IF X<X1 THEN 6060
6050 PRINT CHR$(27);"X ";CHR$(27);"K"            : PRINT LINE ON TTY
6060 RETURN
6190 REM PRINT IBC MEANS & RATIOS (FROM 2ND SCAN)
6200 PRINT "EE";R AS 10F5;"E";S AS 10F5;"E";T AS 10F5;
6210 LET H3=1
6220 PRINT[H3] CHR$(27);"X ";CHR$(27);"K"  : PRINT LINE ON TTY
6230 RETURN
6290 REM PRINT RUNNING MEAN AND STANDARD ERROR
6300 PRINT CHR$(27);"XA";"RUNNING MEAN: ";
6310 PRINT R6 AS 11F5;R7 AS 11F5;R8 AS 11F5;
6320 PRINT CHR$(27);"X ";CHR$(27);"K"            : PRINT LINE ON TTY
6330 PRINT CHR$(27);"XAD;"STD. ERROR: ";
6340 PRINT V1 AS 11I;V2 AS 11I;V3 AS 11I;
6350 PRINT CHR$(27);"X ";CHR$(27);"K"            : PRINT LINE ON TTY
6360 GOTO 1900

6990 REM SUBROUTINE 5: EDIT FACILITY
7000 PRINT "START/END EDIT BLOCK: INPUT B5,E5 (0,0 TO STOP)"
7010 INPUT B5,E5
7020 IF B5>E5 THEN 7045
7025 IF B5<1 THEN 7045                           : CHECK CORRECT INPUT
7030 IF E5>Y2 THEN 7045                          : (7010-7050)
7040 GOTO 7055
7045 PRINT "INCORRECT INPUT: B5>E5, B5<1, E5>Y2?"
7050 GOTO 7010
7055 IF B5>0 THEN 7070
7060 PRINT CHR$(27);"X ";CHR$(27);"K"            : PRINT LINE ON TTY
7065 GOTO 1900
7070 FOR M=B5 TO E5
7075 PRINT "ARRAY POSN: ";M AS 3I;" EDITED RATIO: ";D(M) AS 11F5;
7080 PRINT CHR$(27);"X ";CHR$(27);"K"            : PRINT LINE ON TTY
7085 LET D(M)=D(M)*-1                            : FLAG RATIO IN ARRAY
7090 GOTO 7120
```

```
7095 NEXT M
7100 GOTO 7010

7990 REM SUBROUTINE 6: GRAND MEAN CALCULATION AND PRINT
8000 PRINT "GRAND MEAN CALCULATION";CHR$(27);"X ";CHR$(27);"K"
8010 PRINT "START/END BLOCK: INPUT B6,E6"
8015 PRINT "Y2: ";Y2 AS 3I;
8020 INPUT B6,E6
8025 IF B6>E6 THEN 7045
8030 IF B6<1 THEN 7045                  : CHECK CORRECT INPUT
8035 IF E6>Y2 THEN 7045                 : (8020-8050)
8040 GOTO 8055
8045 PRINT "INCORRECT INPUT: B5>E5, B5<1, E5>Y2?"
8050 GOTO 8020
8055 PRINT "BEGINNING: ";B6 AS 3I;CHR$(27);"X ";CHR$(27);"K"
8060 PRINT "   END    : ";E6 AS 3I;CHR$(27);"X ";CHR$(27);"K"
8080 LET V7=0                           : END OF PURGE CHECK
8090 LET L1=0                           : SUM VARIABLES FOR MEAN
8100 LET P1=0                           : - CALCULATION
8110 LET F5=0                           : COUNTER
8120 FOR M=B6 TO E6
8130 IF D(M)<0 THEN 8165                : IGNORE FLAGGED RATIOS
8135 REM MEAN AND S.E. CALCULATION
8140 LET N1=D(M)
8145 LET K1=D(M)-N1
8150 LET LI=L1+K1
8155 LET P1=P1+(K1*K1)
8160 LET F5=F5+1                        : INCREMENT COUNTER
8165 NEXT M
8170 LET K6=L1/(F5)+N1                  : GRAND MEAN
8180 LET V6=1E06/F5*SQR((F5*P1-(L1*L1))/F5): STANDARD ERROR OF MEAN
8190 IF V7=V6 THEN 8350                 : END WHEN NO MORE REMOVED
8200 REM PRINT GRAND MEAN AND STANDARD ERROR
8210 PRINT "GRAND MEAN: ";K6 AS 11F5;
8220 PRINT CHR$(27);"X ";CHR$(27);"K"   : PRINT LINE ON TTY
8230 PRINT "STD. ERROR: ";INT(V6) AS 12I;
8240 PRINT CHR$(27);"X ";CHR$(27);"K"   : PRINT LINE ON TTY
8250 PRINT "TOTAL NO. SCANS: ";F5 AS 3I;
8260 PRINT CHR$(27);"X ";CHR$(27);"K"   : PRINT LINE ON TTY
8270 GOSUB 8800                         : CALCULATE SKEWNESS
8275 LET V7=V6
8280 REM PURGE OUTLIERS
8285 FOR M=B6 TO E6
8290 IF D(M)<0 THEN 8330                : IGNORE FLAGGED RATIOS
8295 LET A5=ABS(K6-D(M))                : COMPARE EACH RATIO TO MEAN
8300 LET A6=V6/1E06*SQR(F5)*2.5         : 2.5 * STANDARD DEVIATION
8305 IF A5<A6 THEN 8330                 : IGNORE "GOOD" DATA
8310 LET D(M)=D(M)*-1                   : FLAG   "POOR" DATA
8315 PRINT "REMOVED RATIO: ";D(M) AS 11F5;
8320 PRINT "ARRAY POSN: ";Z AS 3I;
8325 PRINT CHR$(27);"X ";CHR$(27);"K"   : PRINT LINE ON TTY
8330 NEXT M
8340 GOTO 8090                          : RE-CALC. GRAND MEAN AND S.E.
8350 PRINT "END OF PURGE"               : NO MORE RATIOS REMOVED
8360 PRINT CHR$(27);"X ";CHR$(27);"K"   : SPACE
8370 IF F3=0 THEN 8390
8380 RETURN
8390 GOTO 1900                          : RETURN TO KEY OPTION LOOP

8480 REM SUBROUTINE 7: CALCULATE AND PRINT GRAND MEAN AND STANDARD ERROR
```

```
8490 REM - OF SUCCESSIVE BLOCKS OF 10 RATIOS
8500 PRINT "BLOCKS OF 10 RATIOS";CHR$(27);"X ";CHR$(27);"K"
8510 FOR M=1 TO INT(Y2/10)
8520 IF M>1 THEN 8560
8525 REM SET BEGINNING AND END OF BLOCK IN GRAND MEAN & S.E. CALCULATION
8530 REM - IN SUBROUTINE 6
8535 LET B6=1
8540 LET E6=10
8550 GOTO 8580
8560 LET B6=B6+10
8570 LET E6=E6+10
8580 LET F3=1
8590 GOSUB 8055                              : BEGIN GRAND MEAN CALC.
8600 NEXT M
8610 LET F3=0                                : END OF BLOCKS
8620 GOTO 1900                               : RETURN TO KEY OPTION LOOP

8790 REM SUBROUTINE 8: CALCULATE SKEWNESS OF RATIOS DISTRIBUTION
8800 LET W1=0
8810 LET W2=0                                : INITIALISE SUMS
8820 LET W3=0
8830 FOR M=B6 TO E6
8840 IF D(M)<0 THEN 8890                     : IGNORE FLAGGED RATIOS
8850 LET W1=(D(M)-K6)*1E05                   : SUM THE CUBE OF THE
8860 LET W2=W2+(W1**3)                       : - DEVIATIONS FROM THE MEAN
8870 NEXT M
8875 REM SKEWNESS=SUM OF THE CUBE OF THE DEVIATIONS FROM THE MEAN
8880 REM - DIVIDED BY THE NUMBER OF RATIOS
8885 REM - DIVIDED BY THE STANDARD DEVIATION
8880 LET W3=W2/(F5*(V6*(SQR(F5)))/1E015      : GIVEN FOR THE FIFTH DECIMAL
8885 PRINT CHR$(27);"X ";CHR$(27);"K"        : SPACE
8890 PRINT "SKEWNESS= ";W3 AS 6F2;
8900 PRINT CHR$(27);"X ";CHR$(27);"K"        : PRINT LINE ON TTY
8910 PRINT CHR$(27);"X ";CHR$(27);"K"        : SPACE
8920 RETURN

9290 SUBROUTINE 9: FINAL HEADINGS
9300 PRINT "Sr ISOTOPIC ANALYSIS: FINAL STATISTICS";
9310 PRINT CHR$(27);"X ";CHR$(27);"K"        : PRINT LINE ON TTY
9320 PRINT "INPUT SAMPLE INFORMATION: INPUT A$=DATE; B$=ANALYST;"
9330 PRINT "INPUT C$=SAMPLE NUMBER; D$=ROCK TYPE; E$=LOCALITY"
9340 PRINT "DATE: ";A$;"   "ANALYST: ";B$;
9350 PRINT CHR$(27);"X ";CHR$(27);"K"        : PRINT LINE ON TTY
9360 PRINT "SAMPLE NUMBER: ";C$;"   ROCK TYPE: ";
9370 PRINT CHR$(27);"X ";CHR$(27);"K"        : PRINT LINE ON TTY
9380 PRINT "LOCALITY: ";E$;
9390 PRINT CHR$(27);"X ";CHR$(27);"K"        : PRINT LINE ON TTY
9400 GOTO 1900                               : RETURN TO KEY LOOP
```

The following alterations and additions to the above program are included in Sr ID program (VERSION 3).

```
1390
1400 LET C4=C(6)/C(3)                         : 84Sr/86Sr
1410 LET C7=C(4)/C(3)                         : 87Sr/86Sr
1420 LET C8=C(5)/C(3)                         : 88Sr/86Sr
1430 REM CALCULATE MATRIX DETERMINANTS
1440 GOSUB 9000
1450 LET R=1/C4                               : 86Sr/88Sr
1460 LET S=B7                                 : 87Sr/86Sr (sample)
1470 LET T=E1                                 : Sr(sample)/Sr(spike)
1500

4390 REM SUBROUTINE 2: HEADINGS
4000 DATA 1,1,"Rb-Sr PROJECT",25,1,"STRONTIUM ISOTOPE DILUTION"
4005 DATA 60,1,"DATE : ",1,2,"SAMPLE NO. : ",60,2,"ANALYST : "
4010 DATA 1,3,"LOCALITY : ",1,4,"ROCK TYPE : "
4015 DATA 1,7,"CHANNEL 1      2       3       4       5       6"
4020 DATA 1,8,"MASS  84.5     85      86      87      88      84"
4025 DATA 60,7,"RATIOS",50,8,"86/88        87/86S  Sr(S)/Sr(T)"

9180 REM SUBROUTINE 10: CALCULATE MATRIX DETERMINANTS
9190 - (AFTER RUSSELL, 1977)
9200 DATA 1786,.125,.95,.0568,8.375          : CONSTANTS (SEE TABLE 2.7)
9210 RESTORE 9200
9220 READ A4,A7,A8,B4,B8
9225 REM SEE FIG.2.4 FOR MATRIX
9230 LET D1=.5*((3*C4*(A8-B8))+(A4*(B8+C8))-(B4*(A8+C8)))
9240 LET D2=(C4*((2*C8)-B8))-(B4*C8)
9250 LET D3=(C4*(A8-(2*C8)))+(A4*C8)
9260 LET B7=((D1/D3)*C7)-((D2/D3)*A7)       : 87Sr/86Sr (sample)
9270 LET E1=(D3*(1+B4+B7+B8))/(D2*(1+A4+A7+A8)) : Sr(sample)/Sr(spike)
9280 RETURN

9490 REM SUBROUTINE 12: CALCULATE AND PRINT Sr CONTENT OF SAMPLE
9500 PRINT "INPUT W1=WEIGHT SPIKE/g, W2=WEIGHT SAMPLE/g"
9510 INPUT W1,W2
9520 PRINT "WEIGHT SPIKE = ";W1 AS 7F5;" g";
9530 PRINT CHR$(27);"X ";CHR$(27);"K"        : PRINT LINE ON TTY
9540 PRINT "WEIGHT SAMPLE= ";W2 AS 7F5;" g";
9550 PRINT CHR$(27);"X ";CHR$(27);"K"        : PRINT LINE ON TTY
9560 PRINT "INPUT Sr CONCENTRATION OF SPIKE (ug/g)"
9570 INPUT A1
9575 REM CALCULATE Sr CONCENTRATION IN SAMPLE USING GRAND MEAN VALUE OF
9580 REM - Sr (sample)/Sr(spike)
9590 LET E6=(K6*A1*W1)/W2
9600 PRINT "Sr CONCENTRATION IN SAMPLE (ug/g)= ";E6 AS 9F2;
9610 PRINT CHR$(27);"X ";CHR$(27);"K"        : PRINT LINE ON TTY
9615 REM CALCULATE ANALYTICAL PRECISION AS: 2-SIGMA ERROR ON DISTRIBUTION
9620 REM - OF K6 + ERROR ON SPIKE CONCENTRATION + ERROR ON WEIGHTS
9630 LET E7=((V6/1E04*2/K6)+.05)/1E02*E6    : ERROR AS % OF Sr CONTENT
9640 PRINT "                 PRECISION          = ";E7 AS 9F2;
9650 PRINT CHR$(27);"X ";CHR$(27);"K"       : PRINT LINE ON TTY
9660 PRINT CHR$(27);"X ";CHR$(27);"K"       : SPACE
9670 GOTO 1900                              : RETURN TO KEY LOOP
```

EDIT and GRAND MEAN calculations are performed on arrays containing B7=87Sr/86Sr(sample) and E1=Sr(spike)/Sr(sample), so requiring the following changes:

```
490 DIM A(27),B(600),C(6),D(200),E(200)

1740 LET D(Y2)=S
1750 LET E(Y2)=T

1835 IF Y2>200 THEN 1860                      : EXCEEDED MAX. ALLOWED SCANS

1909 REM KEY=5 CALCULATE Sr CONCENTRATION OF SAMPLE
1910 ON F4-47 GOTO 1810,1920,6300,7000,8000,9500,9300,500,1950

7000 PRINT "ARRAY TYPE? INPUT D (87/86S) OR E (Sr(S)/Sr(T))"
7005 INPUT D$

7073 IF D$="E" THEN 7100

7100 FOR M=B5 TO E5
7110 PRINT "ARRAY POSN: ";M AS 3I;" EDITED RATIO: ";E(M) AS 11F5;
7120 PRINT CHR$(27);"X ";CHR$(27);"K"       : PRINT LINE ON TTY
7130 LET E(M)=E(M)*-1                       : FLAG RATIO IN ARRAY
7140 NEXT M

8000 PRINT "GRAND MEAN CALCULATION";CHR$(27);"X ";CHR$(27);"K"
8005 PRINT "ARRAY TYPE? INPUT D (87/86S) OR E (Sr(S)/Sr(T))"
8010 INPUT D$
8012 PRINT "START/END BLOCK: INPUT B6,E6"

8120 FOR M=B6 TO E6
8122 IF D$="E" THEN 8150

8140 GOTO 8170
8150 IF E(M)<0 THEN 8170                    : IGNORE FLAGGED RATIOS
8152 IF M>B THEN 8160
8155 LET N1=E(M)
8160 LET K1=E(M)-N1
8170 LET L1=L1+K1

8280 REM PURGE OUTLIERS
8285 FOR M=B6 TO E6
8287 IF D$="E" THEN 8310

8310 IF E(M)<0 THEN 8330                    : IGNORE FLAGGED RATIOS
8312 LET A5=ABS(K6-E(M))                    : COMPARE EACH RATIO TO MEAN
8315 LET A6=V6/1E06*SQR(F5)*2.5             : 2.5 * STANDARD DEVIATION
8318 IF A5<A6 THEN 8330                     : IGNORE "GOOD" DATA
8322 LET E(M)=E(M)*-1                       : FLAG   "POOR" DATA
8325 PRINT "REMOVED RATIO: ";E(M) AS 11F5;
8327 PRINT "ARRAY POSN: ";Z AS 3I;
8329 PRINT CHR$(27);"X ";CHR$(27);"K"       : PRINT LINE ON TTY
8330 NEXT M
```

A4.3: CUBIC LEAST SQUARES REGRESSION ANALYSIS OF Rb-Sr ISOTOPIC DATA

This program was written by Mr R.M.Renner of the Institute of Statistics and Operations Research (ISOR), Victoria University of Wellington. It allows computation of the slope and y-intercept from x-y pairs representing the ratios $^{87}Rb/^{86}Sr$ and $^{87}Sr/^{86}Sr$, taking into account errors on both x and y variables. The principals involved in the program are discussed in Chapter 2.4.

[CLSRA (exec)]

```
&TRACE ALL
*SET BLIP BUSY
GLOBAL TXTLIB CMSLIB VFORTLIB RND
*FORTVS GRAHAMO3
FI 10 DISK COF4 DATA A
FI 11 DISK COF4 LISTING A (RECFM FB LRECL 133 BLOCK 1330
FI 6 TERMINAL
FI 5 TERMINAL
CLRSCRN
LOAD GRAHAMO3 (START
*SET BLIP OFF
&EXIT
```

[CLSRA (main program)]

```
C
C THIS ITERATIVE PROGRAM COMPUTES A SOLUTION TO THE 'LEAST-SQUARES
C CUBIC' AS DEFINED IN DEREK YORK'S 1966 PAPER (CANADIAN J. PHYSICS)
C      THE DATA ARE READ, IN FREEFIELD, IN THE FOLLOWING ORDER,
C      X, THE MAXIMUM ERROR IN X (68.26% PROBABILITY) AS A PERCENTAGE,
C      Y, THE MAXIMUM ERROR IN Y (68.26% PROBABILITY) AS A PERCENTAGE.
C    FIRST, THE PROGRAM DETERMINES ESTMATES OF SLOPE B CORRESPONDING TO
C    (1) NO ERRORS IN X, Y SUBJECT TO ERRORS, AND
C    (2) NO ERRORS IN Y, X SUBJECT TO ERRORS.
C        IT THEN LOOKS ALONG AN INTERVAL WHICH INCLUDES
C        THESE TWO VALUES, FOR SIGN CHANGES IN YORK'S  'CUBIC'
C
C   WRITTEN BY R.M. RENNER INSTITUTE OF STATISTICS AND OPERATIONS
C       RESEARCH, VICTORIA UNIVERSITY OF WELLINGTON 1 JULY 1984
C
      REAL*16 X(100),PX(100),Y(100),PY(100),W(100),WX(100),WY(100),
     1XSUM,YSUM,WSUM,A,B,BB,
     2ZERO,XBAR,YBAR,SUM1,SUM2,SUM3,SUM4,SUM5,TEST1,TEST2,TESTX,DELTA,
     3BMID,U(100),V(100),B1,B2,B3,VARA,VARB,SIGA,SIGB,AGE,
     4RX(100),RY(100)
      COMMON X,Y,WX,WY,U,V,W,ZERO,XBAR,YBAR,A,M
      ZERO=0.00Q+00
C
      M=1
  001 CONTINUE
```

```
      READ (10,*,END=002) X(M),PX(M),Y(M),PY(M)
C
C  COMPUTE RECIPROCAL OF VARIANCE FROM ERROR PERCENT. THIS VALUE
C  BECOMES THE WEIGHT ASSOCIATED WITH THE APPROPRIATE DATA-VALUE. THEN
C  IDEALLY, THE MINIMIZED WEIGHTED SQUARED DEVIATIONS (YORK EQUATION 7)
C  WILL HAVE A CHI-SQUARE DISTRIBUTION WITH  D.O.F. = (DATA-POINTS - 2)
C
      WX(M)=    (100/(X(M)*PX(M)))**2
      WY(M)=    (100/(Y(M)*PY(M)))**2
      M=M+1
      GO TO 001
  002 CONTINUE
      M=M-1
C
      DATA XSUM,YSUM,WSUM,SUM1,SUM2/5*0.0Q+00/
      DO 003 I=1,M
         XSUM=XSUM+WY(I)*X(I)
         YSUM=YSUM+WY(I)*Y(I)
         WSUM=WSUM+WY(I)
  003 CONTINUE
      XBAR=XSUM/WSUM
      YBAR=YSUM/WSUM
      DO 004 I=1,M
         U(I)=X(I)-XBAR
         V(I)=Y(I)-YBAR
         SUM1=SUM1+WY(I)*U(I)*V(I)
         SUM2=SUM2+WY(I)*(U(I)**2)
  004 CONTINUE
      B1=SUM1/SUM2
      CALL CUBIC(B1,TEST1)
      WRITE (6,005) B1,TEST1
  005 FORMAT (/,10X,Q20.10,10X,Q30.20)
C
      XSUM=ZERO
      YSUM=ZERO
      WSUM=ZERO
      SUM1=ZERO
      SUM2=ZERO
      DO 006 I=1,M
         XSUM=XSUM+WX(I)*X(I)
         YSUM=YSUM+WX(I)*Y(I)
         WSUM=WSUM+WX(I)
  006 CONTINUE
      XBAR=XSUM/WSUM
      YBAR=YSUM/WSUM
      DO 007 I=1,M
         U(I)=X(I)-XBAR
         V(I)=Y(I)-YBAR

         SUM1=SUM1+WX(I)*(V(I)**2)
         SUM2=SUM2+WX(I)*U(I)*V(I)
  007 CONTINUE
      B2=SUM1/SUM2
      CALL CUBIC(B2,TEST2)
      WRITE (6,008) B2,TEST2
  008 FORMAT (/,10X,Q20.10,10X,Q30.20,2(/))
      CALL ORDER(B1,B2)
C
C  IF TEST1, TEST2 OF OPPOSITE SIGN, THEIR PRODUCT IS NEGATIVE
C
```

```
      IF (TEST1.GT.1.00Q+35) TEST1=TEST1/1.00Q+35
      IF (TEST2.GT.1.00Q+35) TEST2=TEST2/1.00Q+35
      SUM1=TEST1*TEST2
      IF (SUM1.LT.ZERO) GO TO 011
C
C IF SUM1 GT ZERO, START THE SEARCH ON EITHER SIDE OF INTERVAL (B1,B2)
C TESTX WILL IN GENERAL CHANGE SIGN ON EITHER SIDE OF ROOTS
C
      DELTA=(B1+B2)/10.0
      KOUNT=0
  300 CONTINUE
      B1=B1+DELTA
      B2=B2-DELTA
      CALL CUBIC(B1,TEST1)
      CALL CUBIC(B2,TEST2)
      SUM1=TEST1*TEST2
      IF (SUM1.LT.ZERO) GO TO 011
      KOUNT=KOUNT+1
      IF (KOUNT.GT.100) GO TO 9999
      GO TO 300
C
  011 CONTINUE
      DELTA=(B1-B2)
       BMID=(B1+B2)/2.0
      IF (DELTA.LT.1.00Q-14) GO TO 200
      CALL CUBIC(B1,TEST1)
      CALL CUBIC(B2,TEST2)
      CALL CUBIC(BMID,TESTX)
      IF (TEST1.GT.1.00Q+35) TEST1=TEST1/1.00Q+35
      IF (TEST2.GT.1.00Q+35) TEST2=TEST2/1.00Q+35
      IF (TESTX.GT.1.00Q+35) TESTX=TESTX/1.00Q+35
      SUM1=TEST1*TESTX
      SUM2=TEST2*TESTX
      IF (SUM1.LT.ZERO) B2=BMID
      IF (SUM2.LT.ZERO) B1=BMID
      GO TO 011
C
  200 CONTINUE
      B3=BMID
C
C  COMPUTE VARIANCES OF SLOPE AND INTERCEPT. ALSO COMPUTE RESIDUALS,
C  THE ERROR SUM OF SQUARES (YORK EQUATION 7 PAGE 1080), AND RMSWD
C
      CALL CUBIC(B3,TESTX)
      SUM1=ZERO
      SUM2=ZERO
      SUM3=ZERO
      SUM4=ZERO
      SUM5=ZERO
      DO 015 I=1,M
      SUM1=SUM1+(W(I)*(((B3*U(I))-V(I))**2))
      SUM2=SUM2+(W(I)*(U(I)**2))
      SUM3=SUM3+(W(I)*(X(I)**2))
      SUM4=SUM4+ W(I)
C
C  X AND Y RESIDUALS RX(I),RY(I) SEE YORK PAGE 1084
C
      RX(I)=-(B3)*(W(I)/WX(I))*(A+(B3*X(I))-Y(I))
      RY(I)=      (W(I)/WY(I))*(A+(B3*X(I))-Y(I))
C
```

```
C  MINIMISED WEIGHTED SQUARED DEVIATIONS (RESIDUALS)
C
      SUM5= SUM5+((WX(I)*(RX(I)**2))+(WY(I)*(RY(I)**2)))
  015 CONTINUE
      VARB= (SUM1/SUM2)/(M-2)
      VARA= VARB*(SUM3/SUM4)
      SIGA= QSQRT(VARA)
      SIGB= QSQRT(VARB)
      SUM1 =B3+1
       AGE=(QLOG(SUM1))/(1.42Q-05)
      SUM1 =B3+1+SIGB
      SUM2 =((QLOG(SUM1))/(1.42Q-05))-AGE
      SUM3= SUM5/(M-2)
      SUM4= QSQRT(SUM3)
      WRITE (6,016) M,A,SIGA,B3,SIGB,AGE,SUM2,SUM5,SUM4
  016 FORMAT (1X,'                 NUMBER OF DATA-POINTS=',I7/
     *        1X,'                             INTERCEPT=',F18.10/
     1        1X,'    STANDARD DEVIATION OF INTERCEPT=',F18.10/
     2        1X,'                                 SLOPE=',F18.10/
     3        1X,'         STANDARD DEVIATION OF SLOPE=',F18.10/
     4        1X,'                AGE (MILLIONS YEARS)=',F18.10/
     5        1X,'       ERROR IN AGE (MILLIONS YEARS)=',F18.10/
     6        1X,'                ERROR SUM OF SQUARES=',F18.10/
     7        1X,'ROOT MEAN SQUARE WEIGHTED DEVIATION=',F18.10,2(/),)
      WRITE (11,017) A,SIGA,B3,SIGB,AGE,SUM2,SUM5,SUM4,M
  017 FORMAT (5(/),26X,'YORK: LEAST SQUARES FITTING OF A STRAIGHT LINE'/
     *  1HO,  24X,'                            INTERCEPT =',F18.10/
     1        25X,'  STANDARD DEVIATION OF INTERCEPT =',F18.10/
     2  1HO,  24X,'                                SLOPE =',F18.10/
     3        25X,'      STANDARD DEVIATION OF SLOPE =',F18.10/
     4  1HO,  24X,'               AGE (MILLIONS YEARS) =',F18.10/
     5        25X,'     ERROR IN AGE (MILLIONS YEARS) =',F18.10/
     6  1HO,  24X,'                ERROR SUM OF SQUARES=',F18.10/
     7        25X,'ROOT MEAN SQUARE WEIGHTED DEVIATION=',F18.10/
     8  1HO,  24X,'               NUMBER OF DATA POINTS=',I7)
C
      WRITE (11,500)
  500 FORMAT(1H1,2(/),13X,'NUMBER',14X,'X',13X,'ERROR IN X (%)',
     18X,'Y',13X,'ERROR IN Y (%)',2(/))
      DO 502 I=1,M
      WRITE (11,501) I,X(I),PX(I),Y(I),PY(I)
  501 FORMAT (10X,I6,5X,4F18.5/)
  502 CONTINUE
C
C  COMPUTE THE PERCENTAGE RESIDUAL ERRORS
C
      WRITE (11,600)
  600 FORMAT(1H1,2(/),13X,'NUMBER',11X,'X RESIDUAL',6X,'X RESIDUAL (%)',
     16X,'Y RESIDUAL',6X,'Y RESIDUAL (%)',2(/))
      DO 402 I=1,M
         X(I)=(RX(I)/X(I))*100
         Y(I)=(RY(I)/Y(I))*100
      WRITE (11,601) I,RX(I),X(I),RY(I),Y(I)
  601 FORMAT (10X,I6,5X,4F18.5/)
         X(I)=QABS(X(I))
         Y(I)=QABS(Y(I))
         IF (X(I).LT.PX(I).AND.Y(I).LT.PY(I)) GO TO 401
         WRITE (6,400) I
  400    FORMAT (1X,'PERCENTAGE RESIDUAL ERROR OF POINT NUMBER ',I2,' EX
     1CEEDS SPECIFIED MAXIMUM',/)
```

```
  401 CONTINUE
  402 CONTINUE
 9999 WRITE (6,403)
  403 FORMAT (2(/),25X,'END OF PROGRAM',)
      END
C
      SUBROUTINE ORDER(C1,C2)
      REAL*16 C1,C2,CC
      IF (C1.GT.C2) GO TO 001
         CC=C1
         C1=C2
         C2=CC
  001 CONTINUE
      RETURN
      END
C
      SUBROUTINE CUBIC(B,TEST)
      REAL*16 X(100),Y(100),WX(100),WY(100),W(100),XSUM,YSUM,WSUM,A,B,
     1ZERO,XBAR,YBAR,SUM1,SUM2,SUM3,SUM4,SUM5,TEST1,TEST2,TESTX,DELTA,
     2BMID,U(100),V(100)
      COMMON X,Y,WX,WY,U,V,W,ZERO,XBAR,YBAR,A,M
C
      XSUM=ZERO
      YSUM=ZERO
      WSUM=ZERO
      SUM1=ZERO
      SUM2=ZERO
      SUM3=ZERO
      SUM4=ZERO
      SUM5=ZERO
      DO 001 I=1,M
         W(I)=(WX(I)*WY(I))/(((B**2)*WY(I))+WX(I))
         XSUM=XSUM+W(I)*X(I)
         YSUM=YSUM+W(I)*Y(I)
         WSUM=WSUM+W(I)
  001 CONTINUE
      XBAR=XSUM/WSUM
      YBAR=YSUM/WSUM
         A=YBAR-B*XBAR
      DO 002 I=1,M
         U(I)=X(I)-XBAR
         V(I)=Y(I)-YBAR
         SUM1=SUM1+((W(I)*U(I))**2)/WX(I)
         SUM2=SUM2+((W(I)**2)*U(I)*V(I))/WX(I)
         SUM3=SUM3+W(I)*(U(I)**2)
         SUM4=SUM4+((W(I)*V(I))**2)/WX(I)
         SUM5=SUM5+W(I)*U(I)*V(I)
  002 CONTINUE
      TEST=((B**3)*SUM1)-(2*(B**2)*SUM2)-(B*(SUM3-SUM4))+SUM5
      RETURN
      END
```

Table A5.1: Chemical compositions of ideal minerals used in least squares modelling.

	SiO_2	TiO_2	Al_2O_3	FeO	MgO	CaO	Na_2O	K_2O
Fo90	40.87	.00	.00	9.77	49.36	.00	.00	.00
Fo85	40.01	.00	.00	14.35	45.64	.00	.00	.00
Fo80	39.19	.00	.00	18.74	42.07	.00	.00	.00
En80	56.31	.00	.00	13.47	30.22	.00	.00	.00
En70	54.70	.00	.00	19.62	25.68	.00	.00	.00
CPX1	51.81	.00	2.31	6.52	16.46	22.90	.00	.00
CPX2	51.15	.00	2.28	10.30	15.17	21.10	.00	.00
An90	45.68	.00	34.95	.00	.00	18.25	1.12	.00
An80	48.09	.00	33.35	.00	.00	16.31	2.25	.00
An70	50.54	.00	31.70	.00	.00	14.36	3.40	.00
An60	53.05	.00	30.01	.00	.00	12.38	4.56	.00
An50	55.59	.00	28.30	.00	.00	10.38	5.73	.00
An40	58.19	.00	26.54	.00	.00	8.36	6.91	.00
MT0.0	.00	.00	.00	100.00	.00	.00	.00	.00
MT2.5	.00	2.50	.00	97.50	.00	.00	.00	.00
MT5.0	.00	5.00	.00	95.00	.00	.00	.00	.00
MT7.5	.00	7.50	.00	92.50	.00	.00	.00	.00
MT10.0	.00	10.00	.00	90.00	.00	.00	.00	.00
MT12.5	.00	12.50	.00	87.50	.00	.00	.00	.00
MT15.0	.00	15.00	.00	85.00	.00	.00	.00	.00
MT17.5	.00	17.50	.00	82.50	.00	.00	.00	.00
MELT1	72.00	.50	13.50	3.50	.50	1.00	3.00	6.00
MELT2	76.00	.50	11.50	3.00	.50	2.50	3.00	3.00

NOTES: Fo = olivine (90%, 85% and 80% forsterite);
En = orthopyroxene (80% and 70% enstatite);
CPX = clinopyroxene;
An = plagioclase (90% through 40% anorthite);
MT = magnetite (0% through 17.5% TiO_2)
MELT compositions (MELT1 = K-rich, MELT2 = K-poor) are based on microprobe analyses of xenoliths (c.f. Table 5.16).

****

APPENDIX 5: PETROGENETIC MODELS

****

Each of the following petrogenetic models is constructed using a set of systematic guidelines. These are:

RULE 1: Major elements are normalised volatile-free.

RULE 2: MnO and P_2O_5 are excluded as major elements because they are typically at such low concentrations that precision is unacceptably low (note that the behaviour of these elements is closely similar to that of FeO and Zr respectively).

RULE 3: Fe is expressed as total FeO.

RULE 4: Fractional crystallisation uses ideal mineral compositions (Table A5.1) so as to more accurately determine the composition of phases removed. Also, suitable "natural" phenocryst compositions were difficult to select owing to the wide range observed in most lavas.

RULE 5: Typically, it is assumed that (at most) four minerals are fractionating i.e. plagioclase, olivine or orthopyroxene, clinopyroxene (augite) and titanomagnetite (magnetite) (POAM fractionation; Gill, 1981). The models are restricted in this way because, in general, the more phases that are added to the model the better the resultant fit. Olivine is assumed to be a fractionating phase for the most basic lavas but is replaced by orthopyroxene for more-evolved compositions.

RULE 6: Best fit models are those for which the sum of the squares of the residuals (SSR) is minimised, for which the fractionating phases are compositionally reasonable (i.e. compare well with the compositions of phenocryst cores) and for which the total

Table A5.2: Trace element distribution coefficients.

	ol	opx	cpx	pl	mt
Rb	.01	.02	.02	.07	.01
Ba	.01	.02	.02	.16	.01
Zr	.01	.10	.25	.01	.40
Sr	.01	.03	.08	1.83	.01
V	.08	1.10	1.10	.01	30.00
Cr	1.00	3.00	10.00#	.01	40.00
Ni	12.00*	8.00	6.00	.01	10.00

NOTES: ol =olivine; cpx = clinopyroxene; opx = orthopyroxene; pl = plagioclase; mt = magnetite. All values are averages from Gill (1981) except # = minimum value; * variable, Kd=(124/MgO)-.9 (Hart and Davis, 1978).

amount of crystals removed is similar to, and in proportion to, the phenocryst content of the lava concerned.

RULE 7: Trace element Kd values (Table A5.2) are drawn mainly from the summary in Gill (1981, Table 6.3). Many show a wide range of possible values (Banno and Matsui, 1973; Irving, 1973; Arth, 1976), particularly Cr which is not well known at present for calc-alkaline rocks - the Kd of 10 for clinopyroxene-melt is a minimum value according to Gill (1981), but application of it here indicates that it may be too high for TVC andesites (Mann, 1983, estimates a value of 4.68 for Main Series lavas of Santorini Volcano Greece which may be closer to the true value). Thus because of uncertainty as to the appropriate Kd for Cr, large errors of fit for this element are difficult to assess. Ni Kd for olivine is calculated from Kd=(124/MgO)-.9 (Hart and Davis, 1978). As a general guideline, trace element misfits occur when the error of fit (i.e. % ERROR) is greater than 20%.

Abbreviations used in individual models are:

P	=	observed parent magma.
D	=	observed daughter magma.
MODEL	=	calculated daughter magma.
RESID.	=	residual (D - MODEL).
PHASE	=	phase removed (-) or added (+).
WGT %	=	weight percentage of phases removed/added (compared to P).
%	=	percentage of total crystals removed.
BULK DC	=	bulk distribution coefficient.
% ERROR	=	percentage difference ((MODEL-D)/D).
MISFIT	=	% ERROR greater than 20%? (YES or NO).
nd	=	not determined

In AFC models, where an amount of partial granitic melt is added, trace element contents are calculated with respect to removed crystals only. In POAM fractionation models where some minerals are removed and others added, trace element contents are estimated in two parts:

1. from the fractionating phases (using bulk Kd)
2. from the added phases (by estimating bulk Kd and "adding" an amount from an assumed parent).

The following is a listing of all models referred to in Chapters 4 and 6, including those appearing as Tables.

A5.1 - Basalts of Taupo Volcanic Zone; the models attempt to derive low-alumina and high-alumina basalt from tholeiite, and high-alumina basalt from low-alumina basalt by POAM fractionation (Chapter 4, Part 2) (10 models).

A5.2 - TYPE 1 lavas of Ruapehu and Ngauruhoe 1954; the models attempt to derive evolved compositions from more basic parents by assimilation and fractional crystalisation (AFC, Taylor, 1980; De Paolo, 1981) (Chapter 6.2.1) (30 models).

A5.3 - TYPE 2 lavas of Wahianoa Formation, Ruapehu; the models attempt to derive these plagioclase-enriched lavas from suitable parental magmas by AFC or crystal accumulation (Chapter 6.2.2) (10 models)

A5.4 - TYPE 3 lavas of Ruapehu; the models attempt to derive these pyroxene-olivine-enriched lavas from suitable parental magmas by AFC or crystal accumulation (Chapter 6.2.3) (20 models).

A5.5 - TYPE 4 lavas of Wahianoa and Mangawhero Formations, Ruapehu; the models attempt to derive these mafic-rich, uncontaminated lavas by POAM fractionation of suitable parental magmas (Chapter 6.2.4) (9 models).

A5.6 - TYPE 5 lavas of Hauhungatahi, Ohakune and Pukekaikiore; the models attempt to derive these olivine andesites by POAM fractionation of suitable parental magmas (Chapter 6.2.5) (11 models).

A5.7 - TYPE 6 lavas of Pukeonake and Mangawhero Formation, Ruapehu; the models attempt to derive these hybrid lavas by binary mixing of basic and acidic parents (Chapter 6.2.5) (10 models).

MODEL NO. : A5.1.1
PARENT : 17439 (WAIMARINO BASALT)
DAUGHTER : 14855 (RUAPEHU BASALT)
DESCRIPTION : POAM fractionation

	P	D	MODEL	RESID.	PHASE	WGT%	%
SiO_2	53.0	52.9	53.0	+.08			
TiO_2	.5	.7	.7	-.02			
Al_2O_3	12.9	15.8	15.9	+.16			
FeO	8.5	8.9	9.0	+.09	Fo90	-6.37	67.01
MgO	13.3	8.8	8.9	+.08	CPX1	-3.14	32.99
CaO	9.7	9.8	9.8	+.07	An50	+15.88	0.00
Na_2O	1.7	2.6	2.3	-.27	MT10.0	+2.33	0.00
K_2O	.4	.6	.4	-.19			

SUM SQUARES RESID. = .1631 CRYSTALS REMOVED = 9.51%

	P	D	MODEL	BULK DC	% ERROR	MISFIT
Rb	15	11	17	.01	+ 54.5	YES
Ba	122	185	135	.01	- 27.0	YES
Zr	48	50	53	.09	+ 6.0	NO
Sr	342	201	377	.03	+ 82.6	YES
V	226	251	240	.42	- 4.4	NO
Cr	1037	380	771	3.97	+102.9	YES
Ni	341	142	176	7.61	+ 23.9	YES

MODEL NO. : A5.1.2
PARENT : 17439 (WAIMARINO BASALT)
DAUGHTER : 11965 (RED CRATER BASALT)
DESCRIPTION : POAM fractionation

	P	D	MODEL	RESID.	PHASE	WGT%	%
SiO_2	53.0	53.3	53.4	+.08			
TiO_2	.5	.7	.7	+.00			
Al_2O_3	12.9	15.5	15.7	+.13			
FeO	8.5	9.1	9.2	+.09	Fo90	-10.57	93.55
MgO	13.3	7.8	7.9	+.07	CPX1	-.73	6.45
CaO	9.7	10.5	10.5	+.07	An50	+10.95	0.00
Na_2O	1.7	2.5	2.2	-.20	MT12.5	+2.21	0.00
K_2O	.4	.7	.4	-.24			

SUM SQUARES RESID. = .1428 CRYSTALS REMOVED = 11.30%

	P	D	MODEL	BULK DC	% ERROR	MISFIT
Rb	15	20	17	.01	- 15.0	NO
Ba	122	137	137	.01	+ 0.0	NO
Zr	48	68	54	.03	- 20.6	YES
Sr	342	278	385	.01	+ 38.5	YES
V	226	271	250	.15	- 7.7	NO
Cr	1037	281	967	1.58	+244.1	YES
Ni	341	63	143	8.25	+127.0	YES

MODEL NO. : A5.1.3
PARENT : 17439 (WAIMARINO BASALT)
DAUGHTER : 22998 (ONGAROTO BASALT)
DESCRIPTION : POAM fractionation

	P	D	MODEL	RESID.	PHASE	WGT%	%
SiO_2	53.0	50.9	51.2	+.29			
TiO_2	.5	1.1	1.0	-.14			
Al_2O_3	12.9	15.8	16.1	+.26			
FeO	8.5	9.2	9.5	+.30	Fo90	-3.70	100.00
MgO	13.3	9.4	9.5	+.14	CPX1	+.37	0.00
CaO	9.7	10.5	10.6	+.08	An70	+20.89	0.00
Na_2O	1.7	2.5	1.8	-.71	MT17.5	+4.05	0.00
K_2O	.4	.6	.3	-.23			

SUM SQUARES RESID. = .8438 CRYSTALS REMOVED = 3.70%

	P	D	MODEL	BULK DC	% ERROR	MISFIT
Rb	15	10	16	.01	+ 60.0	YES
Ba	122	nd				
Zr	48	125	50	.01	- 60.0	YES
Sr	342	330	355	.01	+ 7.6	NO
V	226	220	234	.08	+ 6.4	NO
Cr	1037	550	1037	1.00	+ 88.5	YES
Ni	341	160	258	8.40	+ 61.3	YES

MODEL NO. : A5.1.4
PARENT : 17439 (WAIMARINO BASALT)
DAUGHTER : 22996 (K-TRIG BASALT)
DESCRIPTION : POAM fractionation

	P	D	MODEL	RESID.	PHASE	WGT%	%
SiO_2	53.0	49.9	50.0	+.14			
TiO_2	.5	1.0	.9	-.12			
Al_2O_3	12.9	17.5	17.7	+.15			
FeO	8.5	9.6	9.7	+.15	Fo90	-7.86	100.00
MgO	13.3	7.1	7.2	+.09	CPX1	+15.69	0.00
CaO	9.7	12.3	12.4	+.06	An70	+51.81	0.00
Na_2O	1.7	2.2	1.9	-.34	MT12.5	+8.58	0.00
K_2O	.4	.3	.2	-.13			

SUM SQUARES RESID. = .2236 CRYSTALS REMOVED = 7.86%

	P	D	MODEL	BULK DC	% ERROR	MISFIT
Rb	15	8	16	.01	+100.0	YES
Ba	122	94	132	.01	+ 40.4	YES
Zr	48	56	52	.01	- 7.1	NO
Sr	342	344	371	.01	+ 7.8	NO
V	226	244	244	.08	- 0.0	NO
Cr	1037	120	1037	1.00	+764.2	YES
Ni	341	39	186	8.40	+376.9	YES

MODEL NO. : A5.1.5
PARENT : 17439 (WAIMARINO BASALT)
DAUGHTER : 22994 (BEN LOMOND ROAD BASALT)
DESCRIPTION : POAM fractionation

	P	D	MODEL	RESID.	PHASE	WGT%	%
SiO_2	53.0	51.4	51.5	+.12			
TiO_2	.5	1.1	1.3	+.14			
Al_2O_3	12.9	17.6	17.7	+.13			
FeO	8.5	9.8	9.9	+.08	Fo90	-11.67	100.00
MgO	13.3	6.0	6.1	+.07	CPX1	+.20	0.00
CaO	9.7	10.8	10.9	+.05	An60	+31.55	0.00
Na_2O	1.7	2.8	2.4	-.37	MT17.5	+6.16	0.00
K_2O	.4	.5	.3	-.22			

SUM SQUARES RESID. = .2508 CRYSTALS REMOVED = 11.67%

	P	D	MODEL	BULK DC	% ERROR	MISFIT
Rb	15	14	17	.01	+ 21.4	YES
Ba	122	129	138	.01	+ 7.0	NO
Zr	48	84	54	.01	- 35.7	YES
Sr	342	348	387	.01	+ 11.2	NO
V	226	252	253	.08	+ .4	NO
Cr	1037	44	1037	1.00	+2256.8	YES
Ni	341	29	136	8.40	+369.0	YES

MODEL NO. : A5.1.6
PARENT : 22998 (ONGAROTO BASALT)
DAUGHTER : 22996 (K-TRIG BASALT)
DESCRIPTION : POAM fractionation

	P	D	MODEL	RESID.	PHASE	WGT%	%
SiO_2	50.9	49.9	49.8	-.11			
TiO_2	1.1	1.0	1.0	+.00			
Al_2O_3	15.8	17.5	17.4	-.10			
FeO	9.2	9.6	9.5	-.09	Fo90	-3.47	100.00
MgO	9.4	7.1	7.1	-.06	CPX1	+12.40	0.00
CaO	10.5	12.3	12.3	-.03	An70	+25.08	0.00
Na_2O	2.5	2.2	2.5	+.30	MT7.5	+3.69	0.00
K_2O	.6	.3	.4	+.08			

SUM SQUARES RESID. = .1335 CRYSTALS REMOVED = 3.47%

	P	D	MODEL	BULK DC	% ERROR	MISFIT
Rb	10	8	10	.01	+ 25.0	YES
Ba	nd	94				
Zr	125	56	130	.01	+132.1	YES
Sr	330	344	342	.01	- .6	NO
V	220	244	227	.08	- 7.0	NO
Cr	550	120	550	1.00	+358.3	YES
Ni	160	39	107	12.40	+174.4	YES

MODEL NO. : A5.1.7
PARENT : 22998 (ONGAROTO BASALT)
DAUGHTER : 22994 (BEN LOMOND ROAD BASALT)
DESCRIPTION : POAM fractionation

	P	D	MODEL	RESID.
SiO_2	50.9	51.4	51.4	-.07
TiO_2	1.1	1.1	1.2	+.12
Al_2O_3	15.8	17.6	17.5	-.05
FeO	9.2	9.8	9.7	-.07
MgO	9.4	6.0	5.9	-.04
CaO	10.5	10.8	10.8	-.02
Na_2O	2.5	2.8	2.8	+.06
K_2O	.6	.5	.6	+.08

PHASE	WGT%	%
Fo90	-7.03	67.54
CPX1	-3.38	32.46
An70	+.46	0.00
MT7.5	+.55	0.00

SUM SQUARES RESID. = .0378 CRYSTALS REMOVED = 10.41%

	P	D	MODEL	BULK DC	% ERROR	MISFIT
Rb	10	14	11	.01	- 21.4	YES
Ba	nd	129				
Zr	125	84	137	.09	+ 63.1	YES
Sr	330	348	363	.03	+ 4.3	NO
V	220	252	233	.41	- 7.5	NO
Cr	550	44	412	3.92	+836.4	YES
Ni	160	29	64	10.32	+120.7	YES

MODEL NO. : A5.1.8
PARENT : 22998 (ONGAROTO BASALT)
DAUGHTER : 21717 (TARAWERA BASALT)
DESCRIPTION : POAM fractionation

	P	D	MODEL	RESID.
SiO_2	50.9	51.6	51.7	+.16
TiO_2	1.1	.8	1.2	+.32
Al_2O_3	15.8	17.5	17.1	-.41
FeO	9.2	9.6	9.4	-.11
MgO	9.4	6.3	6.1	-.18
CaO	10.5	11.6	11.2	-.31
Na_2O	2.5	2.2	2.6	+.44
K_2O	.6	.6	.6	+.07

PHASE	WGT%	%
Fo90	-7.86	53.87
CPX1	-2.03	13.90
An50	-4.41	30.21
MT17.5	-.29	2.02

SUM SQUARES RESID. = .6305 CRYSTALS REMOVED = 14.59%

	P	D	MODEL	BULK DC	% ERROR	MISFIT
Rb	10	15	12	.03	- 20.0	NO
Ba	nd	nd				
Zr	125	82	145	.05	+ 76.8	YES
Sr	330	318	353	.57	+ 11.0	NO
V	220	256	227	.81	- 11.3	NO
Cr	550	55	418	2.74	+660.0	YES
Ni	160	14	55	7.72	+292.8	YES

MODEL NO. : A5.1.9
PARENT : 22998 (ONGAROTO BASALT)
DAUGHTER : 22993 (ORAKEI-KORAKO BASALT)
DESCRIPTION : OA fractionation

	P	D	MODEL	RESID.
SiO_2	50.9	51.0	51.5	+.45
TiO_2	1.1	1.3	1.2	-.11
Al_2O_3	15.8	17.2	17.4	+.20
FeO	9.2	9.8	9.3	-.46
MgO	9.4	6.4	6.5	+.14
CaO	10.5	10.8	10.7	-.10
Na_2O	2.5	3.1	2.8	-.30
K_2O	.6	.4	.6	+.18

PHASE	WGT%	%
Fo90	-5.89	61.12
CPX1	-3.75	38.88

SUM SQUARES RESID. = .6191 CRYSTALS REMOVED = 9.64%

	P	D	MODEL	BULK DC	% ERROR	MISFIT
Rb	10	8	11	.01	+ 37.5	YES
Ba	nd	145				
Zr	125	147	137	.10	- 6.8	NO
Sr	330	347	364	.04	+ 4.9	NO
V	220	286	232	.48	- 18.9	NO
Cr	550	37	386	4.50	+673.0	YES
Ni	160	33	65	9.91	+ 97.0	YES

MODEL NO. : A5.1.10
PARENT : 14855 (RUAPEHU BASALT)
DAUGHTER : 11965 (RED CRATER BASALT)
DESCRIPTION : POAM fractionation

	P	D	MODEL	RESID.
SiO_2	52.9	53.3	53.3	+.02
TiO_2	.7	.7	.7	-.02
Al_2O_3	15.8	15.5	15.5	-.02
FeO	8.9	9.1	9.1	+.01
MgO	8.8	7.8	7.8	+.00
CaO	9.8	10.5	10.4	-.01
Na_2O	2.6	2.5	2.5	+.07
K_2O	.6	.7	.6	-.05

PHASE	WGT%	%
Fo90	-3.85	45.26
CPX1	+2.22	0.00
An50	-4.52	53.10
MT0.0	-.14	1.64

SUM SQUARES RESID. = .0081 CRYSTALS REMOVED = 8.51%

	P	D	MODEL	BULK DC	% ERROR	MISFIT
Rb	11	20	12	.04	- 40.0	YES
Ba	185	137	201	.09	+ 46.7	YES
Zr	48	68	55	.02	- 19.1	NO
Sr	201	278	201	.98	- 27.7	YES
V	251	271	262	.53	- 3.3	NO
Cr	380	281	376	1.11	+ 33.8	YES
Ni	142	63	90	6.14	+ 42.9	YES

MODEL NO. : A5.2.1
PARENT : 14855 (RUAPEHU BASALT)
DAUGHTER : 29250 (NGAURUHOE 1954 BASIC ANDESITE)
DESCRIPTION : POAM fractionation

	P	D	MODEL	RESID.	PHASE	WGT%	%
SiO_2	52.9	56.5	56.5	+.04			
TiO_2	.7	.8	.8	+.01			
Al_2O_3	15.8	16.7	16.7	+.02			
FeO	8.9	8.3	8.3	+.03	Fo90	-7.65	23.27
MgO	8.8	5.2	5.2	+.02	CPX1	-9.44	28.73
CaO	9.8	8.3	8.4	+.01	An70	-13.72	41.75
Na_2O	2.6	3.1	3.2	+.06	MT7.5	-2.05	6.25
K_2O	.6	1.2	1.0	-.19			

SUM SQUARES RESID. = .0441 CRYSTALS REMOVED = 32.86%

	P	D	MODEL	BULK DC	% ERROR	MISFIT
Rb	11	38	16	.04	- 57.9	YES
Ba	185	214	268	.08	+ 25.2	YES
Zr	50	95	72	.10	- 24.2	YES
Sr	201	247	219	.79	- 11.3	NO
V	251	220	155	2.21	- 29.5	YES
Cr	380	100	60	5.61	- 40.0	YES
Ni	142	29	24	5.42	- 26.9	YES

MODEL NO. : A5.2.2
PARENT : 14855 (RUAPEHU BASALT)
DAUGHTER : 29250 (NGAURUHOE 1954 BASIC ANDESITE)
DESCRIPTION : AFC (K-rich melt)

	P	D	MODEL	RESID.	PHASE	WGT%	%
SiO_2	52.9	56.5	56.5	+.02			
TiO_2	.7	.8	.8	-.00			
Al_2O_3	15.8	16.7	16.7	+.01			
FeO	8.9	8.3	8.3	+.01	Fo90	-6.93	27.40
MgO	8.8	5.2	5.2	+.01	CPX1	-7.72	30.52
CaO	9.8	8.3	8.4	+.00	An70	-9.34	36.92
Na_2O	2.6	3.1	3.1	-.04	MT7.5	-1.31	5.16
K_2O	.6	1.2	1.1	-.02	MELT1	+5.46	0.00

SUM SQUARES RESID. = .0023 CRYSTALS REMOVED = 25.30%

	P	D	MODEL	BULK DC	% ERROR	MISFIT
Rb	11	38	15	.04	- 60.5	YES
Ba	185	214	243	.07	+ 13.6	NO
Zr	50	95	65	.10	- 31.6	YES
Sr	201	247	219	.70	- 11.3	NO
V	251	220	193	1.91	- 12.3	NO
Cr	380	100	106	5.39	+ 6.0	NO
Ni	142	29	33	5.97	+ 13.8	NO

MODEL NO. : A5.2.3
PARENT : 14855 (RUAPEHU BASALT)
DAUGHTER : 29250 (NGAURUHOE 1954 BASIC ANDESITE)
DESCRIPTION : AFC (K-poor melt)

	P	D	MODEL	RESID.	PHASE	WGT%	%
SiO_2	52.9	56.5	56.5	+.06			
TiO_2	.7	.8	.8	-.00			
Al_2O_3	15.8	16.7	16.7	+.04			
FeO	8.9	8.3	8.4	+.05	Fo90	-6.40	30.07
MgO	8.8	5.2	5.2	+.03	CPX1	-7.65	35.94
CaO	9.8	8.3	8.4	+.02	An80	-6.35	29.82
Na_2O	2.6	3.1	3.1	+.01	MT7.5	-.89	4.17
K_2O	.6	1.2	.9	-.21	MELT2	+6.31	0.00

SUM SQUARES RESID. = .0532 CRYSTALS REMOVED = 21.29%

	P	D	MODEL	BULK DC	% ERROR	MISFIT
Rb	11	38	14	.03	- 63.2	YES
Ba	185	214	232	.06	+ 8.4	NO
Zr	50	95	62	.11	- 34.7	YES
Sr	201	247	222	.58	- 10.1	NO
V	251	220	214	1.67	- 2.7	NO
Cr	380	100	127	5.57	+ 27.0	YES
Ni	142	29	38	6.55	+ 31.0	YES

MODEL NO. : A5.2.4
PARENT : 11965 (RED CRATER BASALT)
DAUGHTER : 29250 (NGAURUHOE 1954 BASIC ANDESITE)
DESCRIPTION : AFC (K-rich melt)

	P	D	MODEL	RESID.	PHASE	WGT%	%
SiO_2	53.3	56.5	56.5	+.02			
TiO_2	.7	.8	.8	+.02			
Al_2O_3	15.5	16.7	16.7	+.01			
FeO	9.1	8.3	8.3	+.01	Fo90	-3.85	14.54
MgO	7.8	5.2	5.2	+.01	CPX2	-12.69	47.92
CaO	10.5	8.3	8.3	+.00	An80	-8.67	32.74
Na_2O	2.5	3.1	3.1	-.05	MT12.5	-1.27	4.80
K_2O	.7	1.2	1.1	-.03	MELT1	+3.03	0.00

SUM SQUARES RESID. = .0043 CRYSTALS REMOVED = 26.48%

	P	D	MODEL	BULK DC	% ERROR	MISFIT
Rb	20	38	27	.03	- 29.0	YES
Ba	137	214	183	.06	- 14.5	NO
Zr	68	95	89	.14	- 6.3	NO
Sr	278	247	311	.64	+ 25.9	YES
V	271	220	200	1.98	- 9.1	NO
Cr	281	100	46	6.86	- 54.0	YES
Ni	63	29	16	5.55	- 44.8	YES

MODEL NO. : A5.2.5
PARENT : 17439 (WAIMARINO BASALT)
DAUGHTER : 29250 (NGAURUHOE 1954 BASIC ANDESITE)
DESCRIPTION : AFC (K-rich melt)

	P	D	MODEL	RESID.	PHASE	WGT%	%
SiO_2	53.0	56.5	56.7	+.24			
TiO_2	.5	.8	.7	-.04			
Al_2O_3	12.9	16.7	16.8	+.18			
FeO	8.5	8.3	8.5	+.19	Fo90	-14.81	42.57
MgO	13.3	5.2	5.3	+.12	CPX1	-15.14	43.66
CaO	9.7	8.3	8.4	+.06	An80	-4.32	12.47
Na_2O	1.7	3.1	2.7	-.47	MT7.5	-.40	1.16
K_2O	.4	1.2	.9	-.28	MELT1	+.78	0.00

SUM SQUARES RESID. = .4466 CRYSTALS REMOVED = 34.67%

	P	D	MODEL	BULK DC	% ERROR	MISFIT
Rb	15	38	23	.02	- 39.5	YES
Ba	122	214	184	.03	- 14.0	NO
Zr	48	95	70	.12	- 26.3	YES
Sr	342	247	467	.27	+ 89.1	YES
V	226	220	240	.86	+ 9.1	NO
Cr	1037	100	169	5.26	+ 69.0	YES
Ni	341	29	35	6.33	+ 20.7	YES

MODEL NO. : A5.2.6
PARENT : 17439 (WAIMARINO BASALT)
DAUGHTER : 29250 (NGAURUHOE 1954 BASIC ANDESITE)
DESCRIPTION : AFC (K-rich melt)

	P	D	MODEL	RESID.	PHASE	WGT%	%
SiO_2	53.0	56.5	56.7	+.20			
TiO_2	.5	.8	.7	-.08			
Al_2O_3	12.9	16.7	17.0	+.36			
FeO	8.5	8.3	8.3	-.07	Fo90	-13.91	49.97
MgO	13.3	5.2	5.4	+.18	CPX1	-13.92	50.03
CaO	9.7	8.3	8.5	+.12			
Na_2O	1.7	3.1	2.5	-.60			
K_2O	.4	1.2	1.0	-.12	MELT1	+5.55	0.00

SUM SQUARES RESID. = .5964 CRYSTALS REMOVED = 27.83%

	P	D	MODEL	BULK DC	% ERROR	MISFIT
Rb	15	38	21	.02	- 44.7	YES
Ba	122	214	168	.02	- 21.5	YES
Zr	48	95	64	.13	- 32.6	YES
Sr	342	247	467	.05	+ 89.1	YES
V	226	220	258	.59	+ 17.3	NO
Cr	1037	100	239	5.50	+139.0	YES
Ni	341	29	45	7.21	+ 55.2	YES

MODEL NO. : A5.2.7
PARENT : 22994 (BEN LOMOND ROAD BASALT)
DAUGHTER : 29250 (NGAURUHOE 1954 BASIC ANDESITE)
DESCRIPTION : AFC (K-rich melt; O = olivine)

	P	D	MODEL	RESID.	PHASE	WGT%	%
SiO_2	51.4	56.5	56.4	-.02			
TiO_2	1.1	.8	.8	+.02			
Al_2O_3	17.6	16.7	16.6	-.02			
FeO	9.8	8.3	8.3	-.02	Fo90	-1.88	5.14
MgO	6.0	5.2	5.2	-.01	CPX1	-9.44	25.86
CaO	10.8	8.3	8.3	-.01	An70	-21.08	57.72
Na_2O	2.8	3.1	3.2	+.05	MT15.0	-4.12	11.28
K_2O	.5	1.2	1.2	+.01	MELT1	+4.51	0.00

SUM SQUARES RESID. = .0039 CRYSTALS REMOVED = 36.52%

	P	D	MODEL	BULK DC	% ERROR	MISFIT
Rb	14	38	22	.05	- 42.1	YES
Ba	129	214	194	.10	- 9.3	NO
Zr	84	95	126	.12	+ 32.6	YES
Sr	348	247	336	1.08	+ 36.0	YES
V	252	220	75	3.68	- 65.9	YES
Cr	44	100	3	7.16	- 97.0	YES
Ni	29	29	9	3.71	- 69.0	YES

MODEL NO. : A5.2.8
PARENT : 22994 (BEN LOMOND ROAD BASALT)
DAUGHTER : 29250 (NGAURUHOE 1954 BASIC ANDESITE)
DESCRIPTION : AFC (K-rich melt; O = orthopyroxene)

	P	D	MODEL	RESID.	PHASE	WGT%	%
SiO_2	51.4	56.5	56.4	-.06			
TiO_2	1.1	.8	.8	+.03			
Al_2O_3	17.6	16.7	16.6	-.04			
FeO	9.8	8.3	8.3	-.06	En80	-3.86	9.19
MgO	6.0	5.2	5.2	-.01	CPX1	-9.78	23.32
CaO	10.8	8.3	8.3	-.03	An70	-24.01	57.25
Na_2O	2.8	3.1	3.2	+.12	MT15.0	-4.29	10.23
K_2O	.5	1.2	1.2	+.01	MELT1	+4.23	0.00

SUM SQUARES RESID. = .0289 CRYSTALS REMOVED = 41.9%

	P	D	MODEL	BULK DC	% ERROR	MISFIT
Rb	14	38	24	.05	- 36.8	YES
Ba	129	214	210	.10	- 1.9	NO
Zr	84	95	136	.11	+ 43.2	YES
Sr	348	247	335	1.07	+ 35.6	YES
V	252	220	67	3.43	- 69.5	YES
Cr	44	100	2	6.71	- 98.0	YES
Ni	29	29	9	3.169	- 69.0	YES

MODEL NO. : A5.2.9
PARENT : 14855 (RUAPEHU BASALT)
DAUGHTER : 14858 (MANGAWHERO FORMATION BASIC ANDESITE)
DESCRIPTION : POAM fractionation

	P	D	MODEL	RESID.	PHASE	WGT%	%
SiO_2	52.9	54.3	54.3	-.01			
TiO_2	.7	.7	.7	-.01			
Al_2O_3	15.8	17.2	17.2	-.02			
FeO	8.9	8.5	8.5	-.01	Fo90	-4.05	23.13
MgO	8.8	6.8	6.8	-.01	CPX1	-7.73	44.13
CaO	9.8	9.0	9.0	-.01	An60	-4.65	26.56
Na_2O	2.6	2.9	2.9	+.04	MT10.0	-1.08	6.18
K_2O	.6	.7	.7	+.02			

SUM SQUARES RESID. = .0027 CRYSTALS REMOVED = 17.51%

	P	D	MODEL	BULK DC	% ERROR	MISFIT
Rb	11	18	13	.03	- 27.8	YES
Ba	185	237	222	.05	- 6.3	NO
Zr	50	58	59	.14	+ 1.7	NO
Sr	201	219	220	.52	+ 0.5	NO
V	251	258	193	2.36	- 25.2	YES
Cr	380	140	117	7.12	- 16.4	NO
Ni	142	51	51	6.32	0.0	NO

MODEL NO. : A5.2.10
PARENT : 14855 (RUAPEHU BASALT)
DAUGHTER : 14858 (MANGAWHERO FORMATION BASIC ANDESITE)
DESCRIPTION : AFC (K-rich melt)

	P	D	MODEL	RESID.	PHASE	WGT%	%
SiO_2	52.9	54.3	54.2	-.10			
TiO_2	.7	.7	.7	+.04			
Al_2O_3	15.8	17.2	17.0	-.18			
FeO	8.9	8.5	8.7	+.25	Fo90	-3.25	35.78
MgO	8.8	6.8	6.6	-.12	CPX1	-5.83	64.22
CaO	9.8	9.0	8.9	-.08			
Na_2O	2.6	2.9	2.9	+.02			
K_2O	.6	.7	.9	+.18	MELT1	+4.04	0.00

SUM SQUARES RESID. = .1563 CRYSTALS REMOVED = 9.08%

	P	D	MODEL	BULK DC	% ERROR	MISFIT
Rb	11	18	12	.02	- 33.3	YES
Ba	185	237	203	.02	- 14.3	NO
Zr	50	58	54	.16	- 6.9	NO
Sr	201	219	220	.05	+ .5	NO
V	251	258	257	.74	- .4	NO
Cr	380	140	219	6.78	+ 56.4	YES
Ni	142	51	69	8.58	+ 35.3	YES

MODEL NO. : A5.2.11
PARENT : 14855 (RUAPEHU BASALT)
DAUGHTER : 14850 (MANGAWHERO FORMATION BASIC ANDESITE)
DESCRIPTION : AFC (K-rich melt)

	P	D	MODEL	RESID.	PHASE	WGT%	%
SiO_2	52.9	56.4	56.4	-.01			
TiO_2	.7	.8	.8	+.01	PHASE	WGT%	%
Al_2O_3	15.8	17.7	17.7	+.01			
FeO	8.9	7.7	7.7	-.01	Fo90	-6.50	21.86
MgO	8.8	5.1	5.1	-.00	CPX1	-11.10	37.36
CaO	9.8	8.2	8.2	+.00	An50	-10.14	34.11
Na_2O	2.6	3.0	2.9	-.05	MT5.0	-1.98	6.67
K_2O	.6	1.1	1.2	+.04	MELT1	+5.11	0.00

SUM SQUARES RESID. = .0042 CRYSTALS REMOVED = 29.72%

	P	D	MODEL	BULK DC	% ERROR	MISFIT
Rb	11	34	16	.03	- 52.9	YES
Ba	185	313	257	.06	- 17.9	NO
Zr	50	84	68	.13	- 19.0	NO
Sr	201	251	227	.66	- 9.6	NO
V	251	216	152	2.43	- 29.6	YES
Cr	380	132	52	6.63	- 60.6	YES
Ni	142	49	26	5.80	- 46.9	YES

MODEL NO. : A5.2.12
PARENT : 14855 (RUAPEHU BASALT)
DAUGHTER : 14850 (MANGAWHERO FORMATION BASIC ANDESITE)
DESCRIPTION : AFC (K-poor melt)

	P	D	MODEL	RESID.	PHASE	WGT%	%
SiO_2	52.9	56.4	56.5	+.04			
TiO_2	.7	.8	.8	+.02	PHASE	WGT%	%
Al_2O_3	15.8	17.7	17.7	+.03			
FeO	8.9	7.7	7.7	+.03	Fo90	-6.44	20.70
MgO	8.8	5.1	5.1	+.02	CPX1	-11.88	38.20
CaO	9.8	8.2	8.2	+.01	An50	-10.74	34.55
Na_2O	2.6	3.0	2.9	-.04	MT5.0	-2.04	6.56
K_2O	.6	1.1	1.0	-.12	MELT2	+3.99	0.00

SUM SQUARES RESID. = .0200 CRYSTALS REMOVED = 31.1%

	P	D	MODEL	BULK DC	% ERROR	MISFIT
Rb	11	34	16	.03	- 52.9	YES
Ba	185	313	262	.07	- 16.3	NO
Zr	50	84	69	.13	- 17.9	NO
Sr	201	251	228	.67	- 9.2	NO
V	251	216	149	2.41	- 31.0	YES
Cr	380	132	46	6.65	- 65.2	YES
Ni	142	49	25	5.68	- 49.0	YES

MODEL NO. : A5.2.13
PARENT : 14855 (RUAPEHU BASALT)
DAUGHTER : 14844 (MANGAWHERO FORMATION ACID ANDESITE)
DESCRIPTION : AFC (K-rich melt)

	P	D	MODEL	RESID.	PHASE	WGT%	%
SiO_2	52.9	58.3	58.3	+.00			
TiO_2	.7	.7	.7	-.04			
Al_2O_3	15.8	17.4	17.4	-.00			
FeO	8.9	6.9	6.9	+.01	Fo85	-8.69	19.30
MgO	8.8	4.7	4.7	+.00	CPX2	-14.44	32.06
CaO	9.8	7.6	7.6	+.00	An60	-19.33	42.91
Na_2O	2.6	3.1	3.1	+.03	MT12.5	-2.58	5.73
K_2O	.6	1.2	1.2	+.00	MELT1	+1.98	0.00

SUM SQUARES RESID. = .0024 CRYSTALS REMOVED = 45.02%

	P	D	MODEL	BULK DC	% ERROR	MISFIT
Rb	11	37	20	.04	- 45.9	YES
Ba	185	310	321	.08	+ 3.5	NO
Zr	50	93	85	.11	- 8.6	NO
Sr	201	250	225	.81	- 10.0	NO
V	251	195	131	2.09	- 32.8	YES
Cr	380	92	23	5.70	- 75.0	YES
Ni	142	35	13	5.05	- 62.9	YES

MODEL NO. : A5.2.14
PARENT : 14855 (RUAPEHU BASALT)
DAUGHTER : 14844 (MANGAWHERO FORMATION ACID ANDESITE)
DESCRIPTION : AFC (K-poor melt)

	P	D	MODEL	RESID.	PHASE	WGT%	%
SiO_2	52.9	58.3	58.3	+.00			
TiO_2	.7	.7	.7	+.03			
Al_2O_3	15.8	17.4	17.4	-.01			
FeO	8.9	6.9	6.9	-.00	Fo85	-8.34	19.48
MgO	8.8	4.7	4.7	+.00	CPX2	-14.46	33.77
CaO	9.8	7.6	7.6	-.00	An60	-17.69	41.30
Na_2O	2.6	3.1	3.1	+.03	MT10.0	-2.34	5.46
K_2O	.6	1.2	1.2	-.06	MELT2	+3.20	0.00

SUM SQUARES RESID. = .0058 CRYSTALS REMOVED = 42.83%

	P	D	MODEL	BULK DC	% ERROR	MISFIT
Rb	11	37	19	.04	- 48.6	YES
Ba	185	310	310	.08	+ 0.0	NO
Zr	50	93	82	.11	- 11.8	NO
Sr	201	250	227	.79	- 9.2	NO
V	251	195	141	2.03	- 27.7	YES
Cr	380	92	27	5.76	- 70.7	YES
Ni	142	35	14	5.15	- 60.0	YES

MODEL NO. : A5.2.15
PARENT : 14858 (MANGAWHERO FORMATION BASIC ANDESITE)
DAUGHTER : 14844 (MANGAWHERO FORMATION ACID ANDESITE)
DESCRIPTION : AFC (K-rich melt)

	P	D	MODEL	RESID.	PHASE	WGT%	%
SiO_2	54.3	58.3	58.3	+.00			
TiO_2	.7	.7	.7	+.02			
Al_2O_3	17.2	17.4	17.4	+.01			
FeO	8.5	6.9	6.9	-.00	Fo85	-4.85	16.50
MgO	6.8	4.7	4.7	+.00	CPX2	-6.88	23.39
CaO	9.0	7.6	7.6	+.00	An60	-15.43	52.49
Na_2O	2.9	3.1	3.1	-.03	MT7.5	-2.24	7.62
K_2O	.7	1.2	1.2	+.00	MELT1	+3.84	0.00

SUM SQUARES RESID. = .0016 CRYSTALS REMOVED = 29.40%

	P	D	MODEL	BULK DC	% ERROR	MISFIT
Rb	18	37	25	.04	- 32.4	YES
Ba	237	310	325	.09	+ 4.8	NO
Zr	58	93	80	.10	- 14.0	NO
Sr	219	250	220	.98	- 12.0	NO
V	258	195	150	2.56	- 23.1	YES
Cr	140	92	29	5.56	- 68.5	YES
Ni	51	35	16	4.35	- 54.3	YES

MODEL NO. : A5.2.16
PARENT : 14855 (RUAPEHU BASALT)
DAUGHTER : 14886 (MANGAWHERO FORMATION ACID ANDESITE)
DESCRIPTION : AFC (K-rich melt)

	P	D	MODEL	RESID.	PHASE	WGT%	%
SiO_2	52.9	61.8	61.8	-.03			
TiO_2	.7	.8	.8	+.01			
Al_2O_3	15.8	16.9	16.9	-.03			
FeO	8.9	5.8	5.8	-.03	Fo80	-10.74	22.15
MgO	8.8	3.2	3.2	-.01	CPX2	-15.48	31.91
CaO	9.8	5.9	5.9	-.01	An70	-20.05	41.33
Na_2O	2.6	3.5	3.6	+.07	MT10.0	-2.24	4.61
K_2O	.6	2.0	2.0	+.03	MELT1	+11.52	0.00

SUM SQUARES RESID. = .0081 CRYSTALS REMOVED = 48.51%

	P	D	MODEL	BULK DC	% ERROR	MISFIT
Rb	11	81	21	.04	- 74.1	YES
Ba	185	418	342	.08	- 18.2	NO
Zr	50	158	91	.10	- 42.4	YES
Sr	201	253	232	.78	- 8.3	NO
V	251	162	152	1.76	- 6.2	NO
Cr	380	51	23	5.26	- 54.9	YES
Ni	142	26	8	5.30	- 69.2	YES

MODEL NO. : A5.2.17
PARENT : 14855 (RUAPEHU BASALT)
DAUGHTER : 14886 (MANGAWHERO FORMATION ACID ANDESITE)
DESCRIPTION : AFC (K-poor melt)

	P	D	MODEL	RESID.	PHASE	WGT%	%
SiO_2	52.9	61.8	61.9	+.04			
TiO_2	.7	.8	.8	+.05			
Al_2O_3	15.8	16.9	16.9	+.00			
FeO	8.9	5.8	5.9	+.03	Fo80	-10.89	20.81
MgO	8.8	3.2	3.3	+.02	CPX2	-16.82	32.14
CaO	9.8	5.9	5.9	+.01	An70	-22.24	42.50
Na_2O	2.6	3.5	3.7	+.16	MT10.0	-2.38	4.55
K_2O	.6	2.0	1.7	-.31	MELT2	+5.18	0.00

SUM SQUARES RESID. = .1245 CRYSTALS REMOVED = 52.33%

	P	D	MODEL	BULK DC	% ERROR	MISFIT
Rb	11	81	22	.04	- 72.8	YES
Ba	185	418	366	.08	- 12.4	NO
Zr	50	158	97	.10	- 38.6	YES
Sr	201	253	232	.81	- 8.3	NO
V	251	162	145	1.74	- 10.5	NO
Cr	380	51	16	5.25	- 68.6	YES
Ni	142	26	7	5.13	- 73.1	YES

MODEL NO. : A5.2.18
PARENT : 14858 (MANGAWHERO FORMATION BASIC ANDESITE)
DAUGHTER : 14886 (MANGAWHERO FORMATION ACID ANDESITE)
DESCRIPTION : AFC (K-rich melt)

	P	D	MODEL	RESID.	PHASE	WGT%	%
SiO_2	54.3	61.8	61.8	+.02			
TiO_2	.7	.8	.8	-.02			
Al_2O_3	17.2	16.9	16.9	+.02			
FeO	8.5	5.8	5.9	+.02	Fo80	-7.09	18.92
MgO	6.8	3.2	3.3	+.01	CPX2	-9.05	24.14
CaO	9.0	5.9	5.9	+.01	An70	-18.91	50.45
Na_2O	2.9	3.5	3.5	-.04	MT7.5	-2.44	6.50
K_2O	.7	2.0	2.0	-.02	MELT1	+13.27	0.00

SUM SQUARES RESID. = .0039 CRYSTALS REMOVED = 37.5%

	P	D	MODEL	BULK DC	% ERROR	MISFIT
Rb	18	81	28	.04	- 65.4	YES
Ba	237	418	364	.09	- 12.9	NO
Zr	58	158	89	.09	- 43.7	YES
Sr	219	253	225	.94	- 11.1	NO
V	258	162	144	2.24	- 11.1	NO
Cr	140	51	19	5.21	- 62.7	YES
Ni	51	26	9	4.60	- 65.4	YES

MODEL NO. : A5.2.19
PARENT : 14850 (MANGAWHERO FORMATION BASIC ANDESITE)
DAUGHTER : 14886 (MANGAWHERO FORMATION ACID ANDESITE)
DESCRIPTION : AFC (K-rich melt; O = olivine)

	P	D	MODEL	RESID.	PHASE	WGT%	%
SiO_2	56.4	61.8	61.8	+.01			
TiO_2	.8	.8	.8	+.02			
Al_2O_3	17.7	16.9	16.9	+.01			
FeO	7.7	5.8	5.9	+.01	Fo80	-3.77	15.25
MgO	5.1	3.2	3.2	+.00	CPX2	-5.36	21.67
CaO	8.2	5.9	5.9	+.00	An80	-13.59	54.99
Na_2O	3.0	3.5	3.5	-.03	MT7.5	-2.00	8.09
K_2O	1.1	2.0	2.0	-.01	MELT1	+8.67	0.00

SUM SQUARES RESID. = .0017 CRYSTALS REMOVED = 24.72%

	P	D	MODEL	BULK DC	% ERROR	MISFIT
Rb	34	81	45	.05	- 44.4	YES
Ba	313	418	405	.09	- 3.1	NO
Zr	84	158	109	.09	- 31.0	YES
Sr	251	253	249	1.03	- 1.6	NO
V	216	162	134	2.68	- 17.3	NO
Cr	132	51	36	5.56	- 29.4	YES
Ni	49	26	20	4.13	- 23.1	YES

MODEL NO. : A5.2.20
PARENT : 14850 (MANGAWHERO FORMATION BASIC ANDESITE)
DAUGHTER : 14886 (MANGAWHERO FORMATION ACID ANDESITE)
DESCRIPTION : AFC (K-rich melt; O = orthopyroxene)

	P	D	MODEL	RESID.	PHASE	WGT%	%
SiO_2	56.4	61.8	61.8	-.00			
TiO_2	.8	.8	.8	+.01			
Al_2O_3	17.7	16.9	16.9	-.00			
FeO	7.7	5.8	5.8	-.00	En80	-6.68	18.24
MgO	5.1	3.2	3.2	-.00	CPX2	-6.06	16.54
CaO	8.2	5.9	5.9	-.00	An70	-21.20	57.89
Na_2O	3.0	3.5	3.5	+.00	MT10.0	-2.68	7.33
K_2O	1.1	2.0	2.0	+.00	MELT1	+3.25	0.00

SUM SQUARES RESID. = .0001 CRYSTALS REMOVED = 36.62%

	P	D	MODEL	BULK DC	% ERROR	MISFIT
Rb	34	81	53	.05	- 34.6	YES
Ba	313	418	472	.10	+ 12.9	NO
Zr	84	158	127	.09	- 19.6	NO
Sr	251	253	242	1.08	- 4.3	NO
V	216	162	105	2.59	- 35.2	YES
Cr	132	51	20	5.14	- 60.8	YES
Ni	49	26	18	3.19	- 30.8	YES

MODEL NO. : A5.2.21
PARENT : 14844 (MANGAWHERO FORMATION ACID ANDESITE)
DAUGHTER : 14886 (MANGAWHERO FORMATION ACID ANDESITE)
DESCRIPTION : AFC (K-rich melt)

	P	D	MODEL	RESID.	PHASE	WGT%	%
SiO_2	58.3	61.8	61.8	+.02			
TiO_2	.7	.8	.8	+.01	PHASE	WGT%	%
Al_2O_3	17.4	16.9	16.9	+.02			
FeO	6.9	5.8	5.9	+.02	En70	-5.78	23.73
MgO	4.7	3.2	3.2	+.00	CPX2	-4.11	16.85
CaO	7.6	5.9	5.9	+.01	An70	-13.60	55.82
Na_2O	3.1	3.5	3.5	-.05	MT10.0	-.88	3.61
K_2O	1.2	2.0	1.9	-.03	MELT1	+6.03	0.00

SUM SQUARES RESID. = .0044 CRYSTALS REMOVED = 24.37%

	P	D	MODEL	BULK DC	% ERROR	MISFIT
Rb	37	81	48	.05	- 53.1	YES
Ba	310	418	399	.10	- 4.5	NO
Zr	93	158	120	.09	- 24.1	YES
Sr	250	253	247	1.04	- 2.4	NO
V	195	162	168	1.53	+ 3.7	NO
Cr	92	51	42	3.85	- 17.6	NO
Ni	35	26	19	3.28	- 26.9	YES

MODEL NO. : A5.2.22
PARENT : 14855 (RUAPEHU BASALT)
DAUGHTER : 14889 (MANGAWHERO FORMATION DACITE)
DESCRIPTION : AFC (K-rich melt)

	P	D	MODEL	RESID.	PHASE	WGT%	%
SiO_2	52.9	64.0	64.0	+.01			
TiO_2	.7	.8	.8	+.01	PHASE	WGT%	%
Al_2O_3	15.8	16.8	16.9	+.01			
FeO	8.9	5.1	5.1	+.01	Fo80	-11.38	19.76
MgO	8.8	2.3	2.3	+.01	CPX2	-18.30	31.78
CaO	9.8	4.9	4.9	+.00	An60	-25.24	43.83
Na_2O	2.6	3.4	3.4	-.04	MT10.0	-2.66	4.63
K_2O	.6	2.8	2.8	-.01	MELT1	+17.98	0.00

SUM SQUARES RESID. = .0020 CRYSTALS REMOVED = 57.59%

	P	D	MODEL	BULK DC	% ERROR	MISFIT
Rb	11	120	25	.04	- 79.2	YES
Ba	185	527	408	.08	- 22.6	YES
Zr	50	201	108	.10	- 46.3	YES
Sr	201	260	233	.83	- 10.4	NO
V	251	115	131	1.76	+ 13.9	NO
Cr	380	31	10	5.23	- 67.7	YES
Ni	142	20	5	4.98	- 75.0	YES

MODEL NO. : A5.2.23
PARENT : 14855 (RUAPEHU BASALT)
DAUGHTER : 14889 (MANGAWHERO FORMATION DACITE)
DESCRIPTION : AFC (K-poor melt)

	P	D	MODEL	RESID.	PHASE	WGT%	%
SiO_2	52.9	64.0	63.9	-.01			
TiO_2	.7	.8	.9	+.04			
Al_2O_3	15.8	16.8	16.8	-.02			
FeO	8.9	5.1	5.1	-.02	Fo80	-14.09	14.33
MgO	8.8	2.3	2.3	-.01	CPX2	-18.39	18.70
CaO	9.8	4.9	4.9	-.01	An60	-43.12	43.86
Na_2O	2.6	3.4	3.4	+.04	MT12.5	-4.25	4.33
K_2O	.6	2.8	2.7	-.02	MELT2	-18.46	18.78

SUM SQUARES RESID. = .0043 CRYSTALS REMOVED = 98.31%

NOTE: Trace elements cannot be adequately modelled because melt must be removed to produce the best majors fit.

MODEL NO. : A5.2.24
PARENT : 14858 (MANGAWHERO FORMATION BASIC ANDESITE)
DAUGHTER : 14889 (MANGAWHERO FORMATION DACITE)
DESCRIPTION : AFC (K-rich melt)

	P	D	MODEL	RESID.	PHASE	WGT%	%
SiO_2	54.3	64.0	63.9	-.01			
TiO_2	.7	.8	.8	-.04			
Al_2O_3	17.2	16.8	16.8	-.01			
FeO	8.5	5.1	5.1	-.00	Fo80	-7.54	20.01
MgO	6.8	2.3	2.3	-.00	CPX2	-10.65	28.27
CaO	9.0	4.9	4.9	-.00	An70	-17.08	45.31
Na_2O	2.9	3.4	3.4	+.05	MT5.0	-2.42	6.41
K_2O	.7	2.8	2.8	+.01	MELT1	+32.19	0.00

SUM SQUARES RESID. = .0040 CRYSTALS REMOVED = 37.69%

	P	D	MODEL	BULK DC	% ERROR	MISFIT
Rb	18	120	28	.04	- 76.7	YES
Ba	237	527	366	.08	- 30.6	YES
Zr	58	201	89	.10	- 55.7	YES
Sr	219	260	235	.85	- 9.6	NO
V	258	115	143	2.25	+ 24.3	YES
Cr	140	31	16	5.60	- 48.4	YES
Ni	51	20	8	4.98	- 60.0	YES

MODEL NO. : A5.2.25
PARENT : 14850 (MANGAWHERO FORMATION BASIC ANDESITE)
DAUGHTER : 14889 (MANGAWHERO FORMATION DACITE)
DESCRIPTION : AFC (K-rich melt; 0 = olivine)

	P	D	MODEL	RESID.	PHASE	WGT%	%
SiO_2	56.4	64.0	64.0	+.02			
TiO_2	.8	.8	.8	-.04	PHASE	WGT%	%
Al_2O_3	17.7	16.8	16.9	+.02			
FeO	7.7	5.1	5.1	+.02	Fo80	-4.39	14.84
MgO	5.1	2.3	2.3	+.01	CPX2	-7.89	26.66
CaO	8.2	4.9	4.9	+.01	An70	-15.08	50.94
Na_2O	3.0	3.4	3.4	-.03	MT7.5	-2.24	7.56
K_2O	1.1	2.8	2.7	-.02	MELT1	+24.79	0.00

SUM SQUARES RESID. = .0034 CRYSTALS REMOVED = 29.60%

	P	D	MODEL	BULK DC	% ERROR	MISFIT
Rb	34	120	48	.04	- 60.0	YES
Ba	313	527	431	.09	- 18.2	NO
Zr	84	201	115	.10	- 42.8	YES
Sr	251	260	255	.96	- 1.9	NO
V	216	115	124	2.58	+ 7.8	NO
Cr	132	31	24	5.84	- 22.6	YES
Ni	39	20	15	4.32	- 25.0	YES

MODEL NO. : A5.2.26
PARENT : 14850 (MANGAWHERO FORMATION BASIC ANDESITE)
DAUGHTER : 14889 (MANGAWHERO FORMATION DACITE)
DESCRIPTION : AFC (K-rich melt; 0 = orthopyroxene)

	P	D	MODEL	RESID.	PHASE	WGT%	%
SiO_2	56.4	64.0	63.9	-.04			
TiO_2	.8	.8	.8	+.01	PHASE	WGT%	%
Al_2O_3	17.7	16.8	16.8	-.03			
FeO	7.7	5.1	5.1	-.03	En80	-7.25	19.52
MgO	5.1	2.3	2.2	-.01	CPX2	-7.44	20.03
CaO	8.2	4.9	4.9	-.02	An70	-19.77	53.24
Na_2O	3.0	3.4	3.5	+.09	MT7.5	-2.68	7.22
K_2O	1.1	2.8	2.8	+.04	MELT1	+20.05	0.00

SUM SQUARES RESID. = .0138 CRYSTALS REMOVED = 37.14%

	P	D	MODEL	BULK DC	% ERROR	MISFIT
Rb	34	120	53	.05	- 55.8	YES
Ba	313	527	476	.09	- 9.7	NO
Zr	84	201	127	.10	- 36.8	YES
Sr	251	260	251	1.00	- 3.5	NO
V	216	115	103	2.61	- 10.4	NO
Cr	132	31	17	5.48	- 45.2	YES
Ni	39	20	15	3.49	- 25.0	YES

MODEL NO. : A5.2.27
PARENT : 14844 (MANGAWHERO FORMATION ACID ANDESITE)
DAUGHTER : 14889 (MANGAWHERO FORMATION DACITE)
DESCRIPTION : AFC (K-rich melt)

	P	D	MODEL	RESID.	PHASE	WGT%	%
SiO_2	58.3	64.0	64.0	+.03			
TiO_2	.7	.8	.8	-.02			
Al_2O_3	17.4	16.8	16.9	+.03			
FeO	6.9	5.1	5.1	+.03	En80	-5.62	19.62
MgO	4.7	2.3	2.3	+.01	CPX2	-6.68	23.32
CaO	7.6	4.9	4.9	+.02	An60	-14.82	51.71
Na_2O	3.1	3.4	3.3	-.07	MT5.0	-1.53	5.35
K_2O	1.2	2.8	2.7	-.02	MELT1	+22.32	0.00

SUM SQUARES RESID. = .0097 CRYSTALS REMOVED = 28.65%

	P	D	MODEL	BULK DC	% ERROR	MISFIT
Rb	37	120	51	.05	- 57.5	YES
Ba	310	527	422	.09	- 19.9	NO
Zr	93	201	126	.10	- 37.3	YES
Sr	250	260	252	.97	- 3.1	NO
V	192	115	135	2.08	+ 17.4	NO
Cr	92	31	23	5.07	- 25.8	YES
Ni	35	20	15	3.51	- 25.0	YES

MODEL NO. : A5.2.28
PARENT : 14886 (MANGAWHERO FORMATION ACID ANDESITE)
DAUGHTER : 14889 (MANGAWHERO FORMATION DACITE)
DESCRIPTION : AFC (K-rich melt)

	P	D	MODEL	RESID.	PHASE	WGT%	%
SiO_2	61.8	64.0	64.0	+.03			
TiO_2	.8	.8	.8	+.01			
Al_2O_3	16.9	16.8	16.8	-.03			
FeO	5.8	5.1	5.1	+.01	En70	-2.34	18.92
MgO	3.2	2.3	2.2	-.02	CPX2	-3.17	25.92
CaO	5.9	4.9	4.9	+.01	An40	-6.42	52.00
Na_2O	3.5	3.4	3.5	+.06	MT5.0	-.41	3.36
K_2O	2.0	2.8	2.7	-.08	MELT1	+11.16	0.00

SUM SQUARES RESID. = .0124 CRYSTALS REMOVED = 12.34%

	P	D	MODEL	BULK DC	% ERROR	MISFIT
Rb	81	120	92	.05	- 23.3	YES
Ba	418	527	471	.09	- 10.6	NO
Zr	158	201	178	.10	- 11.4	NO
Sr	253	260	254	.98	- 2.3	NO
V	162	115	152	1.50	+ 32.2	YES
Cr	51	31	32	4.49	+ 3.1	NO
Ni	26	20	19	3.40	- 5.0	NO

MODEL NO. : A5.2.29
PARENT : 14855 (RUAPEHU BASALT)
DAUGHTER : 14737 (TE HERENGA FORMATION BASIC ANDESITE)
DESCRIPTION : POAM fractionation.

	P	D	MODEL	RESID.	PHASE	WGT%	%
SiO_2	52.9	56.7	56.7	-.03			
TiO_2	.7	.7	.7	+.01			
Al_2O_3	15.8	18.2	18.2	-.02			
FeO	8.9	8.1	8.0	-.03	Fo90	-7.24	19.03
MgO	8.8	4.7	4.7	-.02	CPX1	-14.39	37.82
CaO	9.8	7.7	7.7	-.02	An60	-13.91	36.56
Na_2O	2.6	3.2	3.2	-.00	MT10.0	-2.51	6.59
K_2O	.6	.8	.9	+.11			

SUM SQUARES RESID. = .0153 CRYSTALS REMOVED = 38.05%

	P	D	MODEL	BULK DC	% ERROR	MISFIT
Rb	11	20	17	.04	- 15.0	NO
Ba	185	260	289	.07	+ 11.2	NO
Zr	50	63	76	.13	+ 20.6	YES
Sr	201	248	232	.70	- 6.5	NO
V	251	210	128	2.41	- 39.0	YES
Cr	380	38	26	6.61	- 31.6	YES
Ni	142	25	17	5.44	- 32.0	YES

MODEL NO. : A5.2.30
PARENT : 14855 (RUAPEHU BASALT)
DAUGHTER : 14737 (TE HERENGA FORMATION BASIC ANDESITE)
DESCRIPTION : AFC (K-rich melt)

	P	D	MODEL	RESID.	PHASE	WGT%	%
SiO_2	52.9	56.7	56.7	-.00			
TiO_2	.7	.7	.7	+.00			
Al_2O_3	15.8	18.2	18.2	-.00			
FeO	8.9	8.1	8.1	-.00	Fo90	-7.67	16.91
MgO	8.8	4.7	4.7	-.00	CPX1	-14.99	33.04
CaO	9.8	7.7	7.7	-.00	An60	-16.99	37.45
Na_2O	2.6	3.2	3.2	+.01	MT10.0	-2.94	6.47
K_2O	.6	.8	.8	-.00	MELT1	-2.78	6.13

SUM SQUARES RESID. = .0001 CRYSTALS REMOVED = 45.37%

NOTE: Trace elements cannot be adequately modelled because melt must be removed to produce the best majors fit.

MODEL NO. : A5.2.31
PARENT : 14855 (RUAPEHU BASALT)
DAUGHTER : 14737 (TE HERENGA FORMATION BASIC ANDESITE)
DESCRIPTION : AFC (K-poor melt)

	P	D	MODEL	RESID.	PHASE	WGT%	%
SiO_2	52.9	56.7	56.7	+.00			
TiO_2	.7	.7	.6	-.04			
Al_2O_3	15.8	18.2	18.2	+.00			
FeO	8.9	8.1	8.1	+.01	Fo90	-9.67	13.85
MgO	8.8	4.7	4.7	+.00	CPX1	-15.71	22.50
CaO	9.8	7.7	7.7	+.00	An60	-28.76	41.18
Na_2O	2.6	3.2	3.2	+.01	MT10.0	-4.59	6.57
K_2O	.6	.8	.8	+.02	MELT2	-11.10	15.90

SUM SQUARES RESID. = .0022 CRYSTALS REMOVED = 69.83%

NOTE: Trace elements cannot be adequately modelled because melt must be removed to produce the best majors fit.

MODEL NO. : A5.2.32
PARENT : 22998 (ONGAROTO BASALT)
DAUGHTER : 14737 (TE HERENGA FORMATION BASIC ANDESITE)
DESCRIPTION : POAM fractionation.

	P	D	MODEL	RESID.	PHASE	WGT%	%
SiO_2	50.9	56.7	56.6	-.06			
TiO_2	1.1	.7	.7	+.03			
Al_2O_3	15.8	18.2	18.2	-.05			
FeO	9.2	8.1	8.0	-.06	Fo90	-9.02	16.07
MgO	9.4	4.7	4.7	-.04	CPX1	-17.77	31.66
CaO	10.5	7.7	7.6	-.03	An60	-24.89	44.34
Na_2O	2.5	3.2	3.2	-.01	MT17.5	-4.45	7.93
K_2O	.6	.8	1.0	+.22			

SUM SQUARES RESID. = .0605 CRYSTALS REMOVED = 56.13%

	P	D	MODEL	BULK DC	% ERROR	MISFIT
Rb	10	20	22	.04	+ 10.0	NO
Ba	nd	260				
Zr	125	63	259	.12	+311.1	YES
Sr	330	248	377	.84	+ 52.0	YES
V	220	210	52	2.74	- 75.2	YES
Cr	550	38	6	6.50	- 84.0	YES
Ni	160	25	8	4.69	- 68.0	YES

MODEL NO. : A5.2.33
PARENT : 14855 (RUAPEHU BASALT)
DAUGHTER : 14785 (WHAKAPAPA FORMATION ACID ANDESITE)
DESCRIPTION : AFC (K-rich melt)

	P	D	MODEL	RESID.	PHASE	WGT%	%
SiO_2	52.9	57.6	57.6	+.04			
TiO_2	.7	.7	.7	+.01	PHASE	WGT%	%
Al_2O_3	15.8	17.1	17.1	+.03			
FeO	8.9	7.1	7.1	+.03	Fo80	-8.11	25.57
MgO	8.8	5.0	5.0	+.01	CPX2	-11.01	34.71
CaO	9.8	7.8	7.8	+.01	An70	-11.31	35.68
Na_2O	2.6	3.4	3.3	-.08	MT15.0	-1.28	4.04
K_2O	.6	1.4	1.3	-.05	MELT1	+6.85	0.00

SUM SQUARES RESID. = .0115 CRYSTALS REMOVED = 31.71%

	P	D	MODEL	BULK DC	% ERROR	MISFIT
Rb	11	51	16	.03	- 68.6	YES
Ba	185	343	264	.07	- 23.0	YES
Zr	50	98	70	.11	- 28.6	YES
Sr	201	299	227	.68	- 24.1	YES
V	251	192	198	1.62	+ 3.1	NO
Cr	380	74	73	5.35	- 1.4	NO
Ni	142	40	22	5.87	- 45.0	YES

MODEL NO. : A5.2.34
PARENT : 11965 (RED CRATER BASALT)
DAUGHTER : 14785 (WHAKAPAPA FORMATION ACID ANDESITE)
DESCRIPTION : AFC (K-rich melt)

	P	D	MODEL	RESID.	PHASE	WGT%	%
SiO_2	53.3	57.6	57.6	+.06			
TiO_2	.7	.7	.7	-.01	PHASE	WGT%	%
Al_2O_3	15.5	17.1	17.1	+.04			
FeO	9.1	7.1	7.2	+.05	Fo80	-4.23	13.89
MgO	7.8	5.0	5.1	+.02	CPX2	-15.07	49.47
CaO	10.5	7.8	7.8	+.01	An80	-9.33	30.62
Na_2O	2.5	3.4	3.2	-.11	MT15.0	-1.83	6.01
K_2O	.7	1.4	1.3	-.08	MELT1	+4.57	0.00

SUM SQUARES RESID. = .0269 CRYSTALS REMOVED = 30.46%

	P	D	MODEL	BULK DC	% ERROR	MISFIT
Rb	20	51	28	.03	- 45.1	YES
Ba	137	343	193	.06	- 43.7	YES
Zr	68	98	93	.15	- 5.1	NO
Sr	278	299	321	.60	+ 7.4	NO
V	271	192	165	2.36	- 14.1	NO
Cr	281	74	27	7.49	- 63.5	YES
Ni	63	40	12	5.67	- 70.0	YES

MODEL NO. : A5.2.35
PARENT : 14855 (RUAPEHU BASALT)
DAUGHTER : 14781 (WHAKAPAPA FORMATION ACID ANDESITE)
DESCRIPTION : AFC (K-rich melt; O = olivine)

	P	D	MODEL	RESID.	PHASE	WGT%	%
SiO_2	52.9	59.3	59.3	+.00			
TiO_2	.7	.7	.7	+.02			
Al_2O_3	15.8	17.0	17.0	-.00			
FeO	8.9	6.5	6.5	-.00	Fo80	-9.03	22.75
MgO	8.8	4.5	4.5	-.00	CPX2	-13.34	33.62
CaO	9.8	7.0	7.0	-.00	An70	-15.47	38.98
Na_2O	2.6	3.4	3.4	-.01	MT12.5	-1.85	4.65
K_2O	.6	1.6	1.6	-.01	MELT1	+8.34	0.00

SUM SQUARES RESID. = .0007 CRYSTALS REMOVED = 39.69%

	P	D	MODEL	BULK DC	% ERROR	MISFIT
Rb	11	59	18	.04	- 69.5	YES
Ba	185	367	296	.07	- 19.3	NO
Zr	50	116	79	.11	- 57.8	YES
Sr	201	280	229	.74	- 18.2	NO
V	251	177	169	1.79	- 4.5	NO
Cr	380	75	40	5.45	- 46.7	YES
Ni	142	32	15	5.49	- 53.1	YES

MODEL NO. : A5.2.36
PARENT : 14855 (RUAPEHU BASALT)
DAUGHTER : 14781 (WHAKAPAPA FORMATION ACID ANDESITE)
DESCRIPTION : AFC (K-rich melt; O = orthopyroxene)

	P	D	MODEL	RESID.	PHASE	WGT%	%
SiO_2	52.9	59.3	59.2	-.15			
TiO_2	.7	.7	.7	+.01			
Al_2O_3	15.8	17.0	16.9	-.10			
FeO	8.9	6.5	6.4	-.12	En80	-15.35	27.35
MgO	8.8	4.5	4.4	-.02	CPX2	-13.15	23.43
CaO	9.8	7.0	6.9	-.06	An70	-24.78	44.14
Na_2O	2.6	3.4	3.7	+.24	MT12.5	-2.86	5.09
K_2O	.6	1.6	1.8	+.19	MELT1	+6.84	0.00

SUM SQUARES RESID. = .1442 CRYSTALS REMOVED = 56.14%

	P	D	MODEL	BULK DC	% ERROR	MISFIT
Rb	11	59	24	.04	- 59.3	YES
Ba	185	367	394	.08	+ 7.4	NO
Zr	50	116	104	.11	- 10.3	NO
Sr	201	280	230	.84	- 17.9	NO
V	251	177	102	2.09	- 42.4	YES
Cr	380	75	12	5.20	- 84.0	YES
Ni	142	32	11	4.11	- 65.6	YES

MODEL NO. : A5.2.37
PARENT : 11965 (RED CRATER BASALT)
DAUGHTER : 14781 (WHAKAPAPA FORMATION ACID ANDESITE)
DESCRIPTION : AFC (K-rich melt)

	P	D	MODEL	RESID.	PHASE	WGT%	%
SiO_2	53.3	59.3	59.3	+.01			
TiO_2	.7	.7	.7	+.02			
Al_2O_3	15.5	17.0	17.0	+.01			
FeO	9.1	6.5	6.6	+.01	Fo80	-4.99	13.65
MgO	7.8	4.5	4.5	+.01	CPX2	-17.03	46.54
CaO	10.5	7.0	7.0	+.00	An80	-12.27	33.54
Na_2O	2.5	3.4	3.4	-.03	MT12.5	-2.29	6.27
K_2O	.7	1.6	1.6	-.02	MELT1	+7.08	0.00

SUM SQUARES RESID. = .0022 CRYSTALS REMOVED = 36.58%

	P	D	MODEL	BULK DC	% ERROR	MISFIT
Rb	20	59	31	.03	- 47.5	YES
Ba	137	367	210	.06	- 42.8	YES
Zr	68	116	100	.15	- 13.8	NO
Sr	278	280	326	.65	+ 16.4	NO
V	271	177	143	2.41	- 19.2	NO
Cr	281	75	16	7.30	- 78.7	YES
Ni	63	32	8	5.48	- 75.0	YES

MODEL NO. : A5.2.38
PARENT : 14855 (RUAPEHU BASALT)
DAUGHTER : 14804 (WHAKAPAPA FORMATION ACID ANDESITE)
DESCRIPTION : AFC (K-rich melt)

	P	D	MODEL	RESID.	PHASE	WGT%	%
SiO_2	52.9	60.6	60.6	+.01			
TiO_2	.7	.7	.7	+.00			
Al_2O_3	15.8	16.8	16.9	+.02			
FeO	8.9	6.3	6.3	+.01	Fo80	-10.38	20.06
MgO	8.8	3.8	3.9	+.01	CPX2	-15.62	30.19
CaO	9.8	6.6	6.6	+.01	An60	-23.35	45.12
Na_2O	2.6	3.3	3.2	-.06	MT12.5	-2.40	4.63
K_2O	.6	1.8	1.8	-.00	MELT1	+7.19	0.00

SUM SQUARES RESID. = .0044 CRYSTALS REMOVED = 51.65%

	P	D	MODEL	BULK DC	% ERROR	MISFIT
Rb	11	73	22	.04	- 69.9	YES
Ba	185	413	361	.08	- 12.6	NO
Zr	50	139	96	.10	- 30.9	YES
Sr	201	293	224	.85	- 23.5	YES
V	251	164	146	1.74	- 11.0	NO
Cr	380	53	20	5.08	- 62.3	YES
Ni	142	24	8	4.93	- 66.7	YES

MODEL NO. : A5.2.39
PARENT : 11965 (RED CRATER BASALT)
DAUGHTER : 14804 (WHAKAPAPA FORMATION ACID ANDESITE)
DESCRIPTION : AFC (K-rich melt)

	P	D	MODEL	RESID.	PHASE	WGT%	%
SiO_2	53.3	60.6	60.6	+.00			
TiO_2	.7	.7	.7	-.01			
Al_2O_3	15.5	16.8	16.8	+.00			
FeO	9.1	6.3	6.3	+.00	Fo80	-6.13	13.87
MgO	7.8	3.8	3.8	+.00	CPX2	-18.37	41.54
CaO	10.5	6.6	6.6	+.00	An70	-17.09	38.64
Na_2O	2.5	3.3	3.3	+.00	MT12.5	-2.63	5.95
K_2O	.7	1.8	1.8	-.00	MELT1	+8.45	0.00

SUM SQUARES RESID. = .0002 CRYSTALS REMOVED = 44.22%

	P	D	MODEL	BULK DC	% ERROR	MISFIT
Rb	20	73	35	.04	- 52.1	YES
Ba	137	413	235	.07	- 43.1	NO
Zr	68	139	113	.13	- 18.7	NO
Sr	278	293	323	.74	+ 10.2	NO
V	271	164	130	2.26	- 20.7	YES
Cr	281	53	10	6.68	- 81.1	YES
Ni	63	24	6	5.19	- 75.0	YES

MODEL NO. : A5.2.40
PARENT : 14785 (WHAKAPAPA FORMATION ACID ANDESITE)
DAUGHTER : 14804 (WHAKAPAPA FORMATION ACID ANDESITE)
DESCRIPTION : AFC (K-rich melt)

	P	D	MODEL	RESID.	PHASE	WGT%	%
SiO_2	57.6	60.6	60.6	+.00			
TiO_2	.7	.7	.7	-.02			
Al_2O_3	17.1	16.8	16.9	+.02			
FeO	7.1	6.3	6.3	+.01	En80	-6.50	11.61
MgO	5.0	3.8	3.9	+.01	CPX2	-8.69	15.52
CaO	7.8	6.6	6.6	+.00	An50	-28.82	51.48
Na_2O	3.4	3.3	3.3	-.03	MT12.5	-2.58	4.60
K_2O	1.4	1.8	1.9	+.01	MELT1	-9.39	16.78

SUM SQUARES RESID. = .0022 CRYSTALS REMOVED = 55.98%

NOTE: Trace elements cannot be adequately modelled because melt must be removed to produce the best majors fit.

MODEL NO. : A5.3.1
PARENT : 14855 (RUAPEHU BASALT)
DAUGHTER : 14925 (WAHIANOA FORMATION ACID ANDESITE)
DESCRIPTION : AFC (K-rich melt)

	P	D	MODEL	RESID.	PHASE	WGT%	%
SiO_2	52.9	57.2	57.2	-.01			
TiO_2	.7	.7	.7	-.04	PHASE	WGT%	%
Al_2O_3	15.8	17.1	17.0	-.02			
FeO	8.9	7.7	7.7	-.00	Fo90	-7.41	19.65
MgO	8.8	5.3	5.3	-.01	CPX1	-11.29	29.93
CaO	9.8	8.2	8.2	-.00	An60	-16.18	42.90
Na_2O	2.6	2.9	3.0	+.09	MT10.0	-2.84	7.53
K_2O	.6	1.0	1.0	-.01	MELT1	+1.10	0.00

SUM SQUARES RESID. = .0108 CRYSTALS REMOVED = 37.72%

	P	D	MODEL	BULK DC	% ERROR	MISFIT
Rb	11	31	17	.04	- 45.2	YES
Ba	185	268	286	.08	+ 5.2	NO
Zr	50	75	76	.11	+ 1.3	NO
Sr	201	226	220	.81	- 2.7	NO
V	251	225	117	2.61	- 48.0	YES
Cr	380	141	32	6.21	- 77.3	YES
Ni	142	64	20	5.15	- 68.8	YES

MODEL NO. : A5.3.2
PARENT : 14855 (RUAPEHU BASALT)
DAUGHTER : 14911 (WAHIANOA FORMATION ACID ANDESITE)
DESCRIPTION : AFC (K-rich melt)

	P	D	MODEL	RESID.	PHASE	WGT%	%
SiO_2	52.9	58.3	58.3	+.01			
TiO_2	.7	.7	.7	+.00	PHASE	WGT%	%
Al_2O_3	15.8	20.5	20.5	+.01			
FeO	8.9	5.5	5.5	+.00	Fo85	-10.72	30.22
MgO	8.8	2.1	2.1	+.00	CPX2	-16.53	46.61
CaO	9.8	8.0	8.0	+.00	An60	-6.01	16.96
Na_2O	2.6	3.6	3.6	-.03	MT10.0	-2.20	6.21
K_2O	.6	1.3	1.3	-.00	MELT1	+4.73	0.00

SUM SQUARES RESID. = .0009 CRYSTALS REMOVED = 35.47%

	P	D	MODEL	BULK DC	% ERROR	MISFIT
Rb	11	39	17	.02	- 56.4	YES
Ba	185	317	282	.04	- 11.0	NO
Zr	50	95	73	.15	- 23.2	YES
Sr	201	344	267	.35	- 22.4	YES
V	251	167	136	2.40	- 18.6	NO
Cr	380	36	23	7.45	- 36.1	YES
Ni	142	27	9	7.41	- 66.7	YES

MODEL NO. : A5.3.3
PARENT : 14855 (RUAPEHU BASALT)
DAUGHTER : 14901 (WAHIANOA FORMATION ACID ANDESITE)
DESCRIPTION : AFC (K-rich melt)

	P	D	MODEL	RESID.	PHASE	WGT%	%
SiO_2	52.9	58.9	58.9	+.02			
TiO_2	.7	.7	.7	+.00	PHASE	WGT%	%
Al_2O_3	15.8	20.0	20.0	+.02			
FeO	8.9	5.6	5.6	+.02	Fo85	-10.89	26.83
MgO	8.8	2.1	2.1	+.01	CPX2	-16.79	41.38
CaO	9.8	7.6	7.6	+.00	An70	-10.44	25.73
Na_2O	2.6	3.9	3.8	-.05	MT10.0	-2.46	6.06
K_2O	.6	1.2	1.2	-.02	MELT1	+2.65	0.00

SUM SQUARES RESID. = .0036 CRYSTALS REMOVED = 40.58%

	P	D	MODEL	BULK DC	% ERROR	MISFIT
Rb	11	35	18	.03	- 48.6	YES
Ba	185	294	303	.05	+ 3.1	NO
Zr	50	91	79	.13	- 13.2	NO
Sr	201	317	260	.51	- 18.0	NO
V	251	195	128	2.30	- 34.4	YES
Cr	380	15	18	6.83	+ 20.0	NO
Ni	142	20	8	6.63	- 60.0	YES

MODEL NO. : A5.3.4
PARENT : 11965 (RED CRATER BASALT)
DAUGHTER : 14911 (WAHIANOA FORMATION ACID ANDESITE)
DESCRIPTION : AFC (K-rich melt)

	P	D	MODEL	RESID.	PHASE	WGT%	%
SiO_2	53.3	58.3	58.3	+.02			
TiO_2	.7	.7	.7	+.04	PHASE	WGT%	%
Al_2O_3	15.5	20.5	20.5	+.02			
FeO	9.1	5.5	5.5	+.01	Fo85	-7.15	19.85
MgO	7.8	2.1	2.1	+.01	CPX2	-20.69	57.43
CaO	10.5	8.0	8.0	+.00	An70	-5.60	15.53
Na_2O	2.5	3.6	3.6	-.08	MT10.0	-2.59	7.20
K_2O	.7	1.3	1.2	-.03	MELT1	+2.02	0.00

SUM SQUARES RESID. = .0098 CRYSTALS REMOVED = 36.04%

	P	D	MODEL	BULK DC	% ERROR	MISFIT
Rb	20	39	31	.03	- 20.5	YES
Ba	137	317	210	.04	- 33.8	YES
Zr	68	95	98	.18	+ 3.2	NO
Sr	278	344	374	.33	+ 8.7	NO
V	271	167	121	2.81	- 27.5	YES
Cr	281	36	9	8.82	- 75.0	YES
Ni	63	27	4	7.16	- 85.2	YES

MODEL NO. : A5.3.5
PARENT : 22994 (BEN LOMOND BASALT)
DAUGHTER : 14911 (WAHIANOA FORMATION ACID ANDESITE)
DESCRIPTION : AFC (K-rich melt)

	P	D	MODEL	RESID.	PHASE	WGT%	%
SiO_2	51.4	58.3	58.2	-.02			
TiO_2	1.1	.7	.7	-.00	PHASE	WGT%	%
Al_2O_3	17.6	20.5	20.5	-.01			
FeO	9.8	5.5	5.5	-.01	Fo90	-4.18	10.64
MgO	6.0	2.1	2.1	-.01	CPX1	-15.56	39.61
CaO	10.8	8.0	8.0	-.00	An70	-13.92	35.44
Na_2O	2.8	3.6	3.7	+.04	MT12.5	-5.62	14.31
K_2O	.5	1.3	1.3	+.02	MELT1	+5.37	0.00

SUM SQUARES RESID. = .0027 CRYSTALS REMOVED = 39.28%

	P	D	MODEL	BULK DC	% ERROR	MISFIT
Rb	14	39	23	.04	- 41.0	YES
Ba	129	317	206	.07	- 35.0	YES
Zr	84	95	128	.16	+ 32.6	YES
Sr	348	344	408	.68	+ 18.4	NO
V	252	167	39	4.74	- 76.6	YES
Cr	44	36	1	9.79	- 97.2	YES
Ni	29	27	3	5.94	- 88.9	YES

MODEL NO. : A5.3.6
PARENT : 14922 (WAHIANOA FORMATION BASIC ANDESITE)
DAUGHTER : 14911 (WAHIANOA FORMATION ACID ANDESITE)
DESCRIPTION : POAM fractionation.

	P	D	MODEL	RESID.	PHASE	WGT%	%
SiO_2	55.8	58.3	58.4	+.10			
TiO_2	.8	.7	.7	-.01	PHASE	WGT%	%
Al_2O_3	17.9	20.5	20.6	+.05			
FeO	8.0	5.5	5.6	+.08	En80	-8.11	36.14
MgO	5.2	2.1	2.1	+.00	CPX2	-7.06	31.45
CaO	8.7	8.0	8.1	+.03	An90	-5.19	23.15
Na_2O	2.7	3.6	3.4	-.20	MT12.5	-2.08	9.27
K_2O	.9	1.3	1.2	-.07			

SUM SQUARES RESID. = .0677 CRYSTALS REMOVED = 22.44%

	P	D	MODEL	BULK DC	% ERROR	MISFIT
Rb	25	39	32	.03	- 17.9	NO
Ba	243	317	309	.05	- 2.5	NO
Zr	69	95	86	.15	- 9.5	NO
Sr	220	344	252	.46	- 26.7	YES
V	242	167	128	3.53	- 23.4	YES
Cr	72	36	12	7.94	- 66.7	YES
Ni	30	27	9	5.71	- 66.7	YES

MODEL NO. : A5.3.7
PARENT : 14922 (WAHIANOA FORMATION BASIC ANDESITE)
DAUGHTER : 14911 (WAHIANOA FORMATION ACID ANDESITE)
DESCRIPTION : POA fractionation (O = olivine)

	P	D	MODEL	RESID.
SiO_2	55.8	58.3	57.2	-1.05
TiO_2	.8	.7	.8	+.08
Al_2O_3	17.9	20.5	21.1	+.61
FeO	8.0	5.5	6.4	+.87
MgO	5.2	2.1	1.8	-.30
CaO	8.7	8.0	8.3	+.22
Na_2O	2.7	3.6	3.6	-.03
K_2O	.9	1.3	.9	-.40

PHASE	WGT%	%
Fo85	-4.91	41.77
CPX2	-6.85	58.23
An40	+15.40	0.00

SUM SQUARES RESID. =2.5426 CRYSTALS REMOVED = 11.76%

	P	D	MODEL	BULK DC	% ERROR	MISFIT
Rb	25	39	24	.02	- 38.5	YES
Ba	243	317	234	.02	- 26.2	YES
Zr	69	95	63	.15	- 33.7	YES
Sr	220	344	280	.05	- 18.6	NO
V	242	167	207	.67	+ 28.5	YES
Cr	72	36	31	6.24	- 13.9	NO
Ni	30	27	10	8.51	- 50.0	YES

MODEL NO. : A5.3.8
PARENT : 14922 (WAHIANOA FORMATION BASIC ANDESITE)
DAUGHTER : 14911 (WAHIANOA FORMATION ACID ANDESITE)
DESCRIPTION : POA fractionation (O = orthopyroxene)

	P	D	MODEL	RESID.
SiO_2	55.8	58.3	56.6	-1.64
TiO_2	.8	.7	.8	+.12
Al_2O_3	17.9	20.5	21.4	+.91
FeO	8.0	5.5	6.5	+.97
MgO	5.2	2.1	2.3	+.20
CaO	8.7	8.0	7.8	-.21
Na_2O	2.7	3.6	3.6	-.03
K_2O	.9	1.3	.9	-.32

PHASE	WGT%	%
En80	-4.64	31.95
CPX2	-9.88	68.05
An40	+12.20	0.00

SUM SQUARES RESID. =4.6627 CRYSTALS REMOVED = 14.52%

	P	D	MODEL	BULK DC	% ERROR	MISFIT
Rb	25	39	25	.02	- 35.9	YES
Ba	243	317	251	.02	- 20.8	YES
Zr	69	95	68	.20	- 28.4	YES
Sr	220	344	281	.06	- 18.3	NO
V	242	167	206	1.10	+ 23.4	YES
Cr	72	36	22	7.76	- 38.9	YES
Ni	30	27	11	6.64	- 59.3	YES

MODEL NO. : A5.3.9
PARENT : 16721 (WAHIANOA FORMATION ACID ANDESITE)
DAUGHTER : 14901 (WAHIANOA FORMATION ACID ANDESITE)
DESCRIPTION : Plagioclase addition.

	P	D	MODEL	RESID.	PHASE	WGT%	%
SiO_2	60.1	58.9	59.0	+.06			
TiO_2	.7	.7	.5	-.19			
Al_2O_3	18.0	20.0	20.0	+.02			
FeO	6.6	5.6	5.5	-.10			
MgO	3.0	2.1	2.6	+.46			
CaO	6.7	7.6	7.7	+.04	An60	+19.68	0.00
Na_2O	3.7	3.9	3.8	-.05			
K_2O	1.2	1.2	1.0	-.24			

SUM SQUARES RESID. = .3265 CRYSTALS ADDED = 19.68%

	P	D	MODEL	BULK DC	% ERROR	MISFIT
Rb	41	35	32	.07	- 8.6	NO
Ba	328	294	262	.16	- 10.9	NO
Zr	96	91	73	.01	- 19.8	NO
Sr	237	317	277	1.83	- 12.6	NO
V	153	195	116	.01	- 40.5	YES
Cr	23	15	17	.01	+ 13.3	NO
Ni	17	20	13	.01	- 35.0	YES

MODEL NO. : A5.3.10
PARENT : 16867 (WAHIANOA FORMATION ACID ANDESITE)
DAUGHTER : 14901 (WAHIANOA FORMATION ACID ANDESITE)
DESCRIPTION : Plagioclase + magnetite addition.

	P	D	MODEL	RESID.	PHASE	WGT%	%
SiO_2	61.4	58.9	59.1	+.15			
TiO_2	.7	.7	.7	-.02			
Al_2O_3	17.9	20.0	20.3	+.33			
FeO	6.2	5.6	5.7	+.15			
MgO	2.6	2.1	2.0	-.16			
CaO	6.0	7.6	7.2	-.40	An60	+27.13	0.00
Na_2O	3.6	3.9	3.8	-.09	MT12.5	+1.23	0.00
K_2O	1.6	1.2	1.3	+.02			

SUM SQUARES RESID. = .3514 CRYSTALS ADDED = 28.36%

	P	D	MODEL	BULK DC	% ERROR	MISFIT
Rb	56	35	36	.07	+ 2.9	NO
Ba	389	294	262	.15	- 10.9	NO
Zr	119	91	63	.03	- 30.8	YES
Sr	248	317	303	1.75	- 5.0	NO
V	173	195	190	1.31	- 2.6	NO
Cr	10	15	12	1.74	- 20.0	NO
Ni	17	20	13	.44	- 35.0	YES

MODEL NO. : A5.4.1
PARENT : 14883 (MANGAWHERO FORMATION ACID ANDESITE)
DAUGHTER : 14882 (MANGAWHERO FORMATION ACID ANDESITE)
DESCRIPTION : POAM fractionation (O = olivine)

	P	D	MODEL	RESID.	PHASE	WGT%	%
SiO_2	58.0	60.2	60.2	+.02			
TiO_2	.7	.8	.8	+.00			
Al_2O_3	15.6	15.6	15.6	+.02			
FeO	6.9	6.3	6.3	+.02	Fo85	-3.26	18.44
MgO	7.0	5.8	5.9	+.01	CPX2	-4.81	27.15
CaO	7.6	6.7	6.7	+.01	An60	-8.83	49.85
Na_2O	2.7	2.9	2.9	-.04	MT7.5	-.81	4.57
K_2O	1.4	1.8	1.7	-.04			

SUM SQUARES RESID. = .0044 CRYSTALS REMOVED = 17.71%

	P	D	MODEL	BULK DC	% ERROR	MISFIT
Rb	54	73	65	.04	- 12.3	NO
Ba	331	388	395	.09	+ 1.8	NO
Zr	114	142	136	.09	- 4.2	NO
Sr	250	222	253	.94	+ 14.0	NO
V	189	176	165	1.69	- 6.3	NO
Cr	286	240	138	4.73	- 42.1	YES
Ni	110	81	55	4.53	- 32.1	YES

MODEL NO. : A5.4.2
PARENT : 14883 (MANGAWHERO FORMATION ACID ANDESITE)
DAUGHTER : 14882 (MANGAWHERO FORMATION ACID ANDESITE)
DESCRIPTION : POAM fractionation (O = orthopyroxene)

	P	D	MODEL	RESID.	PHASE	WGT%	%
SiO_2	58.0	60.2	60.2	-.03			
TiO_2	.7	.8	.8	-.00			
Al_2O_3	15.6	15.6	15.6	-.01			
FeO	6.9	6.3	6.2	-.02	En80	-6.28	25.41
MgO	7.0	5.8	5.8	-.00	CPX2	-4.91	19.87
CaO	7.6	6.7	6.7	-.01	An60	-12.55	50.84
Na_2O	2.7	2.9	2.9	-.01	MT12.5	-.96	3.88
K_2O	1.4	1.8	1.8	+.08			

SUM SQUARES RESID. = .0084 CRYSTALS REMOVED = 24.70%

	P	D	MODEL	BULK DC	% ERROR	MISFIT
Rb	54	73	71	.05	- 2.7	NO
Ba	331	388	428	.09	+ 10.3	NO
Zr	114	142	147	.10	+ 3.5	NO
Sr	250	222	253	.95	+ 14.0	NO
V	189	176	156	1.67	- 11.4	NO
Cr	286	240	112	4.31	- 53.3	YES
Ni	110	81	52	3.62	- 35.8	YES

MODEL NO. : A5.4.3
PARENT : 14883 (MANGAWHERO FORMATION ACID ANDESITE)
DAUGHTER : 14829 (MANGAWHERO FORMATION DACITE)
DESCRIPTION : POAM fractionation (0 = olivine)

	P	D	MODEL	RESID.	PHASE	WGT%	%
SiO_2	58.0	64.4	64.5	+.16			
TiO_2	.7	.9	.9	-.00	PHASE	WGT%	%
Al_2O_3	15.6	15.6	15.6	+.07			
FeO	6.9	5.1	5.2	+.13	Fo80	-8.32	20.83
MgO	7.0	3.2	3.2	+.05	CPX2	-10.50	26.30
CaO	7.6	4.8	4.8	+.03	An60	-19.89	49.82
Na_2O	2.7	3.1	3.1	-.00	MT15.0	-1.22	3.05
K_2O	1.4	3.1	2.6	-.43			

SUM SQUARES RESID. = .2365 CRYSTALS REMOVED = 39.93%

	P	D	MODEL	BULK DC	% ERROR	MISFIT
Rb	54	132	88	.04	- 33.3	YES
Ba	331	535	527	.09	- 1.5	NO
Zr	114	226	182	.09	- 19.5	NO
Sr	250	215	258	.94	+ 20.0	NO
V	189	151	169	1.23	+ 11.9	NO
Cr	286	113	60	4.06	- 46.9	YES
Ni	110	48	17	4.64	- 64.6	YES

MODEL NO. : A5.4.4
PARENT : 14883 (MANGAWHERO FORMATION ACID ANDESITE)
DAUGHTER : 14829 (MANGAWHERO FORMATION DACITE)
DESCRIPTION : POAM fractionation (0 = orthopyroxene)

	P	D	MODEL	RESID.	PHASE	WGT%	%
SiO_2	58.0	64.4	64.4	+.03			
TiO_2	.7	.9	.9	-.00	PHASE	WGT%	%
Al_2O_3	15.6	15.6	15.6	-.00			
FeO	6.9	5.1	5.1	+.02	En80	-13.31	26.46
MgO	7.0	3.2	3.2	-.00	CPX2	-9.60	19.09
CaO	7.6	4.8	4.8	+.01	An60	-25.59	50.88
Na_2O	2.7	3.1	3.1	+.06	MT15.0	-1.80	3.57
K_2O	1.4	3.1	2.9	-.12			

SUM SQUARES RESID. = .0184 CRYSTALS REMOVED = 50.30%

	P	D	MODEL	BULK DC	% ERROR	MISFIT
Rb	54	132	105	.05	- 20.5	YES
Ba	331	535	625	.09	+ 16.8	NO
Zr	114	226	215	.09	- 4.9	NO
Sr	250	215	258	.95	+ 20.0	NO
V	189	151	126	1.58	- 16.6	NO
Cr	286	113	32	4.14	- 71.7	YES
Ni	110	48	18	3.62	- 62.5	YES

MODEL NO. : A5.4.5
PARENT : 14883 (MANGAWHERO FORMATION ACID ANDESITE)
DAUGHTER : 14829 (MANGAWHERO FORMATION DACITE)
DESCRIPTION : AFC (K-rich melt)

	P	D	MODEL	RESID.	PHASE	WGT%	%
SiO_2	58.0	64.4	64.4	-.01			
TiO_2	.7	.9	.8	-.01			
Al_2O_3	15.6	15.6	15.6	-.01			
FeO	6.9	5.1	5.1	-.01	En80	-12.26	27.72
MgO	7.0	3.2	3.2	-.00	CPX2	-8.61	19.49
CaO	7.6	4.8	4.8	-.00	An60	-21.83	49.38
Na_2O	2.7	3.1	3.1	+.03	MT12.5	-1.51	3.41
K_2O	1.4	3.1	3.1	+.00	MELT1	+10.30	0.00

SUM SQUARES RESID. = .0015 CRYSTALS REMOVED = 44.23%

	P	D	MODEL	BULK DC	% ERROR	MISFIT
Rb	54	132	94	.04	- 28.8	YES
Ba	331	535	563	.09	+ 5.2	NO
Zr	114	226	193	.10	- 14.6	NO
Sr	250	215	261	.93	+ 21.4	YES
V	189	151	137	1.55	- 9.3	NO
Cr	286	113	46	4.15	- 59.3	YES
Ni	110	48	22	3.73	- 54.2	YES

MODEL NO. : A5.4.6
PARENT : 14884 (MANGAWHERO FORMATION ACID ANDESITE)
DAUGHTER : 14829 (MANGAWHERO FORMATION DACITE)
DESCRIPTION : POAM fractionation

	P	D	MODEL	RESID.	PHASE	WGT%	%
SiO_2	59.2	64.4	64.4	+.01			
TiO_2	.7	.9	.8	-.01			
Al_2O_3	15.2	15.6	15.6	+.01			
FeO	6.5	5.1	5.1	+.01	En80	-11.81	25.33
MgO	6.7	3.2	3.2	+.00	CPX2	-9.80	21.03
CaO	7.1	4.8	4.8	+.01	An50	-23.60	50.63
Na_2O	3.0	3.1	3.1	-.01	MT17.5	-1.40	3.01
K_2O	1.6	3.1	3.0	-.03			

SUM SQUARES RESID. = .0015 CRYSTALS REMOVED = 46.61%

	P	D	MODEL	BULK DC	% ERROR	MISFIT
Rb	66	132	120	.05	- 9.1	NO
Ba	342	535	605	.09	+ 13.1	NO
Zr	129	226	228	.10	+ .8	NO
Sr	232	215	239	.95	+ 11.2	NO
V	171	151	132	1.42	- 12.6	NO
Cr	325	113	47	4.07	- 58.4	YES
Ni	101	48	20	3.59	- 58.3	YES

MODEL NO. : A5.4.7
PARENT : 14882 (MANGAWHERO FORMATION ACID ANDESITE)
DAUGHTER : 14829 (MANGAWHERO FORMATION DACITE)
DESCRIPTION : POAM fractionation

	P	D	MODEL	RESID.	PHASE	WGT%	%
SiO_2	60.2	64.4	64.4	+.01			
TiO_2	.8	.9	1.1	+.20			
Al_2O_3	15.6	15.6	15.6	+.04			
FeO	6.3	5.1	5.1	-.03	En70	-11.04	27.29
MgO	5.8	3.2	3.2	+.02	CPX2	-7.31	18.08
CaO	6.7	4.8	4.8	-.00	An50	-21.73	53.72
Na_2O	2.9	3.1	2.9	-.17	MT15.0	-.37	.91
K_2O	1.8	3.1	3.0	-.07			

SUM SQUARES RESID. = .0768 CRYSTALS REMOVED = 40.45%

	P	D	MODEL	BULK DC	% ERROR	MISFIT
Rb	73	132	143	.05	+ 8.3	NO
Ba	388	535	733	.10	+ 37.0	YES
Zr	142	226	271	.08	+ 19.9	NO
Sr	222	215	221	1.01	+ 2.8	NO
V	176	151	206	.78	+ 36.4	YES
Cr	240	113	59	3.00	- 47.8	YES
Ni	81	48	15	3.36	- 68.8	YES

MODEL NO. : A5.4.8
PARENT : 14882 (MANGAWHERO FORMATION ACID ANDESITE)
DAUGHTER : 14829 (MANGAWHERO FORMATION DACITE)
DESCRIPTION : AFC (K-rich melt)

	P	D	MODEL	RESID.	PHASE	WGT%	%
SiO_2	60.2	64.4	64.4	+.01			
TiO_2	.8	.9	.8	-.07			
Al_2O_3	15.6	15.6	15.6	+.00			
FeO	6.3	5.1	5.1	+.02	En80	-7.11	33.71
MgO	5.8	3.2	3.2	-.00	CPX2	-4.14	19.63
CaO	6.7	4.8	4.8	-.01	An60	-9.30	44.12
Na_2O	2.9	3.1	3.1	+.04	MT15.0	-.54	2.54
K_2O	1.8	3.1	3.0	-.02	MELT1	+21.82	0.00

SUM SQUARES RESID. = .0070 CRYSTALS REMOVED = 21.09%

	P	D	MODEL	BULK DC	% ERROR	MISFIT
Rb	73	132	92	.04	- 30.3	YES
Ba	388	535	482	.08	- 9.9	NO
Zr	142	226	176	.10	- 22.1	YES
Sr	222	215	231	.83	+ 7.4	NO
V	176	151	162	1.35	+ 7.3	NO
Cr	240	113	118	3.99	+ 4.4	NO
Ni	81	48	39	4.13	- 18.8	NO

MODEL NO. : A5.4.9
PARENT : 17439 (WAIMARINO BASALT)
DAUGHTER : 14883 (MANGAWHERO FORMATION ACID ANDESITE)
DESCRIPTION : AFC (K-rich melt)

	P	D	MODEL	RESID.	PHASE	WGT%	%
SiO_2	53.0	58.0	58.2	+.14			
TiO_2	.5	.7	.7	-.02			
Al_2O_3	12.9	15.6	15.7	+.11			
FeO	8.5	6.9	7.0	+.10	Fo90	-11.19	36.81
MgO	13.3	7.0	7.1	+.07	CPX1	-13.78	45.35
CaO	9.7	7.6	7.6	+.04	An80	-4.13	13.60
Na_2O	1.7	2.7	2.4	-.32	MT0.0	-1.29	4.25
K_2O	.4	1.4	1.3	-.13	MELT1	+8.90	0.00

SUM SQUARES RESID. = .1666 CRYSTALS REMOVED = 30.39%

	P	D	MODEL	BULK DC	% ERROR	MISFIT
Rb	15	54	21	.02	- 61.1	YES
Ba	122	331	173	.03	- 47.7	YES
Zr	48	114	66	.14	- 42.1	YES
Sr	342	250	443	.29	+ 77.2	YES
V	226	189	169	1.80	- 8.8	NO
Cr	1037	286	136	6.60	- 52.4	YES
Ni	341	110	51	6.25	- 53.6	YES

MODEL NO. : A5.4.10
PARENT : 11965 (RED CRATER BASALT)
DAUGHTER : 14883 (MANGAWHERO FORMATION ACID ANDESITE)
DESCRIPTION : AFC (K-rich melt)

	P	D	MODEL	RESID.	PHASE	WGT%	%
SiO_2	53.3	58.0	58.0	+.01			
TiO_2	.7	.7	.7	-.01			
Al_2O_3	15.5	15.6	15.7	+.02			
FeO	9.1	6.9	6.9	+.01	Fo85	-1.91	4.91
MgO	7.8	7.0	7.1	+.01	CPX2	-15.44	39.62
CaO	10.5	7.6	7.6	+.01	An60	-18.44	47.32
Na_2O	2.5	2.7	2.7	-.06	MT10.0	-3.17	8.15
K_2O	.7	1.4	1.4	+.00	MELT1	+4.11	0.00

SUM SQUARES RESID. = .0043 CRYSTALS REMOVED = 38.96%

	P	D	MODEL	BULK DC	% ERROR	MISFIT
Rb	20	54	32	.04	- 40.7	YES
Ba	137	331	215	.08	- 35.0	YES
Zr	68	114	104	.14	- 8.8	NO
Sr	278	250	292	.90	+ 16.8	NO
V	271	189	107	2.89	- 43.4	YES
Cr	281	286	13	7.28	- 96.5	YES
Ni	63	110	15	3.94	- 86.4	YES

MODEL NO. : A5.4.11
PARENT : 22998 (ONGAROTO BASALT)
DAUGHTER : 14883 (MANGAWHERO FORMATION ACID ANDESITE)
DESCRIPTION : POAM fractionation

	P	D	MODEL	RESID.	PHASE	WGT%	%
SiO_2	50.9	58.0	58.0	-.01			
TiO_2	1.1	.7	.7	+.00	PHASE	WGT%	%
Al_2O_3	15.8	15.6	15.6	-.01			
FeO	9.2	6.9	6.9	-.01	Fo90	-8.11	13.41
MgO	9.4	7.0	7.0	-.01	CPX1	-15.94	26.37
CaO	10.5	7.6	7.6	-.00	An60	-30.94	51.17
Na_2O	2.5	2.7	2.8	+.04	MT15.0	-5.47	9.05
K_2O	.6	1.4	1.4	-.00			

SUM SQUARES RESID. = .0017 CRYSTALS REMOVED = 60.46%

	P	D	MODEL	BULK DC	% ERROR	MISFIT
Rb	10	54	24	.04	- 55.6	YES
Ba	nd	331				
Zr	125	114	286	.11	+152.6	YES
Sr	330	250	343	.96	+ 37.2	YES
V	220	189	34	3.02	- 82.0	YES
Cr	550	286	4	6.40	- 98.6	YES
Ni	160	110	9	4.16	- 91.8	YES

MODEL NO. : A5.4.12
PARENT : 14855 (RUAPEHU BASALT)
DAUGHTER : 14883 (MANGAWHERO FORMATION ACID ANDESITE)
DESCRIPTION : AFC (K-rich melt)

	P	D	MODEL	RESID.	PHASE	WGT%	%
SiO_2	52.9	58.0	58.0	-.02			
TiO_2	.7	.7	.7	+.02	PHASE	WGT%	%
Al_2O_3	15.8	15.6	15.6	-.03			
FeO	8.9	6.9	6.9	-.02	Fo85	-5.27	14.03
MgO	8.8	7.0	7.0	-.01	CPX2	-10.74	28.57
CaO	9.8	7.6	7.6	-.01	An60	-18.84	50.13
Na_2O	2.6	2.7	2.8	+.06	MT7.5	-2.73	7.27
K_2O	.6	1.4	1.4	-.00	MELT1	+6.39	0.00

SUM SQUARES RESID. = .0060 CRYSTALS REMOVED = 37.58%

	P	D	MODEL	BULK DC	% ERROR	MISFIT
Rb	11	54	17	.04	- 68.5	YES
Ba	185	331	284	.09	- 14.2	NO
Zr	50	114	76	.11	- 33.3	YES
Sr	201	250	207	.94	- 17.2	NO
V	251	189	123	2.51	- 34.9	YES
Cr	380	286	38	5.91	- 85.3	YES
Ni	142	110	30	4.30	- 72.7	YES

MODEL NO. : A5.4.13
PARENT : 14855 (RUAPEHU BASALT)
DAUGHTER : 14884 (MANGAWHERO FORMATION ACID ANDESITE)
DESCRIPTION : AFC (K-rich melt)

	P	D	MODEL	RESID.	PHASE	WGT%	%
SiO_2	52.9	59.2	59.2	+.01			
TiO_2	.7	.7	.7	+.04			
Al_2O_3	15.8	15.2	15.2	+.02			
FeO	8.9	6.5	6.5	+.01	Fo85	-6.14	13.93
MgO	8.8	6.7	6.8	+.01	CPX2	-12.01	27.24
CaO	9.8	7.1	7.1	+.00	An60	-22.79	51.71
Na_2O	2.6	3.0	2.9	-.08	MT7.5	-3.14	7.13
K_2O	.6	1.6	1.6	-.01	MELT1	+6.99	0.00

SUM SQUARES RESID. = .0091 CRYSTALS REMOVED = 44.08%

	P	D	MODEL	BULK DC	% ERROR	MISFIT
Rb	11	66	19	.04	- 71.2	YES
Ba	185	342	314	.09	- 8.2	NO
Zr	50	129	84	.10	- 34.9	YES
Sr	201	232	205	.97	- 11.6	NO
V	251	171	108	2.45	- 36.8	YES
Cr	380	325	24	5.72	- 92.6	YES
Ni	142	101	22	4.19	- 78.2	YES

MODEL NO. : A5.4.14
PARENT : 14855 (RUAPEHU BASALT)
DAUGHTER : 14882 (MANGAWHERO FORMATION ACID ANDESITE)
DESCRIPTION : AFC (K-rich melt)

	P	D	MODEL	RESID.	PHASE	WGT%	%
SiO_2	52.9	60.2	60.2	-.00			
TiO_2	.7	.8	.8	-.02			
Al_2O_3	15.8	15.6	15.6	-.01			
FeO	8.9	6.3	6.2	-.00	Fo80	-8.16	16.34
MgO	8.8	5.8	5.8	-.00	CPX2	-13.92	27.89
CaO	9.8	6.7	6.7	-.00	An60	-24.96	49.99
Na_2O	2.6	2.9	2.9	+.04	MT10.0	-2.89	5.78
K_2O	.6	1.8	1.8	-.00	MELT1	+6.88	0.00

SUM SQUARES RESID. = .0018 CRYSTALS REMOVED = 49.93%

	P	D	MODEL	BULK DC	% ERROR	MISFIT
Rb	11	73	21	.04	- 71.2	YES
Ba	185	388	348	.09	- 10.3	NO
Zr	50	142	93	.10	- 34.5	YES
Sr	201	222	210	.94	- 5.4	NO
V	251	176	121	2.06	- 31.3	YES
Cr	380	240	20	5.27	- 91.7	YES
Ni	142	81	13	4.41	- 84.0	YES

MODEL NO. : A5.4.15
PARENT : 17439 (WAIMARINO BASALT)
DAUGHTER : 14882 (MANGAWHERO FORMATION ACID ANDESITE)
DESCRIPTION : AFC (K-rich melt)

	P	D	MODEL	RESID.	PHASE	WGT%	%
SiO_2	53.0	60.2	60.3	+.09			
TiO_2	.5	.8	.7	-.03	PHASE	WGT%	%
Al_2O_3	12.9	15.6	15.7	+.06			
FeO	8.5	6.3	6.3	+.06	Fo85	-14.26	36.34
MgO	13.3	5.8	5.9	+.04	CPX2	-16.87	43.00
CaO	9.7	6.7	6.7	+.02	An90	-7.63	19.44
Na_2O	1.7	2.9	2.7	-.17	MT2.5	-.48	1.23
K_2O	.4	1.8	1.7	-.08	MELT1	+12.80	0.00

SUM SQUARES RESID. = .0547 CRYSTALS REMOVED = 39.24%

	P	D	MODEL	BULK DC	% ERROR	MISFIT
Rb	15	73	24	.03	- 67.1	YES
Ba	122	388	196	.04	- 49.5	YES
Zr	48	142	74	.12	- 47.9	YES
Sr	342	222	462	.39	+108.1	YES
V	226	176	241	.87	+ 36.9	YES
Cr	1037	240	131	5.16	- 45.4	YES
Ni	341	81	32	5.76	- 60.5	YES

MODEL NO. : A5.4.16
PARENT : 14855 (RUAPEHU BASALT)
DAUGHTER : 14829 (MANGAWHERO FORMATION DACITE)
DESCRIPTION : AFC (K-rich melt)

	P	D	MODEL	RESID.	PHASE	WGT%	%
SiO_2	52.9	64.4	64.4	-.00			
TiO_2	.7	.9	.8	-.02	PHASE	WGT%	%
Al_2O_3	15.8	15.6	15.6	-.01			
FeO	8.9	5.1	5.1	+.00	Fo80	-10.25	18.66
MgO	8.8	3.2	3.2	-.00	CPX2	-15.73	28.65
CaO	9.8	4.8	4.8	-.00	An60	-26.13	47.58
Na_2O	2.6	3.1	3.1	+.03	MT7.5	-2.81	5.11
K_2O	.6	3.1	3.1	-.00	MELT1	+26.95	0.00

SUM SQUARES RESID. = .0011 CRYSTALS REMOVED = 54.92%

	P	D	MODEL	BULK DC	% ERROR	MISFIT
Rb	11	132	24	.04	- 81.8	YES
Ba	185	535	384	.08	- 28.2	YES
Zr	50	226	103	.10	- 54.4	YES
Sr	201	215	218	.90	+ 1.4	NO
V	251	151	126	1.87	- 16.6	NO
Cr	380	113	15	5.10	- 86.7	YES
Ni	142	48	8	4.70	- 83.3	YES

MODEL NO. : A5.4.17
PARENT : 14844 (MANGAWHERO FORMATION ACID ANDESITE)
DAUGHTER : 14883 (MANGAWHERO FORMATION ACID ANDESITE)
DESCRIPTION : Olivine + clinopyroxene addition

	P	D	MODEL	RESID.	PHASE	WGT%	%
SiO_2	58.3	58.0	57.3	-.71			
TiO_2	.7	.7	.7	-.05	PHASE	WGT%	%
Al_2O_3	17.4	15.6	16.2	+.56			
FeO	6.9	6.9	7.1	+.18	Fo90	+4.53	0.00
MgO	4.7	7.0	7.0	-.05	CPX1	+3.71	0.00
CaO	7.6	7.6	7.8	+.23			
Na_2O	3.1	2.7	2.9	+.13			
K_2O	1.2	1.4	1.1	-.30			

SUM SQUARES RESID. =1.0170 CRYSTALS ADDED = 8.24%

	P	D	MODEL	BULK DC	% ERROR	MISFIT
Rb	37	54	34	.01	- 37.0	YES
Ba	310	331	283	.01	- 14.5	NO
Zr	93	114	86	.12	- 24.6	YES
Sr	250	250	229	.04	- 8.4	NO
V	195	189	187	.54	- 1.1	NO
Cr	92	286	176	5.05	- 38.5	YES
Ni	35	110	91	9.35	- 17.3	NO

MODEL NO. : A5.4.18
PARENT : 14844 (MANGAWHERO FORMATION ACID ANDESITE)
DAUGHTER : 14883 (MANGAWHERO FORMATION ACID ANDESITE)
DESCRIPTION : AFC (K-rich melt; olivine + clinopyroxene addition)

	P	D	MODEL	RESID.	PHASE	WGT%	%
SiO_2	58.3	58.0	58.0	+.01			
TiO_2	.7	.7	.6	-.08	PHASE	WGT%	%
Al_2O_3	17.4	15.6	15.6	+.02			
FeO	6.9	6.9	6.8	-.04	Fo90	+5.34	0.00
MgO	4.7	7.0	7.1	+.02	CPX1	+5.72	0.00
CaO	7.6	7.6	7.6	+.02			
Na_2O	3.1	2.7	2.8	+.07			
K_2O	1.2	1.4	1.4	-.01	MELT1	+7.03	0.00

SUM SQUARES RESID. = .0150 CRYSTALS ADDED = 11.06%

	P	D	MODEL	BULK DC	% ERROR	MISFIT
Rb	37	54	32	.02	- 40.7	YES
Ba	310	331	272	.02	- 17.8	NO
Zr	93	114	83	.13	- 27.2	YES
Sr	250	250	220	.05	- 12.0	NO
V	195	189	186	.61	- 1.6	NO
Cr	92	286	203	5.65	- 29.0	YES
Ni	35	110	102	9.09	- 7.3	NO

MODEL NO. : A5.4.19
PARENT : 14886 (MANGAWHERO FORMATION ACID ANDESITE)
DAUGHTER : 14882 (MANGAWHERO FORMATION ACID ANDESITE)
DESCRIPTION : Olivine + clinopyroxene addition

	P	D	MODEL	RESID.	PHASE	WGT%	%
SiO_2	61.8	60.2	60.4	+.22			
TiO_2	.8	.8	.7	-.06	PHASE	WGT%	%
Al_2O_3	16.9	15.6	15.4	-.26			
FeO	5.8	6.3	6.0	-.22	Fo90	+4.59	0.00
MgO	3.2	5.8	5.9	+.04	CPX1	+6.08	0.00
CaO	5.9	6.7	6.6	-.06			
Na_2O	3.5	2.9	3.2	+.31			
K_2O	2.0	1.8	1.8	+.03			

SUM SQUARES RESID. = .2747 CRYSTALS ADDED = 10.67%

	P	D	MODEL	BULK DC	% ERROR	MISFIT
Rb	81	73	71	.02	- 2.7	NO
Ba	418	388	369	.02	- 4.9	NO
Zr	158	142	142	.15	+ 0.0	NO
Sr	253	222	224	.05	+ .9	NO
V	162	176	152	.66	- 13.6	NO
Cr	51	240	218	6.13	- 9.2	NO
Ni	26	81	113	9.31	- 39.5	YES

MODEL NO. : A5.4.20
PARENT : 14813 (MANGAWHERO FORMATION DACITE)
DAUGHTER : 14829 (MANGAWHERO FORMATION DACITE)
DESCRIPTION : Olivine + clinopyroxene addition

	P	D	MODEL	RESID.	PHASE	WGT%	%
SiO_2	64.5	64.4	64.1	-.26			
TiO_2	.8	.9	.8	-.05	PHASE	WGT%	%
Al_2O_3	16.2	15.6	15.9	+.30			
FeO	5.0	5.1	5.1	-.02	Fo90	+.95	0.00
MgO	2.5	3.2	3.1	-.02	CPX1	+1.10	0.00
CaO	4.7	4.8	4.9	+.06			
Na_2O	3.4	3.1	3.3	+.23			
K_2O	2.9	3.1	2.8	-.24			

SUM SQUARES RESID. = .2729 CRYSTALS REMOVED = 2.05%

	P	D	MODEL	BULK DC	% ERROR	MISFIT
Rb	115	132	113	.02	- 22.0	YES
Ba	530	535	519	.02	- 3.0	NO
Zr	199	226	195	.14	- 13.7	NO
Sr	228	215	223	.05	+ 3.7	NO
V	136	151	135	.63	- 10.6	NO
Cr	69	113	80	5.82	- 29.2	YES
Ni	32	48	39	8.79	- 18.8	NO

MODEL NO. : A5.5.1
PARENT : 17439 (WAIMARINO BASALT)
DAUGHTER : 14811 (MANGAWHERO FORMATION ACID ANDESITE)
DESCRIPTION : POAM fractionation

	P	D	MODEL	RESID.	PHASE	WGT%	%
SiO_2	53.0	58.2	58.3	+.15			
TiO_2	.5	.7	.7	-.01			
Al_2O_3	12.9	15.6	15.7	+.11			
FeO	8.5	7.1	7.2	+.12	Fo90	-14.76	37.50
MgO	13.3	6.1	6.2	+.08	CPX2	-14.88	37.82
CaO	9.7	8.3	8.3	+.04	An90	-8.55	21.74
Na_2O	1.7	2.9	2.7	-.19	MT7.5	-1.16	2.95
K_2O	.4	1.2	.9	-.30			

SUM SQUARES RESID. = .1841 CRYSTALS REMOVED = 39.35%

	P	D	MODEL	BULK DC	% ERROR	MISFIT
Rb	15	40	24	.03	- 40.0	YES
Ba	122	294	197	.05	- 33.0	YES
Zr	48	90	75	.11	- 16.7	NO
Sr	342	334	455	.43	+ 36.2	YES
V	226	207	191	1.33	- 8.7	NO
Cr	1037	231	118	5.34	- 48.9	YES
Ni	341	73	32	5.72	- 56.2	YES

MODEL NO. : A5.5.2
PARENT : 14855 (RUAPEHU BASALT)
DAUGHTER : 14811 (MANGAWHERO FORMATION ACID ANDESITE)
DESCRIPTION : POAM fractionation

	P	D	MODEL	RESID.	PHASE	WGT%	%
SiO_2	52.9	58.2	58.3	+.02			
TiO_2	.7	.7	.7	+.01			
Al_2O_3	15.8	15.6	15.6	+.02			
FeO	8.9	7.1	7.1	+.02	Fo80	-9.24	19.41
MgO	8.8	6.1	6.2	+.01	CPX2	-11.35	23.83
CaO	9.8	8.3	8.3	+.01	An60	-24.46	51.37
Na_2O	2.6	2.9	2.9	-.02	MT12.5	-2.57	5.39
K_2O	.6	1.2	1.2	-.05			

SUM SQUARES RESID. = .0044 CRYSTALS REMOVED = 47.62%

	P	D	MODEL	BULK DC	% ERROR	MISFIT
Rb	11	40	20	.04	- 50.0	YES
Ba	185	294	333	.09	+ 13.3	NO
Zr	50	90	90	.09	+ 0.0	NO
Sr	201	334	206	.96	- 38.3	YES
V	251	207	140	1.90	- 32.4	YES
Cr	380	231	34	4.74	- 85.3	YES
Ni	142	73	14	4.54	- 80.8	YES

MODEL NO. : A5.5.3
PARENT : 11965 (RED CRATER BASALT)
DAUGHTER : 14811 (MANGAWHERO FORMATION ACID ANDESITE)
DESCRIPTION : POAM fractionation

	P	D	MODEL	RESID.	PHASE	WGT%	%
SiO_2	53.3	58.2	58.2	+.01			
TiO_2	.7	.7	.7	-.01			
Al_2O_3	15.5	15.6	15.6	-.00			
FeO	9.1	7.1	7.1	+.01	Fo80	-4.82	12.30
MgO	7.8	6.1	6.1	+.00	CPX2	-13.36	34.05
CaO	10.5	8.3	8.3	+.00	An70	-18.21	46.44
Na_2O	2.5	2.9	3.0	+.06	MT12.5	-2.83	7.21
K_2O	.7	1.2	1.1	-.07			

SUM SQUARES RESID. = .0083 CRYSTALS REMOVED = 39.22%

	P	D	MODEL	BULK DC	% ERROR	MISFIT
Rb	20	40	32	.04	- 20.0	NO
Ba	137	294	216	.08	- 26.5	YES
Zr	68	90	105	.12	+ 16.7	NO
Sr	278	334	295	.88	- 11.7	NO
V	271	207	125	2.55	- 39.6	YES
Cr	281	231	19	6.42	- 91.8	YES
Ni	63	73	10	4.63	- 86.3	YES

MODEL NO. : A5.5.4
PARENT : 11965 (RED CRATER BASALT)
DAUGHTER : 14811 (MANGAWHERO FORMATION ACID ANDESITE)
DESCRIPTION : AFC (K-rich melt)

	P	D	MODEL	RESID.	PHASE	WGT%	%
SiO_2	53.3	58.2	58.2	-.01			
TiO_2	.7	.7	.6	-.02			
Al_2O_3	15.5	15.6	15.6	-.01			
FeO	9.1	7.1	7.1	-.00	Fo80	-4.42	12.18
MgO	7.8	6.1	6.1	-.00	CPX2	-12.47	34.36
CaO	10.5	8.3	8.3	-.00	An70	-16.70	46.03
Na_2O	2.5	2.9	2.9	+.03	MT12.5	-2.69	7.43
K_2O	.7	1.2	1.2	+.01	MELT1	+2.31	0.00

SUM SQUARES RESID. = .0023 CRYSTALS REMOVED = 36.28%

	P	D	MODEL	BULK DC	% ERROR	MISFIT
Rb	20	40	31	.04	- 22.5	YES
Ba	137	294	207	.08	- 29.6	YES
Zr	68	90	101	.12	+ 12.2	NO
Sr	278	334	295	.87	- 11.7	NO
V	271	207	130	2.62	- 37.2	YES
Cr	281	231	23	6.53	- 90.0	YES
Ni	63	73	12	4.65	- 83.6	YES

MODEL NO. : A5.5.5
PARENT : 17439 (WAIMARINO BASALT)
DAUGHTER : 16722 (WAHIANOA FORMATION ACID ANDESITE)
DESCRIPTION : AFC (K-rich melt)

	P	D	MODEL	RESID.	PHASE	WGT%	%
SiO_2	53.0	61.7	61.8	+.07			
TiO_2	.5	.6	.8	+.17	PHASE	WGT%	%
Al_2O_3	12.9	15.8	15.9	+.04			
FeO	8.5	5.6	5.6	+.03	Fo80	-18.67	38.00
MgO	13.3	4.7	4.8	+.03	CPX2	-18.28	37.20
CaO	9.7	6.5	6.5	+.00	An90	-12.09	24.60
Na_2O	1.7	3.4	3.2	-.22	MT7.5	-.10	.20
K_2O	.4	1.7	1.5	-.11	MELT1	+6.63	0.00

SUM SQUARES RESID. = .0983 CRYSTALS REMOVED = 49.14%

	P	D	MODEL	BULK DC	% ERROR	MISFIT
Rb	15	59	29	.03	- 50.8	YES
Ba	122	353	232	.05	- 34.3	YES
Zr	48	108	88	.10	- 18.5	NO
Sr	342	351	485	.48	+ 38.2	YES
V	226	138	316	.50	+129.0	YES
Cr	1037	106	121	4.18	+ 14.2	NO
Ni	341	54	17	5.45	- 68.5	YES

MODEL NO. : A5.5.6
PARENT : 14855 (RUAPEHU BASALT)
DAUGHTER : 16722 (WAHIANOA FORMATION ACID ANDESITE)
DESCRIPTION : POAM fractionation

	P	D	MODEL	RESID.	PHASE	WGT%	%
SiO_2	52.9	61.7	61.8	+.04			
TiO_2	.7	.6	.6	+.02	PHASE	WGT%	%
Al_2O_3	15.8	15.8	15.9	+.04			
FeO	8.9	5.6	5.6	+.03	Fo80	-10.72	17.63
MgO	8.8	4.7	4.8	+.02	CPX2	-16.14	26.55
CaO	9.8	6.5	6.5	+.01	An60	-30.51	50.19
Na_2O	2.6	3.4	3.3	-.10	MT12.5	-3.42	5.63
K_2O	.6	1.7	1.6	-.07			

SUM SQUARES RESID. = .0196 CRYSTALS REMOVED = 60.79%

	P	D	MODEL	BULK DC	% ERROR	MISFIT
Rb	11	59	27	.04	- 54.2	YES
Ba	185	353	435	.09	+ 23.2	YES
Zr	50	108	117	.10	+ 8.3	NO
Sr	201	351	212	.94	- 39.6	YES
V	251	138	98	2.00	- 29.0	YES
Cr	380	106	8	5.09	- 92.4	YES
Ni	142	54	5	4.49	- 90.7	YES

MODEL NO. : A5.5.7
PARENT : 11965 (RED CRATER BASALT)
DAUGHTER : 16722 (WAHIANOA FORMATION ACID ANDESITE)
DESCRIPTION : AFC (K-rich melt)

	P	D	MODEL	RESID.	PHASE	WGT%	%
SiO_2	53.3	61.7	61.8	+.01			
TiO_2	.7	.6	.6	-.01	PHASE	WGT%	%
Al_2O_3	15.5	15.8	15.8	+.01			
FeO	9.1	5.6	5.6	+.01	Fo80	-6.16	12.19
MgO	7.8	4.7	4.7	+.00	CPX2	-17.89	35.39
CaO	10.5	6.5	6.5	+.00	An70	-22.80	45.09
Na_2O	2.5	3.4	3.4	-.01	MT12.5	-3.71	7.34
K_2O	.7	1.7	1.7	-.00	MELT1	+3.25	0.00

SUM SQUARES RESID. = .0005 CRYSTALS REMOVED = 50.56%

	P	D	MODEL	BULK DC	% ERROR	MISFIT
Rb	20	59	39	.04	- 33.9	YES
Ba	137	353	262	.08	- 25.8	YES
Zr	68	108	126	.12	+ 16.7	NO
Sr	278	351	308	.86	- 12.3	NO
V	271	138	87	2.61	- 37.2	YES
Cr	281	106	5	6.60	- 95.3	YES
Ni	63	54	5	4.70	- 90.7	YES

MODEL NO. : A5.5.8
PARENT : 14811 (MANGAWHERO FORMATION ACID ANDESITE)
DAUGHTER : 16722 (WAHIANOA FORMATION ACID ANDESITE)
DESCRIPTION : POAM fractionation (O = olivine)

	P	D	MODEL	RESID.	PHASE	WGT%	%
SiO_2	58.2	61.7	61.8	+.03			
TiO_2	.7	.6	.6	+.02	PHASE	WGT%	%
Al_2O_3	15.6	15.8	15.8	+.02			
FeO	7.1	5.6	5.6	+.02	Fo80	-2.80	12.31
MgO	6.1	4.7	4.8	+.01	CPX2	-8.49	37.38
CaO	8.3	6.5	6.5	+.01	An70	-9.86	43.40
Na_2O	2.9	3.4	3.3	-.04	MT12.5	-1.57	6.91
K_2O	1.2	1.7	1.6	-.06			

SUM SQUARES RESID. = .0082 CRYSTALS REMOVED = 22.72%

	P	D	MODEL	BULK DC	% ERROR	MISFIT
Rb	40	59	51	.04	- 13.6	NO
Ba	294	353	373	.08	+ 5.7	NO
Zr	90	108	113	.13	+ 4.6	NO
Sr	334	351	349	.83	- .6	NO
V	207	138	141	2.50	+ 2.2	NO
Cr	231	106	54	6.63	- 49.1	YES
Ni	73	54	34	3.97	- 37.0	YES

MODEL NO. : A5.5.9
PARENT : 14811 (MANGAWHERO FORMATION ACID ANDESITE)
DAUGHTER : 16722 (WAHIANOA FORMATION ACID ANDESITE)
DESCRIPTION : POAM fractionation (O = orthopyroxene)

	P	D	MODEL	RESID.	PHASE	WGT%	%
SiO_2	58.2	61.7	61.7	-.01			
TiO_2	.7	.6	.6	+.02			
Al_2O_3	15.6	15.8	15.8	-.02			
FeO	7.1	5.6	5.5	-.01	En80	-4.64	17.37
MgO	6.1	4.7	4.7	-.00	CPX2	-8.36	31.28
CaO	8.3	6.5	6.5	-.01	An70	-11.96	44.75
Na_2O	2.9	3.4	3.4	+.02	MT12.5	-1.76	6.60
K_2O	1.2	1.7	1.7	+.00			

SUM SQUARES RESID. = .0011 CRYSTALS REMOVED = 26.72%

	P	D	MODEL	BULK DC	% ERROR	MISFIT
Rb	40	59	54	.04	- 8.5	NO
Ba	294	353	391	.08	+ 10.8	NO
Zr	90	108	118	.13	+ 9.3	NO
Sr	334	351	350	.85	- .3	NO
V	207	138	129	2.52	- 6.5	NO
Cr	231	106	45	6.29	- 57.5	YES
Ni	73	54	29	3.93	- 46.3	YES

MODEL NO. : A5.6.1
PARENT : 17439 (WAIMARINO BASALT)
DAUGHTER : 14817 (HAUHUNGATAHI ACID ANDESITE)
DESCRIPTION : POAM fractionation

	P	D	MODEL	RESID.	PHASE	WGT%	%
SiO_2	53.0	57.6	57.6	-.00			
TiO_2	.5	.6	.6	-.01			
Al_2O_3	12.9	15.7	15.7	-.00			
FeO	8.5	7.8	7.8	-.00	Fo90	-14.61	40.66
MgO	13.3	6.4	6.4	-.00	CPX1	-12.51	34.81
CaO	9.7	8.8	8.8	-.00	An80	-7.50	20.89
Na_2O	1.7	2.3	2.3	+.02	MT7.5	-1.31	3.64
K_2O	.4	.7	.7	-.01			

SUM SQUARES RESID. = .0007 CRYSTALS REMOVED = 35.93%

	P	D	MODEL	BULK DC	% ERROR	MISFIT
Rb	15	16	23	.03	+ 43.8	YES
Ba	122	183	187	.04	+ 2.2	NO
Zr	48	68	71	.11	+ 4.4	NO
Sr	342	467	444	.41	- 4.9	NO
V	226	215	180	1.51	- 16.3	NO
Cr	1037	195	150	5.35	- 23.0	YES
Ni	341	34	39	5.87	+ 14.7	NO

MODEL NO. : A5.6.2
PARENT : 14855 (RUAPEHU BASALT)
DAUGHTER : 14817 (HAUHUNGATAHI ACID ANDESITE)
DESCRIPTION : POAM fractionation

	P	D	MODEL	RESID.	PHASE	WGT%	%
SiO_2	52.9	57.6	57.6	-.05			
TiO_2	.7	.6	.6	-.02	PHASE	WGT%	%
Al_2O_3	15.8	15.7	15.7	-.01			
FeO	8.9	7.8	7.8	-.04	Fo90	-7.72	15.72
MgO	8.8	6.4	6.3	-.02	CPX1	-11.01	22.43
CaO	9.8	8.8	8.8	-.02	An50	-26.52	54.03
Na_2O	2.6	2.3	2.2	-.07	MT10.0	-3.84	7.82
K_2O	.6	.7	.9	+.22			

SUM SQUARES RESID. = .0601 CRYSTALS REMOVED = 49.09%

	P	D	MODEL	BULK DC	% ERROR	MISFIT
Rb	11	16	21	.04	+ 31.3	YES
Ba	185	183	341	.09	+ 86.3	YES
Zr	50	68	92	.09	+ 35.3	YES
Sr	201	467	200	1.01	- 57.2	YES
V	251	215	85	2.61	- 60.5	YES
Cr	380	195	18	5.53	- 90.8	YES
Ni	142	34	16	4.21	- 52.9	YES

MODEL NO. : A5.6.3
PARENT : 11965 (RED CRATER BASALT)
DAUGHTER : 14817 (HAUHUNGATAHI ACID ANDESITE)
DESCRIPTION : POAM fractionation

	P	D	MODEL	RESID.	PHASE	WGT%	%
SiO_2	53.3	57.6	57.6	-.06			
TiO_2	.7	.6	.6	+.02	PHASE	WGT%	%
Al_2O_3	15.5	15.7	15.7	+.00			
FeO	9.1	7.8	7.8	-.05	Fo90	-4.14	9.03
MgO	7.8	6.4	6.3	-.03	CPX1	-14.15	30.88
CaO	10.5	8.8	8.8	-.02	An50	-23.59	51.48
Na_2O	2.5	2.3	2.2	-.15	MT10.0	-3.94	8.61
K_2O	.7	.7	1.0	+.29			

SUM SQUARES RESID. = .1153 CRYSTALS REMOVED = 45.82%

	P	D	MODEL	BULK DC	% ERROR	MISFIT
Rb	20	16	36	.04	+125.0	YES
Ba	137	183	239	.09	+ 30.6	YES
Zr	68	68	117	.12	+ 72.1	YES
Sr	278	467	283	.97	- 39.4	YES
V	271	215	83	2.94	- 61.4	YES
Cr	281	195	9	6.63	- 95.4	YES
Ni	63	34	10	4.08	- 70.6	YES

MODEL NO. : A5.6.4
PARENT : 22998 (ONGAROTO BASALT)
DAUGHTER : 14817 (HAUHUNGATAHI ACID ANDESITE)
DESCRIPTION : POAM fractionation

	P	D	MODEL	RESID.	PHASE	WGT%	%
SiO_2	50.9	57.6	57.5	-.09			
TiO_2	1.1	.6	.6	-.05	PHASE	WGT%	%
Al_2O_3	15.8	15.7	15.6	-.11			
FeO	9.2	7.8	7.7	-.08	Fo90	-9.21	15.96
MgO	9.4	6.4	6.3	-.07	CPX1	-13.58	23.52
CaO	10.5	8.8	8.8	-.06	An60	-29.87	51.74
Na_2O	2.5	2.3	2.5	+.20	MT17.5	-5.07	8.78
K_2O	.6	.7	1.0	+.26			

SUM SQUARES RESID. = .1431 CRYSTALS REMOVED = 57.73%

	P	D	MODEL	BULK DC	% ERROR	MISFIT
Rb	10	16	23	.04	+ 43.8	YES
Ba	nd	183				
Zr	125	68	271	.10	+298.5	YES
Sr	330	467	339	.97	- 27.4	YES
V	220	215	43	2.91	- 80.0	YES
Cr	550	195	7	6.03	- 96.4	YES
Ni	160	34	10	4.27	- 70.6	YES

MODEL NO. : A5.6.5
PARENT : 22994 (BEN LOMOND BASALT)
DAUGHTER : 14817 (HAUHUNGATAHI ACID ANDESITE)
DESCRIPTION : POAM fractionation

	P	D	MODEL	RESID.	PHASE	WGT%	%
SiO_2	51.4	57.6	57.6	-.06			
TiO_2	1.1	.6	.5	-.08	PHASE	WGT%	%
Al_2O_3	17.6	15.7	15.7	-.08			
FeO	9.8	7.8	7.8	-.05	Fo90	-2.44	4.57
MgO	6.0	6.4	6.3	-.05	CPX1	-11.27	21.10
CaO	10.8	8.8	8.8	-.04	An60	-33.58	62.87
Na_2O	2.8	2.3	2.5	+.15	MT15.0	-6.12	11.46
K_2O	.5	.7	.9	+.20			

SUM SQUARES RESID. = .0824 CRYSTALS REMOVED = 53.41%

	P	D	MODEL	BULK DC	% ERROR	MISFIT
Rb	14	16	29	.05	+ 81.5	YES
Ba	129	183	255	.11	+ 39.3	YES
Zr	84	68	166	.11	+144.1	YES
Sr	348	467	306	1.17	- 34.5	YES
V	252	215	33	3.68	- 84.7	YES
Cr	44	195	1	6.75	- 99.5	YES
Ni	29	34	5	3.33	- 85.3	YES

MODEL NO. : A5.6.6
PARENT : 17439 (WAIMARINO BASALT)
DAUGHTER : 14815 (HAUHUNGATAHI BASIC ANDESITE)
DESCRIPTION : POAM fractionation

	P	D	MODEL	RESID.	PHASE	WGT%	%
SiO_2	53.0	56.1	56.0	-.04			
TiO_2	.5	.6	.6	+.01			
Al_2O_3	12.9	15.2	15.2	-.03			
FeO	8.5	7.6	7.6	-.04	Fo90	-10.12	36.68
MgO	13.3	9.1	9.1	-.03	CPX1	-10.94	39.67
CaO	9.7	9.0	9.0	-.03	An70	-5.16	18.70
Na_2O	1.7	2.1	2.1	+.00	MT5.0	-1.37	4.95
K_2O	.4	.4	.5	+.16			

SUM SQUARES RESID. = .0307 CRYSTALS REMOVED = 27.59%

	P	D	MODEL	BULK DC	% ERROR	MISFIT
Rb	15	8	21	.03	+162.5	YES
Ba	122	128	166	.04	+ 29.7	YES
Zr	48	52	64	.12	+ 23.1	YES
Sr	342	569	418	.38	- 26.5	YES
V	226	190	166	1.95	- 12.6	NO
Cr	1037	342	186	6.32	- 45.6	YES
Ni	341	88	69	5.96	- 21.6	YES

MODEL NO. : A5.6.7
PARENT : 17439 (WAIMARINO BASALT)
DAUGHTER : 14816 (HAUHUNGATAHI BASIC ANDESITE)
DESCRIPTION : POAM fractionation

	P	D	MODEL	RESID.	PHASE	WGT%	%
SiO_2	53.0	56.6	56.6	+.02			
TiO_2	.5	.6	.6	-.01			
Al_2O_3	12.9	15.3	15.3	+.02			
FeO	8.5	7.7	7.7	+.02	Fo90	-13.55	47.62
MgO	13.3	7.3	7.3	+.01	CPX1	-8.73	30.67
CaO	9.7	9.7	9.7	+.01	An80	-5.06	17.77
Na_2O	1.7	2.3	2.3	-.06	MT7.5	-1.12	3.95
K_2O	.4	.6	.6	-.00			

SUM SQUARES RESID. = .0054 CRYSTALS REMOVED = 28.46%

	P	D	MODEL	BULK DC	% ERROR	MISFIT
Rb	15	14	21	.02	+ 50.0	YES
Ba	122	177	168	.04	- 5.1	NO
Zr	48	60	65	.10	+ 8.3	NO
Sr	342	463	425	.35	- 8.4	NO
V	226	226	187	1.56	- 17.3	NO
Cr	1037	234	260	5.12	+ 11.1	NO
Ni	341	39	59	6.24	+ 51.3	YES

MODEL NO. : A5.6.8
PARENT : 17439 (WAIMARINO BASALT)
DAUGHTER : 14798 (OHAKUNE ACID ANDESITE)
DESCRIPTION : POAM fractionation

	P	D	MODEL	RESID.	PHASE	WGT%	%
SiO_2	53.0	57.4	57.4	+.02			
TiO_2	.5	.5	.5	+.01			
Al_2O_3	12.9	14.7	14.7	+.02			
FeO	8.5	8.1	8.1	+.01	Fo90	-14.23	41.42
MgO	13.3	7.1	7.2	+.01	CPX1	-9.85	28.67
CaO	9.7	9.2	9.2	+.01	An80	-9.02	26.26
Na_2O	1.7	2.3	2.3	-.08	MT10.0	-1.26	3.65
K_2O	.4	.7	.7	+.01			

SUM SQUARES RESID. = .0074 CRYSTALS REMOVED = 34.36%

	P	D	MODEL	BULK DC	% ERROR	MISFIT
Rb	15	16	23	.03	+ 43.8	YES
Ba	122	140	182	.05	+ 30.0	YES
Zr	48	62	70	.09	+ 12.9	NO
Sr	342	346	421	.51	+ 21.7	YES
V	226	224	187	1.45	- 16.5	NO
Cr	1037	265	214	4.74	- 19.2	NO
Ni	341	49	50	5.57	+ 2.0	NO

MODEL NO. : A5.6.9
PARENT : 14815 (HAUHUNGATAHI BASIC ANDESITE)
DAUGHTER : 14817 (HAUHUNGATAHI ACID ANDESITE)
DESCRIPTION : POA fractionation

	P	D	MODEL	RESID.	PHASE	WGT%	%
SiO_2	56.1	57.6	57.7	+.07			
TiO_2	.6	.6	.6	+.03			
Al_2O_3	15.2	15.7	15.8	+.05			
FeO	7.6	7.8	7.9	+.03	Fo90	-6.25	46.95
MgO	9.1	6.4	6.4	+.04	CPX1	-2.68	20.09
CaO	9.0	8.8	8.9	+.03	An80	-4.39	32.96
Na_2O	2.1	2.3	2.3	-.04			
K_2O	.4	.7	.5	-.22			

SUM SQUARES RESID. = .0607 CRYSTALS REMOVED = 13.32%

	P	D	MODEL	BULK DC	% ERROR	MISFIT
Rb	8	16	9	.03	- 43.8	YES
Ba	128	183	146	.06	- 20.2	YES
Zr	52	68	60	.06	- 11.8	NO
Sr	569	467	600	.62	+ 28.5	YES
V	190	215	211	.26	- 1.9	NO
Cr	342	195	277	2.48	+ 42.1	YES
Ni	88	34	49	5.15	+ 44.1	YES

MODEL NO. : A5.6.10
PARENT : 14817 (HAUHUNGATAHI ACID ANDESITE)
DAUGHTER : 14815 (HAUHUNGATAHI BASIC ANDESITE)
DESCRIPTION : Olivine + clinopyroxene addition

	P	D	MODEL	RESID.	PHASE	WGT%	%
SiO_2	57.6	56.1	56.6	+.54			
TiO_2	.6	.6	.6	+.00	PHASE	WGT%	%
Al_2O_3	15.7	15.2	14.5	-.70			
FeO	7.8	7.6	7.9	+.33	Fo90	+5.92	69.92
MgO	6.4	9.1	8.9	-.15	CPX1	+2.54	30.08
CaO	8.8	9.0	8.6	-.36			
Na_2O	2.3	2.1	2.1	+.07			
K_2O	.7	.4	.7	+.28			

SUM SQUARES RESID. =1.1372 CRYSTALS ADDED = 8.46%

	P	D	MODEL	BULK DC	% ERROR	MISFIT
Rb	16	8	14	.01	+ 75.0	YES
Ba	183	128	166	.01	+ 29.7	YES
Zr	68	52	62	.08	+ 19.2	NO
Sr	467	569	445	.03	- 20.0	NO
V	215	190	226	.39	+ 18.9	NO
Cr	195	342	268	3.71	- 21.9	YES
Ni	34	88	83	10.20	- 5.6	NO

MODEL NO. : A5.6.11
PARENT : 17439 (WAIMARINO BASALT)
DAUGHTER : 24471 (PUKEKAIKIORE ACID ANDESITE)
DESCRIPTION : POAM fractionation

	P	D	MODEL	RESID.	PHASE	WGT%	%
SiO_2	53.0	57.5	57.6	+.09			
TiO_2	.5	.6	.6	+.01	PHASE	WGT%	%
Al_2O_3	12.9	14.8	14.9	+.07			
FeO	8.5	7.4	7.4	+.07	Fo90	-14.49	42.79
MgO	13.3	6.9	7.0	+.05	CPX1	-9.47	27.97
CaO	9.7	9.4	9.4	+.03	An80	-8.33	24.59
Na_2O	1.7	2.5	2.3	-.18	MT5.0	-1.58	4.66
K_2O	.4	.9	.7	-.14			

SUM SQUARES RESID. = .0745 CRYSTALS REMOVED = 33.87%

	P	D	MODEL	BULK DC	% ERROR	MISFIT
Rb	15	30	22	.03	- 26.7	YES
Ba	122	214	181	.05	- 15.4	NO
Zr	48	90	70	.10	- 22.2	YES
Sr	342	640	425	.48	- 33.6	YES
V	226	201	166	1.74	- 17.4	NO
Cr	1037	276	191	5.09	- 30.8	YES
Ni	341	38	48	5.74	+ 26.3	YES

MODEL NO. : A5.7.1
PARENT1 : 17439 (WAIMARINO BASALT)
PARENT2 : 14813 (MANGAWHERO FORMATION DACITE)
DAUGHTER : 14848 (PUKEONAKE BASIC ANDESITE)
DESCRIPTION : Binary mixing

	P1	P2	D	MODEL	RESID.
SiO_2	53.0	64.5	57.5	57.6	+.08
TiO_2	.5	.8	.7	.6	-.07
Al_2O_3	12.9	16.2	14.4	14.2	-.22
FeO	8.5	5.0	7.1	6.9	-.18
MgO	13.3	2.5	8.7	8.6	-.08
CaO	9.7	4.7	7.3	7.5	+.20
Na_2O	1.7	3.4	2.8	2.4	-.39
K_2O	.4	2.9	1.5	1.5	+.01

SUM SQUARES RESID. = .2859 P1/P2 = 1.316

	P1	P2	D	MODEL	% ERROR	MISFIT
Rb	15	115	49	58	+ 15.5	NO
Ba	122	530	355	296	- 16.6	NO
Zr	48	199	115	112	- 2.6	NO
Sr	342	228	277	291	+ 5.1	NO
V	226	136	181	186	+ 2.8	NO
Cr	1037	69	507	615	+ 21.3	YES
Ni	341	32	237	206	- 13.1	NO

MODEL NO. : A5.7.2
PARENT1 : 17439 (WAIMARINO BASALT)
PARENT2 : 14889 (MANGAWHERO FORMATION DACITE)
DAUGHTER : 14848 (PUKEONAKE BASIC ANDESITE)
DESCRIPTION : Binary mixing

	P1	P2	D	MODEL	RESID.
SiO_2	53.0	64.0	57.5	57.5	-.02
TiO_2	.5	.8	.7	.6	-.07
Al_2O_3	12.9	16.8	14.4	14.5	+.11
FeO	8.5	5.1	7.1	7.0	-.12
MgO	13.3	2.3	8.7	8.6	-.15
CaO	9.7	4.9	7.3	7.6	+.31
Na_2O	1.7	3.4	2.8	2.4	-.37
K_2O	.4	2.8	1.5	1.4	-.04

SUM SQUARES RESID. = .2860 P1/P2 = 1.333

	P1	P2	D	MODEL	% ERROR	MISFIT
Rb	15	120	49	60	+ 22.4	YES
Ba	122	527	355	295	- 16.9	NO
Zr	48	201	115	113	- 1.7	NO
Sr	342	260	277	306	+ 10.5	NO
V	226	115	181	178	- 1.7	NO
Cr	1037	31	507	604	+ 19.1	NO
Ni	341	20	237	203	- 14.3	NO

MODEL NO. : A5.7.3
PARENT1 : 17439 (WAIMARINO BASALT)
PARENT2 : 14829 (MANGAWHERO FORMATION DACITE)
DAUGHTER : 14848 (PUKEONAKE BASIC ANDESITE)
DESCRIPTION : Binary mixing

	P1	P2	D	MODEL	RESID.
SiO_2	53.0	64.4	57.5	57.6	+.13
TiO_2	.5	.9	.7	.6	-.05
Al_2O_3	12.9	15.6	14.4	14.0	-.45
FeO	8.5	5.1	7.1	6.9	-.21
MgO	13.3	3.2	8.7	8.7	-.01
CaO	9.7	4.8	7.3	7.5	+.15
Na_2O	1.7	3.1	2.8	2.3	-.49
K_2O	.4	3.1	1.5	1.6	+.13

SUM SQUARES RESID. = .5461 P1/P2 = 1.228

	P1	P2	D	MODEL	% ERROR	MISFIT
Rb	15	132	49	67	+ 36.7	YES
Ba	122	535	355	305	- 14.1	NO
Zr	48	226	115	127	+ 10.4	NO
Sr	342	215	277	283	+ 2.2	NO
V	226	151	181	191	+ 5.5	NO
Cr	1037	113	507	617	+ 21.7	YES
Ni	341	48	237	208	- 12.2	NO

MODEL NO. : A5.7.4
PARENT1 : 17439 (WAIMARINO BASALT)
PARENT2 : 14885 (MANGAWHERO FORMATION ACID ANDESITE)
DAUGHTER : 14848 (PUKEONAKE BASIC ANDESITE)
DESCRIPTION : Binary mixing

	P1	P2	D	MODEL	RESID.
SiO_2	53.0	62.5	57.5	57.4	-.07
TiO_2	.5	.8	.7	.6	-.06
Al_2O_3	12.9	16.5	14.4	14.6	+.21
FeO	8.5	5.8	7.1	7.2	+.03
MgO	13.3	3.2	8.7	8.4	-.29
CaO	9.7	5.8	7.3	7.9	+.53
Na_2O	1.7	3.3	2.8	2.4	-.33
K_2O	.4	2.1	1.5	1.2	-.25

SUM SQUARES RESID. = .5860 P1/P2 = 1.073

	P1	P2	D	MODEL	% ERROR	MISFIT
Rb	15	84	49	48	- 2.0	NO
Ba	122	410	355	260	- 26.8	YES
Zr	48	161	115	102	- 11.3	NO
Sr	342	256	277	300	+ 8.3	NO
V	226	161	181	194	+ 7.2	NO
Cr	1037	65	507	567	+ 11.8	NO
Ni	341	25	237	188	- 20.7	YES

MODEL NO. : A5.7.5
PARENT1 : 17439 (WAIMARINO BASALT)
PARENT2 : 14886 (MANGAWHERO FORMATION ACID ANDESITE)
DAUGHTER : 14848 (PUKEONAKE BASIC ANDESITE)
DESCRIPTION : Binary mixing

	P1	P2	D	MODEL	RESID.
SiO_2	53.0	61.8	57.5	57.4	-.15
TiO_2	.5	.8	.7	.6	-.06
Al_2O_3	12.9	16.9	14.4	14.9	+.43
FeO	8.5	5.9	7.1	7.2	+.08
MgO	13.3	3.2	8.7	8.4	-.27
CaO	9.7	5.9	7.3	7.9	+.57
Na_2O	1.7	3.5	2.8	2.6	-.20
K_2O	.4	2.0	1.5	1.2	-.28

SUM SQUARES RESID. = .7324 P1/P2 = 1.054

	P1	P2	D	MODEL	% ERROR	MISFIT
Rb	15	81	49	47	- 4.1	NO
Ba	122	418	355	266	- 25.0	YES
Zr	48	158	115	102	- 11.3	NO
Sr	342	253	277	300	+ 8.3	NO
V	226	162	181	195	+ 7.7	NO
Cr	1037	51	507	558	+ 10.1	NO
Ni	341	26	237	188	- 20.7	YES

MODEL NO. : A5.7.6
PARENT1 : 17439 (WAIMARINO BASALT)
PARENT2 : 14813 (MANGAWHERO FORMATION DACITE)
DAUGHTER : 14826 (PUKEONAKE BASIC ANDESITE)
DESCRIPTION : Binary mixing

	P1	P2	D	MODEL	RESID.
SiO_2	53.0	64.5	57.6	57.7	+.08
TiO_2	.5	.8	.7	.6	-.07
Al_2O_3	12.9	16.2	14.5	14.2	-.33
FeO	8.5	5.0	6.9	7.0	+.07
MgO	13.3	2.5	8.9	8.7	-.19
CaO	9.7	4.7	7.3	7.5	+.27
Na_2O	1.7	3.4	2.7	2.4	-.29
K_2O	.4	2.9	1.4	1.5	+.08

SUM SQUARES RESID. = .3213 P1/P2 = 1.339

	P1	P2	D	MODEL	% ERROR	MISFIT
Rb	15	115	54	58	+ 7.4	NO
Ba	122	530	320	295	- 7.8	NO
Zr	48	199	112	112	+ 0.0	NO
Sr	342	228	283	292	+ 3.2	NO
V	226	136	182	187	+ 2.7	NO
Cr	1037	69	572	621	+ 8.6	NO
Ni	341	32	214	208	- 2.8	NO

MODEL NO. : A5.7.7
PARENT1 : 17439 (WAIMARINO BASALT)
PARENT2 : 14889 (MANGAWHERO FORMATION DACITE)
DAUGHTER : 14826 (PUKEONAKE BASIC ANDESITE)
DESCRIPTION : Binary mixing

	P1	P2	D	MODEL	RESID.
SiO_2	53.0	64.0	57.6	57.6	-.02
TiO_2	.5	.8	.7	.6	-.07
Al_2O_3	12.9	16.8	14.5	14.5	-.00
FeO	8.5	5.1	6.9	7.0	+.13
MgO	13.3	2.3	8.9	8.6	-.26
CaO	9.7	4.9	7.3	7.7	+.38
Na_2O	1.7	3.4	2.7	2.4	-.27
K_2O	.4	2.8	1.4	1.4	+.02

SUM SQUARES RESID. = .3056 P1/P2 = 1.356

	P1	P2	D	MODEL	% ERROR	MISFIT
Rb	15	120	54	60	+ 11.1	NO
Ba	122	527	320	294	- 8.1	NO
Zr	48	201	112	113	+ 0.9	NO
Sr	342	260	283	307	+ 8.5	NO
V	226	115	182	179	- 1.6	NO
Cr	1037	31	572	609	+ 6.4	NO
Ni	341	20	214	205	- 4.2	NO

MODEL NO. : A5.7.8
PARENT1 : 17439 (WAIMARINO BASALT)
PARENT2 : 14813 (MANGAWHERO FORMATION DACITE)
DAUGHTER : 14871 (MANGAWHERO FORMATION ACID ANDESITE)
DESCRIPTION : Binary mixing

	P1	P2	D	MODEL	RESID.
SiO_2	53.0	64.5	59.4	59.3	-.12
TiO_2	.5	.8	.6	.7	+.02
Al_2O_3	12.9	16.2	14.3	14.7	+.37
FeO	8.5	5.0	6.3	6.7	+.40
MgO	13.3	2.5	8.0	7.8	-.22
CaO	9.7	4.7	7.0	7.2	+.17
Na_2O	1.7	3.4	2.8	2.6	-.21
K_2O	.4	2.9	1.6	1.7	+.14

SUM SQUARES RESID. = .4576 P1/P2 = .917

	P1	P2	D	MODEL	% ERROR	MISFIT
Rb	15	115	59	68	+ 15.3	NO
Ba	122	530	327	337	+ 3.1	NO
Zr	48	199	117	128	+ 9.4	NO
Sr	342	228	283	284	+ .4	NO
V	226	136	173	180	+ 4.0	NO
Cr	1037	69	426	535	+ 25.6	YES
Ni	341	32	132	175	+ 32.6	YES

MODEL NO. : A5.7.9
PARENT1 : 17439 (WAIMARINO BASALT)
PARENT2 : 14889 (MANGAWHERO FORMATION DACITE)
DAUGHTER : 14871 (MANGAWHERO FORMATION ACID ANDESITE)
DESCRIPTION : Binary mixing

	P1	P2	D	MODEL	RESID.
SiO_2	53.0	64.0	59.4	59.2	-.25
TiO_2	.5	.8	.6	.7	+.02
Al_2O_3	12.9	16.8	14.3	15.1	+.77
FeO	8.5	5.1	6.3	6.8	+.48
MgO	13.3	2.3	8.0	7.7	-.27
CaO	9.7	4.9	7.0	7.3	+.31
Na_2O	1.7	3.4	2.8	2.6	-.20
K_2O	.4	2.8	1.6	1.7	+.07

SUM SQUARES RESID. =1.1000 P1/P2 = .942

	P1	P2	D	MODEL	% ERROR	MISFIT
Rb	15	120	59	70	+ 18.6	NO
Ba	122	527	327	334	+ 2.1	NO
Zr	48	201	117	128	+ 9.4	NO
Sr	342	260	283	303	+ 7.1	NO
V	226	115	173	170	- 1.7	NO
Cr	1037	31	426	524	+ 23.0	YES
Ni	341	20	132	177	+ 34.0	YES

MODEL NO. : A5.7.10
PARENT1 : 17439 (WAIMARINO BASALT)
PARENT2 : 14829 (MANGAWHERO FORMATION DACITE)
DAUGHTER : 14871 (MANGAWHERO FORMATION ACID ANDESITE)
DESCRIPTION : Binary mixing

	P1	P2	D	MODEL	RESID.
SiO_2	53.0	64.4	59.4	59.4	-.05
TiO_2	.5	.9	.6	.7	+.04
Al_2O_3	12.9	15.6	14.3	14.4	+.10
FeO	8.5	5.1	6.3	6.7	+.34
MgO	13.3	3.2	8.0	7.8	-.15
CaO	9.7	4.8	7.0	7.1	+.09
Na_2O	1.7	3.1	2.8	2.4	-.34
K_2O	.4	3.1	1.6	1.9	+.29

SUM SQUARES RESID. = .3626 P1/P2 = .837

	P1	P2	D	MODEL	% ERROR	MISFIT
Rb	15	132	59	79	+ 33.9	YES
Ba	122	535	327	348	+ 6.4	NO
Zr	48	226	117	145	+ 23.9	YES
Sr	342	215	283	274	+ 3.2	NO
V	226	151	173	186	+ 7.5	NO
Cr	1037	113	426	536	+ 25.8	YES
Ni	341	48	132	182	+ 37.9	YES